

R
ADIOLGY
AND
ONCOLOGY

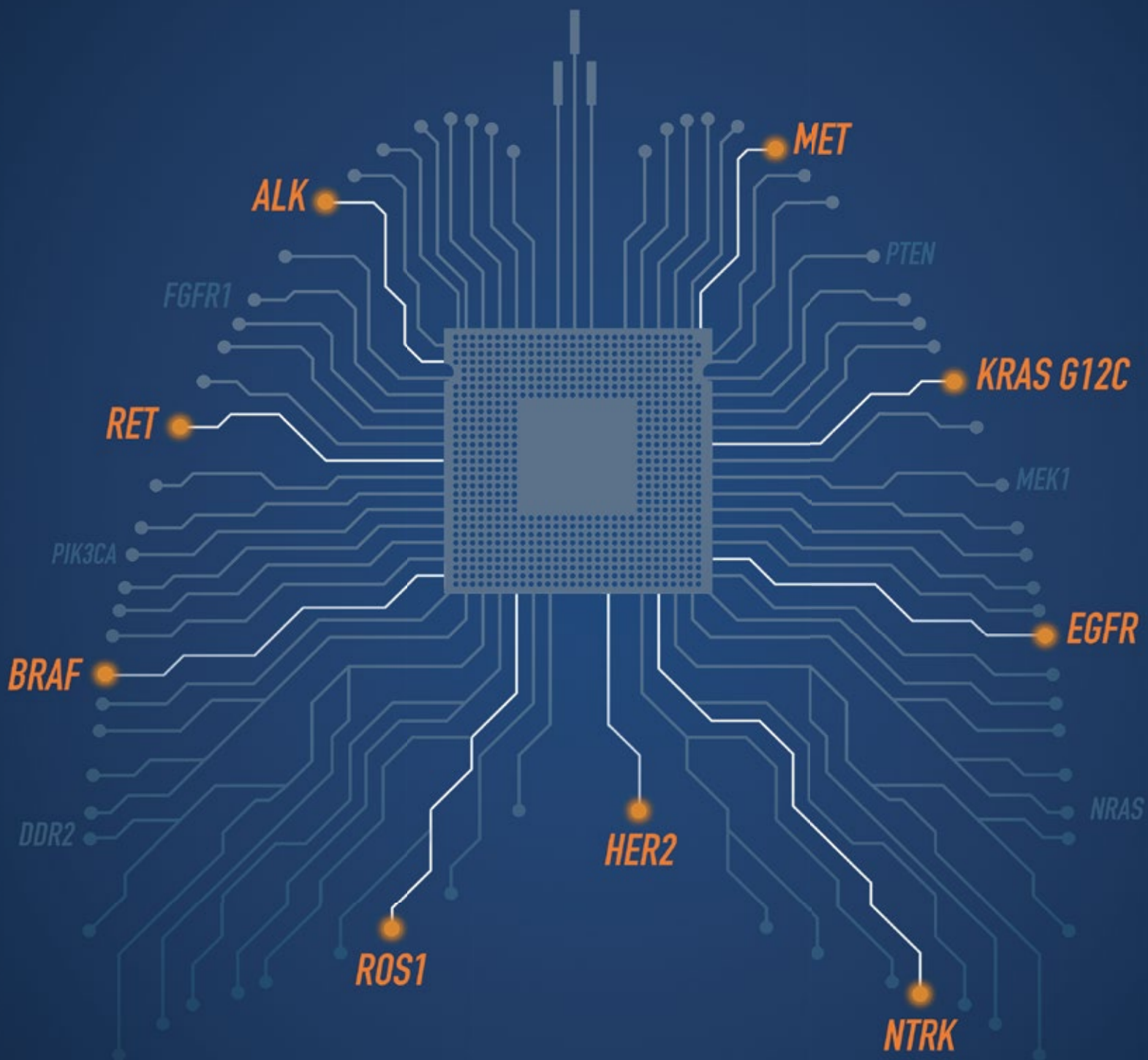
vol.55 no.4

december 2021



DODAJAMO MOČ TARČNEMU ZDRAVLJENJU NEDROBNOCELIČNEGA PLJUČNEGA RAKA

Desetletja inovacij tarčnega zdravljenja pomagajo ljudem s pljučnim rakom živeti dlje.





Publisher

Association of Radiology and Oncology

Aims and Scope

Radiology and Oncology is a multidisciplinary journal devoted to the publishing original and high quality scientific papers and review articles, pertinent to diagnostic and interventional radiology, computerized tomography, magnetic resonance, ultrasound, nuclear medicine, radiotherapy, clinical and experimental oncology, radiobiology, medical physics and radiation protection. Therefore, the scope of the journal is to cover beside radiology the diagnostic and therapeutic aspects in oncology, which distinguishes it from other journals in the field.

Editor-in-Chief

Gregor Serša, Institute of Oncology Ljubljana, Department of Experimental Oncology, Ljubljana, Slovenia (Subject Area: Experimental Oncology)

Executive Editor

Viljem Kovač, Institute of Oncology Ljubljana, Department of Radiation Oncology, Ljubljana, Slovenia (Subject Areas: Clinical Oncology, Radiotherapy)

Editorial Board

Subject Areas:

Radiology and Nuclear Medicine

Sotirios Bisdas, University College London, Department of Neuroradiology, London, UK

Boris Brkljačić, University Hospital "Dubrava", Department of Diagnostic and Interventional Radiology, Zagreb, Croatia

Maria Gódný, National Institute of Oncology, Budapest, Hungary

Gordana Ivanac, University Hospital Dubrava, Department of Diagnostic and Interventional Radiology, Zagreb, Croatia

Luka Ležaić, University Medical Centre Ljubljana, Department for Nuclear Medicine, Ljubljana, Slovenia

Katarina Šurlan Popovič, University Medical Center Ljubljana, Clinical Institute of Radiology, Ljubljana, Slovenia

Jernej Vidmar, University Medical Center Ljubljana, Clinical Institute of Radiology, Ljubljana, Slovenia

Deputy Editors

Andrej Čör, University of Primorska, Faculty of Health Science, Izola, Slovenia (Subject Areas: Clinical Oncology, Experimental Oncology)

Božidar Casar, Institute of Oncology Ljubljana, Department for Dosimetry and Quality of Radiological Procedures, Ljubljana (Subject Area: Medical Physics)

Maja Čemažar, Institute of Oncology Ljubljana, Department of Experimental Oncology, Ljubljana, Slovenia (Subject Area: Experimental Oncology)

Subject Areas:

Clinical Oncology and Radiotherapy

Serena Bonin, University of Trieste, Department of Medical Sciences, Cattinara Hospital, Surgical Pathology Bg, Molecular Biology Lab, Trieste, Italy

Luca Campana, Veneto Institute of Oncology (IOV-IRCCS), Padova, Italy

Christian Dittrich, Kaiser Franz Josef - Spital, Vienna, Austria

Blaž Grošelj, Institute of Oncology Ljubljana, Department of Radiation Oncology, Ljubljana

Luka Milas, UT M. D. Anderson Cancer Center, Houston, USA

Miha Oražem, Institute of Oncology Ljubljana, Department of Radiation Oncology, Ljubljana

Gaber Plavc, Institute of Oncology Ljubljana, Department of Radiation Oncology, Ljubljana

Csaba Polgar, National Institute of Oncology, Budapest, Hungary

Dirk Rades, University of Lubeck, Department of Radiation Oncology, Lubeck, Germany

Luis Souhami, McGill University, Montreal, Canada

Borut Štabuc, University Medical Center Ljubljana, Division of Internal Medicine, Department of Gastroenterology, Ljubljana, Slovenia

Andrea Veronesi, Centro di Riferimento Oncologico- Aviano, Division of Medical Oncology, Aviano, Italy

Branko Zakotnik, Institute of Oncology Ljubljana, Department of Medical Oncology, Ljubljana, Slovenia

Miklós Kásler, National Institute of Oncology, Budapest, Hungary

Maja Osmak, Ruder Bošković Institute, Department of Molecular Biology, Zagreb, Croatia

Igor Kocijančič, University Medical Center Ljubljana, Institute of Radiology, Ljubljana, Slovenia (Subject Areas: Radiology, Nuclear Medicine)

Karmen Stanič, Institute of Oncology Ljubljana, Department of Radiation Oncology, Ljubljana, Slovenia (Subject Areas: Radiotherapy; Clinical Oncology)

Primož Strojjan, Institute of Oncology Ljubljana, Department of Radiation Oncology, Ljubljana, Slovenia (Subject Areas: Radiotherapy, Clinical Oncology)

Subject Area: Experimental Oncology

Metka Filipič, National Institute of Biology, Department of Genetic Toxicology and Cancer Biology, Ljubljana, Slovenia

Janko Kos, University of Ljubljana, Faculty of Pharmacy, Ljubljana, Slovenia

Tamara Lah Turnšek, National Institute of Biology, Ljubljana, Slovenia

Damijan Miklavčič, University of Ljubljana, Faculty of Electrical Engineering, Ljubljana, Slovenia

Ida Ira Skvortsova, EXTRO-lab, Dept. of Therapeutic Radiology and Oncology, Medical University of Innsbruck, Tyrolean Cancer Research Institute, Innsbruck, Austria

Gillian M. Tozer, University of Sheffield, Academic Unit of Surgical Oncology, Royal Hallamshire Hospital, Sheffield, UK

Subject Area: Medical Physics

Robert Jeraj, University of Wisconsin, Carbone Cancer Center, Madison, Wisconsin, USA

Mirjana Josipović, Rigshospitalet, Department of Oncology, Section of Radiotherapy, Copenhagen, Denmark

Håkan Nyström, Skandionkliniken, Uppsala, Sweden

Ervin B. Podgoršak, McGill University, Medical Physics Unit, Montreal, Canada

Matthew Podgorsak, Roswell Park Cancer Institute, Departments of Biophysics and Radiation Medicine, Buffalo, NY, USA

Advisory Committee

Tullio Giraldi, University of Trieste, Faculty of Medicine and Psychology, Department of Life Sciences, Trieste, Italy

Vassil Hadjidekov, Medical University, Department of Diagnostic Imaging, Sofia, Bulgaria

Marko Hočevar, Institute of Oncology Ljubljana, Department of Surgical Oncology, Ljubljana, Slovenia

Editorial office

Radiology and Oncology

Zaloška cesta 2

P. O. Box 2217

SI-1000 Ljubljana

Slovenia

Phone: +386 1 5879 369

Phone/Fax: +386 1 5879 434

E-mail: gsera@onko-i.si

Copyright © Radiology and Oncology. All rights reserved.

Reader for English

Vida Kološa

Secretary

Mira Klemenčič

Zvezdana Vukmirović

Design

Monika Fink-Serša, Samo Rován, Ivana Ljubanović

Layout

Matjaž Lužar

Printed by

Tiskarna Ozimek, Slovenia

Published quarterly in 400 copies

Beneficiary name: DRUŠTVO RADIOLOGIJE IN ONKOLOGIJE

Zaloška cesta 2

1000 Ljubljana

Slovenia

Beneficiary bank account number: SI56 02010-0090006751

IBAN: SI56 0201 0009 0006 751

Our bank name: Nova Ljubljanska banka, d.d.,

Ljubljana, Trg republike 2,

1520 Ljubljana; Slovenia

SWIFT: LJBASIX

Subscription fee for institutions EUR 100, individuals EUR 50

The publication of this journal is subsidized by the Slovenian Research Agency.

Indexed and abstracted by:

- Baidu Scholar
- Case
- Chemical Abstracts Service (CAS) - Cplus
- Chemical Abstracts Service (CAS) - SciFinder
- CNKI Scholar (China National Knowledge Infrastructure)
- CNPIEC - cnpLINKer
- Dimensions
- DOAJ (Directory of Open Access Journals)
- EBSCO (relevant databases)
- EBSCO Discovery Service
- Embase
- Genamics JournalSeek
- Google Scholar
- Japan Science and Technology Agency (JST)
- J-Gate
- Journal Citation Reports/Science Edition
- JournalGuide
- JournalTOCs
- KESLI-NDSL (Korean National Discovery for Science Leaders)
- Medline
- Meta
- Microsoft Academic
- Naviga (Softweco)
- Primo Central (ExLibris)
- ProQuest (relevant databases)
- Publons
- PubMed
- PubMed Central
- PubsHub
- QOAM (Quality Open Access Market)
- ReadCube
- Reaxys
- SCImago (SJR)
- SCOPUS
- Sherpa/RoMEO
- Summon (Serials Solutions/ProQuest)
- TDNet
- Ulrich's Periodicals Directory/ulrichsweb
- WanFang Data
- Web of Science - Current Contents/Clinical Medicine
- Web of Science - Science Citation Index Expanded
- WorldCat (OCLC)

This journal is printed on acid-free paper

On the web: ISSN 1581-3207

<https://content.sciendo.com/raon>

<http://www.radioloncol.com>

contents

review

- 379 **MitomiRs: their roles in mitochondria and importance in cancer cell metabolism**
Andrej Rencelj, Nada Gvozdenovic, Maja Cemazar
- 393 **Target motion management in breast cancer radiation therapy**
Elham Piruzan, Naser Vosoughi, Seied Rabi Mahdavi, Leila Khalafi, Hojjat Mahani

radiology

- 409 **Study of correlations between CT properties of retrieved cerebral thrombi with treatment outcome of stroke patients**
Rebeka Viltuznik, Jernej Vidmar, Andrej Fabjan, Miran Jeromel, Zoran V. Milosevic, Igor J. Kocijancic, Igor Sersa
- 418 **The role of unenhanced phase of the liver in the scanning protocol of metastatic breast cancer: implications for sensitivity, response evaluation and size measurement**
Juan José Arenas-Jiménez, Elena García-Garrigós, Mariana Cecilia Planells-Alduvín

clinical oncology

- 426 **Diagnostic performance of p16/Ki-67 dual immunostaining at different number of positive cells in cervical smears in women referred for colposcopy**
Ursula Salobir Gajsek, Andraz Dovnik, Iztok Takac, Urska Ivanus, Tine Jerman, Simona Sramek Zatler, Alenka Repse Fokter
- 433 **Robotic versus laparoscopic surgery for colorectal cancer: a case-control study**
Jan Grosek, Jurij Ales Kosir, Primož Sever, Vanja Erculj, Ales Tomazic
- 439 **Preoperative intensity-modulated chemoradiotherapy with simultaneous integrated boost in rectal cancer: five-year follow-up results of a phase II study**
Jasna But-Hadzic, Anja Meden Boltezar, Tina Skerl, Vesna Zadnik, Vaneja Velenik
- 449 **The role of haematological parameters in predicting the response to radical chemoradiotherapy in patients with anal squamous cell cancer**
Suzana Stojanovic-Rundic, Mladen Marinkovic, Milena Cavic, Vesna Plesinac Karapandzic, Dusica Gavrilovic, Radmila Jankovic, Richarda M. de Voer, Sergi Castellvi-Bel, Zoran Krivokapic

- 459 **Hypofractionated preoperative radiotherapy for high risk soft tissue sarcomas in a geriatric patient population**
Vlatko Potkrajcic, Frank Traub, Barbara Hermes, Marcus Scharpf, Jonas Kolbenschlag, Daniel Zips, Frank Paulsen, Franziska Eckert
- 467 **Definitive radiotherapy for squamous cell carcinoma of the oral cavity: a single-institution experience**
Kristin Lang, Melissa Baur, Thomas Held, Rami El Shafie, Julius Moratin, Christian Freudlsperger, Karim Zaoui, Nina Bougatf, Jürgen Hoffmann, Peter K. Plinkert, Jürgen Debus, Sebastian Adeberg
- 474 **Acute side effects after definitive stereotactic body radiation therapy (SBRT) for patients with clinically localized or locally advanced prostate cancer: a single institution prospective study**
Kliton Jorgo, Csaba Polgar, Gabor Stelczer, Tibor Major, Laszlo Gesztesi, Peter Agoston
- 482 **Clinical outcomes in stage III non-small cell lung cancer patients treated with durvalumab after sequential or concurrent platinum-based chemoradiotherapy - single institute experience**
Martina Vrankar, Karmen Stanic, Stasa Jelercic, Eva Ciric, Ana Lina Vodusek, Jasna But-Hadzic
- 491 **Disease control with prior platinum-based chemotherapy is prognostic for survival in patients with metastatic urothelial cancer treated with atezolizumab in real-world practice**
Marina Mencinger, Dusan Mangaroski, Urska Bokal

medical physics

- 499 **Non-coplanar volumetric modulated arc therapy for locoregional radiotherapy of left-sided breast cancer including internal mammary nodes**
Yuan Xu, Pan Ma, Zhihui Hu, Yuan Tian, Kuo Men, Shulian Wang, Yingjie Xu, Jianrong Dai
- 508 **Verification of an optimizer algorithm by the beam delivery evaluation of intensity-modulated arc therapy plans**
Tamas Pocza, Domonkos Szegedi, Tibor Major, Csilla Pesznyak

slovenian abstracts

MitomiRs: their roles in mitochondria and importance in cancer cell metabolism

Andrej Rencelj^{1,2}, Nada Gvozdenovic¹, Maja Cemazar^{1,3}

¹ Institute of Oncology Ljubljana, Department of Experimental Oncology, Ljubljana, Slovenia

² Faculty of Medicine, University of Ljubljana, Ljubljana, Slovenia

³ Faculty of Health Sciences, University of Primorska, Izola, Slovenia

Radiol Oncol 2021; 55(4): 379-392.

Received 10 August 2021

Accepted 28 September 2021

Correspondence to: Prof. Maja Čemazar, Ph.D., Institute of Oncology Ljubljana, Ljubljana, Slovenia.

E-mail: MCemazar@onko-i.si

Disclosure: No potential conflicts of interest were disclosed.

This is an open access article under the CC BY-NC-ND license (<http://creativecommons.org/licenses/by-nc-nd/4.0/>).

Background. MicroRNAs (miRNAs) are short non-coding RNAs that play important roles in almost all biological pathways. They regulate post-transcriptional gene expression by binding to the 3' untranslated region (3' UTR) of messenger RNAs (mRNAs). MitomiRs are miRNAs of nuclear or mitochondrial origin that are localized in mitochondria and have a crucial role in regulation of mitochondrial function and metabolism. In eukaryotes, mitochondria are the major sites of oxidative metabolism of sugars, lipids, amino acids, and other bio-macromolecules. They are also the main sites of adenosine triphosphate (ATP) production.

Conclusions. In the review, we discuss the role of mitomiRs in mitochondria and introduce currently well studied mitomiRs, their target genes and functions. We also discuss their role in cancer initiation and progression through the regulation of mRNA expression in mitochondria. MitomiRs directly target key molecules such as transporters or enzymes in cell metabolism and regulate several oncogenic signaling pathways. They also play an important role in the Warburg effect, which is vital for cancer cells to maintain their proliferative potential. In addition, we discuss how they indirectly upregulate hexokinase 2 (HK2), an enzyme involved in glucose phosphorylation, and thus may affect energy metabolism in breast cancer cells. In tumor tissues such as breast cancer and head and neck tumors, the expression of one of the mitomiRs (miR-210) correlates with hypoxia gene signatures, suggesting a direct link between mitomiR expression and hypoxia in cancer. The miR-17/92 cluster has been shown to act as a key factor in metabolic reprogramming of tumors by regulating glycolytic and mitochondrial metabolism. This cluster is deregulated in B-cell lymphomas, B-cell chronic lymphocytic leukemia, acute myeloid leukemia, and T-cell lymphomas, and is particularly overexpressed in several other cancers. Based on the current knowledge, we can conclude that there is a large number of miRNAs present in mitochondria, termed mitomiR, and that they are important regulators of mitochondrial function. Therefore, mitomiRs are important players in the metabolism of cancer cells, which need to be further investigated in order to develop a potential new therapies for cancer.

Key words: microRNAs; mitomiR; mitochondria; cancer; cancer cell metabolism

Introduction

MicroRNAs (miRNAs) are short non-coding RNAs (ncRNAs) of ~18-25 nucleotides that are present in all eukaryotic cells and play important roles in almost all biological signaling pathways.¹⁻⁴ Since the discovery of the first miRNA (lin-4) in *C. elegans*⁵,

approximately 2000 miRNAs have been annotated in the human genome.⁶ Data from genomic studies show that most miRNAs are highly conserved, making them very interesting targets for studying various disease states.⁷ They regulate post-transcriptional gene expression by binding to the 3' UTR of messenger RNAs.⁸⁻¹⁴ A single miRNA

can regulate many mRNA targets, and conversely, a single mRNA target can be regulated by many miRNAs.^{15–17} Therefore, by regulating these fundamental target genes, miRNAs have been implicated in signaling pathways to modulate a large set of important biological processes such as cell proliferation¹², metastasis¹⁸, apoptosis¹⁹, senescence¹², differentiation²⁰, autophagy²¹, and immune response²². Moreover, miRNAs have been found to be dysregulated in many pathological conditions, such as neurodegenerative diseases²³, cardiovascular diseases²⁴, and cancer.^{25–28}

More recently, miRNAs have been found to be specifically present in mitochondria. These mitochondrial miRNAs were named “mitomiR”.^{7,29–32} Most of them have a nuclear origin, but some mitomiRs originate from mRNA molecules derived from the mitochondrial genome. The association of mitomiRs with mitochondria is species- and cell type-specific.^{7,33} They have been found in mitochondria in various tissues and cells and are thought to have different thermodynamic properties than miRNAs.^{7,34} Mitochondria have a discrete and unique pool of mitomiRs, which has been demonstrated with various experiments.²⁹

For the first time, in 2011, Barrey and co-workers demonstrated the presence of pre-miRNAs (precursor-miRNAs) in mitochondria and postulated that some pre-miRNA sequences could be processed into mature miRNAs that could immediately become active on mitochondrial transcripts or exported to the cytosol to disrupt genomic mRNA.³⁵ Barrey's group screened for 742 miRNAs using qRT-PCR and showed that 243 miRNAs had significant expression in mitochondrial RNA samples isolated from human myotubes by *in situ* hybridization. This study was the first to provide evidence that pre-miRNAs can be localized in mitochondria. Subsequently, a number of studies have identified “signatures” of miRNAs localized to mitochondria through various experimental approaches. Mercer *et al.*¹⁵ examined the human mitochondrial transcriptome and demonstrated that 3 miRNAs (miR-146a, miR-103, and miR-16) have quite high expression in the intermembrane region compared to the matrix. Latronico and Condorelli³⁶ found 15 nuclear-encoded miRNAs in mitochondria isolated from rat liver, 20 miRNAs from mouse liver mitochondria, and 13 miRNAs from HeLa cells (isolated from human cervical cancer) by microarray. Some other groups identified novel mitomiRs from HEK293 cells (isolated from human embryonic kidneys)³⁷, 143B cells (isolated from human bone marrow)³⁸, mouse heart³⁹ and HeLa cells.^{37,40}

MitomiRs have been shown to be important regulators of mitochondrial function.^{35,38,41} The regulation of mitochondria by mitomiRs influences the development of many diseases caused by mitochondrial dysfunction, which is responsible for the pathophysiology of numerous diseases, such as cardiovascular and neurodegenerative diseases, diabetes, obesity, and cancer.⁴²

In the first part of this review article, we describe the biosynthesis of mitomiRs and the transport mechanisms from mitomiRs to mitochondria. The next part is dedicated to the role of these small molecules in mitochondria and the presentation of some important mitomiRs, their target genes and functions. In the last part of the review, we discuss the functions of mitomiRs in cancer cell metabolism and introduced mitomiRs in the context of cancer.

Biosynthesis of miRNA/mitomiRs

Most miRNAs/mitomiRs are produced via the canonical biosynthetic pathway, which involves transcription by RNA polymerase II (Pol II) to produce a primary transcript (pri-miRNA/mitomiR). The primary transcript is first cleaved in the nucleus by the nuclear heterodimer Drosha/DGCR8 (DiGeorge syndrome chromosomal region 8), which cleaves the pri-miRNA/mitomiR and produces a pre-miRNA/mitomiR with a hairpin structure that is much more stable than the pri-miRNA/mitomiR due to its characteristic hairpin loop structure.⁴³ Exportin 5 (EXP5) and GTP-binding nuclear protein (RANGTP) then form a transport machinery to export the pre-miRNA from the nucleus to the cytoplasm. After export to the cytoplasm, the pre-miRNA/mitomiR is further cleaved by the enzyme Dicer to form a double-stranded RNA (dsRNA) duplex (Figure 1). Only a single strand of the dsRNA duplex forms the mature miRNA/mitomiR and is incorporated into the RNA-induced silencing complex (RISC), which directs the binding of Argonaute (AGO) proteins in the RISC to the 3'UTR of the target mRNA to either repress protein translation or promote mRNA degradation.^{43–45} After incorporation into RISC, mature miRNA/mitomiRs are transported into mitochondria, back to nucleus by importin 8 (IPO-8) or extracellular environment (Figure 1).^{46,47}

In addition to the canonical miRNAs/mitomiRs biosynthesis pathway, there are also non-canonical, Drosha/DGCR8-independent and Dicer-independent biosynthesis pathways. Prominent

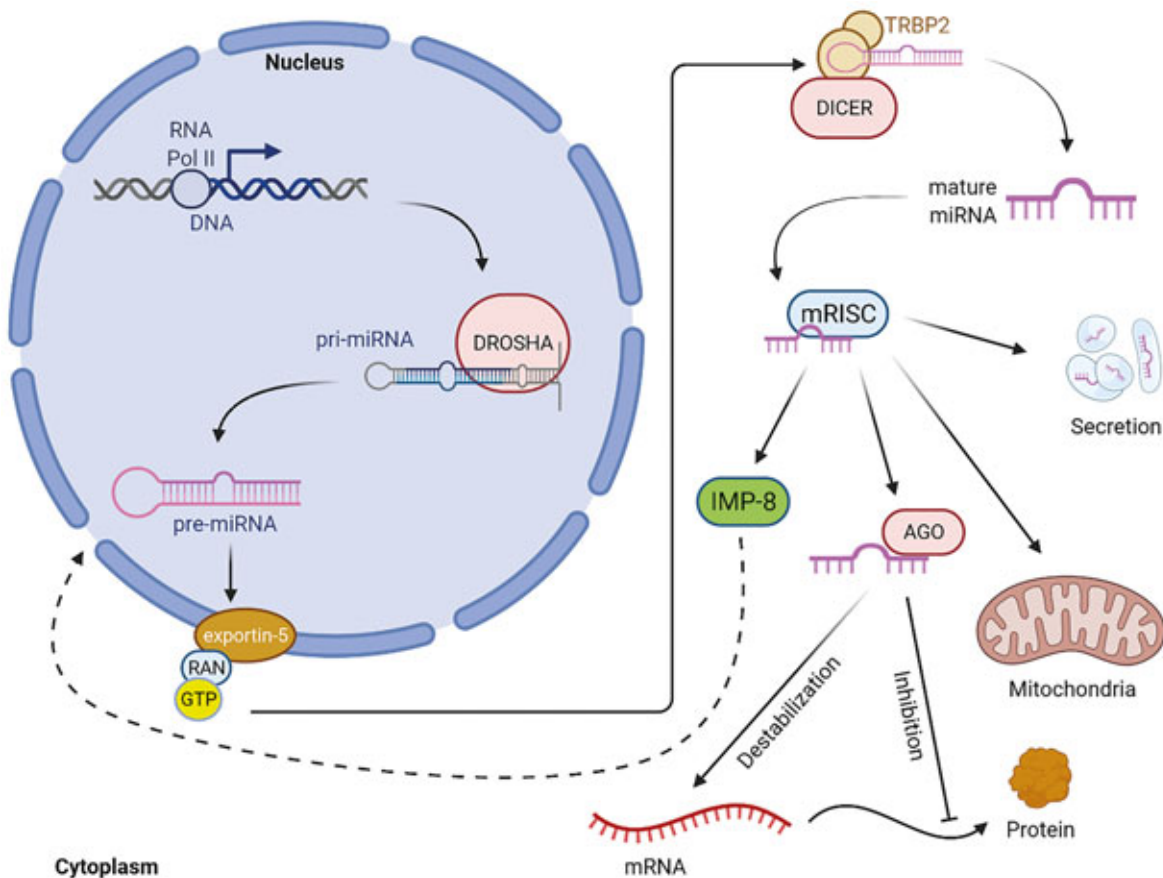


FIGURE 1. Canonical biosynthesis of miRNAs/mitomiRs (adopted from ^{29,43,45}). Mature miRNA can be transported into any part of the cell; but miRNA/mitomiR regulation is possible only after incorporation into RISC. (AGO2 = argonaute 2; DGCR8 = DiGeorge critical region 8; EXP5 = exportin 5; GTP = guanosine triphosphate; IMP8 = importin 8; mRISC = RNA induced silencing complex loaded with mature miRNA; POLII = DNA polymerase II; RANGTP = binding nuclear protein RAN; RISC = RNA-induced silencing complex; TRBP2 = RISC-loading complex subunit TRBP2).

classes of Drosha/DGCR8-independent miRNAs/mitomiRs are the “mirtrons” derived from introns that, once spliced, function as pre-miRNAs and thus do not require cleavage by Drosha/DGCR8 and can be immediately exported to the cytoplasm for processing by Dicer. MiRNAs/mitomiRs can also be processed from hairpins generated directly by Pol II at specific transcription start sites. These pre-miRNAs are capped and exported via the exportin 1 (EXP1) pathway. The Dicer-independent miRNAs/mitomiRs biosynthesis pathway involves the unusually short hairpin of miR-451, which is directly cleaved by argonaute 2 (AGO2).⁴⁵

MitomiRs transport to mitochondria

The discovery of mitomiRs raised the question of elucidating the underlying molecular mechanisms

of their transport into mitochondria. Due to their size and charged nature, mitomiRs are unlikely to cross membranes under their own power. The molecular mechanisms of mitomiR transport into mitochondria may vary between species and are not well understood.²⁹

Some proposals have been published on AGO2 as a potential mitomiR import protein.^{7,29,48} Due to its RNA-binding ability and dual localization in the cytosol and mitochondria, AGO2 might be involved in the trafficking of mitomiRs.⁷ Shepherd *et al.*⁴⁹ showed that the exoribonuclease polyribonucleotide nucleotidyltransferase (PNPT1/ PNPase) has a major role in the import of mitomiRs. Therefore, PNPase could be part of an alternative, AGO2-independent, uptake pathway of mitochondrial miRNA. Furthermore, a possible mechanism could involve the voltage-dependent anion-selective channel protein (VDAC).³⁴ Several studies have suggested that the instability of RISC in the

cytoplasm promotes miRNA translocation to mitochondria, but the molecular components that facilitate this translocation process are not fully understood. Furthermore, the concept that mammalian mitochondria can import cytosolic ncRNAs may facilitate research in another exciting area, long ncRNAs. Clearly, these translocation mechanisms and the identification of pathway components for mitochondrial targeting require further studies.⁷

Roles of mitomiRs in mitochondria

Mitochondria are semi-autonomous cell organelles with their own DNA (mtDNA) encoding 22 tRNAs, 2 rRNAs, and 13 polypeptides. These polypeptides and those encoded by nuclear genes, form 4 protein complexes of the electron transport chain (ETC). Mitochondria are constantly dividing and fusing, and the balance between mitochondrial fission and fusion influences mitochondrial morphology, whose dynamics and turnover are critical for cellular homeostasis and differentiation.⁵⁰ Several proteins are involved in the regulation of mitochondrial dynamics. Deregulation of mitochondrial dynamics is not only associated with deregulation of mitochondrial function, but is also closely related to several biological processes such as proliferation, cell death, apoptosis and production of reactive oxygen species (ROS), since mitochondria are the major sites of oxidative metabolism of sugars, lipids, amino acids and ATP production.^{1,51-53}

It's also worth noting that the mitochondrial matrix has its own set of environmental variables. Because of its thioester bond, acetyl-coenzyme A (acetyl-CoA) is a very abundant metabolite in mitochondria and functions as a powerful acetylation reagent. Protein lysine acetylation and succinylation are caused by acetyl-CoA and mitochondrial matrix pH concentrations. Non-enzymatic acetylation occurs often in mitochondria.⁵⁴ The most of mitochondrial proteins have acetyl groups, which is consistent with this hypothesis. Non-enzymatic acetylation of RNA molecules, including miRNAs, is a logical possibility for mitochondrial modification. An acetyl group covalently attached to a miRNA might change its mRNA recognition behavior. If it happens at the 2 OH group of ribose needed for the cleavage process, it could inhibit spontaneous bond cleavage and therefore increase the half-life of mRNA. Furthermore, post-transcriptional alterations can result in structural changes⁵⁵ as well

as changed interactions with other RNA molecules or proteins.⁵⁶

As stated, mitomiRs are regulators of mitochondrial function, as shown in the following examples. *In silico* analysis identified miR-378, miR-24, and miR-23b in liver mitochondria (Table 1) and these mitomiRs have been shown to regulate systemic energy homeostasis, oxidative capacity, ROS, and mitochondrial lipid metabolism.^{35,57-62} Several reports have indicated that miRNAs such as miR-1291, miR-138, miR-150, miR-199a, and miR-532-5p can alter the expression of some important glycolytic enzymes (Table 1).^{4,63-70} miR-29a, miR-29b and miR-124 (Table 1) regulate the expression of monocarboxylate transporter 1 (SLC16A1) in pancreatic beta cells.⁷¹ miR-33a/b has been shown to regulate lipid metabolism by targeting the cholesterol transporter ATP-binding cassette transporter (ABCA1).⁷² miR-143 and miR-24 have also been shown to regulate mitochondrial lipid metabolism (Table 1).^{73,74} On the other hand, miR-204 accelerates fatty acid oxidation by inhibiting acetyl-coenzyme A carboxylase (ACC).⁷⁵ Ahmad *et al.* (2011) showed that miR-200 is associated with the regulation of phosphoglucose isomerase (PGI), which is an important factor in glycolysis and gluconeogenesis. Overexpression of miR-338 leads to downregulation of the protein level of cytochrome c oxidase IV and reduces mitochondrial oxygen consumption and ATP production.^{77,78} Similarly, overexpression of miR-181c decreases mt-COX1 protein and causes remodeling of the complex IV (*in vitro*)⁴⁸ and a dysfunctional complex IV (*in vivo*)⁷⁹, along with increased production of ROS. It has also been reported that miR-210 modulates the function of the complex IV by targeting the nuclear-encoded mRNA, COX10.^{80,81} It has also been reported that miR-15b, miR-16, miR-195 and miR-338 (Table 1) regulate ATP production by targeting several nuclear genes that play important roles in ETC.^{77,82,83} miR-101-3p regulates the expression of ATP synthase subunit beta (ATP5B) in ETC (Table 1).⁸⁴ In addition, miR-210-5p reduces the expression of iron-sulfur cluster assembly enzyme (ISCU) under hypoxic conditions, which affects the proteins containing iron-sulfur clusters (Fe-S).⁸⁵ It has also been reported that miR-29a-3p⁸⁶ is involved in β -oxidation of lipids (Table 1) and that miR-19b negatively regulates mitochondrial fusion by downregulating mitofusin 1 (MFN1).⁸⁷

The microRNAs listed in Table 1 significantly affect mitochondrial regulation and function, which is why they are classified in the group of mitomiRs, which are crucial regulatory molecules

TABLE 1. Summary of microRNAs and their roles in mitochondria

miR	miR accession number	Target genes	Gene accession number	Function	Functional pathway	Location	Species	References
miR-378	MI0000795	Crat	ENSMUSG00000026853	Downregulation	Mitochondrial oxidative metabolism	Mitochondria in liver cells	Mouse	Carrer <i>et al.</i> , 2012 ⁵⁹
miR-24	MI0000080	H2ax	ENSMUSG00000049932	Downregulation	Insulin signaling pathway	Mitochondria in liver cells	Human	Jeong <i>et al.</i> , 2017 ⁶¹
miR-23b	MI0000439	GLS	ENSG00000115419	Downregulation	Glutamine metabolism	Mitochondria in liver cells	Human	Gao <i>et al.</i> , 2009 ⁶⁰
miR-1291	MI0006353	SLC2A1 CPT1C ESRRA ASS1 GLUT1	ENSG00000117394 ENSG00000169169 ENSG00000173153 ENSG00000130707 ENSG00000117394	Downregulation Downregulation Downregulation Downregulation	Mitochondrial metabolism	Mitochondria in renal cells	Human	Yamasaki <i>et al.</i> , 2013; Chen <i>et al.</i> , 2020, Tu <i>et al.</i> , 2020 ⁶³⁻⁶⁵
miR-138	MI0000455	PDK1	ENSG00000152256	Downregulation	Glucose metabolism	Mitochondria in cardiac cells	Human	Zhu <i>et al.</i> , 2017 ⁶⁶
miR-150	MI0000920 MI0000479	Slc2a4 SLC2A1	ENSRNOG00000017226 ENSG00000117394	Downregulation Downregulation	Metabolism	Mitochondria in cardiac cells	Rat Human	Ju <i>et al.</i> , 2020 ⁶⁷ Li <i>et al.</i> , 2017 ⁶⁸
miR-199a	MI0000941 MI0000242	Slc2a4 HK2 HK2	ENSRNOG00000017226 ENSRNOG00000006116 ENSG00000159399	Upregulation Upregulation	Expression of glucose transporters	Mitochondria in muscle cells Mitochondria in liver cells	Rat Human	Esteves <i>et al.</i> , 2018, Yan <i>et al.</i> , 2014, Guo <i>et al.</i> , 2015 ^{69,70}
miR-532-5p	MI0006154	Slc2a4 HK2	ENSRNOG00000017226 ENSRNOG00000006116	Upregulation Upregulation	Expression of glucose transporters	Mitochondria in muscle cells	Rat	Esteves <i>et al.</i> , 2018 ⁷⁰
miR-29a	MI0000576	Slc16a1	ENSMUSG00000032902	Downregulation	Mitochondrial oxidative metabolism	Mitochondria in pancreatic beta-cells	Mouse	Pullen <i>et al.</i> , 2011 ⁷¹
miR-29b	MI0000143	Slc16a1	ENSMUSG00000032902	Downregulation	Mitochondrial oxidative metabolism	Mitochondria in pancreatic beta-cells	Mouse	Pullen <i>et al.</i> , 2011 ⁷¹
miR-124	MI0000716	Slc16a1	ENSMUSG00000032902	Downregulation	Mitochondrial oxidative metabolism	Mitochondria in pancreatic beta-cells	Mouse	Pullen <i>et al.</i> , 2011 ⁷¹
miR-33a/b	a-MI0002684, b-MI0007603	CROT CPT1A HADHB PRKAA1 ABCA1 SREBF1 FASN ACLY ACACA	ENSANAG00000028065 ENSANAG00000017356 ENSANAG00000027802 ENSANAG00000032687 ENSANAG00000033387 ENSANAG00000021477 ENSANAG00000032055 ENSANAG00000036009 ENSANAG00000035253	Downregulation Downregulation Downregulation Downregulation Upregulation Upregulation Upregulation Upregulation	Lipid metabolism	Mitochondria in liver cells	Monkey	Rayner <i>et al.</i> , 2011 ⁷²
miR-143	MI0000916 MI0000459	Map2k5 APOL6	ENSRNOG00000007926 ENSG00000221963	Downregulation Downregulation	Adipogenesis Adipogenesis	Mitochondria in adipose cells Mitochondria in adipose cells	Rat Human	Chen <i>et al.</i> , 2014 ⁷³ Ye <i>et al.</i> , 2013 ⁷⁴
miR-204	MI0000284	ACACB	ENSG00000076555	Downregulation	Lipid metabolism	Mitochondria in adipose cells	Human	Civelek <i>et al.</i> , 2013 ⁷⁵
miR-200	MI0000737	ZEB1 ZEB2	ENSG00000148516 ENSG00000169554	Upregulation Upregulation	Lipid metabolism	Mitochondria in breast cells	Human	Ahmad <i>et al.</i> , 2011 ⁷⁶
miR-338	MI0000618	COXIV	ENSRNOG00000007827	Downregulation	Mitochondria oxidative metabolism	Mitochondria in neural cells	Rat	Aschrafi <i>et al.</i> , 2008 ⁷⁷
miR-181c	MI0000924	COX1	ENSRNOG00000034234	Downregulation	Mitochondria oxidative metabolism	Mitochondria in cardiac cells	Rat	Das <i>et al.</i> , 2012 ⁸⁸
miR-210	MI0000268	ISCU	ENSG00000136003	Downregulation	Mitochondria oxidative metabolism	Mitochondria in placenta cells	Human	Colleoni <i>et al.</i> , 2013; Qiao <i>et al.</i> , 2013 ^{81,85}
miR-15b	MI0000843	Arl2 Bcl2	ENSRNOG00000021010 ENSRNOG00000002791	Downregulation Downregulation	ATP production	Mitochondria in cardiac cells	Rat	Nishi <i>et al.</i> , 2010 ⁸²
miR-16	MI0000844	Bcl2 Arl2	ENSRNOG00000002791 ENSRNOG00000021010	Downregulation Downregulation	ATP production	Mitochondria in cardiac cells	Rat	Nishi <i>et al.</i> , 2010 ⁸²
miR-195	MI0000939	Arl2	ENSRNOG00000021010	Downregulation	ATP production	Mitochondria in cardiac cells	Rat	Nishi <i>et al.</i> , 2010 ⁸²
miR-29a-3p	MI0000576	Foxa2	ENSMUSG00000037025	Upregulation	Lipid metabolism	Mitochondria in liver cells	Mouse	Kurtz <i>et al.</i> , 2014 ⁸⁶
miR-19b	MI0000074	MFN1	ENSG00000171109	Downregulation	Apoptosis	Mitochondria in bone cells	Human	Li <i>et al.</i> , 2014 ⁸⁷
miR-101-3p	MI0000103	ATP5B	ENSG00000110955	Silencing	Mitochondria metabolism	Mitochondria in heLa cells	Human	Zheng <i>et al.</i> , 2011 ⁸⁴

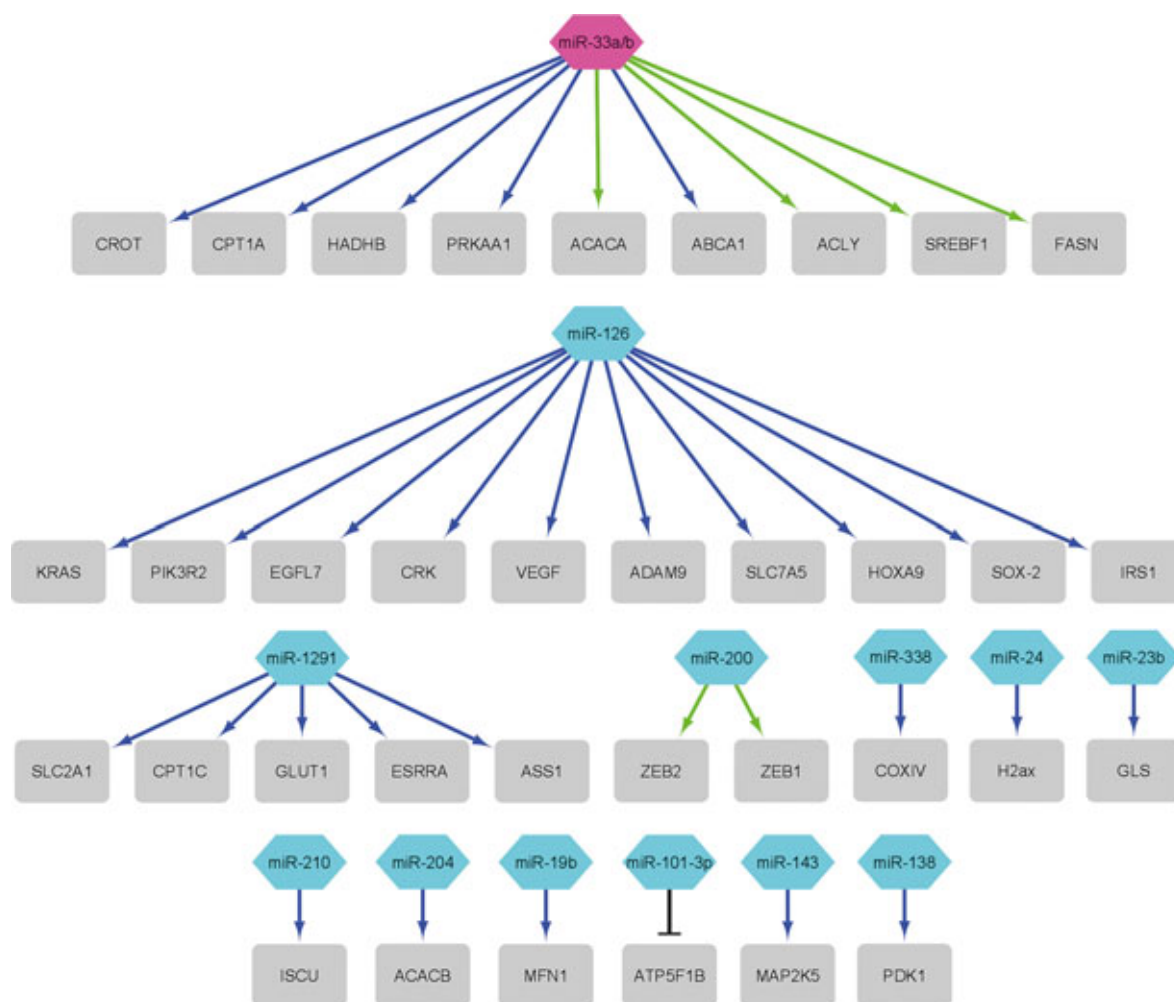


FIGURE 2. The network of the mitomiRs and their target genes (grey rectangle) in primates (data from Table 1). Blue arrows present downregulation, green arrows present upregulation and black T-line present silencing. Purple octagon shape presents monkey miRNA and cyan hexagon presents human miRNAs (figure constructed with Cytoscape Network Data Integration, Analysis, and Visualization in a Box V3.8.2).

of mitochondrial function and regulation of metabolism. In the figures (Figure 2 and Figure 3), we have shown how these mitomiRs are linked to their target genes in primates (Figure 2) and rodents (Figure 3).

In primates, there is no regulation of the same genes by different mitomiRs from Table 1 (Figure 2). Moreover, most mitomiRs target one gene and only a few mitomiRs target a larger number of genes and in most cases mitomiRs downregulate genes.

In contrast to primates, in rodents, some genes are regulated by different mitomiRs (Figure 3). The mitomiRs miR-15b and miR-16 both regulate the *Arl2* gene⁸², which is a nucleotide-binding gene, and the *Bcl2* gene, which regulates apoptosis. In

addition, the mitomiRs miR-199a^{69,70} and miR-532-5p⁷⁰ both regulate the *Hk2* gene, which has an important function in regulating glucose metabolism, and the *Slc2a4* gene, which is a glucose transmembrane transporter. It can be concluded that there is a greater overlap of mitomiRs in rodents than in primates. In most cases, mitomiRs downregulate genes.

From the figures (Figure 2 and Figure 3), we can summarize that some mitomiRs and their target genes are related in primates and rodents. MitomiR miR-199a^{69,70} regulates the same gene in both primates and rodents (Figure 3), the gene *Hk2*, which has an important function in regulating glucose metabolism. MiR-143^{73,74} regulates the same gene *MAP2K5* (Figure 3), which has an important

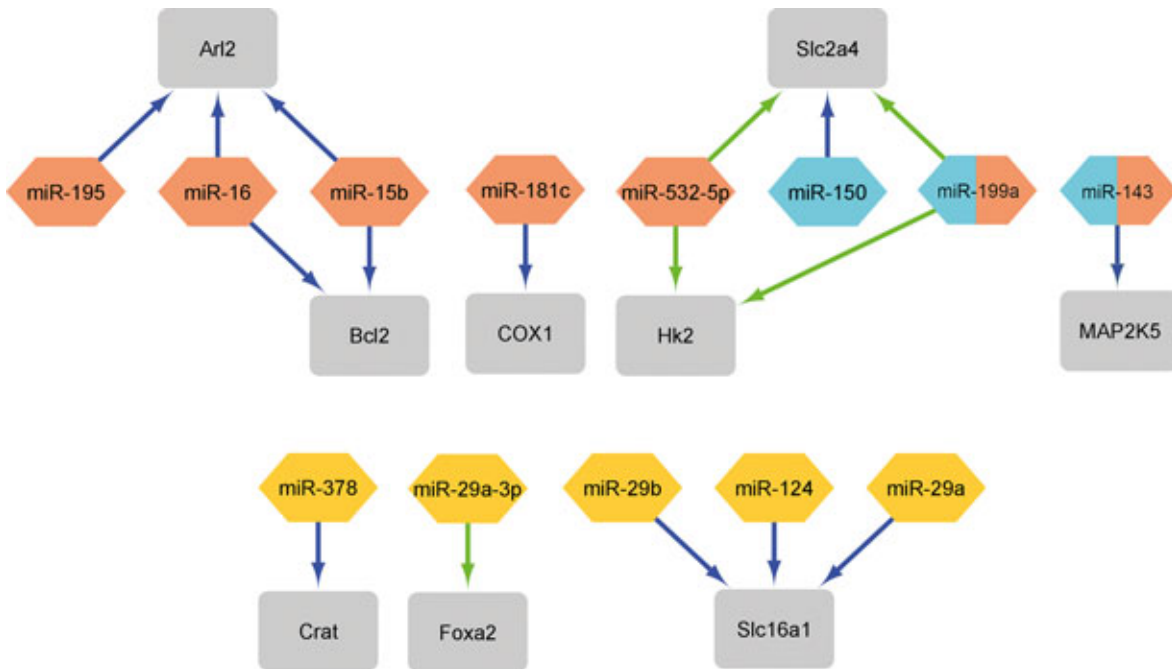


FIGURE 3. The network of the mitomiRs and their target genes (grey rectangle) in rodents (data from Table 1). Blue arrows present downregulation and green arrows present upregulation. Orange diamond shape presents rat miRNAs, yellow rectangle presents mouse miRNAs and cyan hexagon presents human miRNAs. miR-199a and miR-143 show that these two miRNAs regulate (figure constructed with Cytoscape Network Data Integration, Analysis, and Visualization in a Box V3.8.2).

function in signal cascade involved in growth factor stimulated cell proliferation and muscle cell differentiation.

MitomiRs in cancer

Traditional cancer traits include ten biological capabilities gained during the multistage development of human tumors.⁸⁹ These ten traditional cancer traits include resistance to cell death, induction of angiogenesis, maintenance of proliferative signaling, evasion of growth suppressors, activation of invasion and metastasis, facilitation of replicative immortality, altered metabolism, evasion of destruction by the immune system, tumor-promoting inflammation, and genome instability (Figure 4).^{89,90}

An important feature of cancer is the presence of the Warburg effect. Under aerobic conditions, normal cells generate ATP primarily in the mitochondrial oxidative phosphorylation process (OXPHOS), which utilizes the products of glycolysis and the Krebs cycle. Under anaerobic conditions, relatively little pyruvate, the end product of

glycolysis, is added to the Krebs cycle and is instead converted to lactate. However, this metabolic conversion of glucose appears to be energetically detrimental. In tumor cells, ATP deficiency can be compensated to some extent by upregulation of glycolysis.⁹¹ Interestingly, it has been observed that many cancer cells prefer glycolysis over OXPHOS even in the presence of an adequate amount of oxygen. This abnormal energy metabolism is known as the Warburg effect. Reduced OXPHOS and enhanced aerobic glycolysis are the main manifestations of reprogramming of glucose metabolism in tumor cells.^{1,92} Albeit the specific causes and utilitarian outcomes of this metabolic switch are as yet unclear, there is a developing agreement that the impact of Warburg effect is certifiably not an inconsequential result of carcinogenesis, yet is imperative for cancer cells to keep up with their proliferative potential and is driven by a few elements.⁹²⁻⁹⁴

It has been confirmed that abnormal expression of mitomiRs in mitochondria is related to the occurrence of cancer features.⁹⁵ Moreover, mitomiRs play an essential role in the control of cancer cell metabolism by regulating mRNA expression. They regulate several oncogenic signaling pathways and

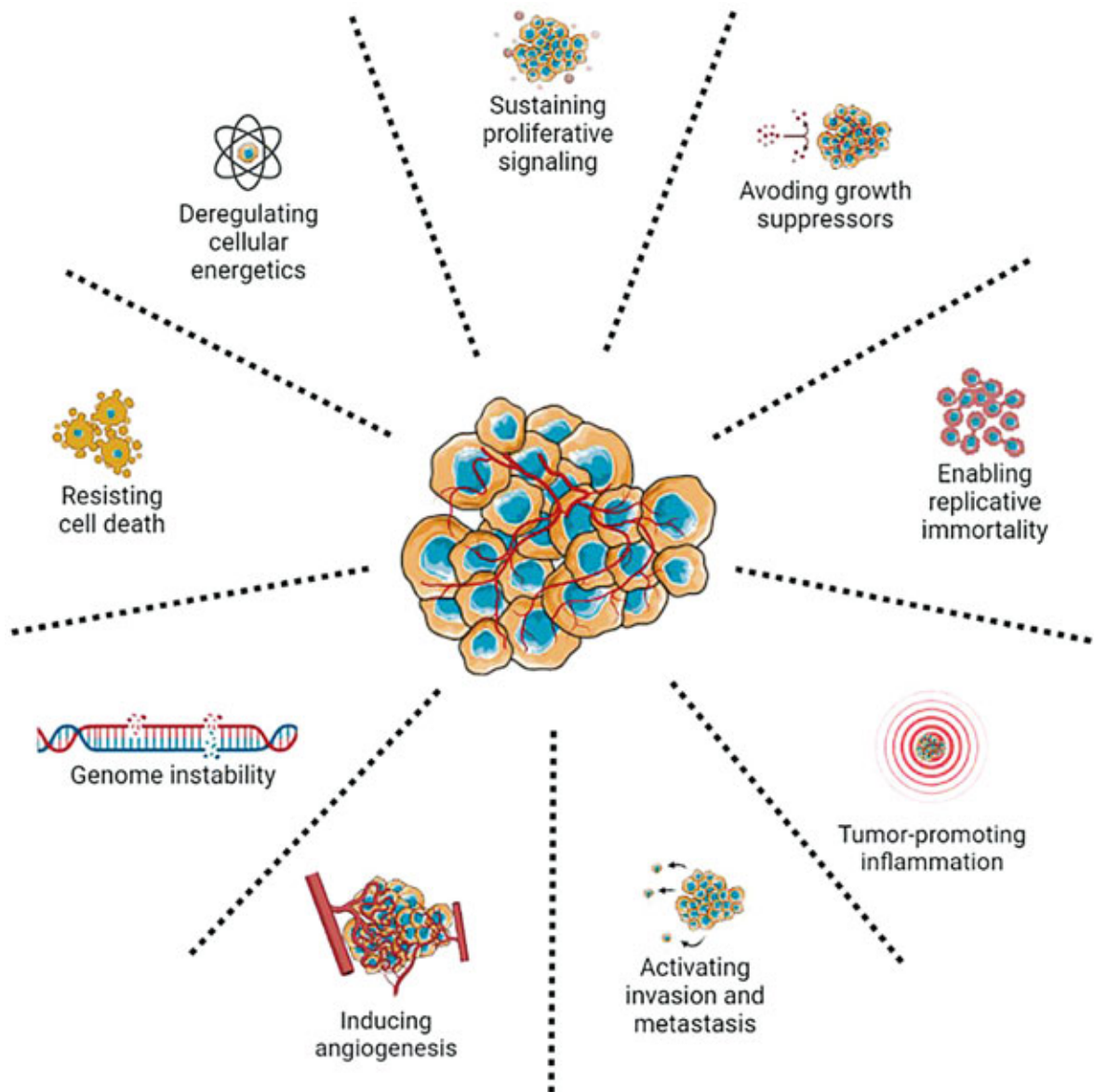


FIGURE 4. Traditional cancer traits.⁸⁹

target key transporters or enzymes in cellular metabolism. In addition, they may have a function as tumor suppressors that inhibit tumor cell proliferation or as oncogenes that induce tumorigenesis.^{96–98} MitomiRs can be isolated from any tissue or body fluid of any organism to study the level of expression in the organism in a diseased state, and thus can function as novel prognostic and predictive biomarkers.⁹⁹

The first evidence of miRNA involvement in human cancers was provided in a study of chronic lymphocytic leukemia (CLL).¹⁰⁰ MiR-15a and miR-16-1 localized to 13q14 were reported to be fre-

quently deleted and/or reduced in patients with B-cell chronic lymphocytic leukemia. This finding provided the first evidence that miRNAs may be involved in the pathogenesis of human cancers, as deletion of chromosome 13q14 resulted in the loss of these two miRNAs. MiR-15a induces apoptosis by regulating mitochondrial function and affecting the activity of Bcl-2 and Mcl-1 in human (Table 2). In addition, miR-15a causes mitochondrial dysfunction, leading to the release of cytochrome c into the cytoplasm and depletion of mitochondrial membrane potential.¹⁰¹ MiR-15a and miR-16a have been shown to be ATP modulators correlated with

TABLE 2. Summary of mitomiRs with roles in cancer

miR	miR accession number	Target genes	Gene accession number	Function	Functional pathway	Type of cancer	Species	References
miR-210	MI0000286	HIF-1	ENSG00000258777	Upregulation	Hypoxia	Breast cancer, neck and head cancer, lung cancer	Human	Qin <i>et al.</i> , 2014; Gee <i>et al.</i> , 2010; Puissegur <i>et al.</i> , 2011 ¹⁰⁹⁻¹¹¹
		ISCU	ENSG00000136003	Upregulation				
		COX10	ENSG00000006695	Upregulation				
		SDHD	ENSG00000204370	Upregulation				
		NDUFA4	ENSG00000189043	Upregulation				
miR-200a	MI0000342	TFAM	ENSG00000108064	Downregulation	Mitochondrial biogenesis, cancer metabolism	Breast cancer	Human	Yao <i>et al.</i> , 2014 ¹¹²
miR-155	MI0000681	HK2	ENSG00000159399	Upregulation	Glucose phosphorylation	Breast cancer	Human	Fang <i>et al.</i> , 2012; Jiang <i>et al.</i> , 2012 ¹⁰⁴
miR-124	MI0000443	PKM	ENSG00000067225	Upregulation	Glucose metabolism	Colorectal cancer	Human	Sun <i>et al.</i> , 2012 ¹⁰⁵
miR-137	MI0000454	PKM	ENSG00000067225	Upregulation	Glucose metabolism	Colorectal cancer	Human	Sun <i>et al.</i> , 2012 ¹⁰⁵
miR-340	MI0000802	PKM	ENSG00000067225	Upregulation	Glucose metabolism	Colorectal cancer	Human	Sun <i>et al.</i> , 2012 ¹⁰⁵
miR-326	MI0000808	PKM2	ENSG00000067225	Downregulation	Glucose metabolism	Glioblastoma	Human	Kefas <i>et al.</i> , 2010 ¹⁰⁶
miR-181-5p	MIMAT0000256	RASSF6	ENSG00000169435	Downregulation	Mitogen-activated protein kinase (MAPK) signaling pathway	Gastric cancer, cervical cancer	Human	Mi <i>et al.</i> , 2017; Zhuang <i>et al.</i> , 2017 ^{108,113}
		INPP5A	ENSG00000068383	Downregulation				
miR-92a-1	MI0000093	BCL2L1	ENSG00000153094	Downregulation	Apoptosis	Lymphoma	Human	Mogilyansky and Rigoutsos, 2013 ⁹⁴
miR-126	MI0000471	PIK3R2	ENSG00000105647	Downregulation	Inflammation, angiogenesis	Breast cancer cells	Human	Zhu <i>et al.</i> , 2011 ¹¹⁴
		PLK2	ENSG00000260410	Downregulation		Acute leukaemia cells		Li <i>et al.</i> , 2008 ¹¹⁵
		EGFL7	ENSG00000172889	Downregulation		Oral squamous cells		Sasahira <i>et al.</i> , 2012 ¹¹⁶
		CRK	ENSG00000167193	Downregulation		Lung cancer cells		Crawford <i>et al.</i> , 2008 ¹¹⁷
		ADAM9	ENSG00000168615	Downregulation		Melanoma cancer cells		Felli <i>et al.</i> , 2013 ¹¹⁸
		HOXA9	ENSG00000078399	Downregulation		Acute leukaemia cells		Shen <i>et al.</i> , 2008 ¹¹⁹
		IRS1	ENSG00000169047	Downregulation		Breast cancer cells		Zhang <i>et al.</i> , 2008 ¹²⁰
		SOX-2	ENSG00000242808	Downregulation		Gastric cancer cells		Otsubo <i>et al.</i> , 2011 ¹²¹
		SLC7A5	ENSG00000103257	Downregulation		Lung cancer cells		Miko <i>et al.</i> , 2011 ¹²²
VEGFA	ENSG00000150630	Downregulation	Oral squamous cells	Sasahira <i>et al.</i> , 2012 ¹¹⁶				
MMP7	ENSG00000137673	Downregulation	Melanoma cancer cells	Felli <i>et al.</i> , 2013 ¹¹⁸				
miR-15a	MI0000069	BCL-2	ENSG00000171791	Downregulation	Apoptosis, ATP production	B-cell chronic lymphocytic leukemia	Human	Gao <i>et al.</i> , 2010 ¹⁰¹
		MCL-1	ENSG00000143384	Downregulation				
		COX4I2	ENSG00000131055	Downregulation				
		COX6A2	ENSG00000156885	Downregulation				
		NDUFB7	ENSG00000099795	Downregulation				
		NDUFV1	ENSG00000167792	Downregulation				
NDUFS4	ENSG00000164258	Downregulation						
miR-16a	MI0000070	COX4I2	ENSG00000131055	Downregulation	Apoptosis, ATP production	B-cell chronic lymphocytic leukemia	Human	Siengdee <i>et al.</i> , 2010 ¹⁰²
		COX6A2	ENSG00000156885	Downregulation				
		NDUFB7	ENSG00000099795	Downregulation				
		NDUFV1	ENSG00000167792	Downregulation				
		NDUFS4	ENSG00000164258	Downregulation				

cytochrome c oxidase subunit 4I2 (Cox4i2), subunit 6A2 (Cox6a2), NADH:ubiquinone oxidoreductase subunit B7 (Ndufb7), NADH:ubiquinone oxidoreductase core subunit V1 (Ndufv1) and NADH:ubiquinone oxidoreductase subunit S4 (Ndufs4) expression.¹⁰²

Glycolysis is the initial step in glucose catabolism, and occurs outside of the mitochondria in the cytoplasm. In the context of miRNAs affecting cell metabolism, miR-155 (Table 2) was found to indirectly upregulate hexokinase 2 (HK2), a glucose phosphorylation enzyme that might affect energy consumption in breast cancer cells. Mir-143 appears to be one of two potential pathways regulating miR-155-dependent HK2 regulation.^{103,104} Alternative splicing of pyruvate kinase isoenzyme (PKM), whose splicing proteins are regulated by miR-124, miR-137, and miR-340, is another pathway regulating glucose metabolism (Table 2). This miRNA-dependent regulation of PKM is able to influence colorectal cancer growth and counteract the Warburg effect.¹⁰⁵ In addition, pyruvate kinase (PK) is a direct target of the tumor suppressor miR-326, making it a potential glucose metabolism regulator.^{94,106,107}

In hepatocellular carcinoma, reduced mRNA levels were detected in 11 of the 13 genes encoded in the mtDNA, including the genes encoding cytochrome B (mt-CYB) and cytochrome C oxidase II (mt-CO2).¹⁰⁸ When miR-181a-5p expression was increased, the levels of mt-CYB and mt-CO2 were reduced in hepatocellular carcinoma cells, while mitochondrial membrane potential (MMP) maintained by electron transfer chain was reduced. *In vivo* experiments, which were done by Zhuang *et al.*¹⁰⁸, have shown to have caused glucose metabolism to reprogram and stimulated tumor growth and early lung metastasis in patients with hepatocellular carcinoma.

Several studies reported that miR-126 has an important role in different human cancers (Table 2) such as breast, lung, gastric cancers, melanoma cancer and acute leukaemia. Tomasetti *et al.*⁸³ reported that miR-126 affects mitochondrial energy metabolism, resulting in malignant mesothelioma tumor suppression. This mitomiR reduce mitochondrial respiration and promote glycolysis in H28 cells, associated with IRS1 modulate ATP-citrate lyase degradation. This leads to an increase in ATP and citrate production which is linked with reducing Akt signaling and inhibiting cytosolic sequestration of Forkhead box O1 (FoxO1), which promote the expression of genes involved in gluconeogenesis and oxidative stress defense.⁸³

Hypoxia has previously been related to altered mitomiR expression, with hypoxia-regulated mitomiRs being found to play a key role in cell survival in oxygen-depleted settings.¹²³ MiR-210 is one of the mitomiRs that is continuously increased in normal and transformed cells during hypoxia, suggesting that miR-210 plays a role in cells' adaptive response to hypoxia.¹⁰⁹ MiR-210 expression corresponds with hypoxia gene signatures in tumor tissues such as breast and head and neck cancers, demonstrating a direct connection between miR-210 expression and hypoxia in cancer.¹¹⁰ MiR-210 has been researched extensively and has a number of functionally significant targets in cell cycle control, cell survival, differentiation, angiogenesis, and metabolism.¹²³ Cell metabolism switches from mitochondrial OXPHOS to glycolysis under hypoxic environments. HIF-1, a hypoxia-inducible factor that upregulates the expression of most glycolytic enzymes as well as pyruvate dehydrogenase kinase while downregulating mitochondrial respiration, plays a key role in this action. Previous research has looked into how miR-210 regulates mitochondrial metabolism under hypoxia. MiR-210 target iron-sulfur cluster assembly proteins (ISCU1/2) and inhibit the activity of iron-sulfur proteins that govern mitochondrial metabolism, such as complex I and aconitase, resulting in lower OXPHOS.¹²³ It acts directly on cytochrome c oxidase assembly factor heme A:farnesyltransferase (COX10), succinate dehydrogenase complex subunit D (SDHD), and NADH dehydrogenase (ubiquinone) 1 alpha subcomplex 4 (NDUFA4) in regulating mitochondrial activity.¹²³ Another study found an abnormal mitochondrial phenotype in A549 lung cells overexpressing miR-210, and mRNA expression profile analysis connecting miR-210 to mitochondrial dysfunction.¹¹² Interestingly, HIF is rapidly destroyed upon reoxygenation of hypoxic cells due to miR-210's high stability, whereas miR-210 stays stable to maintain the glycolytic phenotype. Under normal conditions, this slows mitochondrial metabolism and may contribute to the Warburg effect in cancer cells. This result supports miR-210's involvement in regulating mitochondrial metabolism and promoting cancer cells' adaptability to hypoxic environments.

Another important mitomiR is miR-200, which has been identified as involved in tumor progression.^{124,125} One of miR-200 targets, is transcription factor mitochondria (TFAM) which is one of the most important proteins regulating mitochondrial biogenesis. TFAM has been described as a functional target of miR-200 in breast cancer cells.¹¹³ Its

transcription factor activity is required for mtDNA replication and transcription. In addition to its function in replication and transcription, the presence of TFAM is necessary for mtDNA maintenance.¹²⁶ It has also been implicated as a primary architectural protein of the mitochondrial genome by packaging mtDNA. In addition, TFAM expression has been reported to be involved in tumor progression, cancer cell growth, and chemoresistance.¹²⁷

Regarding the role of miRNAs in cancer and metabolism, the miR-17/92 cluster is one of the best characterized oncogenic miRNAs. This cluster is also known as oncomiR-1, and there is growing evidence of its oncogenic potential.⁹³ It has been shown that miR-17/92 suppresses apoptosis and was originally found amplified in B-cell lymphomas, where ectopically overexpressed truncated versions lacking miR-92a-1 were shown to possess oncogenic properties.¹¹⁰ The MiR-17/92 cluster is deregulated in B-cell lymphomas, T-cell lymphomas, B-cell chronic lymphocytic leukemia, and acute myeloid leukemia. This cluster is particularly overexpressed in several other cancers, including osteosarcoma, neuroblastoma, cervical, pancreatic, breast, lung, colorectal, ovarian, kidney, and liver cancers.^{93,105} Izreig *et al.*¹²⁸ reported that this miRNA cluster is a key factor in metabolic reprogramming of tumors. If oncomiR-1 is absent in Myc+ tumor cells, there is a global decrease in glycolytic and mitochondrial metabolism. If increased oncomiR-1 expression is present, this is sufficient for increased nutrient utilization by tumor cells. Deletion of miR-17/92 promoted changes in gene expression in Myc+ lymphoma which results in global decrease in metabolic pathways including glycolysis, the Krebs cycle, components of the electron transfer chain, amino acid metabolism, the pentose phosphate pathway, serine biosynthesis and nucleotide biosynthesis.¹²⁸

Conclusions

MiRNAs have been found in the mitochondria of many cell types, as shown by an increasing number of studies and they were named mitomiRs. In general, mitomiR populations differ in various tissues and under different pathological circumstances, implying that mitomiR populations are regulated by mechanisms that remain to be discovered. Based on the available information, we can deduce that there are a significant number of miRNAs which are present in mitochondria.^{7,29-33}

In our review, we have shown that various mitomiRs play a role in the initiation and progres-

sion of cancer via the regulation of mitochondria. They are involved in the Warburg effect, which is necessary for cancer cells to maintain their proliferative capacity.⁹¹ MitomiRs also upregulate HK2, a glucose phosphorylation enzyme, in an indirect manner, which may impact energy consumption in breast cancer cells.^{103,104} Expression of one of the mitomiRs (miR-210) corresponds with hypoxia gene signatures in tumor tissues such as breast cancer and head and neck cancers, demonstrating a clear connection between mitomiR expression and hypoxia in cancer.^{108,109,121} MiRNAs have emerged in the last decade as key regulators in cancer-related processes and are classified as either oncogenic or tumor suppressive miRNAs. The miR-17/92 cluster was first discovered to be amplified in diffuse cell lymphoma and B-cell lymphoma. This mitomiR cluster suppresses apoptosis and may act as an oncogene in B-cell lymphomas, B-cell chronic lymphocytic leukemia, acute myeloid leukemia, and T-cell lymphomas. It is also overexpressed in numerous other malignancies. This cluster is a key factor in metabolic reprogramming of tumors by regulating glycolytic and mitochondrial metabolism. Tumor-targeting treatments based on mitomiRs are emerging as a novel diagnostic and therapeutic tool.^{94,106,111,128}

Future perspectives

We have shown that mitomiRs are important players in mitochondria of cancer cell that need to be further investigated to develop a new potential therapies for cancer. Numerous studies that have been published in recent years give promising predictions that mitomiRs will receive more attention in the context of their role in cancer as possible biomarkers or targets for treatment.

Acknowledgement

This work was financially supported by the Slovenian Research Agency (ARRS grant # P3-0003).

References

1. Bienertova-Vasku J, Sana J, Slaby O. The role of microRNAs in mitochondria in cancer. *Cancer Lett* 2013; **336**: 1-7. doi: 10.1016/j.canlet.2013.05.001
2. Jansson MD, Lund AH. MicroRNA and cancer. *Mol Oncol* 2012; **6**: 590-610. doi: 10.1016/j.molonc.2012.09.006
3. Thomson DW, Bracken CP, Goodall GJ. Experimental strategies for microRNA target identification. *Nucleic Acids Res* 2011; **39**: 6845-53. doi: 10.1093/nar/gkr330

4. Zhang X, Zuo X, Yang B, Li Z, Xue Y, Zhuo Y, et al. MicroRNA directly enhances mitochondrial translation during muscle differentiation. *Cell* 2014; **158**: 607-19. doi: 10.1016/j.cell.2014.05.047
5. Lee RC, Feinbaum RL, Ambros V. The C. elegans heterochronic gene lin-4 encodes small RNAs with antisense complementarity to lin-14. *Cell* 1993; **75**: 843-54. doi: 10.1016/0092-8674(93)90529-Y
6. Wang JK, Wang Z, Li G. MicroRNA-125 in immunity and cancer. *Cancer Lett* 2019; **454**: 134-45. doi: 10.1016/j.canlet.2019.04.015
7. Macgregor-Das AM, Das S. A microRNA's journey to the center of the mitochondria. *Am J Physiol Circ Physiol* 2018; **315**: H206-H215. doi: 10.1152/ajpheart.00714.2017
8. Fiore D, Donnarumma E, Roscigno G, Iaboni M, Russo V, Affinito A, et al. miR-340 predicts glioblastoma survival and modulates key cancer hallmarks through down-regulation of NRAS. *Oncotarget* 2016; **7**: 19531-47. doi: 10.18632/oncotarget.6968
9. Pekarsky Y, Balatti V, Palamarchuk A, Rizzotto L, Veneziano D, Bigita G, et al. Dysregulation of a family of short noncoding RNAs, tsRNAs, in human cancer. *Proc Natl Acad Sci* 2016; **113**: 5071-76. doi: 10.1073/pnas.1604266113
10. Quintavalle C, Donnarumma E, Iaboni M, Roscigno G, Garofalo M, Romano G, et al. Effect of miR-21 and miR-30b/c on TRAIL-induced apoptosis in glioma cells. *Oncogene* 2013; **32**: 4001-8. doi: 10.1038/onc.2012.410
11. Roscigno G, Puoti I, Giordano I, Donnarumma E, Russo V, Affinito A, et al. miR-24 induces chemotherapy resistance and hypoxic advantage in breast cancer. *Oncotarget* 2017; **8**: 19507-21. doi: 10.18632/oncotarget.14470
12. Zhang J, He J, Zhang L. The down-regulation of microRNA-137 contributes to the up-regulation of retinoblastoma cell proliferation and invasion by regulating COX-2/PGE2 signaling. *Biomed Pharmacother* 2018; **106**: 35-42. doi: 10.1016/j.biopha.2018.06.099
13. Gebert LFR, MacRae IJ. Regulation of microRNA function in animals. *Nat Rev Mol Cell Biol* 2019; **20**: 21-37. doi: 10.1038/s41580-018-0045-7
14. Ingenito F, Roscigno G, Affinito A, Nuzzo S, Scognamiglio I, Quintavalle C, et al. The role of exo-miRNAs in cancer: a focus on therapeutic and diagnostic applications. *Int J Mol Sci* 2019; **20**: 4687. doi: 10.3390/ijms20194687
15. Mercer TR, Neph S, Dinger ME, Crawford J, Smith MA, Shearwood AMJ, et al. The human mitochondrial transcriptome. *Cell* 2011; **146**: 645-58. doi: 10.1016/j.cell.2011.06.051
16. Breving K, Esquela-Kerscher A. The complexities of microRNA regulation: mirandering around the rules. *Int J Biochem Cell Biol* 2010; **42**: 1316-29. doi: 10.1016/j.biocel.2009.09.016
17. Tétreault N, De Guire V. miRNAs: Their discovery, biogenesis and mechanism of action. *Clin Biochem* 2013; **46**: 842-5. doi: 10.1016/j.clinbiochem.2013.02.009
18. Xiong Y, Wang Y, Wang L, Huang Y, Xu Y, Xu L, et al. MicroRNA-30b targets Snail to impede epithelial-mesenchymal transition in pancreatic cancer stem cells. *J Cancer* 2018; **9**: 2147-59. doi: 10.7150/jca.25006
19. Zhu L, Xue F, Xu X, Xu J, Hu S, Liu S, et al. MicroRNA-198 inhibition of HGF/c-MET signaling pathway overcomes resistance to radiotherapy and induces apoptosis in human non-small-cell lung cancer. *J Cell Biochem* 2018; **119**: 7873-86. doi: 10.1002/jcb.27204
20. Otto T, Candido SV, Pilarz MS, Scinska E, Bronson RT, Bowden M, et al. Cell cycle-targeting microRNAs promote differentiation by enforcing cell-cycle exit. *Proc Natl Acad Sci* 2017; **114**: 10660-5. doi: 10.1073/pnas.1702914114
21. Wen X, Han XR, Wang YJ, Wang S, Shen M, Zhang ZF, et al. MicroRNA-421 suppresses the apoptosis and autophagy of hippocampal neurons in epilepsy mice model by inhibition of the TLR/MyD88 pathway. *J Cell Physiol* 2018; **233**: 7022-34. doi: 10.1002/jcp.26498
22. Yang T, Ge B. miRNAs in immune responses to Mycobacterium tuberculosis infection. *Cancer Lett* 2018; **431**: 22-30. doi: 10.1016/j.canlet.2018.05.028
23. Rosas-Hernandez H, Chigurupati S, Raymick J, Robinson B, Cuevas E, Hanig J, et al. Identification of altered microRNAs in serum of a mouse model of Parkinson's disease. *Neurosci Lett* 2018; **687**: 1-9. doi: 10.1016/j.neulet.2018.07.022
24. Islas JF, Moreno-Cuevas JE. A MicroRNA perspective on cardiovascular development and diseases: an update. *Int J Mol Sci* 2018; **19**: 2075. doi: 10.3390/ijms19072075
25. Hosseinahli N, Aghapour M, Duijf PHG, Baradaran B. Treating cancer with microRNA replacement therapy: a literature review. *J Cell Physiol* 2018; **233**: 5574-88. doi: 10.1002/jcp.26514
26. Acunzo M, Romano G, Wernicke D, Croce CM. MicroRNA and cancer - a brief overview. *Adv Biol Regul* 2015; **57**: 1-9. doi: 10.1016/j.jbior.2014.09.013
27. Iorio MV, Croce CM. microRNA involvement in human cancer. *Carcinogenesis* 2012; **33**: 1126-33. doi: 10.1093/carcin/bgs140
28. Tang Q, Ouyang H, He D, Yu C, Tang G. MicroRNA-based potential diagnostic, prognostic and therapeutic applications in triple-negative breast cancer. *Artif Cells, Nanomedicine, Biotechnol* 2019; **47**: 2800-9. doi: 10.1080/21691401.2019.1638791
29. Geiger J, Dalgaard LT. Interplay of mitochondrial metabolism and microRNAs. *Cell Mol Life Sci* 2017; **74**: 631-46. doi: 10.1007/s00018-016-2342-7
30. Das S, Kohr M, Dunkerly-Eyring B, Lee DI, Bedja D, Kent OA, et al. Divergent Effects of miR-181 Family members on myocardial function through protective cytosolic and detrimental mitochondrial microRNA targets. *J Am Heart Assoc* 2017; **6**: 1-17. doi: 10.1161/JAHA.116.004694
31. Paramasivam A, Vijayashree Priyadharsini J. MitomiRs: new emerging microRNAs in mitochondrial dysfunction and cardiovascular disease. *Hypertens Res* 2020; **43**: 851-3. doi: 10.1038/s41440-020-0423-3
32. Duarte FV, Palmeira CM, Rolo AP. The role of microRNAs in mitochondria: small players acting wide. *Genes* 2014; **5**: 865-86. doi: 10.3390/genes5040865
33. Shinde S, Bhadra U. A complex genome-microRNA interplay in human mitochondria. *Biomed Res Int* 2015; **2015**: 1-13. doi: 10.1155/2015/206382
34. Bandiera S, Matégot R, Girard M, Demongeot J, Henrion-Caude A. MitomiRs delineating the intracellular localization of microRNAs at mitochondria. *Free Radic Biol Med* 2013; **64**: 12-19. doi: 10.1016/j.freeradbiomed.2013.06.013
35. Barrey E, Saint-Auret G, Bonnamy B, Damas D, Boyer O, Gidrol X. Pre-microRNA and mature microRNA in human mitochondria. *PLoS One* 2011; **6**: e20220. doi: 10.1371/journal.pone.0020220
36. Latronico MVG, Condorelli G. The might of microRNA in mitochondria. *Circ Res* 2012; **110**: 1540-2. doi: 10.1161/CIRCRESAHA.112.271312
37. Sripada L, Tomar D, Prajapati P, Singh R, Singh AK, Singh R. Systematic analysis of small RNAs associated with human mitochondria by deep sequencing: detailed analysis of mitochondrial associated miRNA. *PLoS One* 2012; **7**: e44873. doi: 10.1371/journal.pone.0044873
38. Mercer TR, Neph S, Dinger ME, Crawford J, Smith MA, Shearwood AMJ. The human mitochondrial transcriptome. *Cell* 2011; **146**: 645-58. doi: 10.1016/j.cell.2011.06.051
39. Jagannathan R, Thapa D, Nichols CE, Shepherd DL, Stricker JC, Croston TL, et al. Translational regulation of the mitochondrial genome following redistribution of mitochondrial microRNA in the diabetic heart. *Circ Cardiovasc Genet* 2015; **8**: 785-802.
40. Bandiera S, Rüberg S, Girard M, Cagnard N, Hanein S, Chretien D, et al. Nuclear outsourcing of RNA interference components to human mitochondria. *PLoS One* 2011; **6**: e20746. doi: 10.1371/journal.pone.0020746
41. Fan S, Tian T, Chen W, Lv X, Lei X, Zhang H, et al. Mitochondrial miRNA determines chemoresistance by reprogramming metabolism and regulating mitochondrial transcription. *Cancer Res* 2019; **79**: 1069-84. doi: 10.1158/0008-5472.CAN-18-2505
42. Srinivasan H, Das S. Mitochondrial miRNA (MitomiR): a new player in cardiovascular health. *Can J Physiol Pharmacol* 2015; **93**: 855-61. doi: 10.1139/cjpp-2014-0500
43. Di Leva G, Garofalo M, Croce CM. MicroRNAs in cancer. *Annu Rev Pathol Mech Dis* 2014; **9**: 287-314. doi: 10.1146/annurev-pathol-012513-104715
44. Fabian MR, Sonenberg N. The mechanics of miRNA-mediated gene silencing: a look under the hood of miRISC. *Nat Struct Mol Biol* 2012; **19**: 586-93. doi: 10.1038/nsmb.2296
45. Treiber T, Treiber N, Meister G. Regulation of microRNA biogenesis and its crosstalk with other cellular pathways. *Nat Rev Mol Cell Biol* 2019; **20**: 5-20. doi: 10.1038/s41580-018-0059-1
46. Song R, Hu XQ, Zhang L. Mitochondrial miRNA in cardiovascular function and disease. *Cells* 2019; **8**: 1475. doi: 10.3390/cells8121475
47. Geiger J, Dalgaard LT. Interplay of mitochondrial metabolism and microRNAs. *Cell Mol Life Sci* 2017; **74**: 631-646. doi: 10.1007/s00018-016-2342-7

48. Das S, Ferlito M, Kent OA, Fox-Talbot K, Wang R, Liu D, et al. Nuclear miRNA regulates the mitochondrial genome in the heart. *Circ Res* 2012; **110**: 1596-603. doi: 10.1161/CIRCRESAHA.112.267732
49. Shepherd DL, Hathaway QC, Pinti MV, Nichols CE, Durr AJ, Sreekumar S, et al. Exploring the mitochondrial microRNA import pathway through Polynucleotide Phosphorylase (PNPase). *J Mol Cell Cardiol* 2017; **110**: 15-25. doi: 10.1016/j.yjmcc.2017.06.012
50. Chan DC. Fusion and fission: Interlinked processes critical for mitochondrial health. *Annu Rev Genet* 2012; **46**: 265-87. doi: 10.1146/annurev-genet-110410-132529
51. Kushnareva Y, Newmeyer D. Bioenergetics and cell death. *Ann N Y Acad Sci* 2010; **1201**: 50-7. doi: 10.1111/j.1749-6632.2010.05633.x
52. Hudson G, Gomez-Duran A, Wilson IJ, Chinnery PF. Recent mitochondrial DNA mutations increase the risk of developing common late-onset human diseases. *PLoS Genet* 2014; **10**: e1004369. doi: 10.1371/journal.pgen.1004369
53. Dowling DK. Evolutionary perspectives on the links between mitochondrial genotype and disease phenotype. *Biochim Biophys Acta - Gen Subj* 2014; **1840**: 1393-403. doi: 10.1016/j.bbagen.2013.11.013
54. Wagner GR, Payne RM. Widespread and enzyme-independent N-acetylation and N-succinylation of proteins in the chemical conditions of the mitochondrial matrix. *J Biol Chem* 2013; **288**: 29036-45. doi: 10.1074/jbc.M113.486753
55. Pan T. N6-methyl-adenosine modification in messenger and long non-coding RNA. *Trends Biochem Sci* 2013; **38**: 204-9. doi: 10.1016/j.tibs.2012.12.006
56. Li K, Zhang J, Yu J, Liu B, Guo Y, et al. MicroRNA-214 suppresses gluconeogenesis by targeting activating transcription factor 4. *J Biol Chem* 2015; **290**: 8185-95. doi: 10.1074/jbc.M114.633990
57. Brunette TJ, Permezziani F, Huang PS, Bhabha G, Ekiert DC, Tsutakawa SE, et al. Exploring the repeat protein universe through computational protein design. *Nature* 2015; **528**: 580-4. doi: 10.1038/nature16162
58. Fang J, Song XW, Tian J, Chen HY, Li DF, Wang JF, et al. Overexpression of microRNA-378 attenuates ischemia-induced apoptosis by inhibiting caspase-3 expression in cardiac myocytes. *Apoptosis* 2012; **17**: 410-23. doi: 10.1007/s10495-011-0683-0
59. Carrer M, Liu N, Grueter CE, Williams AH, Frisard MI, Hulver MW, et al. Control of mitochondrial metabolism and systemic energy homeostasis by microRNAs 378 and 378*. *Proc Natl Acad Sci* 2012; **109**: 15330-5. doi: 10.1073/pnas.1207605109
60. Gao P, Tchernyshyov I, Chang TC, Lee YS, Kita K, Ochi T, et al. c-Myc suppression of miR-23a/b enhances mitochondrial glutaminase expression and glutamine metabolism. *Nature* 2009; **458**: 762-5. doi: 10.1038/nature07823
61. Jeong JH, Cheol Kang Y, Piao Y, Kang S, Pak YK. miR-24-mediated knockdown of H2AX damages mitochondria and the insulin signaling pathway. *Exp Mol Med* 2017; **49**: e313. doi: 10.1038/emm.2016.174
62. Serguenco A, Grad I, Wennerstrom A, Meza-Zepeda LA, Thiede B, Stratford EW, et al. Metabolic reprogramming of metastatic breast cancer and melanoma by let-7a microRNA. *Oncotarget* 2015; **6**: 2451-65. doi: 10.18632/oncotarget.3235
63. Yamasaki T, Seki N, Yoshino H, Itesako T, Yamada Y, Tatarano S, et al. Tumor-suppressive microRNA-1291 directly regulates glucose transporter 1 in renal cell carcinoma. *Cancer Sci* 2013; **104**: 1411-9. doi: 10.1111/cas.12240
64. Chen Y, Zhou Y, Han F, Zhao Y, Tu M, Wang Y, et al. A novel miR-1291-ERR α -CPT1C axis modulates tumor cell proliferation, metabolism and tumorigenesis. *Theranostics* 2020; **10**: 7193-210. doi: 10.7150/tno.44877
65. Tu MJ, Duan Z, Liu Z, Zhang C, Bold RJ, Gonzalez FJ, et al. MicroRNA-1291-5p sensitizes pancreatic carcinoma cells to arginine deprivation and chemotherapy through the regulation of arginyls and glycolysis. *Mol Pharmacol* 2020; **98**: 686-94. doi: 10.1124/molpharm.120.000130
66. Zhu H, Xue H, Jin QH, Guo J, Chen YD. MiR-138 protects cardiac cells against hypoxia through modulation of glucose metabolism by targeting pyruvate dehydrogenase kinase 1. *Biosci Rep* 2017; **37**: 1-9. doi: 10.1042/BSR20170296
67. Ju J, Xiao D, Shen N, Zhou T, Che H, Li X, et al. miR-150 regulates glucose utilization through targeting GLUT4 in insulin-resistant cardiomyocytes. *Acta Biochim Biophys Sin (Shanghai)* 2020; **52**: 1111-9. doi: 10.1093/abbs/gmaa094
68. Li SJ, Liu HL, Tang SL, Li XJ, Wang XY. MicroRNA-150 regulates glycolysis by targeting von Hippel-Lindau in glioma cells. *Am J Transl Res* 2017; **9**: 1058-66.
69. Guo W, Qiu Z, Wang Z, Wang Q, Tan N, Chen T, et al. MiR-199a-5p is negatively associated with malignancies and regulates glycolysis and lactate production by targeting hexokinase 2 in liver cancer. *Hepatology* 2015; **62**: 1132-44. doi: 10.1002/hep.27929
70. Esteves JV, Yonamine CY, Pinto-Junior DC, Gerlinger-Romero F, Enguita FJ, Machado UF. Diabetes modulates microRNAs 29b-3p, 29c-3p, 199a-5p and 532-3p expression in muscle: Possible role in GLUT4 and HK2 repression. *Front Endocrinol* 2018; **9**: 1-12. doi: 10.3389/fendo.2018.00536
71. Pullen TJ, da Silva Xavier G, Kelsey G, Rutter GA. miR-29a and miR-29b contribute to pancreatic β -cell-specific silencing of monocarboxylate transporter 1 (Mct1). *Mol Cell Biol* 2011; **31**: 3182-94. doi: 10.1128/MCB.01433-10
72. Rayner KJ, Esau CC, Hussain FN, McDaniel AL, Marshall SM, van Gils JM, et al. Inhibition of miR-33a/b in non-human primates raises plasma HDL and lowers VLDL triglycerides. *Nature* 2011; **478**: 404-7. doi: 10.1038/nature10486
73. Chen L, Hou J, Ye L, Chen Y, Cui J, Tian W, et al. MicroRNA-143 regulates adipogenesis by modulating the MAP2K5-ERK5 signaling. *Sci Rep* 2015; **4**: 3819. doi: 10.1038/srep03819
74. Ye Q, Zhao X, Xu K, Li Q, Cheng J, Gao Y, et al. Polymorphisms in lipid metabolism related miRNA binding sites and risk of metabolic syndrome. *Gene* 2013; **528**: 132-8. doi: 10.1016/j.gene.2013.07.036
75. Civelek M, Hagopian R, Pan C, Che N, Yang W, Kayne PS, et al. Genetic regulation of human adipose microRNA expression and its consequences for metabolic traits. *Hum Mol Genet* 2013; **22**: 3023-37. doi: 10.1093/hmg/ddt159
76. Ahmad A, Aboukameel A, Kong D, Wang Z, Sethi S, Chen W, et al. Phosphoglucose isomerase/autocrine motility factor mediates epithelial-mesenchymal transition regulated by miR-200 in breast cancer cells. *Cancer Res* 2011; **71**: 3400-9. doi: 10.1158/0008-5472.CAN-10-0965
77. Aschrafi A, Schwechter AD, Mameza MG, Natera-Naranji O, Gioio AE, Kaplan BB. MicroRNA-338 regulates local cytochrome c oxidase IV mRNA levels and oxidative phosphorylation in the axons of sympathetic neurons. *J Neurosci* 2008; **28**: 12581-90. doi: 10.1523/JNEUROSCI.3338-08.2008
78. Li P, Jiao J, Gao G, Prabhakar BS. Control of mitochondrial activity by miRNAs. *J Cell Biochem* 2012; **113**: 1104-10. doi: 10.1002/jcb.24004
79. Barman RK, Saha S, Das S. Prediction of interactions between viral and host proteins using supervised machine learning methods. *PLoS One* 2014; **9**: e112034. doi: 10.1371/journal.pone.0112034
80. Chen, H, Vermulst M, Wang YE, Chomyn A, Prolla TA, McCaffery JM, et al. Mitochondrial fusion is required for mtDNA stability in skeletal muscle and tolerance of mtDNA mutations. *Cell* 2010; **141**: 280-9. doi: 10.1016/j.cell.2010.02.026
81. Colleoni F, Padmanabhan N, Wung HW, Watson ED, Cetin I, Tissot van Patot M, et al. Suppression of mitochondrial electron transport chain function in the hypoxic human placenta: a role for miRNA-210 and protein synthesis inhibition. *PLoS One* 2013; **8**: e55194. doi: 10.1371/journal.pone.0055194
82. Nishi H, Ono K, Iwanaga Y, Horie T, Nagao T, Takemura G, et al. MicroRNA-15b modulates cellular ATP levels and degenerates mitochondria via Arl2 in neonatal rat cardiac myocytes. *J Biol Chem* 2010; **285**: 4920-30. doi: 10.1074/jbc.M109.082610
83. Tomasetti M, Neuzil J, Dong L. MicroRNAs as regulators of mitochondrial function: role in cancer suppression. *Biochim Biophys Acta* 2014; **1840**: 1441-53. doi: 10.1016/j.bbagen.2013.09.002
84. Zheng S, Li Y, Zhang Y, Li X, Tang H. MiR-101 regulates HSV-1 replication by targeting ATP5B. *Antiviral Res* 2011; **89**: 219-226. doi: 10.1016/j.antiviral.2011.01.008
85. Qiao A, Khechaduri A, Mutharasan RK, Wu R, Nagpal V, Ardehali H. MicroRNA-210 Decreases heme levels by targeting ferrochelatase in cardiomyocytes. *J Am Heart Assoc* 2013; **2**: 1-12. doi: 10.1161/JAHA.113.000121
86. Kurtz CL, Peck BCE, Fannin EE, Beysen C, Miao J, Landstreet SR, et al. MicroRNA-29 Fine-tunes the expression of key FOXA2-activated lipid metabolism genes and is dysregulated in animal models of insulin resistance and diabetes. *Diabetes* 2014; **63**: 3141-8. doi: 10.2337/db13-1015
87. Li X, Wang FS, Wu ZY, Lin JL, Lan WB, Lin JH. MicroRNA-19b targets Mfn1 to inhibit Mfn1-induced apoptosis in osteosarcoma cells. *Neoplasma* 2014; **61**: 265-73. doi: 10.4149/neo_2014_034

88. Das S, Ferlito M, Kent OA, Fox-Talbot K, Wang R, Liu D, et al. Nuclear miRNA regulates the mitochondrial genome in the heart. *Circ Res* 2012; **110**: 1596-603. doi: 10.1161/CIRCRESAHA.112.267732
89. Hanahan D, Weinberg RA. Hallmarks of cancer: The next generation. *Cell* 2011; **144**: 646-74. doi: 10.1016/j.cell.2011.02.013
90. Zhong Z, Yu J, Virshup DM, Madan B. Wnts and the hallmarks of cancer. *Cancer Metastasis Rev* 2020; **39**: 625-45. doi: 10.1007/S10555-020-09887-6
91. Courtney R, Ngo DC, Malik N, Ververis K, Tortorella SM, Karagiannis TC. Cancer metabolism and the Warburg effect: the role of HIF-1 and PI3K. *Mol Biol Rep* 2015; **42**: 841-51. doi: 10.1007/s11033-015-3858-x
92. Zheng J. Energy metabolism of cancer: glycolysis versus oxidative phosphorylation (Review). *Oncol Lett* 2012; **4**: 1151-7. doi: 10.3892/ol.2012.928
93. Fogg VC, Lanning NJ, MacKeigan JP. Mitochondria in cancer: at the crossroads of life and death. *Chin J Cancer* 2011; **30**: 526-39. doi: 10.5732/cjc.011.10018
94. Mogilyansky E, Rigoutsos I. The miR-17/92 cluster: a comprehensive update on its genomics, genetics, functions and increasingly important and numerous roles in health and disease. *Cell Death Differ* 2013; **20**: 1603-14. doi: 10.1038/cdd.2013.125
95. Chen B, Li H, Yen H, Yang P, Liu X, Zhao X, et al. Roles of microRNA on cancer cell metabolism. *J Transl Med* 2012; **10**: 228. doi: 10.1186/1479-5876-10-228
96. Li L, Yuan L, Luo J, Gao J, Guo J, Xie X. MiR-34a inhibits proliferation and migration of breast cancer through down-regulation of Bcl-2 and SIRT1. *Clin Exp Med* 2013; **13**: 109-17. doi: 10.1007/s10238-012-0186-5
97. Buechner J, Tømte E, Haug BH, Henriksen JR, Løkke C, Flægstad T, et al. Tumour-suppressor microRNAs let-7 and miR-101 target the proto-oncogene MYCN and inhibit cell proliferation in MYCN-amplified neuroblastoma. *Br J Cancer* 2011; **105**: 296-303. doi: 10.1007/s10238-012-0186-5
98. Zhang L, Liao Y, Tang L. MicroRNA-34 family: a potential tumor suppressor and therapeutic candidate in cancer. *J Exp Clin Cancer Res* 2019; **38**: 1-13. doi: 10.1186/S13046-019-1059-5
99. Endo K, Naito Y, Ji X, Nakanishi M, Noguchi T, Goto Y, et al. MicroRNA 210 as a biomarker for congestive heart failure. *Biol Pharm Bull* 2013; **36**: 48-54. doi: 10.1248/bpb.12-00578
100. Calin GA, Dumitru CD, Shimizu M, Bichi R, Zupo S, Noch E, et al. Nonlinear partial differential equations and applications: Frequent deletions and down-regulation of micro-RNA genes miR15 and miR16 at 13q14 in chronic lymphocytic leukemia. *Proc Natl Acad Sci* 2002; **99**: 15524-9. doi: 10.1073/pnas.242606799
101. Gao S, Chen C, Wu J, Tan Y, Yu K, Xing CY, et al. Synergistic apoptosis induction in leukemic cells by miR-15a/16-1 and arsenic trioxide. *Biochem Biophys Res Commun* 2010; **403**: 203-8. doi: 10.1016/j.bbrc.2010.10.137
102. Siengdee P, Trakooljul N, Murani E, Schwerin M, Wimmers K, Ponsuksili S. MicroRNAs regulate cellular ATP levels by targeting mitochondrial energy metabolism genes during C2C12 myoblast differentiation. 2015; doi:10.1371/journal.pone.0127850. doi:10.1371/journal.pone.0127850.
103. Fang R, Xiao T, Fang Z, Sun Y, Li F, Gao Y, et al. MicroRNA-143 (miR-143) regulates cancer glycolysis via targeting hexokinase 2 gene. *J Biol Chem* 2012; **287**: 23227-23235. doi: 10.1074/jbc.M112.373084
104. Jiang S, Zhang LF, Zhang HW, Hu S, Lu MH, Liang S, et al. A novel miR-155/miR-143 cascade controls glycolysis by regulating hexokinase 2 in breast cancer cells. *EMBO J* 2012; **31**: 1985-98. doi: 10.1038/emboj.2012.45
105. Sun Y, Zhao X, Zhou Y, Hu Y. miR-124, miR-137 and miR-340 regulate colorectal cancer growth via inhibition of the Warburg effect. *Oncol Rep* 2012; **28**: 1346-52. doi: 10.3892/or.2012.1958
106. Kefas B, Comeau L, Erdle N, Montgomery E, Amos S, Purow B. Pyruvate kinase M2 is a target of the tumor-suppressive microRNA-326 and regulates the survival of glioma cells. *Neuro Oncol* 2010; **12**: 1102-12. doi: 10.1093/neuonc/noon080
107. Olive V, Jiang I, He L. miR-17-92, a cluster of miRNAs in the midst of the cancer network. *Int J Biochem Cell Biol* 2010; **42**: 1348-54. doi: 10.1016/j.biocel.2010.03.004
108. Zhuang X, Chen Y, Wu Z, Xu Q, Chen M, Shao M, et al. Mitochondrial miR-181a-5p promotes glucose metabolism reprogramming in liver cancer by regulating the electron transport chain. *Carcinogenesis* 2020; **41**: 972-83. doi: 10.1093/CARCIN/BGZ174
109. Qin Q, Furong W, Baosheng L. Multiple functions of hypoxia-regulated miR-210 in cancer. *J Exp Clin Cancer Res* 2014; **33**: 50. doi: 10.1186/1756-9966-33-50
110. Gee HE, Camps C, Buffa FM, Patiar S, Winter SC, Betts G, et al. hsa-miR-210 is a marker of tumor hypoxia and a prognostic factor in head and neck cancer. *Cancer* 2010; **116**: 2148-58. doi: 10.1002/cncr.25009
111. Puisségur MP, Mazure NM, Bertero T, Pradelli L, Grosso S, Robbeserment K, et al. miR-210 is overexpressed in late stages of lung cancer and mediates mitochondrial alterations associated with modulation of HIF-1 activity. *Cell Death Differ* 2011; **18**: 465-78. doi: 10.1038/cdd.2010.119
112. Yao J, Zhou E, Wang Y, Xu F, Zhang D, Zhong D. microRNA-200a inhibits cell proliferation by targeting mitochondrial transcription factor A in breast cancer. *DNA Cell Biol* 2014; **33**: 291-300. doi: 10.1089/dna.2013.2132
113. Mi Y, Zhang D, Jiang W, Weng J, Zhou C, Huang K, et al. miR-181a-5p promotes the progression of gastric cancer via RASSF6-mediated MAPK signalling activation. *Cancer Lett* 2017; **389**: 11-22. doi: 10.1016/j.canlet.2016.12.033
114. Zhu N, Zang D, Xie H, Zhou Z, Chen H, Hu T, et al. Endothelial-specific intron-derived miR-126 is down-regulated in human breast cancer and targets both VEGFA and PIK3R2. *Mol Cell Biochem* 2011; **351**: 157-64. doi: 10.1007/s11010-011-0723-7
115. Li Z, Lu J, Sun M, Mi S, Zhang H, Luo RT, et al. Distinct microRNA expression profiles in acute myeloid leukemia with common translocations. *Proc Natl Acad Sci* 2008; **105**: 15535-40. doi: 10.1073/pnas.0808266105
116. Sasahira T, Kurihara M, Bhawal UK, Ueda N, Shimomoto T, Yamamoto K. et al. Downregulation of miR-126 induces angiogenesis and lymphangiogenesis by activation of VEGF-A in oral cancer. *Br J Cancer* 2012; **107**: 700-6. doi: 10.1038/bjc.2012.330
117. Crawford M, Brawner E, Batte K, Yu L, Hunter MG, Otterson GA, et al. MicroRNA-126 inhibits invasion in non-small cell lung carcinoma cell lines. *Biochem Biophys Res Commun* 2008; **373**: 607-12. doi: 10.1016/j.bbrc.2008.06.090
118. Felli N, Felicetti F, Lustrì AM, Errico MC, Bottero L, Cannistraci A, et al. miR-126&126* restored expressions play a tumor suppressor role by directly regulating ADAM9 and MMP7 in melanoma. *PLoS One* 2013; **8**: e56824. doi: 10.1371/journal.pone.0056824
119. Shen WF, Hu YL, Uttarwar L, Passegue E, Largman C. MicroRNA-126 regulates HOXA9 by binding to the homeobox. *Mol Cell Biol* 2008; **28**: 4609-19. doi: 10.1128/MCB.01652-07
120. Zhang J, Du YY, Lin Y, Chen Y, Yang L, Wang H, et al. The cell growth suppressor, miR-126, targets IRS-1. *Biochem Biophys Res Commun* 2008; **377**: 136-40. doi: 10.1016/j.bbrc.2008.09.089
121. Otsubo T, Akiyama Y, Hashimoto Y, Shimada S, Goto K, Tuasa Y. MicroRNA-126 inhibits SOX2 expression and contributes to gastric carcinogenesis. *PLoS One* 2011; **6**: e16617. doi: 10.1371/journal.pone.0016617
122. Miko E, Margitai Z, Zimmerer Z, Varkonyi I, Dezso B, Lanyi A, et al. miR-126 inhibits proliferation of small cell lung cancer cells by targeting SLC7A5. *FEBS Lett* 2011; **585**: 1191-1196. doi: 10.1016/j.febslet.2011.03.039
123. Gee HE, Ivan C, Calin GA, Ivan M. HypoxamiRs and cancer: From biology to targeted therapy. *Antioxid Redox Signal* 2014; **21**: 1220-38. doi: 10.1089/ars.2013.5639
124. Roybal JD, Zang Y, Ahn YH, Yang Y, Gibbons DL, Baird BN, et al. miR-200 inhibits lung adenocarcinoma cell invasion and metastasis by targeting Fli1/VEGFR1. *Mol Cancer Res* 2011; **9**: 25-35. doi: 10.1158/1541-7786.MCR-10-0497
125. Rasheed SAK, Teo CR, Beillard EJ, Voorhoeve PM, Casey PJ. MicroRNA-182 and microRNA-200a control G-protein subunit α -13 (GNA13) expression and cell invasion synergistically in prostate cancer cells. *J Biol Chem* 2013; **288**: 7986-95. doi: 10.1074/jbc.M112.437749
126. Renčelj A, Škrlep M, Čandek-Potokar M, Dovč P. Tissue specific splicing of pre-mRNA porcine mitochondrial transcription factor A. *Czech J Anim Sci* 2018; **63**: 43-50. doi: 10.17221/29/2017-CJAS
127. Han B, Izumi H, Yasuniwa Y, Akiyama M, Yamaguchi T, Fujimoto N, et al. Human mitochondrial transcription factor A functions in both nuclei and mitochondria and regulates cancer cell growth. *Biochem Biophys Res Commun* 2011; **408**: 45-51. doi: 10.1016/j.bbrc.2011.03.114
128. Izreig S, Samborska B, Johnson RM, Sergushichev A, Ma EH, Lussier C, et al. The miR-17-92 microRNA cluster is a global regulator of tumor metabolism. *Cell Rep* 2016; **16**: 1915-28. doi: 10.1016/j.celrep.2016.07.036

Target motion management in breast cancer radiation therapy

Elham Piruzan¹, Naser Vosoughi¹, Seied Rabi Mahdavi^{2,3}, Leila Khalafi^{2,3}, Hojjat Mahani⁴

¹ Department of Energy Engineering, Sharif University of Technology, Tehran, Iran

² Radiation Biology Research Center, Iran University of Medical Sciences, Tehran, Iran

³ Department of Medical Physics, Iran University of Medical Sciences, Tehran, Iran

⁴ Radiation Applications Research School, Nuclear Science and Technology Research Institute, Tehran, Iran

Radiol Oncol 2021; 55(4): 393-408.

Received 10 June 2021

Accepted 4 August 2021

Correspondence to: Hojjat Mahani, Ph.D., Radiation Applications Research School, Nuclear Science and Technology Research Institute, Tehran, Iran. E-mail: hmahani@aeoi.org.ir

Disclosure: No potential conflicts of interest were disclosed.

This is an open access article under the CC BY-NC-ND license (<http://creativecommons.org/licenses/by-nc-nd/4.0/>).

Background. Over the last two decades, breast cancer remains the main cause of cancer deaths in women. To treat this type of cancer, radiation therapy (RT) has proved to be efficient. RT for breast cancer is, however, challenged by intrafractional motion caused by respiration. The problem is more severe for the left-sided breast cancer due to the proximity to the heart as an organ-at-risk. While particle therapy results in superior dose characteristics than conventional RT, due to the physics of particle interactions in the body, particle therapy is more sensitive to target motion.

Conclusions. This review highlights current and emerging strategies for the management of intrafractional target motion in breast cancer treatment with an emphasis on particle therapy, as a modern RT technique. There are major challenges associated with transferring real-time motion monitoring technologies from photon to particles beams. Surface imaging would be the dominant imaging modality for real-time intrafractional motion monitoring for breast cancer. The magnetic resonance imaging (MRI) guidance and ultra high dose rate (FLASH)-RT seem to be state-of-the-art approaches to deal with 4D RT for breast cancer.

Key words: breast cancer; target motion; particle therapy; intrafractional movement

Introduction

Breast cancer is the second most common cancer worldwide.¹⁻⁴ Radiation therapy (RT) is proved to be efficient for breast cancer treatment.⁵⁻⁷ Breast cancer RT is mainly categorized into whole-breast irradiation (WBI) and partial-breast irradiation (PBI), each consisting of a variety of techniques.^{6,8} Although the principal goal of breast cancer RT is to damage tumor while sparing normal tissues, superior treatment outcome is hampered by some uncertainties such as organ motion. Target motion imposes a negative impact on breast cancer RT, particularly for the left-sided breast. Organ motion is generally categorized into three types: (1) pa-

tient motion, (2) interfractional motion occurring between the fractions, and (3) intrafractional motion referring to all involuntary movements during a treatment fraction. Examples of the latter include respiration cycle, heart beating, muscle relaxation/tension, bowel, and rectal/bladder filling. As the intrafractional motion follows approximately a systemic pattern in an intrafractional motion always increases the apparent size of the target resulting in a larger irradiated volume. It, in turn, increases secondary cancer risk, as well. Owing to the importance of breast cancer, several techniques are introduced to address the problem of respiratory-induced target movement.⁹ It should be also noted that for the right-sided breast cancer, the manage-

ment of target motion is not regular mainly due to the larger distance between the heart and the target compared to the left-sided cases. In contrast to lung RT, few studies are focusing on tumor motion management in breast RT. In addition, the literature about addressing breast tumor motion in particle therapy is also sparse. The problem is more challenging in particle therapy than conventional RT mainly due to stricter accuracy requirements and thus mandates special considerations.¹⁰ It should also be noted that this review covers only the external-beam RT techniques for breast cancer. To this end, this literature review aims at providing an overview of current intrafractional target motion management techniques for breast cancer irradiation, highlighting the gaps, and finally presenting future directions in the field of interest.

Literature search strategy

To conduct a comprehensive literature review, all English full-text records indexed in both Scopus and/or PubMed were searched and considered. The published year was limited between 1990 and 2021 to ensure the inclusion of all recent publications. The following keywords were used: “intrafraction”, “intra-fraction”, “intrafractional”, “intra-fractional”, “breast cancer”, “radiotherapy”, “radiation therapy”, “proton therapy”, “proton beam therapy”, “motion”, “particle therapy”, “and respiration”, “prone”, or “supine”. Four identification, screening, eligibility, and inclusion steps were then followed. The selection criteria were as follows: (1) monitoring intrafractional target motion in breast cancer treatment and (2) irradiating moving target in breast cancer treatment. However, some identified articles were excluded since they were either duplicated or irrelevant. Of them, 106 articles fulfilled the inclusion criteria. No specific additional filter was applied. Moreover, additional 45 original articles, reviews, and books were also considered as they were applicable to breast cancer and/or they provided general information on target motion monitoring and management techniques in RT.

The nature and extent of target motion in breast cancer

Breast subjects to intrafractional movement caused by both baseline shift and respiration and therefore breast cancer RT is always challenged by target mo-

tion.⁶ Usually, the amount of breast motion ranges from 1 mm to more than 20 mm displacement in some cases.^{6,11-15} Moreover, studies reported that this motion tends to be non-linear (*i.e.*, it peruses semi-circles rather than a straight line) for many tumors.¹⁶ Most of the tumors (~78%) in the breast move with less than 10 mm peak-to-peak displacement.¹⁶ Smith *et al.* showed the maximum range of intrafractional variation of central lung distance (CLD), as the best predictor of setup uncertainties, for any patient on the day, is 2.5 mm. Maximum changes of lung and heart area during treatment are 270 mm² and 360 mm², respectively.¹⁷ Saliou *et al.* showed that using CLD, mean setup errors are estimated to be 3.8 mm and 3.2 mm for systematic and random errors, respectively. In addition, the breast moves during respiration with a motion amount of 0.8-10 mm in the anterior-posterior (AP) direction.^{18,19} Latifi *et al.* reported the respiratory-induced fiducial motion, based on the mean change in the fiducial's center of mass, was 0.8 ± 0.6 mm with a range of 0-2.2 mm.²⁰ Qi *et al.* estimated that respiratory-induced heart displacement for the left-sided breast irradiation results in variations in dose delivered to the heart up to 39%.²¹ The discrepancy between the reported motion extents arises from several factors such as obesity, body mass index (BMI), the accuracy of the measurement technique, patient stress, the direction of the breast motion measurement, and patient age. It is shown that the target motion extent is more considerable in the AP direction compared to the right-left (RL) and craniocaudal (CC) directions.²²⁻²⁵

Motion monitoring techniques in breast cancer RT

Surface imaging

A promising solution for intrafractional motion monitoring in the chest wall irradiation and breast cancer RT is optical surface imaging.²⁶ Using three optical cameras and light projectors, the 3D map of a patient's topography is generated and allows visualization of the patient in any position or gantry angle (Figure 1).²⁷

Surface imaging provides mobile target monitoring in the case of breast irradiation. Surface imaging is characterized by easy utilization and high temporal frequency without further radiation dose to the patient.²⁶ It can be matched with a variety of RT techniques (for example, breath-hold and respiratory gating) to reduce setup uncertainties

during delivery, which can lead to a reduction in target margins and nearby sparing. Several studies have shown that surface guidance for intrafractional monitoring was mainly utilized for breast breath-hold RT.^{28,29} Additional benefits of surface imaging include (1) reducing interfractional setup error, (2) monitoring intrafractional motion, and (3) using less invasive patient fixation than other immobilization techniques, and more comfortability of patient as well.³⁰ However, surface guidance comes with some limitations. The visibility of the patient's skin surface for surface imaging is essential. Therefore, there is a compromise between surface imaging ability and the degree of immobilization. Also, any obstacle on the skin can lead to impossible reflectivity and restricting the function of surface imaging. An important limitation of surface imaging relevance to target localization is insufficient adaption between the external and internal surfaces. However, in breast cancer RT in which the external surface is the target surface, this problem becomes less important.²⁶ Nonetheless, surface-guided RT (SGRT) technology enables adaptive radiation therapy (ART) in which a motion history related to the patient is applied to perform narrower margins in the next following treatment fractions. Current applications of real-time surface imaging rely on breath-hold, respiratory gating, and tumor tracking deliveries.³¹

Internal/external markers combined with real-time imaging

Accessibility of the breast (compared to deep organs such as liver or prostate) and typically shallow-seated targets, facilitate the application of internal markers.³² Additionally, breast motion is well characterized by external markers.³³ Internal/external markers result in superior performance compared to the surgical clips in terms of both accuracy and detectability on kilovoltage (kV) images.³⁴ Organ displacement and real-time localization during beam delivery can be directly evaluated by employing external surrogate and/or internal radio-opaque fiducial markers. The fiducial marker tracking technique was first introduced for conventional RT and later for particle therapy.³² Target motion tracking using internal markers is usually combined with more than two fluoroscopic imaging examinations. The fiducial markers are implanted near to or inside of the target. Markers (or surgical clips) are usually made from high-Z material such as gold, platinum, carbon-coated zirconium oxide to be visible in X-ray images.³⁵

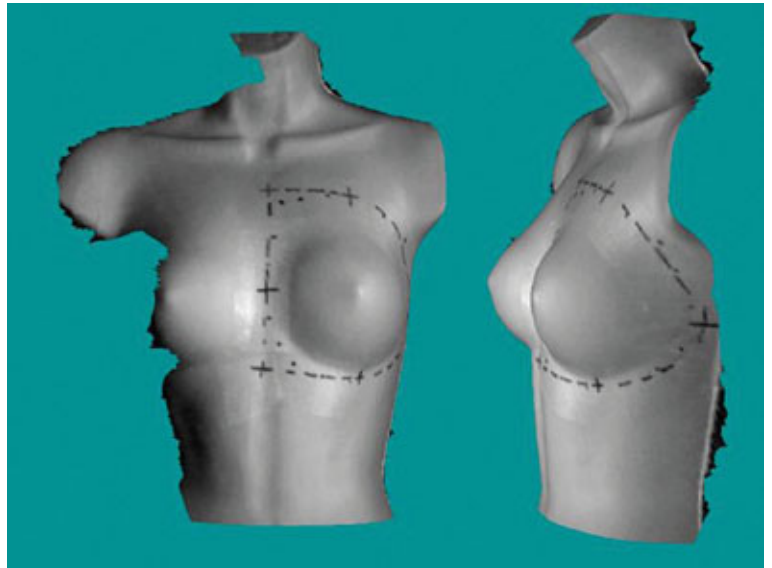


FIGURE 1. Anterior (left) and lateral (right) views of 3D surface images of the target left-sided breast using a 3D surface camera. With permission.²⁷

Using markers for motion monitoring in breast cancer, Kinoshita *et al.* showed the median range of respiratory motion is 1.0 ± 0.6 mm, 1.3 ± 0.5 mm, and 2.6 ± 1.4 mm for the RL, CC, and AP directions, respectively. The range of motion was the largest in the AP direction in all cases.^{23,36-38} In a work by Korreman *et al.*, it was reported that variability in motion patterns for target and surrogate using an internally placed gold marker and a reflective marker implanted on the chest wall can be considerable.^{39,40} However, the difference between the surrogate marker position and the real tumor position in breast cancer is not a shortcoming as of other organs, mainly due to a good correlation between tumor displacement and that of the markers.

While fiducial markers find a wide range of applications in breast cancer due to the existing well signal correlation between tumor site and marker location, their usage is hampered by (1) the invasive nature of marker implantation, (2) possible displacement of the markers even more than few millimeters for tumor volumes far from the skin, (3) lack of volumetric information about anatomy deformations close to organ-at-risks (OARs), and (4) ionizing radiation imaging needed to localize them. Marker displacement from the implanted place, tumor deformation, and tumefaction of surrounding tissues are common reasons leading to such positional error^{41,42} Artifacts in computed tomography (CT) images caused by high-Z fiducial markers are also problematic.⁴³ Electromagnetic

transducers/transponders (ET) are alternatives to high-Z internal markers providing continuous real-time 3D localization of the target without radiation imaging.²⁶ The Calypso system detects the fiducial marker location in real-time without X-ray imaging.⁴⁴ Commonly, three transponders with a variety of resonance frequencies (300-500 kHz) are placed in or close to the tumor. While the implementation techniques for ET are feasible and safe, they cannot be standalone. Several works indicate that interfractional variations of transponder location are significant and therefore hybrid real-time monitoring, for example, real-time tumor tracking is recommended.^{45,46}

4D CT imaging

4D CT provides a high spatial and temporal resolution image of the thorax region during the planning phase to construct the breathing modeling used for managing respiration-induced motion. In other words, 4D CT enables 4D treatment planning. In 4D CT, the respiration cycle is first monitored by an external indicator such as real-time position management (RPM) system followed by dividing the cycle into several gates. Richter *et al.* showed motion amplitude of the chest in the 4D CT scanning is about 1.8 ± 0.9 mm and target coverage was decreased by $< 5\%$, caused by breathing motion.⁴⁷ 4D CT imaging/respiratory-correlated CT procedure is a promising solution for obtaining a time-resolved CT image at the cost of a substantial increase in radiation dose.⁴⁸⁻⁵³

Chan *et al.* showed a better estimation of the real amount of heart in the radiation field is possible using 4D CT imaging of the patient with breast cancer.⁵⁴ Qi *et al.* assessed respiration-induced heart motion by proposing two indices, the maximum heart depth (MHD) and the depth of the left ascending aorta (DLAD) extracted from the 4D CT dataset. They showed the dosimetric variation of the heart is highly correlated with these two metrics in gated RT for the left-sided breast cancer. Larger respiration-induced heart displacements (nearly 1 cm) are observed based on 4D CT scans. Also, a mean maximal dose to the left ventricle reduced from 49.14 (3D conformal RT (CRT)) to 33.97 Gy (intensity-modulated RT (IMRT)) when 4D CT imaging is used. The findings illustrated the potential use of 4D CT-based planning for cardiac sparing.²¹ In a similar work, Yue *et al.* showed the changes (the difference between 4D and conventional plans) in D95, D90, V100, V95, and V90 of the target volume were -5.4%, -3.1%, -13.4%, -5.1%, and

-3.2%, respectively.¹² In addition, V100 decreases from 81.8% in the conventional plan to 74.9% in 4D CT-based planning.¹² For evaluating cardiac sparing in tangential breast IMRT, Mahmoudzadeh *et al.* modeled the breathing-induced motion with deformable registration using 4D CT imaging in RT simulation in order to calculate accumulated heart dose for robust optimized and clinical plans.⁵⁵ Compared to the regular CT, the main drawback of 4D CT imaging for RT is the added radiation dose to the patient. The extra dose from the 4D CT imaging can be compensated by a substantial reduction of the RT dose to the OARs.⁵⁵

4D and cine MR imaging

Recently, 4D magnetic resonance imaging (MRI) has been used to estimate respiratory motion variations and as a procedure to complement and support 4D CT enabling 4D RT planning and simulation.⁵⁶ Owing to superior soft-tissue contrast and radiation-free imaging features, MRI allows frequent multiple data acquisitions than CT. Due to limited time resolution associated with true 4D MRI, 2D cine-MRI is suggested.⁵⁷ Individualization of planning target volume (PTV) margin based on cine MRI data in the simulation seems to be a promising solution for the intrafractional motion problem.⁵⁸ Respiratory-correlated 4D MRI has attained more interest as an alternative to 4D CT for the measurement of respiratory motion.⁵⁹ Cai *et al.* presented the feasibility of 4D MRI using an image-based respiratory surrogate in the planning phase.⁶⁰ They investigated the accuracy of 4D MRI for motion measurement using 4D phantoms, for example, XCAT in terms of stability. Moreover, motion tracks can be estimated based on 4D MRI and 2D cine-MRI with an acceptable difference in motion amplitude up to -0.3 ± 0.5 mm.⁶⁰ 4D MRI provides an estimation of the respiratory motion for the two human subjects as much as 0.88 and 1.32 cm.⁶⁰ Also, Hu *et al.* showed a respiratory amplitude-based system to guide 4D MRI image acquisition is more robust to control irregular breathing compared to phase-based ones.⁶¹

Oar *et al.* performed a comparison between 4D CT and 4D MRI data quality based on the amplitude of motion in abdominal RT planning.⁵² Motion uncertainty due to respiratory was estimated to be less than 0.2 mm in both the 4D CT and the ground truth; the median amplitude of motion was 11.2 mm and 10.1 mm for 4D CT and 4D MRI, respectively.⁶² Paganelli *et al.* showed that the 4D MRI sequence enables describing organ motion and re-

duction of safety margins in RT planning.⁶³ Hurst *et al.* developed and optimized 4D MRI based on respiratory triggering using an external surrogate for abdominal tumors.⁶⁴ They concluded that any irregularity in patient breathing significantly affects 4D MRI performance. In addition, irregular and slow breathing rates deteriorate 4D MRI efficiency. A limitation of 4D MRI is, however, being sensitive to the change of breathing pattern between the preparation and acquisition periods. In addition, low temporal resolution is another limiting factor resulting in frequent scanner halts when breathing is irregular.⁶¹ Long scan time is also uncomfortable for the patients. However, a reduction in acquisition time in a high field 4D MRI scanner is expected.⁶⁴

Gantry-mounted X-ray imaging

Gantry-mounted X-ray imaging refers to those X-ray imaging modalities mounted on the treatment gantry allowing monoscopic and stereoscopic X-ray imaging. Portal imaging using electronic portal imaging devices (EPID) is a popular example of gantry-mounted imaging. Beam's eye view (BEV) portal imaging also enables real-time target motion tracking. Portal imaging is acquired with the help of the therapeutic megavoltage (MV) beam. Recently, gantry-mounted kV X-ray radiographic/fluoroscopic imaging is also available by either kV X-ray tubes or reduction of linac beam energy from MV to kV ranges.⁴⁷ The Vero, ExcaTrac, and CyberKnife systems offer stereoscopic imaging using two kV sources coupled with two flat-panel detectors.²⁶

The acquisition of portal imaging is proved to be fast as well as easy to use in order to measure patient movement during breast cancer RT.⁶⁵ Richer *et al.* presented that tracking breast motion in EPID results in patient-specific maximum motion amplitude of from 0.8 to 2.2 mm, 1.5 mm on average.²⁵ In another work, respiratory motion during daily treatment on the CLD was investigated by EPID. The results of their work showed that intrafractional variation in each patient during treatment day was minimal. The daily maximum range for any patient was 0.25 cm.¹⁷ For evaluating intrafractional and interfractional motion in breast cancer RT using EPID, Kron *et al.* concluded that the largest variation is in the CC direction with 1.3 ± 0.4 mm and 2.6 ± 1.3 mm for intrafractional and interfractional motions, respectively.⁶⁵ In a recent study based upon stereoscopic imaging enabled by the Cyberknife machine, Hoekstra *et al.* evaluated the effect of baseline and breathing motion on

PTV margins for accelerated PBI (APBI) irradiation. They showed that the PTV margin depends on the treatment time.⁶⁶ However, poor image quality because of dominant Compton scattering in MV beams remains a major problem in portal imaging. Furthermore, according to the AAPM Task Group 75 report, a significant disadvantage of kV imaging-based motion monitoring is the extra dose to the patient, particularly at the skin surface.⁶⁷ Depending on the imaging technique, a typical dose of 1–3 mGy per image is delivered in any kV imaging.²⁶

Ultrasound imaging

Rapid imaging along with no ionizing radiation makes ultrasound (US) imaging suitable for estimating intrafractional motion during the planning and simulation phases. The real-time US is also of interest in breast imaging mainly due to the lack of bony structures and also easy accessibility of the organ.^{26,68} 4D US provides almost real-time 3D rendered image data and is considered as a basis of multidimensional imaging of the breast.⁶⁸ In addition, 3D/4D US of the breast provides diagnostic information of the coronal plane.⁶⁸

US imaging typically provides good soft-tissue contrast and therefore allows contouring breast tumors. Furthermore, imaging artifact limits the application of real-time US imaging.⁶⁸⁻⁷⁰ Because of its manual operation, the image quality is also user-dependent as well.⁶⁸ Despite well-established applications of US in diagnostics, target delineation, and pre-treatment localization, the use of real-time US imaging for intrafractional motion estimation and mitigation for breast cancer is limited and there is no commercially available system. The only commercial US system is Clarity Autoscan (Elekta) for monitoring intrafractional motion²⁶ that is approved specifically for prostate and/or prostate bed RT. However, Wong *et al.* applied the Clarity system to breast imaging to evaluate the error between the Clarity and pre-treatment CT images and observed that the errors are clinically insignificant.⁷¹ However, in the era of surface imaging, the US methods cannot hold great advantages over ultrasound techniques for estimating breast intrafractional motion.⁷²

Motion mitigation techniques in breast cancer RT

In the previous section, the main motion monitoring techniques of breast target were presented. The

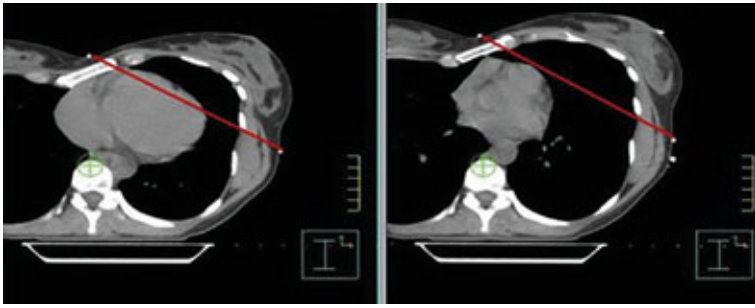


FIGURE 2. Heart position on axial CT slices of the same patient with breast cancer at free-breathing (left) and deep-inspiration breath-hold (DIBH) (right). The red line indicates the tangential treatment field border for whole-breast irradiation (WBI). With permission.⁷⁵

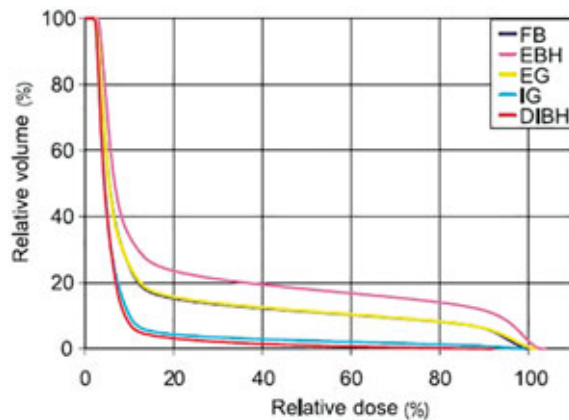


FIGURE 3. Comparison of whole heart dose-volume histogram in breathing adaptive radiotherapy for the same left-sided breast cancer patient for free-breathing (FB), end-expiration breath-hold (EBH), end-expiration gating (EG), end inspiration gating (IG), and DIBH plans. With permission.⁷⁶

next step in the RT workflow is to assist the irradiation of mobile targets with motion monitoring data. Common irradiation approaches addressing the respiration-induced intrafractional motion in breast cancer treatment include breath-hold, respiratory gating, and real-time tumor tracking techniques. The influence of intrafractional target motion is of particular concern in APBI due to high doses per fraction, particularly for target volumes close to inhomogeneities (*i.e.*, skin or chest wall).^{73,33} Therefore, motion mitigation techniques have to be perused in such treatment options.

Breath-hold

Breath-hold techniques refer to the management of target motion from the patient side. The deep-

inspiration breath-hold (DIBH) method is a practical and easy-to-use solution for breast cancer RT.⁶ During inhalation, the diaphragm moves the heart posteriorly and inferiorly away from the breast leading to a potential reduction of both heart and lung toxicities.¹⁶ As illustrated in Figures 2 and 3, the major role of DIBH in motion-addressed breast cancer RT is increasing the distance between tumor volume and the heart leading to less dose to the heart and therefore a lower rate of toxicity.⁷⁴⁻⁷⁶ DIBH is always linked to the beam gating to repeatedly on and off the irradiation beam based upon the patient respiratory cycle.

The DIBH for breast cancer RT is mostly employed in two manners: (1) moderate DIBH and (2) voluntary DIBH (vDIBH).^{76,77} The former is also known as active breathing control (ABC) in the literature.⁷⁹ ABC uses special devices to control airflow during the respiratory cycle^{77,78}, while in vDIBH the patient is partially freely breathing. A decrease in the mean heart dose and the left artery dose to about 67% and 73%, respectively, is observed when using the ABC for breast cancer RT.⁷⁶ In addition, the ABC devices allow a reduction in setup uncertainties to less than 2 mm.⁷⁶ The vDIBH is sometimes used in conjunction with respiratory motion monitoring to capture breath function at certain points in the breathing period. As for the ABC, the vDIBH decreases the time for RT simulation and daily setup.^{76,79} In contrast to ABC, vDIBH offers more patient comfort while it is also inexpensive.^{75,79} Recently, the DIBH treatment using volumetric-modulated arc therapy (VMAT) is utilized for a patient with the left-sided breast cancer to irradiate both whole breast and regional node with superior target coverage and good cardiac sparing.^{80,81}

Fassi *et al.* investigated target position reproducibility in the left-sided breast irradiation with DIBH using multiple optical control points. They compared the performance of optical surface imaging with that of the RPM-based methods and showed that the use of multiple surface fiducials leads to improved target and surface reproducibility.⁸² Betgen *et al.* reported a systematic interfractional translation up to 5 mm and intrafractional errors of about 1.4 mm during voluntary DIBH using 3D surface imaging in patients with the left-sided breast cancer.⁸³ Borst *et al.* quantified the influence of breathing with DIBH in breast cancer RT. The percentage of the left ventricle (LV) irradiated volume was 28% and 71% for DIBH and free-breathing (FB), respectively.⁸⁴

Respiratory gating

An efficient method of dealing with moving targets is to gate the radiation field. Respiratory gating refers to the management of target motion during treatment by rapid beam switching within the breathing cycle synchronized with an internal/external tracking system. Respiratory gating is usually implemented in two fashions: phase-based and amplitude-based gating. The former is accomplished by defining a set of phases (gates) over a complete breathing cycle. The irradiation beam is on in only one or few gates. In contrast, the latter is performed by setting a threshold value on the amplitude of the respiratory signal. Once the respiration signal falls below the predefined threshold, the irradiation beam is on. In a small gating window, the phase-based gating method can result in missing the tumor caused by interfractional position variations.

In contrast to the DIBH, the patient freely breathes while being irradiated with the therapeutic beam in respiratory-gated RT. Therefore, more patient comfort is obtained with respiratory gating.^{85,86} Korreman *et al.* highlighted the dosimetric advantages of free-breathing gated breast cancer RT over vDIBH in terms of cardiopulmonary dose sparing.⁷³ Giraud *et al.* conducted a multicenter prospective study to compare respiratory-gated RT with conventional CRT for patients with breast cancer. They observed a significant reduction in lungs and cardiac toxicities when using the respiratory gating method.⁸⁷ Also, Qi *et al.* reported that the median heart volume receiving at least 50% of the maximum dose was decreased from 19.2% for free-breathing to 2.8% for end-inspiration gating. A substantial coronary artery volume sparing patients with the left-sided breast cancer was also observed. In addition, for both the right- and left-sided breast cancers, the median lung volume receiving 50% of the prescribed target dose reduced from 45.6% for free-breathing to 29.5% for inspiration gating.²¹

Respiratory gating results in two clinical benefits: (1) acceptable levels of target dose conformity and (2) OARs/normal tissues sparing. There are, however, several challenges associated with respiratory gating mandating further researches. First, time latency at the gating process has a result in underdosage and overdosage of proximal tissue. Thus, a successful gating process needs to minimize time latency during the gating window. Another challenge is a long treatment time by respiratory gating. The longer treatment time is in-

convenient for the patients and can result in respiratory pattern variation, such as shift motion.³¹ Another noticeable challenge for gated IMRT delivery is an increase in delivery time. The low efficiency of gated IMRT, as a product of the IMRT efficiency (20% to 30%) and the gating duty cycle (20% to 30%), results in a 10 to 25-fold increase in delivery time than conventional CRT treatments.⁸⁸

To obtain benefits of the respiratory gating method, higher temporal resolution, higher soft-tissue contrast, and lower radiation exposure imaging techniques in the RT planning are mandated.⁶⁷ In some cases, however, motion occurs within the gate window, called residual motion.⁸⁸ Therefore, there is always a compromise between the amount of residual motion and the duty cycle to search for optimal gating parameters.⁸⁹ As heart dose automatically leads to an increase in cardiac mortality⁹⁰, a key question in respiratory gating is, therefore, the selection of optimal gating window parameters. Many studies have proved that the end of inspiration is optimal in terms of heart and lung tissue sparing in the left-sided breast cancer RT.^{74,21} While the absolute lung volume irradiated is largest in respiratory-gated breast RT, the relative lung volume is smallest in the inspiration phases. Thus, the inspiration phases are optimal for beam gating in breast cancer RT by providing the longest distance between the breast and heart and also minimizing the lung density.⁷⁴ Although not implemented yet, respiratory gating based on the data from real-time cine MRI data would be a solution for online motion mitigation.

Real-time tumor tracking

Real-time tumor tracking is generally performed by either robotic radiosurgery, dynamic multi-leaf collimators (DMLCs), or couch movement.⁹¹ Owing to the benefits of stereotactic body RT (SBRT), Cyberknife APBI can be considered as a real-time tumor tracking mitigating the intrafractional respiratory motion.⁹² Methods like kV/MV radiographic imaging with and without markers, US imaging, portal imaging through EPID, kV/MV imaging are real-time tumor tracking methods. A combination of imaging methods with DMLCs (called dynamic IMRT) results in a solution for real-time tumor tracking.⁹³

In breast cancer RT, real-time tumor tracking results in a substantial reduction in the volume of the heart receiving a high radiation dose.^{93,94} Continues portal imaging during RT has shown promising results for estimating intrafractional chest wall mo-

tion of patients with breast cancer by providing time-resolved visualization of the internal organ from BEV.⁹⁵ As an estimate, Hijal *et al.* showed the irradiated volume of the heart of 30 Gy (V30) is 0.03% and 1.14%, and the mean heart dose is 1.35 Gy and 2.22 Gy, for real-time 3D CRT and static 3D CRT, respectively.⁹⁶ Leonardo *et al.* showed that real-time tumor tracking leads to significant heart sparing in a prone position in APBI and provides a daily precision treatment while reducing clinical target volume (CTV) to PTV margin.⁹³ In addition, in patients with abnormal anatomies as the significant volume of the heart may be irradiated, real-time tumor tracking would be useful to avoid extreme doses.⁹⁷

MLC tracking has been successfully performed for IMRT and VMAT deliveries to address intra-fractional target motion.⁹⁸⁻¹⁰⁰ Dynamic IMRT enables dynamically reshaping the treatment field in the BEV based on the actually recorded target motion.¹⁰¹ Furthermore, real-time tumor tracking with IMRT delivery resulted in better cardiopulmonary sparing and improved target coverage for breast cancer treatment.^{102,103} While the dynamic IMRT provides a highly conformal dose distribution, it is usually challenged by the interplay effect that occurs in the time between leaf and the target motions. The interplay effect automatically leads to motion artifacts in dose distributions.^{104,105} Synchronization of real-time tumor tracking based on two sets of fluoroscopy and IMRT delivery is also feasible but at the expense of non-negligible skin surface dose.¹⁰⁶ Real-time tumor tracking could also result in a percentage depth dose of 58% (at 5 cm) of the peak dose for long IMRT treatments.²⁶ In SGRT-based tumor tracking, beam-on and beam-off delays might play a role and vary between the SGRT system and beam delivery.²⁶ Smaller PTV margins are usually appropriate for patients with breast cancer who are actively monitored with surface imaging during RT.¹⁰⁷ Hamming *et al.* showed that SGRT data correlated well with CBCT data in patients with breast cancer.¹⁰⁸ In their study, the left-sided breast cancer was monitored continuously to maintain positional errors within 5 mm with SGRT.¹⁰⁸ The combination of real-time surface-guided DIBH is also successfully implemented in patients with breast cancer, resulting in a reliable and stable DIBH treatment.¹⁰⁹

However, some concerns associated with real-time tumor tracking are the resource-intensive nature of delivery and also imposing the amount of additional radiation dose.¹¹⁰ According to the Report of AAPM Task Group 75⁶⁷, a typical in-

room kV cone-beam CT of the chest (commonly used in the case of breast cancer RT) leads to a maximum skin dose of 85.4 mGy. Real-time CBCT breast imaging results in a dose of 2 mGy and 12 mGy per scan for the right- and left-sided breast cancers, respectively.¹¹⁰ Liu *et al.* showed that using 4D CBCT, PTV margin would be substantially reduced compared to kV CBCT treatments.¹¹¹ Real-time imaging during treatment increases RT irradiation time while the patient lies on the couch.⁶⁷ Real-time tumor tracking increases the complexity of the radiotherapy planning and delivery process, mandating rigid quality assurance at every level for precision and safe treatment.¹⁰¹ Furthermore, the time delay between the real tumor position and the beam positioning system is a major challenge in real-time tumor tracking.¹⁶ Besides, cycle-to-cycle fluctuations in the breathing cycle of the patient add complexity to the problem to some extent.¹¹² However, adaptive filter algorithms are proposed to predict tumor position in advance.¹¹³

The choice between prone and supine positions

Patient positioning (*i.e.*, supine or prone positions) plays a considerable role in motion mitigation techniques in patients with breast cancer.¹¹⁴ Prone position refers to hanging the breast tissue under its weight through a hole at the bottom of the couch. Prone position improves separation between tumor and OARs as heart and lung for some patients. In addition, the prone position results in fewer respiration movements when compared to the supine position. Furthermore, some prone boards allow regional node irradiation, as well. However, the prone positioning is dependent on the position of the original tumor. In addition, patient setup variations can be significantly larger in prone positioning resulting in an increased interfractional variation.¹¹⁵ In contrast, supine positioning is more common for staff and ease of setup. It can match nodal field to chest wall fields if this requires. Nonetheless, there is a lack of skin-sparing in women with large or pendulous breasts. Therefore, breast support by other devices is sometimes required to anteriorly position the breast away from the heart, lung, and abdomen. Referring to Figure 4, it is proven that the prone setup is more optimal for sparing lung volume compared to the supine position.^{115,116}

Because of a significant decrease in irradiated lung volume and even irradiated heart volume in 87% of all patients with the left-sided breast cancer, the prone position outperforms the supine

setup by exhibiting improved dose homogeneity and fewer toxicities. Morrow *et al.* showed that the respiratory motion of the chest wall substantially decreases from 2.3 ± 0.9 mm to -0.1 ± 0.4 mm in supine and prone positions, respectively. They also showed that the prone positioning of patients for breast irradiation reduces the error introduced by intrafractional respiratory motion.¹¹⁶ Veldeman *et al.* reported the 2-year better cosmetic outcome of prone positioning in comparison with supine positioning in large-breast patients.¹¹⁷ To summarize, while supine positioning is the ease of setup, it is suboptimal in terms of lung and heart doses in some cases.¹¹⁷

Target motion considerations in particle therapy

Particle therapy offers promising treatment outcomes and efforts have been continued to become a mature method for breast cancer treatment. Particle therapy commonly refers to the use of light/heavy charged particles such as protons, carbon-ions and helium-ions for cancer treatment. While active scanning and intensity-modulated proton therapy (IMPT) have become increasingly used in proton therapy, a great number of clinical researches are still published in passive scattering particle therapy (PSPT).^{10,118} Compared to photon beam RT, particle beams are more sensitive to in-line geometrical and density changes.^{32,37,119} It is because of the particle interaction mechanism inside of the body.³² In the monitoring of target motion benefiting from implanted surrogates, the high-Z internal markers can significantly alter dose distribution in particle therapy, and therefore thin (less than 0.5 mm in thickness) and low-Z materials, such as carbon-coated zirconium oxide clips, are preferred.¹²⁰ The degree of such an impact on charged particle dose distribution depends on the marker material, its position in the treatment field, and its thickness.¹²⁰ Similarly, Landry *et al.* showed that electromagnetic monitoring suffers from substantial distortions which bounded their utilization in a particle therapy.¹²¹

Breath-hold particle therapy is also an intrafractional motion mitigation technique in breast patients. However, in spot scanning beam delivery, the breath-hold technique cannot significantly reduce the heart dose mainly due to the so-called interplay effect.^{5,6} Respiratory gating is also successfully translated into particle therapy to address the problem of the mobile target in breast cancer treat-

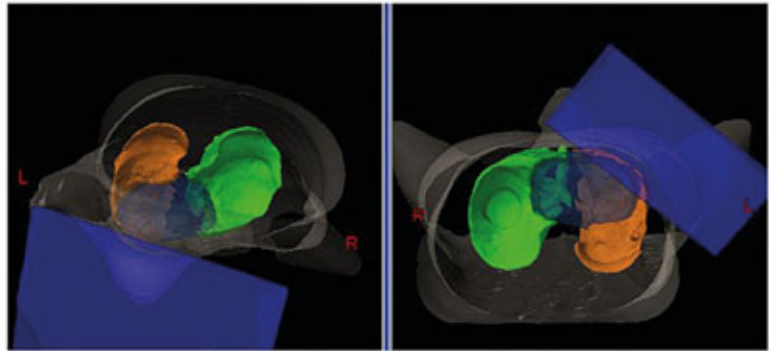


FIGURE 4. Comparison of cardiac sparing in prone (left) and supine (right) positions. The virtual blue box illustrates the in-field volume of the heart and lung by the Eclipse TPS. With permission.¹¹⁵

ment.³⁷ Respiratory gating can be considered as a direct solution to the problem of dose degradation due to target motion as well as less dependency on the properties of the irradiation system. Similar to photon beams, respiratory gating for particle therapy faces two major challenges: (1) time latency that leads to over- and underdosage of the tumor and nearby tissues and (2) treatment prolongation that causes respiratory pattern variation.^{32,122}

Intrafractional target motion management in active scanning particle therapy is hampered by the interplay effect. The interplay effect (interplay between intrafractional target motion and the beam spot position) is however approached by a new generation of particle accelerators, called Cyclinacs, enabling 4D spot scanning in particle therapy.¹²³ In a comparative study by Flejmer *et al.*, respiratory gating proton therapy resulted in a reduction factor of 1.6 (from 0.5 Gy(relative biological effectiveness (RBE)) to 0.3 Gy(RBE)) in mean heart dose in the left-sided breast cancer compared to free-breathing proton therapy.¹²⁴ Siebenthal *et al.* studied the translation of 4D MRI from conventional RT to particle therapy to evaluate motion sensitivity and assess the residual motion under different gating techniques.¹²⁵

Patel *et al.* compared the dosimetric performance of photon and proton deliveries with and without DIBH.¹²⁶ They showed passively scattered proton beam delivery without DIBH results in slightly superior performance compared to the pencil-beam scanning during DBIH in terms of key metrics for avoidance structures. This is probably due to the interplay effect that exists in scanning deliveries. Another key conclusion of their study is that the cardiopulmonary toxicities in motion-managed particle therapy are not as high as those of photon therapy in breast cancer treatment. In another com-

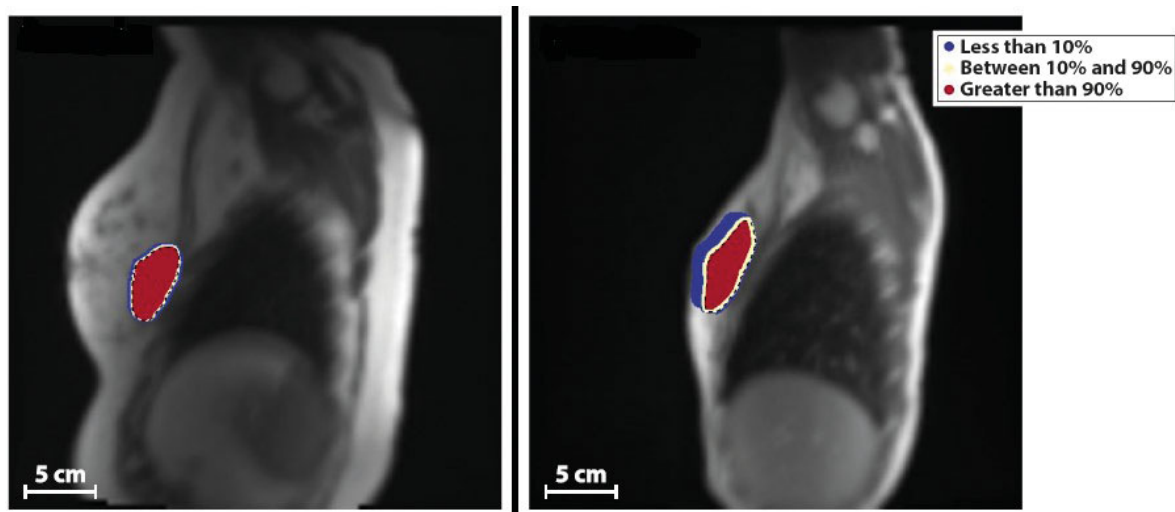


FIGURE 5. Heat map of fractional time that the surgical cavity occupies a given position during the MR-guided accelerated partial-breast irradiation (APBI) for two different patients with small (left) and large (right) displacements during the treatment delivery. With permission.¹⁵⁸

parative study, Mondal *et al.* observed a significant dose reduction with proton DIBH compared to photon DIBH in terms of cardiac and pulmonary toxicities for WBI.¹²⁷

The real-time tumor tracking approach for particle therapy is not well clinically available when compared to advance in-room imaging techniques in conventional photon beam therapy. Since particle therapy is much more sensitive to target motion when compared to conventional photon therapy, a combination of several motion mitigation techniques would be most beneficial.¹²⁸ Though most studies are centered on WBI, the influence of target size, location, breast size, and breathing cycle period is not well understood in APBI with particle beams. The effectiveness of respiratory gating for intrafractional target motion management for left-sided proton APBI needs to be also investigated. In addition, studies should be conducted to assess the impact of prone *versus* supine positions on the therapeutic outcome in terms of cardiopulmonary sparing, especially for thick or pendulous breasts.

Future directions

MRI guidance

MRI guidance is considered the future of image-guided RT (IGRT).¹²⁹ Real-time MR imaging is also safe in terms of radiation doses.¹³⁰ The state-of-the-art MR-linac integration in SBRT can provide tracking of the respiratory motion during the treatment

fraction. A present limitation of an integrated MR-RT gantry is the high installation cost that limits its use in clinical practices. Acharya *et al.* determined intrafractional motion and evaluated delivered dose *versus* planned dose.¹³¹ They demonstrated the mean difference of less than 1% between the planned and delivered dose using MR guidance for APBI delivery (Figure 5). They showed that a reduction in the PTV margin leads to a significant reduction in V50 and V100 for ipsilateral breast cancer MR-guided RT. When no additional PTV margin is applied, the mean cavity displacement in the AP and SI directions reaches 0.6 mm.¹³¹

Nachbar *et al.* in 2019, studied first-in-human APBI performed at a 1.5 T MR-linac for breast cancer using 7-beam IMRT delivery. Additionally, they have also investigated the influence of interactions of the secondary electrons with magnetic field on out-of-field dose.¹³² Individualization of PTV margin based on cine MRI data from the simulation is also a possible motion mitigation method.¹³³ Although not yet implemented, real-time cine MRI-based beam gating seems also to be a promising solution.¹³³ Despite several advantages of MRI guidance, an open question, however, is a dose uncertainty observed in air-tissue interfaces where secondary electrons slightly contribute to total proton dose delivery.¹³³ Electron return and electron stream effects are two main concerns in treatment planning for a hybrid MR-linac delivery.¹³³ Although some existing challenges such as the selection of suitable coils and the above issues for breast cancer remain,

the first breast cancer was successfully treated with a hybrid MR-linac machine using an APBI technique.¹³³ Additionally, the magnetic field has a little negative impact on skin dose in APBI relative to WBI due to the use of smaller fields.¹³⁴

Artificial intelligence in 4D RT

Artificial intelligence (AI) offers a set of key applications in RT workflow, including image segmentation (target and OAR delineation), image registration, radiomics, treatment response assessment/prediction, and tumor tracking. An interesting study showed that using single radiography, a whole 4D data is feasible to predict tumor movement during the treatment fraction using a deep convolutional neural network (DCNN).^{135,136} Another role of AI in 4D RT is to create synthetic 4D CT from the 4D MRI dataset in MR-only treatment planning.¹³⁵ Chen *et al.* pointed out the usefulness of a deep U-net-based approach that synthesizes on-treatment CT-like images with accurate numbers from both planning CT and on-treatment CBCT. Based on their results, the proposed U-net can increase the accuracy of the CT number of CBCT, which makes possible further quantitative tools of CBCT, such as dose calculation and adaptive treatment planning.¹³⁷ The uses of AI in dynamic/4D breast imaging, image registration, and automatic cancer diagnosis are attracting a lot of attention.¹³⁸⁻¹⁴⁰

Rescanning for particle therapy

The rescanning (repainting) approach is proved to be effective in managing motion-induced dose uncertainty in actively scanned particle therapy to address the interplay effect.¹⁴¹ However, some repainting methods mandate monitoring patient breathing to provide respiration parameters like period and rate.¹⁴² For large target movements (> 5 mm), a combination of the repainting techniques with, for example, respiratory gating and breath-hold techniques lead to a superior outcome in terms of target dose uniformity. It should be mentioned that repainting techniques do not eliminate the use of safety margins entirely covering the target along with its movement extent. A potential pitfall of the repainting approach is a significant increase in total irradiation time.¹⁴²⁻¹⁴⁴ Figure 6 shows the respiratory-correlated layered repainting method.³² An iso-energy layer is irradiated in the gating window. The gating window is then divided into three portions, and therefore the number of rescanning is three.³² While this method is proposed to be applied

for lung cancer, its usefulness and applications in APBI are sparse and mandate extra researches.

Robust treatment planning

The term “robust treatment planning” refers to the incorporation of CTV-to-PTV margins into the optimization function during inverse treatment planning in IMRT techniques. The concept of robust treatment planning for breast cancer IMRT is utilized via RayStation TPS, as the sole TPS supporting robust optimization for IMRT.^{54,145-147} Though, studies are shown that internal margin (IM) cannot be entirely eliminated in robust treatment planning.⁵³ Due to some uncertainties in particle therapy, for example, range uncertainty, the definition of simple PTV in particle therapy is suboptimal. Therefore, the role of robust optimization is to effectively address the tumor motion and uncertainties in RT, particularly in particle therapy.¹⁴⁵ Robust planning using VMAT delivery for a moving target in the breast generated clinically acceptable plans and was confirmed by real patient CBCT data.¹⁴⁷ Not directly applied for intrafractional motion management, the robust optimization for intensity-modulated proton therapy was used to address residual setup errors.¹⁴⁸

Ultra high dose rate (FLASH) radiotherapy

FLASH-RT refers to ultra high dose RT with treatment time shorter than 0.1 s enabling excellent intrafractional motion management.¹⁴⁹ While maintaining local tumor control, FLASH-RT reduces normal tissue toxicity. Despite few clinical devices with the capability to deliver ultra-high dose rates, a lot of preclinical studies confirm the effectiveness of this paradigm-shifting technique.¹⁵⁰ In 2019, the first patient with T-cell lymphoma was successfully treated using FLASH-RT with the superior outcome on normal skin and the tumor.¹⁵¹ Despite some technical challenges ahead, the combination of proton therapy (superior conformity) and FLASH-RT (shorter treatment time) can be a viable option for the treatment of breast cancer considering the intrafractional movements.

Conclusions

In this review, a comprehensive overview of the current and the state-of-the-art intrafractional target motion management in breast cancer RT was presented. Particularly, target motion considera-

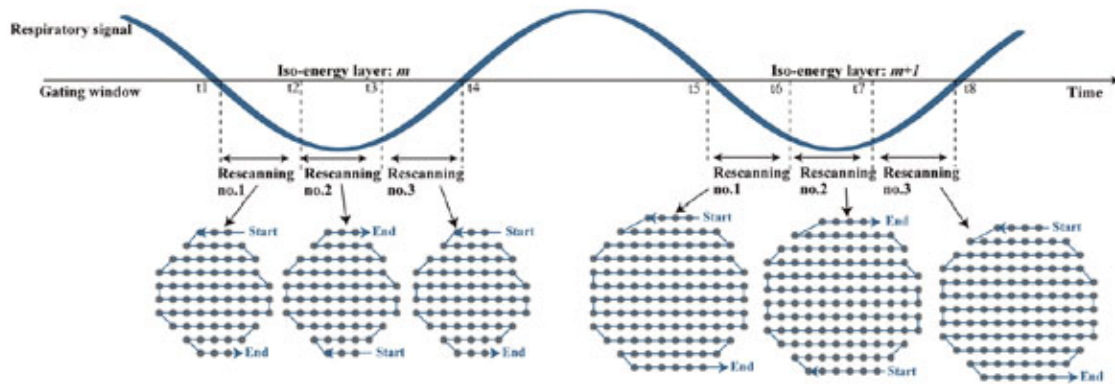


FIGURE 6. Schematics of iso-layered repainting in active scanning particle therapy. Three rescanning is applied within each respiration cycle. The middle rescanning (no. 2) has a reverse scheme as the scanning starts from the bottom and ends at the top. With permission.³³

tion for particle therapy for breast cancer is highlighted. Several techniques available for monitoring intrafractional target movements such as surface imaging, kV/MV imaging with and without markers, 4D CT, 4D MRI, and the real-time US are discussed. Future perspectives for mitigating intrafractional motion, for example, MR guidance, and FLASH-RT are also highlighted. Almost all of the available remedies are directly applicable to breast cancer, mainly since it is an easily accessible organ. However, the SGRT technique seems to be the dominant motion-managed RT strategy for breast cancer. The problem of intrafractional target motion is more challenging in particle therapy, and therefore further research and development efforts still need to be performed to take the full advantages of the presented methods and to address the open questions in technical and clinical issues related to irradiation of mobile targets seated in the breast.

References

- Lin YL. Reirradiation of recurrent breast cancer with proton beam therapy: a case report and literature review. *World J Clin Oncol* 2019; **10**: 256-68. doi: 10.5306/wjco.v10.i7.256
- Momenimovahed Z, Salehiniya H. Epidemiological characteristics of and risk factors for breast cancer in the world. *Breast Cancer (Dove Med Press)* 2019; **11**: 151-64. doi: 10.2147/BCTT.S176070
- The American Cancer Society. *Cancer facts and statistics*. [cited 2021 May 15]. Available at: <https://www.cancer.org/research/cancer-facts-statistics/>
- Bray F, Ferlay J, Soerjomataram I, Siegel RL, Torre LA, Jemal A. Global cancer statistics GLOBOCAN estimates of incidence and mortality worldwide for 36 cancers in 185 countries. *CA Cancer J Clin* 2018; **68**: 394-424. doi: 10.3322/caac.21492
- Kunheri B, Vijaykumar DK. *Management of early stage breast cancer*. Singapore: Springer Nature; 2021.
- Bellon JR, Wong JS, MacDonald SM, Ho AY. *Radiation therapy techniques and treatment planning for breast cancer*. 1st edition. Switzerland: Springer International Publishing; 2016.
- Fadavi P, Nafissi N, Mahdavi SR, Jafarnejadi B, Javadinia SA. Outcome of hypofractionated breast irradiation and intraoperative electron boost in early breast cancer: a randomized non-inferiority clinical trial. *Cancer Rep (Hoboken)* 2021; e1376. doi: 10.1002/cnr2.1376
- Haydaroglu A, Ozyigit G. *Principles and practice of modern radiotherapy techniques in breast cancer*. New York: Springer Science & Business Media; 2013.
- Lagerwaard FJ, Van Sornsens de Koste JR, Nijsen-Visser MR, Schuchhard-Schipper RH, Oei SS, Munne A, et al. Multiple "slow" CT scans for incorporating lung tumor mobility in radiotherapy planning. *Int J Radiat Oncol Biol Phys* 2001; **51**: 932-7. doi: 10.1016/S0360-3016(01)01716-3
- Mohan R, Grosshans D. Proton therapy – present and future. *Adv Drug Deliv Rev* 2016; **109**: 26-44. doi: 10.1016/j.addr.2016.11.006
- AAPM Report No. 91. *The management of respiratory motion in radiation oncology. Report of AAPM Task Group 76*. The American Association of Physicists in Medicine; 2006.
- Yue NJ, Li X, Beriwal S, Heron DE, Sontag MR, Saiful Huq M. The intrafraction motion-induced dosimetric impacts in breast 3D radiation treatment: a 4DCT based study. *Med Phys* 2007; **34**: 2789-800. doi: 10.1118/1.2739815
- De Rose F, Cozzi L, Meattini I, Fogliata A, Franceschini D, Franzese C, et al. The potential role of intensity-modulated proton therapy in the regional nodal irradiation of breast cancer: a treatment planning study. *Clin Oncol* 2020; **32**: 26-34. doi: 10.1016/j.clon.2019.07.016
- Reitz D, Carl G, Schönecker S, Pazos M, Freislederer P, Niyazi M, et al. Real-time intrafraction motion management in breast cancer radiotherapy: analysis of 2028 treatment sessions. *Radiat Oncol* 2018; **13**: 128. doi: 10.1186/s13014-018-1072-4
- George R, Keall PJ, Kini VR, Vedam SS, Siebers JV, Wu Q, et al. Quantifying the effect of intrafraction motion during breast IMRT planning and dose delivery. *Med Phys* 2003; **30**: 552-62. doi: 10.1118/1.1543151
- Keall PJ, Mageras GS, Balter JM, Emery RS, Forster KM, Jiang SB, et al. The management of respiratory motion in radiation oncology report of AAPM Task Group 76. *Med Phys* 2006; **33**: 3874-900. doi: 10.1118/1.2349696
- Smith RP, Bloch P, Harris EE, McDonough J, Sarkar A, Kassaei A, et al. Analysis of interfractional and intrafractional variation during tangential breast irradiation with an electronic portal imaging device. *Int J Radiat Oncol Biol Phys* 2005; **62**: 373-8. doi: 10.1016/j.ijrobp.2004.10.022
- Saliou MG, Giraud P, Simon L, Fournier-Bidoz N, Fouquet A, Dendal R, et al. Radiotherapy for breast cancer: respiratory and set-up uncertainties. *Cancer Radiother* 2005; **9**: 414-21. doi: 10.1016/j.canrad.2005.09.003

19. Böhmer D, Feyer P, Harder C, Korner M, Sternemann M, Dinges S, et al. Verification of set-up deviations in patients with breast cancer using portal imaging in clinical practice. *Strahlenther Onkol* 1998; **174**(Suppl 2): 36-9. PMID: 9810336.
20. Latifi K, Forster K, Harris E. Evaluation of fiducial marker migration and respiratory-induced motion for image-guided radiotherapy in whole breast irradiation. *Cancer Res* 2009; **69**(24 Suppl): 744S. doi: 10.1158/0008-5472.SABCS-09-4113
21. Qi XS, Hu A, Wang K, Newman F, Crosby M, Hu B, et al. Respiration induced heart motion and indications of gated delivery for left-sided breast irradiation. *Int J Radiat Oncol Biol Phys* 2012; **82**: 1605-11. doi: 10.1016/j.ijrobp.2011.01.042
22. Fein D, McGee KP, Schultheiss TE, Fowle BL, Hanks GE. Intrafraction and interfractional reproducibility of tangential breast fields: a prospective on-line portal imaging study. *Int J Radiat Oncol Biol Phys* 1996; **34**: 733-40. doi: 10.1016/0360-3016(95)02037-3
23. Kinoshita R, Shimizu S, Taguchi H, Katoh N, Fujino M, Onimaru R, et al. Three-dimensional intrafractional motion of breast during tangential breast irradiation monitored with high-sampling frequency using a real-time tumor-tracking radiotherapy system. *Int J Radiat Oncol Biol Phys* 2008; **70**: 931-4. doi: 10.1016/j.ijrobp.2007.10.003
24. Seppenwoolde Y, Shirato H, Kitamura K, Shimizu Sh, Van Herk M, Lebesque JV, et al. Precise and real-time measurement of 3D tumor motion in lung due to breathing and heartbeat, measured during radiotherapy. *Int J Radiat Oncol Biol Phys* 2002; **53**: 882-34. doi: 10.1016/s0360-3016(02)02803-1
25. Jones S, Fitzgerald R, Owen R, Ramsay J. Quantifying intra- and interfractional motion in breast radiotherapy. *J Med Radiat Sci* 2015; **62**: 40-6. doi: 10.1002/jmrs.61
26. Bertholet J, Knopf A, Eiben B, McClelland J, Grimwood A, Harris E, et al. Real-time intrafraction motion monitoring in external beam radiotherapy. *Phys Med Biol* 2019; **64**: 1-34. doi: 10.1088/1361-6560/ab2ba8
27. Djajaputra D, Li Sh. Real-time 3D surface-image-guided beam setup in radiotherapy of breast cancer. *Med Phys* 2005; **32**: 65-75. doi: 10.1118/1.1828251
28. Tang X, Zagar TM, Bair E, Jones EL, Fried D, Zhang L, et al. Clinical experience with 3-dimensional surface matching-based deep inspiration breath hold for left-sided breast cancer radiation therapy. *Pract Radiat Oncol* 2014; **4**: e151-8. doi: 10.1016/j.pro.2013.05.004
29. Ma Z, Zhang W, Su Y, Liu P, Pan Y, Zhang G, et al. Optical surface management system for patient positioning in interfractional breast cancer radiotherapy. *Biomed Res Int* 2018; **3**: 1-8. doi: 10.1155/2018/6415497
30. Hoisak JDP, Pawlicki T. The role of optical surface imaging systems in radiation therapy. *Semin Radiat Oncol* 2018; **28**: 185-93. doi: 10.1016/j.semradonc.2018.02.003
31. Freisleder P, Kügele M, Öllers M, Swinnen A, Sauer TO, Bert C, et al. Recent advances in surface guided radiation therapy. *Radiat Oncol* 2020; **15**: 187. doi: 10.1186/s13014-020-01629-w
32. Mori S, Knopf AC, Umegaki K. Motion management in particle therapy. *Med Phys* 2018; **45**: e994-e1010. doi: 10.1002/mp.12679
33. Quirk S, Conroy L, Smith WL. Accounting for respiratory motion in partial breast intensity modulated radiotherapy during treatment planning: A new patient selection metric. *Eur J Cancer* 2014; **50**: 1872-9. doi: 10.1016/j.ejca.2014.04.016
34. Yue NJ, Goyal Sh, Kim LH, Khan A, Haffty BG. Patterns of intrafractional motion and uncertainties of treatment setup reference systems in accelerated partial breast irradiation for right- and left-sided breast cancer. *Pract Radiat Oncol* 2014; **4**: 6-12. doi: 10.1016/j.pro.2012.12.003
35. Habermehl D, Henkner K, Ecker S, Jakel O, Debus J, Combs SE. Evaluation of different fiducial markers for image-guided radiotherapy and particle therapy. *J Radiat Res* 2013; **54**: 161-8. doi: 10.1093/jrr/rrt071
36. Spadea MF, Baroni G, Riboldi M, Tagaste B, Garibaldi C, Orecchia R, et al. Patient set-up verification by infrared optical localization and body surface sensing in breast radiation therapy. *Radiother Oncol* 2006; **79**: 170-8. doi: 10.1016/j.radonc.2006.02.011
37. Minohara S, Kanai T, Endo M, Noda K, Kanazawa M. Respiratory gated irradiation system for heavy-ion radiotherapy. *Int J Radiat Oncol Biol Phys* 2000; **47**: 1097-103. doi: 10.1016/S0360-3016(00)00524-1
38. Juhler Nøttrup T, Korreman SS, Pedersen AN, Aarup LR, Nystrom H, Olsen M, et al. Intrafraction and interfraction breathing variations during curative radiotherapy for lung cancer. *Radiother Oncol* 2007; **84**: 40-8. doi: 10.1016/j.radonc.2007.05.026
39. Korreman SS. Motion in radiotherapy: Photon therapy. *Phys Med Biol* 2012; **57**: R161-91. doi: 10.1088/0031-9155/57/23/R161
40. Bert C, Durante M. Motion in radiotherapy: particle therapy. *Phys Med Biol* 2011; **56**: R113-44. doi: 10.1088/0031-9155/56/16/R01
41. Shirato H, Suzuki K, Sharp GC, Fujita K, Onimaru R, Fujino M, et al. Speed and amplitude of lung tumor motion precisely detected in four-dimensional setup and in real-time tumor-tracking radiotherapy. *Int J Radiat Oncol Biol Phys* 2006; **64**: 1229-36. doi: 10.1016/j.ijrobp.2005.11.016
42. Nicholet AM, Brock KK, Lockwood GA, Moseley DJ, Rosewall T, Warde PR, et al. A magnetic resonance imaging study of prostate deformation relative to implanted gold fiducial markers. *Int J Radiat Oncol Biol Phys* 2007; **67**: 48-56. doi: 10.1016/j.ijrobp.2006.08.021
43. Schlosser J, Salisbury K, Hristov D. Telerobotic system concept for real-time soft tissue imaging during radiotherapy beam delivery. *Med Phys* 2010; **37**: 6357-67. doi: 10.1118/1.3515457
44. Balter JM, Wright JN, Newell LJ, Friemel B, Dimmer S, Cheng Y, et al. Accuracy of a wireless localization system for radiotherapy. *Int J Radiat Oncol Biol Phys* 2005; **61**: 933-7. doi: 10.1016/j.ijrobp.2004.11.009
45. Braide K, Lindencrona U, Welinder K, Götstedt J, Ståhl I, Pettersson N, et al. Clinical feasibility and positional stability of an implanted wired transmitter in a novel electromagnetic positioning system for prostate cancer radiotherapy. *Radiother Oncol* 2018; **128**: 336-42. doi: 10.1016/j.radonc.2018.05.031
46. Vanhanen A, Syrén H, Kapanen M. Localization accuracy of two electromagnetic tracking systems in prostate cancer radiotherapy: a comparison with fiducial marker based kilovoltage imaging. *Phys Med* 2018; **56**: 10-8. doi: 10.1016/j.ejmp.2018.11.007
47. Richter A, Sweeney R, Baier K, Flentje M, Guckenberger M. Effect of breathing motion in radiotherapy of breast cancer: 4D dose calculation and motion tracking via EPID. *Strahlenther Onkol* 2009; **185**: 425-30. doi: 10.1007/s00066-009-1980-1
48. Vedam SS, Kini VR, Keall PJ, Ramakrishnan V, Mohan R. Quantifying the predictability of diaphragm motion during respiration with a noninvasive external marker. *Med Phys* 2003; **30**: 505-13. doi: 10.1118/1.1558675
49. Ford EC, Mageras GS, Yorke E, Ling CC. Respiration-correlated spiral CT: a method of measuring respiratory-induced anatomic motion for radiation treatment planning. *Med Phys* 2003; **30**: 88-97. doi: 10.1118/1.1531177
50. Low DA, Nystrom M, Kalinin E, Parikh P, Dempsey JF, Bradley JD, et al. A method for the reconstruction of four-dimensional synchronized CT scans acquired during free breathing. *Med Phys* 2003; **30**: 1254-63. doi: 10.1118/1.1576230
51. Keall PJ, Starkschall G, Shukla H, Forster KM, Ortiz V, Stevens CW, et al. Acquiring 4D thoracic CT scans using a multislice helical method. *Phys Med Biol* 2004; **49**: 2053-67. doi: 10.1088/0031-9155/49/10/015
52. Rietze E, Chen GT, Doppke KP, Pan T, Choi NC, Willett CG. 4D computed tomography for treatment planning. *Int J Radiat Oncol Biol Phys* 2003; **57**: S232-3. doi: 10.1016/S0360-3016(03)01055-1
53. Ruysscher DD, Sterpin E, Hausermans K, Depuydt T. Tumor movement in proton therapy: solutions and remaining questions: a review. *Cancers* 2015; **7**: 1143-53. doi: 10.3390/cancers7030829
54. Chan TC, Mahmoudzadeh H, Purdie TG. A robust-CvAr optimization approach with 1602 application to breast cancer therapy. *Eur J Oper Res* 2014; **238**: 876-85. doi: 10.1016/j.ejor.2014.04.038
55. Mahmoudzadeh H, Lee J, Chan T C, Purdie TG. Robust optimization methods for cardiac sparing in tangential breast IMRT. *Med Phys* 2015; **42**: 2212-22. doi: 10.1118/1.4916092
56. Meschini G, Vai A, Paganelli Ch, Molinelli S, Fontana G, Pella A, et al. Virtual 4DCT from 4DMRI for the management of respiratory motion in carbon ion therapy of abdominal tumors. *Med Phys* 2019; **47**: 909-16. doi: 10.1002/mp.13992
57. Hugo GD, Rosu M. Advances in 4D radiation therapy for managing respiration: part I – 4D imaging. *Z Med Phys* 2012; **22**: 258-71. doi: 10.1016/j.zemedi.2012.06.009

58. Koerkamp MLG, Vasmel JE, Russell NS, Shaitelman SF, Anandadas CN, Currey A, et al. Optimizing MR-guided radiotherapy for breast cancer patients. *Front Oncol* 2020; **10**: 1107. doi: 10.3389/fonc.2020.01107
59. Stemkens B, Paulson ES, Tijssen RHN. Nuts and bolts of 4D-MRI for radiotherapy. *Phys Med Biol* 2018; **63**: 21TR01. doi: 10.1088/1361-6560/aae56d
60. Cai J, Chang Zh, Wang Zh, Segars WP, Yin FF. Four-dimensional magnetic resonance imaging (4D-MRI) using image-based respiratory surrogate: a feasibility study. *Med Phys* 2011; **38**: 6384-94. doi: 10.1118/1.3658737
61. Hu Y, Caruthers Sh.D, Low DA, Parikh PJ, Mutic S. Respiratory amplitude guided 4-dimensional magnetic resonance imaging. *Int J Radiation Oncol Biol Phys* 2012; **86**: 198-204. doi: 10.1016/j.ijrobp.2012.12.014
62. Oar A, Liney G, Rai R, Deshpande Sh, Pan L, Johnston M, et al. Comparison of four dimensional computed tomography and magnetic resonance imaging in abdominal radiotherapy planning. *Phys Imag Radiat Oncol* 2018; **7**: 70-5. doi: 10.1016/j.phro.2018.09.004
63. Paganelli Ch, Summers P, Bellomi M, Baroni G, Riboldi M. Liver 4DMRI: a retrospective image-based sorting method. *Med Phys* 2015; **42**: 4814-21. doi: 10.1118/1.4927252
64. Glide-Hurst CK, Joshua PK, To D, Hu Y, Kadbi M, Nielsen T, et al. Four dimensional magnetic resonance imaging optimization and implementation for magnetic resonance imaging simulation. *Pract Radiat Oncol* 2015; **5**: 433-42. doi: 10.1016/j.prro.2015.06.006
65. Kron T, Lee Ch, Perera F, Yu E. Evaluation of intra- and inter-fraction motion in breast radiotherapy using electronic portal cine imaging. *Technol Cancer Res Treat* 2004; **3**: 443-9. doi: 10.1177/153303460400300505
66. Hoekstra N, Habraken S, Swaak-Kragten A, Hoogeman M. Intrafraction motion during partial breast irradiation depends on treatment time. *Radiation Oncol* 2021; **159**: 176-82. doi: 10.1016/j.radonc.2021.03.029
67. Murphy MJ, Balter J, Balter S, BenComo JA, Das UJ, Jiang SB, et al. The management of imaging dose during image-guided radiotherapy: Report of the AAPM Task Group 75. *Med Phys* 2007; **34**: 4041-63. doi: 10.1118/1.2775667
68. Weismann Ch, Mayr Ch, Egger H, Auer A. Breast sonography – 2D, 3D, 4D ultrasound or elastography? *Breast Care* 2011; **6**: 98-103. doi: 10.1159/000327504
69. Huang Q, Zeng Zh. A review on real-time 3D ultrasound imaging technology. *Biomed Res Int* 2017; **2017**: 1-20. doi: 10.1155/2017/6027029
70. Acar Ph, Battle L, Dulac Y, Peyre M, Dubourdieu H, Hascoet S, et al. Real-time three-dimensional fetal echocardiography using a new transabdominal xMATRIX array transducer. *Arch Cardiovasc Dis* 2014; **107**: 4-9. doi: 10.1016/j.acvd.2013.10.003
71. Wong Ph, Muanza Th, Reynard E, Robert K, Barker J, Sultanem Kh. Use of three-dimensional ultrasound in the detection of breast tumor bed displacement during radiotherapy. *Int J Radiat Oncol Biol Phys* 2011; **79**: 39-45. doi: 10.1016/j.ijrobp.2009.10.023
72. O'Shea T, Bamber J, Fontanarosa D, van der Meer S, Verhaegen F, Harris E. Review of ultrasound image guidance in external beam radiotherapy part II: intra-fraction motion management and novel applications. *Phys Med Biol* 2016; **61**: R90-137. doi: 10.1088/0031-9155/61/8/R90
73. Korreman SS, Pedersen AN, Nottrup TJ, Specht L, Nystrom H. Breathing adapted radiotherapy for breast cancer: comparison of free-breathing gating with the breath-hold technique. *Radiation Oncol* 2005; **76**: 311-8. doi: 10.1016/j.radonc.2005.07.009
74. Zagar TM, Kaidar-Person O, Tang X, Jones EE, Matney J, Das SK, et al. Utility of deep inspiration breath-hold for left-sided breast radiation therapy in preventing early cardiac perfusion defects: a prospective study. *Int J Radiat Oncol Biol Phys* 2017; **97**: 903-9. doi: 10.1016/j.ijrobp.2016.12.017
75. Macrie BD, Donnelly ED, Hayes JP, Gopalakrishnan M, Philip RT, Reczek J, et al. A cost-effective technique for cardiac sparing with deep inspiration-breath hold (DIBH). *Phys Med* 2015; **31**: 733-7. doi: 10.1016/j.ejmp.2015.06.006
76. Bergom C, Currey A, Desai N, Tai A, Strauss JB. Deep inspiration breath hold: techniques and advantages for cardiac sparing during breast cancer irradiation. *Front Oncol* 2018; **8**: 87. doi: 10.3389/fonc.2018.00087
77. Wong JW, Sharpe MB, Jaffray DA, Kini VR, Robertson JM, Stromberg JS, et al. The use of active breathing control ABC to reduce margin for breathing motion. *Int J Radiat Oncol Biol Phys* 1999; **4**: 911-9. doi: 10.1016/S0360-3016(99)00056-5
78. Remouchamps V, Letts N, Vicini FA, Sharpe MB, Kestin LL, Chen PY, et al. Initial clinical experience with deep inspiration breath-hold using an active breathing control (ABC) device in the treatment of patients with left-sided breast cancer using external beam irradiation. *Int J Radiat Oncol Biol Phys* 2003; **56**: 704-15. doi: 10.1016/S0360-3016(03)00010-5
79. Bartlett FR, Colgan RM, Carr K, Donovan EM, McNair HA, Locke I, et al. The UK Heart Spare Study: randomized evaluation of voluntary deep-inspiration breath-hold in women undergoing breast radiotherapy. *Radiation Oncol* 2013; **108**: 242-7. doi: 10.1016/j.radonc.2013.04.021
80. Holt E, Mantel A, Cokelek M, MBIostat MT, Jassal S, Law M, et al. Volumetric arc therapy: a viable option for right-sided breast with comprehensive regional nodal irradiation in conjunction with deep inspiration breath hold. *J Med Imag and Radiat Sci* 2021; **52**: 223-37. doi: 10.1016/j.jmir.2021.02.007
81. Zhang W, Li R, You D, Su Y, Dong W, Ma Z. Dosimetry and feasibility studies of volumetric modulated arc therapy with deep inspiration breath-hold using optical surface management system for left-Sided breast cancer patients. *Front Oncol* 2020; **10**: 1711. doi: 10.3389/fonc.2020.01711
82. Fassi A, Ivaldi GB, de Fatis PT, Liotta M, Meaglia I, Porcu P, et al. Target position reproducibility in left breast irradiation with deep inspiration breath-hold using multiple optical surface control points. *J Appl Clin Med Phys* 2018; **19**: 35-43. doi: 10.1002/acm2.12321
83. Betgen A, Alderliesten T, Sonke J-J, van Vliet-Vroegindewij C, Bartelink H, Remeijer P. Assessment of set-up variability during deep inspiration breath-hold radiotherapy for breast cancer patients by 3D-surface imaging. *Radiation Oncol* 2013; **106**: 225-30. doi: 10.1016/j.radonc.2012.12.016
84. Borst GR, Sonke JJ, den Hollander S, Betgen A, Remeijer P, van Giersbergen A, et al. Clinical results of image-guided deep inspiration breath hold breast irradiation. *Int J Radiat Oncol Biol Phys* 2010; **78**: 1345-51. doi: 10.1016/j.ijrobp.2009.10.006
85. Yoganathan SA, Maria Das KJ, Agarwal A, Kumar S. Magnitude, impact and management of respiration-induced target motion in radiotherapy treatment: a comprehensive review. *J Med Phys* 2017; **42**: 101-15. doi: 10.4103/jmp.JMP_22_17
86. Keall PJ, Kini VR, Vedam SS, Mohan R. Motion adaptive x-ray therapy: a feasibility study. *Phys Med Biol* 2001; **46**: 1-10. doi: 10.1088/0031-9155/46/1/301
87. Giraud P, Djadi-Prat J, Morelle M, Pourel N, Durdux C, Carrie C, et al. Contribution of respiratory gating techniques for optimization of breast cancer radiotherapy. *Cancer Invest* 2012; **30**: 323-30. doi: 10.3109/07357907.2012.657818
88. Berbeco RI, Nishioka S, Shirato H, Chen GT, Jiang SB. Residual motion of lung tumors in gated radiotherapy with external respiratory motion gates. *Phys Med Biol* 2005; **50**: 3655-67. doi: 10.1088/0031-9155/50/16/001
89. Vedam SS, Keall PJ, Kini V, Mohan R. Determining parameters for respiration gated radiotherapy. *Med Phys* 2001; **28**: 2139-46. doi: 10.1118/1.1406524
90. Gagliardi G, Lax I, Soderstrom S, Gyenes G, Rutqvist LE. Prediction of excess risk of long-term cardiac mortality after radiotherapy of stage I breast cancer. *Radiat Oncol* 1998; **46**: 63-71. doi: 10.1016/S0167-8140(97)00167-9
91. Laaksomaa M, Sarudis S, Rossi M, Lehtonen T, Pehkonen J, Remes J, et al. AlignRT® and Catalyst™ in whole-breast radiotherapy with DIBH: is IGRT still needed? *J Appl Clin Med Phys* 2019; **20**: 97-104. doi: 10.1002/acm2.12553
92. Lozza L, Fariselli L, Sandri M, Rampa M, Pinzi V, De Santis MC, et al. Partial breast irradiation with CyberKnife after breast conserving surgery: a pilot study in early breast cancer. *Radiat Oncol* 2018; **13**: 49. doi: 10.1186/s13014-018-0991-4
93. Leonard CE, Tallhammer M, Johnson T, Hunter K, Howell K, Kercher J, et al. Clinical experience with image-guided radiotherapy in an accelerated partial breast intensity-modulated radiotherapy protocol. *Int J Radiat Oncol Biol Phys* 2010; **76**: 528-34. doi: 10.1016/j.ijrobp.2009.02.001
94. Bourland JD. *Image-guided radiation therapy*. 1st edition. New York: CRC Press; 2020.
95. Thomsen MS, Harrov U, Fledelius W, Poulsen PR. Inter- and intra-fraction geometric errors in daily image-guided radiotherapy of free-breathing breast cancer patients measured with continuous portal imaging. *Acta Oncologica* 2014; **53**: 802-8. doi: 10.3109/0284186X.2014.905700

96. Hijal T, Founier-Bidoz N, Castro-Pena P, Kirova YM, Zefkili S, Bollet MA, et al. Simultaneous integrated boost in breast conservative treatment of cancer: a dosimetric comparison of helical tomotherapy and three-dimensional conformal radiotherapy. *Radiother Oncol* 2010; **94**: 300-6. doi: 10.1016/j.radonc.2009.12.043
97. Hlavka A, Vanasek J, Odrzaka K, Stuk J, Dolezel M, Ulyrch V, et al. Tumor bed radiotherapy in women following breast conserving surgery for breast cancer-safety margin with/without image guidance. *Oncol Lett* 2018; **15**: 6009-14. doi: 10.3892/ol.2018.8083
98. Fast MF, Nill S, Bedford JL, Oelfke U. Dynamic tumor tracking using the Elekta Agility MLC. *Med Phys* 2014; **41**: 111719. doi: 10.1118/1.4899175
99. Lemanski C, Thariat J, Ampil FL, Bose S, Vock J, Davis R, et al. Image-guided radiotherapy for cardiac sparing in patients with left-sided breast cancer. *Front Oncol* 2014; **4**: 1-5. doi: 10.3389/fonc.2014.00257
100. Uhl M, Sterzing F, Habl G, Schubert K, Hof H, Debus J, et al. Breast cancer and funnel chest. Comparing helical tomotherapy and three-dimensional conformal radiotherapy with regard to the shape of pectus excavatum. *Strahlenther Onkol* 2012; **188**: 127-35. doi: 10.1007/s00066-011-0022-y
101. Cherry P, Duxbury A. *Practical radiotherapy physics and equipment*, 2nd edition. New York: John Wiley & Sons; 2009.
102. Latifi K, Pritz J, Zhang GG, Moros EG, Harris EER. Fiducial-based image-guided radiotherapy for whole breast irradiation. *J Radiat Oncol* 2013; **2**: 185-90. doi: 10.1007/s13566-013-0102-y
103. Gupta T, Narayan CA. Image-guided radiation therapy: physician's perspectives. *J Med Phys* 2012; **37**: 174-82. doi: 10.4103/0971-6203.103602
104. Yang JN, Mackie TR, Reckwerdt P, Deasy JO, Thomadsen BR. An investigation of tomotherapy beam delivery. *Med Phys* 1997; **24**: 425-36. doi: 10.1118/1.597909
105. Yu CX, Jaffray DA, Wong JW. The effects of intrafraction organ motion on the delivery of dynamic intensity modulation. *Phys Med Biol* 1998; **43**: 91-104. doi: 10.1088/0031-9155/43/1/006
106. Shirato H, Oita M, Fujita K, Watanabe Y, Miyasaka K. Feasibility of synchronization of real-time tumor-tracking radiotherapy and intensity-modulated radiotherapy from viewpoint of excessive dose from fluoroscopy. *Int J Radiat Oncol Biol Phys* 2004; **60**: 335-41. doi: 10.1016/j.ijrobp.2004.04.028
107. Wiant DB, Wentworth S, Maurer JM, Vanderstraeten CL, Terrell JA, Sintay BJ. Surface imaging-based analysis of intrafraction motion for breast radiotherapy patients. *J App Clin Med Phys* 2014; **15**: 147-59. doi: 10.1120/jacmp.v15i6.4957
108. Hamming VC, Visser C, Batin E, McDermott LN, Busz DM, Both S, et al. Evaluation of a 3D surface imaging system for deep inspiration breath-hold patient positioning and intra-fraction monitoring. *Radiat Oncol* 2019; **14**: 125. doi: 10.1186/s13014-019-1329-6
109. Reitz D, Walter F, Schönecker S, Freislederer P, Pazos M, Niyazi M, et al. Stability and reproducibility of 6013 deep inspiration breath-holds in left-sided breast Cancer. *Radiat Oncol* 2020; **15**: 121. doi: 10.1186/s13014-020-01572-w
110. Donovan EM, Castellano I, Eagle S, Harris E. Clinical implementation of kilovoltage cone beam CT for the verification of sequential and integrated photon boost treatments for breast cancer patients. *Br J Radiol* 2012; **85**: e1051-e7. doi: 10.1259/bjr/28845176
111. Liu WS, Wang BW, Tzeng YD, Tsai MH, Pan CP. The role of 4-dimensional cone beam computerized tomography in breast cancer radiation therapy preliminary report. *Int J Radiat Oncol Biol Phys* 2016; **96**: e23. doi: 10.1016/j.ijrobp.2016.06.6
112. Ozhasoglu C, Murphy MJ. Issues in respiratory motion compensation during external-beam radiotherapy. *Int J Radiat Oncol Biol Phys* 2002; **52**: 1389-99. doi: 10.1016/s0360-3016(01)02789-4
113. Sharp GC, Jiang SB, Shimizu S, Shirato H. Prediction of respiratory tumour motion for real-time image-guided radiotherapy. *Phys Med Biol* 2004; **49**: 425-40. doi: 10.1088/0031-9155/49/3/006
114. Stegman LD, Beal KP, Hunt MA, Fornier MN, McCormick B. Long-term clinical outcomes of whole-breast irradiation delivered in the prone position. *Int J Radiat Oncol Biol Phys* 2007; **68**: 73-81. doi: 10.1016/j.ijrobp.2006.11.054
115. Lymberis SC, deWynngaert JK, Parhar P, Chhabra AM, Fenton-Kerimian M, Chang J, et al. Prospective assessment of optimal individual position (prone versus supine) for breast radiotherapy: volumetric and dosimetric correlations in 100 patients. *Int J Radiat Oncol Biol Phys* 2012; **84**: 902-9. doi: 10.1016/j.ijrobp.2012.01.040
116. Morrow NV, Stepaniak C, White J, Wilson F, Li XA. Intra- and interfraction variations for prone breast irradiation: an indication for image-guided radiotherapy. *Int J Radiat Oncol Biol Phys* 2007; **69**: 910-7. doi: 10.1016/j.ijrobp.2007.06.056
117. Veldeman L, Schiettecatte K, De Sutter C, Monten C, Greveling A. The 2-year cosmetic outcome of a randomized trial comparing prone and supine whole-breast irradiation in large-breasted women. *Int J Radiat Oncol Biol Phys* 2016; **95**: 1210-7. doi: 10.1016/j.ijrobp.2016.03.003
118. Piruzan E, Vosoughi N, Mahani H. Development and validation of an optimal GATE model for double scattering proton beam delivery. *J Instrum* 2021; **16**: 02022. doi: 10.1088/1748-0221/16/02/P02022
119. Galland-Girodet S, Pashtan IM, MacDonald S, Ancukiewicz M, Hirsch AE, Kachnic LA, et al. Long-term cosmetic outcomes and toxicities of proton beam therapy compared to photon-based 3-dimensional conformal accelerated partial breast irradiation: a phase 1 trial. *Int J Radiat Oncol Biol Phys* 2014; **90**: 493-500. doi: 10.1016/j.ijrobp.2014.04.008
120. Habermehl D, Henkner K, Ecker S, Jakel O, Debus J, Combs SE, et al. Evaluation of different fiducial markers for image-guided radiotherapy and particle therapy. *J Radiat Res* 2013; **54**: i61-8. doi: 10.1093/jrr/rrt071
121. Landry G, Hua C. Current state and future applications of radiological image guidance for particle therapy. *Med Phys* 2018; **45**: e1086-95. doi: 10.1002/mp.12744
122. Steidl P, Haberer T, Durante M, Bert C. Gating delays for two respiratory motion sensors in scanned particle radiation therapy. *Phys Med Biol* 2013; **58**: N295-302. doi: 10.1088/0031-9155/58/21/n295
123. Kubiak T. Particle therapy of moving targets—the strategies for tumour motion monitoring and moving targets irradiation. *Br J Radiol* 2016; **89**: 20150275. doi: 10.1259/bjr.20150275
124. Flejmer AM, Edvardsson A, Dohlmar F, Josefsson D, Nilsson M, Witt Nyström P, et al. Respiratory gating for proton beam scanning versus photon 3D-CRT for breast cancer radiotherapy. *Acta Oncol* 2016; **55**: 577-83. doi: 10.3109/0284186X.2015.1120883
125. von Siebenthal M, Szekeley G, Gamper U, Boesiger P, Lomax A, Cattin Ph. 4D MR imaging of respiratory organ motion and its variability. *Phys Med Biol* 2007; **52**: 1547-64. doi: 10.1088/0031-9155/52/6/001
126. Patel SA, Lu HM, Nyamwanda JA, Jimenez RB, Taghian AG, MacDonald SM, et al. Postmastectomy radiation therapy technique and cardiopulmonary sparing: a dosimetric comparative analysis between photons and protons with free breathing versus deep inspiration breath hold. *Pract Radiat Oncol* 2017; **7**: e377-84. doi: 10.1016/j.proro.2017.06.006
127. Mondal D, Jhawar SR, Millevoi R, Haffty BG, Parikh RR. Proton versus photon breath-hold radiation for left-sided breast cancer after breast-conserving surgery: a dosimetric comparison. *Int J Part Ther* 2020; **7**: 24-33. doi: 10.14338/IJPT-20-00026.1
128. MacKay RI. Image guidance for proton therapy. *Clin Oncol* 2018; **30**: 293-8. doi: 10.1016/j.clon.2018.02.004
129. Corradini S, Alongi F, Andratschke N, Belka C, Boldrini L, Cellini F, et al. MR-guidance in clinical reality: current treatment challenges and future perspectives. *Radiat Oncol* 2019; **14**: 92. doi: 10.1186/s13014-019-1308-y
130. Oborn BM, Dowdell S, Metcalfe PE, Crozier S, Mohan R, Keall PJ. Future of medical physics: real-time MRI-guided proton therapy. *Med Phys* 2017; **44**: e77-e90. doi: 10.1002/mp.12371
131. Acharya S, Fischer-Valuck BW, Mazur TR, Curcuru A, Sonka K, Kashani R, et al. Magnetic resonance image guided radiation therapy for external beam accelerated partial-breast irradiation: evaluation of delivered dose and intrafractional cavity motion. *Int J Radiat Oncol Biol Phys* 2016; **96**: 785-92. doi: 10.1016/j.ijrobp.2016.08.006
132. Nachbar M, Mönnich D, Boeke S, Gani C, Weidner N, Heinrich V, et al. Partial breast irradiation with the 1.5 T MR-linac: first patient treatment and analysis of electron return and stream effects. *Radiother Oncol* 2020; **145**: 30-5. doi: 10.1016/j.radonc.2019.11.025
133. Koerkamp MLG, Vasmel JE, Russell NS, Shaitelman SF, Anandadas CN, Currey A, et al. Optimizing MR-guided radiotherapy for breast cancer patients. *Front Oncol* 2020; **10**: 1-13. doi: 10.3389/fonc.2020.01107

134. van Heijst TC, den Hartogh MD, Lagendijk JJ, van den Bongard HJ, van Asselen B. MR-guided breast radiotherapy: feasibility and magnetic-field impact on skin dose. *Phys Med Biol* 2013; **58**: 5917-30. doi:10.1088/0031-9155/58/17/5917
135. Sahiner B, Pezeshk A, Hadjiiski LM, Wang X, Drukker K, Cha KH, et al. Deep learning in medical imaging and radiation therapy. *Med Phys* 2018; **46**: e1-e36. doi: 10.1002/mp.13264
136. Wang C, Zhu X, Hong JC, Zheng D. Artificial intelligence in radiotherapy treatment planning: present and future. *Technol Cancer Res Treat* 2019; **18**: 1-11. doi: 10.1177/1533033819873922
137. Chen L, Liang X, Shen C, Jiang S, Wang J. Synthetic CT generation from CBCT images via deep learning. *Med Phys* 2020; **47**: 1115-25. doi: 10.1002/mp.13978
138. Hickman SE, Baxter GC, Gilbert FJ. Adoption of artificial intelligence in breast imaging: evaluation, ethical constraints and limitations. *Br J Cancer* 2021; **125**: 15-22. doi: 10.1038/s41416-021-01333-w
139. Hayton PM, Brad M, Smith SM, Moore N. A non-rigid registration algorithm for dynamic breast MR images. *Artif Intell* 1999; **114**: 125-56. doi: 10.1016/S0004-3702(99)00073-9
140. Sechopoulos I, Teuwena J, Mann R. Artificial intelligence for breast cancer detection in mammography and digital breast tomosynthesis: state of the art. *Semin Cancer Biol* 2021; **72**: 214-25. doi: 10.1016/j.semcancer.2020.06.002
141. Zenklusen SM, Pedroni E, Meer D. A study on repainting strategies for treating moderately moving targets with proton pencil beam scanning at the new Gantry 2 at PSI. *Phys Med Biol* 2010; **55**: 5103-21. doi: 10.1088/0031-9155/55/17/014
142. Seco J, Robertson D, Trofimov A, Paganetti H. Breathing interplay effects during proton beam scanning: simulation and statistical analysis. *Phys Med Biol* 2009; **54**: N283-94. doi: 10.1088/0031-9155/54/14/N01
143. Phillips MH, Pedroni E, Blattmann H, Boehringer T, Coray A, Scheib S. Effects of respiratory motion on dose uniformity with a charged particle scanning method. *Med Phys Biol* 1992; **37**: 223-34. doi: 10.1088/0031-9155/37/1/016
144. Rietzel E, Bert CH. Respiratory motion management in particle therapy. *Med Phys* 2010; **37**: 449-60. doi: 10.1118/1.3250856
145. Unkelbach J, Alber M, Bangert M, Bokrantz R, Chan TCY, Deasy JO, et al. Robust radiotherapy planning. *Phys Med Biol* 2018; **63**: 22TR02. doi: 10.1088/1361-6560/aae659
146. Byrne M, Hu Y, Archibald-Heeren B. Evaluation of RayStation robust optimization for superficial target coverage with setup variation in breast IMRT. *Australas Phys Eng Sci Med* 2016; **39**: 705-16. doi: 10.1007/s13246-016-0466-6
147. Dunlop A, Colgan R, Kirby A, Ranger A, Blasiak-Wal I. Evaluation of organ motion-based robust optimisation for VMAT planning for breast and internal mammary chain radiotherapy. *Clin Transl Radiat Oncol* 2019; **16**: 60-6. doi: 10.1016/j.ctro.2019.04.004
148. Liang X, Mailhot Vega RB, Li Z, Zheng D, Mendenhall N, Bradley JA. Dosimetric consequences of image guidance techniques on robust optimized intensity-modulated proton therapy for treatment of breast cancer. *Radiat Oncol* 2020; **15**: 47. doi: 10.1186/s13014-020-01495-6
149. Wilson JD, Hammond EM, Higgins GS, Petersson K. Ultra high dose rate (FLASH) radiotherapy: silver bullet or fool's gold? *Front Oncol* 2020; **9**: 1563. doi: 10.3389/fonc.2019.01563
150. Symonds P, Jones GDD. FLASH radiotherapy: the next technological advance in radiation therapy? *Clin Oncol* 2019; **31**: 405-6. doi: 10.1016/j.clon.2019.05.011
151. Bourhis J, Sozzi WJ, Gonçalves Jorge P, Gaide O, Bailat C, Duclos F, et al. Treatment of a first patient with FLASH-radiotherapy. *Radiother Oncol* 2019; **139**: 18-22. doi: 10.1016/j.radonc.2019.06.019

Study of correlations between CT properties of retrieved cerebral thrombi with treatment outcome of stroke patients

Rebeka Viltuznik¹, Jernej Vidmar^{1,2}, Andrej Fabjan^{2,3}, Miran Jeromel^{4,5}, Zoran V. Milosevic⁴, Igor J. Kocijancic⁴, Igor Sersa^{1,2}

¹ Jožef Stefan Institute, Ljubljana, Slovenia

² Institute of Physiology, Medical Faculty, University of Ljubljana, Slovenia

³ Department of Vascular Neurology and Intensive Therapy, University Medical Centre Ljubljana, Slovenia

⁴ Department of Diagnostic and Interventional Neuroradiology, Clinical Institute of Radiology, University Medical Centre Ljubljana, Slovenia

⁵ Department of Diagnostic and Interventional Radiology, General Hospital Slovenj Gradec, Slovenia

Radiol Oncol 2021; 55(4): 409-417.

Received 30 November 2020

Accepted 2 September 2021

Correspondence to: Igor Serša, Ph.D., Jožef Stefan Institute, Jamova 39, SI-1000 Ljubljana, Slovenia. E-mail: igor.sersa@ijs.si

Disclosure: No potential conflicts of interest were disclosed.

This is an open access article under the CC BY-NC-ND license (<http://creativecommons.org/licenses/by-nc-nd/4.0/>).

Background. All the patients with suspected stroke are directed to whole-brain CT scan. The purpose of this scan is to look for early features of ischemia and to rule out alternative diagnoses than stroke. In case of ischemic stroke, CT diagnostics (including CT angiography) is used mainly to locate the occlusion and its size, while the Hounsfield Units (HU) values of the thrombus causing the stroke are usually overlooked on CT scan or considered not important. The aim of this study was to demonstrate that the HU value is relevant and can help in better treatment planning.

Patients and methods. There were 25 patients included in the study, diagnosed with ischemic stroke in the middle cerebral artery (MCA) territory. In all patients, systemic thrombolysis was not successful and the mechanical recanalization was needed. The retrieved thrombi were also analyzed histologically for the determination of red blood cells (RBC) proportion. CT of the proximal MCA (M1) segment was analyzed for average HU value and its variability both in the occluded section and the symmetrical normal site. These CT parameters were then statistically studied for the possible correlations with different clinical, histological and procedure parameters using the Linear Regression and the Pearson correlation coefficient.

Results. Relevant positive correlations were found between average HU value of thrombus and outcome modified Rankin Scale (mRS), initial mRS, number of passes with thrombectomy device as well as RBC proportion.

Conclusions. Results of the present study suggest that measured HU values in CT images of the cerebral thrombi may help in the assessment of thrombus compaction and therefore better treatment planning.

Key words: ischemic stroke; CT images; cerebral thrombi; modified Rankin Scale; RBC proportion

Introduction

The risk for stroke is increasing yearly due to the aging population on a global level and the accumulation of risk factors.¹ Stroke is the second leading cause of death and the main cause for decreased quality of life.² Time is of the essence when it comes to treating the stroke, where thrombolytic

treatment, usually with systemic administration of recombinant tissue plasmin activator (rt-PA), and mechanical thrombectomy are the main approaches; however new experimental treatments are also under consideration.³

The main cause of stroke is the acute cerebral artery occlusion, which leads to ischemic stroke, where the oxygen supply is cut off.⁴ The occlusion

can either be thrombotic or embolic, originating from various locations, which results in various thrombi structures. The structure can also give us information on the age of the thrombi.⁵ On a microscopic level, thrombi are composed of different levels of red and white blood cells intertwined with fibrin meshwork.^{6,7} The structure can strongly influence the permeability which is important for the success of the thrombolytic treatment.⁸

The diagnosis of stroke is a multiple step process, which consists of clinical evaluation and diagnostic imaging. The clinical evaluation includes the assessment of the effect of the stroke, which can be estimated using the modified Rankin Scale (mRS). This is a seven-level stroke scale ranging from 0, which stands for no symptoms to 6, which stands for death.⁹ Another scale serving the same purpose, however, with more grades is National Institutes of Health (NIH) severity stroke scale (NIHss).¹⁰

In diagnostics of stroke, computed tomography (CT) is the main tool in selection of patients that are suitable candidates for stroke treatment: firstly, to exclude hemorrhage, to exclude large areas of hypodense brain tissue, suggesting irreversible ischemia and to exclude stroke mimics. Native CT is complemented by CT angiography (CTA), which provides high diagnostic value in the detection of occlusion in high degree of stenosis as well as CT perfusion (CTP), which provides high specificity in the detection of ischemia and infarcted brain tissue. However, the most accurate assessment for acute stroke involving the site of occlusion, infarction core and salvageable brain tissue is a combination of different CT procedures involving CTA and CTP. In addition, CT scanning is fast, it is widely accessible and its price per scan is relatively low. However, sensitivity of CT to soft tissues cannot match with that of MRI.¹¹⁻¹³ While it has been proven that CT can be used to determine some characteristics of the thrombi¹⁴, the field of connecting CT characteristics to clinical and procedure parameters has yet to be investigated.

The aim of this study is to demonstrate that CT images provide more information than currently used in routine stroke diagnostics. More specifically, mainly geometrical and macroscopic parameters of CT images are used, while information on the HU values of the thrombus causing the ischemic stroke, are usually overlooked or considered not important. In this study we want to show that this information is relevant for assessment of the thrombus microscopic structure and that these parameters correlate with some clinical parameters and can be therefore used for better treatment planning.

Patients and methods

Patient selection and stroke protocol

This study was performed on $n = 25$ patients which were diagnosed with acute ischemic stroke and underwent mechanical thrombectomy procedure with successful removal of the thrombus from the middle cerebral artery (MCA) M1 segment. Mean age of the patients was 73 ± 11 years and the group of patients consisted of 16 males and 9 females. In 11 patients, etiology of the stroke was atherothrombotic and in 14 patients it was cardioembolic. Before the stroke event four patients were receiving antiaggregating drugs, two patients were receiving anticoagulating drugs and one patient was receiving both types of drugs (Table 1).

The patients for the study were admitted to the Neurology Clinic of University Medical Center in Ljubljana for urgent neurological symptoms suggesting brain stroke. These patients were managed according to the standard steps of acute ischemic stroke management in our tertiary center. Firstly, an urgent clinical examination was performed, which was followed by a CT scan (non-contrast enhanced CT scan, CT perfusion and CT angiography) on a Siemens Sensation Open 40 CT scanner, where ischemic stroke caused by the occlusion of the middle cerebral artery, was confirmed. The protocol continued with standard full dose of rt-PA (0.9 mg/kg, maximum 90 mg) systemic thrombolytic treatment. In all studied patients clinical stroke signs persisted after the thrombolytic treatment, therefore further therapy was done by the mechanical thrombectomy. This was performed by skilled interventional neuroradiologist, using the standard mechanical recanalization procedure with the thrombectomy device (Trevor®stent retriever, 4 x 20 mm, Stryker Neurovascular, Kalamazoo, MI). The retrieved thrombi were preserved and additionally examined through histological analysis.

The protocol of the study was approved by the Institutional Review Board and the Ethical Committee of the National Ministry of Health of the Republic of Slovenia, approval No. 0120-99/2021/7. The study was performed in agreement with the informed-consent policy.

CT imaging protocol and image analysis

Stroke patients with qualifying conditions for the study underwent urgent CT scanning of the brain which included non-contrast enhanced (NCE) sequential CT scans and CTA scans. The NCE CT scan is a sequential scan consisting of two parts-the skull

TABLE 1. Experimental data of patients qualified for the study, which include CT, histological, clinical and procedure parameters

#	CT parameters								Histology	Clinical parameters								Procedure parameters		
	HU avg				HU var					L [mm]	RBC [%]	Stroke etiology	Therapy before stroke	NIHSS			mRS		Rd [min]	# pass
	occl	nor	diff	diff [%]	occl	nor	diff	diff [%]						strt	end	diff	strt	end		
1.	29.1	32.4	-3.3	-11.4	4.20	4.42	-0.22	-5.0	20.8	11.5	AT	/	21	1	20	4	1	3	42	1
2.	42.0	29.2	12.8	30.5	4.58	8.98	-4.40	-96.3	16.3	45.1	CE	/	17	8	9	5	4	1	62	2
3.	38.5	35.1	3.4	8.9	3.56	2.75	0.80	22.6	17.0	12.0	CE	/	23	7	16	4	3	1	65	1
4.	36.9	34.3	2.5	6.8	11.66	4.58	7.08	60.7	17.5	41.4	CE	AA	18	3	15	5	2	3	77	1
5.	43.7	44.2	-0.5	-1.2	3.55	3.86	-0.31	-8.7	17.9	65.9	AT	/	26	6	20	5	3	2	97	3
6.	35.8	30.0	5.9	16.4	4.17	2.23	1.95	46.7	16.3	61.0	CE	/	7	0	7	3	0	3	38	3
7.	31.8	36.0	-4.2	-13.2	2.77	3.26	-0.49	-17.8	22.2	57.3	AT	/	13	3	10	4	1	3	90	1
8.	37.8	38.9	-1.1	-2.9	2.82	4.45	-1.63	-58.0	26.9	50.3	CE	/	14	3	11	4	3	1	77	1
9.	32.0	24.0	8.1	25.1	9.50	4.90	4.60	48.4	22.7	56.3	CE	ACAA	5	2	3	3	2	1	115	2
10.	38.5	36.5	2.0	5.1	3.20	2.80	0.40	12.5	19.7	52.4	CE	/	26	42	-16	5	6	-1	82	4
11.	38.3	39.4	-1.1	-2.8	5.49	3.66	1.83	33.4	17.1	19.1	AT	/	12	0	12	3	0	3	60	1
12.	35.7	33.9	1.7	4.9	3.56	5.39	-1.83	-51.2	13.9	31.8	CE	AA	6	3	3	3	1	2	69	1
13.	44.3	31.9	12.3	27.8	4.66	5.11	-0.46	-9.8	22.5	74.7	AT	/	19	12	7	5	4	1	108	2
14.	44.1	37.5	6.6	15.0	2.60	3.92	-1.32	-50.9	19.3	38.9	CE	/	18	20	-2	4	5	-1	63	5
15.	36.0	35.4	0.6	1.6	3.48	2.67	0.81	23.4	17.9	48.8	CE	/	42	42	0	5	6	-1	75	2
16.	38.1	36.4	1.7	4.5	4.16	5.45	-1.30	-31.2	18.6	21.3	AT	/	15	4	11	5	4	1	77	1
17.	42.5	40.7	1.8	4.2	3.11	3.74	-0.63	-20.4	13.5	14.8	CE	AA	14	2	12	5	3	2	53	1
18.	38.7	23.3	15.4	39.8	5.66	4.79	0.87	15.3	19.1	42.4	CE	AC	22	3	19	5	4	1	43	1
19.	34.7	30.9	3.8	11.0	5.61	4.43	1.18	21.1	20.9	37.7	AT	/	3	1	2	1	0	1	60	1
20.	41.2	32.4	8.8	21.4	5.14	4.58	0.56	10.9	19.3	56.0	AT	AC	11	40	-29	4	6	-2	76	3
21.	37.2	28.5	8.7	23.5	3.29	5.27	-1.99	-60.4	29.2	79.1	AT	/	19	10	9	5	5	0	61	1
22.	35.2	32.5	2.6	7.5	3.02	2.79	0.24	7.9	13.6	9.3	CE	/	16	9	7	5	5	0	95	3
23.	41.5	34.5	6.9	16.7	5.14	4.47	0.67	13.0	21.5	80.4	AT	/	16	3	13	4	2	2	65	2
24.	28.9	23.2	5.6	19.5	3.52	4.72	-1.20	-34.1	12.1	57.1	CE	/	13	3	10	4	1	3	55	1
25.	40.2	33.4	6.8	17.0	2.91	4.30	-1.39	-47.8	18.7	46.8	AT	AA	42	42	0	5	6	-1	90	4

AA = antiaggregation; AC = anticoagulant; ACAA = both types of drugs; AT = atherothrombotic; CE = cardioembolic; diff = absolute difference; diff [%] = relative difference in %; HU avg = average Hounsfield units; HU var = variability of Hounsfield units; L [mm] = CT length of the thrombi; mRS = modified Rankin score; NIHSS = NIH Stroke Scale; nor = normal artery; occl = occlusion; RBC [%] = percentage of red blood cells in the thrombi; Rd = duration of mechanical recanalization; # pass = number of passes

base (120 kV, 265 mAs, matrix 1024×1024, slice thickness 3 mm, collimation 20×0.6, rotation time 1 s, window width 90-190, window center 38) and the cerebral part (120 kV, 310 mAs, matrix 1024×1024, slice thickness 4.8 mm, collimation 24×1.2, rotation time 1 s, window width 80, window center 38). Acquired CT images were further analyzed by the ImageJ program (NIH, Bethesda MD, USA) to obtain relevant CT data on brain thrombi of the patients. CTA images were specifically used to determine the position of the thrombi. This information was then used to stack three slices from NCE CT scan containing the thrombus to correctly position the line along the thrombus on the stacked image

as well as the symmetrical non-occluded MCA segment on the opposite side of the brain. Special care was taken to center the lines in the middle of the vessel in order to avoid signals from the vessel wall tissue and therefore reduce a possible partial volume effect and also an increased Hounsfield Units (HU) values due to vessel calcifications. Along the lines the HU intensity profiles were measured in the NCE CT images. NCE CT images were more suitable for the thrombus analysis than CTA images, because they have no contrast enhancement due to the contrast agent that could alter the HU of thrombi. Measured HU intensity profiles were further analyzed by determining average HU val-

ue of the profile HU_{avg} and its standard deviation HU_{var} . HU_{avg} and HU_{var} values of thrombi occluded (ocl) were compared with the corresponding counterpart values of the non-occluded (nor) symmetric MCA segment.

Interventional procedure parameters and clinical parameters

During every interventional procedure, recanalization time and number of passes with the thrombectomy device were registered as the procedure parameters. The recanalization time was considered as the time between the first contact of the thrombectomy device with the thrombus to the successful recanalization through the occluded artery with complete removal of the thrombus.

For clinical parameters, modified Ranking Scale (mRS) for stroke before (mRS_{start} , assessed at admission to the hospital) and after the procedure (mRS_{end} , assessed at discharge from the hospital) was collected and the mRS difference between these two parameters ($mRS_{diff} = mRS_{end} - mRS_{start}$) was calculated.

Histological analysis

Histological analysis was done to determine the percentage of red blood cells (RBC) in the retrieved thrombi (RBC%). The thrombi samples were fixed in 10% buffered formaldehyde for 48 h. After the fixation, they were cut longitudinally as 5- μ m-thick cross-sections and embedded in paraffin. The cross-sections were stained with monoclonal antibodies Anti-Human Glycophorin A (GPA) for RBC content and with anti β -3 integrin Anti-Human CD61 (DakoCytomation, Denmark) for platelet content.

Micro-photography of the stained cross-sections was performed, using a Nikon Eclipse E600 optical microscope (Nikon, Düsseldorf, Germany) equipped with a Nikon 4x Plan Fluor objective and with a high-resolution CCD camera Nikon DS-Fi1. The micro-photography system was controlled by the Nikon NIS Elements software package. The exposure time yielding the optimal image contrast was equal to 10 ms while the in-plane image resolution was equal to 10 μ m (imaging matrix was 1024×1124 and field of view (FOV) 10.24×11.24 mm²).

Histological (hematoxylin-eosin) images of the central cross-section along the thrombi were examined for the RBC proportion by the analysis encompassing the following steps. First, each image was

corrected for uneven illumination (vignetting).¹⁵ Then the corresponding intensity histogram was calculated and used to determine the optimal threshold for the discrimination between the RBC-rich and the platelet-rich regions. The RBC proportion was determined as the ratio between the thresholded RBC area and the total thrombi area.

Statistical analysis

Possible correlations between different groups of data (CT image parameters, histological parameters, clinical parameters and procedure parameters) were tested. Univariate linear regression was the statistical method of choice, where R^2 , linear regression coefficient with its standard error and p -value were calculated for all the possible pairs of data groups. In addition to the regression analysis, Pearson correlation coefficient was calculated for all the tested data pairs. Statistical analysis was performed using Microsoft Excel Analysis ToolPak software.

Results

Histological sections of selected representative retrieved cerebral thrombi are shown in Figure 1. Histological slices were stained by hematoxylin-eosin and then analyzed for RBC proportions using digital image processing of the thrombi images acquired by using optical microscopy of the histological sections. All retrieved thrombi had a distinctly heterogeneous, laminated (multilayer) structure. The structure involves the interweaving of compacted erythrocyte-rich (red) regions with thinner (pink) coatings containing a combination of complementary-linked platelets and a fibrin network. The laminations are often folded and twisted, which is probably due to blood flow turbulence in the environment where the thrombi were formed and their turning as they traveled along the vessel. Among the retrieved thrombi there were no homogeneous single-layered (red only) thrombi. Which can be explain by their high susceptibility to thrombolysis.

Figure 2 shows an example of a CT image of a stroke patient with a clearly visible MCA segment on both hemispheres of the brain. In the example the MCA segment on the right hemisphere is occluded by the cerebral thrombus, while the MCA segment on the opposite hemisphere is normal. Exact location of each thrombus was determined from its CTA image first and then this location was

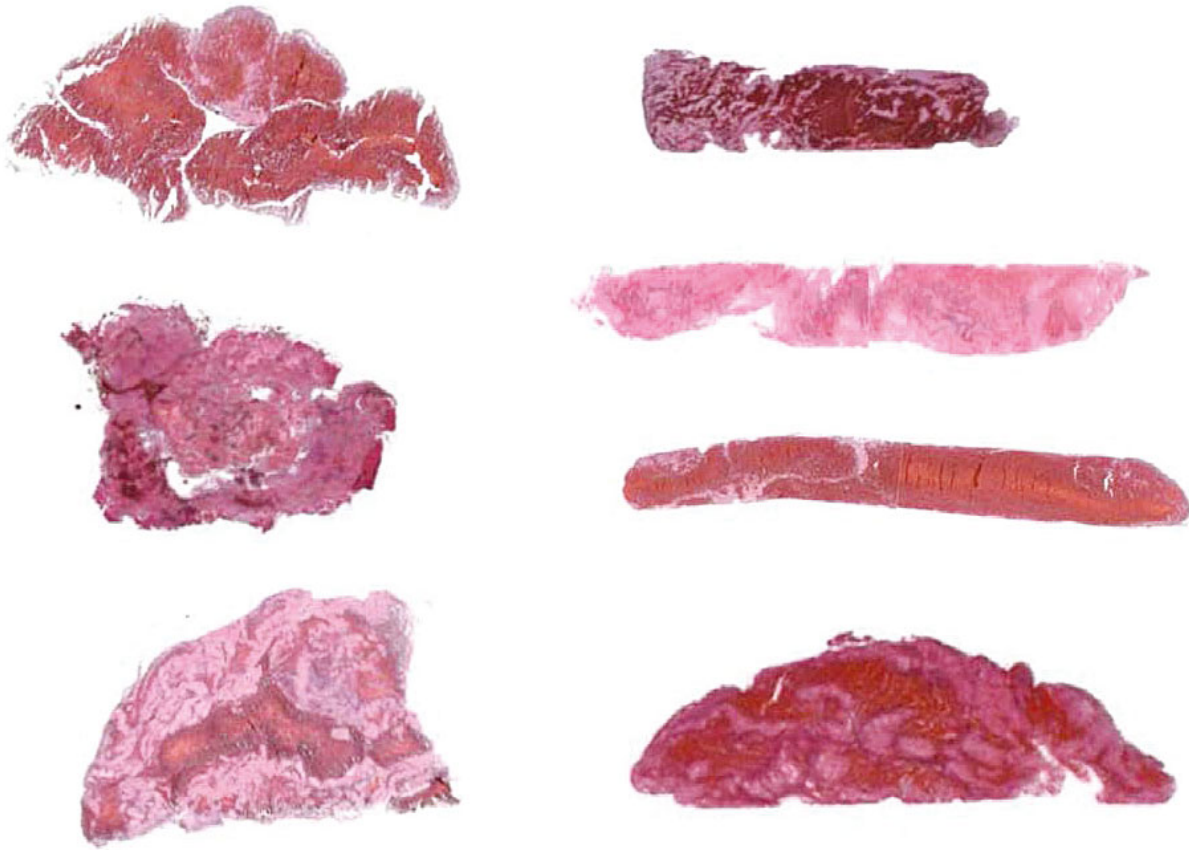


FIGURE 1. Light microscopy images of histological slices along representative retrieved cerebral thrombi. The histological slices were stained by hematoxylin-eosin and then analyzed for the RBS proportion. It can be seen from the images that the structural and compositional diversity among cerebral thrombi is high. All retrieved thrombi had a distinctly heterogeneous, laminated (multilayer) structure which involves the interweaving of compacted erythrocyte-rich (red) regions with thinner (pink) coatings containing a combination of complementary-linked platelets and a fibrin network.

used to obtain HU values along the thrombus from the corresponding CT image. Yellow line on the image is drawn along the thrombus and the symmetrical position of the normal MCA segment. Graphs in Figure 2A correspond to HU intensity profiles along both yellow lines: along the cerebral thrombus in Figure 2B and along the symmetrical section of the normal MCA segment in Figure 2C. For each HU, intensity profile was then calculated by average HU value HU_{avg} and HU value variability HU_{var} . Thus, each patient was characterized by these two CT parameters that were obtained for the occluded (occl) and normal (nor) MCA segment so that it became possible to calculate their absolute (diff) and relative differences (diff [%]), which are equal to: $HU_{avg_diff} = HU_{avg_occl} - HU_{avg_nor}$, $HU_{avg_diff}[\%] = 100 \cdot (1 - HU_{avg_nor} / HU_{avg_occl})$ and $HU_{var_diff} = HU_{var_occl} - HU_{var_nor}$, $HU_{var_diff}[\%] = 100 \cdot (1 - HU_{var_nor} / HU_{var_occl})$. Table 1 shows CT as well as histological (RBC proportion), clinical and procedure parameters of pa-

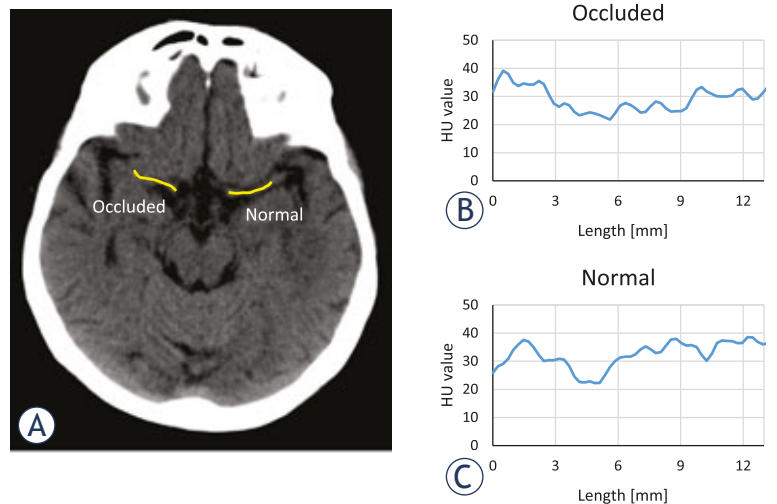


FIGURE 2. CT image of a patient with stroke (A). In the selected slice, Middle Cerebral Artery (MCA) on both hemispheres of the brain is visible. The occluded MCA section on the right hemisphere and its symmetrical normal MCA section is indicated by a yellow line along the cerebral thrombus. Graphs show Hounsfield Units (HU) value profiles of the CT image along the lines for the occluded (B) and the normal (C) MCA segment.

TABLE 2. Linear regression and Pearson correlation coefficient analysis of data group pairs with statistically most significant correlations and linear regression parameters

Data group pair		Linear regression $y = k \cdot x + n$			Pearson coefficient
x-values	y-values	k	p-value	R^2	ρ
HU avg occl	mRS end	0.227 ± 0.086	0.015	0.233	0.483
HU avg occl	# passes	0.119 ± 0.052	0.031	0.186	0.432
HU avg occl	mRS diff	-0.140 ± 0.067	0.049	0.158	-0.398
HU avg diff	RBC [%]	1.646 ± 0.809	0.053	0.153	0.391
HU avg occl	mRS start	0.087 ± 0.045	0.065	0.140	0.374
HU avg diff	mRS diff	-0.104 ± 0.059	0.093	0.118	-0.343

HU avg = average Hounsfield Units; occl = occluded MCA segment; diff = absolute difference; mRS = modified Rankin score; RBC [%] = percentage of red blood cells in the thrombi

tients and their retrieved thrombi included in the study.

Correlation between different pairs of data groups from Table 1 were tested by the Pearson correlation coefficient and the univariate linear regression analysis. Results of this analysis for the pairs with the highest correlation is shown by linear regression graphs in Figure 3 and their corresponding correlation and linear regression parameters are formulated in Table 2. The linear

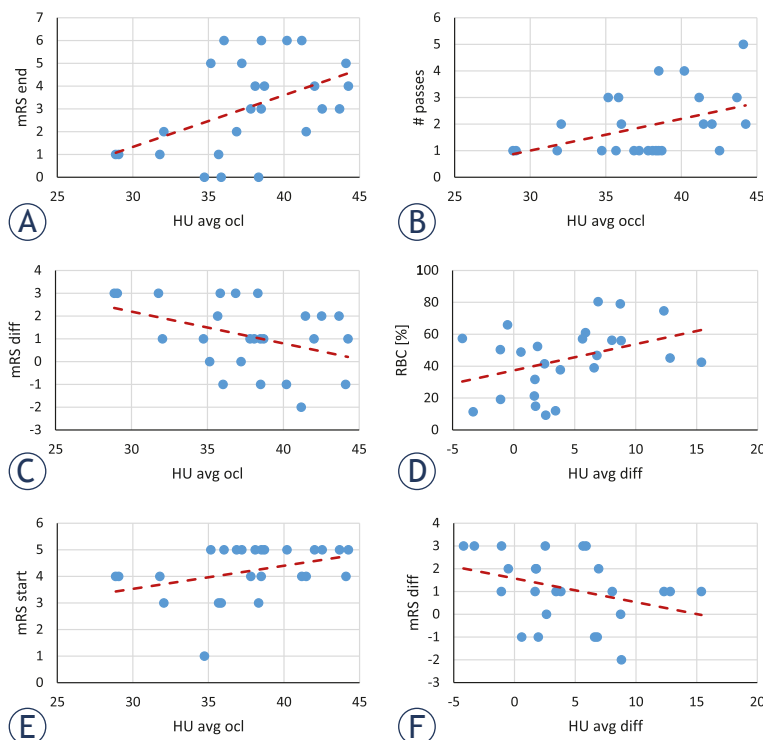


FIGURE 3. Graphs of correlation among different data groups. Shown are six graphs of data group pairs from Table 2 that have the highest Pearson coefficients and also statistically most significant linear regression parameters.

regression statistical analysis showed significant differences ($p < 0.05$) only in three cases, *i.e.*, for the group pairs: outcome mRS *vs.* average HU in the occluded MCA, the number of passes with the thrombectomy device *vs.* the average HU in the occluded MCA, and the difference between the initial and the outcome mRS *vs.* the average HU in the occluded MCA. The next three pairs, also included in Table 2 and Figure 3, had $0.05 < p < 0.1$ which can be considered as borderline significant. These pairs are: thrombus RBC proportion *vs.* the difference between the average HU in the occluded and normal MCA, initial mRS *vs.* the average HU in the occluded MCA and the difference between the initial and the outcome mRS *vs.* difference between average HU in the occluded and normal MCA. From the graphs in Figure 3A,E it can be inferred that the average HU in the occluded MCA is in positive correlation with both the initial and the outcome mRS. As the regression coefficient (slope k) is higher for the outcome mRS than the initial mRS, the correlation between difference of the initial and the outcome mRS ($mRS_{diff} = mRS_{start} - mRS_{end}$) and average HU in the occluded MCA is negative (Figure 3C). The number of passes of the thrombectomy device is also in positive correlation with the average HU in the occluded MCA (Figure 3b). The remaining two of the more significant correlations involve differentiation between the average HU in the occluded and the normal MCA which is in positive correlation with the RBC proportion (Figure 3D); and the negative correlation with the difference of mRSs (Figure 3F). From the results in Table 2, it can also be seen that the data group pairs with higher coefficients of determination R^2 in the linear regression analysis also have higher Pearson coefficients of correlation. Therefore, R^2 can also be considered a measure to the extent of correlation.

Discussion

CT was already employed to study properties of artificially made blood clots. In a study by Kirchhof *et al.* it was concluded that CT has a potential to differentiate between clots with high fibrinogen content and those with low content, but is unable to distinguish between pure plasma clots and low hematocrit clots.¹⁶ In a more recent study by Brinjikji *et al.* single-energy and dual-energy CT were compared in their power to differentiate among different types of artificial blood clots.¹⁷ They confirmed superiority of dual-energy CT in differentiation between high and low RBC content blood clots.

However, studies where CT properties of blood clots *in vivo* are studied are relatively scarce.¹⁸ In our study on correlations between CT properties of MCA thrombi and thrombectomy procedure parameters, treatment outcome, and histology the highest correlation was found between average HU in the occluded MCA (HU_{avg_occl}) and the stroke outcome assessed with mRS (mRS_{end}). According to our findings, higher average HU in the occluded MCA suggests higher mRS. This is because the most important factor among the factors that contribute to the assessment of mRS (such as extent of penumbra tissue, collateral vasculature, time from onset of the occlusion to the intervention, etc.) is the morphology of the thrombus, especially its compaction. Due to their retraction, thrombi with higher compaction, which are often older with low serum content^{19,20} have higher average HU values, while fresh thrombi with more serum spaces²¹, have lower overall HU.

The correlation between the number of passes with the thrombectomy device and average HU of the thrombi can also be associated with the thrombi organization. More organized (hard, fibrin-rich) thrombi can attach strongly with the arterial wall, which may result in the more difficult retrieval of such thrombus during the interventional procedure.²² This suggests, that if higher average HU values in the MCA occlusion are found on the CT scan, it is getting more likely that more than one pass will be needed to successfully retrieve the thrombus during the interventional procedure.

When treating patients with stroke, time is essential.²³ The longer time taken till reestablishment of the normal cerebral blood flow, the less oxygen is present in the brain, which may result in brain cell and nerve connection loss. This contributes to more serious symptoms and a higher mRS classification over time.²³ Outcome after mechanical thrombectomy can be more dependent on the capacity of collateral circulation than on the time from stroke onset.²⁴ However, time still plays an important role in saving tissue at risk (penumbra). In addition, the longer time taken till resolving the occlusion, the thrombus can retract further and therefore becomes more compact with a low serum content. Clot retraction is an important contributing factor for the correlation that was found between the initial mRS (mRS_{start} before the treatment) and the average HU of the thrombus (HU_{avg_occl}). This factor may also explain the correlation between the average HU of the thrombus (HU_{avg_occl}) and the mRS classification difference between the initial and the outcome scores (mRS_{diff}). As already

pointed out, a poorer treatment outcome can be expected in patients with poor collateral status.²⁵ However, time since the formation of thrombus also impacts its properties, especially its retraction, which increases with the time since thrombus formation.²⁶ The correlation between the average HU in the occluded MCA and the difference between the initial and the outcome mRS is negative (Figure 3C). This is because patients with a high average HU in the occluded MCA have usually higher initial mRS classification and their outcome mRS, on average is only slightly lower or even equal to the initial mRS due to the poor treatment results; *e.g.* patients with the initial mRS of 5 have often the outcome mRS of 4 or 5 so that the mRS difference (mRS_{diff}) is 0 or 1, which corresponds to a slim or no treatment improvement. In patients with low average HU in occluded MCA, the initial mRS classification is lower and therefore, their outcome mRS is even much lower, *e.g.*, patients with the initial mRS of 1-3 can recover to mRS of 0 or 1, so that the mRS difference is in the range 0-3. The treatment outcome in these patients is better due to the short time frame from thrombus formation to intervention which is associated with earlier reperfusion and smaller brain tissue damage.²⁷

In addition to average HU in the occluded MCA segment (HU_{avg_occl}), its difference to the corresponding value in normal MCA segment (HU_{avg_diff}) was measured as well. The average HU difference value has in principle advantage over the single-sided MCA values (HU_{avg_occl} and HU_{avg_nor}) as it is insensitive to possible offsets in HU values in CT images. The offsets cancel out in the subtraction of average HU values between the occluded and the normal MCA segments. Possible HU value offset can have an origin in image processing where consecutive three NCE CT image slices in the section with both MCA segments were stacked together. Therefore, the measured HU can in principle contain unwanted contributions from arterial wall and other tissues surrounding the vessel. In addition, the reference HU, that is measured in non-occluded symmetrical MCA segment, can be elevated due to possible arterial wall calcification, hematocrit level.

Positive correlation between RBC proportion ($RBC\ [%]$) and the difference between average HU in the occluded and normal MCA (HU_{avg_diff}) can be explained by the presence of iron in RBCs.²⁸ The thrombi with a higher proportion of RBC have a higher iron content and therefore absorb more X-rays so that an increased HU values are detected in the CT images of these thrombi. In addition,

thrombi with a higher proportion of RBC are also more compact, which further contributes to greater X-ray absorption. Another reason for increased HU values in the MCA region are also calcifications in the vessel wall, which cause higher X-ray absorption. If that is the case MCA may appear hyperdense also without thrombus in it.

Pretreatment thrombus evaluation can be of great clinical importance. Failure of thrombolytic treatment can be expected in fibrin rich thrombi. Thrombus composition can also have an impact on interventional treatment planning (mechanical thrombectomy). Optimal technique (stent retriever *vs.* aspiration) or device type selection can potentially be chosen on the basis of preoperative imaging data.

Major drawback of this study is limited number of cases ($n = 25$) and the use of sequential NCE CT. CT image resolution was insufficient to avoid the partial-volume effect in measurement HU profiles along the thrombi so that the HU profiles can be contaminated with HU values of the surrounding tissues. Specifically, in this study CT image analysis included stacking of three consecutive CT slices could result in inclusion of other brain tissues than the thrombus or normal MCA vessel because of the inferior bend of the MCA that can be anatomically present. Additional problem with the HU values of the vessel wall is that they can vary also due to possible atherosclerotic soft calcifications and these calcifications are often asymmetric, so that using the HU profile of the symmetric non-occluded MCA segment as the reference becomes questionable. If the spiral CT would be used instead of sequential CT, the CT images could also be processed in other (rotated) planes and the stacked slices could then be positioned and oriented ideally parallel to both MCA segments without compromising the quality of the observed vessel. This would make the HU measurements as well as the results more precise.

Conclusions

Routinely acquired CT images of stroke patients provide also information on HU values of thrombi that is usually ignored. In this study a relation between the HU value of a thrombus and its composition was confirmed. As more compact thrombus may represent a bigger problem for the interventional procedure a priori assessment of thrombus compaction is very important for good intervention planning. The present study also provides foundations for further studies where the accuracy

of study could be improved by increasing the number of samples (patients and thrombi) and having more accurate spiral CT images of patients with stroke that would allow improve HU value determination in the targeted region.

Acknowledgment

The authors thank Kanza Awais for proofreading the manuscript. This study was financially supported by the Slovenian Research Agency grant J3-9288.

References

1. Virani SS, Alonso A, Benjamin EJ, Bittencourt MS, Callaway CW, Carson AP, et al. Heart disease and stroke statistics-2020 update: a report from the American heart association. *Circulation* 2020; **141**: e139-596. doi: 10.1161/CIR.0000000000000757
2. Tran J, Mirzaei M, Anderson L, Leeder SR. The epidemiology of stroke in the Middle East and North Africa. *J Neurol Sci* 2010; **295**: 38-40. doi: 10.1016/j.jns.2010.05.016
3. Yamashita T, Abe K. Recent progress in therapeutic strategies for ischemic stroke. *Cell Transplant* 2016; **25**: 893-8. doi: 10.3727/096368916X690548
4. Mozaffarian D, Benjamin EJ, Go AS, Arnett DK, Blaha MJ, Cushman M, et al. Heart disease and stroke statistics-2016 update: a report from the American Heart Association. *Circulation* 2016; **133**: e38-360. doi: 10.1161/CIR.0000000000000350
5. Chernysh IN, Nagaswami C, Kosolapova S, Peshkova AD, Cuker A, Cines DB, et al. The distinctive structure and composition of arterial and venous thrombi and pulmonary emboli. *Sci Rep* 2020; **10**: 5112. doi: 10.1038/s41598-020-59526-x
6. Bajd F, Vidmar J, Fabjan A, Blinc A, Kralj E, Bizjak N, et al. Impact of altered venous hemodynamic conditions on the formation of platelet layers in thromboemboli. *Thromb Res* 2012; **129**: 158-63. doi: 10.1016/j.thromres.2011.09.007
7. Bajd F, Vidmar J, Blinc A, Sersa I. Microscopic clot fragment evidence of biochemo-mechanical degradation effects in thrombolysis. *Thromb Res* 2010; **126**: 137-43. doi: 10.1016/j.thromres.2010.04.012
8. Fang J, Tsui PH. Evaluation of thrombolysis by using ultrasonic imaging: an in vitro study. *Sci Rep* 2015; **5**: 11669. doi: 10.1038/srep11669
9. Broderick JP, Adeoye O, Elm J. Evolution of the modified rankin scale and its use in future stroke trials. *Stroke* 2017; **48**: 2007-12. doi: 10.1161/STROKEAHA.117.017866
10. Kwah LK, Diong J. National Institutes of Health Stroke Scale (NIHSS). *J Physiother* 2014; **60**: 61. doi: 10.1016/j.jphys.2013.12.012
11. Kim BJ, Kang HG, Kim HJ, Ahn SH, Kim NY, Warach S, et al. Magnetic resonance imaging in acute ischemic stroke treatment. *J Stroke* 2014; **16**: 131-45. doi: 10.5853/jos.2014.16.3.131
12. Provost C, Soudant M, Legrand L, Ben Hassen W, Xie Y, Soize S, et al. Magnetic resonance imaging or computed tomography before treatment in acute ischemic stroke. *Stroke* 2019; **50**: 659-64. doi: 10.1161/STROKEAHA.118.023882
13. Dehkharghani S, Andre J. Imaging approaches to stroke and neurovascular disease. *Neurosurgery* 2017; **80**: 991. doi: 10.1093/neuros/nyx268
14. Boodt N, Compagne KCJ, Dutra BG, Samuels N, Tolhuisen ML, Alves H, et al. Stroke etiology and thrombus computed tomography characteristics in patients with acute ischemic stroke: A MR CLEAN Registry Substudy. *Stroke* 2020; **51**: 1727-35. doi: 10.1161/STROKEAHA.119.027749

15. Leong FJ, Brady M, McGee JO. Correction of uneven illumination (vignetting) in digital microscopy images. *J Clin Pathol* 2003; **56**: 619-21. doi: 10.1136/jcp.56.8.619
16. Kirchhof K, Welzel T, Mecke C, Zoubaa S, Sartor K. Differentiation of white, mixed, and red thrombi: value of CT in estimation of the prognosis of thrombolysis phantom study. *Radiology* 2003; **228**: 126-30. doi: 10.1148/radiol.2273020530
17. Brinjikji W, Michalak G, Kadirvel R, Dai D, Gilvarry M, Duffy S, et al. Utility of single-energy and dual-energy computed tomography in clot characterization: an in-vitro study. *Interv Neuroradiol* 2017; **23**: 279-84. doi: 10.1177/1591019917694479
18. Liebeskind DS, Sanossian N, Yong WH, Starkman S, Tsang MP, Moya AL, et al. CT and MRI early vessel signs reflect clot composition in acute stroke. *Stroke* 2011; **42**: 1237-43. doi: 10.1161/STROKEAHA.110.605576
19. Kozak M, Mikac U, Blinc A, Sersa I. Lysability of arterial thrombi assessed by magnetic resonance imaging. *Vasa* 2005; **34**: 262-5. doi: 10.1024/0301-1526.34.4.262
20. Czapliski C, Albadawi H, Partovi S, Gandhi RT, Quencer K, Deipolyi AR, et al. Can thrombus age guide thrombolytic therapy? *Cardiovasc Diagn Ther* 2017; **7**: S186-96. doi: 10.21037/cdt.2017.11.05
21. Sabovic M, Lijnen HR, Keber D, Collen D. Effect of retraction on the lysis of human clots with fibrin specific and non-fibrin specific plasminogen activators. *Thromb Haemost* 1989; **62**: 1083-7. doi: 10.1055/s-0038-1647122
22. Kim BM. Causes and solutions of endovascular treatment failure. *J Stroke* 2017; **19**: 131-42. doi: 10.5853/jos.2017.00283
23. Chugh C. Acute ischemic stroke: management approach. *Indian J Crit Care Med* 2019; **23**: S140-6. doi: 10.5005/jp-journals-10071-23192
24. Jeromel M, Milosevic ZV, Oblak JP. Mechanical recanalization for acute bilateral cerebral artery occlusion—literature overview with a case. *Radiol Oncol* 2020; **54**: 144-8. doi: 10.2478/raon-2020-0017
25. Bang OY, Saver JL, Kim SJ, Kim GM, Chung CS, Ovbiagele B, et al. Collateral flow predicts response to endovascular therapy for acute ischemic stroke. *Stroke* 2011; **42**: 693-9. doi: 10.1161/STROKEAHA.110.595256
26. Ohnson S, Chueh J, Gounis MJ, McCarthy R, McGarry JP, McHugh PE, et al. Mechanical behavior of in vitro blood clots and the implications for acute ischemic stroke treatment. *J Neurointerv Surg* 2020; **12**: 853-7. doi: 10.1136/neurintsurg-2019-015489
27. Hacke W, Donnan G, Fieschi C, Kaste M, von Kummer R, Broderick JP, et al. Association of outcome with early stroke treatment: pooled analysis of ATLANTIS, ECASS, and NINDS rt-PA stroke trials. *Lancet* 2004; **363**: 768-74. doi: 10.1016/S0140-6736(04)15692-4
28. Velasco Gonzalez A, Buerke B, Gorlich D, Fobker M, Rusche T, Sauerland C, et al. Clot analog attenuation in non-contrast CT predicts histology: an experimental study using machine learning. *Transl Stroke Res* 2020; **11**: 940-9. doi: 10.1007/s12975-019-00766-z

The role of unenhanced phase of the liver in the scanning protocol of metastatic breast cancer: implications for sensitivity, response evaluation and size measurement

Juan José Arenas-Jiménez, Elena García-Garrigós, Mariana Cecilia Planells-Alduvín

Department of Radiology, Hospital General Universitario de Alicante, Instituto de Investigación Sanitaria y Biomédica de Alicante (ISABIAL), FISABIO Hospital General Universitario de Alicante, Alicante, Spain

Radiol Oncol 2021; 55(4): 418-425.

Received 13 February 2021
Accepted 1 May 2021

Correspondence to: Juan José Arenas-Jiménez, Ph.D., Department of Radiology, Hospital General Universitario de Alicante, Instituto de Investigación Sanitaria y Biomédica de Alicante (ISABIAL), FISABIO Hospital General Universitario de Alicante, Av Pintor Baeza 12, 03010, Alicante, Spain 03560. E-mail: j.arenasjimenez@gmail.com

Disclosure: No potential conflicts of interest were disclosed.

This is an open access article under the CC BY-NC-ND license (<http://creativecommons.org/licenses/by-nc-nd/4.0/>).

Background. To analyse if performing unenhanced CT of the liver aids in the evaluation of metastatic lesions, response assessment or alter the size of the lesions, compared with portal phase alone, in patients with hepatic metastases from breast carcinoma.

Patients and methods. One-hundred and fifty-three CT scans of 36 women were included. Scans consisted of unenhanced, arterial and portal delayed phases of the liver. Two readers sorted which phase was best for visualization of metastases, evaluated the number of lesions detected in each phase, selected the best phase for assessment of response in two consecutive scans, and measured one target lesion in all the phases. X^2 was used to compare differences among phases and paired t test for measurement differences.

Results. Unenhanced, arterial and portal phases were considered better phases by readers 1/2 in 68/67%, 27/28% and 69/70%, and some lesions were missed in 2%, 11% and 7%, respectively. Sensitivity was significantly better for unenhanced and portal phases compared to arterial phase. Comparison between consecutive scans was considered better in unenhanced (80/79%), followed by portal (70/69%) and arterial phases (31/31%). Maximum diameter of target lesions was 15% greater in unenhanced phase ($p < 0.001$).

Conclusions. Portal and unenhanced phases of the liver allow better detection and delineation of metastatic hepatic lesions from breast carcinoma. In most cases, unenhanced CT is the best phase to assess response and provides the largest diameter. Therefore, we recommend the use of unenhanced CT in the evaluation of patients with breast carcinoma and suspected or known hepatic metastatic disease.

Key words: breast cancer; staging; computed tomography; metastases; hepatic lesion

Introduction

Breast cancer is the neoplasm with the highest incidence and mortality rates among women worldwide, and hepatic metastases appear in more than 50% of patients with advanced disease.^{1,2}

Conspicuity and detection of lesions in multiple phases of contrast enhanced CT of the liver has

been evaluated in patients with metastases.^{3,6} The need of unenhanced CT for detection of metastases has been debated from the early times of oncologic applications of CT^{7,8}, with unenhanced phase being used for scanning breast cancer patients in 21% of the institutions in a survey.⁹

Some studies evaluate the need of multiple phases of dynamic CT of the liver for a better de-

tection of hepatic metastases from breast cancer, but they were performed in the 1990s, with much different technological equipment and therapeutic schemes compared to those used nowadays.^{3,7,8,10,11} In those studies, unenhanced CT added little to the enhanced phases in terms of the amount of lesions detected, although it was demonstrated that some lesions are only or better seen in that phase. Moreover, it has been proved that the size of the lesions is different in unenhanced CT compared to other phases, with one study concluding that the unenhanced CT depicts the maximum volume of hepatic metastases.³ More recently, a Critical Appraised Topic on this subject¹² addressed the need of confirmation of the role of unenhanced CT with modern technology and, more importantly, remarked the need to evaluate the confidence of radiologists to delineate the lesions, that plays a major role in measurement and response evaluation.

In this setting, our hypothesis was that, in patients with breast cancer, unenhanced CT, even with modern equipment, could add information to enhanced CT of the liver in patients with hepatic metastases by increasing the detection of lesions, permitting greater confidence for delineation of the metastases and providing a more accurate depiction of the size of them. For this purpose, we conducted this study, in a series of patients with breast cancer and hepatic metastases detected by CT, comparing tumor conspicuity, sensitivity, comparison on follow-up examination and size of hepatic metastasis in unenhanced, arterial and portal phases of the liver.

Patients and methods

This retrospective observational study was reviewed and approved by the institutional review board and local ethics committee. Informed consent was waived since no intervention was made on the routine institutional protocol for the purpose of the study.

Patient population

From May 2016 to February 2018, patients with already known or newly diagnosed hepatic metastases from breast cancer referred to our department for a CT, either as initial staging or for follow-up, were consecutively included. Patients were excluded if CT wasn't performed according to the scan protocol detailed below, if contrast injection protocol couldn't be achieved as described,

or if they weighted less than 50 or more than 100 kg. A total of 48 patients with hepatic metastases were scanned during that period. Of them, 12 were excluded for the following reasons: contrast protocol couldn't be achieved in 9 patients due to either renal insufficiency or inadequate vein access, 2 for weighing more than 100 kg and one less than 50 kg. Finally, 153 examinations in 36 women (range 1–7) were included, 4 were the initial examination and the remaining 149 were follow-up. Mean age was 59.2 years, range 34–77. Histological confirmation of metastases was available in 2 patients, in the rest, clinical and radiological diagnosis was established taking into consideration radiological presentation and follow-up. No case had to be excluded due to diagnostic uncertainty for presenting indeterminate lesions posing diagnostic doubts at follow-up.

CT protocols

All CT scans were obtained with a 64-MDCT scanner (Philips Brilliance 64, Philips Medical Systems, Cleveland, OH, USA) according to our institutional scanning protocol for breast cancer, consisting of an unenhanced CT of the liver followed by arterial phase at 30 seconds that includes the chest, and portal phase of the abdomen and pelvis at 70 seconds. The protocol changed during the study period after the results of another study underwent at our hospital in patients with lung cancer.¹³ The new protocol consisted in an arterial scan at 35 seconds of the liver, followed by a single delayed acquisition at 65 seconds that included chest, abdomen and pelvis.¹³ Finally, 79 scans were performed with the first protocol, and 74 with the new changes.

All patients received a standardized IV injection through a power injector consisting of iomeprol (Iomeron, Bracco) with an iodine concentration of either 350 or 400 mg I/mL, at a dose of 0.5 g I/kg with a fixed 40-second duration of injection, followed by a 30-mL saline chaser at the same rate as for the contrast medium.

Image analysis

Two radiologists (10 and 20 years experienced) independently reviewed CT images at a PACS workstation (Centricity PACS Universal Viewer 6.0, GE Healthcare). Window settings could be changed as desired. Four reading rounds were performed by each reader that are summarized in Figure 1. Firstly, all phases were assessed independently, and unenhanced, arterial and portal phases were sorted from best to worst according to the subjec-

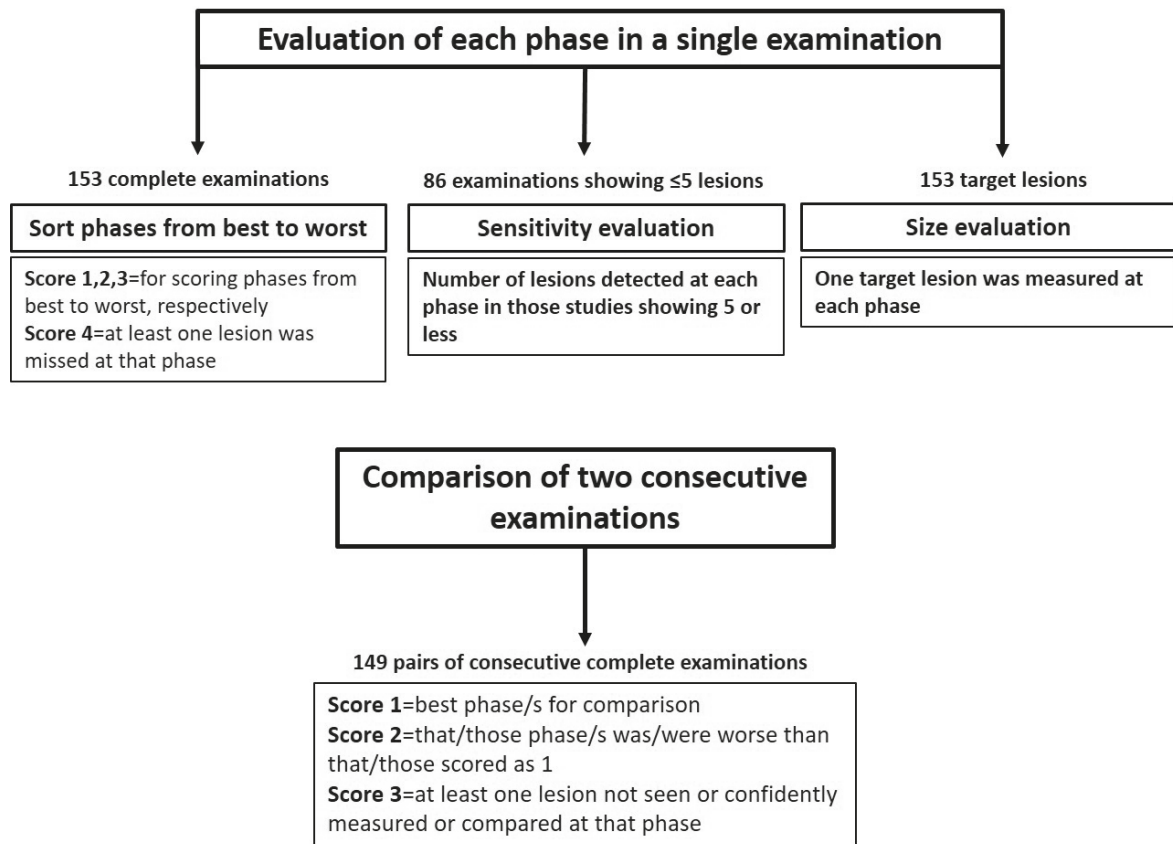


FIGURE 1. Flowchart of the reading protocol. There were four steps: sort of phases from best to worst, sensitivity study based only on the reading of examinations having ≤ 5 metastases, measurement of one target lesion in each examination and evaluation of phases for comparing metastases in 2 consecutive follow-up scans.

tive perception of visualization, conspicuity and delineation of hepatic metastases. If two phases were considered to show lesions in a similar manner, they were scored equally (1 if they were better than the other or 2 if worst). If any lesion was missed by one phase, the score was 4. At this reading, lesions were counted taking into consideration all phases. Lesions were numbered if 5 or less were depicted, and noted if they were more than 5. In a second round, for sensitivity evaluation, readers counted the number of lesions detected in each phase of the 86 examinations that showed 5 lesions or less in the previous reading, randomly presented in a set of 258 complete phases of the liver. The third evaluation round consisted of the comparison of the different phases for assessment of response of hepatic metastases in two paired consecutive scans of the same patient, when available. Both scans were reviewed together, and each phase was scored as 1 if it was the best for compar-

son or 2 if response assessment was judged worse compared to other phase. If two phases performed similarly, they were scored equally and, if any lesion was missed or was impossible to confidently be measured for comparison in any phase, it was scored as 3, and considered to alter the assessment of response. Finally, the fourth reading session was the measurement of a target lesion in each examination. For that purpose, a third radiologist, based on previous radiologic reports and her own evaluation, selected and marked a target lesion from each examination in all phases. The lesion she chose was clearly differentiated from others and, if possible, accurately defined in all phases. Readers measured the maximum diameter of the target lesions in the 3 phases of all examinations.

The number of lesions was calculated taking as the reference standard all phases together as well as the follow-up, as is the clinical standard when treating patients with metastatic breast cancer.

Statistical analysis

Differences in rating among phases were compared by chi-square test. Weighted kappa statistics was used to measure the degree of agreement between observers for rating different phases. Paired t test was used to compare measurements in each phase. Statistical analysis was performed with the software package IBM SPSS Statistics (version 21, IBM). Statistical significance was set at 0.05.

Results

Scoring of individual examinations

The score of each phase for individual assessment of each examination is presented at Table 1. Portal phase was considered a better phase (score 1) in 68 and 67.3% by readers 1 and 2 respectively, score 1 for unenhanced phase was 69.3 and 69.9%, while arterial phase was better in 26.1 and 27.5%, with differences being statistically significant ($p < 0.005$). The percentage of examinations with at least one missed lesion (score 4) was 1.3 and 2% for readers 1 and 2 respectively in unenhanced phase, 6.5% for both readers in portal phase and 10.5 and 11.8 % for arterial phase (Figure 2,3). No lesion was missed in unenhanced and portal phases together. Agreement between observers for this reading was “good” with kappa values of 0.703, 0.726 and 0.793 for unenhanced, arterial and portal phases, respectively.

Sensitivity evaluation

During the first reading session in which all phases were considered, there were 5 metastatic lesions or less in 86 examinations (56.2%), showing 228 lesions. The sensitivities for readers 1/2 were 97.4/96% for unenhanced, 88.6/89% for arterial and 97.8/97.4% for portal phases, respectively.

Scoring of assessment of response

Results of comparison of lesions between two consecutive scans are shown in Table 2. Comparison was considered better in 81.2/79.2% of unenhanced, 30.9/31.5% arterial and 71.1/69.8% of portal phases, by readers 1/2, respectively. Agreement between observers for scoring comparisons was “excellent” with values of 0.917, 0.964 and 0.882 for unenhanced, arterial and portal phases, respectively. Considering all 298 readings, in 154 of them (51.7%), unenhanced and portal phases were together the best phases (score 1), unenhanced phase

TABLE 1. Distribution of scores of each phase by both readers in 153 examinations

		Reader 1					
		UNENHANCED					
		1	2	3	4		
PORTAL	1	ARTERIAL	32	2	2	0	
			16	20	10	1	
			9	10	0	0	
			4	0	0	0	
	2	ARTERIAL	1	0	2	0	
			6	0	0	0	
			15	0	0	1	
			3	0	0	0	
	3	ARTERIAL	1	1	0	0	
			4	0	0	0	
			4	0	0	0	
			0	0	0	0	
4	ARTERIAL	2	1	0	0		
		9	0	0	0		
		Reader 2					
		UNENHANCED					
		1	2	3	4		
PORTAL	1	ARTERIAL	30	5	1	0	
			18	20	7	1	
			7	12	0	0	
			6	0	0	0	
	2	ARTERIAL	1	2	0	2	1
			6	0	0	1	
			14	0	0	0	
			3	0	0	0	
	3	ARTERIAL	1	1	0	0	
			3	0	0	0	
			3	0	0	0	
			1	0	0	0	
4	ARTERIAL	2	1	0	0		
		9	0	0	0		

Scores were 1: best phase; 2: second best; 3: worst; 4: at least one lesion was missed at that phase. Figures are number of examinations.

was considered the only best phase in 85 (28.5%) readings, portal phase in 44 (14.8%), and arterial phase was considered the only best phase for comparison in 3 readings (1%). In 14 examinations, unenhanced phase allowed to compare lesions that could not be evaluated by portal phase (Figure 2). On a per patient basis, this occurred in at least one scan in 6 out of 36 patients along the study.

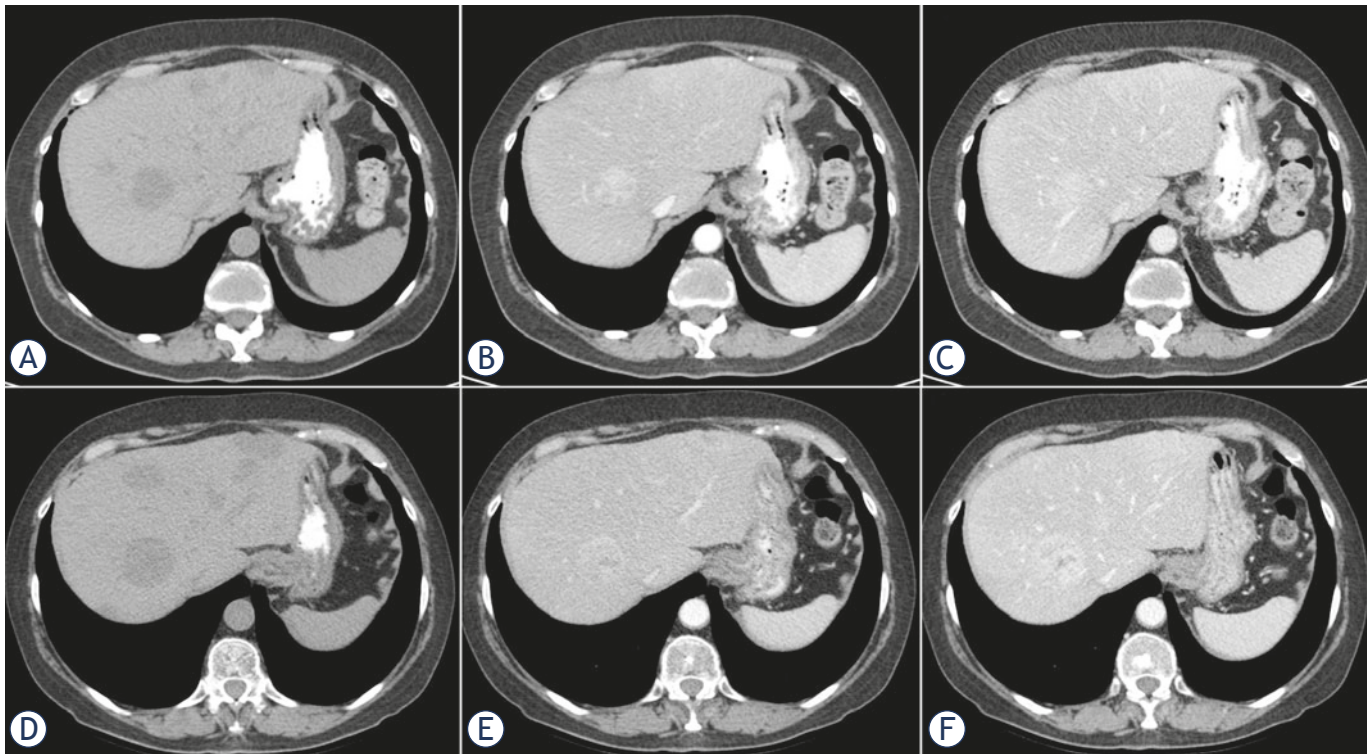


TABLE 2. Distribution of scores of each phase for comparing metastatic lesions in two consecutive scans by both readers in 149 examinations

		Reader 1		UNENHANCED		
				1	2	3
PORTAL	1	ARTERIAL	1	35	6	1
			2	42	20	0
			3	2	0	0
	2	ARTERIAL	1	3	0	1
			2	23	0	0
			3	2	0	0
3	ARTERIAL	2	1	0	0	
		3	13	0	0	
		Reader 2		UNENHANCED		
				1	2	3
PORTAL	1	ARTERIAL	1	39	4	1
			2	34	24	0
			3	2	0	0
	2	ARTERIAL	1	1	0	2
			2	26	0	0
			3	2	0	0
3	ARTERIAL	2	1	0	0	
		3	13	0	0	

Scores were 1: best phase/s for comparison; 2: that phase was worse for comparing lesions than that scored as 1; 3: at least one lesion was not seen or could not be confidently measured or compared at that phase. Figures are number of examinations.

FIGURE 2. 48-year-old woman with hepatic metastases from breast cancer. Upper row corresponds to previous study and lower row is follow-up. Previous unenhanced phase (A) show more lesions than either the arterial (B) and portal (C) phases. At follow-up 6 weeks later, worsening seen in unenhanced phase (D) cannot be confidently confirmed only by arterial (E) and portal (F) phases.

Size of target lesions

Maximum diameter of target lesions was statistically significant larger in unenhanced phase than in either arterial or portal phases ($p < 0.001$) for both observers, as shown in Table 3 (Figure 3). Differences of measurements in unenhanced phase were $\geq 20\%$ compared to portal phase in 29.7% of measurements by reader 1, and in 30.1% by reader 2.

Discussion

Hepatic metastasis from breast cancer appear in more than 50% of patients with advanced disease, for that reason an adequate detection of the lesions is desirable.

Oncologic guidelines about imaging evaluation of patients with breast cancer lack recommendations about the scanning protocol¹⁴, while specific radiological recommendations consider only the need of a portal phase.^{15,16} However, some authors

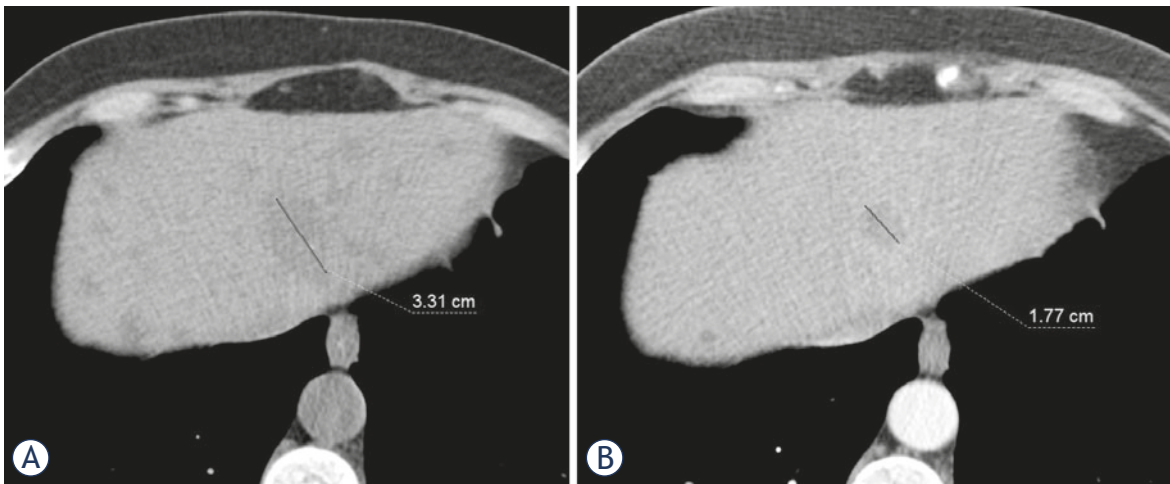


FIGURE 3. 56-year-old woman with hepatic metastases from breast cancer. Measurement of target lesion in unenhanced phase (A) is 33 mm and in the portal phase (B) is 18 mm, that represent a 45% difference. A part of the metastatic lesion posteriorly is scarcely seen as a subtle increase attenuation in the portal phase, but both readers failed to consider that area as part of the lesion, and measured only the hypoattenuating component. Note how unenhanced phase also shows other small lesions not seen in the portal phase.

recommend unenhanced phase for these patients¹⁷ and, in a survey⁹, unenhanced CT was used in 21% of institutions for breast cancer evaluation. These variations make necessary clarification of this issue.

The primary role of imaging in patients with hepatic metastasis is to get the best delineation of the lesions for their detection and adequate comparison in follow-up. The goal of contrast enhanced CT of the liver is to get the optimal lesion-to-liver contrast, and for that purpose, different phases after contrast administration may be useful. In our experience, hepatic metastases from breast cancer are sometimes very difficult to differentiate from normal liver in portal phase, while unenhanced images depict them surprisingly well. This fact had already been studied and discussed in several studies carried out in the 1990s.^{3,7,8,10,11} More recently, a Critically Appraised Topic Review by Sadigh *et al.*¹², concluded that unenhanced CT adds a small incremental value to contrast enhanced CT for the detection of hypervascular metastases, however they remarked that those studies were performed with older CT scanners and contrast infusion technologies which may limit the interpretation of data. Moreover, radiologist's confidence level for detecting lesions hasn't been evaluated in most studies, and it was not clear in most of them whether the CT scan was used as initial staging or for follow-up after treatment. It is also important to consider that the therapeutic arsenal available has expanded and could change the way lesions are seen.

In this setting, our purpose was to evaluate if, with modern equipment and chemotherapy regimens in patients with hepatic metastases from breast cancer, unenhanced CT played any role for detection of lesions, aided in the comparison of studies for response evaluation and if there were significant differences in the size of the lesions.

When readers were asked which phases better showed the lesions, both agreed that portal and unenhanced phases were better than arterial phase in most patients. This is in agreement with older studies evaluating lesion conspicuity in unenhanced phase compared with contrast enhanced⁷, and with arterial and portal phases.³ It is important to note that sensitivity of the unenhanced phase was very similar to that of portal phase both in the joined evaluation and in the number of lesions detected, and that unenhanced and portal phases together didn't miss any lesion detected by arterial phase. That has practical implications, since arterial phase could be eliminated in our series maintaining a

TABLE 3. Measurements of target lesions by phase

	Unenhanced	Arterial	Portal
Reader 1	27.6 ± 18.7	23.9 ± 18.9	24.2 ± 18.2
Reader 2	27.4 ± 18.6	24.0 ± 18.7	24.1 ± 18.0

Figures are mean ± standard deviation, in millimeters. Differences between unenhanced and arterial, and unenhanced and portal phases $p < 0.0001$ for both readers; differences between arterial and portal phases $p = 0.510$ for reader 1 and $p = 0.620$ for reader 2.

perfect detection rate. Except for one study¹⁰, that shows a significant greater sensitivity of portal compared to unenhanced phase, the rest of studies evaluating sensitivity for detection of hepatic metastases from breast cancer find similar sensitivities for unenhanced and portal phases, with slight differences favouring one phase or another^{3,7,8,11}, as in our case. All these studies, and others including metastases from breast cancer as a proportion of patients included¹⁸, agree that arterial phase adds less than does unenhanced phase.

In contrast with all the other studies previously referred, this is the first one examining the role of unenhanced phase for evaluating response in follow-up studies of patients with breast cancer, that is one of the most frequent uses of CT in this population. Since most patients have multiple lesions, detection of any lesion is enough to make a correct diagnosis at the patient level, however, when evaluating response, all the lesions should be detected, and an optimal delineation of them in both examinations being compared is desirable. At this point, the role of unenhanced CT gains relevance, since it was the only phase which allowed to compare all the lesions in 8.7% of the readings, and was the single best phase in 28.5%. Again, unenhanced and portal phase were both the best phases for comparison in more than 50%, while the arterial phase played a marginal role for this purpose. According to our results, addition of only unenhanced phase of the liver, and not an arterial phase, to a single acquisition portal phase of the chest, abdomen and pelvis is the optimal protocol for better evaluating metastatic disease of the liver in follow-up comparisons in patients with breast cancer. We think that recommendations suggesting the elimination of all phases except for the portal phase^{15,16} do not have in consideration this important role of unenhanced phase in follow-up, and only consider its marginal role in the overall detection of lesions.

One study³ reported that unenhanced CT provided the maximal tumor volume, and our results agreed, obtaining approximately 15% larger diameter over portal phase. This contrasts with the results of one study¹⁹ in the evaluation of unenhanced CT in patients with gastric and colon cancer, in which lesions are shown to be significantly smaller and with much lower sensitivity than in portal phase. Conversely, for the measurement of hepatic metastases of neuroendocrine tumour, unenhanced phase has been suggested as the most reliable.²⁰ It must be taken in mind, that when evaluating response by RECIST 1.1, the longest diameter of the target lesions in the phase that it is better

shown and more confidently measurable must be used²¹, and in our study it was unenhanced phase in many cases. Moreover, differences in measurements between portal and unenhanced phases are clinically significant since roughly a 30% of patients showed differences of $\geq 20\%$.

Our study has several limitations. First, we did not have a pathological confirmation of most lesions as occurs in the usual clinical practice, however, clinical diagnosis and follow-up provided unequivocal behaviour as metastases in all cases. Second, for sensitivity evaluation we lacked a pathological or other imaging technique reference standard, instead we took the evaluation of all phases together as the reference. Although this is a major weakness of our investigation, this approach is nearer to the radiologist's daily work and the real clinical scenario, where radiologists can evaluate all phases together, and some subtle lesions can only be considered after confirming their presence in other phases or in follow-up. Although substantial bias could be derived from this approach, the degree of agreement shown by kappa values supported the reproducibility of our results. It could be argued that some lesions might be missed by all phases, however, their clinical relevance is unknown. Third, a formal sensitivity evaluation was performed only in examinations with 5 lesions or less. The reason for this was that many of the remaining studies had uncountable lesions, and counting all the metastases could be an arduous task, not necessarily representing the real number of detectable lesions, due to confluent metastases and different appearance depending of the phases. However, the proportion of lesions examined by choosing this cut-off of 5 lesions, might give us an approach to the real sensitivity of each phase. Fourth, regarding the measurement differences, whether the greater size in unenhanced images corresponds to tumour infiltration or to other parenchymal changes is not clear. In many cases, with lesions clearly larger in unenhanced phase, margins of the lesions in the other phases were difficult to ascertain and some lesions were actually not visible as shown in the figures. As Zimmerman *et al.*³, we lack a pathologic correlation, except for only one recent case not included in the study, with pathological measurements of resected metastases being much closer to those obtained at unenhanced than at portal phase. Finally, although we have evaluated an adequate number of examinations, the number of patients is limited and they were being treated with a variety of chemotherapy schemes, limiting to take more general conclu-

sions about the possible role of different therapeutic regimens on the visualization of lesions in one phase or another. In conclusion, our results showed that unenhanced and portal phases of the liver permitted better detection and delineation of metastatic lesions from breast carcinoma, and that unenhanced phase provided the largest diameter and in most cases was the best phase for comparing consecutive CT scans to assess response. For these reasons, our recommendation for institutions that don't do so, is that they use unenhanced CT in addition to the portal phase of the liver for evaluation for patients with breast carcinoma and suspected or known hepatic metastatic disease.

Acknowledgement

This investigation has been supported by Instituto de Investigación Sanitaria y Biomédica de Alicante (ISABIAL)- (grant no. 19-0259).

References

- Bray F, Ferlay J, Soerjomataram I, Siegel RL, Torre LA, Jemal A. Global cancer statistics 2018: GLOBOCAN estimates of incidence and mortality worldwide for 36 cancers in 185 countries. *CA Cancer J Clin* 2018; **68**: 394-424. doi: 10.3322/caac.21492
- Chikarmane SA, Tirumani SH, Howard SA, Jagannathan JP, DiPiro P. Metastatic patterns of breast cancer subtypes: what radiologists should know in the era of personalized cancer medicine. *Clin Radiol* 2015; **70**: 1-10. doi: 10.1016/j.crad.2014.08.015
- Zimmerman P, Lu DS, Yang LY, Chen S, Sayre J, Kadell B. Hepatic metastases from breast carcinoma: comparison of noncontrast, arterial-dominant, and portal-dominant phase spiral CT. *J Comput Assist Tomogr* 2000; **24**: 197-203. doi: 10.1097/00004728-200003000-00003
- Sica GT, Ji H, Ros PR. CT and MR imaging of hepatic metastases. *AJR Am J Roentgenol* 2000; **174**: 691-8. doi: 10.2214/ajr.174.3.1740691
- Francis IR, Cohan RH, McNulty NJ, Platt JF, Korobkin M, Gebremariam A, et al. Multidetector CT of the liver and hepatic neoplasms: effect of multiphase imaging on tumor conspicuity and vascular enhancement. *AJR Am J Roentgenol* 2003; **180**: 1217-24. doi: 10.2214/ajr.180.5.1801217
- Soyer P, Pocard M, Boudiaf M, Abitbol M, Hamzil, Panis Y, et al. Detection of hypovascular hepatic metastases at triple-phase helical CT: sensitivity of phases and comparison with surgical and histopathologic findings. *Radiology* 2004; **231**: 413-20. doi: 10.1148/radiol.2312021639
- DuBrow RA, David CL, Libshitz HI, Lorigan JG. Detection of hepatic metastases in breast cancer: the role of nonenhanced and enhanced CT scanning. *J Comput Assist Tomogr* 1990; **14**: 366-9. doi: 10.1097/00004728-199005000-00008
- Patten RM, Byun JY, Freeny PC. CT of hypervascular hepatic tumors: are unenhanced scans necessary for diagnosis? *AJR Am J Roentgenol* 1993; **161**: 979-84. doi: 10.2214/ajr.161.5.8273641
- O'Malley ME, Halpern E, Mueller PR, Gazelle GS. Helical CT protocols for the abdomen and pelvis: a survey. *AJR Am J Roentgenol* 2000; **175**: 109-13. doi: 10.2214/ajr.175.1.1750109
- Frederick MG, Paulson EK, Nelson RC. Helical CT for detecting focal liver lesions in patients with breast carcinoma: comparison of noncontrast phase, hepatic arterial phase, and portal venous phase. *J Comput Assist Tomogr* 1997; **21**: 229-35. doi: 10.1097/00004728-199703000-00012
- Sheafor DH, Frederick MG, Paulson EK, Keogan MT, DeLong DM, Nelson RC. Comparison of unenhanced, hepatic arterial-dominant, and portal venous-dominant phase helical CT for the detection of liver metastases in women with breast carcinoma. *AJR Am J Roentgenol* 1999; **172**: 961-8. doi: 10.2214/ajr.172.4.10587129
- Sadigh G, Applegate KE, Baumgarten DA. Comparative accuracy of intravenous contrast-enhanced CT versus noncontrast CT plus intravenous contrast-enhanced CT in the detection and characterization of patients with hypervascular liver metastases: a critically appraised topic. *Acad Radiol* 2014; **21**: 113-25. doi: 10.1016/j.acra.2013.08.023
- García-Garrigós E, Arenas-Jiménez JJ, Sánchez-Payá J. Best Protocol for combined contrast-enhanced thoracic and abdominal CT for lung cancer: a single-institution randomized crossover clinical trial. *AJR Am J Roentgenol* 2018; **210**: 1226-34. doi: 10.2214/ajr.17.19185
- Cardoso F, Senkus E, Costa A, Papadopoulos E, Aapro M, Andre F, et al. 4th ESO-ESMO International Consensus Guidelines for Advanced Breast Cancer (ABC 4). *Ann Oncol* 2018; **29**: 1634-57. doi: 10.1093/annonc/mdy192
- Barter S, Britton P. Breast cancer. In: Nicholson T, editor. *Recommendations for cross-sectional imaging in cancer management*. Second edition. London: The Royal College of Radiologists; 2014.
- Johnson PT, Bello JA, Chatfield MB, Flug JA, Pandharipande PV, Rohatgi S, et al. New ACR choosing wisely recommendations: judicious use of multiphase abdominal CT protocols. *J Am Coll Radiol* 2019; **16**: 56-60. doi: 10.1016/j.jacr.2018.07.026
- Siewert B, Sosna J, McNamara A, Raptopoulos V, Kruskal JB. Missed lesions at abdominal oncologic CT: lessons learned from quality assurance. *Radiographics* 2008; **28**: 623-38. doi: 10.1148/rg.283075188
- Oliver JH 3rd, Baron RL, Federle MP, Jones BC, Sheng R. Hypervascular liver metastases: do unenhanced and hepatic arterial phase CT images affect tumor detection? *Radiology* 1997; **205**: 709-15. doi: 10.1148/radiology.205.3.9393525
- Jee HB, Park MJ, Lee HS, Park MS, Kim MJ, Chung YE. Is non-contrast CT adequate for the evaluation of hepatic metastasis in patients who cannot receive iodinated contrast media? *PLoS One* 2015; **10**: e0134133. doi: 10.1371/journal.pone.0134133
- Huh J, Park J, Kim KW, Kim HJ, Lee JS, Lee JH, et al. Optimal phase of dynamic computed tomography for reliable size measurement of metastatic neuroendocrine tumors of the liver: comparison between pre- and post-contrast phases. *Korean J Radiol* 2018; **19**: 1066-76. doi: 10.3348/kjr.2018.19.6.1066
- Eisenhauer EA, Therasse P, Bogaerts J, Schwartz LH, Sargent D, Ford R, et al. New response evaluation criteria in solid tumours: revised RECIST guideline (version 1.1). *Eur J Cancer* 2009; **45**: 228-47. doi: 10.1016/j.ejca.2008.10.026

Diagnostic performance of p16/Ki-67 dual immunostaining at different number of positive cells in cervical smears in women referred for colposcopy

Ursula Salobir Gajsek¹, Andraz Dovnik², Iztok Takac^{2,3}, Urska Ivanus^{4,5}, Tine Jerman⁴, Simona Sramek Zatler⁶, Alenka Repse Fokter⁶

¹ Department of Obstetrics and Gynecology, General Hospital Celje, Celje, Slovenia

² University Department of Gynecology and Perinatology, University Medical Center Maribor, Maribor, Slovenia

³ Department of Gynecology and Obstetrics, Faculty of Medicine, University of Maribor, Maribor, Slovenia

⁴ National Cervical Cancer Screening Programme and Registry ZORA, Cancer Screening Department, Institute of Oncology Ljubljana, Ljubljana, Slovenia

⁵ Faculty of Medicine, University of Ljubljana, Ljubljana, Slovenia

⁶ Department of Pathology and Cytology, General Hospital Celje, Celje, Slovenia

Radiol Oncol 2021; 55(4): 426-432.

Received 7 July 2020

Accepted 28 September 2021

Correspondence to: Uršula Salobir Gajšek, M.D., Department of Obstetrics and Gynecology, General Hospital Celje, Oblakova 5, 3000 Celje, Slovenia. E-mail: urska.salobir.gajsek@gmail.com

Disclosure: No potential conflicts of interest were disclosed.

This is an open access article under the CC BY-NC-ND license (<http://creativecommons.org/licenses/by-nc-nd/4.0/>).

Background. The aim of the study was to evaluate the diagnostic accuracy of p16/Ki-67 dual immunostaining (p16/Ki-67 DS) in cervical cytology and the number of positive p16/Ki-67 cells to diagnose high grade cervical intraepithelial neoplasia (CIN2+) in colposcopy population.

Subjects and methods. We performed an analysis on a subset cohort of 174 women enrolled within a large-scale randomised controlled human papillomavirus (HPV) self-sampling project organised as part of the population-based Cervical Cancer Screening Programme ZORA in Slovenia. This subset cohort of patients was invited to the colposcopy clinic, underwent p16/Ki-67 DS cervical cytology and had the number of p16/Ki-67 positive cells determined.

Results. Among analysed women, 42/174 (24.1%) had histologically confirmed CIN2+. The risk for CIN2+ was increasing with the number of positive cells ($p < 0.001$). The sensitivity of p16/Ki-67 DS for detection of CIN2+ was 88.1%, specificity was 65.2%, positive predictive value was 44.6% and negative predictive value was 94.5%.

Conclusions. Dual p16/Ki-67 immunostaining for the detection of CIN2+ has shown high sensitivity and high negative predictive value in our study, which is comparable to available published data. The number of p16/Ki-67 positive cells was significantly associated with the probability of CIN2+ detection. We observed a statistically significant and clinically relevant increase in specificity if the cut-off for a positive test was shifted from one cell to three cells.

Key words: cervical cytology; high-grade dysplasia; p16/Ki-67 immunostaining

Introduction

For many decades, cervical cancer prevention has been based on screening with cervical cytology.¹ This method has two major drawbacks: high variability in interpretation among cytopathologists and

relatively low sensitivity, which requires shorter screening intervals.² The interpretation of cervical cytology requires experience and long-term training.³

Inevitable factor in development of cervical cancer is infection with high-risk human papillomavi-

rus (HPV)⁴, but it is not sufficient. However, other cofactors, such as smoking, have been identified to increase the risk of cervical cancer in HPV positive women as well.^{5,6} Some European countries have already implemented primary HPV screening in women aged 30–35 years and older due to the higher sensitivity of validated HPV tests compared to cytology, taking into account the lower specificity of HPV tests due to high HPV prevalence in younger women.^{1,7}

Due to the challenges of cytology and HPV cervical screening, novel biomarkers have been studied. Dual p16/Ki-67 immunostaining (p16/Ki-67 DS) has shown promising sensitivity and specificity for the detection of high-grade cervical intraepithelial neoplasia (CIN2+).^{8–12} Tjama *et al.* reported in a systematic literature review that in the Belgian screening population (age 25–65), p16/Ki-67 DS cytology was significantly more sensitive and slightly less specific than cytology, but in the population with low-grade changes (atypical squamous cells of undetermined significance [ASC-US], low-grade intraepithelial lesion [LSIL]) and the population referred to colposcopy dual-stain with p16/Ki-67 specificity was statistically significantly higher (+25–30%) and sensitivity statistically significantly lower (–5–6%) than HPV testing.¹³ p16/Ki-67 DS is based on simultaneous detection of p16 and Ki67 proteins in cervical smears. p16 protein is an important cyclin-dependent kinase (CDK) inhibitor which directly controls the progression of the cell cycle from the G1 phase to the S phase and induces cell cycle arrest under physiological conditions. It is expressed in cells, which are infected by HPV, a sign of HPV E7 action on tumour suppressor gene Rb.^{14–18} Ki-67 is a cell proliferation marker, strongly associated with tumour cell proliferation and growth and is widely used as a proliferation marker. It is a nuclear non-histone protein and is expressed in all phases of the cell cycle, except during the G0 phase.^{2,19,20} Normally, over-expression of p16 and expression of Ki-67 should not occur in the same cell under physiological conditions. Simultaneous detection of tumour-suppressor protein p16 and a proliferation marker Ki-67 co-expression within the same cell should indicate deregulation of the cell cycle as the consequence of oncogenic transformation after long term infection induced by high-risk HPV.^{2,10}

The presence of 1 or more cervical epithelial cell(s) showing p16/Ki-67 double immunoreactivity is defined as a positive test result for p16/Ki-67 DS cytology, independent from morphology interpretation.¹⁰ This study has been designed to

evaluate the diagnostic accuracy of p16/Ki-67 DS for detection of high-grade cervical intraepithelial neoplasia (CIN2+) and the possible diagnostic role of the number of p16/Ki-67 positive cells. The goal was to determine whether taking a different number of positive cells as the cut-off in the p16/Ki-67 DS test has a statistically significantly different result in detection of CIN2+.

Subjects and methods

We performed the analysis on a subset cohort of women enrolled within a large-scale HPV self-sampling project within the organised, population-based Cervical Cancer Screening Programme ZORA in Slovenia that was conducted in 2013–2016 in two Slovenian regions.²¹ The project was approved by the National ethics committee (Approval Nos. 154/03/13, 136/04/14 and 102/11/15). All enrolled women with permanent residence in the Celje region, who had p16/Ki-67 DS of the cervical smear and colposcopy in the Celje General Hospital region were included in the analysis.

Women were invited to colposcopy to Celje General Hospital either due to high-grade cytology or HPV-positive triage test after low-grade cytology or during follow-up after treatment of CIN2+ according to national cervical cancer screening guidelines or due to a positive HPV-self sampling result from an open label, multi-arm trial with a randomised design. A cervical smear was taken prior to the colposcopy. Conventional cytology with split sample technique was used. The first smear was stained with the standard Papanicolaou method and assessed according to national guidelines (Bethesda classification). The second smear was stained with p16/Ki-67 DS (CINtec PLUS, Cytology CE; Ventana Medical Systems, Inc 2015, Tucson, Arizona USA) according to the manufacturer's instructions.^{22,23} All women underwent colposcopy. In the case of an abnormal colposcopy result, a biopsy was taken, and the result was included in the analysis. If the patient had a negative colposcopy, no biopsy was taken, and she was regarded as negative for CIN2+. All patients were managed according to the national guidelines.²⁴

p16/Ki-67 DS was performed in the cytopathology laboratory of the Institute of Oncology Ljubljana and sent to the cytopathology laboratory of Celje General Hospital for assessment. All slides were blinded at the Institute of Oncology Ljubljana and independently assessed by a cytotechnologist and cytopathologist in Celje General Hospital.

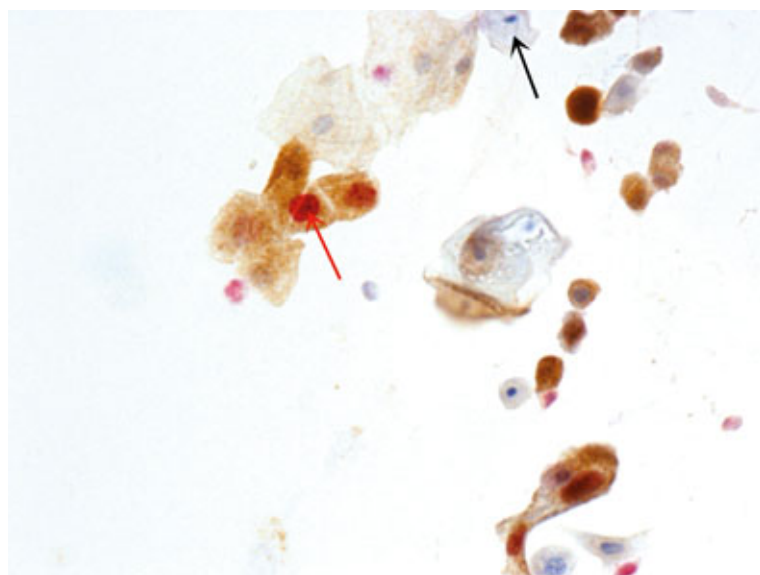


FIGURE 1. Positive reaction was defined as p16 brown signal and Ki-67 red signal (red arrow) present in the same cell with red stained nucleus and brown stained cytoplasm. Note: negative p16/Ki-67 dual immunostaining (p16/Ki-67 DS) reaction (black arrow) (p16/Ki-76 DS, magnification 400x).

The cytopathologist's result was included in the analysis. A positive reaction was defined as a p16 signal (brown) and a Ki-67 signal (red) present in the same cell with red stained nucleus and brown stained cytoplasm (Figure 1). One dual-stained cell was an indicator of a positive result.¹⁰ All evaluators recorded the number of positive or suspicious cells (one to five). A suspicious category was introduced to identify cases that were difficult to interpret. For the purpose of these analyses, suspicious DS results were considered positive, and inadequate as negative.^{22,23}

Number of p16/Ki-67 DS positive cells and CIN2+ according to Pap test results were calculated. The diagnostic accuracy of p16/Ki-67 DS for the detection of CIN2+ was assessed with sensitivity (true positive rate), specificity (true negative rate), positive predictive value (PPV) and negative predictive value (NPV). The association between the number of p16/Ki-67 positive cells and the detection of CIN2+ was evaluated with Mann-Whitney U test. Statistical analysis was performed with R version 4.0.5. A p value of less than 0.05 was considered statistically significant.

Results

Of 212 enrolled women from the Celje region, 38 were excluded due to the lack of p16/Ki-67 DS, leaving 174 women who had both p16/Ki-67 DS and colposcopy performed to be included in the analysis. The average age of women was 45.1 years. 73 women (42.0%) had a pathologic smear, and 101 women (58.0%) had a normal smear. The types of pathologic smears were high-grade intraepithelial lesion (HSIL) in 29 women (16.7%), ASC-US in 24 women (13.8%), LSIL in 14 women (8.0%), atypical squamous cells-cannot exclude high-grade squamous intraepithelial lesion (ASC-H) in 4 women (2.3%), invasive squamous cell carcinoma in 1 woman (0.6%) and atypical glandular cells, not otherwise specified (AGC-N) in 1 woman (0.6%).

The smear was interpreted as p16/Ki-67 DS positive in 83 women (11 of which were originally evaluated as suspicious) and negative in 91 (1 of which was initially inadequate). The analysis of p16/Ki-67 DS positivity among different smear results is presented in Table 1.

TABLE 1. p16/Ki-67 dual immunostaining (p16/Ki-67 DS) positivity and number of positive cells among different smear results

Cervical cytology	Number of p16/Ki-67 positive cells (n, [%])						1+ (Total Positive)	Total
	0 (Negative)	1	2	3	4	≥ 5		
Normal	70 (69.3)	13 (12.9)	9 (8.9)	1 (1.0)	1 (1.0)	7 (6.9)	31 (30.7)	101
ASC-US	14 (58.3)	0 (0.0)	1 (4.2)	2 (8.3)	1 (4.2)	6 (25.0)	10 (41.7)	24
LSIL	7 (50.0)	3 (21.4)	0 (0.0)	0 (0.0)	1 (7.1)	3 (21.4)	7 (50.0)	14
AGC-N	0 (0.0)	0 (0.0)	0 (0.0)	0 (0.0)	0 (0.0)	1 (100.0)	1 (100.0)	1
HSIL	0 (0.0)	1 (3.4)	0 (0.0)	0 (0.0)	0 (0.0)	28 (96.6)	29 (100.0)	29
ASC-H	0 (0.0)	0 (0.0)	0 (0.0)	1 (25.0)	0 (0.0)	3 (75.0)	4 (100.0)	4
Inv. cancer	0 (0.0)	0 (0.0)	0 (0.0)	0 (0.0)	0 (0.0)	1 (100.0)	1 (100.0)	1
Total	91 (52.3)	17 (9.8)	10 (5.7)	4 (2.3)	3 (1.7)	49 (28.2)	83 (47.7)	174

ASC-H = high-grade squamous intraepithelial lesion; AGC-N = atypical glandular cells, not otherwise specified; ASC-US = atypical squamous cells of undetermined significance; HSIL = high-grade intraepithelial lesion; LSIL = low-grade intraepithelial lesion

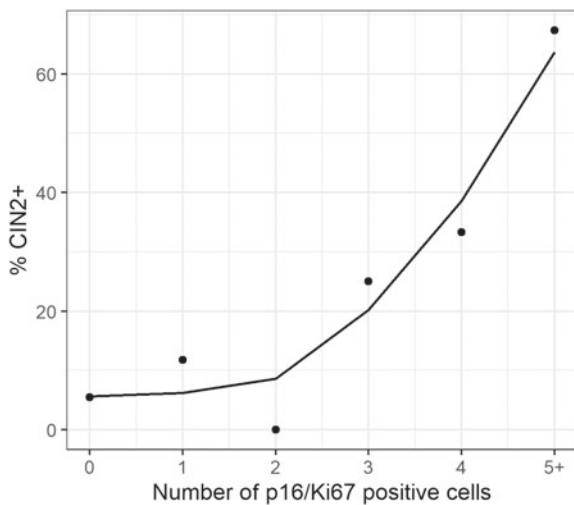


FIGURE 2. The association between the number of p16/Ki-67 dual immunostaining (p16/Ki-67 DS) positive cells and the risk for cervical intraepithelial neoplasia (CIN2+). Observed values are marked as points. Smoothed line (Method spline) is added for better trend representation.

Among the 83 women with a positive p16/Ki-67 DS result, 17 women (20.5%) had one positive cell, 10 women (12.0%) had two positive cells, 4 women (4.8%) had three positive cells, 3 women (3.6%) had four positive cells, and 49 women (59.0%) had at least five positive cells (Table 1).

Among analysed women, 42/174 (24.1%) had histologically confirmed CIN2+, 92 women (52.9%) had CIN1 or normal histology and 40 (23.0%) women had only colposcopy performed. Among the CIN2+ women, 37 (88.1%) had a p16/Ki-67 DS positive smear, and among the women without CIN2+, 46 (34.8%) had a p16/Ki-67 DS positive smear.

The analysis of the number of p16/Ki-67 DS positive cells according to CIN2+ outcome is present-

TABLE 2. Cervical intraepithelial neoplasia (CIN2+) according to the number of p16/Ki-67 dual immunostaining (p16/Ki-67 DS) positive cells

p16/Ki-67		Histology	
Positive cells	n	< CIN2 n (%)	CIN2+ n (%)
0	91	86 (94.5)	5 (5.5)
1	17	15 (88.2)	2 (11.8)
2	10	10 (100.0)	0 (0.0)
3	4	3 (75.0)	1 (25.0)
4	3	2 (66.7)	1 (33.3)
≥ 5	49	16 (32.7)	33 (67.3)
Total	174	132 (75.9)	42 (24.1)

ed in Table 2 and Figure 2. Among the 91 women with negative p16/Ki-67 DS, 5 women (5.5%) had CIN2+. Among p16/Ki-67 DS positive women, the risk for CIN2+ was higher in those with more positive cells ($p < 0.001$: one cell: 2/17 [11.8%], two cells: 0/10 [0.0%]; three cells: 1/4 [25.0%]; four cells: 1/3 [33.3%], five or more cells: 33/49 [67.3%]).

The diagnostic accuracy of p16/Ki-67 DS for the detection of CIN2+ is presented in Table 3. For the total population, sensitivity was 88.1% (50% for women with ASC-US or LSIL), specificity was 65.2% (61.1% for women with ASC-US and 50% for LSIL), PPV was 44.6% and NPV was 94.5%.

Discussion

We evaluated the diagnostic accuracy of p16/Ki-67 DS to detect CIN2+ at different cut-offs defined by the number of positive cells.

Our analysis showed 88.1% sensitivity of p16/Ki-67 DS for the detection of CIN2+, which is comparable to several other studies that reported sensitivity between 86.4 and 98.2%^{3,10,12,25-28} and somewhat higher than some other reported data, including previous data from our group where were analysed postmenopausal women with low-grade cytology.^{9,29,30} Our group also reported that additional training contributes to higher sensitivity of p16/Ki-67 DS for detecting CIN 2+ without a decrease in specificity.^{22,23} Additional analyses showed only 50% sensitivity in women with LSIL, which might reflect the low number of enrolled patients (95% CI: 1.3–98.7%). Other authors reported p16/Ki-67 DS as an effective triage of patients with LSIL.^{2,10,26} Peeters *et al.* reported in a meta-analysis that sensitivity of p16/Ki-67 DS for detection of CIN 2+ in triaging women with ASC-US and LSIL was similar - 84% (95% CI: 77–89%) and 86% (95% CI: 82–89%) - than that of the HPV test - 93% in ASC-US (95% CI: 91–95%) and 95% (95% CI: 94–96%) in LSIL. Specificity of p16/Ki-67 DS for detection of CIN 2+ in ASC-US and LSIL were 77% (95% CI: 70–77%) and 66% (95% CI: 59–72%). In contrast, the HPV test was less specific: in ASC-US 45% (95% CI: 38–53%) and LSIL 27% (95% CI: 23–33%), respectively.²⁸ In cases of ASC-US and LSIL, the recommended subsequent follow-up strategy is HPV triage. However, this strategy has its limitations because of the high HPV positivity in women with low-grade cytology.^{28,31} According to Frega *et al.* the sensitivity and specificity in the ASC-US group were high for CIN 2 (90.09% CI: 89.4–92.4%; 81.8% CI: 74.2–89.4) and CIN 3 (99.9% CI: 92.2–99.9%;

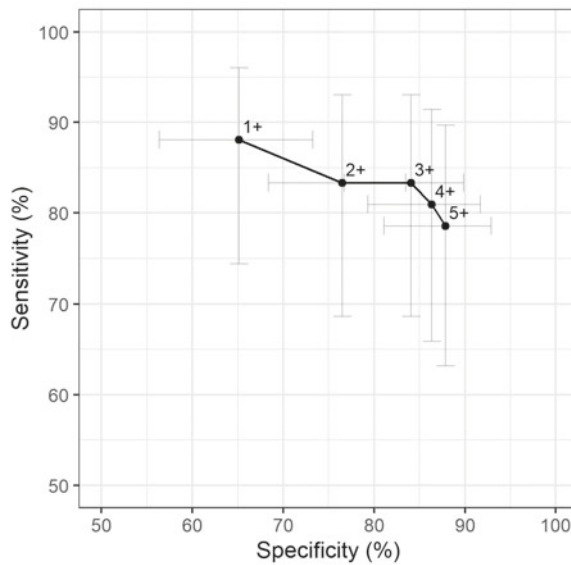


FIGURE 3. Diagnostic performance of p16/Ki-67 dual immunostaining (p16/Ki-67 DS) at different cut-offs (number of positive cells).

73.7% CI: 65.0–82.4%). In LSIL group the sensitivity was 95.2% for CIN 2 (CI: 88.7–99.9%) and 94.1% for CIN 3 (CI: 82.9–99.9%), however specificity was only 61.8% for CIN 2 (CI: 54.4–69.2%) and 49% for

TABLE 3. Diagnostic performance of p16/Ki-67 dual immunostaining (p16/Ki-67 DS) according to cytology results and according to different cut-offs (number of positive cells) in detecting cervical intraepithelial neoplasia (CIN2+)

CIN2+ (n)	p16/Ki-67				
	Sensitivity (%; 95% CI)	Specificity (%; 95% CI)	PPV [†] (%; 95% CI)	NPV [‡] (%; 95% CI)	
Cytology result					
Negative (n = 101)	3	66.7 (9.4–99.2)	70.4 (60.3–79.2)	6.5 (0.8–21.4)	98.6 (92.3–100.0)
ASC-US (n = 24)	6	50.0 (11.8–88.2)	61.1 (35.7–82.7)	30.0 (6.7–65.2)	78.6 (49.2–95.3)
LSIL (n = 14)	2	50.0 (1.3–98.7)	50.0 (21.1–78.9)	14.3 (0.4–57.9)	85.7 (42.1–99.6)
HSIL (n = 29)	26	100.0 (86.8–100.0)	0.0 (0.0–70.8)	89.7 (72.6–97.8)	/
Number of positive p16/Ki-67 cells cut-off					
1+ (n = 174)	42	88.1 (74.4–96.0)	65.2 (56.4–73.2)	44.6 (33.7–55.9)	94.5 (87.6–98.2)
2+ (n = 174)	42	83.3 (68.6–93.0)	76.5 (68.4–83.5)	53.0 (40.3–65.4)	93.5 (87.1–97.4)
3+ (n = 174)	42	83.3 (68.6–93.0)	84.1 (76.7–89.9)	62.5 (48.5–75.1)	94.1 (88.2–97.6)
4+ (n = 174)	42	81.0 (65.9–91.4)	86.4 (79.3–91.7)	65.4 (50.9–78.0)	93.4 (87.5–97.1)
5+ (n = 174)	42	78.6 (63.2–89.7)	87.9 (81.1–92.9)	67.3 (52.5–80.1)	92.8 (86.8–96.7)

[†]positive predictive value; [‡]negative predictive value; ASC-US = atypical squamous cells of undetermined significance; HSIL = high-grade intraepithelial lesion; LSIL = low-grade intraepithelial lesion; NPV = negative predictive value; PPV = positive predictive value

CIN 3 (CI: 41.4–56.6%), respectively. In contrast, the HPV test was more sensitive in all groups but far less specific (17.5% [CI: 2.2–32.8%] – 29.7% [CI: 22.7–36.7%]) in their study group of young women aged 21–24 years.³² It has been reported that by combining high sensitivity and specificity, p16/Ki-67 DS could decrease referrals to colposcopy by 50% in women with ASC-US and LSIL.^{8,10,33–35} Previous studies in women older than 30 years have shown statistically significantly higher sensitivity of p16/Ki-67 DS compared to Pap cytology. However, HPV was statistically significantly more sensitive than dual-stained cytology (93.3% vs. 84.7%; $P = 0.03$), but statistically significantly less specific (93.0% vs. 96.2%; $P < 0.001$).¹²

In our study, the specificity of p16/Ki-67 DS was 65.2%, while the specificity in ASC-US was 61.1% and the specificity in LSIL was 50.0%. Triage studies reported similar results.^{2,25,26,33,35,36} Schmidt *et al.* reported specificity of 80.6% for the detection of CIN2+ in the ASC-US group and 68.0% in the LSIL group, respectively.¹⁰ Danish researchers reported 51.3% specificity of p16/Ki56 DS for the detection of CIN2+ and 48.2% for the detection of CIN 3+.²⁵ In other studies, the reported specificity for the detection of CIN2+ were 59.5% (Wentzensen), 60.0% (Luttmer), 61.9% (Killeen), 82.5% (Zhu), and 95.2% (Ikenberg).^{2,3,12,26,37} Studies involved different populations, which is the reason for the range of specificities reported for the p16/Ki-67 DS test results. Wentzensen and Killeen have similar studies of women referred to colposcopy, Luttmer enrolled HPV-positive women referred to colposcopy, Zhu enrolled only women with ASC-US cytological diagnosis, and Ikenberg involved women 18 years or older undergoing routine cytology-based cervical cancer screening.

PPV and NPV for the detection of CIN2+ in our study were 44.6% and 94.5%, respectively. Killeen *et al.* reported in a group of women with abnormal Pap smear PPV and NPV of 30.6% and 98.4%, respectively.² Waldstrom *et al.* reported 29.3% PPV and 95.2% NPV for p16/Ki-67 DS LSIL smear for the detection of CIN2+.²⁵ Zhu Y. *et al.* reported 55.2% PPV and 99.25% NPV for p16/Ki-67 DS ASC-US smear for detection of CIN2+.³

The major limitation of our study is the small number of participants.

Only one positive cell is required for a positive result of the p16/Ki-67 DS.¹⁰ Ziemke reported in his study that using a score of 10 p16/Ki-76 DS positive cells as a positive result instead of one led to significantly higher specificity (89.0 vs. 70.2%, $p < 0.001$) and that this threshold offers better risk assessment

in LISL.³⁸ In our study, we report the association of the number of p16/Ki-67 DS positive cells with the detection of CIN2+ that could be used to improve real-time diagnostic performance without long-term data. We have investigated the threshold of the number of positive cells where we achieve a statistically significant better specificity but do not lose the sensitivity of the test. We have shown that women with a positive p16/Ki-67 DS result have a significantly higher risk for CIN2+ when the number of p16/Ki-67 DS positive cells is increasing. The probability of detecting a CIN2+ result in a patient with five or more p16/Ki-67 DS positive cells was 67.3% compared to only 11.8% in a patient with only one positive cell. A few longitudinal studies exist that are not directly comparable with ours since they are concerned with long-term cumulative risk rather than current diagnostic implications. They investigated the long-term predictive value of p16/Ki-67 DS cytology and explored additional assessments using different numbers of dual stained positive cells as a cut-off for a positive test result. The cumulative risk of CIN2+ increased with the increasing number of positive dual-stained cells.³⁹ A similar result was observed by Uijterwaal *et al.* in the study of triaging HPV-positive women with normal cytology by p16/Ki-67 DS cytology testing.⁴⁰

We have observed a statistically significant increase in p16/Ki-67 DS specificity at the cut-off for p16/Ki-67 DS positivity at 3 cells compared to 1 cell, with statistically insignificant decrease in sensitivity (Figure 3). This finding opens a new research question, whether changing the cut-off in p16/Ki-67 DS test could improve performance of p16/Ki-67 DS triage in terms of a further increase in specificity, which would lower the colposcopy referrals even further without a significant loss in longitudinal sensitivity and NPV, which would still enable a safe prolongation of follow-up intervals.

References

- Maver PJ, Poljak M. Primary HPV-based cervical cancer screening in Europe: implementation status, challenges, and future plans. *Clin Microbiol Infect* 2020; **26**: 579-5. doi: 10.1016/j.cmi.2019.09.006
- Killeen JL, Dye T, Grace C, Hiraoka M. Improved abnormal Pap smear triage using cervical cancer biomarkers. *J Low Genit Tract Dis* 2014; **18**: 1-7. doi: 10.1097/LGT.0b013e31828aeb39
- Zhu Y, Ren C, Yang L, Zhang X, Liu L, Wang Z. Performance of p16/Ki-67 immunostaining, HPV E6/E7 mRNA testing, and HPV DNA assay to detect high-grade cervical dysplasia in women with ASCUS. *BMC Cancer* 2019; **19**: 271. doi: 10.1186/s12885-019-5492-9
- Sawaya GF, Smith-McCune K, Kuppermann M. Cervical cancer screening: more choices in 2019. *JAMA* 2019; **321**: 2018-9. doi: 10.1001/jama.2019.4595
- White CM, Bakhiet S, Bates M, Ruttle C, Pilkington LJ, Keegan H, et al; CERVIVA consortium. Exposure to tobacco smoke measured by urinary nicotine metabolites increases risk of p16/Ki-67 co-expression and high-grade cervical neoplasia in HPV positive women: A two year prospective study. *Cancer Epidemiol* 2020; **68**: 101793. doi: 10.1016/j.canep.2020.101793
- Gavrić Lovrec V, Eriah T, Dobnik S, Takač I. The influence of smoking on the frequency and characteristics of complications following large loop excision of the transformation zone (LLETZ). *Acta medico-biotechnica* 2019; **1**: 40-6.
- Arbyn M, Ronco G, Anttila A, Meijer CJ, Poljak M, Ogilvie G, et al. Evidence regarding human papillomavirus testing in secondary prevention of cervical cancer. *Vaccine* 2012; **30**(Suppl): F88-99. doi: 10.1016/j.vaccine.2012.06.095. Erratum in: *Vaccine* 2013; **31**: 6266. doi: 10.1016/j.vaccine.2012.06.095
- Petry KU, Schmidt D, Scherbring S, Luyten A, Reinecke-Lüthge A, Bergeron C, et al. Triaging Pap cytology negative, HPV positive cervical cancer screening results with p16/Ki-67 dual-stained cytology. *Gynecol Oncol* 2011; **121**: 505-9. doi: 10.1016/j.ygyno.2011.02.033
- Wright TC Jr, Behrens CM, Ranger-Moore J, Rehm S, Sharma A, Stoler MH, et al. Triaging HPV-positive women with p16/Ki-67 dual-stained cytology: results from a sub-study nested into the ATHENA trial. *Gynecol Oncol* 2017; **144**: 51-6. doi: 10.1016/j.ygyno
- Schmidt D, Bergeron C, Denton KJ, Ridder R; European CINtec Cytology Study Group. p16/Ki-67 dual-stain cytology in the triage of ASCUS and LISL papanicolaou cytology: results from the European equivocal or mildly abnormal Papanicolaou cytology study. *Cancer Cytopathol* 2011; **119**: 158-66. doi: 10.1002/cncy.20140
- Bergeron C, Ikenberg H, Sideri M, Denton K, Bogers J, Schmidt D, et al; PALMS Study Group. Prospective evaluation of p16/Ki-67 dual-stained cytology for managing women with abnormal Papanicolaou cytology: PALMS study results. *Cancer Cytopathol* 2015; **123**: 373-81. doi: 10.1002/cncy.21542
- Ikenberg H, Bergeron C, Schmidt D, Griesser H, Alameda F, Angeloni C, et al; PALMS Study Group. Screening for cervical cancer precursors with p16/Ki-67 dual-stained cytology: results of the PALMS study. *J Natl Cancer Inst* 2013; **105**: 1550-7. doi: 10.1093/jnci/djt235
- Tjalma WAA. Diagnostic performance of dual-staining cytology for cervical cancer screening: a systematic literature review. *Eur J Obstet Gynecol Reprod Biol* 2017; **210**: 275-80. doi: 10.1016/j.ejogrb
- Khleif SN, DeGregori J, Yee CL, Otterson GA, Kaye FJ, Nevins JR, et al. Inhibition of cyclin D-CDK4/CDK6 activity is associated with an E2F-mediated induction of cyclin kinase inhibitor activity. *Proc Natl Acad Sci U S A* 1996; **93**: 4350-4. doi: 10.1073/pnas.93.9.4350
- Wentzensen N, von Knebel Doeberitz M. Biomarkers in cervical cancer screening. *Dis Markers* 2007; **23**: 315-30. doi: 10.1155/2007/678793
- Sano T, Oyama T, Kashiwabara K, Fukuda T, Nakajima T. Expression status of p16 protein is associated with human papillomavirus oncogenic potential in cervical and genital lesions. *Am J Pathol* 1998; **153**: 1741-8. doi: 10.1016/S0002-9440(10)65689-1
- Klaes R, Friedrich T, Spitkovsky D, Ridder R, Rudy W, Petry U, et al. Overexpression of p16(INK4A) as a specific marker for dysplastic and neoplastic epithelial cells of the cervix uteri. *Int J Cancer* 2001; **92**: 276-84. doi: 10.1002/ijc.1174
- Wang HR, Li YC, Guo HQ, Yu LL, Wu Z, Yin J, et al. A cocktail of p16INK4a and Ki-67, p16INK4a and minichromosome maintenance protein 2 as triage tests for human papillomavirus primary cervical cancer screening. *Oncotarget* 2017; **8**: 83890-9. doi: 10.18632/oncotarget.19870
- Schlüter C, Duchrow M, Wohlenberg C, Becker MH, Key G, Flad HD, et al. The cell proliferation-associated antigen of antibody Ki-67: a very large, ubiquitous nuclear protein with numerous repeated elements, representing a new kind of cell cycle-maintaining proteins. *J Cell Biol* 1993; **123**: 513-22. doi: 10.1083/jcb.123.3.513
- Yu L, Fei L, Liu X, Pi X, Wang L, Chen S. Application of p16/Ki-67 dual-staining cytology in cervical cancers. *J Cancer* 2019; **10**: 2654-60. doi: 10.7150/jca.32743
- Ivanus U, Jerman T, Fokter Repše A, Takac I, Prevodnik VK, Marcec M, et al. Randomised trial of HPV self-sampling among non-attenders in the Slovenian cervical screening programme ZORA: comparing three different screening approaches. *Radiol Oncol* 2018; **52**: 399-412. doi: 10.2478/raon-2018-0036

22. Kloboves Prevodnik V, Jerman T, Nolde N, Repše Fokter A, Jezeršek S, Pohar Marinšek Ž, et al. Interobserver variability and accuracy of p16/Ki-67 dual immunocytochemical staining on conventional cervical smears. *Diagn Pathol* 2019; **1**: 48. doi: 10.1186/s13000-019-0821-5
23. Prevodnik VK, Marinsek ZP, Zalar J, Rozina H, Kotnik N, Jerman T, et al. Evaluation of the training program for p16/Ki-67 dual immunocytochemical staining interpretation for laboratory staff without experience in cervical cytology and immunocytochemistry. *Radiol Oncol* 2020; **2**: 201-8. doi: 10.2478/raon-2020-0018
24. *Guidelines for management of women with cervical precancerous lesions*. Ursic-Vrscaj M, Rakar S, Možina A, Kobal B, Takač I, Deisinger I, et al, editors. [Slovenian]. Ljubljana: Institute of Oncology Ljubljana; 2011. [Accessed 2021 Feb 5]. Available at: https://zora.onko-i.si/fileadmin/user_upload/dokumenti/strokovna_priporocila/2011_Smernice_web.pdf
25. Waldstrøm M, Christensen RK, Ørnskov D. Evaluation of p16(INK4a)/Ki-67 dual stain in comparison with an mRNA human papillomavirus test on liquid-based cytology samples with low-grade squamous intraepithelial lesion. *Cancer Cytopathol* 2013; **121**: 136-45. doi: 10.1002/cncy.21233
26. Wentzensen N, Schwartz L, Zuna RE, Smith K, Mathews C, Gold M A, et al. Performance of p16/Ki-67 immunostaining to detect cervical cancer precursors in a colposcopy referral population. *Clin Cancer Res* 2012; **18**: 4154-62. doi: 10.1158/1078-0432.CCR-12-0270
27. Šekoranja D, Repše Fokter A. Triaging atypical squamous cells-cannot exclude high-grade squamous intraepithelial lesion with p16/Ki-67 dual stain. *J Low Genit Tract Dis* 2017; **21**: 108-11. doi: 10.1097/LGT.0000000000000297
28. Peeters E, Wentzensen N, Bergeron C, Arbyn M. Meta-analysis of the accuracy of p16 or p16/Ki-67 immunocytochemistry versus HPV testing for the detection of CIN2+/CIN3+ in triage of women with minor abnormal cytology. *Cancer Cytopathol* 2019; **127**: 169-80. doi: 10.1002/cncy.22103
29. Edgerton N, Cohen C, Siddiqui MT. Evaluation of CINtec PLUS® testing as an adjunctive test in ASC-US diagnosed SurePath® preparations. *Diagn Cytopathol* 2013; **41**: 35-40. doi: 10.1002/dc.21757
30. Dvornik A, Repše Fokter A. p16/Ki-67 Immunostaining in the triage of postmenopausal women with low-grade cytology results. *J Low Genit Tract Dis* 2020; **24**: 235-7. doi: 10.1097/LGT.0000000000000539
31. Dvornik A, Repše-Fokter A. p16/Ki-67 immunostaining in the triage of young women with LSIL, ASC-US, and ASC-H cytology. *Diagn Cytopathol* 2020; **48**: 96-7. doi: 10.1002/dc.24339
32. Frega A, Pavone M, Sesti F, Leone C, Bianchi P, Cozza G, et al. Sensitivity and specificity values of high-risk HPV DNA, p16/Ki-67 and HPV mRNA in young women with atypical squamous cells of undetermined significance (ASCUS) or low-grade squamous intraepithelial lesion (LSIL). *Eur Rev Med Pharmacol Sci* 2019; **24**: 10672-7. doi: 10.26355/eurrev-201912-19765
33. Wentzensen N, Clarke MA, Bremer R, Poitras N, Tokugawa D, Goldhoff PE, et al. Clinical evaluation of human papillomavirus screening with p16/Ki-67 dual stain tri-age in a large organized cervical cancer screening program. *JAMA Intern Med* 2019; **179**: 881-8. doi: 10.1001/jamainternmed.2019.0306
34. Stoler MH, Baker E, Boyle S, Aslam S, Ridder R, Huh WK, et al. Approaches to triage optimization in HPV primary screening: Extended genotyping and p16/Ki-67 dual-stained cytology-Retrospective insights from ATHENA. *Jr. Int J Cancer* 2020; **146**: 599-607. doi: 10.1002/ijc.32669
35. Giorgi Rossi P, Carozzi F, Ronco G, Allia E, Bisanzio S, Gillio-Tos A, et al; the New Technology for Cervical Cancer 2 Working Group. p16/Ki-67 and E6/E7 mRNA accuracy and prognostic value in triaging HPV DNA-positive women. *J Natl Cancer Inst*. 2021; **3**: 292-300. doi: 10.1093/jnci/djaa105
36. Han Q, Guo H, Geng L, Wang Y. p16/Ki-67 dual-stained cytology used for triage in cervical cancer opportunistic screening. *Chin J Cancer Res* 2020; **2**: 208-17. doi: 10.21147/j.issn.1000-9604.2020.02.08
37. Luttmmer R, Dijkstra MG, Snijders PJF, Berkhof J, van Kemenade FJ, Rozendaal L, et al. p16/Ki-67 dual-stained cytology for detecting cervical (pre)cancer in a HPV-positive gynecologic outpatient population. *Mod Pathol* 2016; **29**: 870-8. doi: 10.1038/modpathol.2016.80
38. Ziemke P. p16/Ki-67 Immunocytochemistry in gynecological cytology: limitations in practice. *Acta Cytologica* 2017; **61**: 230-6. doi: 10.1159/000475979
39. Clarke MA, Cheung LC, Castle PE, Schiffman M, Tokugawa D, Poitras N, et al. Five-year risk of cervical precancer following p16/Ki-67 dual-stain triage of HPV-positive women. *JAMA Oncol* 2019; **5**: 181-6. doi:10.1001/jamaoncol.2018.4270
40. Uijterwaal MH, Polman NJ, Witte BI, van Kemenade FJ, Rijkaart D, Berkhof J, et al. Triage HPV-positive women with normal cytology by p16/Ki-67 dual-stained cytology testing: baseline and longitudinal data. *J Cancer* 2015; **136**: 2361-8. doi: 10.1002/ijc.29290

Robotic versus laparoscopic surgery for colorectal cancer: a case-control study

Jan Grosek^{1,2}, Jurij Ales Kosir¹, Primoz Sever¹, Vanja Erculj³, Ales Tomazic^{1,2}

¹ Department of Abdominal Surgery, Ljubljana University Medical Center, Ljubljana, Slovenia

² Medical Faculty, University of Ljubljana, Ljubljana, Slovenia

³ Faculty of Criminal Justice and Security, University of Maribor, Ljubljana, Slovenia

Radiol Oncol 2021; 55(4): 433-438.

Received 29 January 2020

Accepted 20 April 2021

Correspondence to: Prof. Aleš Tomažič, M.D., Ph.D., Department of Abdominal Surgery, Ljubljana University Medical Center, Zaloška cesta 7, SI-1000 Ljubljana, Slovenia; E-mail: ales.tomazic@kclj.si

Disclosure: No potential conflicts of interest were disclosed.

This is an open access article under the CC BY-NC-ND license (<http://creativecommons.org/licenses/by-nc-nd/4.0/>).

Background. Robotic resections represent a novel approach to treatment of colorectal cancer. The aim of our study was to critically assess the implementation of robotic colorectal surgical program at our institution and to compare it to the established laparoscopically assisted surgery.

Patients and methods. A retrospective case-control study was designed to compare outcomes of consecutively operated patients who underwent elective laparoscopic or robotic colorectal resections at a tertiary academic centre from 2019 to 2020. The associations between patient characteristics, type of operation, operation duration, conversions, duration of hospitalization, complications and number of harvested lymph nodes were assessed by using univariate logistic regression analysis.

Results. A total of 83 operations met inclusion criteria, 46 robotic and 37 laparoscopic resections, respectively. The groups were comparable regarding the patient and operative characteristics. The operative time was longer in the robotic group ($p < 0.001$), with fewer conversions to open surgery ($p = 0.004$), with less patients in need of transfusions ($p = 0.004$) and lower reoperation rate ($p = 0.026$). There was no significant difference between the length of stay ($p = 0.17$), the number of harvested lymph nodes ($p = 0.24$) and the overall complications ($p = 0.58$).

Conclusions. The short-term results of robotic colorectal resections were comparable to the laparoscopically assisted operations with fewer conversions to open surgery, fewer blood transfusions and lower reoperation rate in the robotic group.

Key words: robotic surgery; laparoscopic surgery; minimally invasive surgery; colorectal cancer

Introduction

Surgical resection is still the main treatment modality for resectable colorectal cancer. Advances in surgery have allowed the widespread use of minimally invasive surgical techniques, which are represented by laparoscopic and robotic approaches as opposed to open approach.

Laparoscopic colorectal resections (LCR) are safe and offer patients better short-term results as open surgery with less postoperative pain, faster recovery, shorter hospitalization and better cosme-

sis. Furthermore, they are oncologically equivalent to open surgery, as evidenced by multiple randomized studies.¹⁻³ There is even some evidence that LCR result in better median overall survival for patients with stage II colon cancer, older than 75 years, when compared to open surgery.⁴

Robotic surgical systems were designed to overcome the limitations of laparoscopic surgery, offering better visualization with three-dimensional magnified view and stable camera platform, stabilization of tremors and greater dexterity of movements. Moreover, they also improve the ergonom-

ics, possibly reducing fatigue of the operating surgeon.⁵ Key drawbacks include loss of haptic control, longer operative time and above all, increased financial costs.

Shortly after the introduction of robotic platforms, surgeons have begun to utilize robotic surgery for management of colorectal diseases and the number of procedures performed annually has steadily increased.⁶ The evolution and usage of robotic platform is well illustrated by bibliometric data, as more and more manuscripts are being published each year, from feasibility studies to case series and reviews, and, finally, more and more multi-centre trials. The abundance of published research clearly shows, how robotic assisted surgery has gained acceptance not only in the field of colorectal surgery, but across many surgical specialities.⁷ However, most of the studies have not demonstrated a major advantage of robotic colorectal resections (RCR) in comparison to laparoscopic resections.⁸ Some studies have shown a benefit of the robotic approach with fewer conversions.⁹ The ROLARR study has also shown this for the difficult rectal resections involving obese men with low rectal cancers.¹⁰

To evaluate the implementation of robotic platform at a tertiary medical centre we designed a retrospective case-control study to compare outcomes of patients who underwent elective laparoscopic or robotic colorectal resections.

Patients and methods

Patients

A retrospective review of patients that underwent either robotic or laparoscopic surgery for colorectal carcinoma was performed. Patients in both groups were consecutively operated in a two-year period; in 2019 (laparoscopic group) and 2020 (robotic group). All the operations were performed by a two-member surgical team. The data source was a prospectively maintained database in a single academic institution with previous history of performing laparoscopic assisted surgeries for many years.^{11,12} Approval for the study was obtained from the Medical Ethics Committee of the Republic of Slovenia.

A total of 83 patients were identified and included in the study; of these, 46 underwent robotic and 37 laparoscopic resections, respectively. The inclusion criteria were as follows: histologically proven adenocarcinoma of colon or upper rectum (> 10 cm from the anal verge); no previous or concurrent malignancy at other site; no evidence of distant

metastasis at the time of the surgery; minimally invasive (*i.e.*, laparoscopic, or robotic) operation. Patients with low or middle rectal cancer and those presenting as acute emergent cases (*i.e.*, perforation, obstruction) were excluded from the study.

Preoperative (age, sex, body mass index [BMI], American Society of Anaesthesiologists [ASA] score and tumour location), intraoperative (operative time, conversion rate) and postoperative complications according to the Clavien-Dindo (CD) classification, number of all harvested lymph nodes (LN) and number of positive LN, length of hospital stay and pathologic stage according to the 8th edition of the American Joint Committee on Cancer [AJCC]-TNM classification, reoperation and mortality rates were reviewed.^{13,14} The primary outcomes were conversion rates and hospital length of stay. Secondary outcomes were operative time, postoperative morbidity, and number of harvested lymph nodes.

Surgical technique

All operations were performed by a two-member surgical team. Both surgeons were highly experienced in open and laparoscopic colorectal surgery and underwent thorough training with proctorship before starting the robotic colorectal program.

Early in 2020 we started a robotic abdominal program, focusing at first on colorectal resections, both for benign and malignant diseases. As safety and feasibility of robotic colorectal surgery (RCS) are well established, most of currently published data focuses on evaluating perioperative data, comparing it to its laparoscopic counterpart.¹⁵

Patients in both groups underwent identical, standard preoperative workup and preparation, according to our institutional practice. This included full colonoscopy (partial in case of obstructive carcinoma) and contrast-enhanced computed tomography (CT) of the chest and the abdomen. Full mechanical bowel preparation was employed as per standard for all left sided lesions, while enema alone was employed for all right sided and for completely obstructive left sided lesions as well, respectively. Preoperative intravenous antibiotics were given to cover intestinal flora.

Patients were secured on a special no-slip foam in a modified lithotomy position for left-sided colectomies and rectal resections, while for right colectomies legs were extended and secured by wrapping circumferentially with a roller bandage.

All RCR were performed by a single-docking, totally robotic technique using da Vinci Robotic

Surgical System Xi (Intuitive Surgical System, Sunnyvale, CA, USA). All cases were operated with a dual console system. The robotic cart was docked on the side of the tumour, either on the left or right side of patients. Four 8 mm robotic ports were placed diagonally, lying on an imaginary linear line. Configuration of two-left handed instruments and one right-handed instrument was employed. Additional 12 mm port (Airseal[®], Applied Medical, USA) was inserted for the assistant at the patient site.

In both left and right sided colectomies primary vascular control with high-tie of the appropriate vessels was obtained at first. After that, a medial to lateral dissection was performed, respecting the avascular embryological planes.¹⁵ After resecting the bowel with tumour, intracorporeal anastomosis was fashioned: side-to-side anastomosis for right and left colectomies, and end-to-end for sigmoid or anterior rectal resections using circular stapling device and the double-stapling technique. Bowel was safely extracted through small Pfannenstiel incision, with wound-protector inserted for protection from faecal or tumour spillage.

For laparoscopic resection four or five trocar technique placed in a rhomboid fashion was used. Primary vascular control, followed by medial-to-lateral dissection was used, like already described in robotic technique. The specimen was exteriorised through mini-median incision with wound-protector, and, after resecting the bowel with tumour, the anastomosis was performed. A combination of intracorporeal and extracorporeal anastomoses were utilized, as per surgeon's discretion. The former was performed as previously described for robotic operation. When extracorporeal anastomoses were chosen for right or left colectomies, they were hand sewn (side-to-side or end-to-side for right sided-anastomoses and end-to-end for left-sided anastomoses) under direct visualizations.

Postoperative complications were stratified according to the CD classification system.¹³ Accordingly severe morbidity was identified when at least CD grade III or more occurred. Anastomotic leak was considered along with all conditions with clinical or radiological features of anastomotic dehiscence. Hence, it was defined, as per the International study group definition.¹⁶ Conversion was defined as the unplanned change from laparoscopy to open procedure or from robotic surgery to either laparoscopic or open approach. Operative time was considered as the time from the first skin incision until the last scar was sutured.

Early and frequent mobility was encouraged, and venous thromboembolism prophylaxis was

started approx. 12 hours after the operation. Nasogastric tube was removed prior to the end of the operation, while drainage tube and Foley catheter were removed on postoperative day one. Patients were offered clear liquids in the evening on the day of the operation. In the absence of nausea, vomiting or abdominal discomfort they were quickly advanced from liquid to regular diet.

Statistical analysis

Categorical variables were described by frequencies and percentages, normally distributed continuous variables by means and standard deviations, others by medians and interquartile ranges (IQR). Normality of the distribution of continuous variables per treatment group was assessed by Shapiro-Wilk test. The association between patient characteristics, operation duration, conversions, duration of hospitalization, complications, reoperation, and type of operation was assessed by using univariate logistic regression analysis. When there were zero cases present in any of the cells of the contingency table, likelihood ratio test was used. All statistical testing was performed at 0.05 significance level. Statistical program SPSS version 27 was used to perform all statistical analyses.

Results

There was no statistically significant association between demographic variables, concomitant diseases, the severity of disease and the type of the operation (Table 1). Patient characteristics did not differ significantly between groups as there was no statistically significant association between demographic variables, concomitant diseases, and severity of disease and the type of the operation.

Associations between several variables of the performed operation, patient course of recovery after the operation, procedure (type of resection) and the type of the operation performed (laparoscopic or robotic) were analysed by univariate logistic regression and results are presented in Table 2. Operative time was statistically significantly longer ($p < 0.001$) in robotic group. Five (13.5%) patients had operation conversion within the laparoscopic group, while there were no conversions to open surgery in the robotic group of patients ($p = 0.004$). While the groups were comparable regarding the duration of hospitalization ($p = 0.168$) and the number of harvested lymph nodes ($p = 0.240$), the transfusion was to higher extent given to patients

TABLE 1. Association between demographic characteristics, concomitant diseases, severity of the disease, and type of operation (results of univariate logistic regression)

	Laparoscopic (n = 37)	Robotic (n = 46)	OR (95 % CI)	P
Male gender	23 (62.2)	26 (56.5)	0.79 (0.33; 1.92)	0.604
Mean age (SD)	67.5 (10.1)	66.8 (11)	0.99 (0.95; 1.04)	0.770
Median (IQR) BMI	27.2 (25.1–29.4)	27.5 (25.7–31.3)	1.01 (0.92; 1.12)	0.808
ASA				0.262 ^a
1	0 (0)	2 (4.3)		
2	20 (54.1)	24 (52.2)		
3	16 (43.2)	20 (43.5)		
4	1 (2.7)	0 (0)		
Procedure				0.273
Right colectomy	15 (40.5)	21 (45.7)	-	-
Left colectomy	4 (10.8)	3 (6.5)	-	-
Rectosigmoid/sigmoid/anterior resection	16 (43.2)	22 (47.8)	-	-
Total colectomy	2 (5.4)	0 (0)	-	-
T stage				
T1	9 (24.3)	7 (15.2)	-	-
T2	7 (18.9)	13 (28.3)	2.39 (0.69;9.2)	0.206
T3	15 (40.5)	20 (43.5)	1.71 (0.52;5.65)	0.376
T4	6 (16.2)	6 (13)	1.29 (0.29;5.77)	0.743
Stage				
1	16 (43.2)	12 (26.1)	1	-
2	9 (24.3)	18 (39.1)	2.67 (0.89; 7.98)	0.079
3	12 (32.4)	16 (34.8)	1.78 (0.62; 5.12)	0.287

^a = likelihood ratio test; ASA = American Society of Anaesthesiologists score; BMI = body mass index; CI = confidence interval; IQR = interquartile range; OR = odds ratio; SD = standard deviation

in laparoscopic group of patients ($p = 0.004$). Five (13.5%) patients within laparoscopic group needed transfusion, while there were no patients in need of transfusion within the robotic group of patients. The groups were comparable both with regards to overall complications ($p = 0.576$) as well as to type of complications according to the CD classification ($p = 0.12$). Reoperation was performed in three (8.1%) patients from the laparoscopic and none of the patients within the robotic group of patients ($p = 0.026$).

Discussion

This analysis of minimally invasive colorectal resections is, to the best of our knowledge, the first comparison of robotic versus laparoscopic resections for colon and upper rectal cancer in Slovenia. Safety of our patients and quality of surgical care

was of utmost importance when we implemented a new robotic abdominal program. Hence, treatment results were not to be compromised. Consequently, only patients with colon and upper rectal cancer were operated at first, because we deemed middle and low rectal cancers not suitable at the beginning of the new program, due to technical demands of pelvic surgery.

Many studies, comparing RCR and LCR, have shown the new technology to be safe, feasible and at least equivalent with respect to short-term outcomes and oncological results.¹⁷ The most relevant finding of our study were significantly lower rates of conversion to open with the robotic platform compared to LCR ($p = 0.004$), which is consistent with findings of other studies.¹⁸ Only slightly shorter hospital length of stay was seen in robotic group, the difference not reaching statistical significance ($p = 0.168$). Some studies agree with our findings, others, on the other hand, demonstrate

TABLE 2. Association between the operation and hospitalization duration, conversion, number of lymph nodes, transfusion, complications, reoperation, and the type of the operation (results of univariate logistic regression)

	Laparoscopic (n = 37)	Robotic (n = 46)	OR (95 % CI)	P
Median (IQR) operation duration (min)	150 (130–184)	262 (201–300)	1.03 (1.02; 1.05)	< 0.001
Conversion	5 (13.5)	0 (0)		0.004 ^a
Median (IQR) hospitalization duration	7 (6–8)	6 (5–7)	0.91 (0.81; 1.04)	0.168
Lymph nodes	20 (15–26)	24 (21–30)	1.03 (0.98; 1.08)	0.24
Transfusion	5 (13.5)	0 (0)		0.004 ^a
Complications	10 (27)	10 (21.7)	0.75 (0.27; 2.06)	0.576
Clavien-Dindo				0.12 ^a
0	27 (73)	36 (78.3)		
1	0 (0)	3 (6.5)		
2	7 (18.9)	6 (13)		
3	2 (5.4)	0 (0)		
5	1 (2.7)	1 (2.2)		
Reoperation	3 (8.1)	0 (0)		0.026 ^a

^a = likelihood ratio test; CI = confidence interval; IQR = interquartile range; OR = odds ratio

clinically significant shorter length of stay associated with robotic colorectal resections.^{19–21} In our study, there were three cases of anastomotic leakage in laparoscopic group. All three patients had to be reoperated, one of them died due to the septic shock. In the robotic group, there was no anastomotic leakage, however, one patient died because of acute thrombosis of superior mesenteric artery and coeliac axis. It is reasonable to assume that our study was underpowered to detect differences in postoperative morbidity, either overall or specific complications. However, other studies also demonstrate inconsistencies when comparing laparoscopic and robotic complication rates. Halabi *et al.*, in their analysis argue, that there is no difference in postoperative morbidity between LCR and RCR.²² On the other hand, there are studies, showing better results in terms of postoperative morbidity and mortality for either laparoscopic or robotic colorectal resections.^{23,24} Nevertheless, some reports in literature show variable differences in complication rates, *i.e.*, more anastomotic complications in one group and more general postoperative morbidity in the other.²⁰

Another limitation of our study is its retrospective observational nature with all the inherent biases. Important issue to be addressed are the operative costs, which is one of the biggest criticisms of robotic surgery and has been a subject of discussion since its introduction. Our database does not

include the cost data, so we did not address this issue in our study. Also, the intention of study being primarily the safety and oncologic equivalency of our new robotic surgical program, we did not assess the quality of life of operated patients. This, together with comprehensive cost analysis as well as long-term oncological results represents a very good potential for future studies.

The strength of our study is that the operations were performed by only two surgeons that reduces the heterogeneity of surgical techniques. Both surgeons had years of experience in laparoscopic surgery for all the patients included in the study and it can be assumed that they were already on top of their learning curve in laparoscopic surgery. This probably also played a role in faster acquisition of skills on the robotic platform. However, since the included robotic operations represent the start of our robotic program, there may still be room for improvement. It has been shown that the operating time decreases with the number of cases and this could have impacted the results of our study as well.^{25,26}

Conclusions

With this study, we sought to offer an outcome-based assessment of implemented robotic colorectal program at our academic institution. Based on

the results, it is appropriate to conclude, that our program is safe, has equivalent postoperative results compared to classic laparoscopy and is even associated with decreased conversion rates.

References

- Weeks JC, Nelson H, Gelber S, Sargent D, Schroeder G. Clinical outcomes of surgical therapy (COST) study group. Short-term quality-of-life outcomes following laparoscopic-assisted colectomy vs open colectomy for colon cancer: a randomized trial. *JAMA* 2020; **287**: 321-8. doi: 10.1001/jama.287.3.321
- Green BL, Marshall HC, Collinson F, Quirke P, Guillou P, Jayne DG, et al. Long-term follow-up of the medical research council CLASICC trial of conventional versus laparoscopically assisted resection in colorectal cancer. *Br J Surg* 2013; **100**: 75-82. doi: 10.1002/bjs.8945
- Deijen CL, Vasmel JE, de Lange-de Klerk ESM, Cuesta MA, Coene PLO, Lange JF, et al. Ten-year outcomes of a randomised trial of laparoscopic versus open surgery for colon cancer. *Surg Endosc* 2017; **31**: 2607-15. doi: 10.1007/s00464-016-5270-6
- Fan CZ, Chu YP, Wei P, Dai H, Chen W. Comparison of survival of patients receiving laparoscopic and open radical resection for stage II colon cancer. *Radiol Oncol* 2011; **45**: 273-8. doi: 10.2478/v10019-011-0029-0
- Wee IUY, Kuo LJ, NGU JCU. A systematic review of the true benefits of robotic surgery: ergonomics. *Int J Med Robotics Comput Assist Surg* 2020; **16**: e2113. doi: 10.1002/rcs.2113
- Sheetz KH, Claflin J, Dimick JB. Trends in the adoption of robotic surgery for common surgical procedures. *JAMA Netw Open* 2020; **3**: e1018911. doi: 10.1001/jamanetworkopen.2019.18911
- Connelly TM, Malik Z, Sehgal R, Byrnes G, Coffey JC, Peirce C. The 100 most influential manuscripts in robotic surgery: a bibliometric analysis. *J Robot Surg* 2020; **14**: 155-65. doi: 10.1007/s11701-019-00956-9
- Delaney CP, Lynch AC, Senagore AJ, Fazio VW. Comparison of robotically performed and traditional laparoscopic colorectal surgery. *Dis Colon Rectum* 2003; **46**: 1633-9. doi: 10.1007/BF02660768
- Speicher PJ, Englum BR, Ganapathi AM, Nussbaum DP, Mantyh CR, Migaly J. Robotic low anterior resection for rectal cancer: a national perspective on short-term oncologic outcomes. *Ann Surg* 2015; **262**: 1040-5. doi: 10.1097/SLA.0000000000001017
- Jayne D, Pigazzi A, Marshall H, Croft J, Corrigan N, Copeland J, et al. Effect of robotic-assisted vs conventional laparoscopic surgery on risk of conversion to open laparotomy among patients undergoing resection for rectal cancer: The ROLARR randomized clinical trial. *JAMA* 2017; **318**: 1569-80. doi: 10.1001/jama.2017.7219
- Grosek J, Tomazic A. Key clinical applications for indocyanine green fluorescence imaging in minimally invasive colorectal surgery. *J Minim Access Surg* 2020; **16**: 308-14. doi: 10.4103/jmas.JMAS_312_18
- Janež J, Korać T, Kodre AR, Jelenc F, Ihan A. Laparoscopically assisted colorectal surgery provides better short-term clinical and inflammatory outcomes compared to open colorectal surgery. *Arch Med Sci* 2015; **11**: 1217-26. doi: 10.5114/aoms.2015.56348
- Dindo D, Demartines N, Clavien PA. Classification of surgical complications: a new proposal with evaluation in a cohort of 6336 patients and results of a survey. *Ann Surg* 2004; **240**: 205-13. doi: 10.1097/01.sla.0000133083.54934.ae
- Weiser MR. AJCC 8th edition: Colorectal cancer. *Ann Surg Oncol* 2018; **25**: 1454-5. doi: 10.1245/s10434-018-6462-1
- Grosek J. How I do it: right colectomy with the Da Vinci Xi Robotic Platform. *Surg Endosc* 2020; **2**: 61-8.
- Rahbari NN, Weitz J, Hohenberger W, Heald RJ, Moran B, Ulrich A, et al. Definition and grading of anastomotic leakage following anterior resection of the rectum: a proposal by the International study group of rectal cancer. *Surgery* 2010; **147**: 339-51. doi: 10.1016/j.surg.2009.10.012
- Ng KT, Tsia AKV, Chong VYL. Robotic versus conventional laparoscopic surgery for colorectal cancer: a systematic review and meta-analysis with trial sequential analysis. *World J Surg* 2019; **43**: 1146-61. doi: 10.1007/s00268-018-04896-7
- Liao G, Zhao Z, Lin S, Li R, Yuan Y, Du S, et al. Robotic-assisted versus laparoscopic colorectal surgery: a meta-analysis of four randomized controlled studies. *World J Surg* 2014; **12**: 1-11. doi: 10.1186/1477-7819-12-122
- Rawlings AL, Woodland JH, Vegunta RK, Crawford DL. Robotic versus laparoscopic colectomy. *Surg Endosc* 2007; **21**: 1701-8. doi: 10.1007/s00464-007-9231-y
- Tam MS, Kaoutzanis C, Mullard AJ, Regen SE, Franz MG, et al. A population-based study comparing laparoscopic and robotic outcomes in colorectal surgery. *Surg Endosc* 2016; **30**: 455-63. doi: 10.1007/s00464-015-4218-6
- Kim CW, Kim CH, Baik SH. Outcomes of robotic-assisted colorectal surgery compared with laparoscopic and open surgery: a systematic review. *J Gastrointest Surg* 2014; **18**: 816-30. doi: 10.1007/s11605-014-2469-5
- Halabi WJ, Kang CY, Jafari MD, Nguyen VQ, Carmichael JC, Mills S, et al. Robotic-assisted colorectal surgery in the United States: a nationwide analysis of trend and outcomes. *World J Surg* 2013; **37**: 2782-90. doi: 10.1007/s00268-013-2024-7
- Salman M, Bell T, Martin J, Bhuva K, Grim R, Ahuja V. Use, cost, complications and mortality of robotic versus nonrobotic general surgery procedures based on a nationwide database. *Ann Surg* 2013; **79**: 553-60
- Tyler JA, Fox JP, Desai MM, Perry WB, Glasgow SC. Outcome and cost associated with robotic colectomy in the minimally invasive era. *Dis Colon Rectum* 2013; **56**: 458-66. doi: 10.1097/DCR.0b013e31827085ec
- Mushtaq HH, Shah SK, Agarwal AK. The current role of robotics in colorectal surgery. *Curr Gastroenterol Rep* 2019; **21**: 11. doi: 10.1007/s11894-019-0676-7.
- Shaw DD, Wright M, Taylor L, Bertelson NL, Shashidharan M, Menon P, et al. Robotic Colorectal Surgery Learning Curve and Case Complexity. *J Laparoendosc Adv Surg Tech A* 2018; **28**: 1163-8. doi: 10.1089/lap.2016.0411

Preoperative intensity-modulated chemoradiotherapy with simultaneous integrated boost in rectal cancer: five-year follow-up results of a phase II study

Jasna But-Hadzic^{1,2}, Anja Meden Boltezar¹, Tina Skerl¹, Vesna Zadnik^{2,3}, Vaneja Velenik^{1,2}

¹ Institute of Oncology Ljubljana, Division of Radiotherapy, Ljubljana, Slovenia

² Faculty of Medicine, University of Ljubljana, Ljubljana, Slovenia

³ Institute of Oncology Ljubljana, Epidemiology and Cancer Registry, Ljubljana, Slovenia

Radiol Oncol 2021; 55(4): 439-448.

Received 17 February 2021

Accepted 26 April 2021

Correspondence to: Assist. Prof. Jasna But-Hadžić, M.D., Ph.D., Institute of Oncology Ljubljana, Zaloška 2, 1000 Ljubljana, Slovenia.

E-mail: jbut@onko-i.si

Disclosure: No potential conflicts of interest were disclosed.

This is an open access article under the CC BY-NC-ND license (<http://creativecommons.org/licenses/by-nc-nd/4.0/>).

Background. We conducted a phase II study to investigate the feasibility and safety of preoperative radiochemotherapy experimental fractionation, using intensity-modulated radiation therapy with simultaneous integrated boost (IMRT SIB) to shorten the overall treatment time without dose escalation in intermediate/locally advanced rectal cancer with the aim to improving treatment outcome.

Patients and methods. A total of 51 patients with operable stage II–III rectal carcinoma were included between January 2014 and January 2015. Fifty patients completed preoperative IMRT treatment with an elective dose of 41.8 Gy and simultaneously delivered 46.2 Gy to T2/T3 and 48.4 Gy to T4 tumour in 22 fractions, with concomitant capecitabine (825 mg/m²/12 h, including at weekends). Median follow-up was 70 months (range 11–80 m).

Results. Forty-seven patients completed treatment per protocol. Acute toxicity occurred in 2 (4%) patients. R0 resection was achieved in all but 1 and pathologic complete response (pCR) in 12 (25.5%) patients who had 5-year overall survival (OS), disease-free survival (DFS) and local control (LC) of 91.7%, 100% and 100%, respectively. The intention-to-treat analysis showed that the type of surgery significantly moderated OS and DFS, while total downstaging and pN were predictive for DFS only. For treatment per protocol 5-year OS, DFS and LC were 80.9% (95% confidence interval [CI] 69.7–92.1), 77.1% (95% CI 65.1–89.1) and 95.2% (95% CI 88.7–100), respectively. The proportion of patients with severe late (CTCAE G ≥ 3) gastrointestinal, urinary and sexual toxicity was 15%, 2% and 8% respectively, with one reported secondary carcinoma.

Conclusions. Preoperative IMRT-SIB without dose escalation was well tolerated, with a low acute toxicity profile, we achieved a high rate of pCR and showed encouraging 5-year OS, DFS and LC.

Key words: rectal cancer; IMRT; simultaneous integrated boost; preoperative radiochemotherapy; acute toxicity; pathologic complete response; overall survival; disease-free survival; local control; late toxicity; quality of life

Introduction

In recent years, many different treatment strategies have been tested to improve outcomes for patients with locally advanced rectal cancer, with toxicity being the main obstacle for intensification of the

standard treatment.¹⁻⁴ Changing the preoperative radiotherapy (RT) technique from 3D conformal (3D CRT) to intensity-modulated radiotherapy (IMRT) allowed better sparing of normal tissue in dosimetric analyses⁵⁻⁸ and was used in several phase II studies to achieve dose escalation with si-

multaneous integrated boost (SIB) with or without another drug in addition to standard concomitant capecitabine.⁹⁻¹⁴ The published reports showed encouraging results for pathologic complete response (pCR) and local control (LC)^{9,11}, but with no impact on gastrointestinal toxicity with the addition of oxaliplatin¹⁵ and important late toxicity with dose escalation.¹⁰

Due to the promising impact on clinical outcome, but, conflicting toxicity results of treatment intensification with IMRT-SIB dose escalation in preoperative locally advanced rectal cancer (LARC) treatment, we conducted a prospective phase II study, where we kept the biologically effective dose (BED) of experimental IMRT SIB fractionation similar to the standard 3D CRT protocol of 45 Gy elective dose and boost of 4.5 Gy to T3 and 9 Gy to T4 tumour.

Our previously published results have shown that radiochemotherapy with IMRT-SIB without dose escalation, concomitantly with capecitabine, achieved a high rate of pCR (25.5%) and downstaging rate, with favourable acute toxicity profile and excellent compliance.¹⁶ In this paper, we report LC, disease-free survival (DFS), overall survival (OS), late toxicity and quality of life (QoL) after median follow-up of 70 months.

Patients and methods

Study design and inclusion criteria

Details about the trial (the eligibility criteria, treatment details and trial design) are available elsewhere.^{16,17} In short, to enter the study patients had to present with operable, histologically proven, intermediate/locally advanced (cT \geq 3 and/or cN \geq 1 on MRI), non-metastatic (M0 confirmed on CT thorax and abdomen) rectal adenocarcinoma, located up to 15 cm from the anal verge with no contraindications for systemic therapy. Written consent was signed before entering the trial, which was approved by the National Medical Ethics Committee of the Republic of Slovenia (No. 41/12/13) and complied with the Declaration of Helsinki. The study was registered in the ClinicalTrials.gov database (NCT02268006).

Treatment protocol

The target volumes and dose prescription were described in detail.¹⁶ Visible primary tumour was contoured as the gross tumour volume (GTV) and was extended with a 1 cm margin to represent a

boost volume (clinical target volume 2 – CTV2). Clinical target volume 1 (CTV1) encompassed CTV2, mesorectum, and regional lymph nodes. The nodes along the *arteria iliaca externa* were included in case of substantial genitourinary structure infiltration, and the ischioanal fossa and anal canal if the *musculus levator ani* or anal canal were involved. CTV 1 was extended anteriorly due to bowel movement as internal target volume (ITV). ITV + 1cm (7 mm posterior/lateral) represented the planning target volume (PTV). PTV 1 received 41.8 Gy in 22 fractions and SIB was prescribed to tumour (PTV 2) concomitantly to doses of 46.2 Gy and 48.4 Gy to T \leq 3 and T4 tumours in 22 fractions, respectively, 5 times per week (Monday to Friday). Concomitant capecitabine was prescribed from the first to the last day of the radiation treatment (including at weekends) at a daily dose of 825 mg/m²/12 h. The treatment was delivered on Clinac 2100 CDI (Varian, Palo Alto, USA) using the dynamic multileaf collimator technique with 6MV photons and a daily position verification (ExacTrac X-ray 6D system, BrainLAB AG, Feldkirchen, Germany).

After total mesorectal excision (TME), that was scheduled 6–8 weeks after preoperative treatment, six cycles of adjuvant chemotherapy with capecitabine were offered to patients with residual tumour on pathologic examination. Pathologic stage and tumour regression grade (TRG) were recorded according to the American Joint Committee on Cancer (AJCC) 7th edition¹⁸ and criteria by Dworak *et al.*¹⁹, respectively.

All patients were followed up with clinical and serum CEA evaluation every 3 months for two years, and later on a bi-annual basis with abdominal ultrasound every 6 months and a chest radiograph annually.

Statistics

This prospective phase II study in patients with intermediate/locally advanced rectal cancer was designed to evaluate the pathologic complete response after experimental preoperative treatment as a primary endpoint. The key secondary endpoints were to evaluate the acute toxicity of preoperative treatment, tumour response, local control (LC), disease-free survival (DFS) and overall survival (OS). In this report, we focus on survival, late toxicity and quality of life (QoL) after a 5-year follow-up.

A statistical analysis was performed with the Statistical Package for Social Sciences, v. 25.0 (SPSS

Inc., Chicago, IL, USA). Descriptive statistics were used to present frequencies. Survival was calculated with the Kaplan-Meier method and the influence of possible prognostic factors verified by means of the log-rank test. Time intervals were defined from the end of treatment (operation or radiotherapy completion for non-operated patients) until the last follow-up or death for OS and additionally until local or distant recurrence for DFS. For the intention-to-treat analysis (all patients), LC and DFS were counted as 0m for non-operated patients and DFS as 0m for M1 patients. Patients surgically treated after chemoradiotherapy completion (N = 47) entered treatment per protocol analysis.

Late adverse events data were available in the medical records for all patients and telephone interviews were additionally performed in November 2020, discussing patients' late adverse effects and quality of life, following the Common Terminology Criteria for Adverse Events (CTCAE) v 5.0.²⁰

QoL was recorded with the EORTC cancer-specific core questionnaire QLQ-C30²¹ and colorectal-specific questionnaire QLQ-C29²², that were collected before treatment (T0), and 1 year (T1) and 5 years (T5) after treatment. Data from all questionnaires were available for 31 patients for which the recorded answers were transformed into dimensions in the range 1–100.²³ Higher scores represented a higher level of functioning (for functional scales and single items) and lower scores displayed a lower symptom level (for symptom scales and single items). Statistical significance for QLQ scores changes over time was verified by comparing means with the Wilcoxon signed-rank test and with the t-test for EORTC reference value comparison. A p-value < 0.05 was considered statistically significant.

Results

Between January 2014 and January 2015, 51 (N = 51) patients were included. The patients' characteristics are described in detail elsewhere¹⁶, but briefly – median age was 66 years (range: 33–81 years) and nearly half of the tumours were located in the lower third of the rectum. The tumour invaded the mesorectal fascia in 20 patients and 15 patients had suspicious extramesorectal lymph nodes on MRI. Clinical stages were: T2N1M0 (n = 1), T3N0M0 (n = 6), T3N1M0 (n = 15), T3N2M0 (n = 22), T4N1M0 (n = 4), T4N2M0 (n = 2), and T3N1M1¹⁸, with small lung lesion prior to inclusion revealed as lung metastasis on control CT after the treatment in the last patient.

Preoperative radiochemotherapy was completed by 50 patients and 1 received preoperative short-course radiotherapy due to ischaemic stroke.

Altogether, 48 patients underwent surgery (47 treated per protocol). In 3 patients, surgery was omitted due to patient refusal, synchronous pancreatic cancer and rectal varices haemorrhage. Low anterior resection (LAR) was performed in 40 patients, abdominoperineal resection (APE) in 7, and pelvic exenteration in 1. One patient had a positive circumferential margin. Extramesorectal nodes exploration was based upon surgeon discretion and nodes were removed in 4 patients.

The total downstaging rate was 87% (41/47 patients), with a decrease in T and N stage observed in 32 and 39 patients, respectively. Pathologic complete response was achieved in 12 patients.

In median follow-up of 70 months (range 11–80 m) we recorded 13 deaths, 7 due to rectal cancer. Among the 6 remaining patients, 3 died of cardiovascular disease and one each of pancreatic cancer, alcohol hepatic cirrhosis and grade 5 (G5) ileus. One isolated local relapse and 1 with synchronous distant metastasis occurred 41 and 42 months after LAR and APE, respectively. Time to distant relapses was 0 m and 18 m (lung), 6 and 11 m (liver), 41 m (adrenal gland) and 42 m (abdominal lymph nodes). At the latest date of follow-up on 30.1.2021, there were 37 patients alive without disease and one patient on systemic treatment for disseminated rectal cancer.

Survival

We performed an intention-to-treat analysis for all 51 patients and for 47 patients that were treated according to protocol (Table 1). For the entire cohort, cumulative 5-year OS, 5-year DFS and 5-year LC were 76.5% (95% CI 64.9–88.1), 72.4% (95% CI 60.4–84.6), and 89.7% (95% CI 81.1–98.3), respectively. In the treatment per protocol group 5-year OS, 5-year DFS and 5-year LC were 80.9% (95% CI 69.7–92.1), 77.1% (95% CI 65.1–89.1) and 95.2% (95% CI 88.7–100), respectively. Five-year colostomy-free survival was 76% (29/38).

The potential influence of prognostic factors on survival was determined by means of the log-rank test (Table 2). There was no association between age at diagnosis, performance status, tumour grade, positive mesorectal fascia or suspicious extramesorectal lymph nodes, removal of extramesorectal lymph nodes, clinical stage (cT, cN), decrease in T and N stage or pathologic T stage on survival. We found no predictive value for pCR, TRG prognostic

TABLE 1. Number of events after median follow-up of 70 months (11–80 m) and 5-year survival

	Intention to treat (N = 51)	Per protocol (N = 47)
5-year OS*	76.5%	80.9%
5-year DFS	72.5%	76.5%
5-year LC	90.2%	95.7%
	Number of events (%)	Number of events (%)
OS status		
Alive	38 (74.5)	37 (78.7) *
Dead	13 (25.5)	10 (21.3)
DFS status		
Alive without disease	37 (72.5)	36 (76.5)
Local/distant relapse/death	14 (27.5)	11 (23.5)
LC status		
Local relapse -	46 (90.2)	45 (95.7)
Local relapse +	5 (9.8)	2 (4.3)

* = Numbers differ from OS status due to one noncancer death > 5-year after surgery; DFS = disease-free survival; LC = local control; OS = overall survival; for non-operated patients and patient with M+ disease local or distant recurrence was calculated as 0 months.

group or NAR prognostic group as survival surrogates. Significantly better DFS was found in patients where total downstaging was achieved and in patients with pathologically negative lymph nodes (Figure 1). There was significantly better OS and DFS with LAR compared with APE or pelvic exenteration ($p = 0.000$ and 0.013 , respectively). Gender was a predictive prognostic factor for OS and treatment per protocol was associated with better OS and DFS.

We recorded no local or distant relapses in the group of patients with pCR, with one death due to G5 adverse event, leading to 91.7% 5-year OS and 100% 5-year DFS and 5-year LC for this group of patients.

Late toxicity

Late toxicity data are available for all patients and are listed in Table 3. Patients reported mean 5 late adverse events (range 0–19) at last follow up. Major adverse events (CTCAE version 5.0 $G \geq 3$)²⁰

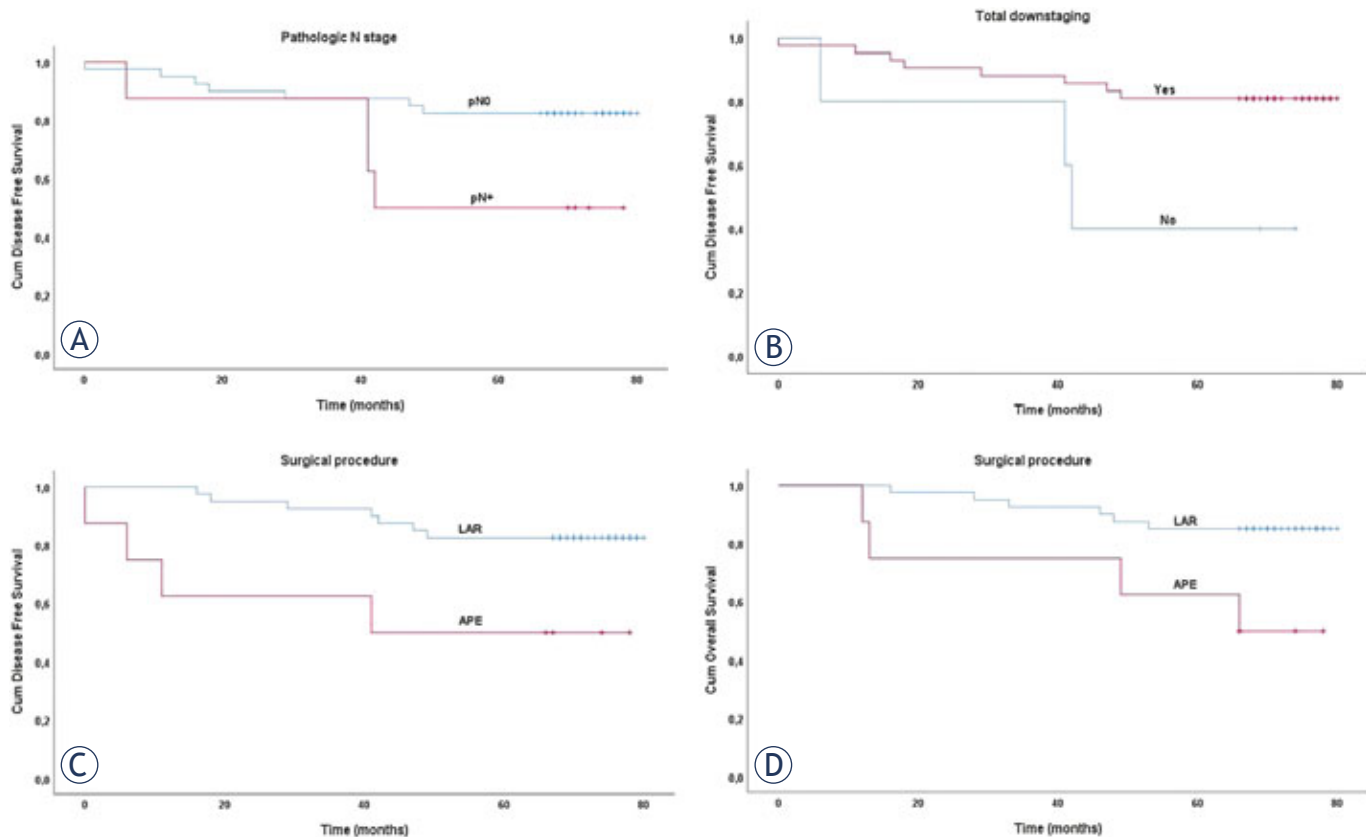


FIGURE 1. Prognostic significance of (A) pathologic nodal stage (pN) and (B) total downstaging on 5-year disease-free survival, (C) prognostic significance of surgery procedure on 5-year disease-free survival and (D) overall survival in rectal cancer after preoperative radiochemotherapy and surgery.

APE = abdominoperineal excision; LAR = low anterior resection

occurred in 12 patients (23%), of which 7 patients had one, 3 patients two and 1 patient had three G3 toxicities. Following protective stoma closure, 1 patient died due to G5 ileus complication 29 months after LAR. Gastrointestinal toxicity (GI) ≥ 3 was recorded in 7 (15%) and genitourinary (GU) in 5 (10%) patients. Two men have erectile dysfunction and two women are reporting problems due to dyspareunia, vaginal dryness and vaginal stricture. Due to complete faecal incontinence, permanent stoma was required in two patients, 10 and 36 months after LAR. Urgent surgical intervention was required for anastomotic dehiscence and hernia incarceration in one case where the patient later developed enterocutaneous fistula. In the remaining two patients with anastomotic dehiscence, protective stoma closure was omitted in one patient and permanent stoma was placed 23 months after LAR in the other patient. Permanent stoma placement was also required due to rectoprostatic fistula in one patient 36m after LAR. Altogether, 6 patients with sphincter-preserving surgery had stoma closure omitted or later placed as permanent due to late toxicity (faecal incontinence, anastomotic dehiscence and fistula). The last recorded serious adverse event possibly related to treatment was recorded after 60m of follow up in a patient with bladder carcinoma (Figure 2).

Quality of life evaluation (QoL)

Of 38 eligible patients, 31 (81.6%) completed the EORTC QLQ-C30 and QLQ-C29 questionnaires before treatment (T0), 1 year (T1) and ≥ 5 years (T5) after treatment at median age 75 years (range 37–86 years). The global QoL mean scores have not significantly changed over time (mean T0 vs. T5 was 57.0 vs. 60.8; $p = 0.384$), but were significantly lower compared to the general Slovenian population ($p = 0.035$). Also, no significant differences in mean scores over time were observed for any of the core functional and physical scales (data shown in Supplement 1). Significant changes in CR29 scales occurred 1 year after treatment and remain significant > 5 -year post treatment. There was a significant drop in reported blood and mucus (mean T0 vs. T1 vs. T5 was 33.9 vs.7.5 vs.4.3; T0/T1 and T0/T5 $p < 0.000$) and anxiety score (mean T0 vs. T1 vs. T5 was 67.7 vs. 39.3 vs. 42.2; T0/T1 $p = 0.000$ and T0/T5 $p = 0.005$), but higher scores were recorded for faecal incontinence/leakage, hair loss, and body image (T0/T1 $p = 0.027, 0.046,$ and 0.007 , respectively). There was no difference in mean scores for urinary incontinence between T0/T1, but mean scores rose

TABLE 2. Influence of probable prognostic factors on OS and DFS

Prognostic factor	Intention to treat (N = 51)		Per protocol (N = 47)	
	OS	DFS	OS	DFS
Age at diagnosis (≥ 65 years vs. <65 years)	ns	ns	ns	ns
Gender (male vs. female)	$p = 0.044$	ns	$p = 0.064$	ns
PS WHO	ns	ns	ns	ns
Tumour grade	ns	ns	ns	ns
Tumour location (upper/middle/lower rectal third)	ns	ns	ns	ns
MRI +	ns	ns	ns	ns
Extramesorectal lymph nodes (positive/negative)	ns	ns	ns	ns
Time to treatment ($\leq 7w / > 7w$)	$p = 0.045$	ns	ns	ns
Surgery procedure (APE and pelvic exenteration/LAR)	$p = 0.000$	$p = 0.013$	$p = 0.020$	$p = 0.016$
cT stage ^a	ns	ns	ns	ns
cN stage ^a	ns	ns	ns	ns
Decrease in T stage	ns	ns	ns	ns
Decrease in N stage	ns	ns	ns	ns
Total downstaging	ns	$p = 0.029$	ns	$p = 0.029$
pT stage (0-2 vs. 3-4)	ns	ns	ns	ns
pN stage (0 vs. +)	ns	$p = 0.044$	ns	$p = 0.019$
Ekstramesorectal lymph node removal	ns	ns	ns	ns
pCR	ns	ns	ns	ns
TRG prognostic group	ns	ns	ns	ns
NAR prognostic group	ns	ns	ns	ns
Adjuvant chemotherapy ^b (5-6 / ≤ 4 cycles)	ns	ns	ns	ns
Treatment per protocol	$p = 0.006$	$p = 0.001$	/	/

^a according to AJCC, 7th edition¹⁸; ^b calculated for 36 patients with indication for adjuvant chemotherapy; APE = abdominoperineal excision; DFS = disease free survival; LAR = low anterior resection; MRI+ = positive mesorectal fascia; N = nodal; NAR = neoadjuvant rectal cancer score³²; ns = not specific ($p > 0.05$). OS = overall survival; pCR = pathologic complete response; PS WHO = WHO performance status; T = tumour; TRG = tumour regression grade¹⁹

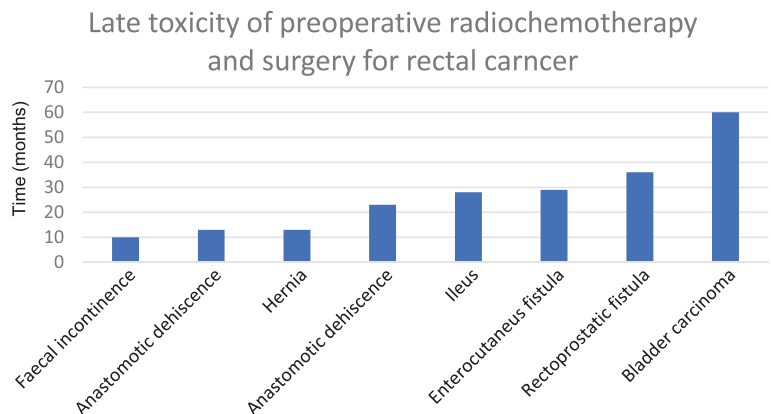


FIGURE 2. Time to occurrence of G ≥ 3 adverse events.

TABLE 3. Late toxicity after preoperative radiochemotherapy, surgery and adjuvant chemotherapy according to CTCAE version 5.0²⁰

	G1, n (%)	G2, n (%)	G3, n (%)	G4, n (%)	G5, n (%)
Anastomotic dehiscence	-	1 (2.1)	3 (6.3)	-	-
Anastomotic stenosis	4 (10.0)	-	-	-	-
Ileus	-	-	-	-	1 (2.1)
Hernia	4 (8.3)	1 (2.1)	1 (2.1)	-	-
Abdominal or pelvic pain	11 (22.9)	3 (6.3)	-	-	-
Anal stenosis	5 (10.4)	-	-	-	-
Fistula	-	1 (2.1)	2 (4.2)	-	-
Bloating	21 (43.8)	3 (6.3)	-	-	-
Constipation	10 (20.8)	4 (8.3)	-	-	-
Diarrhoea	9 (18.8)	5 (10.4)	-	-	-
Faecal incontinence	6 (15.4)	12 (30.8)	3 (7.7)	-	-
Faecal urgency*	5 (13.2)	1 (2.6)	-	-	-
Flatulence	25 (52.1)	6 (12.5)	-	-	-
Haemorrhoidal haemorrhage	1 (2.1)	-	-	-	-
Haemorrhoids	3 (6.3)	-	-	-	-
Proctitis	1 (2.1)	-	-	-	-
Intestinal stoma leak	2 (8.3)	-	-	-	-
Dysuria	1 (2.1)	-	-	-	-
Urinary frequency	13 (27.1)	-	-	-	-
Urinary incontinence	9 (18.8)	4 (8.3)	1 (2.1)	-	-
Urinary retention	1 (2.1)	1 (2.1)	-	-	-
Urinary urgency	21 (43.8)	1 (2.1)	-	-	-
Ejaculation disorder (n = 20)	5 (25)	1 (5)	-	-	-
Erectile dysfunction (n=20)	2 (10.0)	6 (30.0)	2 (10.0)	-	-
Dyspareunia (n=18)	1 (5.6)	2 (11.1)	1 (5.6)	-	-
Vaginal dryness (n = 18)	1 (5.6)	3 (16.7)	1 (5.6)	-	-
Vaginal stricture (n = 18)	1 (5.6)	1 (5.6)	1 (5.6)	-	-
Treatment-related secondary malignancy	-	-	1 (2.0)	-	-
Other**	-	-	-	-	-

* = data not available for all patients; ** = other: anal pain, anal, rectal or colonic haemorrhage, anal necrosis, anal or rectal fissure, anal ulcer, rectal obstruction or stenosis

CTCAE = Common Terminology Criteria for Adverse Events version 5.0.; G = grade

from 7.5 pre-treatment to 21.5 with > 5-year follow up ($p = 0.008$). T1 and T5 comparison showed a small but significant deterioration of pain, fatigue and nausea ($p = 0.09$, 0.017 and 0.033 , respectively) after treatment with longer follow-up.

According to QLQ-C30, our patient cohort had significantly lower QoL in comparison to the general Slovenian population (Table 4). Nearly all

functional scales' mean scores were lower with the exception of emotional function. Patients reported more fatigue, constipation, diarrhoea and financial problems. Compared to EORTC reference values for colorectal (CRC) cancer patients, our cohort had borderline significant lower cognitive functioning and reported higher financial problems.

TABLE 4. Health-related quality of life analysis: Mean scores comparisons 5 years after treatment with general Slovenian population³⁸ and with EORTC reference values for colorectal cancer patients³⁹ for all scales of EORTC QLQ-C30

Scale	5-year post-surgery mean (SD)	General Slovenian population mean (SD)	p value*	Colorectal reference values mean (SD)	p value*
Global health status/QoL	60.8 (26.1)	71.1 (21.4)	0.035	62.1 (23.4)	0.759
Functional scales					
Physical function	78.9 (24.5)	91.8 (14.0)	0.006	83.0 (21.1)	0.285
Role function	77.4 (26.0)	88.7 (20.1)	0.022	70.4 (32.8)	0.238
Emotional function	74.7 (25.0)	82.0 (18.5)	0.115	68.9 (24.5)	0.192
Cognitive function	78.0 (24.5)	90.2 (16.0)	0.009	85.2 (20.4)	0.052
Social function	78.5 (24.8)	90.9 (17.3)	0.009	76.0 (28.6)	0.629
Symptom scales					
Fatigue	29.4 (23.2)	19.8 (19.8)	0.029	34.7 (28.4)	0.302
Nausea/vomiting	6.5 (10.3)	3.3 (10.6)	0.097	7.3 (17.2)	0.796
Pain	21.0 (23.2)	14.5 (20.2)	0.130	24.0 (29.6)	0.575
Dyspnoea	10.8 (23.4)	5.3 (15.3)	0.204	17.4 (26.3)	0.160
Insomnia	30.1 (30.3)	19.8 (25.1)	0.067	30.5 (32.6)	0.946
Appetite loss	12.9 (22.2)	5.3 (15.5)	0.067	19.1 (30.2)	0.256
Constipation	20.4 (26.8)	6.9 (16.9)	0.009	15.8 (27.9)	0.363
Diarrhoea	16.1 (22.6)	4.2 (13.6)	0.006	16.6 (27.6)	0.920
Financial problems	22.6 (29.0)	6.6 (17.5)	0.005	13.6 (26.3)	0.059

* = values (p < 0.050) are bolded

Discussion

Preoperative use of IMRT for LARC is increasing rapidly with great variations in clinical practice among centres²⁴ indicating a lack of quality clinical studies reporting treatment outcome and toxicity for different fractionation regimes. To date, only four prospective phase II studies have been published with short-term outcome data after preoperative IMRT concomitant with capecitabine in patients with LARC^{9,16,25,26}, but none of them reported long-term results. Our study is the first to report a 5-year treatment outcome with late toxicity and QoL.

With shorter treatment time and no dose escalation with SIB to primary tumour only, our pCR rate improved from 10% to 25.5%.^{16,27} With dose escalation in a Chinese study (41 Gy elective; 56 Gy tumour/lymph node; 22 fractions) and a Spanish study (46 Gy elective; 57.5 Gy tumour/lymph nodes; 23 fraction) they reported 31% and 30.6% pCR, respectively.^{9,11} The higher pCR rate can reflect higher BED in these trials, but pCR of 32.6% recently reported by Simson *et al.* in a prospec-

tive observational study with single target dose of 50.4 Gy in 28 fractions suggests other possible factors influencing treatment results, since there are important differences in target definition and treatment verification between studies.²⁸ With no boost to pathologic lymph nodes, but with detailed contouring guidelines, added internal safety margin and image-guided radiation therapy (IGRT), we have achieved an equal or better N downstaging rate (83%) in comparison to the Chinese and Spanish trials (79.2% and 47.2%, respectively) where a 5 mm uniform margin was used.

The encouraging total downstaging rate of 87% in our study translated into excellent 5-year OS, DFS and LC of 80.9%, 77.1% and 95.2%, respectively. OS and DFS were significantly higher compared to our historic cohort²⁹ (OS 61.4%, p = 0.03 and DFS 52.4%, p = 0.01). Studies with more intensified escalated IMRT regimes with added concurrent oxaliplatin^{12,30}, are reporting 5-year OS of 63–82% and 5-year DFS of 60–66%, that are comparable to our study.

A reported death from cardiovascular disease in three male patients can probably explain why

male gender is significant prognostic factor for OS but not for DFS. Surprisingly, the type of operation significantly affected OS and DFS. In concordance with other studies, we found significant association between total downstaging and pN0 with the improvement of DFS³¹, but we found no predictive value for pCR, TRG prognostic group¹⁹ or NAR prognostic group³² as survival surrogates. However, we found excellent prognosis for the group of patients with pCR who had 91.7% 5-year OS and 100% 5-year DFS and 100% 5-year LC, confirming observations from other studies.³³

Previously, we reported low acute toxicity of preoperative treatment and postoperative complications ($G \geq 3$ of 4% and 8% respectively). All patients with LAR had protective stoma placement, so we recorded no anastomotic leakage, but with time, 4 (8%) cases of anastomotic dehiscence were detected, as expected from the published literature.³⁴ In median follow-up of 70 months, we recorded 17 $G \geq 3$ late adverse events in 12 patients (25% of patients who underwent surgery), with 15% of GI, 2% urinary and 8% sexual late toxicity, significantly lower than to our historic cohort (40%, 19.2% and 51.7%, respectively)²⁹ and less than 35% reported late surgical complications after 3D CRT concomitant with 5-Fu/oxaliplatin.³⁵ The only comparable IMRT study reporting late adverse events is a Belgian study, with preoperative IMRT-SIB to 46/55.2 Gy in 23 fractions and median 54 months of follow-up.¹⁰ Their estimated $G \geq 3$ late toxicity was 13% and is lower than the 25% observed in our study with much lower GI and GU toxicity rates (9% *vs.* 15% and 4% *vs.* 10%, respectively) compared to ours. With different recording of late effects in our study, the late toxicity could have been overestimated. Anastomotic dehiscence was discovered late, when protective stoma closure was planned and was not counted as a postoperative complication. Late events were recorded with the actuarial method, so faecal incontinence, although not present at the time of the last follow-up, occurred previously in two patients. Also, we had no data on sexual activity and GI disorder prior to treatment, so all GI events are counted as late sequelae, although no difference in sexual functioning before and 5 years after treatment was found on QoL analysis. Exclusion of anastomotic dehiscence and two cases of faecal incontinence decreases our rate of GI $G \geq 3$ toxicity to 8%, which is in concordance with 9% in the Belgian study and 9% reported after 3D CRT.³⁴ The occurrence of $G \geq 2$ late diarrhoea (10%) is also within the range of reported rates in the literature, with 9.5% of patients

from the EORTC 22921 trial who reported grade 2 diarrhoea or higher after 5-year follow-up.³⁴ The Spanish and Chinese investigators reported 2 and 4 fistulas in median follow-up at 17 m and 22 m. The occurrence of fistula in our study is similar, with 3 fistulas that occurred 29, 34 and 36 months after surgery, showing the importance of longer follow-up and subsequently underreporting of long toxicity events in clinical studies. Since the first publication with a reported sphincter preservation rate of 62% in our series, 6 patients with LAR ended up with permanent stoma due to faecal incontinence, anastomotic dehiscence and fistula, but still, we report a high rate of 5 y colostomy-free survival of 76%, comparable to other studies.³⁵ Regarding major toxicity, 1 patient (2%) died due to treatment-related toxicity, consistent with a 1.4% and 2% death rate in the EORTC 22921 and German CAO/ARO/AIO-94 trial, respectively.^{34,36}

Our patient cohort have significantly lower quality of life compared to the general Slovenian population³⁷ according to EORTC QLQ-C30 scores comparison, with inferior global function and functional mean scales with problems with fatigue, constipation, diarrhoea and finance. However, comparison to EORTC reference scores³⁸ for CRC patients shows no difference in any of the QLQ-C30 items with borderline lower cognitive function, reflecting advanced patient age (median 75 years) at 5-year data collection. Time analysis of EORTC QLQ-C30 and QLQ-C29 median scores showed that improvement or deterioration of function/symptom appeared one year after treatment and remained stable with longer follow-up. We recorded improvement in body image and a drop of anxiety and as expected after surgery, there was less mucus/blood in stool, and after radiation patients reported hair loss. A significant rise in reported faecal incontinence/leakage, is in concordance with the reported late toxicity but late detection of urinary incontinence (significant after 5 but not 1 year) indicates the importance of long follow-up for reliable reporting of late toxicity. Contrary to 8% sexual late toxicity findings, there were no differences in sexual end points in the QoL analysis, reflecting the possibility of overestimation of these late events in our cohort.

Together with uncertainty in the reporting of late toxicity, the main limitation of our study design is the small sample size and lack of randomization. According to definition of "locally advanced rectal cancers" before new subgroup division consensus in 2013, we used the term locally advanced also for the intermediate/bad group, without additional

subdivision of T3 tumours. Nevertheless, our results are comparable to above mentioned studies, for they used the same definition in that time. The advantages of our study are the very strict radiotherapy protocol and quality control with the precise recording of acute and late toxicity events. In comparison to other IMRT studies for preoperative LARC, we were the only one not to intensify treatment with dose escalation and/or novel drug addition.

By shortening the overall treatment time using SIB, we reported excellent 25.5% pCR and after 5-year follow-up, our OS and DFS (80.9% and 77.1%, respectively) are in the survival range of more intensified treatments^{12,30}, suggesting possible overtreatment for certain patients with LARC. In the era of high local control, more effort should be directed to reducing acute and late toxicity. Our fractionation regime showed a very low acute toxicity profile with a non-negligible late events rate. More high-quality data with longer follow-up is needed to determine the true effect on QoL and possibly determine relevant tolerances of the organ at risk for late consequences to optimize treatment planning.

Conclusions

The results of this long-term study confirm that IMRT SIB is feasible for preoperative treatment of intermediate/locally advanced rectal cancer. By shortening the overall treatment time, without dose escalation, we achieved high pCR, five-year overall survival, disease-free survival and local control. Due to the favourable acute toxicity profile, our treatment regime is suitable for treatment intensification with another drug in addition to capecitabine. More long-term data is needed for late toxicity assessment.

References

- Gérard JP, Azria D, Gourgou-Bourgade S, Martel-Lafay I, Hennequin C, Etienne PL, et al. Clinical outcome of the ACCORD 12/0405 PRODIGE 2 randomized trial in rectal cancer. *J Clin Oncol* 2012; **30**: 4558-65. doi: 10.1200/JCO.2012.42.8771
- Rödel C, Liersch T, Becker H, Fietkau R, Hohenberger W, Hothorn T, et al. Preoperative chemoradiotherapy and postoperative chemotherapy with fluorouracil and oxaliplatin versus fluorouracil alone in locally advanced rectal cancer: initial results of the German CAO/ARO/AIO-04 randomised phase 3 trial. *Lancet Oncol* 2012; **13**: 679-87. doi: 10.1016/S1470-2045(12)70187-0
- O'Connell MJ, Colangelo LH, Beart RW, Petrelli NJ, Allegra CJ, Sharif S, et al. Capecitabine and oxaliplatin in the preoperative multimodality treatment of rectal cancer: surgical end points from National Surgical Adjuvant Breast and Bowel Project trial R-04. *J Clin Oncol* 2014; **32**: 1927-34. doi: 10.1200/JCO.2013.53.7753
- Bahadoer RR, Dijkstra EA, van Etten B, Marijnen CAM, Putter H, Kranenbarg EM, et al. Short-course radiotherapy followed by chemotherapy before total mesorectal excision (TME) versus preoperative chemoradiotherapy, TME, and optional adjuvant chemotherapy in locally advanced rectal cancer (RAPIDO): a randomised, open-label, phase 3 trial. *Lancet Oncol* 2021; **22**: 29-42. doi: 10.1016/S1470-2045(20)30555-6
- Arbea L, Ramos LI, Martínez-Monge R, Moreno M, Aristu J. Intensity-modulated radiation therapy (IMRT) vs. 3D conformal radiotherapy (3DCRT) in locally advanced rectal cancer (LARC): dosimetric comparison and clinical implications. *Radiat Oncol* 2010; **5**: 17. doi: 10.1186/1748-717X-5-17
- Guerrero Urbano MT, Henrys AJ, Adams EJ, Norman AR, Bedford JL, Harrington KJ, et al. Intensity-modulated radiotherapy in patients with locally advanced rectal cancer reduces volume of bowel treated to high dose levels. *Int J Radiat Oncol Biol Phys* 2006; **65**: 907-16. doi: 10.1016/j.ijrobp.2005.12.056
- Engels B, De Ridder M, Tournel K, Sermeus A, De Coninck P, Verellen D, et al. Preoperative helical tomotherapy and megavoltage computed tomography for rectal cancer: impact on the irradiated volume of small bowel. *Int J Radiat Oncol Biol Phys* 2009; **74**: 1476-80. doi: 10.1016/j.ijrobp.2008.10.017
- Mok H, Crane CH, Palmer MB, Briere TM, Beddar S, Delclos ME, et al. Intensity modulated radiation therapy (IMRT): differences in target volumes and improvement in clinically relevant doses to small bowel in rectal carcinoma. *Radiat Oncol* 2011; **6**: 63. doi: 10.1186/1748-717X-6-63
- Li JL, Ji JF, Cai Y, Li XF, Li YH, Wu H, et al. Preoperative concomitant boost intensity-modulated radiotherapy with oral capecitabine in locally advanced mid-low rectal cancer: a phase II trial. *Radiother Oncol* 2012; **102**: 4-9. doi: 10.1016/j.radonc.2011.07.030
- Engels B, Platteaux N, Van den Begin R, Gevaert T, Sermeus A, Storme G, et al. Preoperative intensity-modulated and image-guided radiotherapy with a simultaneous integrated boost in locally advanced rectal cancer: report on late toxicity and outcome. *Radiother Oncol* 2014; **110**: 155-9. doi: 10.1016/j.radonc.2013.10.026
- Hernando-Requejo O, López M, Cubillo A, Rodríguez A, Ciervide R, Valero J, et al. Complete pathological responses in locally advanced rectal cancer after preoperative IMRT and integrated-boost chemoradiation. *Strahlenther Onkol* 2014; **190**: 515-20. doi: 10.1007/s00066-014-0650-0
- Picardi V, Macchia G, Guido A, Giaccherini L, Deodato F, Farioli A, et al. Preoperative chemoradiation with VMAT-SIB in rectal cancer: a phase II study. *Clin Colorectal Cancer* 2017; **16**: 16-22. doi: 10.1016/j.clcc.2016.06.004
- Hong YS, Nam BH, Kim KP, Kim JE, Park SJ, Park YS, et al. Oxaliplatin, fluorouracil, and leucovorin versus fluorouracil and leucovorin as adjuvant chemotherapy for locally advanced rectal cancer after preoperative chemoradiotherapy (ADORE): an open-label, multicentre, phase 2, randomised controlled trial. *Lancet Oncol* 2014; **15**: 1245-53. doi: 10.1016/S1470-2045(14)70377-8
- Zhu J, Liu F, Gu W, Lian P, Sheng W, Xu J, et al. Concomitant boost IMRT-based neoadjuvant chemoradiotherapy for clinical stage II/III rectal adenocarcinoma: results of a phase II study. *Radiat Oncol* 2014; **9**: 70. doi: 10.1186/1748-717X-9-70
- Hong TS, Moughan J, Garofalo MC, Bendell J, Berger AC, Oldenburg NB, et al. NRG Oncology Radiation Therapy Oncology Group 0822: a phase 2 study of preoperative chemoradiation therapy using intensity modulated radiation therapy in combination with capecitabine and oxaliplatin for patients with locally advanced rectal cancer. *Int J Radiat Oncol Biol Phys* 2015; **93**: 29-36. doi: 10.1016/j.ijrobp.2015.05.005
- But-Hadzic J, Anderlüh F, Breclj E, Ethemovic I, Secerov-Ermenc A, Hudej R, et al. Acute toxicity and tumor response in locally advanced rectal cancer after preoperative chemoradiation therapy with shortening of the overall treatment time using intensity-modulated radiation therapy with simultaneous integrated boost: a phase 2 trial. *Int J Radiat Oncol* 2016; **96**: 1003-10. doi: 10.1016/j.ijrobp.2016.08.031
- But-Hadzic J, Velenik V. Preoperative intensity-modulated chemoradiation therapy with simultaneous integrated boost in rectal cancer: 2-year follow-up results of phase II study. *Radiat Oncol* 2018; **52**: 23-29. doi: 10.1515/raon-2018-0007
- Edge SB, Compton CC. The American Joint Committee on Cancer: the 7th edition of the AJCC cancer staging manual and the future of TNM. *Ann Surg Oncol* 2010; **17**: 1471-4. doi: 10.1245/s10434-010-0985-4

19. Dworak O, Keilholz L, Hoffmann A. Pathological features of rectal cancer after preoperative radiochemotherapy. *Int J Colorectal Dis* 1997; **12**: 19-23. doi: 10.1007/s003840050072
20. Cancer Institute N. *Common Terminology Criteria for Adverse Events (CTCAE) v5.0.*; 2017. [cited 2021 Feb 04]. Available at https://ctep.cancer.gov/protocoldevelopment/electronic_applications/docs/ctcae_v5_quick_reference_5x7.pdf
21. Aaronson NK, Ahmedzai S, Bergman B, Bullinger M, Cull A, Duez NJ, et al. The European Organization for Research and Treatment of Cancer QLQ-C30: a quality-of-life instrument for use in international clinical trials in oncology. *J Natl Cancer Inst* 1993; **85**: 365-76. doi: 10.1093/jnci/85.5.365
22. van der Hout A, Neijenhuijs KI, Jansen F, van Uden-Kraan CF, Aaronson NK, Groenvold M, et al. Measuring health-related quality of life in colorectal cancer patients: systematic review of measurement properties of the EORTC QLQ-CR29. *Support Care Cancer* 2019; **27**: 2395-412. doi: 10.1007/s00520-019-04764-7
23. Fayers P, Aaronson NK, Bjordal K, Groenvold M, Curran D, Bottomley A. *EORTC QLQ-C30 Scoring Manual*. European Organisation for Research and Treatment of Cancer; 2001. [cited 2021 Feb 04]. Available at <https://abdn.pure.elsevier.com/en/publications/eortc-qlq-c30-scoring-manual-3rd-edition>.
24. Hanna CR, Slevin F, Appelt A, Beavon M, Adams R, Arthur C, et al. Intensity-modulated radiotherapy for rectal cancer in the UK in 2020. *Clin Oncol* 2021; **33**: 214-23. doi: 10.1016/j.clon.2020.12.011
25. Fernández-Martos C, Pericay C, Aparicio J, Salud A, Safont M, Massuti B, et al. Phase II, randomized study of concomitant chemoradiotherapy followed by surgery and adjuvant capecitabine plus oxaliplatin (CAPOX) compared with induction CAPOX followed by concomitant chemoradiotherapy and surgery in magnetic resonance imaging-defined, locally advanced rectal cancer: Grupo cancer de recto 3 study. *J Clin Oncol* 2010; **28**: 859-65. doi: 10.1200/JCO.2009.25.8541
26. Tey J, Leong CN, Cheong WK, Sze TG, Yong WP, Tham IWK, et al. A phase II trial of preoperative concurrent chemotherapy and dose escalated intensity modulated radiotherapy (IMRT) for locally advanced rectal cancer. *J Cancer* 2017; **8**: 3114-21. doi: 10.7150/jca.21237
27. Velenik V, Anderluh F, Oblak I, Strojanc P, Zakotnik B. Capecitabine as a radiosensitizing agent in neoadjuvant treatment of locally advanced resectable rectal cancer: prospective phase II trial. *Croat Med J* 2006; **47**: 693-700.
28. Simson DK, Mitra S, Ahlawat P, Saxena U, Sharma MK, Rawat S, et al. Prospective study of neoadjuvant chemoradiotherapy using intensity-modulated radiotherapy and 5 fluorouracil for locally advanced rectal cancer – Toxicities and response assessment. *Cancer Manag Res* 2018; **10**: 519-26. doi: 10.2147/CMAR.S142076
29. Velenik V, Oblak I, Anderluh F. Long-term results from a randomized phase II trial of neoadjuvant combined-modality therapy for locally advanced rectal cancer. *Radiat Oncol* 2010; **5**: 88. doi: 10.1186/1748-717X-5-88
30. Garofalo M, Moughan J, Hong T, J. Bendell, A. Berger, F. Lerna, et al. RTOG 0822: a phase II study of preoperative (PREOP) chemoradiotherapy (CRT) utilizing IMRT in combination with capecitabine (C) and oxaliplatin (O) for patients with locally advanced rectal cancer. *Int J Radiat Oncol* 2011; **81**: S3-S4. doi: 10.1016/j.ijrobp.2011.06.008
31. Fokas E, Liersch T, Fietkau R, Hohenberger W, Beissbarth T, Hess C, et al. Tumor regression grading after preoperative chemoradiotherapy for locally advanced rectal carcinoma revisited: updated results of the CAO/ARO/AIO-94 trial. *J Clin Oncol* 2014; **32**: 1554-62. doi: 10.1200/JCO.2013.54.3769
32. George TJ, Allegra CJ, Yothers G. Neoadjuvant Rectal (NAR) Score: a new surrogate endpoint in rectal cancer clinical trials. *Curr Colorectal Cancer Rep* 2015; **11**: 275-80. doi: 10.1007/s11888-015-0285-2
33. Maas M, Nelemans PJ, Valentini V, Das P, Rödel C, Kuo LJ, et al. Long-term outcome in patients with a pathological complete response after chemoradiation for rectal cancer: a pooled analysis of individual patient data. *Lancet Oncol* 2010; **11**: 835-44. doi: 10.1016/S1470-2045(10)70172-8
34. Sauer R, Becker H, Hohenberger W, Rödel C, Wittekind C, Fietkau R, et al. Preoperative versus postoperative chemoradiotherapy for rectal cancer. *N Engl J Med* 2004; **351**: 1731-40. doi: 10.1056/NEJMoa040694
35. Urso E, Serpentine S, Pucciarelli S, De Salvo GL, Friso ML, Fabris G, et al. Complications, functional outcome and quality of life after intensive preoperative chemoradiotherapy for rectal cancer. *Eur J Surg Oncol* 2006; **32**: 1201-8. doi: 10.1016/j.ejso.2006.07.003
36. Bosset JF, Collette L, Calais G, Mineur L, Maingon P, Radosevic-Jelic L, et al. Chemotherapy with preoperative radiotherapy in rectal cancer. *N Engl J Med* 2006; **355**: 1114-23. doi: 10.1056/NEJMoa060829
37. Velenik V, Secerov-Ermenc A, But-Hadzic J, Zadnik V. Health-related quality of life assessed by the EORTC QLQ-C30 questionnaire in the general slovenian population. *Radiat Oncol* 2017; **51**: 342-50. doi: 10.1515/raon-2017-0021
38. Scott NW, Fayers PM, Aaronson NK, Bottomley A, de Graeff A, Groenvold M, et al; EORTC Quality of Life Group. *EORTC QLQ-C30 Reference Values*; 2008. [cited 2021 Feb 04]. Available at https://www.eortc.org/app/uploads/sites/2/2018/02/reference_values_manual2008.pdf

The role of haematological parameters in predicting the response to radical chemoradiotherapy in patients with anal squamous cell cancer

Suzana Stojanovic-Rundic^{1,2}, Mladen Marinkovic¹, Milena Cavic³,
Vesna Plesinac Karapandzic^{1,2}, Dusica Gavrilovic⁴, Radmila Jankovic³,
Richarda M. de Voer⁵, Sergi Castellvi-Bel⁶, Zoran Krivokapic^{2,7}

¹ Clinic for Radiation Oncology and Diagnostics, Department of Radiation Oncology, Institute for Oncology and Radiology of Serbia, Belgrade, Serbia

² Faculty of Medicine, University of Belgrade, Belgrade, Serbia

³ Department of Experimental Oncology, Institute for Oncology and Radiology of Serbia, Belgrade, Serbia

⁴ Data Center, Institute for Oncology and Radiology of Serbia, Belgrade, Serbia

⁵ Department of Human Genetics, Radboud Institute of Molecular Life Sciences, Radboud University Medical Center, Nijmegen, the Netherlands

⁶ Gastroenterology Department, Institut d' Investigacions Biomèdiques August Pi i Sunyer (IDIBAPS), Centro de Investigación Biomédica en Red de Enfermedades Hepáticas y Digestivas (CIBERehd), Hospital Clínic, Barcelona, Spain

⁷ Clinic for Digestive Surgery, Clinical Center of Serbia, Belgrade, Serbia

Radiol Oncol 2021; 55(4): 449-458.

Received 18 May 2021
Accepted 16 July 2021

Correspondence to: Assoc. Prof. Suzana Stojanović-Rundić, M.D., Ph.D., Institute for Oncology and Radiology of Serbia, Clinic for Radiation Oncology and Diagnostics, Department of Radiation Oncology, Pasterova 14, 11000 Belgrade, Serbia. E-mail: stojanovics@ncrc.ac.rs

Disclosure: No potential conflicts of interest were disclosed.

This is an open access article under the CC BY-NC-ND license (<http://creativecommons.org/licenses/by-nc-nd/4.0/>).

Background. Historically, the treatment of choice for anal cancer had been abdominoperineal resection (APR). Radical radiotherapy with concurrent 5-fluorouracil plus mitomycin C chemotherapy was later established as standard therapy, although with a failure rate of 20–30%. The aim of this study was to evaluate the outcomes after radical chemoradiotherapy (CRT), prognostic and predictive factors and patterns of failure.

Patients and methods. This study included 47 patients treated with radical CRT for pathohistologically confirmed anal squamous cell carcinoma. Analysed haematological parameters included: neutrophil-to-lymphocyte ratio (NLR), platelet-to-lymphocyte ratio (PLR), and haemoglobin level. The final logistic regression model included treatment break period. Tumour response was assessed at 24 weeks from CRT completion. Follow-up was performed every 3 months during the first two years, and every 6 months thereafter.

Results. A complete clinical response (CR) was detected in 30 patients (63.8%). Patients who did not achieve a 6-months CR and those who had a CR after 6 months but then relapsed were referred to surgical treatment. With combined CRT and surgical salvage treatment the CR rate was 80.9%. Patients with CR after 6 months had significantly longer disease-free survival (DFS), progression-free survival (PFS), and overall survival (OS). A significant effect on the 6-month response was confirmed for PLR ($p = 0.03$).

Conclusions. Important prognostic factors associated with CR were baseline haemoglobin level and period of treatment interruptions. Potential haematological prognostic factors could be PLR and NLR, which can be routinely determined by low-cost and minimally invasive methods.

Key words: anal cancer; chemoradiotherapy; haematological parameters

Introduction

The anal cancer is a rare malignancy in the general population globally. According to the latest official reports from 2018, it represented only 0.23% of all malignancies in Serbia.¹ However, over the last two decades there has been a steady increase in anal cancer incidence. This might be related to an increased spread of human papilloma virus (HPV) and human immunodeficiency virus (HIV) through sexual transmission, which are established risk factors of this.^{2,3}

Historically, the treatment of choice for the anal cancer had been abdominoperineal resection (APR). The upfront use of surgical treatment was associated with a high percentage of local recurrence (around 40%) and a five-year survival of about 40–70%.⁴ This approach also leads to serious morbidity due to permanent colostomy.⁵ Studies on the application of concurrent preoperative chemoradiotherapy (CRT) treatment during the 1970s gave space for further research focused on preserving the function of the anal sphincter, with better locoregional control and longer survival.⁶ As a result of multiple randomized trials, radical radiotherapy (RT) with concurrent 5-fluorouracil (5-FU) plus mitomycin C (MMC) chemotherapy was established as a standard therapy for patients diagnosed with anal cancer.^{7–9} Treatment with CRT leads to preservation of the anal sphincter and a 5-year survival rate up to 80%.¹⁰ However, failure of CRT occurs in 20–30% of patients, resulting in persistent or recurrent anal cancer.¹¹ Radical surgery is reserved for salvage treatment in case of partial response or recurrence.¹² Although molecular targeted therapies have redefined treatment strategies in colorectal cancer, they have shown little potential in anal cancer.^{13–16}

The optimal total dose, schedule of RT and radiation delivery techniques for the anal cancer continue to be evaluated. Current state-of-the-art does not provide uniform recommendations regarding the mentioned RT parameters.¹⁷ According to the ACCORD-03 trial no benefit was achieved using doses of > 59 Gy.¹⁸ Due to the need to apply high RT doses to a large volume area, with combined toxicity of concomitant chemotherapy, adverse events requiring a treatment break of CRT are reported in up to 80% of patients.¹⁹ On the other hand, some studies have shown that limited breaks in treatment are associated with increased local disease control.²⁰ The split-course approach with a planned treatment break can be an option to reduce treatment-related toxicity and avoid required interruptions.²¹

The aim of this study was to evaluate the outcomes after radical CRT for patients with anal squamous cell cancer, and to investigate prognostic and predictive factors using the logistic regression model, as well as patterns of failure.

Patients and methods

Patients

We retrospectively reviewed medical records of 53 patients who were treated with radical CRT for anal cancer between January 2009 and December 2019 at the Institute for Oncology and Radiology of Serbia. Patients who underwent palliative therapy ($n = 6$) were excluded, so the final analysis was conducted on 47 patients. All patients had a pathological diagnosis of anal squamous cell cancer confirmed by endoscopic biopsy. Prior to treatment, patients underwent physical examination, conventional radiography or computed tomography (CT) of the chest and CT or magnetic resonance imaging (MRI) of the abdomen and pelvis. Ethylenediaminetetraacetic acid (EDTA) peripheral blood was drawn by venipuncture and haematological parameters were derived from the absolute differential counts of a complete blood count (CBC). The neutrophil-to-lymphocyte ratio (NLR) was calculated as a ratio of circulating neutrophil and lymphocyte counts, and the platelet-to-lymphocyte ratio (PLR) was defined as the absolute count of platelets divided by the absolute lymphocyte count. Patients' pre-treatment haemoglobin levels were obtained from medical history. The staging of the tumour was re-evaluated according to the eighth edition of the Union for International Cancer Control (UICC) TNM staging system for cancer of the anal canal.²² The general condition of the patients was classified using the ECOG Scale of Performance Status.²³

Chemoradiotherapy

RT began on the first day of chemotherapy and was administered 5 times a week with a daily fraction of 1.8 Gy. External beam RT was performed with either an anteroposterior-posteroanterior (2D technique) or three-dimensional conformal RT (3D-CRT).²⁴ The target volumes and dose prescription were defined according to the International Commission on Radiation Units and Measurements (ICRU) Reports 50 and 62.^{25,26} The gross tumour volume (GTV) encompassed the visible primary tumour on physical examination

and imaging. Gross disease clinical target volume (CTV3) includes GTV with a 2 cm margin expansion but excluding uninvolved bone, muscle, or air. Nodal GTV was defined as all nodes that are ≥ 1.5 cm, or biopsy proven nodes. The clinical target volume (CTV1) included the gross disease CTV, areas at risk for microscopic spread, and regional lymph nodes (presacral, internal and external iliac, and inguinal nodes). The prescribed dose for this volume was 36 Gy in 20 fractions. After a two-week break in treatment according to the split course approach, RT was continued with a boost dose of 14.4 Gy in 8 fractions to CTV2, for a total prescribed dose of 50.4 Gy. The CTV2 included the gross disease CTV in addition with areas at risk for microscopic spread, and regional lymph nodes inferior to the sacroiliac joint. In cases with inguinal lymph node metastases, inguinal nodes were also included in this volume. The planning target volume (PTV) was extended from CTV with margins of 1 cm in all directions. After administration of 50.4 Gy, an additional boost of 9 Gy in 5 fractions was applied to the gross disease CTV (CTV3 = PTV3). Radiation was delivered with a 10 MV linear accelerator.

Chemotherapy consisted of two cycles of 5-FU and MMC. MMC (12 mg/m^2) was administered on the first day of both parts of RT. 5-FU infusion (1000 mg/m^2) was given on days 1 to 4 at the first and the second part of RT.

The treatment compliance and acute toxicity were evaluated weekly according to the common terminology criteria for adverse events (CTCAE) v.5.0.²⁷

Assessment of tumour response

Tumour response was assessed at 24 weeks from CRT completion. The response to treatment was evaluated by a digital rectal examination, rectosigmoidoscopy, and radiologic evaluation (pelvic CT or MRI). Results of the clinical assessment were reported as complete clinical response (CR) or incomplete response (partial regression [PR], stable disease [SD] or progression [PD]).²⁸ Patients with incomplete clinical response were referred to surgical treatment, as well as those with initial complete response who relapsed. In case of distant disease progression, patients were selected for chemotherapy.

Patient follow-up

Follow-up of patients was performed every 3 months during the first two years after comple-

tion of treatment, and every 6 months thereafter. Clinical examination and rectosigmoidoscopy were done at each follow-up. CT/MRI of the pelvis was performed every 3 months in the first year of follow-up and every 6 months thereafter.

Overall survival (OS) was defined as time from the date of beginning of CRT to the date of the last clinical control or the date of death. Anal cancer specific overall survival (ACSOS) excluded patients in whom death occurred for other reasons, and was calculated like OS. Progression-free survival (PFS) was calculated for patients whose response was assessed as PR, CR, or SD on initial evaluation 6 months after treatment completion, and was defined as time from the date of follow-up 6 months after treatment until the onset of progression, death or last follow-up for patients who did not progress. Disease-free survival (DFS) was based on the time from achieving a CR to the onset of progression, death, or the date of the last follow-up for patients who did not progress. Colostomy-free survival (CFS) was calculated only for patients in whom no colostomy was placed at the time of beginning of CRT, and was defined as the time from the start of treatment to the date of placement of a colostomy, death, or the date of the last follow-up for patients who did not have a colostomy. Overall treatment time (OTT) was measured as the number of days from the start of CRT to the end of treatment.

Statistical analysis

For normal distribution data testing, the Kolmogorov-Smirnov and Shapiro-Wilk tests were used. Descriptive methods (frequencies, percent, mean, median, standard deviation [SD] and range) were used to summarize the data. The statistical significance level was set at $p < 0.05$. For comparison of disease and treatment characteristics among different risk subgroups the Wilcoxon rank sum, Pearson chi-square and Fisher exact tests were used. Methods of survival analysis were used for DFS, OS, PFS, ACSOS, CFS (median with corresponding 95% confidence interval [CI] for description, Kaplan-Meier product-limit method for illustration and log-rank test). Also, for evaluating potential predictors of the response, univariate and multivariate logistic regression was used (odds ratio [OR] with 95% CI for description, Likelihood Ratio and Wild test), and the CR after 6 months (coded as 0) *vs.* non-CR (coded as 1) was set as a dependent variable. The receiver operating characteristics (ROC) curve methods were applied to investigate the discriminative potential of NLR and

TABLE 1. Patients' disease, treatment and outcomes characteristics

Characteristics	N (%)	Characteristics	N (%)
Age (years)		NLR	
Mean (SD)	61.9 (10.0)	Mean (SD)	2.7 (1.7)
Median (Range)	63.0 (40.0–81.0)	Median (Range)	2.1 (0.8–7.0)
Gender		PLR	
Female	36 (76.6%)	Mean (SD)	159.4 (92.1)
Male	11 (23.4%)	Median (Range)	132.9 (51.7–401.2)
Performance status (PS)¹		RT technique	
ECOG 0	13 (27.7%)	2D	23 (48.9%)
ECOG 1	33 (70.2%)	3D	24 (51.1%)
ECOG 2	1 (2.1%)	The first RT part-dose (Gy)	
T in clinical TNM		Mean (SD)	36.1 (1.6)
T2	18 (38.3%)	Median (Range)	36 (30–45)
T3	24 (51.1%)	The second RT part-dose (Gy)	
T4	5 (10.6%)	Mean (SD)	22.8 (2.5)
N in clinical TNM		Median (Range)	23.4 (9–26)
N0	17 (36.2%)	Total dose (Gy)	
N1	30 (63.8%)	Mean (SD)	58.9 (1.6)
UICC staging		Median (Range)	59.4 (52–59.4)
IIA	10 (21.3%)	OTT (days)	
IIB	7 (14.9%)	Mean (SD)	74.7 (14.2)
IIIA	8 (17.0%)	Median (Range)	77 (51–134)
IIIC	22 (46.8%)	Acute toxicity-first part	
Tumour differentiation		Without or gr. I/II	26 (55.3%)
well	24 (51.1%)	Grade III/IV	21 (44.7%)
moderate	13 (27.7%)	Acute toxicity-second part	
poor	4 (8.5%)	Without or gr. I/II	32 (68.1%)
without data	6 (12.8%)	Grade III/IV	15 (31.9%)
Tumour size (cm)		Tumour response at 6 months	
Mean (SD)	5.2 (2.0)	CR	30 (63.8%)
Median (Range)	5.4 (2.1–10.0)	PR	15 (31.9%)
Initial haemoglobin level (g/L)		SD	1 (2.1%)
Mean (SD)	116.3 (20.3)	PD	1 (2.1%)
Median (Range)	124 (66–154)	Follow-up period (months)	
Pretreatment colostomy		Mean (SD)	53.0 (30.9)
No	42 (89.4%)	Median (Range)	44 (11–136)
Yes	5 (10.6%)	Total	47 (100%)

CR = complete clinical response; NLR = neutrophil-to-lymphocyte ratio; OTT = overall treatment time; PD = disease progression; PR = partial regression; PLR = platelet-to-lymphocyte ratio; RT = radiotherapy; SD = stable disease; SD = standard deviation; UICC = Union for International Cancer Control; ¹ ECOG PS = The Eastern Cooperative Oncology Group performance status

PLR for the presence/absence of CR (Area Under the ROC curve [AUC ROC] according DeLong's method; Likelihood ratio test for AUC ROC; the best cut-off value was set as value with maximum

sensitivity and specificity). The statistical analysis was performed using the program R (version 3.3.2 (2016-10-31) –“Sincere Pumpkin Patch”; Copyright (C) 2016 The R Foundation for Statistical

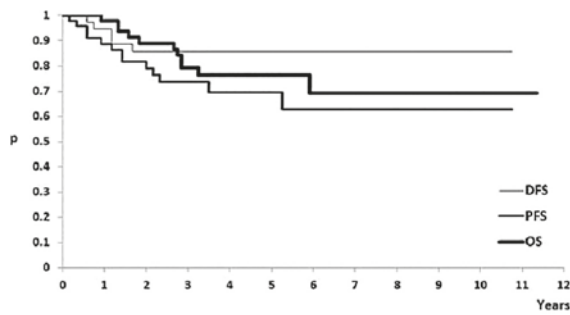


FIGURE 1. Disease-free survival (DFS), progression-free survival (PFS), and overall survival (OS) for the whole patient group.

Computing; Platform: x86_64-w64-mingw32/x 64 (64-bit); downloaded: January 21, 2017).

Ethics approval

All analyses presented in this study are part of routine clinical practice approved by the Ethics Committee of the Institute for Oncology and Radiology of Serbia and were performed in accordance with the Helsinki Declaration of 1975, as revised in 2013.

Results

Patients' disease, treatment and outcomes characteristics are presented in Table 1. Radical CRT according to protocol was completed in 39 patients. All 47 patients completed the planned RT treatment. RT alone was performed in 3 patients. Two of them didn't receive chemotherapy due to significant medical comorbidities, and 1 patient refused the proposed chemotherapy treatment. Five patients didn't receive a second cycle of chemotherapy due to toxicities Grade 3 or 4 after the first course. The three-dimensional conformal radiotherapy (3D-CRT) was delivered in twenty-four patients, while the remaining 23 patients received the 2D technique. In the first part, majority of patients (95.7%) received the dose of 36 Gy. After a two-week break in treatment according to the split course approach, median planned dose of radiation was 23.4 Gy. The median total dose of radiation was 59.4 Gy. (Table 1).

Most patients (80.85%) had treatment pause due to toxicities. Because of treatment interruptions the median OTT was 77 days. The most common non-haematological acute toxicity was radiation dermatitis. Any grade of haematological acute complications was registered in 33 patients (70.21%). The

TABLE 2. Comparison of characteristics of complete responders (CR) and non-complete responders (non-CR) to chemoradiotherapy

Characteristic	The response to treatment after 6 months		Wilcoxon rank sum test
	CR	non-CR	
Age (years)			
Mean (SD)	60 (10.7)	65.1 (7.8)	
Median (Range)	59.5 (40.0–80.0)	65.0 (52.0–81.0)	ns
Gender			
Male	6 (20%)	5 (29.4%)	ns*
Female	24 (80%)	12 (70.6%)	
T in clinical TNM			
T2	13 (43.3%)	5 (29.4%)	ns#
T3	14 (46.7%)	10 (58.2%)	
T4	3 (10.0%)	2 (11.8%)	
N in clinical TNM			
N0	15 (50.0%)	2 (11.8%)	p* < 0.05
N1	15 (50.0%)	15 (88.2%)	
Tumour size (cm)			
Mean (SD)	4.7 (1.8)	6.0 (2.1)	p < 0.05
Median (Range)	4.9 (2.1–8.0)	5.8 (2.3–10.0)	
Initial haemoglobin level (g/L)			
Mean (SD)	124.2 (16.9)	103.0 (18.8)	p < 0.01
Median (Range)	127.0 (66.0–154.0)	101.0 (68.0–132.0)	
Pretreatment colostomy			
No	28 (93.3%)	14 (82.3%)	ns#
Yes	2 (6.7%)	3 (17.6%)	
Neutrophil-to-lymphocyte ratio			
N (%)	16/30 (50%)	16/17 (50%)	ns
Mean (SD)	2.4 (1.8)	3.1 (1.6)	
Median (Range)	1.9 (0.8–7.0)	3.2 (0.9–5.6)	
Platelet-to-lymphocyte ratio			
N (%)	16/30 (50%)	16/17 (50%)	p < 0.05
Mean (SD)	118.3 (54.9)	200.5 (104.4)	
Median (Range)	108.3 (51.7–256.6)	158.9 (79.5–401.2)	
DFS (months)			
Median (95% CI)	NR	NR	p‡ < 0.05
PFS (months)			
Median (95% CI)	NR	26 (> 17)	p‡ < 0.01
OS (months)			
Median (95% CI)	NR	71 (> 33)	p‡ < 0.01
ACSOS (months)			
Median (95% CI)	NR	NR	p‡ < 0.05
CFS (months)			
Median (95% CI)	NR	11 (> 10)	p‡ < 0.01
Total	30 (100%)	17 (100%)	-

ACSOS = anal cancer specific overall survival; CFS = colostomy-free survival; DFS = disease-free survival; CI = confidence interval; DFS = disease-free survival; NR = not reached; ns = not statistically significant; OS = overall survival; PFS = progression-free survival; SD = standard deviation; * = Pearson χ^2 test; # = Fisher exact test; ‡ = log-rank test

TABLE 3. Logistic regression analysis of the response to treatment after 6 months

Characteristic	Logistic regression			
	Univariate		Multivariate	
	OR (95%CI)	Wild test	OR (95%CI)	Likelihood Ratio test
Age				
> 63 y vs. ≤ 63 y	1.7 (0.4–6.6)	p = 0.213	-	p = 0.884
Gender				
Male vs. Female	2.1 (0.6–7.2)	p = 0.468	-	p = 0.082
T in clinical TNM				
T3 vs. T2	1.9 (0.5–6.9)	p = 0.634	-	p = 0.940
T4 vs. T2	1.7 (0.2–13.7)			
N in clinical TNM				
N1 vs. N0	7.5 (1.4–38.7)	p = 0.006	-	p = 0.133
Tumour size (cm)				
> 4 cm vs. ≤ 4 cm	6.6 (1.3–33.8)	p = 0.011	-	p = 0.602
Initial haemoglobin level (g/L)				
< 120 g/L vs. ≥ 120 g/L	8.9 (2.2–35.6)	p = 0.001	13.4 (2.4–74.3)	p* = 0.003
RT technique				
2D vs. 3D	1.3 (0.4–4.2)	p = 0.679	-	p = 0.784
Treatment break				
> 10 days vs. ≤ 10 days	6.0 (1.6–22.3)	p = 0.005	9.6 (1.7–52.5)	p* = 0.009
Completed chemotherapy				
No vs. Yes	2.0 (0.4–9.3)	p = 0.379	-	p = 0.555

CI = confidence interval; OR = odds ratio; RT = radio therapy; * = wild test

most frequent serious haematological toxicity (gr. III/IV) was leukopenia.

Survival curves for the whole patient group are presented in Figure 1. The follow up period had a median of 44 months. The median times for DFS, PFS and OS were not reached.

Evaluation of response after 6 months

The response to treatment was evaluated after 6 months of completion of therapy. The CR was detected in 30 patients (63.8%), 24 females (80%) and 6 males.

Comparison of characteristics of complete responders and non-complete responders to chemoradiotherapy are presented in Table 2. Patients with N0 responded to treatment significantly better than patients with N1. Primary tumour size also influenced the response.

Although median times to events for DFS/PFS/OS were not reached, patients with CR after 6 months had significantly increased DFS, PFS, and OS after treatment completion compared to patients with non-CR response (Figure 2, Table 2).

Predicting the response to treatment after 6 months

A logistic regression model included nine variables (gender, age, clinical T stage, clinical N stage, tumour size, haemoglobin level, RT technique, treatment break period, and chemotherapy completion) (Table 3). It was found that patients with shorter period of treatment interruptions, a tumour size ≤ 4cm, the initial haemoglobin level more than 120 g/L, and lymph node negative patients, responded significantly better to treatment. The final model included pretreatment haemoglobin level and treatment break period.

Evaluating the potential of NLR and PLR in predicting the response to treatment after 6 months

Next, we examined if there were differences in the response to treatment after 6 months according to the cut-off values obtained by ROC analysis for NLR and PLR. (Figure 3, Table 4) According to the cut-off value obtained by ROC analysis (145.2), a

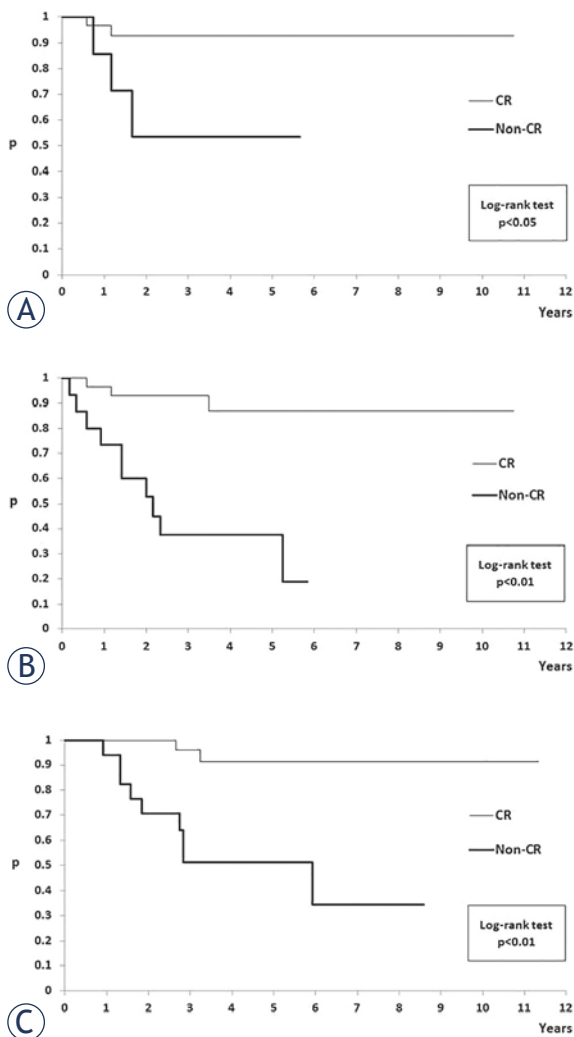


FIGURE 2. (A) Kaplan-Meier plots for Disease-free survival (DFS), (B) progression-free survival (PFS), and (C) overall survival (OS) in relation to response to treatment after 6 months.

statistically significant difference in the response was confirmed for PLR ($p = 0.03$). For NLR, a statistically significant effect on the response was not confirmed ($p = 0.23$). The patients were further divided into two groups based on literature cut-off value for NLR in rectal cancer (0–3 vs. ≥ 3).²⁹ A positive trend ($p = 0.06$) was found when 0–3 vs. ≥ 3 groups were tested, in regard to the nonCR vs. CR response. (Table 5)

Evaluation of long term outcomes

The one patient who had disease progression was selected for chemotherapy. All other patients ($n = 16$) who did not achieve a CR after 6 months were referred to surgical treatment, as well as two pa-

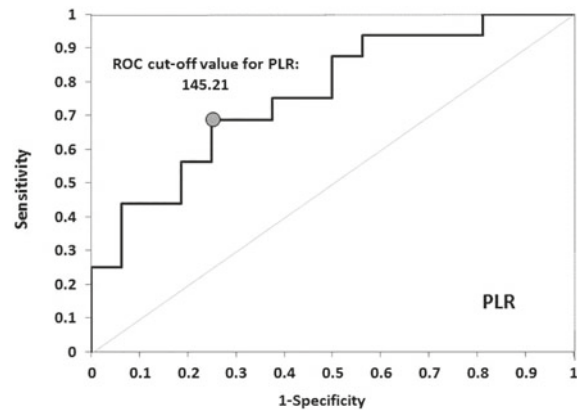


FIGURE 3. Receiver Operating Characteristics (ROC) curve for the platelet-to-lymphocyte ratio (PLR) in relation to response to treatment after 6 months.

tients who had a CR after 6 months but then relapsed. From the 11 patients that underwent surgery (APR), 9 were incomplete responders to CRT and 2 initial complete responders that relapsed. Within this surgically treated group, 9 patients (82%) achieved a complete response after surgical treatment. One patient died in early postsurgical period due to acute renal failure. Four patients relapsed after surgery, 3 of them were initial complete responders to surgery, but presented with distant metastases within two years of follow-up. All patients who relapsed after surgery were treated with postoperative chemotherapy and continued follow-up. With combined CRT and surgical salvage treatment CR rate was 80.9%. Two patients had palliative postCRT colostomy, due to medical comorbidities which didn't allow radical surgical treatment. The remaining five patients were closely followed-up without any additional treatment because they had a poor general condition or refused surgery.

Six patients developed distant metastasis during the follow-up period and five of them were referred to chemotherapy. Two of them had dissemination to the lungs, 2 to the liver and the other sites were retroperitoneum, bones, and peritoneal metastasis. Three patients had multiple metastases.

Discussion

To the best of our knowledge, no study has evaluated the long-term outcomes after CRT, as well as predictors of the response after 6 months of CRT completion in patients with anal cancer in the Balkan region. In this study, we focused on the as-

TABLE 4. Results of the ROC analysis for neutrophil-to-lymphocyte ratio (NLR) and platelet-to-lymphocyte ratio (PLR) and relevant events

Characteristics	NLR	PLR
AUC ROC ^a (95% CI)	65.2% (45.3–85.2%)	76.2% (59.5–92.9%)
Likelihood ratio test ^b	ns	$p < 0.05$
ROC-cut-off value ^c	-	145.2
Sensitivity (95% CI)	-	68.7% (43.7–87.5%)
Specificity (95% CI)	-	75.0% (56.1–93.7%)

AUC ROC^a = Area Under the Receiver Operating Characteristics Curve (DeLong's method);
^b = Likelihood ratio test for AUC ROC; ^c = Value with maximum sensitivity and specificity; CI = confidence interval; ns = not statistically significant

TABLE 5. The value of neutrophil-to-lymphocyte ratio (NLR) and platelet-to-lymphocyte ratio (PLR) in prediction of CR vs. non-CR

Characteristic	The response to treatment after 6 months		
	CR	non-CR	Fisher Exact Test
NLR (literature cut-off value)			
< 3.0	13 (81.2%)	7 (43.8%)	$p = 0.06$
≥ 3.0	3 (18.8%)	9 (56.2%)	
PLR (literature cut-off value)			
< 160.0	13 (81.2%)	9 (56.2%)	$p = 0.25$
≥ 160.0	3 (18.8%)	7 (43.8%)	
PLR (ROC cut-off value)			
< 145.2	12 (75%)	5 (31.3%)	$p = 0.03$
≥ 145.2	4 (25%)	11 (68.7%)	
Total	16 (100%)	16 (100%)	-

CR = complete clinical response, non-CR = non-complete clinical response; ROC = Receiver Operating Characteristics

assessment of new prognostic and predictive factors for CRT, evaluating demographic, clinico-pathological and haematological parameters.

There is no precise information about the optimal waiting time period for complete response after CRT. The ACT II trial showed that, in the 29% of patients who did not achieve a complete response at 11 weeks, a complete response occurred at 26 weeks.³⁰ In this study, the assessment of tumour response was performed 6 months after completion of CRT and CR was found in 63.8% of patients. CR was confirmed as a strong predictor of favourable long term clinical outcome. Moreover, it was also found that baseline haemoglobin level and period of treatment interruptions were independent predictors, as low initial haemoglobin level and prolonged period of treatment were related with significantly lower likelihood for CR response.

The optimal dose and schedule of RT for anal cancer also continue to be explored. The median dose in our study was 59.4 Gy, and all patients got the split-course approach. All patients included in our study were in II or III stadium of disease. Recent research suggested that for early-stage tumours < or = 10 mm, optimal radiotherapy dose should be between 40 and 50 Gy for subclinical lesions and 50–60 Gy for T1.³¹ For patients with locally advanced disease (T3, T4, or lymph node-positive tumours) doses of ≥ 54 Gy administered with limited treatment breaks (less than 60 days) were associated with increased local control.²⁰ The results from the RTOG 92-08 trial¹⁴⁷ suggested that doses of > 59 Gy provide no additional benefit to patients with anal cancer.^{18,32}

In our study the majority of patients had treatment interruptions due to acute toxicities, which might correlate with the used RT technique. The development of an advanced technique of RT has enabled the safe application of high RT doses while reducing the dose to surrounding normal tissues like skin, small bowel, bladder, femoral heads, external genitalia, and bone marrow.³³ This leads to low rates of acute and late toxicity and excellent local control, disease-free survival, and overall survival.³⁴

The relationship between inflammation and cancer has been investigated in many studies. Systemic inflammation-based scores extracted from the absolute blood cell count of peripheral blood have the potential to predict the response to various therapeutic approaches, but have still not been validated in larger patient cohorts. Advantages of blood biomarkers lay in the inexpensiveness of analyses and quick availability, as well as minimal invasiveness, and availability in initial assessment. Our recent study successfully evaluated the role of haematological parameters in predicting the survival and toxicity to specific treatment in the lung cancer setting.³⁵ Several studies have reported that an elevated NLR is associated with poor clinical outcome in patients with colorectal cancer.³⁶ To the best of our knowledge, this is the first study which aimed to analyse the prognostic role of NLR and PLR in patients with anal cancer. We analysed the discriminative potential of NLR and PLR in regard to CR vs. non-CR 6 months after CRT completion. It was found that patients with PLR higher than 145.2 had significantly worse CR rate after 6 months. Meta-analysis conducted by Zhnag *et al.* found that elevated NLR, PLR and platelet counts may be associated with worse survival in colorectal cancer patients.³⁷ However, in this study, lower NLR was

not correlated with better response, which might be due to a low number of patients, population-specific differences or differences in the analysed cancer type.

The limitations of the study include the retrospective approach, the fact that this was a single institution analysis and that the sample size was relatively low, which calls for caution in data interpretation. However, the number of analysed patients is considerable taking into consideration that anal cancer is a rare disease. Further studies should be performed on patients treated with novel RT techniques considering shorter treatment interruptions and taking into account both clinical parameters and genetic characteristics of patients, as has been suggested for other cancer types.^{38,39}

Conclusions

Based on the logistic regression model important prognostic factors associated with CR in this study were baseline haemoglobin level and period of treatment interruptions. Potential haematological prognostic factors could be PLR and NLR, which can be routinely determined by low-cost and minimally invasive methods.

Acknowledgements

This study is supported by the Ministry of Education and Science of the Republic of Serbia (Agreement No. 451-03-9/2021-14/200043). This article is based upon work from COST Action CA17118, supported by COST (European Cooperation in Science and Technology); www.cost.eu. MC is supported by the Science Fund of the Republic of Serbia (PROMIS TRACEPIGEN project No. 6060876).

References

- Bray F, Ferlay J, Soerjomataram I, Siegel RL, Torre LA, Jemal A. Global cancer statistics 2018: GLOBOCAN estimates of incidence and mortality worldwide for 36 cancers in 185 countries. *CA Cancer J Clin* 2018; **68**: 394-424. doi: 10.3322/caac.21492
- van der Zee RP, Richel O, de Vries HJC, Prins JM. The increasing incidence of anal cancer: can it be explained by trends in risk groups? *Neth J Med* 2013; **71**: 401-11. PMID: 24127500
- Ouhoumane N, Steben M, Coutlée F, Vuong T, Forest P, Rodier C, et al. Squamous anal cancer: patient characteristics and HPV type distribution. *Cancer Epidemiol* 2013; **37**: 807-12. doi: 10.1016/j.canep.2013.09.015
- Klas JV, Rothenberger DA, Wong WD, Madoff RD. Malignant tumors of the anal canal: the spectrum of disease, treatment, and outcomes. *Cancer* 1999; **85**:1686-93. doi: 10.1002/(sici)1097-0142(19990415)85:8<1686::aid-cncr7>3.0.co;2-7
- Ryan DP, Compton CC, Mayer RJ. Carcinoma of the anal canal. *N Engl J Med* 2000; **342**: 792-800. doi: 10.1056/NEJM200003163421107
- Nigro ND, Vaitkevicius VK, Considine BJ. Combined therapy for cancer of the anal canal: a preliminary report. *Dis Colon Rectum* 1974; **17**: 354-6. doi: 10.1007/BF02586980
- Czito BG, Willett CG. Current management of anal canal cancer. *Curr Oncol Rep* 2009; **11**: 186-92. doi: 10.1007/s11912-009-0027-1
- Bartelink H, Roelofsens F, Eschwege F, Rougier P, Bosset JF, Gonzalez DG, et al. Concomitant radiotherapy and chemotherapy is superior to radiotherapy alone in the treatment of locally advanced anal cancer: results of a phase III randomized trial of the European Organization for Research and Treatment of Cancer Radiotherapy and Gastrointestinal Cooperative Groups. *J Clin Oncol* 1997; **15**: 2040-9. doi: 10.1200/JCO.1997.15.5.2040
- Flam M, John M, Pajak TF, Petrelli N, Myerson R, Doggett S, et al. Role of mitomycin in combination with fluorouracil and radiotherapy, and of salvage chemoradiation in the definitive nonsurgical treatment of epidermoid carcinoma of the anal canal: results of a phase III randomized intergroup study. *J Clin Oncol* 1996; **14**: 2527-39. doi: 10.1200/JCO.1996.14.9.2527
- Shridhar R, Shibata D, Chan E, Thomas CR. Anal cancer: current standards in care and recent changes in practice. *CA Cancer J Clin* 2015; **65**: 139-62. doi: 10.3322/caac.21259
- Hagemans JAW, Blinde SE, Nuytens JJ, Morshuis WG, Mureau MAM, Rothbarth J, et al. Salvage abdominoperineal resection for squamous cell anal cancer: a 30-year single-institution experience. *Ann Surg Oncol* 2018; **25**: 1970-9. doi: 10.1245/s10434-018-6483-9
- Hagemans JAW. ASO Author reflections: salvage surgery for anal cancer. *Ann Surg Oncol* 2018; **25**: 852-3. doi: 10.1245/s10434-018-7025-1
- Jakovljevic K, Malisic E, Cavic M, Krivokuca A, Dobricic J, Jankovic R. KRAS and BRAF mutations in Serbian patients with colorectal cancer. *J BUON* 2012; **17**: 575-80. PMID: 23033302
- Cavic M, Krivokuca A, Boljevic I, Brotto K, Jovanovic K, Tanic M, et al. Pharmacogenetics in cancer therapy – 8 years of experience at the Institute for Oncology and Radiology of Serbia. *J BUON* 2016; **21**: 1287-95. PMID: 27837635
- Serup-Hansen E, Linnemann D, Høgdall E, Geertsen PF, Havsteen H. KRAS and BRAF mutations in anal carcinoma. *APMIS* 2015; **123**: 53-9. doi: 10.1111/apm.12306
- Brotto K, Malisic E, Cavic M, Krivokuca A, Jankovic R. The usability of allele-specific PCR and reverse-hybridization assays for KRAS genotyping in serbian colorectal cancer patients. *Dig Dis Sci* 2013; **58**: 998-1003. doi: 10.1007/s10620-012-2469-9
- Lim F, Glynne-Jones R, Lim F, Glynne-Jones R. Chemotherapy/chemoradiation in anal cancer: a systematic review. *Cancer Treat Rev* 2011; **37**: 520-32. doi: 10.1016/j.ctrv.2011.02.003
- Peiffert D, Tournier-Rangear L, Gérard J-P, Lemanski C, François E, Giovannini M, et al. Induction chemotherapy and dose intensification of the radiation boost in locally advanced anal canal carcinoma: final analysis of the randomized UNICANCER ACCORD 03 trial. *J Clin Oncol* 2012; **30**: 1941-8. doi: 10.1200/JCO.2011.35.4837
- Roohipour R, Patil S, Goodman KA, Minsky BD, Wong WD, Guillem JG, et al. Squamous-cell carcinoma of the anal canal: predictors of treatment outcome. *Dis Colon Rectum* 2008; **51**: 147-53. doi: 10.1007/s10350-007-9125-z
- Huang K, Haas-Kogan D, Weinberg V, Krieg R. Higher radiation dose with a shorter treatment duration improves outcome for locally advanced carcinoma of anal canal. *World J Gastroenterol* 2007; **13**: 895-900. doi: 10.3748/wjg.v13.i6.895
- Hannoun-Levi JM, Ortholan C, Resbeut M, Teissier E, Ronchin P, Cowen D, et al. High-dose split-course radiation therapy for anal cancer: outcome analysis regarding the boost strategy (CORS-03 study). *Int J Radiat Oncol Biol Phys* 2011; **80**: 712-20. doi: 10.1016/j.ijrobp.2010.02.055
- O'Sullivan B, Brierley J, Byrd D, Bosman F, Kehoe S, Kossary C, et al. The TNM classification of malignant tumours-towards common understanding and reasonable expectations. *Lancet Oncol* 2017; **18**: 849-51. doi: 10.1016/S1470-2045(17)30438-2
- Oken MM, Creech RH, Tormey DC, Horton J, Davis TE, McFadden ET, et al. Toxicity and response criteria of the Eastern Cooperative Oncology Group. *Am J Clin Oncol* 1982; **5**: 649-55. PMID: 7165009

24. Matzinger O, Roelofsens F, Mineur L, Koswig S, Van Der Steen-Banasik EM, Van Houtte P, et al. Mitomycin C with continuous fluorouracil or with cisplatin in combination with radiotherapy for locally advanced anal cancer (European Organisation for Research and Treatment of Cancer phase II study 22011-40014). *Eur J Cancer* 2009; **45**: 2782-91. doi: 10.1016/j.ejca.2009.06.020
25. Landsberg T, Chavaudra J, Dobbs J, Hanks G, Johansson K-A, Möller T, et al. Report 50. *J Int Comm Radiat Units Meas* 2016; **os26**: NP-NP. doi: 10.1093/jicru/os26.1.Report50
26. Landsberg T, Chavaudra J, Dobbs J, Gerard JP, Hanks G, Horiot JC, et al. Report 62. *J Int Comm Radiat Units Meas* 2016; **os32**: NP-NP. doi: 10.1093/jicru/os32.1.Report62
27. US Department of Health and Human Services, National Institutes of Health National Cancer Institute 2017. *Common Terminology Criteria for Adverse Events (CTCAE) Version 5.0*. [cited 2021 Mar 15]. Available at https://ctep.cancer.gov/protocoldevelopment/electronic_applications/docs/ctcae_v5_quick_reference_5x7.pdf
28. Schwartz LH, Litière S, de Vries E, Ford R, Gwyther S, Mandrekas S, et al. RECIST 1.1-Update and clarification: from the RECIST committee. *Eur J Cancer* 2016; **62**: 132-7. doi: 10.1016/j.ejca.2016.03.081
29. Lino-Silva LS, Salcedo-Hernández RA, Ruiz-García EB, García-Pérez L, Herrera-Gómez Á. Pre-operative Neutrophils/Lymphocyte Ratio in rectal cancer patients with preoperative chemoradiotherapy. *Med Arch (Sarajevo, Bosnia Herzegovina)* 2016; **70**: 256-60. doi: 10.5455/medarh.2016.70.256-260
30. Glynne-Jones R, Nilsson PJ, Aschele C, Goh V, Peiffert D, Cervantes A, et al. Anal cancer: ESMO-ESSO-ESTRO clinical practice guidelines for diagnosis, treatment and follow-up. *Radiother Oncol* 2014; **111**: 330-9. doi: 10.1016/j.radonc.2014.04.013
31. Ortholan C, Ramaïoli A, Peiffert D, Lusinchi A, Romestaing P, Chauveinc L, et al. Anal canal carcinoma: early-stage tumors < or =10 mm (T1 or Tis): therapeutic options and original pattern of local failure after radiotherapy. *Int J Radiat Oncol Biol Phys* 2005; **62**: 479-85. doi: 10.1016/j.ijrobp.2004.09.060
32. John M, Pajak T, Flam M, Hoffman J, Markoe A, Wolkov H, et al. Dose escalation in chemoradiation for anal cancer: preliminary results of RTOG 92-08. *Cancer J Sci Am* 1996; **2**: 20511. PMID: 9166533
33. Pepek JM, Willett CG, Czito BG. Radiation therapy advances for treatment of anal cancer. *J Natl Compr Canc Netw* 2010; **8**: 123-9. doi: 10.6004/jnccn.2010.0008
34. Mitchell MP, Abboud M, Eng C, Beddar AS, Krishnan S, Delclos ME, et al. Intensity-modulated radiation therapy with concurrent chemotherapy for anal cancer: outcomes and toxicity. *Am J Clin Oncol* 2014; **37**: 461-6. doi: 10.1097/COC.0b013e31827e52a3
35. Jokic V, Savic-Vujovic K, Spasic J, Stanic N, Marinkovic M, Radosavljevic D, et al. Hematological parameters in EGFR-mutated advanced NSCLC patients treated with TKIs: predicting survival and toxicity. *Expert Rev Anticancer Ther* 2021; **6**: 673-9. doi: 10.1080/14737140.2021.1893694
36. Shibutani M, Maeda K, Nagahara H, Noda E, Ohtani H, Nishiguchi Y, et al. A high preoperative neutrophil-to-lymphocyte ratio is associated with poor survival in patients with colorectal cancer. *Anticancer Res* 2013; **33**: 3291-4. PMID: 23898094
37. Zhang J, Zhang HY, Li J, Shao XY, Zhang CX. The elevated NLR, PLR and PLT may predict the prognosis of patients with colorectal cancer: a systematic review and meta-analysis. *Oncotarget* 2017; **8**: 68837-46. doi: 10.18632/oncotarget.18575
38. Tanić M, Krivokuća A, Čavić M, Mladenović J, Plesinac Karapandžić V, Beck S, et al. Molecular signature of response to preoperative radiotherapy in locally advanced breast cancer. *Radiat Oncol* 2018; **13**: 193. doi: 10.1186/s13014-018-1129-4
39. Bergom C, West CM, Higginson DS, Abazeed ME, Arun B, Bentzen SM, et al. The Implications of genetic testing on radiation therapy decisions: a guide for radiation oncologists. *Int J Radiat Oncol Biol Phys* 2019; **105**: 698-712. doi: 10.1016/j.ijrobp.2019.07.026

Hypofractionated preoperative radiotherapy for high risk soft tissue sarcomas in a geriatric patient population

Vlatko Potkrajcic¹, Frank Traub^{2,3,4}, Barbara Hermes^{2,5}, Marcus Scharpf^{2,6}, Jonas Kolbenschlag^{2,7}, Daniel Zips^{1, 8}, Frank Paulsen^{1,2}, Franziska Eckert^{1,2,8}

¹ Department of Radiation Oncology, Eberhard-Karls-University Tuebingen, Tuebingen, Germany

² Centre for Soft Tissue Sarcoma, GIST and bone tumours, Eberhard-Karls-University Tuebingen, Tuebingen, Germany

³ Department of Orthopaedics and Traumatology, University Medical Center Mainz, Johannes Gutenberg-University Mainz, Mainz, Germany

⁴ Department of Orthopaedic Surgery, Eberhard-Karls-University Tuebingen, Tuebingen, Germany

⁵ Department of Medical Oncology, Eberhard-Karls-University Tuebingen, Tuebingen, Germany

⁶ Institute for Pathology, Eberhard-Karls-University Tuebingen, Tuebingen, Germany

⁷ Department of Hand-, Plastic, Reconstructive and Burn Surgery, Eberhard-Karls-University Tuebingen, Tuebingen, Germany

⁸ German Cancer Consortium (DKTK) Partnersite Tuebingen, German Cancer Research Center (DKFZ), Heidelberg, Germany

Radiol Oncol 2021; 55(4): 459-466.

Received 18 May 2021

Accepted 17 August 2021

Correspondence to: Franziska Eckert, M.D., Department of Radiation Oncology, Eberhard-Karls-University of Tuebingen, Hoppe-Seyler-Str. 3, D-72076 Tuebingen, Germany. E-mail: franziska.eckert@med.uni-tuebingen.de

Disclosure: VP, DZ, FP, FE have research and educational grants from Elekta, Philips, Siemens, Sennewald. The other authors declare that they have no conflict of interest.

This is an open access article under the CC BY-NC-ND license (<http://creativecommons.org/licenses/by-nc-nd/4.0/>).

Background. Standard therapy for localised, resectable high risk soft tissue sarcomas consists of wide excision and radiotherapy over several weeks. This treatment schedule is hardly feasible in geriatric and frail patients. In order not to withhold radiotherapy from these patients, hypofractionated radiotherapy with 25 Gy in 5 fractions was evaluated in a geriatric patient population.

Patients and methods. A retrospective analysis was performed of 18 geriatric patients with resectable high risk soft tissue sarcomas of extremities and thoracic wall. Wound healing and short term oncologic outcome were analysed. In addition, dose constraints for radiotherapy of the extremities were transferred from normofractionated to hypofractionated radiotherapy regimens.

Results. Feasibility was good with 17/18 patients completing treatment as planned. Wound healing complication rate was in the range of published data. Two patients developed local and distant recurrence, two patients isolated distant recurrences. No isolated local recurrences were observed. Keeping the constraints was possible in all cases without compromising the coverage of the target volume.

Conclusions. Hypofractionated radiotherapy and surgery was well tolerated even in this specific patient population. With feasibility concerning early wound healing problems and adapted constraints, which allow for the treatment of most resectable extremity tumours, the concept warrants further evaluation in patients unfit for standard radiotherapy.

Key words: sarcoma; radiotherapy; preoperative; geriatric patients; wound healing; hypofractionation

Introduction

Standard treatment for localised high risk soft tissue sarcomas (subfascial, large tumours with in-

termediate or high French Federation of Cancer Centers Sarcoma Group [FNCLCC] grading) consists of wide excision plus radiotherapy over approximately 5 weeks preoperatively or 6–7 weeks

postoperatively.¹ This results in a treatment period of approximately 12 weeks, including the recovery phases after radiation or wound healing before the adjuvant radiotherapy. In select cases and at specialized centers chemotherapy and / or locoregional hyperthermia are added.²⁻⁴ With this approach, local control is rather high for extremity tumours reaching 90%.⁵ Oncologic outcome is mostly determined by distant metastases, especially in the lungs.⁶

This standard approach is almost not feasible in geriatric, frail patients with daily appointments at the radiotherapy department over 5–7 weeks and an overall treatment time of approximately three months, rehabilitation not included. Thus, radiotherapy is omitted in this patient population in a large proportion of cases. Even in patients over 65 years of age, 20% did not receive radiotherapy.^{7,8} For geriatric patients, hypofractionated radiotherapy (with or without stereotactic treatment approaches) has been proposed as a feasible option.⁹

For localised high risk soft tissue sarcoma, different radiotherapy fractionations have been reported as summarized by Haas *et al.*¹⁰ For example, in analogy to hypofractionated regimens in rectal cancer, a fractionation of 25 Gy in 5 fractions on consecutive days has been used.¹¹ A retrospective analysis of 272 patients describes local recurrences in 19% of patients with 7% of patients developing toxicities requiring a second surgery.¹² For the subgroup of myxoid liposarcoma local recurrence rate was even lower.¹³ 25 Gy in 5 fractions in combination with chemotherapy has been reported as a phase 2 trial protocol.¹⁴ The advantage for geriatric patients is the significantly reduced overall treatment time and the limited daily visits to the radiation oncology department making it more feasible as an outpatient treatment. Thus, radiotherapy is an option even in frail geriatric patients who otherwise would undergo surgery alone due to the high burden of daily visits to radiation treatment units over several weeks.

With altered radiotherapy fractionation regimens, normal tissue constraints developed for normofractionated radiotherapy with doses of 1.8 Gy to 2.0 Gy per fraction have to be revisited or newly developed. Especially with higher doses per fraction such as used in stereotactic radiotherapy, dose constraints have to be reconsidered.¹⁵

The aim of this study was to assess the feasibility concerning completion of treatment and early wound healing after preoperative hypofractionated radiotherapy for high risk soft tissue sarcomas in a geriatric patient population. In addition, dose

constraints for radiotherapy of sarcomas of the extremities have been transferred from normofractionated radiation schedules to hypofractionated treatment.

Patients and methods

Starting in 2018, hypofractionated preoperative radiotherapy was introduced at our institution for geriatric patients with newly diagnosed high risk soft tissue sarcomas with an indication for additive radiotherapy (large, deep seated, intermediate or high grade tumours) not eligible for normofractionated (neo) adjuvant radiotherapy over several weeks. In 2020 the regimen was introduced in the second center which included patients in the analysis. All geriatric patients (> 75 years, frail, not eligible for normofractionated radiotherapy) treated with 25 Gy in 5 fractions for preoperative radiotherapy were included in this analysis. The analysis was approved by the Ethics Committee of both centers (508/2020 BO).

Eighteen patients presenting with large soft tissue masses suspicious of soft tissue sarcoma underwent biopsy of the lesion and staging with at least computed tomography (CT) of the lungs and local contrast enhanced magnetic resonance imaging (MRI) or CT after confirmation of the diagnosis. After surgical and anaesthesiological evaluation of the patients, the treatment schedule was discussed in a multidisciplinary tumour board including confirmation that patients were unfit for normofractionated radiotherapy. Given the resectability of the tumour and the operability of the patient, preoperative hypofractionated radiotherapy was offered to the patients. Surgery was planned approximately 3–4 weeks after completion of radiotherapy. Additional preoperative imaging between the end of radiation therapy and surgical resection was not obligatory. However, preoperative staging was carried out in selected cases. In order to limit the loss of quality of life and avoid complications of hospitalization for geriatric patients, most radiotherapy treatments were planned and performed on an outpatient basis.

Radiation treatment planning was performed after informed consent by the patient and/or the legal guardian. 3D conformal radiotherapy as well as intensity modulated radiotherapy (IMRT) was planned based on a planning CT with individual patient positioning depending on the anatomical localisation of the sarcoma. Target volume delineation followed the recommendations for radiother-

apy of high risk soft tissue sarcomas.¹⁶ The gross tumour volume (GTV) was contoured on the planning CT by the aid of diagnostic contrast-enhanced MR and / or CT imaging. In most cases a clinical target volume (CTV) was created with a margin of 3 cm around the GTV in a longitudinal direction and 1.5 cm in a radial direction in case of extremity sarcomas. The CTV was corrected for anatomical borders. The planning target volume (PTV) margin was chosen between 0.5 and 1.0 cm according to the expected positioning precision.

Dose prescription followed the respective International Commission on Radiation Units and Measurements (ICRU) recommendations. For the coverage of the target volume a dose of 95%–107% of the prescribed dose was aimed at for the GTV. The PTV was to be covered with dose to 98% of the contoured volume (D98) \geq 90% and dose to 2% of the contoured volume D2 \leq 107% of the prescribed dose, respectively. Most patients were treated with 3D conformal radiotherapy (n = 15). In case of better sparing of organs at risks (OARs) IMRT techniques were used, mostly volumetric arc therapy (VMAT), n = 3. Radiation planning parameters were recorded for seven patients with lower extremity sarcomas. For two patients with lower limb sarcomas radiotherapy planning parameters are missing. Analysis was focussed on lower extremity sarcomas as these pose the highest risk for pathologic fractures after radiotherapy and the published dose constraints also were limited to lower extremity. D98 was recorded for GTV and CTV. Dose constraints were evaluated according to the re-calculated constraints. The whole femur and tibia were contoured for the analysis of constraints for bone concerning pathologic fractures for thigh and calf tumours, respectively.

Surgical approaches also had to be tailored to the specific patient population of elderly and frail patients. Wide resection taking into account resulting functional deficits or the resulting necessity of plastic surgery was omitted in select cases accepting R1 or even R2 resection if patients would have been endangered with more radical surgical procedures.

Local MRI examinations (or CT for not MRI-eligible patients) and lung imaging were carried out during the follow-up. Clinical and pathological data were collected and analysed. Resection status as well as percentage of vital cells in the surgical specimen was recorded. Wound healing complications were recorded and graded according to the need for additional surgical interventions during the postoperative period.

Statistical analysis was performed with IBM SPSS Version 26 and GraphPad Version 8. Means were compared by two-sided Student's t-test. Survival times were estimated with the Kaplan Meier method. Correlations of continuous variables were described using Pearson correlation coefficients. Chi-square test was used to describe correlations between categorized variables.

Results

Patient population

Median patient age was 83.7 years (range 79.4–91.4 years). All patients included showed at least two features of high risk soft tissue sarcomas (subfascial localisation, intermediate or high grading according to FNCLCC or size > 5 cm). All tumours were located in extremities or superficial trunk wall, no retroperitoneal sarcomas were included. The most common histology was undifferentiated sarcoma, not otherwise specified (NOS). All patients had undergone biopsy for histopathologic confirmation of the diagnosis and had been staged with CT of the lungs prior to therapy to exclude pulmonary metastases. An overview of the patients is provided in Table 1. General condition and frailty of patients were assessed interdisciplinary with surgeons, anaesthesiologists and radiation oncologists. In case patients with extremity and superficial trunk wall sarcomas were not fit for several weeks of treatment or patients and legal guardians would have declined radiotherapy at all in case of five week treatment, hypofractionated irradiation was offered as an alternative.

Feasibility

All patients finished the five planned radiotherapy sessions. No radiation toxicity > grade 1 (Common Terminology Criteria for Adverse Events [CTCAE] V4.0) was observed. All but one patient underwent wide resection after a median of 29 days (range 15–45 days) after end of radiotherapy. One patient deteriorated in the Eastern Cooperative Oncology Group (ECOG) performance status after radiotherapy. Thus, the patient and the legal guardian opted against moving forward to surgery and preferred a best supportive care strategy which left the patient with a good palliative radiotherapy treatment. All patients undergoing surgery were released from hospital, 30 day mortality rate after surgery was 0%. Five of 17 patients undergoing surgery de-

TABLE 1. Patient characteristics and postoperative complications

Age at diagnosis	Localisation	Size [cm]	Histology	Grading	Days to resection	Resection status	Postoperative complication	Follow up
85	forearm	7.5	NOS	2	45	1	hematoma	alive, NED
91	lower leg	5.4	NOS		no surgery			lost to follow up
82	thigh	7.0	myxofibrosarcoma	2–3	25	0		alive, NED
84	forearm	6.0	epithelioid myxofibrosarcoma	3	18	0		alive, NED
91	thigh	5.5	NOS	3	15	2		local and distant recurrence
79	thoracic wall	7.7	liposarcoma	2	29	0		alive, NED
80	gluteus	10.0	NOS	3	30	0		alive, NED
84	thigh	3.7	leiomyosarcoma	3	34	0		alive, NED
83	thigh	10.0	liposarcoma	3	21	1	wound healing complication	local and distant recurrence
80	thigh	8.0	NOS	3	31	0	wound healing complication, seroma	alive, distant recurrence lower leg, curative treatment
90	thigh	8.5	leiomyosarcoma	2	29	0	wound healing complication	alive, NED
85	axilla	9.2	liposarcoma	2	31	1		alive, NED
82	thigh	17.0	liposarcoma	2	23	0		alive, NED
87	thoracic wall	5.0	NOS	3	20	0		alive, NED
82	thoracic wall	9.0	NOS	3	23	0	wound healing complication	alive, NED
91	upper arm	5.2	NOS	3	31	0		distant recurrence
81	thigh	8.3	myxoid fibrosarcoma	3	31	0		alive, NED
81	upper arm	8.3	NOS	2	32	0		alive, NED

NED = no evidence of disease; NOS = not otherwise specified

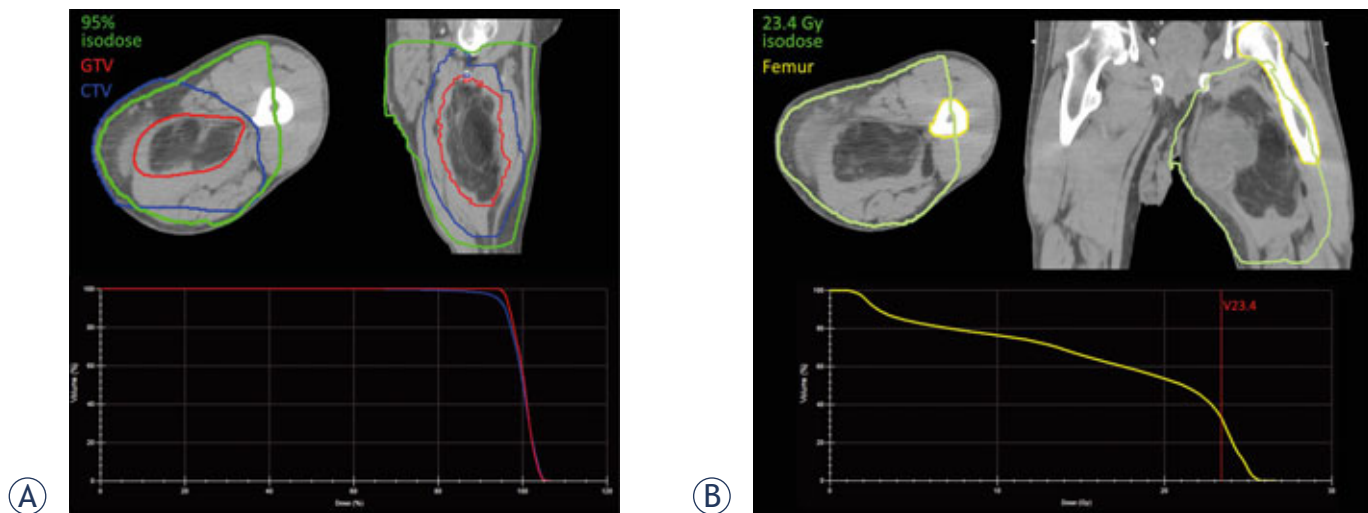


FIGURE 1. Example of a radiation plan for a thigh sarcoma. The 3D conventional radiotherapy plan shows a good dose coverage for the target volumes (even for this case of the largest tumour in our series with 17 cm) (A). The dose constraints for bones concerning pathologic fractures described below were kept (B).

TABLE 2. Dose constraints

Constraints			
Bone	$\alpha/\beta = 1.8 \text{ Gy}$	$\alpha/\beta = 2.8 \text{ Gy}$	
V40 < 64%	V23.4 < 64%	V24.8 < 64%	[18]
Dmean < 37 Gy	Dmean < 22.4	Dmean < 23.6 Gy	[18]
D2 < 59 Gy	D2 < 29.3 Gy	D2 < 31.3 Gy	[18]
Circumferential < 50 Gy	Circumferential < 26.4 Gy	Circumferential < 28.3 Gy	Institutional standard
Soft tissue	$\alpha/\beta = 2.0 \text{ Gy}$		
Circumferential < 40 Gy	Circumferential < 23.7 Gy		Institutional standard

veloped wound healing complications requiring a second surgical intervention. In 4 additional patients, minor wound complications occurred (three times seroma requiring puncture, once protracted wound healing and hematoma). An example of a treatment plan for a thigh sarcoma (the largest tumour in our cohort) shows good feasibility and dose coverage of the target volume while keeping all dose constraints described below (Figure 1).

Oncologic outcomes

Median follow up for all patients was 5.1 ± 1.6 months. Three tumours were resected with microscopically positive margins. In one patient a wide resection without major functional deficits was not feasible. Therefore, a planned positive margin resection was performed. None of the tumours developed a pathologic remission with < 10% vital tumour cells in the resection specimen. Percentage of vital tumour cells was 50% median with a range of 20–95%. The percentage of vital tumour cells did not correlate with the time from end of radiotherapy to surgery (Pearson correlation coefficient $r = -0.01$). Two patients developed a local recurrence, one patient with simultaneous distant metastases five months after start of treatment, one patient 3 months after start of treatment after having developed distant metastases 2 months after start of therapy. All patients developing local recurrences had positive surgical margins. One patient developed pulmonary metastases 3 months after treatment. One patient developed one new distant sarcoma lesion which was treated curatively (Table 1). Thus, estimated local control and disease free survival at 6 months was $92 \pm 8\%$ and $84 \pm 10\%$, respectively. All tumours which developed local and/or distant recurrence showed poorly differentiated histologies (G3).

Dose constraints

As the dose constraints used for radiotherapy of extremity sarcomas (especially for bone concerning pathologic fractures and soft tissue concerning lymphedema) have been developed for normofractionated radiotherapy with 1.8–2.0 Gy per fraction, the question arises, what the corresponding dose constraints for hypofractionated radiotherapy with 25.0 Gy in 5 fractions are. In order to get an estimate of equivalent doses, a literature search was performed to find α/β values for bone fracture and soft tissue. For pathologic rib fractures after radiotherapy for breast cancer α/β values between 1.8 Gy and 2.8 Gy were described.¹⁷ To our knowledge, α/β values for soft tissue concerning lymph oedema have not yet been reported, for the calculation we opted for a value of 2.0 Gy (typically assumed for late radiation toxicity). With an estimate of the α/β values, corresponding doses for institutional constraints as well as published constraints for bone fractures in the radiotherapy of soft tissue sarcomas were calculated as shown in Figure 2. Dose per fraction for the constraints for normofractionated radiotherapy was fixed to 2 Gy, although dose per fraction varies with the number of fractions for the same total dose (e.g. 40 Gy circumferential would refer to a dose per fraction of 1.6 Gy for 25 fractions in preoperative radiotherapy or 1.2 Gy for postoperative radiotherapy in 33 fractions).

With our institutional constraint for bone irradiation at extremities, including the whole bone in the irradiated volume, is unproblematic as the corresponding constraint to 50.0 Gy for the whole bone circumference is between 26.4 Gy and 28.3 Gy depending on the assumed α/β value and thus above the prescribed dose. The corresponding dose constraints based on the constraints reported by Dickie *et al.*, are shown in Table 2.¹⁸ With our in-

$$\text{EQD2} = \frac{d + \alpha/\beta}{2 Gy + \alpha/\beta} \times 5d$$

$$\frac{5d^2 + 5\alpha/\beta \times d}{2 Gy + \alpha/\beta} = \text{EQD2}$$

$$5 \times d^2 + 5 \alpha/\beta \times d = \text{EQD2} \times (2 Gy + \alpha/\beta)$$

$$d^2 + \alpha/\beta \times d - \frac{\text{EQD2} \times (2 Gy + \alpha/\beta)}{5} = 0$$

$$d = -\frac{\alpha/\beta}{2} + \sqrt{\frac{(\alpha/\beta)^2}{4} + \frac{\text{EQD2} \times (2 Gy + \alpha/\beta)}{5}}$$

$$\text{constr}_{\text{HFX}} = 5 \times \left(-\frac{\alpha/\beta}{2} + \sqrt{\frac{(\alpha/\beta)^2}{4} + \frac{\text{constr}_{\text{NFX}} \times (2 Gy + \alpha/\beta)}{5}} \right)$$

FIGURE 2. Starting from the equation for equivalent dose 2 Gy (EQD2) for a hypofractionated radiation regimen in 5 fractions, the quadratic equation for the single dose in five fractions corresponding to the known EQD2 was derived. Solving the quadratic equation leads to the dose per fraction for five fractions corresponding to the given EQD2 (assuming a known α/β value for tumour control or side effects in OARs, respectively). Dose per fraction for the constraints for normofractionated radiotherapy was fixed to 2 Gy, although dose per fraction varies with the number of fractions for the same total dose (e.g. 40 Gy circumferential dose would refer to a dose per fraction of 1.6 Gy for 25 fractions in preoperative radiotherapy or 1.2 Gy for postoperative radiotherapy in 33 fractions). As dose constraints for normofractionated radiotherapy normally are not corrected for number of fractions in clinical plan evaluation, they were not corrected to EQD2 for the transfer to the hypofractionated regimen. $\text{constr}_{\text{HFX}}$ = constraint for hypofractionated radiotherapy. $\text{constr}_{\text{NFX}}$ = constraint for normofractionated radiotherapy.

stitutional standard for the whole circumferential soft tissue to avoid lymphedema of circumferential 40.0 Gy, corresponding dose for 25.0 Gy in 5 fractions is 23.7 Gy (with an assumed α/β value of 2.0 Gy). Thus sparing of at least a part of the circumferential soft tissue is crucial to keep the constraint during hypofractionated radiotherapy with 25.0 Gy in 5 fractions (for details see Table 2).

Radiotherapy planning results

For seven patients with lower extremity sarcomas dose coverage of the target volume as well as the newly established dose constraints for bone were recorded. GTV coverage was good in all cases. CTV coverage was below the dose aimed for in one of the six patients (large calf sarcoma with a CTV reaching the skin in large areas). All dose constraints described in Table 2 were met in all patients (Figure 3). Circumferential dose constraints

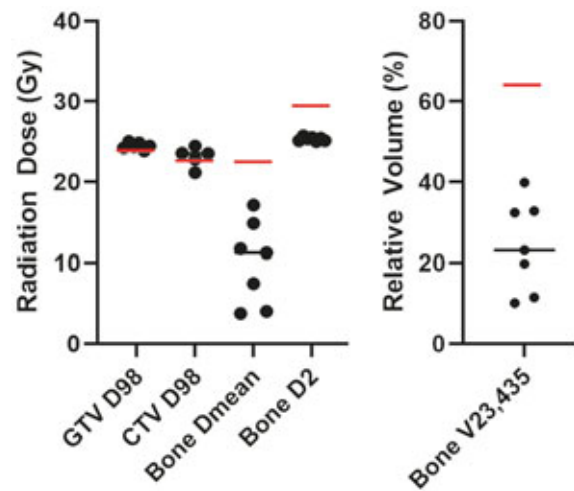


FIGURE 3. Radiation planning parameters were evaluated for seven of nine patients with sarcomas of the lower extremity. For bone constraints concerning pathologic fracture the whole femur or the whole tibia were contoured for thigh and calf sarcomas, respectively. Black bars indicate the median values, red bars indicate the assumed constraints as described in Tbl 2 and in the main text (for bone with $\alpha/\beta = 1.8$ Gy, worst case scenario). Gross tumour volume (GTV) coverage was reached in all cases. D98 for clinical target volume (CTV) fell short in one patient with a large calf sarcoma with a CTV reaching the skin in large areas. Re-calculated dose constraints for pathologic fracture were not reached in any case.

to the bone and soft tissue circumference were met in all cases (data not shown).

Discussion

High risk soft tissue sarcomas in geriatric patients pose difficult treatment decisions.^{7,19} Standard therapy for these tumours consisting of multimodal therapy over several weeks to months is hardly feasible.^{20,21} Surgical approaches are also limited by the functional reserves of patients. Additional radiotherapy significantly reduces the risk of local recurrence.²² In an analysis of geriatric patients with a lower age than in our group including also low risk tumours (American Joint Committee on Cancer [AJCC] stage I) only 22% received radiotherapy. The recurrence rate was comparable or even higher than in our cohort with 27%.²³ Thus, the strategy of hypofractionated preoperative radiotherapy followed by wide resection of the tumour was adopted for this specific patient population.

With pre-treatment interdisciplinary patient evaluation, feasibility of the multimodal concept was good with 17 of 18 (94%) patients completing treatment (radiotherapy and surgery). One

patient did not undergo surgery after completing radiotherapy which resulted in palliative radiotherapy to reduce symptoms caused by the tumour. Postoperative complication rate is not significantly higher than reported for soft tissue sarcomas in general with 5 of 17 (30%) patients requiring surgical intervention compared to 29 of 122 (24%) in a large retrospective analysis (Chi-square: $p = 0.17$).²⁴ In a systematic review and metaanalysis, lower rates for re-surgeries of 16% were reported. However, the specific patient population in our study represents a high risk population for wound complication concerning the described risk factors of age, comorbidities and deep-seated high-grade tumours.²⁵

Our early oncologic results with a local control rate of 92% and a disease-free survival of 84% after 6 months, respectively, were comparable to published data of 87% and 76%, respectively in a dataset of 188 patients with longer follow up.²⁶ None of the patients in our analysis developed an isolated local recurrence. Although the reported dataset is limited in number of patients and short follow-up, our data do not hint at an excessive risk for local recurrence taking into account compromised surgical approaches and chemotherapy options in this specific patient cohort.

To our knowledge, this is the first presentation of the transfer of dose constraints for radiotherapy of the extremities (focusing on bone and soft tissue) for the altered fractionation schedule with 25.0 Gy in 5 fractions. To our knowledge, the quantitative analyses of normal tissue effects in the clinic (QUANTEC) publications do not comment on dose constraints for bone concerning pathologic fracture or soft tissue related to lymph edema.²⁷ We calculated adjusted dose constraints from our institutional constraints for normofractionated radiotherapy as well as from dose constraints published as risk factors for pathologic fractures in sarcoma radiotherapy.¹⁸ Keeping the adjusted institutional constraints was possible in all cases treated in this series without compromising target volume coverage. The constraints listed in the table are a starting point to develop guidance for the altered fractionation in hypofractionated preoperative radiotherapy for extremity soft tissue sarcomas. However, with assumptions to be made such as the α/β value that is hardly known for pathologic fractures or lymph oedema (to our knowledge the only report is on rib fractures after radiotherapy to the thoracic wall), long term side effects of this treatment schedule will need further evaluation.¹⁷

Another field for further development of dose constraints (even for normofractionated radio-

therapy) would be taking into account the number of fractions and calculating dose constraints with equivalent dose 2 Gy (EQD2) correction. This strategy would allow for better comparison of dose constraints and side effects between different radiotherapy fractionation schedules as reported by Jaikuna *et al.*²⁸

Conclusions

In conclusion, hypofractionated preoperative radiotherapy is a feasible and (at least concerning acute wound complications) safe treatment option for geriatric patients with high risk soft tissue sarcoma after critical interdisciplinary evaluation by the surgeon and anesthesiologist as well as the radiation oncologist. The treatment concept warrants further evaluation in this distinct patient population in order to enable perioperative radiotherapy for high risk soft tissue sarcomas.

Acknowledgment

F. Eckert was partly supported by the Deutsche Krebshilfe under grant 70114187.

References

- O'Sullivan B, Davis AM, Turcotte R, Bell R, Catton C, Chabot P, et al. Preoperative versus postoperative radiotherapy in soft-tissue sarcoma of the limbs: a randomised trial. *Lancet* 2002; **359**: 2235-41. doi: 10.1016/S0140-6736(02)09292-9
- Eckert F, Braun LH, Traub F, Kopp HG, Sipos B, Lamprecht U, et al. Radiotherapy and hyperthermia with curative intent in recurrent high risk soft tissue sarcomas. *Int J Hyperthermia* 2018; **34**: 980-7. doi: 10.1080/02656736.2017.1369174
- Eckert F, Gani C, Kluba T, Mayer F, Kopp HG, Zips D, et al. Effect of concurrent chemotherapy and hyperthermia on outcome of preoperative radiotherapy of high-risk soft tissue sarcomas. *Strahlenther Onkol* 2013; **189**: 482-5. doi: 10.1007/s00066-013-0312-7
- Le Cesne A, Ouali M, Leahy MG, Santoro A, Hoekstra HJ, Hohenberger P, et al. Doxorubicin-based adjuvant chemotherapy in soft tissue sarcoma: pooled analysis of two STBSG-EORTC phase III clinical trials. *Ann Oncol* 2014; **25**: 2425-32. doi: 10.1093/annonc/mdu460
- Crompton JG, Ogura K, Bernthal NM, Kawai A, Eilber FC. Local control of soft tissue and bone sarcomas. *J Clin Oncol* 2018; **36**: 111-7. doi: 10.1200/JCO.2017.75.2717
- Pervaiz N, Colterjohn N, Farrokhkar F, Tozer R, Figueredo A, Ghert M. A systematic meta-analysis of randomized controlled trials of adjuvant chemotherapy for localized resectable soft-tissue sarcoma. *Cancer* 2008; **113**: 573-81. doi: 10.1002/cncr.23592
- Greto D, Saieva C, Loi M, Desideri I, Delli Paoli C, Lo Russo M, et al. Patterns of care and survival in elderly patients with locally advanced soft tissue sarcoma. *Am J Clin Oncol* 2019; **42**: 749-54. doi: 10.1097/COC.0000000000000594
- Jones RL. Sarcomas and old age: few options for such a large patient population. *Future Oncol* 2019; **15**: 11-5. doi: 10.2217/fon-2019-0489

9. Pfeffer MR, Blumenfeld P. The changing paradigm of radiotherapy in the elderly population. *Cancer J* 2017; **23**: 223-30. doi: 10.1097/PPO.0000000000000271
10. Haas RL, Miah AB, LePechoux C, DeLaney TF, Baldini EH, Alektiar K, et al. Preoperative radiotherapy for extremity soft tissue sarcoma; past, present and future perspectives on dose fractionation regimens and combined modality strategies. *Radiother Oncol* 2016; **119**: 14-21. doi: 10.1016/j.radonc.2015.12.002
11. Siegel R, Burock S, Wernecke KD, Kretschmar A, Dietel M, Loy V, et al. Preoperative short-course radiotherapy versus combined radiochemotherapy in locally advanced rectal cancer: a multi-centre prospectively randomised study of the Berlin Cancer Society. *BMC Cancer* 2009; **9**: 50. doi: 10.1186/1471-2407-9-50
12. Kosela-Paterczyk H, Szacht M, Morysinski T, Lugowska I, Dziewirski W, Falkowski S, et al. Preoperative hypofractionated radiotherapy in the treatment of localized soft tissue sarcomas. *Eur J Surg Oncol* 2014; **40**: 1641-7. doi: 10.1016/j.ejso.2014.05.016
13. Kosela-Paterczyk H, Szumera-Cieckiewicz A, Szacht M, Haas R, Morysinski T, Dziewirski W, et al. Efficacy of neoadjuvant hypofractionated radiotherapy in patients with locally advanced myxoid liposarcoma. *Eur J Surg Oncol* 2016; **42**: 891-8. doi: 10.1016/j.ejso.2016.02.258
14. Spencer RM, Aguiar Junior S, Ferreira FO, Stevanato Filho PR, Kupper BE, Silva ML, et al. Neoadjuvant hypofractionated radiotherapy and chemotherapy in high-grade extremity soft tissue sarcomas: Phase 2 Clinical Trial Protocol. *JMIR Res Protoc* 2017; **6**: e97. doi: 10.2196/resprot.6806
15. Emami B. Tolerance of normal tissue to therapeutic radiation. *Reports Radiother Oncol* 2013; **1**: 35-48. doi: 10.1016/0360-3016(91)90171-y
16. Wang D, Bosch W, Roberge D, Finkelstein SE, Petersen I, Haddock M, et al. RTOG sarcoma radiation oncologists reach consensus on gross tumor volume and clinical target volume on computed tomographic images for preoperative radiotherapy of primary soft tissue sarcoma of extremity in Radiation Therapy Oncology Group studies. *Int J Radiat Oncol Biol Phys* 2011; **81**: e525-8. doi: 10.1016/j.ijrobp.2011.04.038
17. Overgaard M. Spontaneous radiation-induced rib fractures in breast cancer patients treated with postmastectomy irradiation. A clinical radiobiological analysis of the influence of fraction size and dose-response relationships on late bone damage. *Acta Oncol* 1988; **27**: 117-22. doi: 10.3109/02841868809090331
18. Dickie CI, Parent AL, Griffin AM, Fung S, Chung PW, Catton CN, et al. Bone fractures following external beam radiotherapy and limb-preservation surgery for lower extremity soft tissue sarcoma: relationship to irradiated bone length, volume, tumor location and dose. *Int J Radiat Oncol Biol Phys* 2009; **75**: 1119-24. doi: 10.1016/j.ijrobp.2008.12.006
19. Garbay D, Maki RG, Blay JY, Isambert N, Piperno Neumann S, Blay C, et al. Advanced soft-tissue sarcoma in elderly patients: patterns of care and survival. *Ann Oncol* 2013; **24**: 1924-30. doi: 10.1093/annonc/mdt059
20. Hoefkens F, Dehandschutter C, Somville J, Meijnders P, Van Gestel D. Soft tissue sarcoma of the extremities: pending questions on surgery and radiotherapy. *Radiat Oncol* 2016; **11**: 136. doi: 10.1186/s13014-016-0668-9
21. Larrier NA, Czito BG, Kirsch DG. Radiation Therapy for Soft Tissue Sarcoma: Indications and controversies for neoadjuvant therapy, adjuvant therapy, intraoperative radiation therapy, and brachytherapy. *Surg Oncol Clin N Am* 2016; **25**: 841-60. doi: 10.1016/j.soc.2016.05.012
22. Callegaro D, Miceli R, Bonvalot S, Ferguson P, Strauss DC, Levy A, et al. Impact of perioperative chemotherapy and radiotherapy in patients with primary extremity soft tissue sarcoma: retrospective analysis across major histological subtypes and major reference centres. *Eur J Cancer* 2018; **105**: 19-27. doi: 10.1016/j.ejca.2018.09.028
23. Tsuda Y, Ogura K, Kobayashi E, Hiruma T, Iwata S, Asano N, et al. Impact of geriatric factors on surgical and prognostic outcomes in elderly patients with soft-tissue sarcoma. *Jpn J Clin Oncol* 2017; **47**: 422-9. doi: 10.1093/jjco/hyx016
24. Moore J, Isler M, Barry J, Mottard S. Major wound complication risk factors following soft tissue sarcoma resection. *Eur J Surg Oncol* 2014; **40**: 1671-6. doi: 10.1016/j.ejso.2014.10.045
25. Slump J, Bastiaannet E, Halka A, Hoekstra HJ, Ferguson PC, Wunder JS, et al. Risk factors for postoperative wound complications after extremity soft tissue sarcoma resection: A systematic review and meta-analyses. *J Plast Reconstr Aesthet Surg* 2019; **72**: 1449-64. doi: 10.1016/j.bjps.2019.05.041
26. Sabolch A, Feng M, Griffith K, Rzaa C, Gadzala L, Feng F, et al. Risk factors for local recurrence and metastasis in soft tissue sarcomas of the extremity. *Am J Clin Oncol* 2012; **35**: 151-7. doi: 10.1097/COC.0b013e318209cd72
27. Bentzen SM, Constine LS, Deasy JO, Eisbruch A, Jackson A, Marks LB, et al. Quantitative Analyses of Normal Tissue Effects in the Clinic (QUANTEC): an introduction to the scientific issues. *Int J Radiat Oncol Biol Phys* 2010; **76**(3 Suppl): S3-9. doi: 10.1016/j.ijrobp.2009.09.040
28. Jaikuna T, Khadsiri P, Chawapun N, Saekho S, Tharavichitkul E. Isobio software: biological dose distribution and biological dose volume histogram from physical dose conversion using linear-quadratic-linear model. *J Contemp Brachytherapy* 2017; **9**: 44-51. doi: 10.5114/jcb.2017.66082

Definitive radiotherapy for squamous cell carcinoma of the oral cavity: a single-institution experience

Kristin Lang^{1,2,3}, Melissa Baur¹, Thomas Held^{1,2,3}, Rami El Shafie^{1,2,3}, Julius Moratin⁴, Christian Freudlsperger⁴, Karim Zaoui⁵, Nina Bougatf^{1,2,6}, Jürgen Hoffmann⁴, Peter K. Plinkert⁵, Jürgen Debus^{1,2,3,6,7}, Sebastian Adeberg^{1,2,3,6}

¹ Department of Radiation Oncology, Heidelberg University Hospital, Heidelberg, Germany

² Heidelberg Institute of Radiation Oncology (HIRO), Heidelberg University Hospital, Heidelberg, Germany

³ National Center for Tumor diseases (NCT), Heidelberg University Hospital, Heidelberg, Germany

⁴ Department of Oral and Maxillofacial Surgery, Heidelberg University Hospital, Heidelberg, Germany

⁵ Department of Otorhinolaryngology, Head and Neck Surgery, Heidelberg University Hospital, Heidelberg, Germany

⁶ Heidelberg Ion beam Therapy Center (HIT), Department of Radiation Oncology, Heidelberg University Hospital, Heidelberg, Germany

⁷ Clinical Cooperation Unit Radiation Oncology, German Cancer Research Center (DKFZ), Heidelberg, Germany

Radiol Oncol 2021; 55(4): 467-473.

Received 13 May 2021

Accepted 21 September 2021

Correspondence to: Kristin Lang, M.D., Department of Radiation Oncology, Heidelberg University Hospital, Im Neuenheimer Feld 400, D-69120 Heidelberg, Germany. E-mail: Kristin.lang@med.uni-heidelberg.de

Disclosure: No potential conflicts of interest were disclosed.

This is an open access article under the CC BY-NC-ND license (<http://creativecommons.org/licenses/by-nc-nd/4.0/>).

Background. Surgery is standard of care for oral cavity cancer (OCC). We provide a single-institution experience using definitive radiotherapy (RT) with or without concurrent systemic therapy for primary unresectable OCC.

Patients and methods. We retrospectively examined 49 patients with non-metastatic primary unresectable OCC treated with definitive RT between 2000 and 2019. The majority of patients (63.3%) were treated with definitive chemoradiotherapy while 26.5% were given single-agent cetuximab weekly simultaneous to definitive RT. Five patients were treated with definitive RT alone because of limited disease and no nodal involvement.

Results. Median follow-up was 73 months (range, 6–236 months), median progression free survival (PFS) was 42 months (range, 2–157 months), median local disease-free survival (LDFS) was 44 months (range, 2–157 months) and median overall survival (OS) from the time of RT initiation was 52 months (range, 5–236 months). There were 65.3% locoregional failures, 84.4% local and 15.6% distant metastasis. The majority of patients with local failure presented with American Joint Committee on Cancer (AJCC) Stage III–IV disease (59.2%). The 5-year Kaplan-Meier estimates for OS (III–IV vs. I–II) was 22.8% vs. 54.2% ($p = 0.03$, HR 2.090, 1.1–4.2). Patients who were treated with systemic therapy had a significant better 5-year overall survival compared to those with RT alone (43.9% vs. 23.1%, $p = 0.05$, 1.0–4.1). RT with doses less than 70 Gy ($p = 0.046$, HR 2.1 (1.0–4.5) was associated with worse overall survival. Mucositis was the most common \geq grade 3 acute toxicity and occurred in 19 patients (39%). Incidences of chronic toxicities were loss of taste, trismus, osteoradionecrosis and xerostomia.

Conclusions. Definitive RT with or without concurrent systemic agents in patients with unresectable OCC resulted in an eloquent rate of locoregional control and good overall survival rates and is currently the best available treatment option in this patient collective.

Key words: oral cancer; systemic therapy; definitive radiotherapy; local failure

Introduction

Oral cancer includes cancers of all subsites of the oral cavity (oral tongue, floor of mouth, buccal mucosa, upper lip, lower lip, upper gum, lower gum, palate, and retromolar area) and is the eighth most common cancer worldwide.^{1,2} Worldwide incidence of oral cancer in 2018 was four cases per 100,000 people.³ Most related risk factors for oral cancer belong to tobacco and alcohol use.⁴

Treatment of oral cavity cancer (OCC) includes single modality surgery, radiotherapy (RT) or various combinations of these modalities with or without systemic agents. The selection of treatment is based on disease stage, considerations of disease control, anticipated functional and cosmetic outcomes and expertise. Standard treatment option for OCC is surgery.⁵ Primary RT with or without systemic therapy is not used routinely. There are less prospective trials available which directly compared primary surgery *vs.* primary RT in oral squamous cell carcinoma (OSCC) specifically.⁵⁻⁸ In literature 5-year overall survival rate since first diagnosis in patients treated with RT alone was 15%.^{6,9} To improve local control and overall survival rates intensified treatment with concurrent chemotherapy to RT is necessary instead of RT alone.^{9,10} Stenson *et al.* reported in a retrospective series overall survival rates with 66.9% in locally advanced oral cancer patients (stage III-IV) undergoing concurrent chemoradiotherapy (CCRT).¹⁰ In a meta-analysis from Pignon *et al.* of individual patient data from clinical trials comparing RT *vs.* CCRT (MACH-NC) in locally advanced head and neck cancers, OCC comprised 21% of cases. Results showed an improvement of survival in OCC with CCRT compared to RT alone.⁹⁻¹¹

To examine the clinical significance and outcome in patients who do not undergo surgery we retrospectively reviewed our experience in treating OCC with primary RT with or without concurrent systemic therapies.

Patients and methods

This study was performed following institutional guidelines and the Declaration of Helsinki of 1975 in its most recent version. Ethical approval for the study was given from the local ethics committee at University Hospital Heidelberg (S421-2015).

Clinical, operative, and hospital course records were reviewed. We analyzed data from Nationales Centrum für Tumorerkrankungen (NCT) Cancer

Registry in Heidelberg and imported data into our HIRO Research Database.¹² All patients underwent systemic workup including cross-sectional imaging with referring providers prior to commencing RT. Afterwards, the patients underwent CT simulation with a standard immobilization 5-point mask. Target volume definition was based on CT and MRI scans with contrast agents, included the primary tumor region as well as nodal involvement according to the International Commission on Radiation Units and Measurements (ICRU) definition.¹¹⁻¹⁶ Patients underwent regular follow-up, including CT examinations every three months in the first two years after definitive treatment, in year three and four every 6 months and year five and six once a year as well as regularly clinical examinations at the Department of Oral and Maxillofacial Surgery. All follow-up CT-scans were reviewed by an experienced radiologist by the institutions own diagnostics. We excluded all patients with a metastatic disease (M1) at initial diagnosis.

Treatment toxicity

Acute toxicity was evaluated during and at the end of RT. Late toxicity was evaluated minimum 90 days after completion of RT and was described according to the Common Terminology Criteria for Adverse Events (CTCAE) criteria (version 4.03, U.S. Department of Health and Human Services, Washington, DC, USA).

Statistical analysis and outcome evaluation

Overall survival (OS), progression free survival (PFS) and local disease-free survival (LDFS) were calculated using Kaplan-Meier analysis. OS was calculated from the time of RT initiation until death or the date of last follow-up. PFS was calculated as the time from RT initiation to tumor progression or death/ date of last follow-up, whichever occurred first. LRFS was defined as the time from RT initiation until local tumor progression at the primary tumor site. Patients still alive at the time of analysis, without tumor progression, or patients lost to follow-up were censored. Kaplan-Meier estimates were calculated using IBM SPSS software version 24. Subgroups were compared using the log-rank test. *p*-values of 0.05 or less were considered statistically significant. For comparison between groups, the Chi-squared test was performed in categorical and continuous variables. Kaplan-Meier estimates of potential prognostic factors were compared us-

ing the log-rank test for univariate analysis and the cox-regression model for multivariate analysis.

Results

Patient characteristics

There were 49 patients treated either with definitive RT alone or in combination with chemotherapy/immunotherapy at the Department of Radiation Oncology, University Hospital of Heidelberg. Only patients with cancer of the oral tongue (23 patients), floor of mouth (21 patients) and buccal mucosa (4 patients) were included (ICD-O-3 topography codes C02-C06).

Information regarding a risk factor history was available for all patients, there were 19 patients current and former smokers, 10 patients with alcohol consumption and 61 patients had a smoking and drinking history. Detailed patient characteristics are shown in Table 1.

Treatment characteristics

RT was carried out using photon irradiation with either 3D-planned (17 patients, 34.7%), IMRT (32 patients, 65.3%) (TomoTherapy®, Accuray, Sunnyvale, CA, USA) or volume-modulated RT (VMAT) (Elekta, Sweden), with treatment delivered one fraction per day with 5 fractions per week. The main RT treatment features are listed in Table 2.

There were 5 patients (10.2%) treated with RT alone because of limited disease or no nodal involvement. The majority of patients (31 patients, 63.3%) were treated with single-agent cisplatin 40 mg/m² chemotherapy weekly and 13 patients (26.5%) were given single-agent cetuximab 400 mg/m² one week prior to start of treatment followed by 250 mg/m² weekly as an alternative to chemotherapy.

Treatment results for the whole cohort

After a median follow-up of 73 months (range, 6–236 months), 11 patients (22.4%) were still alive, while 38 patients (77.6%) had died: 31 (81.6%) due to disease progression and 7 (18.4%) due to pulmonary infection, cardiac disease, secondary carcinoma or other comorbidities. There were 32 patients (65.3%) with locoregional failures in this cohort, 27 patients (84.4%) of which were local failures alone and 5 patients (15.6%) were distant. The majority of patients who failed locally presented with American Joint

TABLE 1. Patient characteristics

Characteristic	Number of patients (percentage)
Gender	
Male	30 (61.2%)
Female	19 (38.8%)
Age, years	
Median (range)	61 years (17–85 years)
T-stage	
T1	8 (16.3%)
T2	12 (24.5%)
T3	7 (14.3%)
T4	22 (44.9%)
N-stage	
N0	20 (40.8%)
N+	29 (59.2%)
Grading	
1	5 (10.2%)
2	10 (20.4%)
3	34 (69.4%)
Risk factors	
Smoking history	29 (59.2%)
Alcohol consumption	6 (12.2%)
none	14 (28.6%)

TABLE 2. RT treatment characteristics

Technique	
3D-CRT	17 (34.7%)
IMRT	32 (65.3%)
RT-Dose	
Median total dose base plan (without boost)	57.5 Gy (range: 50.0–65.9 Gy)
Median single dose base plan (without boost)	1.9 Gy (range: 1.7–2.1 Gy)
Boost	
Yes	45 (91.8%)
SIB	38 (84.4%)
Sequential	7 (15.6%)
no	4 (8.2%)
Median total dose boost plan	12.0 Gy (range: 8.0–20.0 Gy)
Median single dose boost plan	2.2 Gy (range: 2.0–2.2 Gy)
Cumulative total dose (base + boost plan)	70.0 Gy (range: 60.0–72.0 Gy)
RT-Volume	
CTV dimension base plan	829.6 ccm (range: 61.7–1554.4 ccm)
CTV dimension boost plan	178.5 ccm (range: 31.4–535.8 ccm)

CTV = clinical target volume; Gy = gray; IMRT = intensity modulated radiotherapy, RT = radiotherapy, SIB = simultaneous integrated boost; 3D-CRT = three dimensional-conformal radiotherapy

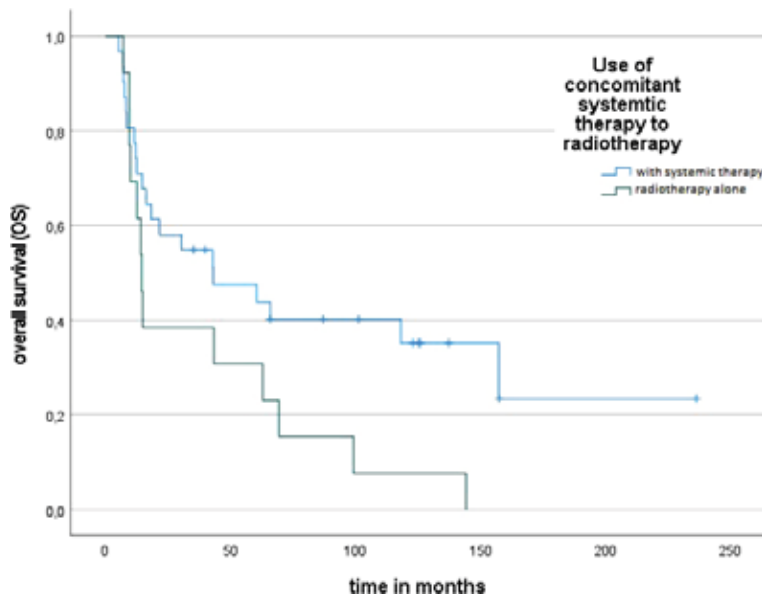


FIGURE 1. The 5-year Kaplan-Meier estimates for overall survival (OS) with systemic treatment (blue) was 43.9% vs. 23.1% with radiotherapy alone (green) ($p = 0.05$, HR 2.1, 1.1–4.2).

Committee on Cancer (AJCC) Stage III–IV disease ($n = 29$, 59.2%), while there were 20 patients (40.8%) that occurred in patients with early (Stage I–II) disease. The 5- and 10-year Kaplan-Meier estimates for OS, PFS, and LDFS were 37.9%, 35.9%, and 44.9%,

and 23.0%, 28.6%, and 36.0% respectively. The median time to development of distant metastases was 66 months (range, 3.0–236 months).

The 5-year Kaplan Meier estimates for OS using systemic treatment versus RT alone was 43.9% vs. 23.1% ($p = 0.05$, Figure 1, HR 2.1, 1.1–4.2), there was no significant difference for PFS and LDFS.

Results of univariate analysis

The 5-year Kaplan-Meier estimates for OS (III–IV vs. I–II) was 22.8% vs. 54.2% ($p = 0.03$, HR 2.090, 1.1–4.2).

On univariate analysis, treatment with RT alone ($p = 0.005$), RT doses < 70Gy ($p = 0.05$) and nodal positive stage ($p = 0.036$) were associated with a greater risk of death (Table 3). For LDFS and PFS only positive nodal stage ($p = 0.026$ and 0.027) was associated with a significantly worse outcome.

Results of multivariate analysis

Multivariate analysis was performed using the following variables: type of treatment, RT concept and nodal tumor stage. RT with doses less than 70Gy ($p = 0.046$, HR 2.1 (1.0–4.5)) was associated with worse overall survival. Table 3 summarizes univariable cox Regression analysis for OS, PFS, LDFS and metastasis free survival (MFS).

TABLE 3. Overview about univariable cox regression analysis for overall survival (OS), progression free survival (PFS), local disease-free survival (LDFS), and metastasis free survival (MFS) in patients with oral squamous cell carcinoma (OSCC) undergoing definitive radiotherapy

Parameter	OS		PFS		LDFS		MFS	
	HR (95% CI)	p-value	HR (95% CI)	p-value	HR (95% CI)	p-value	HR (95% CI)	p-value
Age (< 60 years)	1.2 (0.6–2.2)	0.637	0.9 (0.4–1.7)	0.647	0.6 (0.3–1.3)	0.224	3.4 (0.7–16.8)	0.120
Sex male vs. female	1.2 (0.6–2.4)	0.570	0.9 (0.5–2.0)	0.950	1.1 (0.5–2.4)	0.881	1.3 (0.3–5.1)	0.741
T stage T1/2 vs. T3/4	2.1 (1.1–4.2)	0.036	1.3 (1.0–1.8)	0.077	1.4 (0.9–2.0)	0.072	2.1 (0.9–4.5)	0.071
N stage N0 vs. N+	2.1 (1.1–4.2)	0.036	2.4 (1.1–5.3)	0.026	2.7 (1.1–6.3)	0.027	2.8 (0.8–5.4)	0.071
RT dose < 70.0 Gy vs. \geq 67.0 Gy	1.9 (1.0–3.8)	0.05	1.5 (0.7–3.1)	0.267	1.4 (0.6–3.1)	0.393	1.7 (0.4–7.0)	0.428
Concomitant therapies	2.1 (1.0–4.1)	0.05	1.2 (0.9–1.5)	0.227	1.5 (0.7–3.5)	0.294	0.4 (0.1–3.3)	0.409
Concomitant therapies CHT vs. IT	1.2 (0.9–1.5)	0.216	1.5 (0.7–3.3)	0.296	1.2 (0.6–2.7)	0.586	0.7 (0.2–2.7)	0.580
RT technique IMRT vs. 3D	0.6 (0.4–1.2)	0.183	0.7 (0.3–1.3)	0.258	0.7 (0.3–1.4)	0.282	1.2 (0.3–5.0)	0.765
Risk factor history	1.1 (0.8–1.4)	0.536	0.9 (0.7–1.3)	0.690	0.9 (0.6–1.1)	0.328	1.5 (0.7–3.0)	0.295

CHT = chemotherapy; CTV = clinical target volume; Gy = gray; IMRT = intensity modulated radiotherapy; IT = immunotherapy; LDFS = local disease-free survival; RT = radiotherapy, SIB = simultaneous integrated boost; 3D = three dimensional-conformal radiotherapy

Toxicity

Mucositis was the most common grade > 3 acute toxicity present in 19 patients (39.0%) followed by dysphagia grade 3 in 12 patients (24.0%). Other significant acute toxicities grade 1/2 included dermatitis (56.3%) and xerostomia (39.7%). There were no treatment-related deaths. Late RT-related complications (grade 3) included xerostomia (64.4%), loss of taste (60.3%), trismus (26.0%) and osteoradionecrosis (9.6%). A total of 27 (56.0%) patients received a percutaneous endoscopic gastrostomy (PEG) tube: 5 (19.2%) prophylactically (reflecting the prior institutional practice of routine PEG placement prior to treatment), 22 acutely during treatment (80.8%). Toxicities are summarized in Table 4.

Discussion

The primary purpose of the present study was to evaluate the outcome and prognostic factors for patients with unresectable OCC who underwent definitive RT. Several studies reported local control rates and 5-year OS for definitive RT in OCC ranging between 27% to 70%^{9,11,13} and 37–67%¹⁴, which goes in line with our results.

In our study 59.2% of patients had advanced-stage disease III–IV with significant OS in stage I–II. Over the last decades the role of concomitant systemic therapy has become clearer. Pignon *et al.* reported in MACH-NC about better outcome and locoregional control rates when using concurrent chemotherapy and RT with a better absolute benefit of 4.5% at 5 years.^{9,16} In our study there were

TABLE 4. Early and late toxicity after radiotherapy

Early treatment toxicity (< 90 days)	No of patients n (%)	Late treatment toxicity (> 90 days)	No of patients n (%)
CTCAE grade		CTCAE grade	
Mucositis			
1	6 (13.0)		
2	19 (39.7)		
3	17 (35.6)		
4	2 (3.4)		
Dermatitis			
1	12 (24.7)		
2	15 (31.5)		
3	5 (11.0)		
Xerostomia			
1	15 (30.8)	1	19 (39.7)
2	4 (8.9)	2	17 (35.6)
3	1 (2.1)	3	1 (2.1)
Dysphagia			
1	9 (19.2)	1	15 (30.8)
2	17 (34.9)	2	5 (11.0)
3	12 (24.0)	3	4 (8.9)
Loss of taste (late toxicity)			
		29 (60.0)	
Trismus (late toxicity)			
		13 (26.0)	
Osteoradionecrosis (late toxicity)			
		4 (8.9)	

CTCAE = Common Terminology Criteria for Adverse Events

10.2% patients treated with RT alone due to either comorbidities, worse performance status or because of denied surgery. Patients who were treated with systemic treatment had a significantly better 5-year OS compared to those without (43.9% *vs.*

TABLE 5. Summary of the most important studies for definitive radiotherapy in patients with oral cavity cancer as an overview radiotherapy

Study Period	Radiotherapy	No. of patients	CHT/IT	LDFS	PFS	OS
Lin <i>et al.</i> ¹⁸	42% IMRT	115	48% CHT	27% (3yr)	n/a	15% (3yr)
Foster <i>et al.</i> ¹⁷	54% IMRT	140	100% CHT	79% (5yr)	59% (5yr)	63% (5yr)
Studer <i>et al.</i> ⁸	100% IMRT	54	68% CHT/IT	n/a	37% (4yr)	37% (4yr)
Pederson <i>et al.</i> ⁹	100% IMRT	21	100% CHT	76% (5yr)	71% (5yr)	76% (5yr)
Hosny <i>et al.</i> ¹⁹	100% IMRT	21	35% CHT	42% (5yr)	78% (5yr)	50% (5yr)
Present Study	74% IMRT	119	86.5% CHT/IT	61.9% (5yr)	52.1% (5yr)	47.2% (5yr)

CHT = chemotherapy; IMRT = intensity modulated radiotherapy; IT = immunotherapy; LDFS = local disease-free survival; n/a = not applicable; OS = overall survival; PFS = progression free survival; yr = years

23.1%) ($p = 0.05$, HR 2.1, 1.1–4.2) but no significant difference for PFS and LDFS.

While other studies found T-stage, age, grading and gender to be prognostic factors for PFS and LC¹⁴⁻²⁰, the present study did not find these to have a significant effect in uni- or multivariate analysis. In our collective treatment with RT alone, cumulative total RT doses < 70 Gy and positive nodal stage were associated with a greater risk of death and worse local control. For LDFS and PFS only positive nodal stage was associated with a significant worse outcome.

Cumulative total doses of less than 70 Gy is standard in patients who underwent postoperative treatment and not suggested as definitive RT treatment concept which goes in line with literature.¹⁵

Early and late toxicity from definitive RT to the oral cavity of our collective is comparable to data from other published series.^{7,9,19,21,22,23} Most common acute RT-related complications (CTCAE grade > 3) in our study were oral mucositis (39.0%) and dysphagia (24.0%). Other significant acute toxicities grade 1/2 included dermatitis (56.2%) and xerostomia (39.7%). Late RT-related complications included xerostomia (64.4%), loss of taste (60.3%), trismus (26.0%), edema (47.3%). These late complications appear similar in other series.^{7,9,16,19,22} The rate of osteoradionecrosis in the present study was 9.6%, which falls in line with other studies – ranging from 1% to 56%²³⁻²⁸ in which both conventional and IMRT were utilized. Reuther *et al.* reported that a total dose above 60 Gy was a significant parameter for osteoradionecrosis (ORN).²⁹ This is similar with our study, all patients with ORN had a cumulative total dose of more than 66 Gy.

The limitations of this study include its retrospective nature, which led to a shortage of necessary data on some single cases. However, we were able to retrieve follow-up data covering a lengthy time period for all patients at a large department with a lot of experience in field of oral tumor diseases.

The power of this study is that we were able to show in a dedicated collective of patients with OCC undergoing definitive RT and an extended follow up of 73 months good control and overall survival rates with moderate toxicity.

References

1. Scully C, Bagan J. Oral squamous cell carcinoma overview. *Oral Oncol* 2009; **45**: 301-8. doi: 10.1016/j.oraloncology.2009.01.004
2. Warnakulasuriya S. Global epidemiology of oral and oropharyngeal cancer. *Oral Oncol* 2009; **45**: 309-16. doi: 10.1016/j.oraloncology.2008.06.002
3. Ferlay J, Colombet M, Soerjomataram I, Mathers C, Parkin DM, Pineros M, et al. Estimating the global cancer incidence and mortality in 2018: GLOBOCAN sources and methods. *Int J Cancer* 2019; **144**: 1941-53. doi: 10.1002/ijc.31937
4. Chaturvedi AK, Anderson WF, Lortet-Tieulent J, Curado MP, Ferlay J, Franceschi S, et al. Worldwide trends in incidence rates for oral cavity and oropharyngeal cancers. *J Clin Oncol* 2013; **31**: 4550-9. doi: 10.1200/JCO.2013.50.3870
5. Sutton DN, Brown JS, Rogers SN, Vaughan ED, Woolgar JA. The prognostic implications of the surgical margin in the oral squamous cell carcinoma. *Int J Oral Maxillofac Surg* 2003; **32**: 30-4. doi: 10.1054/ijom.2002.03135
6. Scher ED, Romesser PB, Chen C, Ho F, Wu Y, Sherman EJ, et al. Definitive chemoradiation for primary oral cavity carcinoma: a single institution experience. *Oral Oncol* 2015; **51**: 709-15. doi: 10.1016/j.oraloncology.2015.04.007
7. Foster CC, Melotek JM, Brisson RJ, Seiwert TY, Cohen EEW, Stenson KM, et al. Definitive chemoradiation for locally-advanced oral cavity cancer: a 20-year experience. *Oral Oncol* 2018; **80**: 16-22. doi: 10.1016/j.oraloncology.2018.03.008
8. Lyer N, Tan DSW, Tan VKM, Wang W, Hwang J, Tan NC, et al. Randomized trial comparing surgery and adjuvant radiotherapy versus concurrent chemoradiotherapy in patients with advanced, nonmetastatic squamous cell carcinoma of the head and neck: 10-year update and subset analysis. *Cancer* 2015; **121**: 1599-607. doi: 10.1002/cncr.29251
9. Pignon JP, le Maitre A, Maillard E, Bourhis J, Group M-NC. Meta-analysis of chemotherapy in head and neck cancer (MACH-NC): an update on 93 randomised trials and 17,346 patients. *Radiother Oncol* 2009; **92**: 4-14. doi: 10.1016/j.radonc.2009.04.014
10. Stenson KM, Kunnavakkam R, Cohen EE, Portugal LD, Blair E, Haraf DJ, et al. Chemoradiation for patients with advanced oral cavity cancer. *Laryngoscope* 2010; **120**: 93-9. doi: 10.1002/lary.20716
11. Studer G, Brown M, Bredell M, Graetz KW, Huber G, Linsenmeier C, et al. Follow up after IMRT in oral cavity cancer: update. *Radiat Oncol* 2012; **7**: 84. doi: 10.1186/1748-717X-7-84
12. Kessel KA, Bohn C, Engelmann U, Oetzel D, Bougatf N, Bendl R, et al. Five-year experience with setup and implementation of an integrated database system for clinical documentation and research. *Comput Methods Programs Biomed* 2014; **114**: 206-17. https://doi.org/10.1016/j.cmpb.2014.02.002
13. Lang K, Akbaba S, Held T, Kargus S, Horn D, Bougatf N, et al. Definitive radiotherapy vs. postoperative radiotherapy for lower gingival carcinomas of the mandible: a single-center report about outcome and toxicity. *Strahlenther Onkol* 2019; **195**: 819-29. doi: 10.1007/s00066-019-01484-z
14. Eisbruch A. Intensity-modulated radiation therapy in the treatment of head and neck cancer. *Nat Clin Pract Oncol* 2005; **2**: 34-9. doi: 10.1038/nponc0058
15. Huang SH, O'Sullivan B. Oral cancer: current role of radiotherapy and chemotherapy. *Med Oral Patol Oral Cir Bucal* 2013; **18**: e233-40. doi: 10.4317/medoral.18772
16. Pignon JP, Bourhis J, Domenge C, Designe L. Chemotherapy added to locoregional treatment for head and neck squamous-cell carcinoma: three meta-analyses of updated individual data. MACH-NC Collaborative Group. Meta-analysis of chemotherapy on head and neck cancer. *Lancet* 2000; **355**: 949-55. doi: 10.1016/S0140-6736(00)90011-4
17. Bernier J, Cooper JS, Pajak TF, van Glabbeke M, Bourhis J, Forastiere A, et al. Defining risk levels in locally advanced head and neck cancers: a comparative analysis of concurrent postoperative radiation plus chemotherapy trials of the EORTC (#22931) and RTOG (# 9501). *Head Neck* 2005; **27**: 843-50. doi: 10.1002/hed.20279
18. Lin CY, Wang HM, Kang CJ, Lee LY, Huang SF, Fan KH, et al. Primary tumor site as a predictor of treatment outcome for definitive radiotherapy of advanced-stage oral cavity cancers. *Int J Radiat Oncol Biol Phys* 2010; **78**: 1011-9. doi: 10.1016/j.ijrobp.2009.09.074
19. Hosni A, Chiu K, Huang SH, Xu W, Huang J, Bayley A, et al. Non-operative management for oral cavity carcinoma: definitive radiation therapy as a potential alternative treatment approach. *Radiother Oncol* 2020; **154**: 70-5. doi: 10.1016/j.radonc.2020.08.013
20. Murthy V, Agarwal JP, Laskar SG, Gupta T, Budrukkar A, Pai P, et al. Analysis of prognostic factors in 1180 patients with oral cavity primary cancer treated with definitive or adjuvant radiotherapy. *J Cancer Res Ther* 2010; **6**: 282-9. doi: 10.4103/0973-1482.73360

21. Zelefsky MJ, Harrison LB, Fass DE, Armstrong JG, Shah JP, Strong EW. Postoperative radiation therapy for squamous cell carcinomas of the oral cavity and oropharynx: impact of therapy on patients with positive surgical margins. *Int J Radiat Oncol Biol Phys* 1993; **25**: 17-21. doi: 10.1016/0360-3016(93)90139-m
22. Salama JK, Seiwert TY, Vokes EE. Chemoradiotherapy for locally advanced head and neck cancer. *J Clin Oncol* 2007; **25**: 4118-26. doi: 10.1200/JCO.2007.12.2697
23. Tobias JS, Monson K, Gupta N, Macdougall H, Glaholm J, Hutchison I, et al. Chemoradiotherapy for locally advanced head and neck cancer: 10-year follow-up of the UK Head and Neck (UKHAN1) trial. *Lancet Oncol* 2010; **11**: 66-74. doi:10.1016/S1470-2045(09)70306-7
24. Pederson AW, Salama JK, Witt ME, Stenson KM, Blair EA, Vokes EE, et al. Concurrent chemotherapy and intensity-modulated radiotherapy for organ preservation of locoregionally advanced oral cavity cancer. *Am J Clin Oncol* 2011; **34**: 356-61. doi: 10.1097/COC.0b013e3181e8420b
25. Gebre-Medhin M, Brun E, Engstrom P, Haugen Cange H, Hammarstedt-Nordenvall L, Reizenstein J, Nyman J, et al. ARTSCAN III: a randomized Phase III study comparing chemoradiotherapy with cisplatin versus cetuximab in patients with locoregionally advanced head and neck squamous cell cancer. *J Clin Oncol* 2021; **39**: 38-47. doi: 10.1200/JCO.20.02072
26. Shah JP, Gil Z. Current concepts in management of oral cancer – surgery. *Oral Oncol* 2009; **45**: 394-401. doi: 10.1016/j.oraloncology.2008.05.017
27. Kerr P, Myers CL, Butler J, Alessa M, Lambert P, Cooke AL. Prospective functional outcomes in sequential population based cohorts of stage III/ IV oropharyngeal carcinoma patients treated with 3D conformal vs. intensity modulated radiotherapy. *J Otolaryngol Head Neck Surg* 2015; **44**: 17. doi: 10.1186/s40463-015-0068-429.
28. Blanchard P, Baujat B, Holostenco V, Bourredjem A, Baey C, Bourhis J, et al. Meta-analysis of chemotherapy in head and neck cancer (MACH-NC): a comprehensive analysis by tumour site. *Radiother Oncol* 2011; **100**: 33-40. doi: 10.1016/j.radonc.2011.05.036
29. Reuther T, Schuster T, Mende U, Kübler A. Osteoradionecrosis of the jaws as a side effect of radiotherapy of head and neck tumour patients – a report of a thirty year retrospective review. *Int J Oral Maxillofac Surg* 2003; **32**: 289-95. doi: 10.1054/ijom.2002.0332

Acute side effects after definitive stereotactic body radiation therapy (SBRT) for patients with clinically localized or locally advanced prostate cancer: a single institution prospective study

Kliton Jorgo^{1,2}, Csaba Polgar^{1,2}, Gabor Stelczer^{1,3}, Tibor Major^{1,2}, Laszlo Gesztesi¹, Peter Agoston^{1,2}

¹ Centre of Radiotherapy, National Institute of Oncology, Budapest, Hungary

² Department of Oncology, Semmelweis University, Budapest, Hungary

³ Institute of Nuclear Techniques, Budapest University of Technology and Economy, Budapest, Hungary

Radiol Oncol 2021; 55(4): 474-481.

Received 10 March 2021

Accepted 30 May 2021

Correspondence to: Dr. Jorgo Kliton, M.D., Ph.D., Centre of Radiotherapy, National Institute of Oncology, Ráth György u. 7-9, Budapest, H-1122, Hungary. E-mail: jorgokliton@gmail.com

Disclosure: No potential conflicts of interest were disclosed.

This is an open access article under the CC BY-NC-ND license (<http://creativecommons.org/licenses/by-nc-nd/4.0/>).

Background. The aim of the study was to evaluate acute side effects after extremely hypofractionated intensity-modulated radiotherapy (IMRT) with stereotactic body radiation therapy (SBRT) for definitive treatment of prostate cancer patients.

Patients and methods. Between February 2018 and August 2019, 205 low-, intermediate- and high-risk prostate cancer patients were treated with SBRT using "CyberKnife M6" linear accelerator. In low-risk patients 7.5–8 Gy was delivered to the prostate gland by each fraction. For intermediate- and high-risk disease a dose of 7.5–8 Gy was delivered to the prostate and 6–6.5 Gy to the seminal vesicles by each fraction with a simultaneous integrated boost (SIB) technique. A total of 5 fractions (total dose 37.5–40 Gy) were given on every second working day. Acute radiotherapy-related genitourinary (GU) and gastrointestinal (GI) side effects were assessed using Radiation Therapy Oncology Group (RTOG) scoring system.

Results. Of the 205 patients (28 low-, 115 intermediate-, 62 high-risk) treated with SBRT, 203 (99%) completed the radiotherapy as planned. The duration of radiation therapy was 1 week and 3 days. The frequencies of acute radiotherapy-related side effects were as follows: GU grade 0 – 17.1%, grade I – 30.7%, grade II – 50.7%, grade III – 1.5%; and GI grade 0 – 62.4%, grade I – 31.7%, grade II – 5.9%, grade III – 0%. None of the patients developed grade ≥ 4 acute toxicity.

Conclusions. SBRT with a total dose of 37.5–40 Gy in 5 fractions appears to be a safe and well tolerated treatment option in patients with prostate cancer, associated with slight or moderate early side effects. Longer follow-up is needed to evaluate long-term toxicity and biochemical control.

Key words: prostate cancer; stereotactic radiotherapy; CyberKnife; extreme hypofractionation

Introduction

Prostate cancer is the most common malignancy among men of European western countries.¹ In the male population, the incidence of prostate cancer ranks third in Hungary.² Based on the available evidence, treatment options for organ-confined

prostate cancer include radical prostatectomy, external beam radiation therapy, brachytherapy, and active follow-up.³⁻⁵ In a three-arm, phase III, randomized trial (ProtecT), active monitoring, radical prostatectomy and external beam radiation therapy (EBRT) were compared in patients with non-metastatic, lymph node negative prostate cancer.^{6,7}

After a median follow-up of 10 years there was no significant difference in prostate cancer specific mortality and overall survival. Significant differences were recognized only in the late side effects regarding bowel-, urinary- and sexual function. Therefore, the toxicity after any curative treatment, and the length and burden of the treatment itself are of great importance. Since Brenner and Hall⁸ suggested a low α/β ratio (1.5) for prostate adenocarcinoma, two treatment options have been investigated for external beam irradiation therapy of prostate cancer patients: moderate hypofractionation (2.2–4Gy/fraction)⁹ and extreme hypofractionation (3.5–15Gy/fraction).¹⁰ Three non-inferiority, phase III randomized trials compared conventional fractionation (CF) with moderate hypofractionation (MH), enrolling more than 5500 patients with prostate cancer.^{11–13} At 5-year follow-up these two modalities were shown to be equivalent in terms of tumor control and late side effects, supporting MH as a standard-of-care. In addition to MH, another method of hypofractionation can be used in the radiation treatment of prostate cancer mainly for patients with low- and intermediate-risk. The extreme hypofractionation (stereotactic body radiation therapy, SBRT) can be performed with either a conventional linear accelerator^{14,15} or a robotic arm (CyberKnife, Accuray Incorporated, Sunnyvale, CA) linear accelerator.¹⁶ Currently, more and more results are reported on the effectiveness and tolerability of SBRT, predominantly from retrospective and prospective, non-randomized trials. The advantage of SBRT lies in the use of high and precise ablative doses. In addition, overall treatment-time is relatively short (1–2 weeks) compared to conventional or moderately hypofractionated EBRT, and in contrast to surgery or brachytherapy the treatment is non-invasive.

At our institution we have been performing robotic-arm stereotactic radiation treatments since February 2018. The aim of our prospective study was to implement extreme hypofractionated, robotic-arm based SBRT for the treatment of low-, intermediate- and high-risk, lymph node negative prostate cancer patients and to investigate the acute radiotherapy-related side effects.

Patients and methods

Our prospective study was initiated in February 2018 after approval by our institutional Ethics Committee. Histologically confirmed, low-, intermediate- and high-risk prostate cancer patients

were enrolled. Before radiation therapy staging was required (CT scan or pelvic MRI and bone scan). Lymph node or distant metastasis and previous pelvic irradiation were exclusion criteria. Gold fiducial markers were implanted into the prostate of each patient for image-guided radiotherapy (IGRT). The method is described in details in our previous studies.^{17,18} Briefly, patients received 100 mg tramadol and 5 mg metoclopramide intramuscularly half an hour prior to the procedure. Subsequently, patients were laid down in lithotomy position and 4 gold markers were transperineally inserted into the prostate under rectal ultrasound (US) guidance. In the same plane, two markers were placed near the prostate base, two in the apex. For treatment planning, 14–20 days after marker implantation a topometric CT (TOP CT) was performed in supine position using knee fixation support system for immobilization of the legs. Axial images were obtained with 1.25 mm slice thickness from L1 vertebra to about 3 cm below the ischial tuberosities. A Metal Artefact Reduction (MAR) corrected CT scan was also acquired to reduce the artefact effects of implanted gold markers. Prior to TOP CT, patients were instructed to have moderately, comfortably filled bladder by drinking 0.5 litre of water (after having it emptied) half an hour prior to CT and an empty rectum. In case of habitual constipation light laxative was recommended. In our study, patients were treated according to D'Amico's classification in 3 risk groups.¹⁹ In low-risk patients the clinical target volume for prostate (CTV_{pros}) was the prostate gland. For intermediate-risk two clinical target volumes were created. CTV_{pros} was the same as above. The prostate and seminal vesicles CTV (CTV_{psv}) was generated by 5 mm expansion of CTV_{pros} in all directions except posteriorly at the prostate-rectum interface + proximal 1 cm of the seminal vesicles. For high-risk patients CTV_{pros} was the same as above. CTV_{psv} was defined by 5 mm expansion of CTV_{pros} in all directions except posteriorly + proximal 2 cm of seminal vesicles (in case of cT3b the entire seminal vesicles were included).

Planning target volumes (PTV_{pros}, PTV_{psv}) were formed from CTVs with 3mm extensions in each direction. Depending on the performance status and age of the patients for low-risk patients 7.5–8 Gy fraction dose was applied to PTV_{pros}. In case of intermediate- and high-risk disease 7.5–8 Gy fraction dose to PTV_{pros} and a 6–6.5 Gy fraction dose to PTV_{psv}, with a simultaneous integrated boost (SIB) technique was given. A total of 5 fractions (total dose for prostate 37.5–40 Gy) were

TABLE 1. Dose constraints for organs at risk

Rectum	D0.04ccm < 38 Gy, D20ccm < 25 Gy
Bladder	V26% < 65%
Bladder wall	D0.04ccm < 44 Gy
Sigma	D0.04ccm < 44 Gy, V30Gy < 1ccm
Small intestine	D0.04ccm < 35 Gy, V30Gy < 1ccm, D5ccm < 19.5 Gy
Hip joint	V40% < 5%, D10ccm < 30 Gy
Testicle	D20% < 2Gy
Penis root	V29.5Gy < 50%, D0.04ccm < 50 Gy

Dxxccm or Dxx% = an absolute dose value covering exactly XX ccm or XX % of the given organ at risk; VxxGy or Vxx% = volume of a given OAR receiving XX Gy or XX % of the prescribed dose

administered every other day. The dose constraints for the organs at risk are detailed in Table 1.

The treatment plans were prepared using the Accuray Precision 1.1.1.1 planning system. The dose was prescribed to the 80–85% isodose curve. Dose-coverage requirement for target volumes (PTVpros, PTVpsv) was V100% > 95%. Irradiation from non-coplanar fields was performed using a multileaf collimator with a CyberKnife M6 (Accuray, Sunyvale, CA) robotic accelerator. Based on planning CT digitally reconstructed X-ray images (DRRs) from 45 and 315 degrees were generated and served as reference images for patient alignment. At the start of the treatment, x-rays of the same directions were taken showing the position of gold markers in the prostate. Subsequently, the images were matched by a software and the inaccuracy of the alignment was determined based on the position of the markers in three directions (lateral, longitudinal, vertical) and rotation (roll, pitch, rotation). If the inaccuracy of the set-up was greater

than 10 mm or 3 degrees, we automatically corrected the deviation by moving the treatment couch. In case of a smaller set-up inaccuracy, the corrections were applied by the robotic arm during operation. This verification course was repeated every 20–60 seconds during the treatments, depending on the intra-fractional prostate movements. Patients were followed-up during radiation treatment, after the second and last fractions, then every 3 months. In the present study, maximal acute toxicity data were reported up to the last day of radiotherapy and 3 months after treatment. Acute genitourinary (GU) and gastrointestinal (GI) side effects were classified according to the Radiation Therapy Oncology Group (RTOG) scoring system (Table 2).²⁰ In Statistica software (StatSoft, Inc., USA) Spearman rank order tests were used to evaluate the correlations between risk groups, total dose (37.5 Gy vs. 40 Gy), age of patients, hormonal therapy, volume of CTVpros, PTVpros, CTVpsv, PTVpsv, dosimetric parameters of rectum (D0.04ccm, D20ccm), bladder (V26Gy, D0.04ccm), pre-treatment transurethral resection of prostate (TURP) and acute GI, GU side effects. Statistical significance was set at $p < 0.05$.

Results

Between February 2018 and August 2019, 205 patients with prostate cancer were treated definitively with SBRT. Median follow-up was 8 months. The mean age of the patients was 71 years (range: 58–78 years). The patient, tumor and treatment characteristics are summarized in Table 3. No peri- and postoperative complications were observed after implantation of the gold markers. 179 patients (87.3%) received a total dose of 40 Gy (8 Gy/

TABLE 2. Radiation Therapy Oncology Group acute radiation morbidity scoring scheme²⁰

Organ tissue	Grade 0	Grade 1	Grade 2	Grade 3	Grade 4
Gastrointestinal including pelvis	No change	Increased frequency or change in quality of bowel habits not requiring medication/rectal discomfort not requiring analgesics	Diarrhea requiring parasymphatholytic drugs/mucous discharge not necessitating sanitary pads/rectal or abdominal pain requiring analgesics	Diarrhea requiring parenteral support/severe mucous or blood discharge necessitating sanitary pads/abdominal distention (flat plate radiograph demonstrates distended bowel loops)	Acute or subacute obstruction, fistula or perforation; GI bleeding requiring transfusion; abdominal pain or tenesmus requiring tube decompression or bowel diversion
Genitourinary	No change	Frequency of urination or nocturia twice pretreatment habit/dysuria, urgency not requiring medication	Frequency of urination or nocturia that is less frequent than every hour. Dysuria, urgency, bladder spasm requiring local anesthetic	Frequency with urgency and nocturia hourly or more frequently/dysuria, pelvis pain or bladder spasm requiring regular, frequent narcotic/gross hematuria with/ without clot passage	Hematuria requiring transfusion/acute bladder obstruction not secondary to clot passage, ulceration, or necrosis

fraction[fx]) and 26 patients (12.7%) 37.5 Gy (7.5 Gy/fx). Dose volumes parameters of the rectum and bladder, volumes and dose coverage of the prostate and seminal vesicles clinical- and planning target volumes (CTVpros, CTVpsv, PTVpros, PTVpsv) of patients are summarized in Tables 4 and 5. The duration of radiation treatment was 1 week and 3 days (3 fractions per week). The delivery of a fraction took 25–45 minutes, depending on the complexity of the treatment plan and the frequency of verification X-rays. The frequency of control imaging was related to intra-fractional prostate movements. During control imaging, all the implanted gold markers were clearly visible with a sufficient distance from each other. No marker migration was detected.

In our patients, acute grade 3 side effects were rare, most of acute toxicity resolved spontaneously or with the administration of medications. 202 patients (98.5%) completed radiation therapy at the planned dose and did not require a therapeutic interruption due to radiotherapy-related adverse events. Three patients (1.5%) had to have an urethral catheter inserted due to a complete retention of urine. One of them underwent transurethral resection of prostate (TURP) two months after treatment. After that the radiation therapy was completed with conventional fractionation. The second one refused to complete the radiation treatment, he is currently receiving hormone therapy. The third patient had a urethral catheter only for one week, after that urinary complaints resolved by using α -blockers and the treatment was completed with the planned dose. Acute grade 2 and 3 GU toxicity was reported in 104 (50.7%) and 3 (1.5%) cases, respectively. Acute grade 2 and 3 GI adverse events occurred in 12 (5.9%) and 0 (0%) patients, respectively. None of the patients developed \geq grade 4 acute side effect. At 3 months after the treatment the incidence of grade 2 and 3 GI toxicity was 0.5% (n = 1) and 0% (n = 0), while grade 2 and 3 GU side effects occurred in 9.7% (n = 20) and 1% (n = 2) of the patients, respectively. Frequency of radiotherapy-related toxicities according to the RTOG grading system during radiation therapy and 3 months after treatment are detailed in Table 6. Acute side effects at the end of radiotherapy according to the risk groups are shown in Table 7.

No statistical correlation was detected between risk groups, age of patients, hormone therapy, pre-treatment TURP and acute GI, GU side effects.

Significant correlation was observed between acute \leq 2 GU toxicities and pre-treatment TURP, delivered dose, volumes of CTVpros, CTVpsv,

TABLE 3. Patient, tumour and treatment characteristics

Characteristic	Number (%)
Age (years)	
Median	73
Range	54–85
T stage	
T1	45 (22%)
T2a	35 (17.1%)
T2b	52 (25.3%)
T2c	58 (28.3%)
T3a	7 (3.4%)
T3b	8 (3.9%)
Gleason score	
\leq 6	60 (29.3%)
7	108 (52.7%)
\geq 8	37 (17%)
Initial PSA¹	
Median	15
Range	2–137
< 10	108 (52.7%)
10–20	67 (32.7%)
\geq 20	30 (14.6%)
Risk groups	
Low	23 (11.2%)
Intermediate	120 (58.6%)
High	62 (30.2%)
Hormonal therapy	
No	88 (42.9%)
Short (\leq 6 months)	61 (29.8%)
Long (> 6 months)	56 (27.3%)
TURP² before SBRT³	22 (10.7%)
Total dose	
37.5 Gy ⁴	26 (12.7%)
40 Gy	179 (87.3%)

¹PSA = prostate specific antigen, ²TURP = transurethral resection of the prostate; ³SBRT = stereotactic body radiation therapy, ⁴Gy = Gray

TABLE 4. Dose-volume parameters of rectum and bladder with constraints

Organs at risks	Dose constrain	Mean	Median (range)
Rectum			
D 0.04cm ³ (Gy)	38	37.6	37.8 (32.3–41.5)
D 20cm ³ (Gy)	26	18.8	19.2 (8.0–27.6)
Bladder wall			
D 0.04cm ³ (Gy)	44	40.4	40.4 (30.7–48.6)
D 15cm ³ (Gy)	18.3	29.1	18.9 (6.9–29.1)
Bladder			
V 26Gy (%)	65	9.1	7.3 (0.9–41.9)

Dxxcm³ or Dxx% = an absolute dose value covering exactly XX cm³ or XX % of the given organ at risk; VxxGy or Vxx% = volume of a given OAR receiving XX Gy or XX % of the prescribed dose

TABLE 5. Median volumes and dose coverages of prostate and seminal vesicles clinical- and planning target volumes (CTVpros, CTVpsv, PTVpros, PTVpsv) of 205 prostate cancer patients treated with stereotactic radiation therapy

	CTVpros	PTVpros	CTVpsv	PTVpsv
Volume, cm ³ (range)	52.1 (15.9–134.7)	70.6 (25.1–166.6)	80.4 (30.8–208.5)	108.1 (45.4–259.3)
Dose coverage % (range)	99.1 (94.7–100)	95.8 (88.8–99.9)	100 (97.6–100)	99.5 (95.2–100)

TABLE 6. Acute toxicities after prostate and seminal vesicles intensity-modulated, stereotactic irradiation with SIB technique (N = 205)

Toxicity	Grade	Toxicity at the end of treatment N = 205 (%)	Toxicity 3 months after treatment N = 205 (%)
Gastrointestinal	0	128 (62.4)	195 (95)
	1	65 (31.7)	9 (4.5)
	2	12 (5.9)	1 (0.5)
	3	0 (0)	0 (0)
Genitourinary	0	35 (17.1)	153 (74.6)
	1	63 (30.7)	30 (14.7)
	2	104 (50.7)	20 (9.7)
	3	3 (1.5)	2 (1)

TABLE 7. Acute side effects at the end of radiation therapy according to the risk groups

Toxicity	Grade	Low risk N = 23 (%)	Intermediate risk N = 120 (%)	High risk N = 62 (%)
Gastrointestinal	0	8 (35)	83 (69)	37 (60)
	1	14 (61)	29 (24)	22 (35)
	2	1 (4)	8 (7)	3 (5)
	3	0 (0)	0 (0)	0 (0)
Genitourinary	0	1 (4)	26 (74.6)	8 (13)
	1	10 (43)	25 (14.7)	28 (45)
	2	12 (54)	66 (9.7)	26 (42)
	3	0 (0)	3 (2)	0 (0)

PTVpros, PTVpsv, bladder V26Gy, D0.04ccm ($p < 0.05$). No other parameters had a significant correlation with toxicity.

Discussion

Organ confined prostate cancer is usually treated with EBRT. Data from phase III, randomized studies support MH to be non-inferior to CF. Recently a great interest is shown in SBRT. According to

surveys, the biggest disadvantage of CF is the long treatment time.²¹ Due to the low fraction number, on our opinion SBRT may have the potential to increase patient satisfaction with treatment. This is supported by the fact that it is a non-invasive treatment option.²² Compared with conventional EBRT stereotactic irradiation treatment of prostate cancer seems to be the most cost-effective management option.²³ Also taking into account the radiobiological benefit of hypofractionation, the acceptance of extreme hypofractionation with SBRT is increasing in medical communities.

Recently, Brand *et al.*²⁴ first reported acute toxicity from a randomized, non-inferiority, phase III study (PACE-B). A total of 847 low- and intermediate risk patients were randomly assigned to CF/MH (78 Gy in 39 fractions/62 Gy in 20 fractions) or SBRT (36.25 Gy in 5 fractions). The frequency of acute grade 1, 2, 3 and 4 GU toxicity in the CF/MH arm versus the SBRT arm was 59%, 26%, 1% and < 1%, versus 57%, 21%, 2% and < 1%, respectively. Acute grade 1,2,3 and 4 GI side effects occurred in CF/MH arm in 61%, 11%, 1% and 0% versus in the SBRT arm in 53%, 10%, <1% and 0%, respectively. These results suggest that shortened treatment time (SBRT) does not increase neither acute GI nor GU toxicity.

Immediately after that, the second phase III, non-inferiority, randomized trial (HYPO-RT-PC) was published comparing CF radiotherapy with SBRT in intermediate- and high-risk prostate cancer patients.²⁵ In contrast with PACE-B trial in HYPO-RT-PC patients were treated mostly with 3D conformal technique. In the SBRT arm acute grade 1–2 and 3 GU toxicity was recorded in 48% and 5% of the patients. Acute grade 1–2 and 3 GI side effects occurrence was 51% and 1%. Acute GU toxicity was significantly worse in the SBRT arm, but no significant difference was recorded in acute GI or late GU/GI toxicities and failure free survival (84% vs. 84%) at 5-year median follow up, conforming the non-inferiority of SBRT to CF radiotherapy.

In the last 10–15 years several prospective and retrospective studies reported low rates of severe

TABLE 8. Summary of acute genitourinary (GU) and gastrointestinal (GI) toxicities published in trials using SBRT for prostate cancer treatment

Study	No. of patients	Dose	Grade 1–2 GU (%)	Grade ≥ 3 GU (%)	Grade 1–2 GI (%)	Grade ≥ 3 GI (%)
Madsen, 2007 ²⁶	40	6.7 Gy x 5 fx	49	2.5	39	0
Katz, 2010 ²⁷	304	7/7.25 Gy x 5 fx	79	0	78	0
Boike, 2011 ²⁸	45	9.5/10 Gy x 5 fx	51	0	55	0
Freeman, 2011 ²⁹	41	7/7.25 Gy x 5 fx	32	2.5	16	0
Jabarri, 2012 ³⁰	38	9.5 Gy x 4/2 fx	71	0	32	0
McBride, 2012 ³¹	45	7.5/7.25 Gy x 5 fx	74	0	38	0
Loblaw, 2013 ¹⁵	84	7 Gy x 5 fx	88	1	77	0
Bolzicco, 2013 ³²	100	7 Gy x 5 fx	46	0	45	0
Oliai, 2013 ³³	70	7–7.4 Gy x 5 fx	63	4	26	3
Mantz, 2014 ³⁴	102	8 Gy x 5 fx	58	2	0	0
Chen, 2014 ³⁵	100	7/7.25 Gy x 5 fx	71	0	21	0
Anwar, 2016 ³⁶	50	9.5 Gy x 2 fx and 10.5 Gy x 2 fx boost	85	0	52	0
Hannan, 2016 ³⁷	91	9–10 Gy x 5 fx	70	0	58	2
Brand, 2019 ¹²⁴	415	7.25 Gy x 5 fx	78	3	63	1
¹ Widmark, 2019 ²⁵	589	6.1 Gy x 7 fx	48	5	51	1
Present study	205	7.5/8 Gy x 5 fx	81	1.5	38	0
All studies	2319	Total dose: 33.5–50 Gy Number of fxs: 5–7	32–88	0–5	0–78	0–3

¹ = phase III, randomized trial; fx = fraction

acute toxicity with the use of SBRT for extreme hypofractionation applying commonly a total of 5 fractions with 7–8 Gy fraction doses.^{15,26–37} The frequency of acute ≥ grade 3 GU and GI side effects was 0–5% and 0–3%, respectively (Table 8).

In our phase II prospective study, we reported acute toxicity after extremely hypofractionated, intensity-modulated radiotherapy with SBRT technique for prostate cancer patients. Patients with low- (n = 23), intermediate- (n = 120) and high-risk (n = 62) prostate cancer patients were treated with SBRT, in every second working day and 7.5–8 Gy to the prostate and 6–6.5 Gy to the seminal vesicles was delivered with SIB technique, in a total of 5 fractions (total dose 37.5–40 Gy). Of the 205 patients treated, grade 1–2 GU and GI side effects occurred in 81% and 38%. Three months after treatment, these side effects were present only in 24% and 5%, respectively. The frequency of grade 3 GU toxicity was 1.5%. In the case of extreme hypofractionation, due to pelvic anatomy and radiation sensitivity, the most critical organ at risk is the rectum. In our study, no grade 3 GI acute side effect was observed, and at 3 months after irradiation 95% of patients had no gastrointestinal complaints (GI

Gr.0). Our results regarding acute toxicity are similar to those of reported in the literature using similar total doses and fractionation schemes (Table 8).

Because of the lack of prospective data and paucity of the literature, the effect of pre-treatment TURP on side effects after SBRT currently needs to be investigated. One of the most important data on this issue was reported by Murthy *et al.*³⁸ Fifty prostate cancer patients with pre-treatment TURP were propensity score matched to a similar non-TURP cohort. No significant difference was recorded regarding acute ≥ grade 2 GU side effects (8% vs. 6%, P = 0.45). Wang *et al.*³⁹ concluded that a pre-treatment TURP increases the incidence of urinary incontinence and worsens urinary quality of life. In our patient cohort 22 patients (10.7%) underwent prior TURP. There was no difference between TURP and non-TURP patients with respect to acute GU toxicity. However, the impact of prior TURP on GU toxicity after SBRT is still controversial.

Based on our statistical analyses, a significant correlation was shown between the volume of the prostate gland (CTVpros), CTVpsv, PTVpros, PTVpsv and acute GU toxicities. These findings draw our attention to the fact that a large volume

of prostate or a large safety margin can affect GU side effects. According several studies, patients with a large prostate volume before SBRT experienced worse GU side effects.⁴⁰⁻⁴² Katz *et al.*⁴¹ reported in 336 patients that the rate of late grade 2 and 3 GU toxicity was 15% versus 8% in patients with prostate volume greater than versus less than 60 cm³, respectively.

Three large randomized trials are ongoing to establish SBRT as the preferred standard option for localized disease. The NRG GU-005 trial (NCT03367702) compares SBRT (36.25 Gy in 5 fractions) with moderately hypofractionated radiation therapy (70 Gy in 28 fractions) and is designed to confirm the superiority of SBRT. The PACE series trials (A–C) aim to assess whether SBRT (36.25 Gy in 5 fractions) offers a therapeutic benefit over prostatectomy or conventional radiation therapy (78 Gy in 39 fractions) for patients with localized disease (NCT01584258). The MIRAGE trial is randomized phase III trial comparing MRI-guided SBRT (40 Gy in five fractions) with CT-guided SBRT for organ-confined prostate cancer. The purpose of this study is to demonstrate the benefit of using MRI-guided SBRT in terms of acute grade ≥ 2 GU side effects when compared to CT-guided SBRT (NCT04384770).

One limitation of our single arm phase II prospective study is that SBRT was not compared with CF or MH in a randomized manner. Another factor slightly reducing the value of this study is that the side effects were graded by the physician, which increases the subjectivity of the assessment and may differ in the proportion and severity of the patient-reported toxicities. Further follow-up is needed to validate late side effects and tumor control.

At our institute, treatment with CF (2 Gy/day) or MH (2.5 Gy/day) takes 39 or 28 working days. During SBRT, radiation treatment can be delivered in less than 2 weeks, thus reducing the total radiation treatment time by up to 6 weeks. Routine application of SBRT can reduce waiting time and total treatment time. Shorter treatment times are also beneficial for patients.

Conclusions

The treatment of clinically localized prostate cancer patients using SBRT with 7.5–8 Gy fractions delivered every other working day, with a total dose of 37.5–40 Gy, appears to be a safe treatment and can be introduced into daily routine. Acute GI and GU side effects were moderate, with rare grade 3

GU side effects and no acute grade 3–4 GI side effects. In the majority of cases, toxicities resolved spontaneously by 3 months after treatment. The total treatment time with SBRT is more than 6 weeks shorter compared to EBRT with conventional fractionation.

References

1. Bray F, Ferlay J, Soerjomataram I, Siegel RL, Torre LA, Jemal A. Global cancer statistics 2018: GLOBOCAN estimates of incidence and mortality worldwide for 36 cancers in 185 countries. *Cancer J Clin* 2018; **68**: 394-24. doi: 10.3322/caac.21492
2. Ferlay J, Colombet M, Soerjomataram I, Dyba T, Randi G, Bettio M, et al. Cancer incidence and mortality patterns in Europe: estimates for 40 countries and 25 major cancers in 2018. *Eur J Cancer* 2018; **103**: 356-87. doi: 10.1016/j.ejca.2018.07.005
3. Attard G, Parker C, Eeles R, Schröder F, Tomlins S, Tannock I, et al. Prostate cancer. *Lancet* 2016; **387**: 70-82. doi: 10.1016/S0140-6736(14)61947-4
4. Torre LA, Siegel RL, Ward EM, Jemal A. Global cancer incidence and mortality rates and trends – an update. *Cancer Epidemiol Biomarkers Prev* 2016; **25**: 16-27. doi: 10.1158/1055-9965
5. Heidenreich A, Bastian PJ, Bellmunt J, Bolla M, Joniau S, van der Kwast T, et al. EAU guidelines on prostate cancer. Part 1: screening, diagnosis, and local treatment with curative intent-update 2013. *Eur Urol* 2014; **65**: 124-37. doi: 10.1016/j.eururo.2013.09.046
6. Donovan JL, Hamdy FC, Lane JA, Mason M, Metcalfe C, Walsh E, et al. Patient-reported outcomes after monitoring, surgery, or radiotherapy for prostate cancer. *N Engl J Med* 2016; **375**: 1425-37. doi: 10.1056/NEJMoa1606221
7. Hamdy FC, Donovan JL, Lane JA. 10-year outcomes after monitoring, surgery, or radiotherapy for localized prostate cancer. *N Engl J Med* 2016; **375**: 1415-24. doi: 10.1056/NEJMoa1606220
8. Brenner DJ, Hall EJ. Fractionation and protraction for radiotherapy of prostate carcinoma. *Int J Radiat Oncol Biol Phys* 1999; **43**: 1095-101. doi: 10.1016/S0360-3016(98)00438-6
9. Arcangeli S, Greco C. Hypofractionated radiotherapy for organ-confined prostate cancer: is less more? *Nat Rev Urol* 2016; **13**: 400-8. doi: 10.1038/nrurol.2016.106
10. Zaorsky NG, Studenski MT, Dicker AP, Gomella L, Den R. Stereotactic body radiation therapy for prostate cancer: is the technology ready to be the standard of care? *Cancer Treat Rev* 2013; **39**: 212-8. doi: 10.1016/j.ctrv.2012.10.003
11. Dearnaley D, Syndikus I, Mossop H, Bidmead M, Bloomfield D, Clark C, et al. Conventional versus hypofractionated high-dose intensity-modulated radiotherapy for prostate cancer: 5-year outcomes of the randomised, non-inferiority, phase 3 CHHiP trial. *Lancet Oncol* 2016; **17**: 1047-60. doi: 10.1016/S1470-2045(16)30102-4
12. Catton CN, Lukka H, Gu CS, Martin J, Supiot S, Chung P, et al. Randomized trial of a hypofractionated radiation regimen for the treatment of localized prostate cancer. *J Clin Oncol* 2017; **35**: 1884-90. doi: 10.1200/JCO.2016.71.7397
13. Lee WR, Dignam JJ, Amin MB, Bruner D, Low D, Swanson G, et al. Randomized phase III noninferiority study comparing two radiotherapy fractionation schedules in patients with low-risk prostate cancer. *J Clin Oncol* 2016; **34**: 2325-32. doi: 10.1200/JCO.2016.67.0448
14. Aluwini S, van Rooij P, Hoogeman M, Kirkels W, Kolkman-Deurloo I, Bangma C. Stereotactic body radiotherapy with a focal boost to the MRI-visible tumor as monotherapy for low- and intermediate-risk prostate cancer: early results. *Radiat Oncol Lond Engl* 2013; **8**: 84. doi: 10.1186/1748-717X-8-84
15. Loblaw A, Cheung P, D'Alimonte L, Deabreu A, Mamedov A, Zhang L, et al. Prostate stereotactic ablative body radiotherapy using a standard linear accelerator: toxicity, biochemical, and pathological outcomes. *Radiother Oncol J Eur Soc Ther Radiol Oncol* 2013; **107**: 153-8. doi: 10.1016/j.radonc.2013.03.022

16. King CR, Brooks JD, Gill H, Presti Jr J. Long-term outcomes from a prospective trial of stereotactic body radiotherapy for low-risk prostate cancer. *Int J Radiat Oncol Biol Phys* 2012; **82**: 877-82. doi: 10.1016/j.ijrobp.2010.11.054
17. Jorgo K, Ágoston P, Szabó Z, Major T, Polgár Cs. [Use of gold radionuclide markers implanted into the prostate for image-guided radiotherapy in prostate cancer: side effects caused by the marker implantation]. [Hungarian]. *Magy Onkol* 2014; **58**: 182-87.
18. Jorgo K, Agoston P, Major T, Takácsi-Nagy Z, Polgár Cs. Transperineal gold marker implantation for image-guided external beam radiotherapy of prostate cancer. A single institution, prospective study. *Strahlenther Onkol* 2017; **193**: 452-58. doi: 10.1007/s00066-017-1104-2.
19. D'Amico AV, Moul J, Carroll PR, Sun L, Lubeck D, Chen M. Cancer-specific mortality after surgery or radiation for patients with clinically localized prostate cancer managed during the prostate-specific antigen era. *J Clin Oncol* 2003; **21**: 2163-72. doi: 10.1200/JCO.2003.01.075
20. Cox JD, Stetz J, Pajak TF. Toxicity criteria of the Radiation Therapy Oncology Group (RTOG) and the European Organization for Research and Treatment of Cancer (EORTC). *Int J Radiat Oncol Biol Phys* 1995; **30**: 1341-46. doi: 10.1016/0360-3016(95)00060-C
21. Holmboe ES, Concato J. Treatment decisions for localized prostate cancer: asking men what's important. *J Gen Intern Med* 2000; **15**: 694-701. doi: 10.1046/j.1525-1497.2000.90842.x
22. Dandapani SV, Sanda MG. Measuring health-related quality of life consequences from primary treatment for early-stage prostate cancer. *Semin Radiat Oncol* 2008; **18**: 67-72. doi: 10.1016/j.semradonc.2007.10.001
23. Hodges JC, Lotan Y, Boike TP, Benton R, Barrier A, Timmerman R. Cost-effectiveness analysis of SBRT versus IMRT: an emerging initial radiation treatment option for organ-confined prostate cancer. *Am J Manag Care* 2012; **18**: e186-93. doi: 10.1200/JOP.2012.000548
24. Brand DH, Tree AC, Ostler P, van der Voet H, Loblaw A, Chu W, et al. Intensity-modulated fractionated radiotherapy versus stereotactic body radiotherapy for prostate cancer (PACE-B): acute toxicity findings from an international, randomised, open-label, phase 3, non-inferiority trial. *Lancet Oncol* 2019; **20**: 1531-43. doi: 10.1016/S1470-2045(19)30569-8
25. Widmark A, Gunnlaugsson A, Beckman L, Thellenberg-Karlsson C, Hoyer M, Lagerlund M, et al. Ultra-hypofractionated versus conventionally fractionated radiotherapy for prostate cancer: 5-year outcomes of the HYPO-RT-PC randomised, non-inferiority, phase 3 trial. *Lancet* 2019; **394**: 385-95. doi: 10.1016/S0140-6736(19)31131-6
26. Madsen BL, Hsi RA, Pham HT, Fowler J, Esagui L, Corman J. Stereotactic hypofractionated accurate radiotherapy of the prostate (SHARP), 33.5Gy in five fractions for localized disease: first clinical trial results. *Int J Radiat Oncol Biol Phys* 2007; **67**: 1099-105. doi: 10.1016/j.ijrobp.2006.10.050
27. Katz AJ, Santoro M, Ashley R, Diblasio F, Witten M, et al. Stereotactic body radiotherapy for organ-confined prostate cancer. *BMC Urol* 2010; **10**: 1. doi: 10.1186/1471-2490-10-1
28. Boike TP, Lotan Y, Cho LC, Brindle J, DeRose P, Xie X, et al. Phase I dose-escalation study of stereotactic body radiation therapy for low- and intermediate-risk prostate cancer. *J Clin Oncol* 2011; **29**: 2020-26. doi: 10.1200/JCO.2010.31.4377
29. Freeman DE, King CR. Stereotactic body radiotherapy for low-risk prostate cancer: five-year outcomes. *Radiat Oncol* 2011; **6**: 3. doi: 10.1186/1748-717X-6-3
30. Jabbari S, Weinberg VK, Kaprelian T, Hsu I, Ma L, Chuang C, et al. Stereotactic body radiotherapy as monotherapy or post-external beam radiotherapy boost for prostate cancer: technique, early toxicity, and PSA response. *Int J Radiat Oncol Biol Phys* 2012; **82**: 228-34. doi: 10.1016/j.ijrobp.2010.10.026
31. McBride SM, Wong DS, Dombrowski JJ, Harkins B, Tapella P, Hanscom H, et al. Hypofractionated stereotactic body radiotherapy in low-risk prostate adenocarcinoma: preliminary results of a multi-institutional phase 1 feasibility trial. *Cancer* 2012; **118**: 3681-90. doi: 10.1002/cncr.26699
32. Bolzicco G, Favretto MS, Satariano N, Scremin E, Tambone C, Tasca A. A single-center study of 100 consecutive patients with localized prostate cancer treated with stereotactic body radiotherapy. *BMC Urol* 2013; **13**: 49. doi: 10.1186/1471-2490-13-49
33. Oliai C, Lanciano R, Sprandio B, Yang J, Lamond J, Arrigo S, et al. Stereotactic body radiation therapy for the primary treatment of localized prostate cancer. *J Radiat Oncol* 2013; **2**: 63-70. doi: 10.1007/s13566-012-0067-2
34. Mantz C. A Phase II trial of stereotactic ablative body radiotherapy for low-risk prostate cancer using a non-robotic linear accelerator and real-time target tracking: Report of toxicity, quality of life, and disease control outcomes with 5-year minimum follow-up. *Front Oncol* 2014; **4**: 279. doi: 10.3389/fonc.2014.00279
35. Chen LN, Suy S, Wang H, Bhagat A, Woo J, Moures R, et al. Patient-reported urinary incontinence following stereotactic body radiotherapy (SBRT) for clinically localized prostate cancer. *Radiat Oncol* 2014; **9**: 148. doi: 10.1186/1748-717X-9-148
36. Anwar M, Weinberg V, Seymour Z, Hsu J, Roach M 3rd, Gottschalk A. Outcomes of hypofractionated stereotactic body radiotherapy boost for intermediate and high-risk prostate cancer. *Radiat Oncol* 2016; **11**: 8. doi: 10.1186/s13014-016-0585-y
37. Hannan R, Tumati V, Xie XJ, Cho LC, Kavanagh B, Brindle J, et al. Stereotactic body radiation therapy for low and intermediate risk prostate cancer-Results from a multi-institutional clinical trial. *Eur J Cancer* 2016; **59**: 142-51. doi: 10.1016/j.ejca.2016.02.014
38. Murthy V, Sinha S, Kannan S, Datta D, Das R, Bakshi G, et al. Safety of prostate stereotactic body radiation therapy after Transurethral Resection of Prostate (TURP): A propensity score matched pair analysis. *Pract Radiat Oncol* 2019; **5**: 347-53. doi: 10.1016/j.prrro.2019.04.003
39. Wang K, Chen RC, Kane B, Medbery C, Underhill K, Gray J, et al. Patient and dosimetric predictors of genitourinary and bowel quality of life after prostate SBRT: Secondary analysis of a multi-institutional trial. *Int J Radiat Oncol Biol Phys* 2018; **102**: 1430-37. doi: 10.1016/j.ijrobp.2018.07.191
40. Bolzicco G, Favretto MS, Satariano N, Scremin E, Tambone C, Tasca A. A single-center study of 100 consecutive patients with localized prostate cancer treated with stereotactic body radiotherapy. *BMC Urol* 2013; **13**: 49. doi: 10.1186/1471-2490-13-49
41. Katz AJ, Kang J. Quality of life and toxicity after SBRT for organ-confined prostate cancer, a 7-year study. *Front Oncol* 2014; **4**: 301. doi: 10.3389/fonc.2014.00301
42. Gurka MK, Chen LN, Bhagat A, Moures R, Kim SJ, Yung T, et al. Hematuria following stereotactic body radiation therapy (SBRT) for clinically localized prostate cancer. *Radiat Oncol* 2015; **10**: 44. doi: 10.1186/s13014-015-0351-6

Clinical outcomes in stage III non-small cell lung cancer patients treated with durvalumab after sequential or concurrent platinum-based chemoradiotherapy - single institute experience

Martina Vrankar^{1,2}, Karmen Stanic^{1,2}, Stasa Jelercic¹, Eva Ciric¹, Ana Lina Vodusek¹, Jasna But-Hadzic^{1,2}

¹ Institute of Oncology Ljubljana, Department of Radiotherapy, Ljubljana, Slovenia

² University of Ljubljana, Faculty of Medicine, Ljubljana, Slovenia

Radiol Oncol 2021; 55(4): 482-490.

Received 19 August 2021

Accepted 7 October 2021

Correspondence to: Jasna But-Hadzic, M.D., Ph.D., Institute of Oncology Ljubljana, Zaloska 2, SI-1000 Ljubljana, Slovenia.
E-mail: jbut@onko-i.si;

Disclosure: No potential conflicts of interest were disclosed.

This is an open access article under the CC BY-NC-ND license (<http://creativecommons.org/licenses/by-nc-nd/4.0/>).

Background. Chemoradiotherapy (ChT-RT) followed by 12-month durvalumab is the new standard treatment for unresectable stage III non-small cell lung cancer. Survival data for patients from everyday routine clinical practice is scarce, as well as potential impact on treatment efficacy of sequential or concomitant chemotherapy and the usage of gemcitabine.

Patients and methods. We retrospectively analysed unresectable stage III NSCLC patients who were treated with durvalumab after radical concurrent or sequential chemotherapy (ChT) from December 2017 and completed treatment until December 2020. We assessed progression free survival (PFS), overall survival (OS) and toxicity regarding baseline characteristic of patients.

Results. Eighty-five patients with median age of 63 years of which 70.6% were male, 56.5% in stage IIIB and 58.8% with squamous cell carcinoma, were included in the analysis. Thirty-one patients received sequential ChT only, 51 patients received induction and concurrent ChT and 3 patients received concurrent ChT only. Seventy-nine patients (92.9%) received gemcitabine and cisplatin as induction chemotherapy and switched to etoposide and cisplatin during concurrent treatment with radiotherapy (RT). Patients started durvalumab after a median of 57 days (range 12–99 days) from the end of the RT and were treated with the median of 10.8 (range 0.5–12 months) months. Forty-one patients (48.2%) completed treatment with planned 12-month therapy, 25 patients (29.4%) completed treatment early due to the toxicity and 16 patients (18.8%) due to the disease progression. Median PFS was 22.0 months, 12- and estimated 24-month PFS were 71% (95% CI: 61.2–80.8%) and 45.8% (95% CI: 32.7–58.9%). With the median follow-up time of 23 months (range 2–35 months), median OS has not been reached. Twelve- and estimated 24-month OS were 86.7% (95% CI: 79.5–93.9%) and 68.6% (95% CI: 57.2–79.9%).

Conclusions. Our survival data are comparable with published research as well as with recently published real-world reports. Additionally, the regimen with gemcitabine and platinum-based chemotherapy as induction treatment was efficient and well tolerated.

Key words: non-small cell lung cancer; stage III; chemoradiotherapy; durvalumab

Introduction

In the last few years, standard treatment of unresectable stage III non-small cell lung cancer (NSCLC) changed considerably after the publication of improved survival results with maintenance 12-month treatment with Programmed Death Ligand 1 (PD-L1) antibody durvalumab following standard concurrent chemoradiotherapy (ChT-RT).^{1,3} In the PACIFIC trial, the median progression-free survival (PFS) from randomization was 17.2 months in durvalumab arm versus 5.6 months in placebo arm, while median overall survival (OS) was 47.5 months *vs.* 29.1 months, respectively. Reported 48-month OS rates were 49.6% for durvalumab *vs.* 36.3% for placebo.⁴ However, survival data for stage III NSCLC patients treated with durvalumab after ChT-RT in every day routine clinical practice is scarce, as well as the survival data of patients treated with sequential ChT-RT followed by durvalumab. Patients with unresectable stage III NSCLC are highly heterogeneous regarding age, performance status (PS) and comorbidity and high proportion of them are not fit for concurrent ChT-RT.^{5,6} Here we present single centre survival and safety results for the treatment of unresectable stage III NSCLC patients with sequential or concurrent ChT-RT and maintenance durvalumab.

Patients and methods

Patients and treatment

We retrospectively analysed unresectable stage III NSCLC patients (according to the 8th TNM classification) who were considered for maintenance treatment with durvalumab (intention to treat population, ITT) after radical ChT-RT and completed treatment until December 2020.⁷ First 61 patients were included in early access program (EAP) which started in December 2017 and ended in September 2019 when reimbursement was introduced. Afterwards patients were treated with durvalumab as a standard of care. During EAP, patients were treated with durvalumab after at least stable disease with ChT-RT was achieved regardless of PD-L1 expression level, but from September 2019, during standard of care treatment, only patients with PD-L1 $\geq 1\%$ received adjuvant durvalumab according to European Medicines Agency (EMA) registration.

Before treatment, patients underwent a physical examination, computed tomography (CT) of the chest, abdomen and head as well as the

¹⁸F-fluorodeoxyglucose positron emission tomography/computed tomography (¹⁸F-FDG PET/CT) and brain magnetic resonance imaging (MRI) when indicated. All patients had histologically or cytologically confirmed NSCLC from primary tumour or regional lymph nodes, N stage mostly confirmed with endobronchial ultrasound (EBUS). PD-L1 immunohistochemistry was evaluated with a rabbit monoclonal antibody SP263 as part of the Ventana PD-L1 SP263 assay (Ventana/Roche, USA) on an automated platform (Benchmark, Ventana/Roche, USA). According to our institutional clinical practice most patients started treatment with platinum based ChT combined with gemcitabine or pemetrexed and continued with platinum based ChT with the addition of etoposide or pemetrexed concurrently with RT. The prescribed radiation dose ranged from 54 Gray (Gy) to 66 Gy in 2 Gy daily fractions. Treatment was planned with Three-Dimensional Conformal Radiotherapy (3D-CRT) or Volumetric Modulated Arc Therapy (VMAT) with four-dimensional CT (4D CT) simulation in case of extensive target motion. Daily cone-beam CT was used for set-up correction. After completion of ChT-RT patients were evaluated with CT scan of the chest and abdomen, and when indicated, CT of the brain. Patients without progression and with resolved toxic effects of previous treatment started durvalumab within 3 months after ChT-RT for 12 months until progression or until unacceptable toxicity. Evaluation thoracic CT was done 6 and 12 months after durvalumab introduction and when clinically indicated.

Statistical analysis

Baseline characteristics of patients, including age, gender, pathological features, TNM stage, Eastern Cooperative Oncology Group performance status (ECOG PS), smoking status, PD-L1 expression, mutational status of EGFR, KRAS, ALK, ROS 1, BRAF and NTRK in adenocarcinoma, time to durvalumab start from the end of the RT, treatment completion, PFS and OS from the start of ChT-RT and the start of durvalumab were collected for the analysis. Response rate after ChT-RT was assessed using RECIST 1.1 and during immunotherapy iRECIST.⁸ Immune related adverse events were assessed by their highest reported grade using Common Terminology Criteria for Adverse Events (CTCAE) Version 5.0.⁹

PFS was calculated from the beginning of the durvalumab to disease progression or death and OS as the time from the start of the durvalumab to

TABLE 1. Baseline characteristics of patients treated with durvalumab

		N = 85
Gender	Female	25 (29.4 %)
	Male	60 (70.6 %)
Age	Median (range)	
	< 63	63 (36 – 73)
	≥ 63	
ECOG PS	0	37 (43.5 %)
	1	46 (54.1 %)
	2	2 (2.4 %)
Smoking history	Never	2 (2.4 %)
	Ex-smokers	35 (41.6 %)
	Smoking at diagnosis	47 (56.0 %)
Histology	Adenocarcinoma	31 (36.5 %)
	Squamous Cell	50 (58.8 %)
	Other	4 (4.7 %)
AJCC 8th Edition Stage	IIIA	26 (30.6%)
	IIIB	48 (56.5 %)
	IIIC	11 (12.9 %)
PD-L1 Expression	< 1%	13 (15.3 %)
	1%-49%	33 (38.8 %)
	> 50%	32 (37.7 %)
	Unavailable	7 (8.2 %)
Mutational status	No mutations	65 (76.5 %)
	KRAS	16 (18.8 %)
	Unavailable	4 (4.7 %)

Abbreviation: N-number, ECOG PS- Eastern Cooperative Oncology Group performance status, PD-L1-programmed dead-ligand 1

death from any cause. Data from the patients who had not progressed or had not died were censored at the date of last follow-up (February 3, 2021).

The association between the PFS, OS and the basic clinicopathological variables of patients were tested using the log-rank test. OS and PFS curves were estimated using Kaplan-Meier method. The Cox proportional hazards model was used to assess the association between PFS, OS and treatment characteristics. All tests were two tailed. A p-value less than 0.05 was considered statistically significant. All p values reported were based on the two-sided hypothesis. The statistical analyses were calculated using SPSS -21 (IBM Corporation, Armonk, NY, USA).

This study was conducted in accordance with the Declaration of Helsinki. The study was approved by Institutional Review Board Committee and Institutional Ethics Committee (ERIDNPVO-0004/2021).

Results

In total, 118 patients had been identified as candidates for maintenance treatment with durvalumab from December 2017 who completed treatment until December 2020. Of those, 85 (72.0%) patients continued treatment with maintenance durvalumab after ChT-RT and in 33 durvalumab was omitted due to persistent toxicity in 6, treatment refusal in 11 and progressive disease in 16 patients.

Baseline characteristics of 85 patients included in the analyses are detailed in Table 1. Most were male (70.6%) in stage IIIB (56.5%) with squamous cell carcinoma (58.8%), ECOG PS 1 (54.1%). Median age was 63 years (range 36-73 years). PD-L1 expression was positive in 65 (76.5%) patients, in 13 (15.3%) patients was negative and not available in 7 patients (8.2%). No EGFR, ALK, ROS 1, BRAF and TNFRK mutations were detected in 65 (76.5%) patients, KRAS mutation was present in 16 (18.8%) patients and for 4 patients mutational status was not available.

Treatment with chemoradiotherapy

Eighty-two (96.5%) patients started treatment with induction ChT and 54 (63.5%) patients received ChT during RT (Table 2). Thirty-one (36.5%) patients were treated with sequential ChT only. Patients received median 3 cycles (range 1–5) of ChT altogether. Seventy-nine patients (92.9%) received gemcitabine and cisplatin as induction ChT and 52 (61.2%) of those switched to etoposide and cisplatin during concurrent treatment with RT. Only 3 patients (3.5%) with adenocarcinoma were treated with pemetrexed and cisplatin as induction as well as concurrent regimen. Patients were treated with the median RT dose of 60 Gy (range 54 Gy–66 Gy), and in most of them (82.3%) partial response was observed after ChT-RT.

Treatment with durvalumab

Patients started first cycle of durvalumab after a median of 57 days (range 12–99 days) from the end of the RT and were treated with the median of 10.8 months (range 0.5–12 months) (Table 3). Forty-one

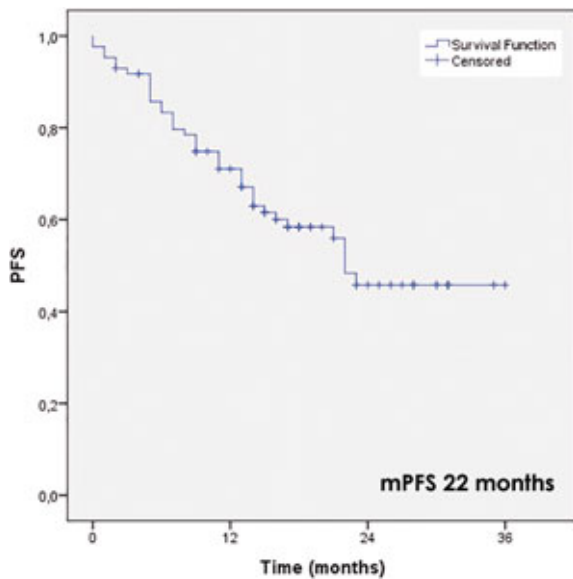


FIGURE 1. Progression free survival of patients treated with durvalumab after sequential or concurrent platinum-based chemoradiotherapy.

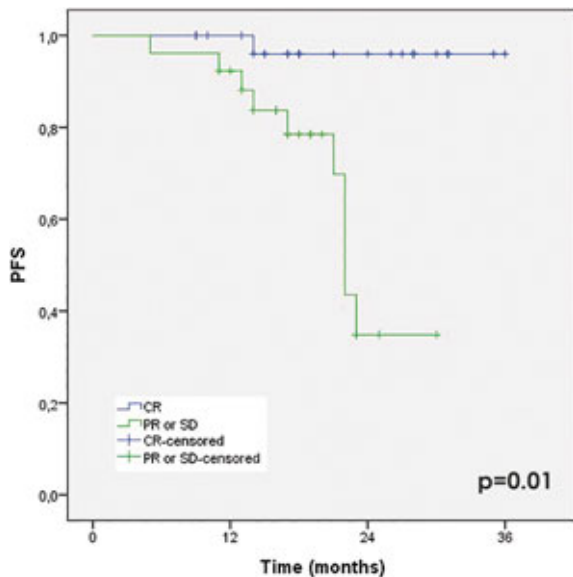


FIGURE 2. Progression free survival regarding response after durvalumab completion.

patients (48.2%) completed treatment with planned 12-month therapy, 25 patients (29.4%) completed treatment early due to the toxicity of durvalumab and 16 patients (18.8%) due to the disease progression. One patient died suddenly after two months of treatment without progression and no known cause of death. One patient stopped treatment after

TABLE 2. Chemoradiotherapy treatment characteristics

		N = 85 (%)
N of ChT	1	3 (3.5%)
	2	13 (15.3%)
	3	41 (48.2%)
	4	27 (31.8%)
	5	1 (1.2%)
ChT	Gem/cis	79 (92.9%)
	Etop/cis	52 (61.2%)
	Pem/cis	3 (3.5%)
ChT	Induction	82 (96.5%)
	Sequential only	31 (36.5%)
	Concurrent	54 (63.5%)
	Concurrent only	3 (3.5%)
RT dose (Gy)	Median (range)	60 (5–66)
V20 (Gy)	Median (range)	27.2 (7.0–35.6)
MLD (Gy)	Median (range)	15.7 (4.0–20.2)
PTV (cm ³)	Median (range)	416.6 (172.3–1282.6)
Evaluation after ChT-RT	CR	10 (11.8%)
	PR	70 (82.3%)
	SD	5 (5.9%)
Time between RT-IT (days)	Median (range)	57 (12–99)

ChT = chemotherapy, CR = complete response; etop/cis = etoposide/cisplatin; gem/cis = gemcitabine/cisplatin; IT = immunotherapy; MLD = mean lung dose; N = number of patients; PD = progressive disease; PR = partial response; PTV = planning target volume; RT = radiotherapy; pem/cis = pemetrexed/cisplatin; SD = stable disease; V20 = volume of the lung that receive radiation dose of 20 Gy

one month due to newly diagnosed prostate cancer and one due to cerebral infarction unrelated to durvalumab treatment.

Toxicity of durvalumab treatment

Twenty-five patients (29.4%) discontinued durvalumab early due to the toxicity after the median treatment time of 6.0 months (range 0.5–11 months). Twelve patients (14.1%) had pneumonitis that started significantly earlier after introduction of durvalumab than other AE (2.0 months *vs.* 7.2 months, $p = 0.012$). Other AE leading to discontinuation of durvalumab treatment included dermatological toxicity ($n = 5$), arthralgia ($n = 4$), colitis ($n = 2$) and uncontrolled hypothyroidism ($n = 2$). Most immune related AE leading to discontinuation of durvalumab were grade 1-2 (68%), 32% were grade 3. No grade 4 of 5 AE were observed.

TABLE 3. Durvalumab treatment characteristics and influence on overall survival

Treatment characteristics		N (%)	P
Time between RT-IT	Median (days)		
	< 57	57 (12-99)	0.689
Treatment time of IT*	Median (months)		
	< 10.8	10.8 (0.5-12.0)	< 0.001
Treatment with IT	Completed	41 (48.2%)	0.095
	Early stopped due to AE	25 (29.4%)	
	Progression	16 (18.8%)	
	Other	3 (3.6%)	
Response after IT**	CR	29 (34.1%)	0.213
	PR	11 (12.9%)	
	SD	15 (17.6%)	
	PD	10 (11.8%)	
Progression***	Loco-regional	21 (24.7%)	0.217
	Metastatic	10 (11.7%)	
	Metastatic and local	5 (5.9%)	
Metastatic spread	CNS	5 (5.9%)	0.101
	Other	10 (11.7%)	

*difference in overall survival between patients treated with immunotherapy less or more than median time;

** including evaluation up to 4 months after completed immunotherapy in patients with 12-month therapy as well as in early stopped due to adverse events, later progression is not included. Two patients were not evaluable;

*** observed progression until the last evaluation date;

AE = adverse events; CNS = central nerve system; CR = complete response; IT = immunotherapy; PD = progressive disease; PR = partial response; RT = radiotherapy; SD = stable disease

In total, 42 (49.6%) patients experienced 47 AE, 38 patients had 1 AE, three patients had 2 and one patient had 3 AE. Pneumonitis was found in 15 (17.6%), arthralgia in 5 (5.9%), skin toxicity in 13 (15.3%), colitis in 6 (7.1%) and hypothyroidism in 8 (9.4%) patients.

Treatment results

Median PFS from the durvalumab start was 22.0 months, estimated 12- and 24-month PFS were 71% (95% CI: 61.2-80.8%) and 45.8% (95% CI: 32.7-58.9%) (Figure 1). During durvalumab treatment, 16 patients progressed after the durvalumab treatment median time of 6.1 months (range 0.5-11.0 months), 7 with loco-regional and 9 with distant metastases. Altogether, 36 (42.4%) patients have progressed until the last follow-up date, 21 (24.7%) patients with loco-regional failure only and 15 (17.6%) patients with distant metastatic disease. Of those, 5 patients had also local progression.

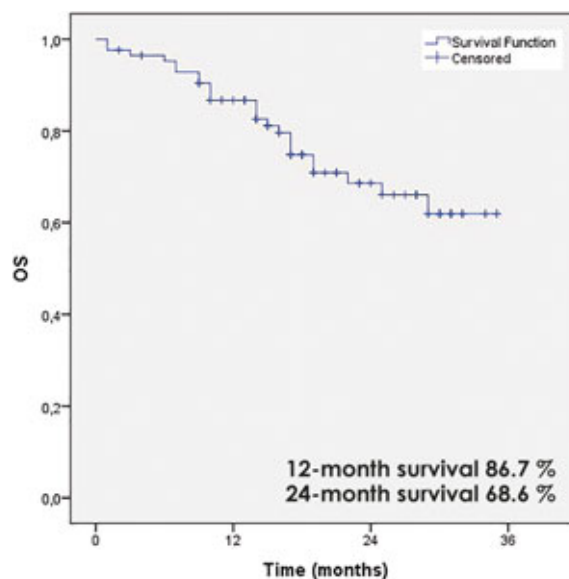


FIGURE 3. Overall survival of patients treated with durvalumab after sequential or concurrent platinum-based chemoradiotherapy.

Age, gender, ECOG PS, stage, histology, PD-L1 expression, mutational status, smoking status, RT dose, time between end of RT and start of durvalumab, time of durvalumab treatment in non-progressive patients during durvalumab, ChT sequential *vs.* concurrent, did not predict poorer PFS in univariate analysis (Table 4). Patients who had complete response (CR) on CT evaluation after durvalumab treatment had significantly longer PFS compared to those with partial response (PR) or stable disease (SD) (mPFS not reached *vs.* 22 months, $p = 0.01$) and this was affirmed in multivariate analysis (Figure 2).

Regarding the pattern of progression, we found more loco-regional only progression in squamous cell carcinoma (79.4%) and distant metastases in adenocarcinoma (81.8%), the difference was significant ($p = 0.002$) (Table 5). In addition, all patients with KRAS mutation that progressed, had distant metastases only ($p < 0.001$). On the contrary, all patients that discontinued treatment early due to AE and progressed later ($n = 8$), had loco-regional failure only ($p = 0.024$).

Median OS from the durvalumab start has not been reached after the median follow-up time of 23 months (range 2-35 months). Twelve- and estimated 24-month OS were 86.7% (95% CI: 79.5-93.9%), and 68.6% (95% CI: 57.2-79.9%), respectively (Figure 3). In total, 25 patients (29.4%) have died until the last follow-up date.

TABLE 4. Univariate and multivariate analysis of predictors for progression free survival

Variable	Univariate analysis		Multivariate analysis	
	HR (95% CI)	p	HR (95% CI)	p
Age	< 63 years	0.67 (0.35–1.29)		0.231
	≥ 63 years			
Gender	Male	0.62 (0.32–1.20)		0.156
	Female			
ECOG PS	0	0.66 (0.34–1.28)		0.226
	1–2			
Stage	IIIA	0.89 (0.54–1.48)		0.663
	IIIB			
	IIIC			
Histology	Adenocarcinoma	0.84 (0.41–1.70)		0.635
	Squamous Cell			
Smoking status	Never	0.59 (0.33–1.07)		0.084
	Ex-smokers			
	Smoking at diagnosis			
Mutational status	No	0.99 (0.87–1.12)		0.881
	KRAS			
PD-L1	< 1%	1.03 (0.67–1.59)		0.882
	1%–49%			
	> 50%			
Time to durvalumab	< 57 days	0.63 (0.32–1.24)		0.186
	≥ 57 days			
RT dose	< 60 Gy	1.10 (0.43–2.84)		0.838
	≥ 60 Gy			
No of ChT	Up to 3	2.06 (0.94–4.51)		0.069
	4–5			
ChT	Sequential	1.51 (0.79–2.85)		0.209
	Concurrent			
Response after IT	CR	0.066 (0.008–0.518)		0.010
	PR/SD			
Durvalumab treatment time	< 10.8 months	3.16 (1.62–6.17)		0.001
	≥ 10.8 months			

CR = complete response; ECOG PS = Eastern Cooperative Oncology Group performance status; ChT = chemotherapy, RT = radiotherapy, IT = immunotherapy; PD = progressive disease; PD-L1 = programmed dead-ligand 1; PR = partial response; SD = stable disease

Age, gender, ECOG PS, stage, histology, PD-L1 expression, mutational status, smoking status, RT dose, ChT sequential *vs.* concurrent, the time between end of RT and start of durvalumab did not predict poorer OS in univariate analysis. Patients with CR after ChT-RT had significant longer survival with Kaplan-Meier method than patients with PR or SD ($p = 0.045$), however, survival was not different according to response after dur-

valumab treatment. In the multivariate Cox proportional hazards model CR after ChT-RT as well as after completion of durvalumab was not predictor of better OS.

Treatment after progression

After progression, six patients had no additional treatment, mostly due to progressive deterioration

TABLE 5. Pattern of progression

Progression (N of patients)		Loco-regional only	Metastatic	p
Gender	Male	12	10	0.563
	Female	9	5	
Stage	IIIA	7	3	0.663
	IIIB	11	9	
	IIIC	3	3	
Histology	Adenocarcinoma	2	9	0.002
	Squamous cell	19	5	
	Other	0	1	
Mutation	KRAS	0	7	< 0.001
	No mutation	21	8	
PD-L1	< 1%	3	4	0.435
	1%–49 %	8	6	
	50%	10	4	

N = number; PD-L1 = programmed dead-ligand 1

of patient's performance. Fourteen patients were treated with RT only and eleven with ChT, of those six received additional RT and one of them also immunotherapy. Two patients had surgery of brain metastases and three patients had salvage surgery of primary tumour.

Discussion

The results of PFS and OS in our series of patients with stage III NSCLC treated with durvalumab after ChT-RT confirmed improved survival compared to our historical data of treatment before durvalumab introduction.¹⁰⁻¹² After the median follow-up time of 23 months, 12- and 24-month PFS (71% and 45.8%, respectively) and OS (86.7% and 68.6%, respectively) in our series were comparable with those in the PACIFIC trial (PFS 55.3% and 44.8% and OS 83.1% and 66.3%).¹⁻⁴ In addition, data from other real-world reports have confirmed the advantage of maintenance treatment with durvalumab over ChT-RT only.¹³⁻¹⁶ In a series of 62 patients in the report of Offin *et al.*, the 12-month PFS and OS were 65% and 85%, respectively.¹⁴ In the Canadian multicentre analysis with 147 patients included, 12-month OS rate of 92.5% was reported after a median follow-up of 15.8 months.¹⁵ Report from the German group encompassed 56 centres with altogether 126 patients treated in expanded access programme, revealed the 12- and 24-month

PFS of 56.0% and 46.7%, and 12- and 24-month OS of 78.6% and 66.0%, respectively.¹⁶

The broad usage of induction ChT before RT, and ChT selection of gemcitabine in our group of stage III NSCLC patients offered comparable survival rates and safety as reported with other schedules in recent publications.¹⁴⁻¹⁶ Some patients with stage III NSCLC are not candidates for concurrent ChT-RT due to the age and comorbidity.^{5,6} Most patients (96.5 %) in our series started treatment with ChT, majority of them with platinum-based ChT including gemcitabine and 63.5% of all continued platinum-based ChT during RT. In the PACIFIC study, only 25.8% of patients were treated with induction ChT and 99.8% of patients with concurrent platinum-based ChT with etoposide, vinblastine, vinorelbine, taxans or pemetrexed.^{1,17} Only few patients in PACIFIC trial were treated with gemcitabine, and additionally, gemcitabine was not used in none of the recently published real-world durvalumab treatment reports. In the real-world reports of durvalumab treatment, platinum-based ChT with etoposide was used in 11.0% to 21.8% of all patients concurrent with RT, and induction ChT was used in up to 32.5% of patients.¹⁴⁻¹⁶

Treatment with induction gemcitabine in our historical analysis had not revealed excessive AE¹⁰⁻¹². Induction, sequential and concomitant regimes were well tolerated also in the present series (data not shown). In present analysis, there were no differences in PFS and OS between the patients treated with sequential ChT only or concurrent ChT. Additionally, the effectiveness of platinum-based ChT with induction gemcitabine was not inferior to other ChT schedules when comparing PFS and OS. Comparing the best response to ChT-RT, we observed a higher rate of CR and PR (11.8% and 82.3%) than the PACIFIC trial (1.9% and 48.7%).¹⁻⁴ The median time to first cycle of durvalumab from the end of RT in our series was 57 days (range 12–99 days) which is considerably longer than in PACIFIC trial (range 1–42 days), and longer as reported by Offin with a median time of 1.5 months (range 0.3–7.7 months), and Desilets with 33 days (range 1–94 days).^{14,15} Early completed durvalumab treatment due to progression in our analysis was observed in 18.8% of patients as compared to 30.2% in PACIFIC trial and 34.1% reported by Faehling.^{1,16} At the evaluation up to 4 months after the completion of durvalumab treatment (planned 12-month therapy or early completed due to AE), we observed CR, PR and SD in 34.1%, 12.9% and 17.6% of patients. Notably, the only predictor for improved PFS in our series was CR compared to

PR/SD after durvalumab treatment that was confirmed in multivariate analysis ($p = 0.032$).

Baseline characteristics of patients in our series differed from patients in PACIFIC trial. In our analysis, more patients in stage IIIB and IIIC (69.4% vs. 47.0%) were included and more patients had squamous cell carcinoma (58.1% vs. 47.1%). Both characteristics are known predictors for worse prognosis.^{18,19} Two real-world analysis similarly reported 72% and 68.3% of patients included in stage IIIB and IIIC NSCLC, but lower proportion of squamous cell carcinoma, ranged from 31% to 42.6%.^{14,16} Squamous cell lung carcinoma is associated with inferior OS in all stage groups including unresectable stage III NSCLC.²⁰ Some reports indicated that patients with squamous-cell carcinoma typically presented with bulky locally advanced disease and in those patients, it might be an advantage to start treatment with induction ChT as it was the case in our series.¹⁶ In our analysis, no difference in PFS and OS regarding histology was revealed, but significantly more loco-regional progression was observed compared to metastatic progression in squamous cell carcinoma ($p = 0.002$) as in adenocarcinoma. Altogether, 24.7% of patients had loco-regional progression only and 17.6% had progression with metastatic disease. On the contrary, Offin *et al.* reported the 12-month incidence of loco-regional and distant failures of 18% and 30%.¹⁴ High proportion of loco-regional progression in our series might be due to high proportion of squamous cell carcinoma.

The salvage treatment for most patients with loco-regional progression was reirradiation with or without reinduction ChT. Three patients in our series had salvage surgery due to progressive primary tumour with observed regression of the lymph nodes. In all, the histology revealed down-staging of the lymph nodes and persistent malignant cells in the primary tumour. The high proportion of loco-regional failures only opens the important emerging issue how to deal with the patients after completion of ChT-RT and maintenance durvalumab with PR or SD. Regarding our results, surgery might be an appropriate additional treatment option in selected patients with PR, especially in patients with squamous cell carcinoma. Further clinical trials are investigating incorporation of immunotherapy at different time point in treatment with ChT-RT in stage III NSCLC patients. Additionally, the research in modulating the immune response by interfering with specific alternative immune receptors, pathways and mediators is ongoing and might offer additional knowledge

that would affect the treatment of stage III NSCLC patients.²¹ However, as demonstrated in advanced NSCLC, one treatment might not be suitable for all and in the future, it could be revealed that personalized multimodality approach for selected stage III NSCLC patients might enable better survival results.

Our results presented here were collected as a single institution experience. Due to small number of patients, this series might be underpowered to detect significant impact on survival for different treatment regimens and probable prognostic variable. Also, some information in statistical analysis might be lost, due to dichotomisation of continuous data. Due to retrospective nature of the analysis, some data were not available for all patients. However, despite more advanced stage III NSCLC and squamous cell histology, our results are consistent with the PACIFIC trial. Additionally, further studies are warranted assessing management of patients with loco-regional SD or PR after durvalumab treatment.

Conclusions

The survival data in present analysis confirmed the advantage of maintenance durvalumab in the treatment of unresectable stage III NSCLC patients over ChT-RT only and our results are in line with the PACIFIC trial as well as with recently published real-world reports. Additionally, with mostly gemcitabine as induction platinum-based ChT, the survival outcomes confirmed our treatment regimen as efficient and well tolerated.

Acknowledgments

We thank all the patients who participated in this study.

References

1. Antonia SJ, Villegas A, Daniel D, Vicente D, Murakami S, Hui R, et al. Durvalumab after chemoradiotherapy in stage III Non-Small-Cell Lung Cancer. *N Engl J Med* 2017; **377**: 1919-29. doi: 10.1056/NEJMoa1709937
2. Antonia SJ, Villegas A, Daniel D, Vicente D, Murakami S, Hui R, et al. Overall survival with durvalumab after chemoradiotherapy in stage III NSCLC. *N Engl J Med* 2018; **379**: 2342-50. doi: 10.1056/NEJMoa1809697
3. Hui R, Ozguroglu M, Villegas A, Daniel D, Vicente D, Murakami S, et al. Patient-reported outcomes with durvalumab after chemoradiotherapy in stage III, unresectable non-small cell lung cancer (PACIFIC): a randomised, controlled, phase 3 study. *Lancet Oncol* 2019; **20**: 1670-80. doi: 10.1016/S1470-2045(19)30519-4

4. Faivre-Finn C, Vicente D, Kurata T, Planchard D, Paz-Ares L, Vansteenkiste JH, et al. Four-year survival with durvalumab after chemoradiotherapy in stage III NSCLC-an update from the PACIFIC Trial. *J Thorac Oncol* 2021; **16**: 860-7. doi: 10.1016/j.jtho.2020.12.015
5. Yusuf D, Walton RN, Hurry M, Farrer D, Bebb DG, Cheung WY, et al. Population-based treatment patterns and outcomes for stage III non-small cell lung cancer patients. *Am J Clin Oncol* 2020; **43**: 615-20. doi: 10.1097/COC.0000000000000716
6. Yoon SM, Shaikh T, Hallman M. Therapeutic management options for stage III non-small cell lung cancer. *World J Clin Oncol* 2017; **8**: 1-20. doi: 10.5306/wjco.v8.i1.1
7. Brierly DJ, Gospodarowicz MK, Wittekind C, editors. TNM classification of malignant tumours. 8th edition. *Oxford*: Wiley-Blackwell; 2017. p. 114-20.
8. Seymour L, Bogaerts J, Perrone A, Ford R, Schwartz LH, Mandrekar S, et al. iRECIST: guidelines for response criteria for use in trials testing immunotherapeutics. *Lancet Oncol* 2017; **18**: e143-52. doi: 10.1016/S1473-2045(17)30074-8
9. NIH. National Cancer Institute. DCTD Division of Cancer Treatment & Diagnosis. *Common Terminology Criteria for Adverse Events (CTCAE). Version 5.0*. U.S. Department of Health and Human Services; 2017. [cited 2021 Jul 07]. Available at: https://ctep.cancer.gov/protocoldevelopment/electronic_applications/docs/ctcae_v5_quick_reference_5x7.pdf
10. Vrankar M, Zwitter M, Bavcar T, Milic A, Kovac V. Induction gemcitabine in standard dose or prolonged low-dose with cisplatin followed by concurrent radiochemotherapy in locally advanced non-small cell lung cancer: a randomized phase II clinical trial. *Radiol Oncol* 2014; **48**: 369-80. doi: 10.2478/raon-2014-0026
11. Vrankar M, Stanic K. Long-term survival of locally advanced stage III non-small cell lung cancer patients treated with chemoradiotherapy and perspectives for the treatment with immunotherapy. *Radiol Oncol* 2018; **52**: 281-8. doi: 10.2478/raon-2018-0009
12. Vrankar M, Kern I, Stanic K. Prognostic value of PD-L1 expression in patients with unresectable stage III non-small cell lung cancer treated with chemoradiotherapy. *Radiat Oncol* 2020; **15**: 247. doi: 10.1186/s13014-020-01696-z
13. Taugner J, Käsmann L, Eze C, Tufman A, Reinmuth N, Duell T, et al. Durvalumab after chemoradiotherapy for PD-L1 expressing inoperable stage III NSCLC leads to significant improvement of local-regional control and overall survival in the real-world setting. *Cancers* 2021; **13**: 1613. doi: 10.3390/cancers13071613
14. Offin M, Shaverdian N, Rimner A, Lobaugh S, Shepherd AF, Simone CB 2nd, et al. Clinical outcomes, local-regional control and the role for metastasis-directed therapies in stage III non-small cell lung cancers treated with chemoradiation and durvalumab. *Radiother Oncol* 2020; **149**: 205-11. doi: 10.1016/j.radonc.2020.04.047
15. Desilets A, Blanc-Durand F, Lau S, Hakozaki T, Kitadai R, Malo J, et al. Durvalumab therapy following chemoradiation compared with a historical cohort treated with chemoradiation alone in patients with stage III non-small cell lung cancer: A real-world multicentre study. *Eur J Cancer* 2021; **142**: 83-91. doi: 10.1016/j.ejca.2020.10.008
16. Faehling M, Schumann C, Christopoulos P, Hoffknecht P, Alt J, Horn M, et al. Durvalumab after definitive chemoradiotherapy in locally advanced unresectable non-small cell lung cancer (NSCLC): real-world data on survival and safety from the German expanded-access program (EAP). *Lung Cancer* 2020; **150**: 114-22. doi: 10.1016/j.lungcan.2020.10.006
17. Faivre-Finn C, Spigel DR, Senan S, Langer C, Perez BA, Özgüroğlu M, et al. Impact of prior chemoradiotherapy-related variables on outcomes with durvalumab on unresectable Stage III NSCLC (PACIFIC). *Lung Cancer* 2021; **151**: 30-8. doi: 10.1016/j.lungcan.2020.11.024
18. Jin G, Wang X, Xu C, Sun J, Yuan Z, Wang J, et al. Disparities in survival following surgery among patients with different histological types of N2-III non-small cell lung cancer: a Surveillance, Epidemiology and End Results (SEER) database analysis. *Ann Transl Med* 2020; **8**: 1288. doi: 10.21037/atm-20-4357
19. Morgensztern D, Waqar S, Subramanian J, Gao F, Trinkaus K, Govindan R, et al. Prognostic significance of tumor size in patients with stage III non-small-cell lung cancer: a surveillance, epidemiology, and end results (SEER) survey from 1998 to 2003. *J Thorac Oncol* 2012; **7**: 1479-84. doi: <https://doi.org/10.1097/JTO.0b013e318267d032>
20. Wang BY, Huang JY, Chen HC, Lin CH, Lin SH, Hung WH, et al. The comparison between adenocarcinoma and squamous cell carcinoma in lung cancer patients. *J Cancer Res Clin Oncol* 2020; **146**: 43-52. doi: 10.1007/s00432-019-03079-8
21. Attili I, Tarantino P, Passaro A, Stati V, Curigliano G, de Marinis F. Strategies to overcome resistance to immune checkpoint blockade in lung cancer. *Lung Cancer* 2021; **154**: 151-60. doi: 10.1016/j.lungcan.2021.02.035

Disease control with prior platinum-based chemotherapy is prognostic for survival in patients with metastatic urothelial cancer treated with atezolizumab in real-world practice

Marina Mencinger^{1,2}, Dusan Mangaroski¹, Urska Bokal¹

¹ Institute of Oncology Ljubljana, Ljubljana, Slovenia

² Faculty of Medicine, University of Ljubljana, Ljubljana, Slovenia

Radiol Oncol 2021; 55(4): 490-498.

Received 27 September 2021

Accepted 07 March 2021

Correspondence to: Assist. Marina Mencinger, M.D., Ph.D., Institute of Oncology Ljubljana, Zaloška 2, 1000 Ljubljana, Slovenia.
Phone: +386 1 5879 286; Fax: +386 1 5879 303; E-mail: mmencinger@onko-i.si

Disclosure: Roche Farmaceutvska Družba d.o.o has funded the statistical analysis for this study. The interpretation of the results and the content of this publication express the author's independent professional opinion and were not influenced by Roche. Marina Mencinger and Urska Bokal received honoraria for consultancy from Roche, all authors received speaker's honoraria from Roche.

Background. Atezolizumab, a programmed-death ligand-1 (PD-L1) inhibitor, is a novel treatment option for patients with metastatic urothelial cancer (mUC). Clinical prognostic factors, survival outcomes, and the safety of patients with mUC treated with atezolizumab, in a real-world setting, were investigated.

Patients and methods. 62 patients with mUC, treated at the Institute of Oncology Ljubljana between May 8th 2018 and Dec 31st 2019, were included. Response rates and immune-related adverse events (irAE) were collected. Progression-free survival and overall survival times were assessed using the Kaplan-Meier method. The Cox proportional hazards model was applied to identify the factors affecting survival.

Results. Of 62 patients, five (8.1%) have not yet been evaluated and 20 (32%) died prior to the first radiographic evaluation. We observed clinical benefit in 19 (33%), objective response in 12 (21%), and complete response in five (9%) patients. Median overall survival for the whole population was 6.8 (95% CI, 2.6–11.0), for platinum-naïve 8.7 (95% CI: 0.8–16.5), and for the platinum-treated group 6.8 (95% CI, 3.7–10) months. At the 5.8 (0.3–23.1) month median follow-up, the median duration of the response was not reached. IrAE occurred in 20 (32%) patients and seven (11%) of them discontinued the treatment. Multivariate analysis in platinum-treated patients showed that a treatment-free interval of more than six months was prognostic for overall survival (OS).

Conclusions. Responses to atezolizumab led to long disease remission in a subset of our patients. The median OS in our real-world population was compromised by a large percentage of patients with poor ECOG performance status (PS). A treatment-free interval from chemotherapy was associated with the longer survival of platinum-treated patients with mUC receiving further atezolizumab.

Key words: PD-L1 inhibitor; urothelial cancer; bladder; atezolizumab; overall survival; immune checkpoint inhibitor; prognostic factors

Introduction

Metastatic urothelial carcinoma (mUC) is an aggressive malignancy with poor prognosis among urological cancers.¹ Standard cisplatin-based

chemotherapy as a first-line regimen for mUC remains a challenge for many patients due to numerous comorbidities.² Patients with mUC not eligible for combination therapy with cisplatin commonly receive carboplatin and have an expected medi-

an overall survival (mOS) of only nine months.³ Moreover, there is a lack of evidence for improved outcomes for second-line therapeutic options: vinflunine is approved only in Europe and taxanes or gemcitabine are commonly used in the USA with only modest efficacy.^{4,5}

Recently, programmed death-ligand 1 (PD-L1) and programmed death-1 (PD-1) inhibitors have become the new systemic therapies for patients with mUC with disease progression after platinum-based chemotherapy.⁶⁻⁹ Two of them, pembrolizumab and atezolizumab, are also approved for the first-line treatment of cisplatin-ineligible patients whose tumors express PD-L1.^{10,11} Recently, the large III phase study IMVIGOR 130, investigating atezolizumab as a first-line therapy, alone or in combination with platinum-based chemotherapy, revealed a significant improvement in the progression-free survival (PFS) of atezolizumab added to platinum-based chemotherapy versus platinum-based chemotherapy alone.¹²

Prognostic factors (Eastern Cooperative Oncology Group Performance status, ECOG PS; haemoglobin level and liver metastasis) in patients with mUC after the failure of platinum-based chemotherapy have already been identified.¹³ Recently, novel prognostic factors (high C reactive protein, poor response to previous chemotherapy and poor ECOG PS) for OS in patients with bladder carcinoma receiving second-line chemotherapy have been proposed.¹⁴

It was shown that PD-L1-positive mUC had a significantly better response to PD-1/PD-L1 targeted treatment.¹⁵ It is not clear if PD-L1 has a predictive role for survival benefit with atezolizumab in patients with mUC.¹⁶ Other clinical and biological parameters beyond PD-L1 expression could affect the benefit from an immune checkpoint blockade.

The aim of this retrospective single-centre study was to identify novel clinical prognostic factors for OS in patients with mUC who received atezolizumab as monotherapy in a real-world setting. Furthermore, response rates in different patient populations, efficacy outcomes and the safety of these patients are reported.

Patients and methods

A retrospective study on patients with mUC who were treated with atezolizumab at the Institute of Oncology, Ljubljana, from May 8th 2018 to December 31st 2019 was performed. Patients received atezolizumab after the failure of platinum-

based chemotherapy or were cisplatin-ineligible as estimated by the treating oncologist. Patients who were cisplatin-ineligible and initiated atezolizumab after August 8th 2018 were tested for PD-L1.

The study was approved by the Institutional Review Board Committee (No. 478, date of approval 2019 Apr 25) and was carried out according to the Declaration of Helsinki. All necessary consents required by applicable law from any relevant patient whose information is included in the article have been obtained.

Patients with a confirmed histological diagnosis of inoperable mUC received atezolizumab at a dose of 1200 mg every three weeks until discontinuation. The therapy was discontinued because of death, radiographic disease progression, or unacceptable toxic adverse events. The relevant clinical and laboratory data were obtained from patients' data charts: age, sex, ECOG PS, tumor histology type, number and types of prior systemic therapies, surgery, location of metastasis in different organs at the initiation of atezolizumab, number of atezolizumab applications, the date of the first and last chemotherapy/atezolizumab cycle, PD-L1 status, if available, immune-related adverse events (irAE) as recorded by the treating oncologist. Considering chemotherapy exposure, two groups have been predefined: the first group, platinum-treated, consisted of patients that had received chemotherapy either as neoadjuvant, adjuvant, or as a first- or second-line therapy, and the second group, defined as platinum-naïve, had not received any chemotherapy before atezolizumab.

The objective response rate (ORR) was defined as the proportion of patients with a complete or partial response according to the Response Evaluation Criteria in Solid Tumors (RECIST v 1.1) of all patients that had had at least one radiographic evaluation or who had died before the first radiographic evaluation. Response to treatment was evaluated using a computed tomography of chest and abdomen at baseline and then every 3–4 months or at the discretion of the treating oncologist. ORR was computed separately for platinum-treated and chemotherapy-naïve groups, and for patients with good (0, 1) and poor (2, 3) ECOG PS.

Clinical benefit (CB) comprised complete, partial response, or stable disease (CR, PR; SD). Duration of the response was defined as the time between the initial response to therapy and subsequent disease progression or death. A treatment-free interval (TFI) was defined as the time between the last chemotherapy cycle to the first cycle of atezolizumab.

Median PFS and mOS for the whole group and mOS for the platinum-treated and the platinum-naïve cohorts were computed separately. Progression of the disease was defined as radiographic progression according to RECIST 1.1 or death, whichever occurred first. We presumed that patients who died before the first radiographic evaluation had progressive disease as their best response. PFS and OS were estimated using Kaplan-Meier methods, and the differences were evaluated using the log-rank test. PFS was defined as the time from the first administration of atezolizumab to radiographic or clinical progression or death. OS time was analyzed from the start of atezolizumab until death from any cause or until the last follow-up examination. Duration of response was defined as the time from response (CR or PR) to progression/death.

P values < 0.05 were considered significant, and 95% confidence intervals (CI) were calculated.

IrAE as assessed by the treating oncologist and graded according to the Common Terminology Criteria for Adverse Events (CTCAE) version 5.0 were assembled.

Results

Sixty two patients with locally advanced or mUC initiated treatment with atezolizumab at the Institute of Oncology Ljubljana between May 8th 2018 and December 31st 2019. According to prior exposure to chemotherapy, platinum-treated and platinum-naïve groups were formed. The characteristics for these patient groups are displayed in Table 1. The group of platinum-treated patients had 44 patients with a median age of 65 (48–80), whereas the group of platinum-naïve patients totaled 18 patients with a median age of 75 (62–85) years. The majority of the patients in both groups were males. Good ECOG PS (0, 1) according to the WHO classification was determined in more than half of them (26 or 59%; 10 or 56%) in each group. Primary metastatic disease was detected in 23 (52%) of platinum-treated patients and in 14 (78%) of platinum-naïve patients. PD-L1 staining (Ventana SP142 test) was positive according to the published criteria in 12 (67%) patients initiating first-line treatment with atezolizumab; but in more than half (25, 57%) of platinum-treated patients testing was not performed and PD-L1 status remained unknown (Table 1). All 18 patients with liver metastasis belong to the platinum-naïve group.

TABLE 1. Patients' characteristics

	Platinum-treated N = 44 (%)	Platinum-naïve N = 18 (%)
Median age, years (range)	65 (48–80)	75 (62–85)
Age ≥ 75 years	7 (16)	12 (67)
Sex		
Male/ Female	27 (61)/17 (39)	11 (61)/ 7 (39)
ECOG PS		
0,1/ 2,3	26 (59)/18 (41)	10 (56)/8 (44)
Primary metastatic disease	23 (52)	14 (78)
Metastatic site nonvisceral/visceral/hepatic	14 (32)/30 (68)/18 (41)	13 (72)/5 (28)/0
Pure urothelial histology	35 (80)	15 (83)
PD-L1 status		
0–4%	9 (20)	1 (5)
≥ 5%	10 (23)	12 (67)
Unknown	25 (57)	5 (28)
Treatment modalities before atezolizumab		
Perioperative chemotherapy	14 (32)	
Surgery	25 (57)	10 (56)
Chemotherapy for metastatic disease	30 (68)	
Number of chemotherapy lines for metastatic disease before atezolizumab		
1/2	28 (93)/2 (7)	

ECOG PS = performance status according to WHO classification

Before the initiation of atezolizumab, more than half the patients in each group underwent a cystectomy. Fourteen platinum-treated patients (32%) received chemotherapy in perioperative, and 30 (68%) in a first-line setting. Most, 28 (93%), received only one line of chemotherapy for metastatic disease before commencing atezolizumab.

Among the 62 included, 57 patients had available data for response analysis. A complete response was obtained in five (9%), a partial response in seven (12%), and a clinical benefit in 19 (33%) patients. The majority, 38 (67%), had progressive disease as their best response as assessed radiographically or/and clinically. Liver metastases were detected in 16 (26%) patients with available data for response analysis. No complete response was observed among patients with liver metastases (Table 2).

Median PFS was 4.2 (95% CI, 1.9–6.5) and mOS 6.8 (95% CI, 2.6–11.0) months (Figure 1). Of the 62 patients included, 18 (29%) were platinum-naïve and had mOS of 8.7 (95% CI, 0.8–16.5) months

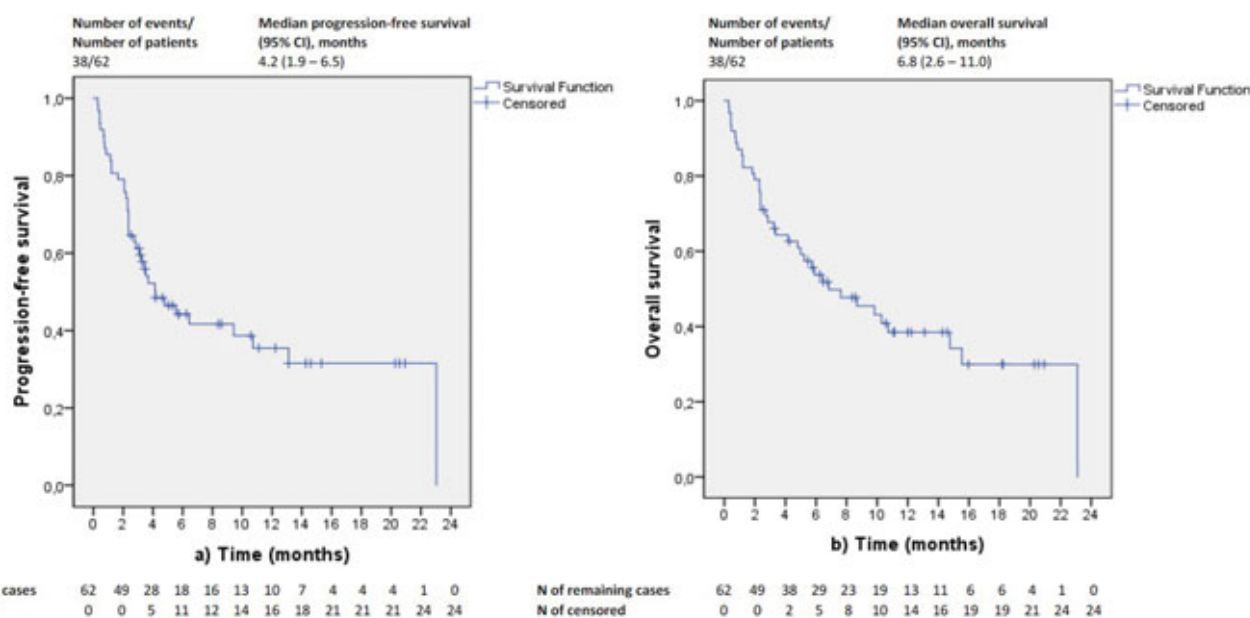


FIGURE 1. Kaplan-Meier curves of progression-free survival (A) and overall survival (B) of all study population.

TABLE 2. Responses to treatment with atezolizumab

Type of response	All patients N=57 (%)	Patients with liver metastases N=16 (28%)	Platinum-naïve N=17 (30%)	Platinum-treated N=40 (70%)	ECOG PS 0+1 N=33 (58%)	ECOG PS 2+3 N=24 (42%)
CR	5 (9)	0 (0)	3 (17.5)	2 (5)	4 (12)	1 (4.2)
PR	7 (12)	1 (6)	3 (17.5)	4 (10)	5 (15)	2 (8.3)
SD	7 (12)	4 (25)	1 (6)	6 (15)	6 (18)	1 (4.2)
PD	38 (67)	11 (69)	10 (59)	28 (70)	18 (55)	20 (83.3)

CR = complete response; PR = partial response; SD = stable disease; PD = progressive disease

TABLE 3. Univariate and multivariate analysis of prognostic factors (correlation with overall survival)

Subgroup	Univariate HR	p	Multivariate HR	p	Reference category
Age	0.861 (0.428-1.731)	0.675			≥ 75 years
ECOG PS	2.883 (1.495-5.559)	0.002	3.449 (1.358-8.761)	0.009	2 or 3
Visceral metastases*	0.965 (0.502-1.853)	0.914			Yes
Clinical benefit to previous chemotherapy	0.319 (0.133-0.765)	0.010	0.355 (0.131-0.961)	0.042	Yes
TfI	0.140 (0.032-0.604)	0.008	0.113 (0.014-0.877)	0.037	> 6 months
IrAE	0.566 (0.266-1.202)	0.139			Yes

Clinical benefit (complete, partial response or stable disease); ECOG PS = Eastern Cooperative Oncology Group performance status; HR = hazard ratio; IrAE = immune related adverse events; TfI = treatment free interval; * = defined as presence of non lymph node and non bone metastases

whereas 44 (71%) were platinum-treated with mOS of 6.8 (95% CI, 3.7–10) months (Figure 2).

The median duration of response was not estimable at a median follow-up of 5.8 (0.3–23.1) months (Figure 3).

A proportional Cox hazard model was used to identify prognostic factors associated with OS. Variables that were found to be significant in univariate analysis were selected for further evaluation in a multivariate model. According to uni-

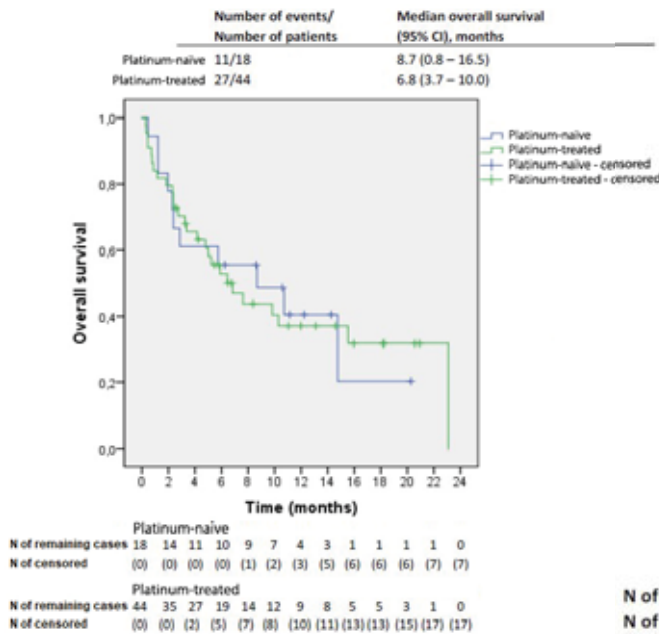


FIGURE 2: Kaplan-Meier curves of overall survival according to the previous exposure to chemotherapy.

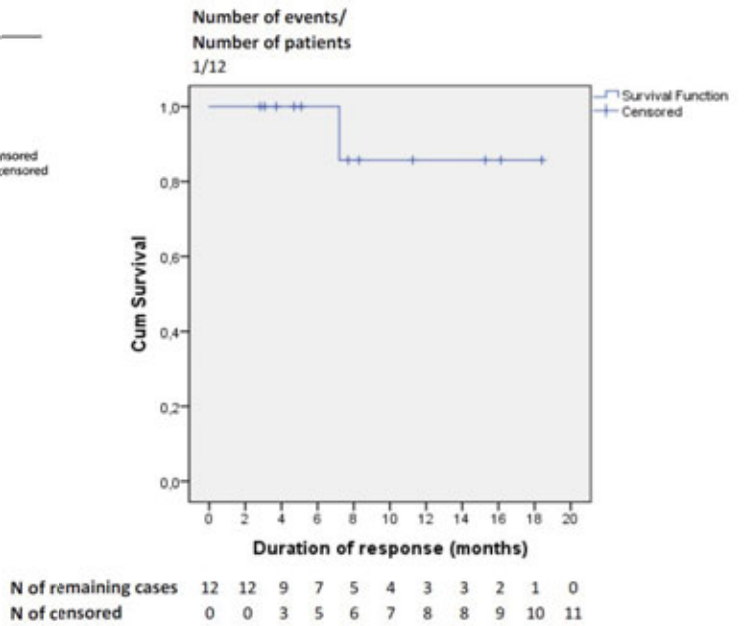


FIGURE 3. Duration of responses at a median follow up of 5.8 (0.3–23.1) months.

TABLE 4. Immune-related adverse events

IrAE of any grade	20 (32%)
IrAE ≥ Grade 3/4	7 (11%)
Systemic corticosteroid use	5 (8%)
Atezolizumab discontinuation due to IrAE	7 (11%)

IrAE = immune related adverse events

variate analysis the negative prognostic factors for overall survival were ECOG PS 2–3, no CB to prior chemotherapy, and TFI less than six months. Only TFI of less than six months impacted poor survival in multivariate analysis. Age, non-visceral disease (defined as metastases in lymph nodes and/or bones only) and the presence of irAE were not proven to be statistically significant in univariate analysis (Table 3).

Safety

The type and severity of irAE were collected. Twenty patients (32%) suffered from irAE, and seven (11%) of them had grade 3–4 irAE as estimated by the treating oncologist and according to the CTCAE v. 5.0. All seven (11%) patients with 3–4 grade toxicity discontinued the therapy. Five (8%) patients were treated with systemic corticosteroids and one patient received only topical corticosteroid therapy (Table 4).

The most common irAE was skin toxicity (eight, 40% of the affected patients), followed by hepatopathy (four, 20%), arthritis, and central nervous toxicity (two, 10%). Hypothyroidism, nephropathy, low platelet count, and gastrointestinal adverse events were annotated in one patient each.

Discussion

The results of our study show that atezolizumab induced long-lasting responses in a subset of patients with mUC. The median duration of response was not reached at a median follow-up of 5.8 months (0.3–23.1), similarly to what was observed in other prospective trials studying the efficacy of atezolizumab in patients with mUC.^{8,12,17,18}

The ORR in our platinum-naïve and platinum-treated groups were comparable to ORR of similar patient groups in prospective trials; however, this did not translate to the same extent of survival benefits as seen in prospective trials, where the selection of patients is stricter.

Notably, a higher proportion of platinum-naïve patients achieved OR (35%) compared to the platinum-treated cohort (15%). This is, however, in line with the reported ORR of similar patient groups in two other trials. In the nonrandomized IMVIGOR 210 trial, the ORR in cohort 1 (cisplatin-ineligible) was 23% and in cohort 2 (platinum-

treated) 15%.^{10,17} Similarly, in a larger phase III clinical trial IMVIGOR 211, which assigned 931 platinum-treated patients, the ORR was only 13.4% in the ITT population regardless of PDL-1 testing.⁸ Although PDL-1 testing has not been performed in all our patients, it was true that the platinum-naive cohort was enriched with PD-L1 positive patients (Table 1). Namely, during our study the label for atezolizumab has been updated by the US Food and Drug Administration (FDA) and the European Medicines Agency (EMA), which restricted the use of atezolizumab to cisplatin-ineligible patients who have a positive PD-L1 score. This selection of patients for first-line atezolizumab therapy at least partially explains the higher ORR in our platinum-naive group. Our platinum-naive cohort corresponded to the cisplatin-ineligible population as defined by the Galsky criteria which, among others, include poor ECOG PS commonly encountered among these patients.³ The predictive value of PD-L1 for atezolizumab in patients with urothelial cancer is controversial.¹⁶ More data on this issue are expected from the IMVIGOR 130 study.

As anticipated, an important difference in ORR was found between the cohort of patients with poor (12%) in comparison to good ECOG PS (27%). Similarly, poor ORR in patients with ECOG PS 2 have been reported in the SAUL trial, which recruited real-world patients with mUC, rarely included in prospective trials.¹⁹ Previous studies have shown that only a subset of patients with mUC are able to receive more lines of therapies as their ECOG PS rapidly deteriorates.²⁰ Therefore, more research efforts need to be put into optimizing the selection of first-line therapy.

Only one patient with liver metastases responded to atezolizumab 1 (6%). Liver metastases were associated with reduced marginal CD8⁺T-cell infiltration, providing a potential mechanism for this outcome.²¹ A similar proportion of our patients with poor and good PS by the WHO had liver metastasis (in poor PS 10/26, 28%, *vs.* in good PS 8/18, 31%) Therefore, the reduced benefit in our population with poor ECOG PS could not be attributed to the site of metastasis, but rather to other uninvestigated factors.

Overall, the mOS of our patient groups was shorter than the mOS of similar patient groups reported in prospective studies. The mOS of our platinum-treated group was shorter in comparison to the intention to treat the population (all platinum-treated) in IMVIGOR 211 or to the platinum-treated cohort 2, in IMVIGOR 210 (6.8 *vs.* 8.6 and 7.8 months), respectively. An even larger difference in

mOS was observed among our platinum-naive cohort and cisplatin-ineligible patients in cohort 1 of IMVIGOR 210 and the randomized large group of 451 patients receiving first-line monotherapy with atezolizumab in IMVIGOR 130 (8.7 *vs.* 15.8 and 16 months), respectively.^{12,22} Very short mOS of only 2.3 m was reported in patients with poor ECOG PS in the prospective SAUL real-world analysis.¹⁹ In total, we had 42% of patients with ECOG PS of two or more, which was four times higher than the proportion of patients with poor ECOG PS represented in the SAUL study population. Almost 30% of our patients died within the first two months after receiving the first dose of atezolizumab (Figure 2). It was reported that nearly double as many cancer patients initiated systemic therapy near the end of life mainly due to increased immune checkpoint inhibitor (ICI) use.²³ Possibly medical oncologists do not fear toxicities of chemotherapy and may prescribe ICI even to patients who are not fit or eligible for chemotherapy.²⁴

We may conclude that the mOS of our whole group was compromised by a large cohort of patients with poor ECOG PS who died even before the first radiographic evaluation. Of interest is the fact that no consensus could be reached by the ESMO Guidelines Committee on whether immune checkpoint inhibitors could be recommended for first-line therapy of PD-L1 negative patients not eligible for any chemotherapy as stated on an e-update in 2019.²⁵ Based on our study, the initiation of second-line systemic therapy with an immune checkpoint inhibitor in patients with poor ECOG PS should be discussed on an individual patient-therapist basis. For the majority of these patients providing best supportive care may be the best option.

Another explanation of a large proportion of patients dying after one or two cycles of atezolizumab may be a potential hyperprogression of the disease. As hyperprogression of cancer by definition needs at least a well-defined course of the disease before initiation of ICI, this hypothesis could not be resolved in a retrospective trial.²⁶

We report clinical prognostic factors for OS in platinum-treated patients with mUC receiving an immune checkpoint inhibitor, atezolizumab, in a real-world practice. In univariate analysis three parameters: ECOG PS 1, 0, TFI more than six months, and CB with chemotherapy, showed a statistically significant correlation with longer survival. Poor ECOG PS has been identified as a poor prognostic factor in other studies with immune checkpoint.^{23,27} Such patients are often excluded from the randomized clinical trials, therefore real-world data

are important for this population. Poor ECOG PS, however, did not retain the prognostic significance for survival in multivariate analysis in our patient cohort, which may be due to the poor reliability of this score.^{15,28}

Furthermore, we found that disease control with chemotherapy was important for the efficiency of the immune checkpoint inhibitor. Disease control parameters, represented by TFI and CB to prior therapy, both showed a prognostic value for survival in univariate analysis. In multivariate analysis only TFI of less than six months retained a negative prognostic value for OS (Table 3). This finding may help in designing future prospective clinical trials. In fact, the JAVELIN 100 phase III trial permitted only patients that achieved CB with chemotherapy to continue with maintenance therapy with avelumab or best supportive care. The addition of avelumab to best supportive care was associated with a significant 31% reduction in the risk of death, with the median OS durations of 21.4 and 14.3 months for the avelumab and BSC alone groups, respectively.²⁹

Response to cisplatin-based chemotherapy or immunotherapy, especially checkpoint blockade, has been shown to correlate with molecular subtype.^{30,31} Whether these molecular subtypes were shared in patients that were not responsive to either therapy is currently unknown. So far, no known molecular markers showing clinical utility to select patients that are not responsive to cisplatin based chemotherapy or ICI are available.³² Moreover, molecular alterations induced by chemotherapy were poorly characterized. Chemotherapy probably plays an important role in enhancing the immunogenicity of tumor, making it more susceptible to therapy with ICI.³³ Based on the results of IMVIGOR 130 the concomitant effect of chemotherapy and atezolizumab is important as a combination of these two significantly prolonged PFS compared to chemotherapy alone.¹²

Nevertheless, it is important that clinicians foresee which patients have a poor prognosis even with ICI. Such patients need careful monitoring when treated with ICI or should perhaps be offered an alternative treatment, if available, or even best supportive treatment instead.

The rate grade 3–4 of immune adverse events we observed was similar to that reported in the prospective SAUL trial (11 % *vs.* 13%). The latter trial included a wide selection of patients. Due to the retrospective nature of our investigation the grading of AE was not exact, nor has the potential im-

mune-related condition been appropriately tested. One of our patients suffered severe neurologic deterioration that we attributed to probable autoimmune encephalitis. The types of immune adverse events we describe (Table 4) were already reported elsewhere.^{12,18}

The present study has several limitations. First, the number of patients was too low to be able to draw definitive conclusions. Second, the retrospective study design has weak points such as a heterogeneous group of patients, non-consistent timing of radiographic evaluation, unconfirmed reporting of, possibly, irAE and missing data such as PD-L1 testing scores.

Conclusions

In total, we have confirmed a long-lasting response to atezolizumab in a proportionally similar subset of patients with mUC treated in daily practice comparable to prospective trials. The mOS of all platinum-naive and platinum-treated patients was shorter than the mOS of similar patient groups reported in prospective studies, mainly due to a high percentage of our patients with poor ECOG PS. Significantly, TFI of less than six months is a clinically-important poor prognostic factor for OS. It would be of clinical value to investigate if patients with FGFR mutation or fusion acquiring disease control with chemotherapy benefit more from an immune checkpoint inhibitor or a FGFR inhibitor. In conclusion, whether disease control with chemotherapy is also predictive of an atezolizumab treatment effect, or not, can only be assessed in a valid comparative setting such as in a randomized trial. If it is predictive, then these patients may share a common molecular genetic profile.

Acknowledgments

We thank Assistant Prof. Janja Jerebic, Ph.D., Faculty of Organizational Sciences, University in Maribor, who performed the statistical analysis

Author contributions

All authors contributed with the study design, data collection, data analysis, and writing of the manuscript. All authors have read and approved the final manuscript.

References

- Torre LA, Siegel RL, Ward EM, Jemal A. Global Cancer Incidence and Mortality Rates and Trends—An Update. *Cancer Epidemiol Biomarkers Prev* 2016; **25**: 16-27. doi: 10.1158/1055-9965.EPI-15-0578
- Oing C, Rink M, Oechsle K, Seidel C, von Amsberg G, Bokemeyer C. Second line chemotherapy for advanced and metastatic urothelial carcinoma: vinflunine and beyond – a comprehensive review of the current literature. *J Urol* 2016; **195**: 254-63. doi: 10.1016/j.juro.2015.06.115
- Galsky MD, Hahn NM, Rosenberg J, Sonpavde G, Hutson T, Oh WK, et al. Treatment of patients with metastatic urothelial cancer “unfit” for cisplatin-based chemotherapy. *J Clin Oncol* 2011; **29**: 2432-8. doi: 10.1200/JCO.2011.34.8433
- Bellmunt J, Théodore C, Demkov T, Komyakov B, Sengelov L, Daugaard G, et al. Phase III trial of vinflunine plus best supportive care compared with best supportive care alone after a platinum-containing regimen in patients with advanced transitional cell carcinoma of the urothelial tract. *J Clin Oncol* 2009; **27**: 4454-61. doi: 10.1200/JCO.2008.20.5534
- Bamias A, Tzannis K, Harshman LC, Crabb SJ, Wong Y-N, Kumar Pal S, et al. Impact of contemporary patterns of chemotherapy utilization on survival in patients with advanced cancer of the urinary tract: a Retrospective International Study of Invasive/Advanced Cancer of the Urothelium (RISC). *Ann Oncol* 2018; **29**: 361-9. doi: 10.1093/annonc/mdx692
- Apolo AB, Infante JR, Balmanoukian A, Patel MR, Wang D, Kelly K, et al. Avelumab, an anti-programmed death-ligand 1 antibody, in patients with refractory metastatic urothelial carcinoma: results from a multicenter, phase Ib study. *J Clin Oncol* 2017; **35**: 2117-24. doi: 10.1200/JCO.2016.71.6795
- Massard C, Gordon MS, Sharma S, Rafii S, Wainberg ZA, Luke J, et al. Safety and efficacy of durvalumab (MED14736), an anti-programmed cell death ligand-1 immune checkpoint inhibitor, in patients with advanced urothelial bladder cancer. *J Clin Oncol* 2016; **34**: 3119-25. doi: 10.1200/JCO.2016.67.9761
- Powles T, Durán I, van der Heijden MS, Loriot Y, Vogelzang NJ, De Giorgi U, et al. Atezolizumab versus chemotherapy in patients with platinum-treated locally advanced or metastatic urothelial carcinoma (IMvigor211): a multicentre, open-label, phase 3 randomised controlled trial. *Lancet* 2018; **391**: 748-57. doi: 10.1016/S0140-6736(17)33297-X
- Sharma P, Retz M, Siefker-Radtke A, Baron A, Necchi A, Bedke J, et al. Nivolumab in metastatic urothelial carcinoma after platinum therapy (CheckMate 275): a multicentre, single-arm, phase 2 trial. *Lancet Oncol* 2017; **18**: 312-22. doi: 10.1016/S1470-2045(17)30065-7
- Balar AV, Galsky MD, Rosenberg JE, Powles T, Petrylak DP, Bellmunt J, et al. Atezolizumab as first-line treatment in cisplatin-ineligible patients with locally advanced and metastatic urothelial carcinoma: a single-arm, multicentre, phase 2 trial. *Lancet* 2017; **389**: 67-76. doi: 10.1016/S0140-6736(16)32455-2
- Balar AV, Castellano D, O'Donnell PH, Grivas P, Vuky J, Powles T, et al. First-line pembrolizumab in cisplatin-ineligible patients with locally advanced and unresectable or metastatic urothelial cancer (KEYNOTE-052): a multicentre, single-arm, phase 2 study. *Lancet Oncol* 2017; **18**: 1483-92. doi: 10.1016/S1470-2045(17)30616-2
- Galsky MD, Arijá JÁ, Bamias A, Davis ID, De Santis M, Kikuchi E, et al. Atezolizumab with or without chemotherapy in metastatic urothelial cancer (IMvigor130): a multicentre, randomised, placebo-controlled phase 3 trial. *Lancet* 2020; **395**: 1547-57. doi: 10.1016/S0140-6736(20)30230-0
- Bellmunt J, Choueiri TK, Fougeray R, Schutz FAB, Salhi Y, Winquist E, et al. Prognostic factors in patients with advanced transitional cell carcinoma of the urothelial tract experiencing treatment failure with platinum-containing regimens. *J Clin Oncol* 2010; **28**: 1850-5. doi: 10.1200/JCO.2009.25.4599
- Matsumoto R, Abe T, Ishizaki J, Kikuchi H, Harabayashi T, Minami K, et al. Outcome and prognostic factors in metastatic urothelial carcinoma patients receiving second-line chemotherapy: an analysis of real-world clinical practice data in Japan. *Jpn J Clin Oncol* 2018; **48**: 771-6. doi: 10.1093/jcco/hyy094
- Ding X, Chen Q, Yang Z, Li J, Zhan H, Lu N, et al. Clinicopathological and prognostic value of PD-L1 in urothelial carcinoma: a meta-analysis. *Cancer Manag Res* 2019; **11**: 4171-84. doi: 10.2147/CMAR.S176937
- Rouanne M, Radulescu C, Adam J, Allory Y. PD-L1 testing in urothelial bladder cancer: essentials of clinical practice. *World J Urol* 2020; [Ahead of print]. doi: 10.1007/s00345-020-03498-0
- Rosenberg JE, Hoffman-Censits J, Powles T, Van Der Heijden MS, Balar AV, Necchi A, et al. Atezolizumab in patients with locally advanced and metastatic urothelial carcinoma who have progressed following treatment with platinum-based chemotherapy: a single-arm, multicentre, phase 2 trial. *Lancet* 2016; **387**: 1909-20. doi: 10.1016/S0140-6736(16)00561-4
- Stewart TF, Petrylak DP. Atezolizumab in understudied populations with bladder cancer. *Nat Rev Urol* 2019; **16**: 449-50. doi: 10.1038/s41585-019-0200-8
- Sternberg CN, Loriot Y, James N, Choy E, Castellano D, Lopez-Rios F, et al. Primary results from SAUL, a multinational single-arm safety study of atezolizumab therapy for locally advanced or metastatic urothelial or nonurothelial carcinoma of the urinary tract. *Eur Urol* 2019; **76**: 73-81. doi: 10.1016/j.eururo.2019.03.015
- Flannery K, Boyd M, Black-Shinn J, Robert N, Kamat AM. Outcomes in patients with metastatic bladder cancer in the USA: a retrospective electronic medical record study. *Future Oncol* 2019; **15**: 1323-34. doi: 10.2217/fon-2018-0654
- Tumeh PC, Hellmann MD, Hamid O, Tsai KK, Loo KL, Gubens MA, et al. Liver metastasis and treatment outcome with anti-PD-1 monoclonal antibody in patients with melanoma and NSCLC. *Cancer Immunol Res* 2017; **5**: 417-24. doi: 10.1158/2326-6066.CIR-16-0325
- Rosenberg J, Petrylak D, Abidoye O, Van der Heijden MS, Hofman-Censits J, Necchi A, et al. 21LBA Atezolizumab in patients (pts) with locally-advanced or metastatic urothelial carcinoma (mUC): results from a pivotal multicenter phase II study (IMvigor 210). *Eur J Cancer* 2015; **51**(Suppl 3): S720. [abstract]. doi: 10.1016/s0959-8049(16)31942-6
- Parikh RB, Galsky MD, Gyawali B, Riaz F, Kaufmann TL, Cohen AB, et al. Trends in checkpoint inhibitor therapy for advanced urothelial cell carcinoma at the end of life: insights from real-world practice. *Oncologist* 2019; **24**: e397-9. doi: 10.1634/theoncologist.2019-0039
- Schnipper LE, Smith TJ, Raghavan D, Blayney DW, Ganz PA, Mulvey TM, et al. American Society of Clinical Oncology identifies five key opportunities to improve care and reduce costs: the top five list for oncology. *J Clin Oncol* 2012; **30**: 1715-24. doi: 10.1200/JCO.2012.42.8375
- Bellmunt J, Orsola A, Leow JJ, Wiegel T, De Santis M, Horwich A. Bladder cancer: ESMO practice guidelines for diagnosis, treatment and follow-up. *Ann Oncol* 2014; **25**: iii40-8. doi: 10.1093/annonc/mdu223
- Frelaut M, Le Tourneau C, Borcoman E. Hyperprogression under immunotherapy. *Int J Mol Sci* 2019; **20**: 2674. doi: 10.3390/ijms20112674
- Khaki AR, Li A, Diamantopoulos LN, Bilen MA, Santos V, Esther J, et al. Impact of performance status on treatment outcomes: a real-world study of advanced urothelial cancer treated with immune checkpoint inhibitors. *Cancer* 2020; **126**: 1208-16. doi: 10.1002/cncr.32645
- Sørensen JB, Klee M, Palshof T, Hansen HH. Performance status assessment in cancer patients. an inter-observer variability study. *Br J Cancer* 1993; **67**: 773-5. doi: 10.1038/bjc.1993.140
- Powles T, Park SH, Voog E, Caserta C, Valderrama BP, Gurney H, et al. Avelumab maintenance therapy for advanced or metastatic urothelial carcinoma. *N Engl J Med* 2020; **383**: 1218-30. doi: 10.1056/nejmoa2002788
- Choi W, Porten S, Kim S, Willis D, Plimack ER, Hoffman-Censits J, et al. Identification of distinct basal and luminal subtypes of muscle-invasive bladder cancer with different sensitivities to frontline chemotherapy. *Cancer Cell* 2014; **25**: 152-65. doi: 10.1016/j.ccr.2014.01.009
- Seiler R, Ashab HAD, Erho N, van Rhijn BWG, Winters B, Douglas J, et al. Impact of molecular subtypes in muscle-invasive bladder cancer on predicting response and survival after neoadjuvant chemotherapy. *Eur Urol* 2017; **72**: 544-54. doi: 10.1016/j.eururo.2017.03.030
- Buttiglierio C, Tucci M, Vignani F, Scagliotti GV, Di Maio M. Molecular biomarkers to predict response to neoadjuvant chemotherapy for bladder cancer. *Cancer Treat Rev* 2017; **54**: 1-9. doi: 10.1016/j.ctrv.2017.01.002
- Luo Q, Zhang L, Luo C, Jiang M. Emerging strategies in cancer therapy combining chemotherapy with immunotherapy. *Cancer Lett* 2019; **454**: 191-203. doi: 10.1016/j.canlet.2019.04.017

Non-coplanar volumetric modulated arc therapy for locoregional radiotherapy of left-sided breast cancer including internal mammary nodes

Yuan Xu, Pan Ma, Zhihui Hu, Yuan Tian, Kuo Men, Shulian Wang, Yingjie Xu, Jianrong Dai

Department of Radiation Oncology, National Cancer Center/National Clinical Research Center for Cancer/Cancer Hospital, Chinese Academy of Medical Sciences and Peking Union Medical College, Beijing, China

Radiol Oncol 2021; 55(4): 499-507.

Received 27 April 2021

Accepted 28 September 2021

Correspondence to: Yingjie Xu, Department of Radiation Oncology, National Cancer Center/National Clinical Research Center for Cancer/Cancer Hospital, Chinese Academy of Medical Sciences and Peking Union Medical College, 100021 Beijing, China. E-mail: xuyingjie08@126.com and Jianrong Dai, Department of Radiation Oncology, National Cancer Center/National Clinical Research Center for Cancer/Cancer Hospital, Chinese Academy of Medical Sciences and Peking Union Medical College, 100021 Beijing, China. E-mail: Dai_jianrong@cicams.ac.cn

Disclosure: No potential conflicts of interest were disclosed

This is an open access article under the CC BY-NC-ND license (<http://creativecommons.org/licenses/by-nc-nd/4.0/>).

Background. Non-coplanar volumetric modulated arc therapy (ncVMAT) is proposed to reduce toxicity in heart and lungs for locoregional radiotherapy of left-sided breast cancer, including internal mammary nodes (IMN).

Patients and methods. This retrospective study included 10 patients with left-sided breast cancer who underwent locoregional radiotherapy after breast-conserving surgery. For each patient, the ncVMAT plan was designed with four partial arcs comprising two coplanar arcs and two non-coplanar arcs, with a couch rotating to 90°. The prescribed dose was normalized to cover 95% of planning target volume (PTV), with 50 Gy delivered in 25 fractions. For each ncVMAT plan, dosimetric parameters were compared with the coplanar volumetric modulated arc therapy (coVMAT) plan.

Results. There were improvements in conformity index, homogeneity index and V_{55} of total target volume (PTVall) comparing ncVMAT to coVMAT ($p < 0.001$). Among the organs at risk, the average V_{30} , V_{20} , V_{10} , V_5 , and mean dose (D_{mean}) of the heart decreased significantly ($p < 0.001$). Furthermore, ncVMAT significantly reduced the mean V_{20} , V_{10} , V_5 , and D_{mean} of left lung and the mean V_{10} and V_5 and D_{mean} of contralateral lung ($p < 0.001$). An improved sparing of the left anterior descending coronary artery and right breast were also observed with ncVMAT ($p < 0.001$).

Conclusions. Compared to coVMAT, ncVMAT provides improved conformity and homogeneity of whole PTV, better dose sparing of the heart, bilateral lungs, left anterior descending coronary artery (LAD), and right breast for locoregional radiotherapy of left-sided breast cancer with IMN, potentially reducing the risk of normal tissue damage.

Key words: non-coplanar; volumetric modulated arc therapy; left-sided breast cancer; internal mammary nodes

Introduction

Adjuvant radiotherapy after breast-conserving surgery has been proven to be effective in reducing the risk of recurrence and death from breast cancer.¹⁻² In radiotherapy for breast cancer, internal mammary nodes (IMN) and supraclavicular nodes (SCN) are often included in planning target volume

(PTV) to improve local control.³⁻⁶ However, irradiation of IMN inevitably increases the dose delivered to heart and lungs, raising the risk of radiation pneumonitis and cardiac mortality.⁷ Indeed, approximately 1%–5% of patients with breast cancer develop radiation pneumonitis after radiotherapy as predicted by the normal tissue complication probability model.⁸ In a study of 61 patients with

early breast cancer who received radiotherapy, approximately 12.5% developed > grade 1 radiation pneumonitis at 12 months.⁹ Additionally, cardiac diseases, such as ischemic heart disease is another major concern associated with radiotherapy in breast cancer¹⁰⁻¹² and controversies remain concerning IMN irradiation.^{7,13} Therefore, reducing the dose to organs at risk during irradiation of nodal regions is crucial for improving the benefits of treatment while reducing associated toxicity.

Several techniques are used for locoregional breast irradiation. While modified wide tangential beam with forward planning used to be the most common technique¹⁴, intensity-modulated radiotherapy (IMRT) was introduced for radiotherapy of left-sided breast cancer with IMN with the development of technology.¹⁵ Conformity and homogeneity were improved and the proportion of volume receiving 30 Gy (V_{30}) for the heart and the proportion of volume receiving 20 Gy (V_{20}) for the left lung was reduced with IMRT using inverse optimization compared to conventional planning. The recently implemented volumetric modulated arc therapy (VMAT) technology for left-sided breast cancer with IMN can achieve similar PTV coverage and organ-at-risk (OAR) sparing compared to IMRT.¹⁶⁻¹⁸ Helical tomotherapy (HT) is another potential solution; however, beam delivery is time consuming compared with conventional linear accelerator.¹⁹ Furthermore, HT does not provide significant improvement to the mean dose delivered to heart compared with VMAT.²⁰ However, new technologies such as IMRT, VMAT, and HT can reduce the dose to OARs compared with wide tangential beams and it remains important to explore approaches that can improve OAR sparing.

Non-coplanar VMAT (ncVMAT) can extend beam angle arrangements and is therefore potentially better in sparing OARs.²¹ With non-coplanar techniques, different fixed fields or arcs do not employ the same geometric plane, which significantly increases the space of solution for optimizing. This can be realized with a C-arm linear accelerator by rotating the treatment couch around the isocenter. The implementation of ncVMAT has already been studied in partial-breast, complicated whole-breast radiotherapy, and postmastectomy radiotherapy.²²⁻²⁴ However, no studies to date have reported the utility of non-coplanar technique in the treatment of left-sided breast cancer after breast-conserving surgery including the internal mammary and supraclavicular nodal regions. In the present study, ncVMAT plans using four arcs were designed to explore the feasibility of ncVMAT for

locoregional radiotherapy of left-sided breast cancer. Additionally, dosimetric parameters, such as target coverage, conformity index, homogeneity index, and OAR sparing ability, were compared between ncVMAT and coplanar VMAT (coVMAT).

Patients and methods

Patient selection

The present retrospective study was approved by the institutional review board, and informed consent was waived. Ten patients with left-sided breast cancer and IMN after breast-conserving surgery were included in the study. The mean patient age was 52 (range, 34–68) years. The planning computed tomography (CT) data were acquired by a Brilliance CT Big Bore (Philips Healthcare, Best, The Netherlands) using 5-mm thick slices. Both arms of patients were above the head scanning in the supine position. The clinical target volume (CTV) comprised the whole breast, SCN, and IMN. The PTV was generated by expanding a 5-mm margin to CTV, with the exclusion of the most superficial 5-mm area. Therefore, breast planning target volume (PTVbreast), supraclavicular nodes planning target volume (PTVscn), and internal mammary nodes planning target volume (PTVimn) were separately delineated for the breast, SCN, and IMN, respectively, which were then combined to generate the total target volume (PTVall). The volume of PTVall varied from 582.6 cc to 1166.1 cc with an average value of 874.8 cc (standard deviation 191.6 cc). The OARs were also contoured on the planning CT images, which included left and right lungs, heart, left anterior descending coronary artery (LAD), right breast, esophagus, spinal cord, left humeral head, and left brachial plexus.

Treatment planning

All plans were designed with the Pinnacle treatment planning system (version 9.1, Philips Healthcare, Eindhoven, Netherlands) and 6-MV X-ray delivered by an Elekta Versa HD accelerator (Elekta Oncology Systems, Crawley, UK). The multi-leaf collimator (MLC) width was 5 mm at the isocenter, and the treatment couch could rotate from -90° to 90° . The prescribed dose was 50 Gy delivered in 25 fractions for all patients.

All patients were planned with both ncVMAT and coVMAT for comparisons. The ncVMAT was optimized with four arcs, comprising two coplanar arcs and two non-coplanar arcs. The two co-

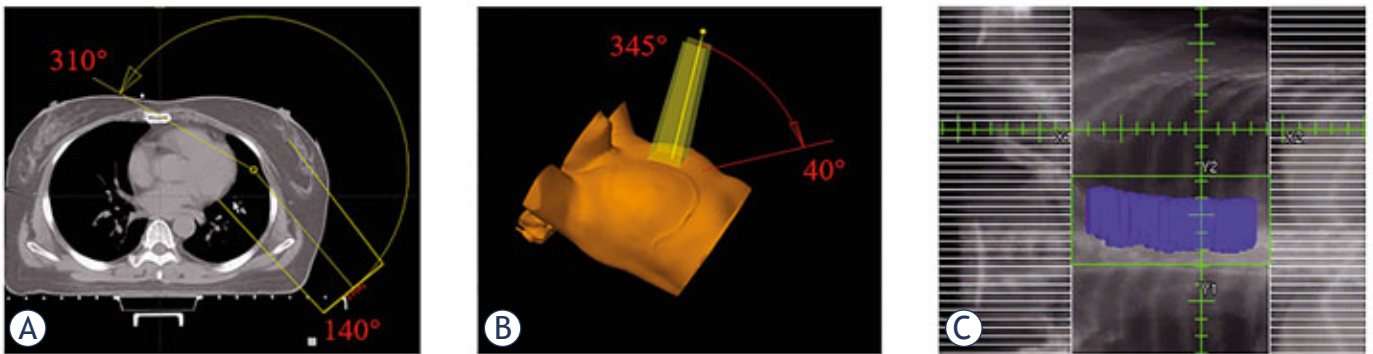


FIGURE 1. Illustration of the arc angle for coplanar arc (A), non-coplanar arc (B), maximum jaw position for non-coplanar arc (C). (Slate blue, internal mammary nodes planning target volume [PTVimn])

planar arcs ranged from 310° to 140° with both clockwise and counterclockwise rotation illustrated in Figure 1 A, and the collimator angles were adjusted slightly according to the shape of each PTV. The non-coplanar arc angle varied from 345° to 40° (both clockwise and counterclockwise) with the couch rotating to 90° shown in Figure 1 B. According to the anatomic location of IMN, the extra dose to heart and bilateral lungs is not avoidable and usually increases with increasing PTVimn coverage. Thus, two non-coplanar arcs were designed to deliver the dose to the internal mammary chains. This was realized by limiting the maximum position of the jaw for non-coplanar arc as shown in Figure 1 C. To protect patients from collision with gantry and to spare the heart, the maximum arc angle was set to 40° in the inferior direction. Additionally, the maximal arc angle in the superior direction was 345° to protect the jaw and arms from irradiation. The four arcs were optimized with an inverse optimizer in the planning system. For coVMAT plans, identical coplanar arc angles (310° to 140°) were used, with two coplanar arcs used for optimization, for all patients.

All plans were normalized to cover at least 95% of the PTVall with the prescribed dose 50 Gy, and the proportion of volume receiving more than 55 Gy (V_{55}) in PTVall was limited to as low as possible while meeting the constraints of the heart and lungs. For the OARs, the proportion of volume of left lung receiving more than 20 Gy (V_{20}) was restricted to lower than 30%,²⁵ and the mean dose of left lung was required to be lower than 15 Gy. The dose constraints for heart were $V_{20} < 15\%$ and mean dose lower than 10 Gy.²⁶ The dose delivery to right lung, and right breast were limited with $V_5 < 10\%$ and mean dose lower than 2-3 Gy. The maximum dose of LAD was restricted to be lower than 55 Gy,

and the mean dose of LAD was limited to be lower than 25 Gy. For all patients, the optimization of parameters was similar between ncVMAT and coVMAT planning, with minor adjustments.

Plan evaluation

Several parameters such as conformity index (CI) and homogeneity index (HI) of PTV were evaluated to compare the ncVMAT and coVMAT plans. CI was based on Paddick's formula:²⁷ $CI = (TVPV)^2 / (TV \times PV)$, where TV is PTV volume, PV is the volume covered by the prescribed dose, and TVPV is the volume of PTV covered by the prescribed dose. A CI value close to 1 represents better conformity. HI was defined as follows:²⁸ $HI = D_{5\%} / D_{95\%}$, where $D_{5\%}$ and $D_{95\%}$ are doses to 5% and 95% of the target volume, and a smaller HI indicates better homogeneity. Prescription dose coverage V_{50} and hot spot V_{55} for PTVall, PTVbreast, PTVscn, and PTVimn were individually evaluated.

Regarding OARs, mean dose (D_{mean}) and proportions of volume receiving 5 Gy (V_5), 10 Gy (V_{10}), and 20 Gy (V_{20}) were calculated for the left lung. Additionally, D_{mean} , V_5 , V_{10} , V_{20} , and V_{30} for the heart; D_{mean} , V_5 , and V_{10} for the right lung and right breast; D_{mean} and maximum dose (D_{max}) for the LAD, esophagus, and left brachial plexus; D_{mean} and V_{30} for left humeral head; D_{mean} , D_{max} , and V_{30} for the thyroid gland; and D_{max} for the spinal cord were also evaluated. Monitor units (MU) for each plan were also calculated, and treatment delivery time was estimated by the treatment planning system.

All statistical analyses were performed with SPSS (version 19.0, IBM, New York, USA). If the data was normally distributed, independent samples *t* test was utilized for the analysis of data; otherwise, nonparametric Wilcoxon signed-rank test

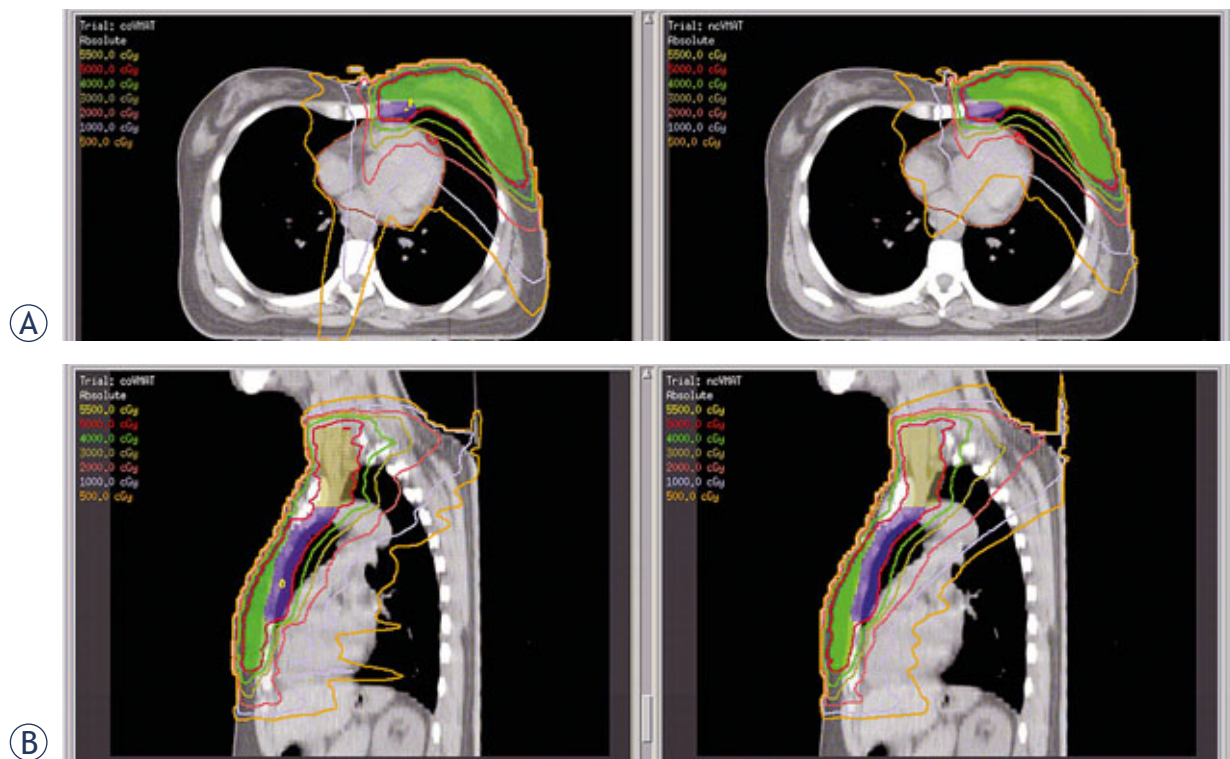


FIGURE 2. Comparison of transverse (A) and sagittal (B) distribution between coplanar volumetric modulated arc therapy [coVMAT] (left) and non-coplanar volumetric modulated arc therapy [ncVMAT] (right). (Color wash: green, breast planning target volume [PTVbreast]; slate blue, internal mammary nodes planning target volume [PTVimn]; olive, supraclavicular nodes planning target volume [PTVscn]; Contour: red, descending coronary artery [LAD]; brown, heart).

was used to compare parameters for significance. Results with a p value of < 0.05 were considered statistically significant.

Results

Figure 2 shows an example of dose distribution by ncVMAT and coVMAT, demonstrating that the dose lines from 500 cGy to 4000 cGy with ncVMAT provided better conformity for PTVbreast and PTVimn. A similar difference could also be observed in the dose-volume histogram of PTV and selected OARs (Figure 3). In this particular patient, ncVMAT provided better sparing of the LAD, heart, bilateral lungs, and right breast and better homogeneity for PTVimn.

Dosimetric evaluation of PTV

All plans were normalized to cover 95% of PTVall with the prescribed dose of 50 Gy. The dosimetric parameters of PTVbreast, PTVscn, PTVimn, and PTVall are shown in Table 1. The mean coverage

was approximately 95% for PTVbreast, PTVscn, and PTVimn, and there was no significant difference between ncVMAT and coVMAT ($p > 0.05$). Additionally, the proportion of volume receiving 110% prescribed dose V_{55} in PTVbreast, PTVscn, PTVimn, and PTVall decreased significantly comparing ncVMAT with coVMAT ($p = 0.005$). Furthermore, improved CI and HI of PTVall were achieved with ncVMAT compared to coVMAT.

Heart

In breast cancer radiotherapy, the heart should be preferentially spared. As summarized in Table 2, the average heart V_{30} , V_{20} , V_{10} , and V_5 declined significantly when using ncVMAT ($p < 0.01$). The mean dose to the heart was significantly reduced from 11.16 ± 3.45 Gy to 9.22 ± 2.98 Gy ($p < 0.001$), and the heart D_{mean} showed a decrease of 17.4%.

Lungs

As shown (Table 2), the left lung mean V_{20} , V_{10} , and V_5 declined significantly when compared ncVMAT

with coVMAT ($p < 0.001$). The contralateral lung mean V_5 and V_{10} also improved with ncVMAT ($p < 0.005$). Both the mean lung doses (MLDs) of the left and right lungs were reduced when compared with ncVMAT with coVMAT ($p < 0.001$), respectively. These results demonstrated that ncVMAT provided an improved sparing strategy for bilateral lungs when compared with coVMAT.

Right breast and LAD

The evaluation of dosimetric parameters of the right breast and LAD (Table 3) showed that the mean contralateral breast V_{10} and V_5 , and D_{mean} declined with ncVMAT ($p < 0.001$). Accordingly, the right breast V_{10} was close to 0 when planned with ncVMAT. The LAD D_{max} and D_{mean} were also improved with ncVMAT, when compared with coVMAT. The reductions in LAD D_{max} and D_{mean} were both statistically significant comparing coVMAT with ncVMAT ($p < 0.001$).

Other OARs

The evaluation of other OARs included in the study is shown in Table 3. Briefly, the D_{mean} of esophagus increased slightly with ncVMAT when compared with coVMAT ($p < 0.001$) and there was also a small decrease in the V_{30} , D_{max} , and D_{mean} of the thyroid gland, and D_{max} and D_{mean} of left brachial plexus with ncVMAT ($p < 0.05$). In addition, there were no significant differences in the V_{30} and D_{mean} of left humeral head, the D_{max} of spinal cord and esophagus ($p > 0.05$). Moreover, all dosimetric parameters of these OARs were clinically acceptable.

MU and treatment delivery time

The average MU values were 797 ± 149 and 803 ± 132 MU for ncVMAT and coVMAT, respectively, which were not significantly different ($p > 0.05$). The average treatment delivery time increased from 233 ± 25 s with coVMAT to 370 ± 31 s (include rotating the couch, approximately 60 s) with ncVMAT. The time was significantly increased with ncVMAT ($p < 0.001$).

Discussion

In the present study, ncVMAT was designed for locoregional radiotherapy of left-sided breast cancer including irradiation of IMN. For coVMAT, the heart was inevitably irradiated to cover the PTVimn

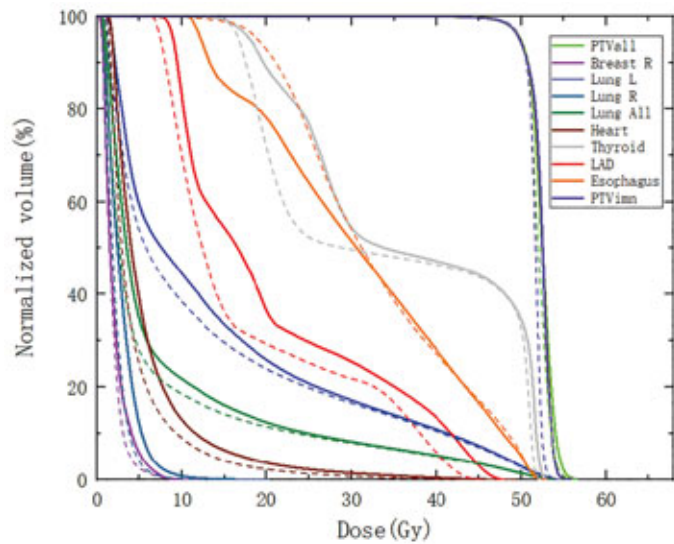


FIGURE 3. Dose-volume histogram of planning target volume (PTV) and selected organs-at-risk (OARs) (Solid line, coplanar volumetric modulated arc therapy [coVMAT]; dashed line, non-coplanar volumetric modulated arc therapy [ncVMAT]).

which was deeply located and anatomically adjacent to the heart. This was observed in Figure 2 A (left) as several sharp peak dose lines across the heart. As the dose constraints were very strict for lungs and the contralateral breast, the beam only irradiated the internal mammary chains, primarily via the vertical direction. By rotating the treatment couch to 90° , the beam irradiated internal mammary chains, more through the ipsilateral breast, the prethoracic muscles and bones, and also through

TABLE 1. Comparison of dosimetric parameters between coplanar volumetric modulated arc therapy (coVMAT) and non-coplanar volumetric modulated arc therapy (ncVMAT) for planning target volume (PTV)

	Parameters	coVMAT	ncVMAT	p
PTVall	CI	0.84 ± 0.04	0.86 ± 0.03	0.028
	HI	1.10 ± 0.02	1.09 ± 0.01	0.019
	V_{55} (%)	6.32 ± 6.35	3.46 ± 3.02	0.011
PTVimn	V_{45} (%)	99.85 ± 0.14	99.85 ± 0.21	0.67
	V_{50} (%)	95.62 ± 0.39	95.67 ± 0.73	0.94
	V_{55} (%)	4.25 ± 4.53	1.08 ± 1.88	< 0.001
PTVscn	V_{50} (%)	95.31 ± 0.43	95.37 ± 0.61	0.681
	V_{55} (%)	1.46 ± 2.89	0.22 ± 0.48	0.001
PTVbreast	V_{50} (%)	95.20 ± 0.52	94.98 ± 0.38	0.054
	V_{55} (%)	8.09 ± 8.84	4.71 ± 4.19	0.028

PTVall= total target volume; PTVbreast = breast planning target volume; PTVimn = internal mammary nodes planning target volume; PTVscn = supraclavicular nodes planning target volume

TABLE 2. Comparison of dosimetric parameters between coplanar volumetric modulated arc therapy (coVMAT) and non-coplanar volumetric modulated arc therapy (ncVMAT) for heart and lung

	Parameters	coVMAT	ncVMAT	p
Heart	V ₅ (%)	61.48 ± 19.63	48.70 ± 18.88	< 0.001
	V ₁₀ (%)	35.50 ± 15.05	26.64 ± 11.97	< 0.001
	V ₂₀ (%)	16.70 ± 8.70	13.07 ± 6.75	< 0.001
	V ₃₀ (%)	8.53 ± 5.28	6.68 ± 3.75	0.001
	Dmean (Gy)	11.16 ± 3.45	9.22 ± 2.98	< 0.001
Left lung	V ₅ (%)	71.67 ± 12.23	59.48 ± 10.51	< 0.001
	V ₁₀ (%)	47.59 ± 8.06	40.48 ± 6.41	< 0.001
	V ₂₀ (%)	26.43 ± 3.95	23.55 ± 3.05	< 0.001
	Dmean (Gy)	15.27 ± 2.03	13.59 ± 1.76	< 0.001
Contralateral lung	V ₅ (%)	9.67 ± 5.35	6.10 ± 4.19	< 0.001
	V ₁₀ (%)	0.87 ± 0.78	0.46 ± 0.50	0.003
	Dmean (Gy)	2.82 ± 0.54	2.43 ± 0.49	< 0.001

the superior and inferior direction of PTV_{imn}. Hence, the conformity of doselines from 500 cGy to 2000 cGy around PTV_{imn} was improved with ncVMAT. We clarify this in the revised manuscript. (Figure 2 A, right). This observation was character-

TABLE 3. Comparison of dosimetric parameters between coplanar volumetric modulated arc therapy (coVMAT) and non-coplanar volumetric modulated arc therapy (ncVMAT) for other organ-at-risk (OAR)

	Parameters	coVMAT	ncVMAT	p
Contralateral breast	V ₅ (%)	9.06 ± 5.22	4.98 ± 2.63	< 0.001
	V ₁₀ (%)	1.53 ± 1.60	0.23 ± 0.27	< 0.001
	Dmean (Gy)	2.62 ± 0.60	2.16 ± 0.41	< 0.001
LAD	Dmax (Gy)	48.90 ± 8.19	46.03 ± 8.20	< 0.001
	Dmean (Gy)	27.39 ± 8.20	23.25 ± 7.16	< 0.001
Left humeral head	V ₃₀ (%)	14.47 ± 16.06	13.50 ± 13.26	0.845
	Dmean (Gy)	19.96 ± 5.11	20.32 ± 5.23	0.737
Esophagus	Dmax (Gy)	51.61 ± 4.64	51.24 ± 3.90	0.052
	Dmean (Gy)	31.22 ± 5.92	33.33 ± 6.09	< 0.001
Left brachial plexus	Dmax (Gy)	54.32 ± 1.05	53.44 ± 0.98	0.004
	Dmean (Gy)	49.77 ± 2.79	49.36 ± 2.74	0.019
Thyroid	V ₃₀ (%)	45.96 ± 8.83	46.10 ± 12.47	0.044
	Dmax (Gy)	54.13 ± 0.77	53.64 ± 0.86	0.009
	Dmean (Gy)	30.79 ± 3.39	29.60 ± 4.71	0.015
Spinal cord	Dmax (Gy)	26.88 ± 5.53	29.38 ± 4.76	0.073

LAD = descending coronary artery

istic of the non-coplanar technique in delivering a higher dose from the superior and inferior direction of the target volume to increase conformity of the target. For the same reason, an improved sparing of the lungs and the contralateral breast was generated with ncVMAT as the beam irradiated more through the middle line. Another possible explanation for an increased sparing of OARs with ncVMAT was that the non-coplanar technique provided more freedom for plan optimization.

Encompassing the IMN is challenging in breast cancer radiotherapy, as it introduces extra irradiation to the heart and lungs. Approaches to reduce toxicity in adjacent OARs compromise the coverage of PTV_{imn}, and 85%²⁹ to 90%³⁰ of the prescribed dose is acceptable in clinical practice. However, the present study investigating the potential utility of ncVMAT in sparing OARs without impacting local control revealed that the coverage of PTV_{imn} was around 95% with both coVMAT and ncVMAT. A tradeoff between target coverage and possible harmful effects is inevitable, and lower coverage of the PTV_{imn} can also be utilized during planning to further reduce the dose to heart and lungs. With ncVMAT, the hot spots V₅₅ for PTV_{imn} were improved, which might provide a potential advantage in protecting anatomically adjacent vessels and nerves from high-dose irradiation.³¹ Moreover, the conformity and homogeneity of PTV_{all} were similar between ncVMAT and coVMAT plans.

Cardiac mortality associated with radiotherapy is a major concern in patients with left-sided breast cancer^{32,33}, who are at higher risk of radiation-induced ischemic heart disease and cardiovascular disease compared to patients with right-sided breast cancer. The rate of major coronary events has been reported to increase by 7.4% with every 1-Gy increase in the dose to the heart.³⁴ Therefore, it is crucial to reduce the dose delivered to heart to the greatest possible extent. In the present study, a reduction of 1.94 Gy in mean heart dose was achieved with ncVMAT; the heart V₃₀, V₂₀, V₁₀ and V₅ were significantly reduced as well. The D_{mean} of the heart with non-coplanar arcs was 9.22 ± 2.98 Gy, which was higher than data reported by Tyran *et al.*¹⁶ and Pham *et al.*³⁵; our data suggested that the dose constraints for bilateral lungs and contralateral breast used in this study were much stricter than the aforementioned studies. Equally, coverage of nodal regions by the prescription dose was reduced in their studies, when compared to a 95% coverage of 50 Gy in this study. Further, ncVMAT was compared with coVMAT with similar optimization parameters without decreasing the cov-

erage of nodal regions, while limiting the dose to lungs and contralateral breast strictly to reduce the risk of harmful effects. Obviously, the dose to the heart could be further reduced if reducing the dose constraints for lungs and contralateral breast while compromising the coverage of nodes. Some studies recommend that certain sensitive areas in heart, injury to which might cause functional damage, should be evaluated separately.³⁶ Marks *et al.* reported that the probability of cardiac perfusion defects increased significantly with the increasing volume of irradiated left ventricle using single-photon emission CT.³⁷ In a retrospective study of patients with breast cancer undergoing radiotherapy from the 1950s to 1990s, Taylor *et al.* found that the irradiation of anterior heart and LAD might have increased the risk of death from cardiac disease.³⁸ Interestingly, improved sparing of $V_{5\gamma}$, V_{10} delivered to the anterior heart, left ventricle, and LAD was possible with ncVMAT in the present study, as illustrated in Figures 2 and 3. With ncVMAT, the maximum and mean doses of LAD were also lower comparing with coVMAT ($p < 0.001$). Although further evidence is necessary to demonstrate radiation-induced dysfunction in different parts of the heart, protection of these related areas still presents potential benefits.

Radiation pneumonitis is a well-known risk of thoracic tumor radiotherapy.³⁹ For breast radiotherapy, moderate symptomatic radiation pneumonitis was not observed if the V_{20} of the ipsilateral lung was $<30\%$, as reported by Lind *et al.*⁴⁰ Furthermore, a high V_{13} indicated a worse recovery after chemotherapy for patients undergoing breast cancer radiotherapy.²⁵ For the ipsilateral lung, Wen *et al.* recommended a $V_{20} < 39.8\%$ and a $V_{30} < 25.7\%$ for patients receiving local-regional irradiation.⁴¹ Thus far, the relationship between V_5 in both the ipsilateral and the contralateral lung, and the risk of radiation pneumonitis for patients after breast cancer radiotherapy is unclear. But according to the experiences in thoracic irradiation treatment, in the present study V_5 was strictly limited to as low as possible.⁴²

In addition to pulmonary and cardiac toxicities induced by radiotherapy, a second primary breast cancer in the long term is another critical concern in young patients with breast cancer.⁴³ Stovall *et al.* reported that the risk of a second primary breast cancer in patients younger than 40 years of age increased with treatment with more than 1 Gy in the contralateral breast.⁴³ Boice *et al.* also illustrated that the risk of a second cancer was associated with age and that patients younger than 45 years

of age had a higher risk of a second cancer after irradiation of the contralateral breast.⁴⁴ Popescu *et al.*⁴⁵ and Xu *et al.*²⁰ demonstrated that VMAT had the ability to reduce irradiation of the contralateral breast compared to IMRT. In the present study, the dose delivered to contralateral breast can be reduced further with ncVMAT. Thus, ncVMAT might be preferred to reduce the risk of a second cancer in young patients.

In the present study, the doses delivered to other OARs were clinically acceptable. Clinicians always face a conflict between effective coverage of the target volume and sparing of the OARs. It remains possible to further reduce the dose delivered to specific OARs with ncVMAT by sacrificing either other OARs or coverage of the target volume, which requires further evaluation on a case-by-case basis. The treatment delivery time, including couch rotation, which was approximately 2.5 min longer with ncVMAT than with coVMAT, was still more efficient than HT (around 1000 s).²⁰ The decline in treatment efficiency with ncVMAT is acceptable to an extent with improving plan quality. Deep inspiration breath-hold (DIBH) is another effective method in reducing dose delivery to the heart.³⁵ The concept was not discussed here because free-breathing is still used in clinical practice, and DIBH was only suitable for patients capable of holding their breath to 70%–80% of the maximum inspiration capacity for a minimum 20–30 s.⁴⁶ For patients incapable of DIBH, ncVMAT is an alternative technique, which better spares the heart and other OARs.

Conclusions

The present retrospective study comparing ncVMAT with normal coVMAT for locoregional radiotherapy of left-sided breast cancer, including IMN revealed that the $V_{5\gamma}$ conformity, and homogeneity for PTVall were improved with similar coverage by introducing of two additional non-coplanar arcs. Regarding the OARs, ncVMAT provided better dose sparing in the heart, bilateral lungs, LAD, and right breast, with no significant differences for most other OARs. In conclusion, ncVMAT is potentially beneficial in reducing the risk of toxicity in left-sided breast cancer.

Acknowledgments

This work is supported by the National Natural Science Foundation of China (Grant No. 11875320)

and the National Key Projects of Research and Development of China [2017YFC0107501].

References

1. Early Breast Cancer Trialists' Collaborative Group (EBCTCG), Darby S, McGale P, Correa C, Taylor C, Arriagada R, Clarke M, et al. Effect of radiotherapy after breast-conserving surgery on 10-year recurrence and 15-year breast cancer death: meta-analysis of individual patient data for 10,801 women in 17 randomised trials. *Lancet* 2011; **378**: 1707-16. doi: 10.1016/S0140-6736(11)61629-2
2. Corradini S, Niyazi M, Niemoeller OM, Li M, Roeder F, Eckel R, et al. Adjuvant radiotherapy after breast conserving surgery—a comparative effectiveness research study. *Radiother Oncol* 2014; **114**: 28-34. doi: 10.1016/j.radonc.2014.08.027
3. Cody HS, Urban JA. Internal mammary node status: a major prognosticator in axillary node-negative breast cancer. *Ann Surg Oncol* 1995; **2**: 32-7. doi: 10.1007/BF02303699
4. Poortmans PM, Collette S, Kirkove C, Limbergen EV, Budach V, Struikmans H, et al. Internal mammary and medial supraclavicular irradiation in breast cancer. *N Engl J Med* 2015; **373**: 317-27. doi: 10.1056/NEJMoa1415369
5. Taghian A, Jagsi R, Makris A, Goldberg S, Ceilley E, Grignon L, et al. Results of a survey regarding irradiation of internal mammary chain in patients with breast cancer: practice is culture driven rather than evidence based. *Int J Radiat Oncol Biol Phys* 2004; **60**: 706-14. doi: 10.1016/j.ijrobp.2004.04.027
6. Thorsen LB, Offersen BV, Dano H, Berg M, Jensen I, Pedersen AN, et al. DBCG-IMN: a population-based cohort study on the effect of internal mammary node irradiation in early node-positive breast cancer. *J Clin Oncol* 2016; **34**: 314-20. doi: 10.1200/JCO.2015.63.6456
7. Verma V, Vicini F, Tendulkar RD, Khan AJ, Wobb J, Edwards-Bennett S, et al. Role of internal mammary node radiation as a part of modern breast cancer radiation therapy: a systematic review. *Int J Radiat Oncol Biol Phys* 2016; **95**: 617-31. doi: 10.1016/j.ijrobp.2016.01.058
8. Marks LB, Yorke ED, Jackson A, Haken RKT, Constine LS, Eisbruch A, et al. The use of normal tissue complication probability models in the clinic. *Int J Radiat Oncol Biol Phys* 2010; **76**: S10-S9. doi: 10.1016/j.ijrobp.2009.07.1754
9. Fragkandrea I, Kouloulis V, Mavridis P, Zettos A, Betsou S, Georgolopoulou P, et al. Radiation induced pneumonitis following whole breast radiotherapy treatment in early breast cancer patients treated with breast conserving surgery: a single institution study. *Hippokratia* 2013; **17**: 233-8. PMID: 24470733
10. Roychoudhuri R, Robinson D, Putcha V, Cuzick J, Darby S, Møller H, et al. Increased cardiovascular mortality more than fifteen years after radiotherapy for breast cancer: a population-based study. *BMC Cancer* 2007; **7**: 9. doi: 10.1186/1471-2407-7-9
11. Pierce SM, Recht A, Lingos TI, Abner A, Vicini F, Silver B, et al. Long-term radiation complications following conservative surgery (CS) and radiation therapy (RT) in patients with early stage breast cancer. *Int J Radiat Oncol Biol Phys* 1992; **23**: 915-23. doi: 10.1016/0360-3016(92)90895-o
12. Paszat LF, Mackillop WJ, Groome PA, Schulze K, Holowaty E. Mortality from myocardial infarction following postlumpectomy radiotherapy for breast cancer: a population-based study in Ontario, Canada. *Int J Radiat Oncol Biol Phys* 1999; **43**: 755-62. doi: 10.1016/s0360-3016(98)00412-x
13. Marks LB, Hebert ME, Bentel G, Spencer DP, Sherouse GW, Prosnitz LR. To treat or not to treat the internal mammary nodes: a possible compromise. *Int J Radiat Oncol Biol Phys* 1994; **29**: 903-9. doi: 10.1016/0360-3016(94)90584-3
14. Stranzl H, Zurl B, Langsenlehner T, Kapp KS. Wide tangential fields including the internal mammary lymph nodes in patients with left-sided breast cancer. Influence of respiratory-controlled radiotherapy (4D-CT) on cardiac exposure. *Strahlenther Onkol* 2009; **185**: 155-60. doi: 10.1007/s00066-009-1939-2
15. Popescu CC, Olivetto I, Patenaude V, Wai E, Beckham WA. Inverse-planned, dynamic, multi-beam, intensity-modulated radiation therapy (IMRT): a promising technique when target volume is the left breast and internal mammary lymph nodes. *Med Dosim* 2006; **31**: 283-91. doi: 10.1016/j.meddos.2006.05.003
16. Tyrn M, Mailleux H, Tallet A, Fau P, Gonzague L, Minsat M, et al. Volumetric-modulated arc therapy for left-sided breast cancer and all regional nodes improves target volumes coverage and reduces treatment time and doses to the heart and left coronary artery, compared with a field-in-field technique. *J Radiat Res* 2015; **56**: 927-37. doi: 10.1093/jrr/rrv052
17. Pasler M, Lutterbach J, Björnsgård M, Reichmann U, Bartelt S, Georg D. VMAT techniques for lymph node-positive left sided breast cancer. *Z Med Phys* 2015; **25**: 104-11. doi: 10.1016/j.zemedi.2014.03.008
18. Yu PC, Wu CJ, Nien HH, Lui LT, Shaw S, Tsai YL. Tangent-based volumetric modulated arc therapy for advanced left breast cancer. *Radiat Oncol* 2018; **13**: 236. doi: 10.1186/s13014-018-1167-y
19. Caudrelier JM, Morgan SC, Montgomery L, Lacelle M, Nyiri B, Macpherson M. Helical tomotherapy for locoregional irradiation including the internal mammary chain in left-sided breast cancer: dosimetric evaluation. *Radiol Oncol* 2009; **90**: 99-105. doi: 10.1016/j.radonc.2008.09.028
20. Xu YJ, Wang JB, Hu ZH, Tian Y, Ma P, Li S, et al. Locoregional irradiation including internal mammary nodal region for left-sided breast cancer after breast conserving surgery: dosimetric evaluation of 4 techniques. *Med Dosim* 2019; **44**: e13-e8. doi: 10.1016/j.meddos.2018.09.004
21. Smyth G, Evans PM, Bamber JC, Bedford JL. Recent developments in non-coplanar radiotherapy. *Br J Radiol* 2019; **92**: 20180908. doi: 10.1259/bjr.20180908
22. Fogliata A, Clivio A, Nicolini, Vanetti E, Cozzi L. A treatment planning study using non-coplanar static fields and coplanar arcs for whole breast radiotherapy of patients with concave geometry. *Radiother Oncol* 2007; **85**: 346-54. doi: 10.1016/j.radonc.2007.10.006
23. Yoo S, Blitzblau R, Yin FF, Horton JK. Dosimetric comparison of preoperative single-fraction partial breast radiotherapy techniques: 3D CRT, noncoplanar IMRT, coplanar IMRT, and VMAT. *J Appl Clin Med Phys* 2015; **16**: 5126. doi: 10.1120/jacmp.v16i1.5126
24. Xie Y, Bourgeois D, Guo B, Zhang R. Postmastectomy radiotherapy for left-sided breast cancer patients: comparison of advanced techniques. *Med Dosim* 2020; **45**: 34-40. doi: 10.1016/j.meddos.2019.04.005
25. Goldman UB, Wennberg B, Svane G, Bylund H, Lind P. Reduction of radiation pneumonitis by V20-constraints in breast cancer. *Radiat Oncol* 2010; **5**: 99. doi: 10.1186/1748-717X-5-99
26. Gagliardi G, Constine LS, Moiseenko V, Correa C, Pierce LJ, Allen AM, et al. *Int J Radiat Oncol Biol Phys* 2010; **76**(Suppl 3): S77-85. doi: 10.1016/j.ijrobp.2009.04.093
27. Paddick I. A simple scoring ratio to index the conformity of radiosurgical treatment plans. Technical note. *J Neurosurg* 2000; **93**(Suppl 3): S219-22. doi: 10.3171/jns.2000.93.supplement
28. Wang X, Zhang X, Dong L, Liu H, Gillin M, Ahamad A, Ang K, et al. Effectiveness of noncoplanar IMRT planning using a parallelized multiresolution beam angle optimization method for paranasal sinus carcinoma. *Int J Radiat Oncol Biol Phys* 2005; **63**: 594-601. doi: 10.1016/j.ijrobp.2005.06.006
29. Thorsen LB, Thomsen MS, Berg M, Jensen I, Josipovic M, Overgaard M, et al. CT-planned internal mammary node radiotherapy in the DBCG-IMN study: benefit versus potentially harmful effects. *Acta Oncologica* 2014; **53**: 1027-34. doi: 10.3109/0284186X.2014.925579
30. Poortmans PMP, Venselaar JLM, Struikmans H, Hurkmans CW, Davis JB, Huyskens D, et al. The potential impact of treatment variations on the results of radiotherapy of the internal mammary lymph node chain: a quality-assurance report on the dummy run of EORTC Phase III randomized trial 22922/10925 in Stage I-III breast cancer. *Int J Radiation Oncology Biol Phys* 2001; **49**: 1399-408. doi: 10.1016/s0360-3016(00)01549-2
31. Donovan E, Bleakley N, Denholm E, Evans P, Gothard L, Hanson J, et al. Randomised trial of standard 2D radiotherapy (RT) versus intensity modulated radiotherapy (IMRT) in patients prescribed breast radiotherapy. *Radiother Oncol* 2007; **82**: 254-64. doi: 10.1016/j.radonc.2006.12.008
32. Clarke M, Collins R, Darby S, Davies C, Elphinstone P, Evans V, et al. Effects of radiotherapy and of differences in the extent of surgery for early breast cancer on local recurrence and 15-year survival: an overview of the randomized trials. *Lancet* 2005; **366**: 2087-106. doi: 10.1016/S0140-6736(05)67887-7
33. Vallis KA, Pintilie M, Chong N, Holowaty E, Douglas PS, Kirkbride P, et al. Assessment of coronary heart disease morbidity and mortality after radiation therapy for early breast cancer. *J Clin Oncol* 2002; **20**: 1036-42. doi: 10.1200/JCO.2002.20.4.1036

34. Darby SC, Ewertz M, McGale P, Bennet AM, Blom-Goldman U, Brønnum D, et al. Risk of ischemic heart disease in women after radiotherapy for breast cancer. *N Engl J Med* 2013; **368**: 987-98. doi: 10.1056/NEJMoa1209825
35. Pham TT, Ward R, Latty D, Owen C, Gebiski V, Chojnowski J, et al. Left-sided breast cancer loco-regional radiotherapy with deep inspiration breath-hold: does volumetric-modulated arc radiotherapy reduce heart dose further compared with tangential intensity-modulated radiotherapy? *Radiat Oncol* 2016; **60**: 545-53. doi: 10.1111/1754-9485.12459
36. Gagliardi G, Lax I, Ottolenghi A, Rutqvist LE. Long-term cardiac mortality after radiotherapy of breast cancer – application of the relative seriality model. *Br J Radiol* 1996; **69**: 839-46. doi: 10.1259/0007-1285-69-825-839
37. Marks LB, Yu X, Prosnitz RG, Zhou SM, Hardenbergh PH, Blazing M. The incidence and functional consequences of RT-associated cardiac perfusion defects. *Int J Radiat Oncol Biol Phys* 2005; **63**: 214-23. doi: 10.1016/j.ijrobp.2005.01.029
38. Taylor CW, Nisbet A, McGale P, Darby SC. Cardiac exposures in breast cancer radiotherapy: 1950s-1990s. *Int J Radiat Oncol Biol Phys* 2007; **69**: 1484-95. doi: 10.1016/j.ijrobp.2007.05.034
39. Jain V, Berman AT. Radiation pneumonitis: old problem, new tricks. *Cancers* 2018; **10**: 222. doi: 10.3390/cancers10070222
40. Lind PA, Svane G, Gagliardi G, Svensson C. Abnormalities by pulmonary regions studied with computer tomography following local or localregional-radiotherapy for breast cancer. *Int J Radiat Oncol Biol Phys* 1999; **43**: 489-96. doi: 10.1016/s0360-3016(98)00414-3
41. Wen G, Tan YT, Lan XW, He ZC, Huang JH, Shi JT, et al. New clinical features and dosimetric predictor identification for symptomatic radiation pneumonitis after tangential irradiation in breast cancer patients. *J Cancer* 2017; **8**: 3795-802. doi: 10.7150/jca.21158
42. Bongers EM, Botticella A, Palma DA, Haasbeek CJA, Warner A, Verbakel WFAR, et al. Predictive parameters of symptomatic radiation pneumonitis following stereotactic or hypofractionated radiotherapy delivered using volumetric modulated arcs. *Radiother Oncol* 2013; **109**: 95-9. doi: 10.1016/j.radonc.2013.10.011
43. Stovall M, Smith SA, Langholz BM, Jr Boice JD, Shore RE, Andersson M, et al. Dose to the contralateral breast from radiotherapy and risk of second primary breast cancer in the WECARE study. *Int J Radiat Oncol Biol Phys* 2008; **72**: 1021-30. doi: 10.1016/j.ijrobp.2008.02.040
44. Boice JD Jr, Harvey EB, Blettner M, Stovall M, Flannery JT. Cancer in the contralateral breast after radiotherapy for breast cancer. *N Engl J Med* 1992; **326**: 781-5. doi: 10.1056/NEJM199203193261201
45. Popescu CC, Olivetto IA, Beckham WA, Ansbacher W, Zavgorodni S, Shaffer R, et al. Volumetric modulated arc therapy improves dosimetry and reduces treatment time compared to conventional intensity-modulated radiotherapy for locoregional radiotherapy of left-sided breast cancer and internal mammary nodes. *Int J Radiat Oncol Biol Phys* 2010; **76**: 287-95. doi: 10.1016/j.ijrobp.2009.05.038
46. Yamauchi R, Mizuno N, Itazawa T, Saitoh H, Kawamori J. Dosimetric evaluation of deep inspiration breath hold for left-sided breast cancer: analysis of patient-specific parameters related to heart dose reduction. *J Radiat Res* 2020; **61**: 447-56. doi: 10.1093/jrr/rraa006

Verification of an optimizer algorithm by the beam delivery evaluation of intensity-modulated arc therapy plans

Tamas Pocza^{1,2}, Domonkos Szegedi¹, Tibor Major^{1,3}, Csilla Pesznyak^{1,2}

¹ Center of Radiotherapy, National Institute of Oncology, Budapest, Hungary

² Institute of Nuclear Techniques, Budapest University of Technology and Economics, Hungary

³ Department of Oncology, Semmelweis University, Budapest, Hungary

Radiol Oncol 2021; 55(4): 508-515.

Received 25 June 2021

Accepted 17 August 2021

Correspondence to: Tamas Pocza, National Institute of Oncology, Hungary. E-mail: pocza.tamas@oncol.hu

Disclosure: No potential conflicts of interest were disclosed

This is an open access article under the CC BY-NC-ND license (<http://creativecommons.org/licenses/by-nc-nd/4.0/>).

Background. In the case of dynamic radiotherapy plans, the fractionation schemes can have dosimetric effects. Our goal was to define the effect of the fraction dose on the plan quality and the beam delivery.

Materials and methods. Treatment plans were created for 5 early-stage lung cancer patients with different dose schedules. The planned total dose was 60 Gy, fraction dose was 2 Gy, 3 Gy, 5 Gy, 12 Gy and 20 Gy. Additionally renormalized plans were created by changing the prescribed fraction dose after optimization. The dosimetric parameters and the beam delivery parameters were collected to define the plan quality and the complexity of the treatment plans. The accuracy of dose delivery was verified with dose measurements using electronic portal imaging device (EPID).

Results. The plan quality was independent from the used fractionation scheme. The fraction dose could be changed safely after the optimization, the delivery accuracy of the treatment plans with changed prescribed dose was not lower. According to EPID based measurements, the high fraction dose and dose rate caused the saturation of the detector, which lowered the gamma passing rate. The aperture complexity score, the gantry speed and the dose rate changes were not predicting factors for the gamma passing rate values.

Conclusions. The plan quality and the delivery accuracy are independent from the fraction dose, moreover the fraction dose can be changed safely after the dose optimization. The saturation effect of the EPID has to be considered when the action limits of the quality assurance system are defined.

Key words: treatment planning system; fractionation scheme; dose optimization; plan normalization

Introduction

Lung cancer is one of the leading causes of cancer death in the world.¹ An early diagnosed non-small cell lung cancer (NSCLC) patient nowadays has a chance for longer survival, because of the emerging treatment techniques. In radiotherapy the rapid technical development allows to perform more effective treatments using higher doses for better tu-

mor control. The standard radiotherapy treatment for patients was carried out by applying only a total dose of 60 Gy with 2 Gy per fraction (biological effective dose $BED_{10} = 72$ Gy). The stereotactic body radiation therapy (SBRT) is the standard radiation treatment for early stage, nodal negative lung cancer that can be irradiated with up to 60 Gy in 3 fractions ($BED_{10} = 180$ Gy).²⁻⁵ The local tumor control of SBRT treatments is comparable with the surgical

resection, and can be performed also for patients judged inoperable due to other comorbidities.⁶⁻⁹

The dose prescription according to recommendations has to be risk adapted, and the size and location of tumor influence the maximum deliverable doses; that way fractionation schemes are used multifariously as well as the daily fraction dose.¹⁰⁻¹⁶

During SBRT planning the main goal is to reach high dose conformity and steep dose gradient around the target volume to spare the dose to the organs at risk. In case of stereotactic treatments to ensure acceptable dose gradient, there is a dose prescription for an isodose line (IDL), and with this method, steeper dose fall-off can be achieved in return for higher dose maximum.¹⁷⁻²¹ Many studies recommend various methods for the optimal selection of the prescribed IDL.²²⁻²⁴

Earlier, in the era of static fields, delivery discrepancies were not caused by the change of the prescribed IDL in clinical practice. SBRT techniques are performed with intensity modulated dynamic fields²⁵ and in this case if the original fraction dose or the prescribed IDL is changed, the delivery parameters are modified - compared to the original optimized ones - which can have an effect on the accuracy of beam delivery.

The uncertainties in radiotherapy are widely presented in the literature, but the effect of the fraction dose value has not been examined deeply.²⁶ In our experience, discrepancies can be caused in the operation of the optimizer by the application of extremely low or high fraction dose values (e.g. few cGy). The aim of our work is to compare plan quality and the deliverability of radiotherapy treatment plans with different dose per fraction values used in clinical practice. We have examined the effect of changing the normalization values from the original optimized ones to other dose per fraction values. The potential pitfalls of the variation of the dose per fraction values were also determined.

Materials and methods

Case selection

Five lung SBRT patients were selected for the study and a set of treatment plans with various parameters were created. 4D CT scan was performed for all patients with a Siemens Definition AS Open (Siemens AG, Erlangen, Germany) scanner and the breathing motion was monitored using the adjustable belt of AZ-733V (Anzai Medical, Tokyo, Japan). The scan parameters were based on the clinically used protocol with 120 kVp without kV modulation, and 2 mm slice thickness. According to the breathing pattern 7 (+1 average) image sets were created with retrospective reconstruction. For target definition the internal target volume (ITV) concept was used. The radiation oncologist delineated the gross tumor volume (GTV) on each of the 7 image sets. No margin was applied between the GTV and the clinical target volume (CTV). The accumulated GTV was created on the average CT and 5 mm additional margin was used to create the planning target volume (PTV). All of the lesions were peripheral, at least 1 cm from the rib cage and mediastinum. During the selection we have strived to create a heterogeneous group, the parameters of the patients and the targets can be found in Table 1.

Treatment planning

5 different fractionation schemes were defined for all patients, 60 Gy total dose with 2, 3, 6, 12, and 20 Gy fraction dose, that way the number of fractions were 30, 20, 12, 5 and 3, respectively. The treatment plans were created with Eclipse 13.6 treatment planning system's Photon Optimizer 13.6 algorithm (Varian Medical Systems, Palo Alto, CA, USA), and delivered on a TrueBeam (Varian Medical Systems, Palo Alto, CA, USA) machine. The isocenter was placed in the geometrical center of the PTV, 4 restricted arcs were defined using 6 MV-flattening

TABLE 1. The parameters of the selected patients and irradiated volumes

Sex	Age [years]	Lobe	GTV_volume [ccm]	Tumor movement [mm]	ITV_volume [ccm]	PTV_volume [ccm]
Male	84	Right-lower	3.7	20	10.7	33.3
Male	66	Left-upper	1.3	4	2.2	11.5
Male	72	Left-upper	4.8	5	7.2	24.9
Female	61	Right-mid	2.6	4	3.9	15.1
Female	67	Right-mid	0.7	2	1.1	7.6

GTV = gross tumor volume; ITV = internal target volume; PTV = planning target volume

TABLE 2. The mean values and the standard deviations of the plan quality parameters

	2 Gy/fraction	3 Gy/fraction	6 Gy/fraction	12 Gy/fraction	20 Gy/fraction
PTV_D _{mean} (cGy)	6706±96	6713±85	6701±97	6715±91	6686±96
PTV_V95 (%)	98.17±2.34	98.44±1.61	98.32±1.72	98.43±1.67	98.22±1.93
PTV_V100 (%)	91.12±5.29	91.85±4.34	91.31±4.63	91.82±4.54	90.78±4.93
PTV_V98 (%)	94.9±4.24	95.47±3.28	94.97±3.54	95.39±3.48	94.75±3.84
PTV_D98 (cGy)	5759±141	5771±116	5760±128	5773±126	5755±128
PTV_D50 (cGy)	6749±128	6762±107	6750±125	6760±119	6726±125
PTV_D2 (cGy)	7515±114	7472±94	7461±106	7487±91	7454±87
ITV_D _{mean} (cGy)	7234±150	7229±126	7113±301	7124±262	7106±272
ITV_D98 (cGy)	6867±130	6901±101	6862±152	6877±125	6848±144
ITV_D50 (cGy)	7242±154	7229±134	7221±145	7238±117	7219±105
ITV_D2 (cGy)	7581±164	7556±162	7531±150	7561±142	7539±166
BODY_V100 (ccm)	17.1±9.56	17.25±9.64	17.13±9.66	17.24±9.72	17.16±9.57
BODY_V50 (ccm)	75.02±35.16	75.09±35.17	74.96±35.68	75.31±35.79	74.74±35.45
BODY_V98 (ccm)	18.2±10.03	18.34±10.11	18.22±10.13	18.34±10.19	18.1±10.16
D _{max} (cGy)	7816±128	7777±106	7731±106	7794±16	7691±288
Lung_V5Gy (%)	15.57±7.25	15.51±7.31	15.59±7.24	15.57±7.3	15.56±7.26
Lung_V20Gy (%)	4.25±2.32	4.28±2.33	4.25±2.33	4.27±2.34	4.26±2.34
Lung_D _{mean} (cGy)	342±148	343±149	342±149	343±149	342±149
# MU / cGy	2.84±0.15	2.81±0.1	2.8±0.12	2.81±0.11	2.81±0.12
R50%	4.27±0.52	4.27±0.51	4.25±0.51	4.27±0.5	4.24±0.49
CI98%_PTV	0.93±0.06	0.94±0.05	0.93±0.06	0.94±0.05	0.94±0.06
CN98%_PTV	0.9±0.03	0.91±0.02	0.91±0.02	0.91±0.02	0.91±0.03

CI = conformity index; CN = conformity number; ITV = internal target volume; MU = monitor units; PTV = planning target volume; R50% = calculated dose gradient

filter-free (FFF) energy and the maximal (1400 MU/min) dose rate. The primary jaws were fitted with 5 mm margin to the PTV, the jaw tracking was enabled. The final dose was calculated by AcurosXB algorithm with dose-to-water setting and 0.125 cm grid size. The optimization parameters were different patient by patient, but were kept the same between the different fractionations. The final results of optimizations were not changed, the minimum PTV coverage was V95% > 99 % and V98% > 95%, and the dose to organs at risk had to be fit for clinically used limitations, based on the European Organization for Research and Treatment of Cancer (EORTC) recommendations¹¹. After that, the original optimized plans were copied and the prescribed doses were changed for all the 4 other values. This way every patient had 25 different plans with 5 different fractionation schemes.

Data collection

For every plan the PTV coverage parameters were evaluated. The dose to the lung and the whole-

body volume were also examined. The statistical analysis of plan quality was performed with GraphPad 8.0.1 (GraphPad Software, San Diego, CA) using ANOVA and post-hoc Dunn's test. The delivery parameters such as the number of monitor units (MU), gantry speed and dose rate values were also collected. To characterize the multi-leaf collimator (MLC) motions aperture complexity metric (ACM) was determined for all beams by using a homemade software, according to the definition of Younge *et al.*²⁷ The score was calculated as:

$$ACM = \frac{1}{MU} \sum_{i=1}^N MU_i \times \frac{y_i}{A_i}$$

whereas

- MU is the total number of MUs in the plan,
- i = 1 to N control point apertures,
- MU_i is the number of MU delivered through aperture i,
- A_i is the open area of aperture i,
- y_i is the aperture perimeter excluding the MLC leaf ends,

and to calculate the score of a given arc, the metrics of all apertures have to be summed.

To evaluate the deliverability of the treatment plans, electronic portal imaging device (EPID) based dose measurement was performed with the portal dosimetry system using Portal Dose Image Prediction (PDIP) 13.6 algorithm (Varian Medical Systems, Palo Alto, CA, USA). The linear accelerator was equipped with an aS1200 Digital Megavolt Imager. Just before the measurements the linear accelerator and the EPID absolute were calibrated to ensure the most accurate results. The gamma analysis was performed for the 500 arcs in absolute mode with 2%, 1 mm parameters, 10% threshold, and the auto alignment was allowed. The maximum and central axis calibrated unit (CU) values of portal dose predictions and measurements were also collected and evaluated.

The meaning of phrases used in the Results section:

- Optimization dose: The dose per fraction value set before (during) the optimization.
- Normalization dose: The dose per fraction value set after the optimization.
- Optimized plan: The optimization dose and the normalization dose are equal.
- Renormalized plans: The optimization dose and the normalization dose are different.

Results

Renormalization does not change the *dose-volume histogram* (DVH) parameters compared to optimized plans. That way for the comparison of the

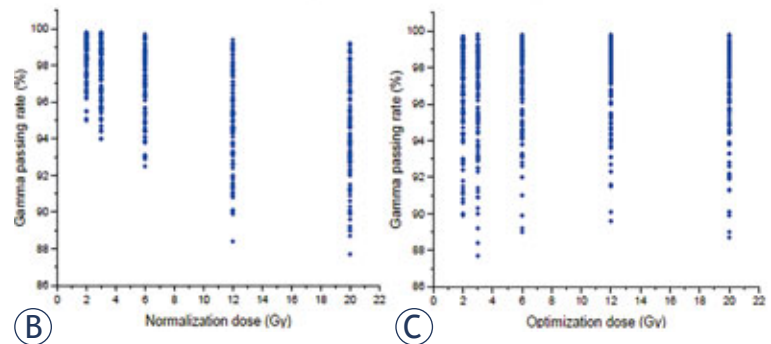
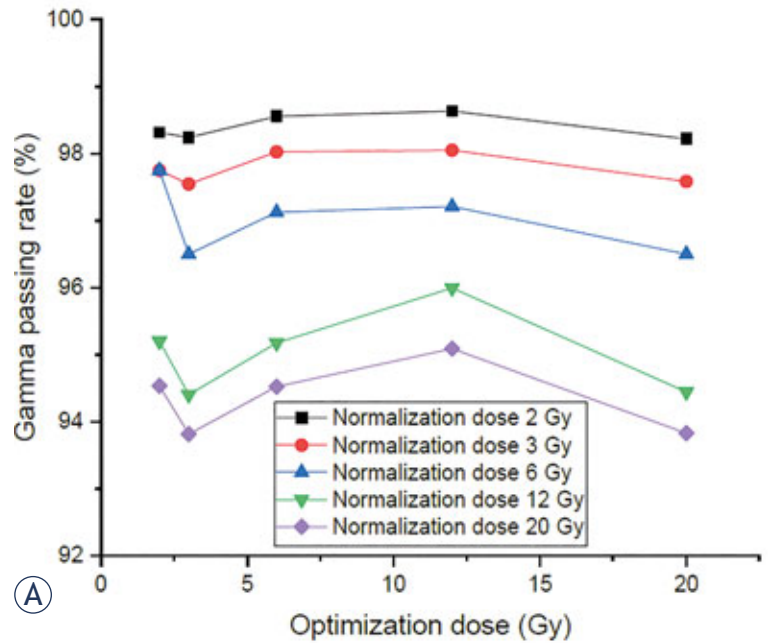


FIGURE 1. (A) The average value of gamma passing rates according to the used optimization separated by normalization, and the gamma passing rates according to the normalization (B) and optimization (C) dose values.

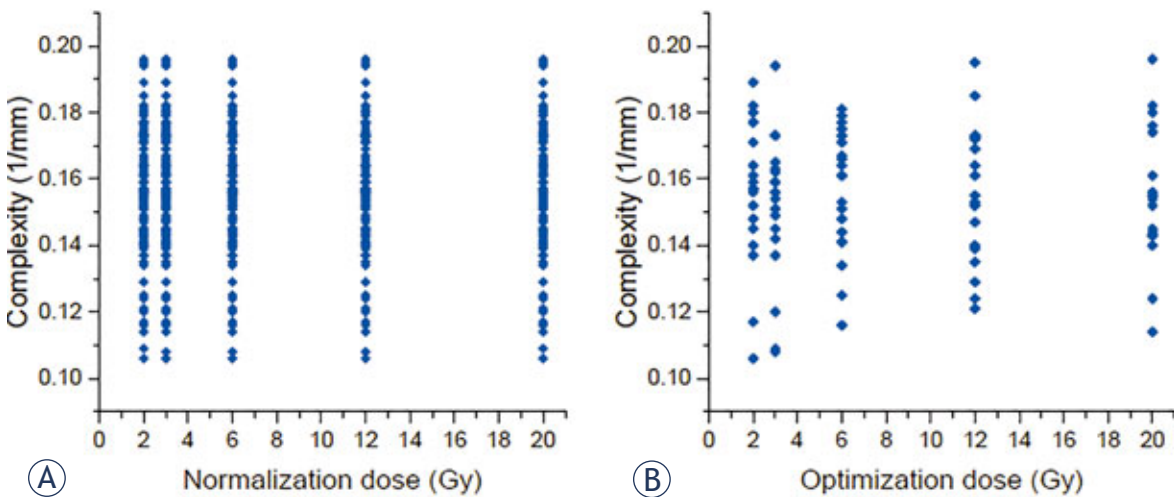


FIGURE 2. The effect of the normalization dose (A) and the optimization dose (B) values on the aperture complexity metric (ACM) score.

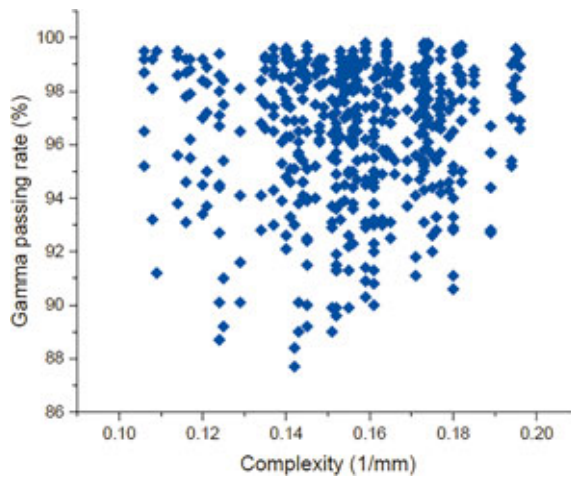


FIGURE 3. The connection between the complexity score and the gamma passing rate.

plan quality metrics, only the optimized plans have to be included. We compared the mean values of the dosimetric parameters of the five patients. PTV and ITV coverage parameters, dose to

lung and whole body parameters were evaluated.²⁸ Conformity index (CI) and conformity number (CN) were calculated for the PTV.²⁹ The dose gradient was described by R50% which is calculated as the ratio of the volume enclosed by the 50% isodose surface and the volume of the PTV.²⁹ There was no significant difference between any of the daily fraction size plans. The average values and the standard deviations of the parameters are summarized in Table 2. Based on the statistical tests, there was no significant difference between the optimization schedules.

The dependence of gamma values on the optimization and the normalization dose values were also investigated. Figure 1 presents that the gamma passing rates are independent from the optimization values, renormalization has no effect on the results. However, the higher fraction dose reduces the passing rates, independently of the used original optimization dose value.

Figure 2A indicates that the renormalization has no effect on the MLC motions. This can be concluded from the same pattern of ACM scores for differ-

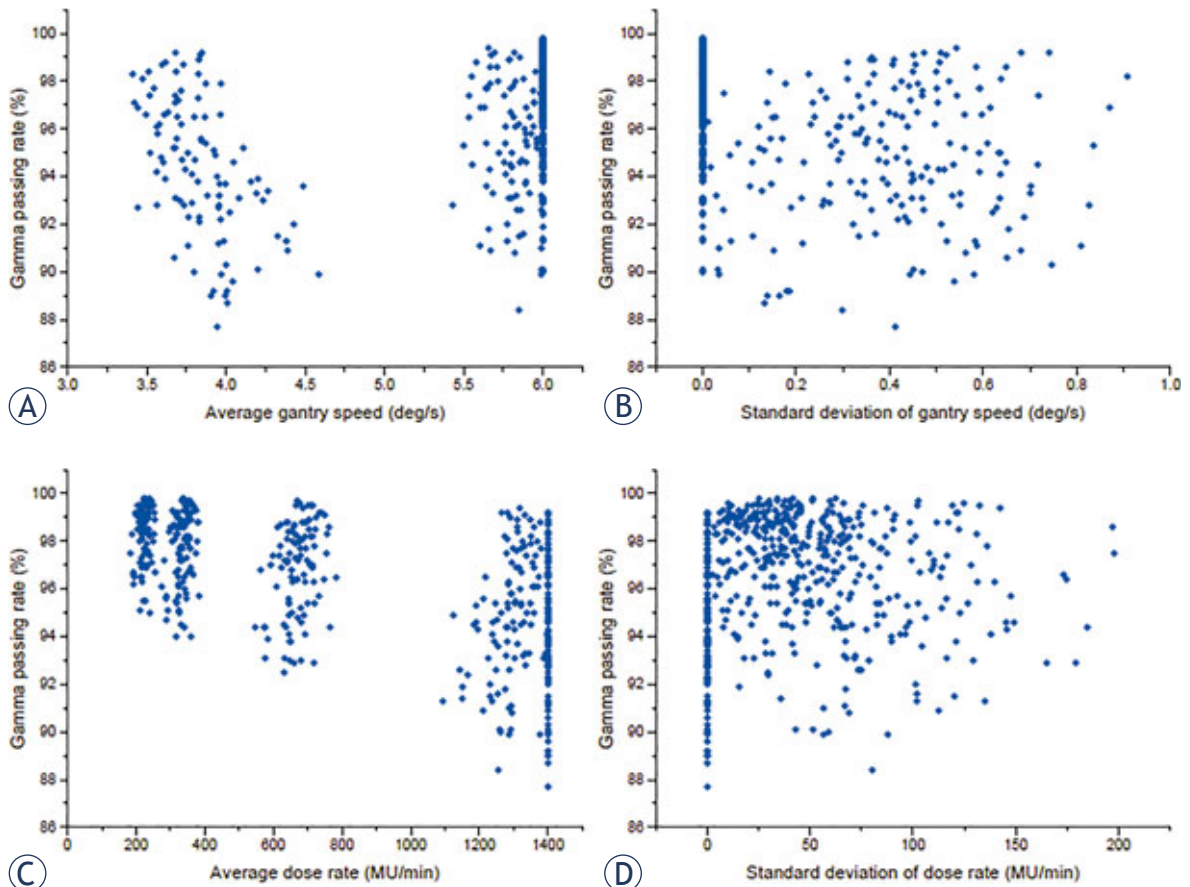


FIGURE 4. The effect of the average gantry speed (A) and standard deviation (B), and the average dose rate (C) and standard deviation (D) on the gamma passing rates.

ent normalization doses. Only the speed of delivery (gantry speed and dose rate) is changed with renormalization. According to Figure 2B, there is no connection between the optimization dose and the complexity metric.

The implementation of the calculated dose maps has no crucial effect on the accuracy of delivery. The optimizer tries to maximize the gantry speed and the enabled dose rate. For higher dose per fraction cases these limits are reached, which can be concluded from the constant mean and zero standard deviation values. In case of high MLC modulation, it is necessary to lower the speed of the delivery. The deviations of gantry speed and dose rate can be used as the describing parameters of the modulation of delivery. According to our data ACM, gantry speed and dose rate values do not correlate with gamma passing rates, as shown in Figure 3 and 4.

The predicted and measured CU values were separately evaluated to define the origin of the differences at high fraction dose. As Figure 5 shows, the deviation of predicted values is low, the CU/Gy values are quasi constant with the changing fraction dose. Meanwhile the measured maximum and the central-axis values are decreasing with the increasing fraction dose, which means the detector has a saturation effect.

Discussion

As can be shown in Table 2, the different optimization fractional dose has no significant effect on plan quality. To our knowledge, this is the first study to examine the effect of prescription dose on the plan quality for volumetric modulated radiotherapy treatment plans.

Figure 1 shows that the accuracy of the beam delivery does not change after changing normalization values. According to average gamma passing rate values there was a slight trend for reducing passing rates compared to the original optimization in case of the renormalization of 5 times 12 Gy plans. In case of 3 Gy per fraction the average gamma values were higher after renormalization. The data was analyzed even patient by patient, but we did not find any trend. As can be seen more clearly in Figure 1B, the higher fraction doses are decreasing, meanwhile the used optimization dose has no well-defined effect on the gamma passing rates, as can be seen in Figure 1C. The lower passing rates in case of high fraction dose can be caused by the limitation of the EPID detection for high dose levels.

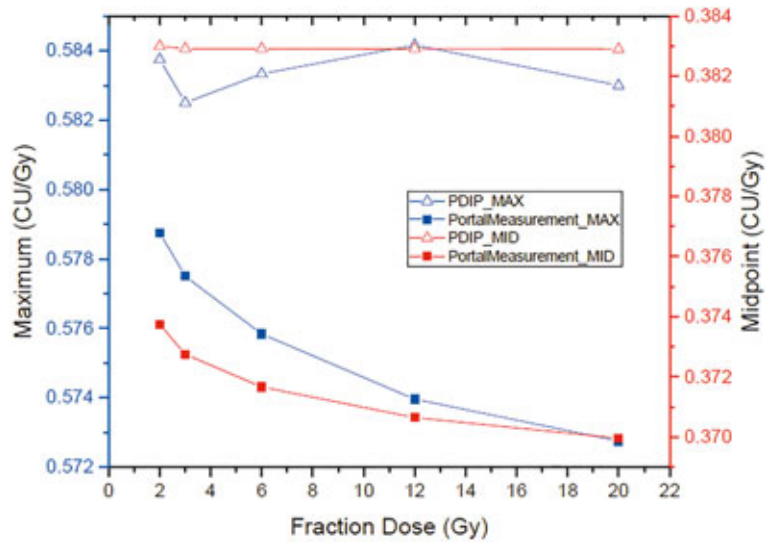


FIGURE 5. The predicted and measured number of maximum (blue) and the central-axis (red) calibrated units (CU) for 1 Gy according to the fraction dose.

PDIP = portal dose image prediction;

This saturation effect is more expressed than the impact of changing fraction dose. Former studies have verified the usability of the Portal Dosimetry system by testing the EPID based dose measurements.³⁰⁻³² Barbeiro *et al.* have demonstrated with synthetic tests that a slight decrease in response linearity can be observed at the high exposures with FFF beams.³³ Xu *et al.* found that the detector panel has a saturation in case of high dose-rate beams, but it was clinically insignificant even at the maximum dose rate of 2400 MU/min.³⁴ Pardo *et al.* and Miri *et al.* investigated FFF beam dosimetry plans and found no clinically relevant deviations, but in these studies plans were not included using beams over ca. 1000 MU.^{35,36} Our test plans have high dose and high dose-rate values, that way the two small effects are summed and lead to increased deviations. Keeping the same optimization and using renormalization it was possible to evaluate the pure effect of the fraction size. According to our results the saturation effect can be clinical relevant using 6 MV-FFF energy with high dose-rate (1400 MU/min) and high fraction dose values, because it decreases the absolute CU values and the gamma passing rates. During the definition of action limits this effect has to be considered.³⁷⁻⁴⁰

Renormalization is a conservative, more rough diversion of the original, optimized plan, than changing prescribed isodose line. In that way any clinically relevant isodose level can be used for prescription, even a different fractionation scheme

can be safely applied without reoptimization. The change of the normalization after optimization keeps the DVH parameters, and the accuracy of dose delivery has no relevant diversion according to gamma passing rate results.

Hernandez *et al.* concluded that Varian machines prefer using MLCs or changing dose rates for dose modulation instead of gantry rotation speed.⁴¹ To describe the complexity of a treatment plan many types of metrics are used in radiotherapy.^{42,43} The ACM, which is applied for evaluation in this study, is related only to the MLC movement. According to our results the changed dose normalization does not change the MLC sequence, as can be concluded from Figure 2A. Meanwhile as Figure 2B shows, the used fraction dose during optimization has no effect on the ACM score. There is no consensus in the literature about the predictive usage of complexity metrics; for example, Park *et al.* have found correlation between metrics and gamma passing rates, but according to the study of Glenn *et al.* for a different metric there is no correlation.^{44–46} Based on our results, which can be seen in Figure 3, there is no clear connection between the complexity of the MLC pattern (ACM) and the gamma passing rates.

The changes (mean values and deviations) of gantry speed and dose rate or control point analysis can also be used to describe the modulation level of a treatment plan.⁴⁷ Huang *et al.* have made comparisons for cranial irradiation plans, focused on the changing dose rate and MU values and they found that plans with low daily dose, very high dose rate have to be handled carefully.⁴⁸ Our results show that the speed parameters of delivery do not predict the results of gamma analysis, as it is illustrated in Figure 4.

The strength of our study was the systematic and comprehensive analysis of the effect of different fraction dose values. The limitation of our results is caused by using only one measurement system (Portal Dosimetry), but this way it was possible to reach excellent spatial resolution and eliminate the additional errors from the usage of different measurement systems. Further investigation can be applied for in-vivo measurements and other beam energies.^{49–52}

The fraction dose used for optimization and the quality of the plan are independent from each other. Varying the prescribed isodose line can be applied safely, the delivery accuracy of the treatment plan is constant, moreover, the fraction dose can be changed after the dose optimization. Plan delivery parameters such as ACM, gantry speed and

dose rate changes do not predict the gamma passing rate values. According to the EPID-based dose measurements the gamma passing rate decreases in the case of high fraction dose and high dose-rate beams. This effect is caused by the saturation of the MV detector panel which has to be considered when the action limits of quality assurance system are defined.

Acknowledgments

This study was supported by the Hungarian Thematic Excellence Program of the Hungarian National Research Development and Innovation Office under grant Nr. TKP2020-NKA-26.

References

1. Ferlay J, Colombet M, Soerjomataram I, Mathers C, Parkin DM, Piñeros M, et al. Estimating the global cancer incidence and mortality in 2018: GLOBOCAN sources and methods. *Int J Cancer* 2019; **144**: 1941-53. doi: 10.1002/ijc.31937
2. Maciejczyk A, Skrzypczyńska I, Janiszewska M. Lung cancer. Radiotherapy in lung cancer: actual methods and future trends. *Reports Pract Oncol Radiother* 2014; **19**: 353-60. doi: 10.1016/j.rpor.2014.04.012
3. Videtic GMM., Donington J., Giuliani M., et al. Stereotactic body radiation therapy for early-stage non-small cell lung cancer: executive summary of an ASTRO Evidence-Based Guideline. *Pract Radiat Oncol* 2017; **7**: 295-301. doi: 10.1016/j.prro.2017.04.014
4. Cheng M, Jolly S, Quarshie WO, Kapadia N, Vigneau FD, Kong FM. Modern radiation further improves survival in non-small cell lung cancer: an analysis of 288,670 patients. *J Cancer* 2019; **10**: 168-77. doi: 10.7150/jca.26600
5. Vinod SK, Hau E. Radiotherapy treatment for lung cancer: current status and future directions. *Respirology* 2020; **25**(Suppl 2): 61-71. doi: 10.1111/resp.13870
6. Shah JL, Loo BW. Stereotactic ablative radiotherapy for early-stage lung cancer. *Semin Radiat Oncol* 2017; **27**: 218-28. doi: 10.1016/j.semradonc.2017.03.001
7. Tian S, Higgins KA, Curran WJ, Cassidy RJ. Stereotactic body radiation therapy vs. surgery in early-stage nonsmall cell lung cancer: lessons learned, current recommendations, future directions. *J Thorac Dis* 2018; **10**: 1201-4. doi: 10.21037/jtd.2018.01.161
8. Shinde A, Li R, Kim J, Salgia R, Hurria A, Amini A. Stereotactic body radiation therapy (SBRT) for early-stage lung cancer in the elderly. *Semin Oncol* 2018; **45**: 2010-9. doi: 10.1053/j.seminoncol.2018.06.002
9. Chi A, Fang W, Sun Y, Wen S. Comparison of long-term survival of patients with early-stage non-small cell lung cancer after surgery vs stereotactic body radiotherapy. *JAMA Netw Open* 2019; **2**: e1915724. doi: 10.1001/jamanetworkopen.2019.15724
10. Lagerwaard FJ, Haasbeek CJA, Smit EF, Slotman BJ, Senan S. Outcomes of risk-adapted fractionated stereotactic radiotherapy for stage I non-small-cell lung cancer. *Int J Radiat Oncol Biol Phys* 2008; **70**: 685-92. doi: 10.1016/j.ijrobp.2007.10.053
11. De Ruysscher D, Faivre-Finn C, Moeller D, Nestle U, Hurkmans CW, Le Péchoux C, et al. European Organization for Research and Treatment of Cancer (EORTC) recommendations for planning and delivery of high-dose, high precision radiotherapy for lung cancer. *Radiother Oncol* 2017; **124**: 1-10. doi: 10.1016/j.radonc.2017.06.003
12. Guckenberger M, Andratschke N, Dieckmann K, Hoogeman MS, Hoyer M, Hurkmans C, et al. ESTRO ACROP consensus guideline on implementation and practice of stereotactic body radiotherapy for peripherally located early stage non-small cell lung cancer. *Radiother Oncol* 2017; **124**: 11-7. doi: 10.1016/j.radonc.2017.05.012

13. Temming S, Kocher M, Stoelben E, Hagemeyer L, Chang DH, Frank K, et al. Risk-adapted robotic stereotactic body radiation therapy for inoperable early-stage non-small-cell lung cancer. *Strahlentherapie Und Onkol* 2018; **194**: 91-7. doi: 10.1007/s00066-017-1194-x
14. de Jong EEC, Guckenberger M, Andratschke N, Dieckmann K, Hoogeman MS, Milder M, et al. Variation in current prescription practice of stereotactic body radiotherapy for peripherally located early stage non-small cell lung cancer: Recommendations for prescribing and recording according to the ACROP guideline and ICRU report 91. *Radiother Oncol* 2020; **142**: 217-23. doi: 10.1016/j.radonc.2019.11.001
15. Ruggieri R, Stavrev P, Naccarato S, Stavreva N, Alongi F, Nahum AE. Optimal dose and fraction number in SBRT of lung tumours: A radiobiological analysis. *Phys Medica* 2017; **44**: 188-95. doi: 10.1016/j.ejmp.2016.12.012
16. Atalar B, Mustafayev TZ, Sio TT, Sahin B, Gungor G, Aydin G, et al. Long-term toxicity and survival outcomes after stereotactic ablative radiotherapy for patients with centrally located thoracic tumors. *Radiol Oncol* 2020; **54**: 480-7. doi: 10.2478/raon-2020-0039
17. Widder J, Hollander M, Ubbels JF, Bolt RA, Langendijk JA. Optimizing dose prescription in stereotactic body radiotherapy for lung tumours using Monte Carlo dose calculation. *Radiother Oncol* 2010; **94**: 42-6. doi: 10.1016/j.radonc.2009.11.008
18. Ewing MM, Desrosiers C, Fakiris AJ, DeBlik CR, Kiszka DN, Stinson ER, et al. Conformality study for stereotactic radiosurgery of the lung. *Med Dosim* 2011; **36**: 14-20. doi: 10.1016/j.meddos.2009.10.004
19. Chan M, Wong M, Leung R, Cheung S, Blanck O. Optimizing the prescription isodose level in stereotactic volumetric-modulated arc radiotherapy of lung lesions as a potential for dose de-escalation. *Radiat Oncol* 2018; **13**: 1-11. doi: 10.1186/s13014-018-0965-6
20. Meng MB, Wang HH, Zaorsky NG, Sun BS, Zhu L, Song YC, et al. Risk-adapted stereotactic body radiation therapy for central and ultra-central early-stage inoperable non-small cell lung cancer. *Cancer Sci* 2019; **110**: 3553-64. doi: 10.1111/cas.14185
21. Tsurugai Y, Takeda A, Sanuki N, Eriguchi T, Aoki Y, Oku Y, et al. Stereotactic body radiotherapy for patients with non-small-cell lung cancer using RapidArc delivery and a steep dose gradient: prescription of 60% isodose line of maximum dose fitting to the planning target volume. *J Radiat Res* 2019; **60**: 364-70. doi: 10.1093/jrr/rry112
22. Oku Y, Takeda A, Kunieda E, Sudo Y, Oooka Y, Aoki Y, et al. Analysis of suitable prescribed isodose line fitting to planning target volume in stereotactic body radiotherapy using dynamic conformal multiple arc therapy. *Pract Radiat Oncol* 2012; **2**: 46-53. doi: 10.1016/j.proro.2011.06.001
23. Ding C, Solberg T, Xing L, Heinzerling J, Timmerman R. SU-E-T-451: optimization of normalized prescription isodose selection for stereotactic radiation therapy: conventional vs. robotic linac. *Med Phys* 2012; **39**: 3808-9. doi: 10.1118/1.4735540
24. Zheng D, Zhang Q, Liang X, Zhu X, Verma V, Wang S, et al. Effect of the normalized prescription isodose line on the magnitude of Monte Carlo vs. pencil beam target dose differences for lung stereotactic body radiotherapy. *J Appl Clin Med Phys* 2016; **17**: 48-58. doi: 10.1120/jacmp.v17i4.5965
25. Dickey M, Roa W, Drodge S, Ghosh S, Murray B, Scrimger R, et al. A planning comparison of 3-dimensional conformal multiple static field, conformal arc, and volumetric modulated arc therapy for the delivery of stereotactic body radiotherapy for early stage lung cancer. *Med Dosim* 2015; **40**: 347-51. doi: 10.1016/j.meddos.2015.04.006
26. Schwarz M, Cattaneo GM, Marrazzo L. Geometrical and dosimetric uncertainties in hypofractionated radiotherapy of the lung: a review. *Phys Medica* 2017; **36**: 126-39. doi: 10.1016/j.ejmp.2017.02.011
27. Younge KC, Roberts D, Janes LA, Anderson C, Moran JM, Matuszak MM. Predicting deliverability of volumetric-modulated arc therapy (VMAT) plans using aperture complexity analysis. *J Appl Clin Med Phys* 2016; **17**: 124-31. doi: 10.1120/jacmp.v17i4.6241
28. Yaparalvi R, Garg MK, Shen J, Bodner WR, Mynampati DK, Gafar A, et al. Evaluating which plan quality metrics are appropriate for use in lung SBRT. *Br J Radiol* 2018; **91**: 1-8. doi: 10.1259/bjr.20170393
29. Feuvret L, Noël G, Mazeron JJ, Bey P. Conformity index: a review. *Int J Radiat Oncol Biol Phys* 2006; **64**: 333-42. doi: 10.1016/j.ijrobp.2005.09.028
30. Esch A Van, Huyskens DP, Hirschi L, Scheib S, Baltas C. Optimized varian aSi portal dosimetry: development of datasets for collective use. *J Appl Clin Med Phys* 2013; **14**: 82-99. doi: 10.1120/jacmp.v14i6.4286
31. Moghadam SE, Nasserri S, Seyedi SS, Gholamhosseinian H, Momennezhad M. Evaluation of application of EPID for rapid QC testing of linear accelerator. *Reports Pract Oncol Radiother* 2018; **23**: 369-77. doi: 10.1016/j.rpor.2018.07.008
32. Min S, Choi YE, Kwak J, Cho B. Practical approach for pretreatment verification of IMRT with flattening filter-free (FFF) beams using varian portal dosimetry. *J Appl Clin Med Phys* 2015; **16**: 40-50. doi: 10.1120/jacmp.v16i1.4934
33. Barbeiro AR, Parent L, Vieilleveigne L, Ferrand R, Franceries X. Dosimetric performance of continuous EPID imaging in stereotactic treatment conditions. *Phys Medica* 2020; **78**: 117-22. doi: 10.1016/j.ejmp.2020.09.009
34. Xu Z, Kim J, Han J, Hsia AT, Ryu S. Dose rate response of digital megavolt imager detector for flattening filter-free beams. *J Appl Clin Med Phys* 2018; **19**: 141-7. doi: 10.1002/acm2.12358
35. Pardo E, Novais JC, López MYM, Maqueda SR. On flattening filter-free portal dosimetry. *J Appl Clin Med Phys* 2016; **17**: 132-45. doi: 10.1120/jacmp.v17i4.6147
36. Miri N, Keller P, Zwan BJ, Greer P. EPID-based dosimetry to verify IMRT planar dose distribution for the aS1200 EPID and FFF beams. *J Appl Clin Med Phys* 2016; **17**: 292-304. doi: 10.1120/jacmp.v17i6.6336
37. Xia Y, Adamson J, Zlateva Y, Giles W. Application of TG-218 action limits to SRS and SBRT pre-treatment patient specific QA. *J Radiosurgery SBRT* 2020; **7**: 135-47. PMID: 33282467
38. Alharthi T, Arumugam S, Vial P, Holloway L, Thwaites D. EPID sensitivity to delivery errors for pre-treatment verification of lung SBRT VMAT plans. *Phys Medica* 2019; **59**: 37-46. doi: 10.1016/j.ejmp.2019.02.007
39. Son J, Baek T, Lee B, Shin D, Park SY, Park J, et al. A comparison of the quality assurance of four dosimetric tools for intensity modulated radiation therapy. *Radiol Oncol* 2015; **49**: 307-13. doi: 10.1515/raon-2015-0021
40. Radojic DS, Rajlic D, Casar B, Kolacio MS, Obajdin N, Faj D, et al. Evaluation of two-dimensional dose distributions for pre-treatment patient-specific IMRT dosimetry. *Radiol Oncol* 2018; **52**: 346-52. doi: 10.2478/raon-2018-0019
41. Hernandez V, Saez J, Pasler M, Jurado-Bruggeman D, Jorner N. Comparison of complexity metrics for multi-institutional evaluations of treatment plans in radiotherapy. *Phys Imaging Radiat Oncol* 2018; **5**: 37-43. doi: 10.1016/j.phro.2018.02.002
42. Chiavassa S, Bessieres I, Edouard M, Mathot M, Moignier A. Complexity metrics for IMRT and VMAT plans: a review of current literature and applications. *Br J Radiol* 2019; **92**. doi: 10.1259/bjr.20190270
43. Xu Z, Wang IZ, Kumaraswamy LK, Podgorsak MB. Evaluation of dosimetric effect caused by slowing with multi-leaf collimator (MLC) leaves for volumetric modulated arc therapy (VMAT). *Radiol Oncol* 2016; **50**: 121-8. doi: 10.1515/raon-2016-0008
44. Park JM, Park SY, Kim H. Modulation index for VMAT considering both mechanical and dose calculation uncertainties. *Phys Med Biol* 2015; **60**: 7101-25. doi: 10.1088/0031-9155/60/18/7101
45. Park JM, Wu HG, Kim JH, Carlson JNK, Kim K. The effect of MLC speed and acceleration on the plan delivery accuracy of VMAT. *Br J Radiol* 2015; **88**: 16-24. doi: 10.1259/bjr.20140698
46. Glenn MC, Hernandez V, Saez J, Followill DS, Howell RM, Pollard-Larkin JM, et al. Treatment plan complexity does not predict IROC Houston anthropomorphic head and neck phantom performance. *Phys Med Biol* 2018; **63**. doi: 10.1088/1361-6560/aae29e
47. Abdellatif A, Gaede S. Control Point Analysis comparison for 3 different treatment planning and delivery complexity levels using a commercial 3-dimensional diode array. *Med Dosim* 2014; **39**: 174-9. doi: 10.1016/j.meddos.2013.12.005
48. Huang L, Zhuang T, Mastroianni A, Djemil T, Cui T, Xia P. Impact of small MU/segment and dose rate on delivery accuracy of volumetric-modulated arc therapy (VMAT). *J Appl Clin Med Phys* 2016; **17**: 203-10. doi: 10.1120/jacmp.v17i3.6046
49. Esposito M, Villaggi E, Bresciani S, Cilla S, Falco MD, Garibaldi C, et al. Estimating dose delivery accuracy in stereotactic body radiation therapy: A review of in-vivo measurement methods. *Radiother Oncol* 2020; **149**: 158-67. doi: 10.1016/j.radonc.2020.05.014
50. Olaciregui-Ruiz I, Beddar S, Greer P, Jorner N, McCurdy B, Paiva-Fonseca G, et al. In vivo dosimetry in external beam photon radiotherapy: Requirements and future directions for research, development, and clinical practice. *Phys Imaging Radiat Oncol* 2020; **15**: 108-16. doi: 10.1016/j.phro.2020.08.003
51. Consorti R, Fidanzio A, Brainovich V, Mangiacotti F, De Spirito M, Mirri MA, et al. EPID-based in vivo dosimetry for stereotactic body radiotherapy of non-small cell lung tumors: Initial clinical experience. *Phys Medica* 2017; **42**: 157-61. doi: 10.1016/j.ejmp.2017.09.133
52. McCurdy BMC, McCowan PM. In vivo dosimetry for lung radiotherapy including SBRT. *Phys Medica* 2017; **44**: 123-30. doi: 10.1016/j.ejmp.2017.05.065

Radiol Oncol 2021; 55(4): 379-392.
doi: 10.2478/raon-2021-0042

MitomiR: njihova vloga v mitohondrijih in njihov pomen v metabolizmu rakavih celic

Renčelj A, Gvozdenović N, Čemažar M

Izhodišča. MikroRNA (miRNA) so kratke nekodirajoče RNA, ki imajo pomembno vlogo v skoraj vseh bioloških poteh. Urejajo post-transkripcijsko izražanje genov z vezavo na 3' neprevedeno regijo (3'UTR) informacijske RNA (mRNA). MitomiR so miRNA jedrnega ali mitohondrijskega izvora, ki so lokalizirane v mitohondrijih in so pomembni regulatorji mitohondrijske funkcije in presnove. Pri evkariontih so mitohondriji glavna mesta oksidativne presnove sladkorjev, lipidov, aminokislin in drugih biomakromolekul. So tudi glavna mesta proizvodnje adenozin trifosfata (ATP).

Zaključki. V prispevku razpravljamo o vlogi mitomiR-jev v mitohondrijih in predstavimo pomembne mitomiR-je, njihove ciljne gene in funkcije. Prav tako razpravljamo o njihovi vlogi pri zagonu in napredovanju raka z regulacijo izražanja mRNA v mitohondrijih. MitomiR-ji neposredno ciljajo na ključne molekule, kot so transporterji ali encimi v celičnem metabolizmu, in uravnavajo več onkogenih signalnih poti. Imajo tudi pomembno vlogo pri Warburgovem učinku, ki je ključnega pomena za ohranitev proliferacijskega potenciala v rakavih celicah. Razpravljamo tudi, kako posredno regulirajo heksokinazo 2 (HK2), encim, ki sodeluje pri fosforilaciji glukoze, in tako lahko vplivajo na energetske presnovo v celicah raka dojke. V tumorskih tkivih, kot so rak dojke in tumorji glave in vratu, je izražanje enega od mitomiR (miR-210) korelirano z geni hipoksije, kar kaže na neposredno povezavo med izražanjem mitomiR-jev in hipoksijo pri raku. Dokazano je, da grozd miR-17/92 deluje kot onkogen z zaviranjem apoptoze in je dereguliran pri limfomih B-celic, kronični limfocitni levkemiji B-celic, akutni mieloični levkemiji in limfomih T-celic ter je še posebej prekomerno izražen pri več vrstah raka. Na podlagi dosedanjih spoznanj lahko sklepamo, da je v mitohondrijih prisotno veliko miRNA, imenovanih mitomiR in da so pomembni regulatorji delovanja mitohondrijev. Zato so mitomiR pomembni akterji v presnovi rakavih celic, ki jih je potrebno nadalje raziskati, da bi lahko razvili potencialne nove terapije za zdravljenje raka.

Radiol Oncol 2021; 55(4): 393-408.
doi: 10.2478/raon-2021-0040

Nadzor gibanja tarče pri radioterapiji raka dojke

Piruzan E, Vosoughi N, Mahdavi SR, Khalafi L, Mahani H

Izhodišča. V zadnjih dveh desetletjih rak dojke ostaja glavni vzrok smrti zaradi raka pri ženskah. Pokazalo se je, da je radioterapija (RT) učinkovita tudi pri zdravljenju te vrste raka. Spopada pa se z gibanjem organov znotraj obsevalnih frakcij, kar je posledica dihanja. Problem je pri raku leve dojke hujši zaradi bližine srca, ki spada med t.i. rizične organe. Razporeditev doze pri obsevanju z delci je boljša kot pri konvencionalni RT, vendar je zaradi fizikalnih interakcij delcev v telesu takšno obsevanje bolj pogojeno z gibanjem tarče.

Zaključki. Osvetljujemo obstoječe in razvijajoče načine za obvladovanje gibanja tarče med intrafrakcijami pri obsevanju raka dojke. Poseben pomen ima terapiji z delci, ki je najsodobnejša tehnika obsevanja. Prenos tehnologij za spremljanje gibanja v realnem času s fotonskih žarkov na žarke delcev prinaša veliko izzivov. Površinsko slikanje se kaže kot prevladujoč način slikanja za spremljanje znotrajfrakcijskega gibanja raka dojke v realnem času. Zdi se, da sta slikovni nadzor z magnetno resonanco in RT z zelo visoko hitrostjo doze (FLASH-RT) najsodobnejša pristopa 4-dimenzionalne RT raka dojke.

Radiol Oncol 2021; 55(4): 409-417.
doi: 10.2478/raon-2021-0037

Raziskava korelacije med računalniškotomografskimi lastnostmi možganskih trombov z izidom zdravljenja pri bolnikih z možgansko kapjo

Viltušnik R, Vidmar J, Fabjan A, Jeromel M, Milošević ZV, Kocijančič IJ, Serša I

Izhodišča. Bolniki s sumom na možgansko kap diagnosticiramo z računalniško tomografijo (CT) možganov. Želeli smo preveriti možnost ugotavljanja zgodnje ishemije in pri tem ovreči druge diagnoze. V primeru ishemične možganske kapi uporabljamo CT (vključno s CT angiografijo) predvsem za določanje okluzije in njene velikosti. Vrednosti Hounsfieldovih enot (HU) pri trombu, ki povzroča možgansko kap, pa običajno spregledamo ali štejeemo za nepomembne. Namen raziskave je bil pokazati, da je vrednost HU pomembna in lahko pomaga pri boljšem načrtovanju zdravljenja.

Bolniki in metode. V raziskavo smo vključili 25 bolnikov z diagnozo ishemične možganske kapi v segmentu srednje možganske arterije (MCA). Pri nekaterih bolnikih namreč sistemska tromboliza ni uspešna in potrebna je bila mehanska rekanalizacija. Trombe smo histološko analizirali za določitev deleža eritrocitov. Iz slik CT-ja smo določili povprečno vrednost HU in njihovo variabilnost v proksimalnem segmentu MCA M1, tako v zaprtem odseku žile kot tudi na simetričnem normalnem mestu. Ta dva parametra CT-ja smo nato statistično preučili. Iskali smo možne korelacije z različnimi kliničnimi, histološkimi in postopkovnimi parametri ter uporabili linearno regresijo in Pearsonov korelacijski koeficient.

Rezultati. Ugotovili smo pozitivne korelacije med povprečno vrednostjo HU tromba in spremenjeno Rankinovo lestvico (mRS), številom trombektomijskih posegov in z deležem eritrocitov v trombu.

Zaključki. Rezultati raziskave kažejo, da lahko izmerjene vrednosti HU na slikah CT-ja možganskih trombov pomagajo pri oceni gostote trombov in s tem boljšemu načrtovanju zdravljenja.

Radiol Oncol 2021; 55(4): 418-425.
doi: 10.2478/raon-2021-0029

Vloga native faze računalniške tomografije jeter v protokolu za slikanje metastatskega raka dojke. Vpliv na senzitivnost, oceno odziva in meritve velikosti

Arenas-Jiménez JJ, García-Garrigós E, Planells-Alduvín MC

Izhodišča. Namen raziskave je bil analizirati, ali izvedba native računalniške tomografije (CT) jeter v primerjavi s samo portalno fazo prispeva k vrednotenju metastatskih lezij, oceni odziva in razliki v meritvah velikosti lezij pri bolnicah z jetrnimi metastazami raka dojke.

Bolniki in metode. V analizo smo vključili 153 preiskav CT pri 36 bolnicah. Preiskave smo izvedli v nativni, arterijski in zakasneni portalni fazi jeter. Dva ocenjevalca sta opredelila, katera faza je bila najboljša za prikaz metastaz in ocenila število lezij, zaznanih v vsaki fazi. Izbrala sta najboljšo fazo za oceno odziva v dveh zaporednih preiskavah in izmerila eno tarčno lezijo v vseh fazah. Za primerjavo razlik med fazami smo uporabili X^2 (Hi-kvadrat test), za razlike med meritvami pa t-test.

Rezultati. Ocenjevalca (1/2) sta nativno, arterijsko in portalno fazo štela kot boljšo možnost v 68/67 %, 27/28 % in 69/70 %. Posamezne lezije so bile spregledane v 2 %, 11 % in 7 %. Senzitivnost je bila pri nativni in portalni fazi bistveno boljša kot pri arterijski fazi. Primerjava med zaporednimi preiskavami je bila najboljša pri nativni fazi (80/79 %), sledili sta portalna faza (70/69 %) in arterijska faza (31/31 %). Največji premer tarčnih lezij je bil v nativni fazi za 15 % večji ($p < 0.001$).

Zaključki. Portalna in nativna faza sta omogočila boljšo zaznavo in zamejitev metastaz raka dojke v jetrih. V večini primerov je bil nativni CT najboljša faza za oceno odziva in je prikazal največji premer lezij. Priporočamo uporabo nativega CT pri oceni bolnic z rakom dojke ob sumu na metastaze oz. znanih jetrnih metastazah.

Radiol Oncol 2021; 55(4): 426-432.

doi: 10.2478/raon-2021-0043

Diagnostični pomen števila obarvanih celic s p16/Ki-67 v brisu materničnega vratu pri ženskah, ki smo jih obravnavali v kolposkopski ambulanti

Salobir Gajšek U, Dovnik A, Takač I, Ivanuš U, Jerman T, Šramek Zatler S, Repše Fokter A

Izhodišča. Namen raziskave je bil opredeliti pomen dvojnega imunocitokemičnega barvanja p16/Ki-67 in pomen števila pozitivnih celic v brisu materničnega vratu pri diagnosticiranju intraepitelijske lezije visoke stopnje na materničnem vratu (CIN 2+) pri ženskah, ki smo jih obravnavali v kolposkopski ambulanti.

Subjekti in metode. V raziskavo smo vključili 174 žensk, ki so bile že obravnavane v randomizirani nadzorovani raziskavi *Humani papilomavirus (HPV) test doma* v okviru Slovenskega organiziranega presejalnega programa za odkrivanje raka materničnega vratu, programa ZORA. Analizirali smo dvojno imunocitokemično barvanje p16/Ki-67 brisa materničnega vratu ter število pozitivno obarvanih celic s p16/Ki-67 pri 174 ženskah pregledanih v kolposkopski ambulanti.

Rezultati. Med obravnavanimi ženskami jih je 42 od 174 (24,1 %) imelo histološki izvid CIN 2+. Tveganje prisotnosti CIN 2+ je rastlo s številom s p16/Ki-67 obarvanih celic v brisu materničnega vratu ($p < 0,001$). Skupna občutljivost p16/Ki-67 za odkrivanje CIN2+ je bila 88,1 %, specifičnost 65,2 %, pozitivna napovedna vrednost 44,6 %, negativna napovedna vrednost pa 94,5 %.

Zaključki. Dvojno imunocitokemično barvanje p16/Ki-67 je v pričujoči raziskavi pokazalo visoko občutljivost in visoko negativno napovedno vrednost pri odkrivanju CIN 2+ in je primerljivo z nam dostopnimi objavljenimi raziskavami. Določitev števila pozitivnih celic v brisu materničnega vratu, obarvanih s p16/Ki-67 ima dodatno statistično značilen vpliv v odkrivanju CIN 2+. Sprememba meje pozitivnega testa p16/Ki-67 iz ene obarvane celice na tri obarvane celice statistično pomembno zviša specifičnost in klinično uporabnost testa.

Radiol Oncol 2021; 55(4): 433-438.
doi: 10.2478/raon-2021-0026

Primerjava robotsko asistirane in laparoskopske kirurgije raka debelega črevesa in danke. Raziskava s kontrolno skupino

Grosek J, Košir JA, Sever P, Erčulj V, Tomažič A

Izhodišča. Robotsko asistirane operacije predstavljajo novejši pristop h kirurškemu zdravljenju raka debelega črevesa in danke. Namen raziskave je bil kritično ovrednotiti implementacijo abdominalnega robotskega kirurškega programa ter ga primerjati z uveljavljenim laparoskopskim pristopom.

Bolniki in metode. V retrospektivni raziskavi s kontrolno skupino smo primerjali rezultate zdravljenja po robotskih in laparoskopskih operacijah. Vključili smo bolnike z rakom debelega črevesa in zgornje tretjine danke, ki sta jih dva kirurga operirala na Univerzitetnem kliničnem centru v Ljubljani v obdobju 2019–2020. S pomočjo univariatne logistične regresije smo ugotavljali povezave med značilnostmi bolnikov, vrsto in dolžino operacije, preklpom v odprti kirurški poseg, trajanjem hospitalizacije, pooperativno obolevnostjo ter številom odstranjenih bezgavk.

Rezultati. Vključitvenim kriterijem je ustrezalo 86 bolnikov, 46 po robotskih in 37 po laparoskopskih resekcijah. Obe skupini bolnikov sta bili primerljivi tako glede značilnosti bolnikov kot tudi samega operativnega zdravljenja. Robotske operacije so trajale statistično pomembno dlje od laparoskopskih ($p < 0,001$), hkrati pa so imeli ti bolniki manjše tveganje za preklp v odprti kirurški poseg ($p = 0,004$). Po robotskih resekcijah je manj bolnikov potrebovalo transfuzijo krvnih derivatov ($p = 0,004$) in manj bolnikov je bilo ponovno operiranih ($p = 0,026$). Med obema skupinama ni bilo statistično pomembnih razlik v dolžini hospitalizacije ($p = 0,026$), številu odstranjenih bezgavk ($p = 0,24$) kot tudi ne v deležu zapletov po operaciji ($p = 0,58$).

Zaključki. Kratkoročni rezultati robotsko asistiranih resekcij debelega črevesa in danke so bili primerljivi laparoskopskim resekcijam. Manj bolnikov v robotski skupini je potrebovalo transfuzijo krvnih derivatov, prav tako so imeli ti bolniki manjše tveganje tako za preklp v odprti kirurški poseg, kot tudi za ponovno operacijo.

Radiol Oncol 2021; 55(4): 439-448.

doi: 10.2478/raon-2021-0028

Predoperativna intenzitetno-modulirana radiokemoterapija s sočasnim dodatkom doze pri raku danke. 5-letni rezultati klinične raziskave II. faze

But-Hadžić J, Meden Boltežar A, Škerl T, Zadnik V, Velenik V

Izhodišča. V klinični raziskavi II. faze smo preverili učinkovitost in varnost predoperativne radiokemoterapije pri lokalno napredovalem raku danke z namenom izboljšati izid zdravljenja. Izvedli smo eksperimentalno frakcionacijo in uporabili intenzitetno modulirano radioterapijo (IMRT) s simultano integriranim dodatkom doze. Želeli smo skrajšati celokupni čas obsevanja brez povišanja celokupna doze.

Bolniki in metode. Med januarjem 2014 in januarjem 2015 smo v raziskavo vključili 51 bolnikov z operabilnim rakom danke stadija II-III. Petdeset bolnikov je zaključilo predoperativno obsevanje z IMRT in elektivno dozo 41,8 Gy ter simultanim dodatkom doze 46,2 Gy na T2/T3 in 48,4 Gy na T4 tumor v 22 frakcijah. Sočasno so prejeli tudi kapecitabin (825 mg/m²/12 ur, vključno z vikendi). Srednji čas sledenja je bil 70 mesecev.

Rezultati. Zdravljenje po protokolu je končalo 47 bolnikov. Akutna toksičnost se je pojavila pri 2 (4 %) bolnikih. Resekcija R0 je bila dosežena pri 98 % bolnikov in patološko popoln odgovor pri 12 (25,5 %) bolnikih. Pri bolnikih s patološko popolnim odgovorom je bilo petletno celokupno preživetje 91,7 %, preživetje brez bolezni 100-odstotno in lokalna kontrola 100-odstotna. Analiza vpliva dejavnikov na preživetje je pokazala pomemben vpliv tipa operacije na celokupno preživetje in preživetje brez bolezni, medtem ko sta se celokupno znižanje stadija in pN izkazala za pomembni napovedni dejavnik samo za preživetje brez bolezni. Bolniki, ki so bili zdravljeni po protokolu, so imeli celokupno preživetje 80,9 % (95 % interval zaupanja [IZ] 69,7–92,1), preživetje brez bolezni 77,1 % (95 % IZ, 65,1–89,1) in lokalno kontrolo bolezni 95,2 % (95 % IZ 88,7–100). Delež bolnikov s hudo pozno (EORTC G ≥ 3) toksičnostjo prebavil, sečil in spolne funkcije je bil 15 %, 2 % in 8 %. Pri enem bolniku smo ugotovili pojav sekundarnega raka.

Zaključki. Predoperativno IMRT s simultano integriranim dodatkom doze in brez dviga celokupne doze so bolniki dobro prenašali. Akutna toksičnost je bila sprejemljiva. Dosegli smo visoko stopnjo patološko popolnih odgovorov in prikazali vzpodbudno 5-letno celokupno preživetje, preživetje brez bolezni in lokalno kontrolo.

Radiol Oncol 2021; 55(4): 449-458.
doi: 10.2478/raon-2021-0039

Vloga hematoloških parametrov pri napovedovanju odziva na radikalno kemoradioterapijo pri bolnikih s ploščatoceličnim rakom analnega kanala

Stojanović-Rundić S, Marinković M, Čavić M, Plešinac Karapandžić V, Gavrilović D, Janković R, de Voer RM, Castellvi-Bel S, Krivokapić Z

Izhodišča. V preteklosti je bila izbira zdravljenja raka analnega kanala abdominoperinealna resekcija. Radikalna radioterapija s sočasno kemoterapijo 5-fluorouracila in mitomicina C je bila kasneje uveljavljena kot standardno zdravljenje, čeprav je bil delež neuspešnosti 20–30 %. Cilj pričujoče raziskave je bil ovrednotiti rezultate po radikalni kemoradioterapiji, napovedne dejavnike za odgovor na zdravljenje in za potek bolezni ter vzorce neuspešnosti.

Bolniki in metode. V raziskavo smo vključili 47 bolnikov, ki smo jih zdravili z radikalno kemoradioterapijo zaradi patohistološko potrjenega ploščatoceličnega raka anusa. Analizirali smo hematološke parametre: razmerje nevtrofilcev in limfocitov, razmerje trombocitov in limfocitov in raven hemoglobina. Odziv tumorja na zdravljenje smo ocenili 24 tednov po zaključku kemoradioterapije. V prvih dveh letih smo bolnike pregledali vsake 3 mesece, nato pa vsakih 6 mesecev.

Rezultati. Popoln klinični odgovor na kemoterapevtsko zdravljenje smo ugotovili pri 30 bolnikih (63,8 %). Bolnike, ki niso dosegli 6-mesečnega popolnega odgovora, in tiste, ki so imeli popoln odgovor po 6 mesecih, a se je bolezen nato ponovila, smo napotili na kirurško zdravljenje. S kombinirano kemoradioterapijo in kirurškim reševalnim zdravljenjem smo dosegli popolno remisijo pri 80,9 % bolnikov. Bolniki s popolnim odgovorom na zdravljenje po 6 mesecih so imeli bistveno daljši čas brez ponovitve bolezni, čas brez napredovanja bolezni in celokupno preživetje. Končni logistični regresijski model je vključeval raven hemoglobina pred zdravljenjem in obdobje prekinitve zdravljenja. Statistično pomemben učinek na 6-mesečni odgovor je bil potrjen pri razmerju trombocitov in limfocitov ($p = 0,03$).

Zaključki. Pomembni napovedni dejavniki, povezani s popolnim odgovorom, so bili izhodiščna raven hemoglobina in obdobje prekinitve zdravljenja. Potencialna hematološka napovedna dejavnika poteka bolezni sta lahko razmerje trombocitov in limfocitov ter razmerje nevtrofilcev in limfocitov, ki ju je mogoče rutinsko določiti z nizkocenovnimi in minimalno invazivnimi metodami.

Radiol Oncol 2021; 55(4): 459-466.

doi: 10.2478/raon-2021-0038

Hipofrakcionirana predoperativna radioterapija za visoko tvegane sarkome mehkih tkiv pri geriatričnih bolnikih

Potkrajčić V, Traub F, Hermes B, Scharpf M, Kolbenschlag J, Zips D, Paulsen F, Eckert F

Izhodišča. Standardna terapija za lokalizirane, resektabilne sarkome mehkih tkiv z visokim tveganjem obsega široko resekcijo in večtedensko radioterapijo. Ta načrt zdravljenja je pri geriatričnih in šibkih bolnikih komaj izvedljiv. Da pri teh bolnikih ne bi odlašali z radioterapijo, smo pri populaciji geriatričnih bolnikov ovrednotili hipofrakcionirano obsevanje z dozo 25 Gy v 5 frakcijah.

Bolniki in metode. Opravili smo retrospektivno analizo 18 geriatričnih bolnikov z resektabilnimi sarkomi mehkih tkiv ekstremitet in prsne stene z visokim tveganjem. Analizirali smo celjenje ran in pooperativni potek bolezni. Poleg tega smo dozne omejitve za radioterapijo okončin prenesli iz standardno frakcioniranih na hipofrakcionirane sheme obsevanja.

Rezultati. Izvedljivost je bila dobra, saj je 17/18 bolnikov zaključilo načrtovano zdravljenje. Stopnja zapletov pri celjenju ran je bila primerljiva z objavljenimi podatki drugih raziskav. Pri dveh bolnikih se je pojavila lokalna in oddaljena ponovitev, dva bolnika sta imela le oddaljene ponovitve. Izoliranih lokalnih recidivov nismo opazili. V vseh primerih smo lahko upoštevali dozne omejitve in pri tem nismo ogrožali pokritosti tarčnega volumna.

Zaključki. Hipofrakcionirano obsevanje in operativno zdravljenje so dobro prenašali tudi geriatrični bolniki. Izvedljivost ob upoštevanju zgodnjega celjenja ran in prilagojenih doznih omejitvah je bila velika. Tako smo lahko zdravili večino resektabilnih tumorjev okončin. Takšen način zdravljenja bo smiselno oceniti tudi pri drugih bolnikih, ki niso primerni za standardno radioterapijo.

Radiol Oncol 2021; 55(4): 467-473.
doi: 10.2478/raon-2021-0041

Radikalna radioterapija skvamoznega raka ustne votline. Izkušnje posamičnega centra

Lang K, Baur M, Held T, El Shafie R, Moratin J, Freudlsperger C, Zaoui K, Bougatf N, Hoffmann J, Plinkert PK, Debus J, Adeberg S

Izhodišča. Kirurgija je metoda izbora zdravljenja raka ustne votline. Primarno neresektibilno obliko bolezni pa lahko zdravimo z radikalno radioterapijo z ali brez sočasne sistemske terapije. Poročamo o izkušnji posamičnega onkološkega centra.

Bolniki in metode. V retrospektivno analizo smo zajeli 49 bolnikov z nemetastatskim primarnim rakom ustne votline, ki je bil neoperabilen. Bolnike smo zdravili z radikalno radioterapijo v letih med 2000 in 2019. Večina bolnikov je prejela tudi sočasno sistemske terapijo, radiokemoterapijo 63,3 % bolnikov, monokemoterapijo s cetuximabom enkrat tedensko pred radikalno radioterapijo pa 26,5 % bolnikov. Pet bolnikov je bilo zdravljenih samo z radikalno radioterapijo zaradi omejene bolezni brez invazije v bezgavke.

Rezultati. Srednji čas spremljanja bolnikov je bil 73 mesecev (6–236 mesecev), srednji čas do napredovale bolezni 42 mesecev (2–157 mesecev), srednji čas brez lokalne ponovitve bolezni 44 mesecev (2–157 mesecev) in srednje preživetje bolnikov od radioterapije je bilo 52 mesecev (5–236 mesecev). Po zdravljenju smo zabeležili 65,3 % lokoregionalnih, 84,4 % lokalnih in 15,6 oddaljenih primerov ponovitve bolezni. Večina bolnikov z lokalnimi ponovitvami je imelo po kriterijih Ameriškega združenja za raka (*angl. American Joint Committee on Cancer; AJCC*) stadij bolezni III–IV (59,2 %). Ocena za petletno celokupno preživetje po Kaplan-Meierjevi metodi je bila za bolnike s stadijem bolezni III–IV 22,8 % za bolnike s stadijem I–II pa 54,2 % ($p = 0,03$; razmerje obetov [HR] 2,090; 1,1–4,2). Bolniki, ki so bili zdravljeni s sočasno sistemske terapijo, so imeli statistično značilno boljše celokupno preživetje v primerjavi z tistimi zdravljenimi samo z radioterapijo (43,9 % vs. 23,1 %; $p = 0,05$; 1,0–4,1). Radioterapija z dozami pod 79 Gy je bila povezana s slabšim celokupnim preživetjem bolnikov ($p = 0,046$, HR 2,1; 1,0–4,5). Mukozitis gradusa 3 je bil najpogostejši akutni stranski učinek, ki smo ga opazili pri 19 bolnikih (39 %). Kronični stranski učinki so bili izguba okusa, trizmus, osteoradionekroza in kserostomija.

Zaključki. Radikalna radioterapija z ali brez sočasnega sistemskega zdravljenja pri bolnikih z neoperabilnim rakom ustne votline zagotavlja trenutno najboljše možno zdravljenje, s sorazmerno dobro lokalno kontrolo rasti tumorjev in dobrim celokupnim preživetjem.

Radiol Oncol 2021; 55(4): 474-481.
doi: 10.2478/raon-2021-0031

Akutni stranski učinki radikalne stereotaktične telesne radioterapije (SBRT) pri bolnikih s klinično lokalno omejenim ali lokalno napredujočim rakom prostate. Prospektivna raziskava posamične ustanove

Jorgo K, Polgar C, Stelczer G, Major T, Gesztesi L, Agoston P

Izhodišča. Ocena akutnih stranskih učinkov po skrajno hipofrakcionirani intenzitetno modulirani radioterapiji (IMRT) s stereotaktično telesno radioterapijo (*angl. stereotactic body radiation therapy, SBRT*) kot edinim načinom zdravljenjem bolnikov z rakom prostate.

Bolniki in metode. Med februarjem 2018 in avgustom 2019 smo s stereotaktično telesno radioterapijo in z uporabo linearnega pospeševalnika »CyberKnife M6« zdravili 205 bolnikov, ki so zboleli za rakom prostate z nizkim, srednjim in visokim tveganjem. Pri bolnikih z nizkim tveganjem je prostatična žleza ob vsaki frakciji obsevanja prejela 7,5–8 Gy. Pri bolnikih s srednjim in visokim tveganjem smo uporabili tehniko simultane integrirane dodatne doze (*angl. simultaneous integrated boost, SIB*). Prostata je z vsako frakcijo obsevanja prejela 7,5–8 Gy in seminalni vezikli 6–6,5 Gy. Bolnike smo obsevali vsak drugi delovni dan in so skupaj prejeli 5 frakcij (skupna doza 37,5–40 Gy). Akutne, z radioterapijo povezane genitourinarnne in gastrointestinalne stranske učinke smo ocenjevali s klasifikacijskim sistemom Onkološke skupine za radioterapijo (*angl. Radiation Therapy Oncology Group, RTOG*).

Rezultati. Od 205 bolnikov (28 z nizkim, 115 srednjim in 62 z visokim tveganjem), ki smo jih zdravili s stereotaktično telesno radioterapijo, je 203 (99 %) zaključilo načrtovano radioterapijo. Obsevanje je trajalo 1 teden in 3 dni. Pogostnost akutnih, z radioterapijo povezanih stranskih učinkov je bila naslednja: genitourinarni stopnje 0 – 17,1 %, stopnje I – 30,7 %, stopnje II – 50,7 % in stopnje III – 1,5 %; ter gastrointestinalni stopnje 0 – 62,4 %, stopnje I – 31,7 %, stopnje II – 5,9 % in stopnje III – 0 %.

Zaključki. Stereotaktična telesna radioterapija s skupno dozo 37,5–40 Gy v 5 frakcijah se kaže kot varna terapevtska možnost, ki jo bolniki z rakom prostate dobro prenašajo, povzroča blage ali zmerne zgodnje stranske učinke. Potrebno je daljše obdobje sledenja, da bi lahko ocenili kasno toksičnost in biokemično kontrolo bolezni.

Radiol Oncol 2021; 55(4): 482-490.
doi: 10.2478/raon-2021-0044

Klinični rezultati obravnave bolnikov z nedrobnoceličnim rakom pljuč stadija III, ki smo jih po obsevanju in po zaporedni ali sočasni kemoterapiji na osnovi platine zdravili z durvalumabom. Izkušnje terciarnega centra.

Vrankar M, Stanič K, Jelerčič S, Čirić E, Vodusek AL, But-Hadžić J

Izhodišča. Zdravljenje z obsevanjem in sočasno kemoterapijo, ki mu sledi 12-mesečno zdravljenje z durvalumabom, je novo standardno zdravljenje za bolnike z neresektabilnim nedrobnoceličnim pljučnim rakom stadija III. Podatkov o preživetju teh bolnikov iz vsakodnevne klinične prakse je malo. Prav tako je malo podatkov o možnem vplivu na učinkovitost zdravljenja bolnikov, ki prejemajo zaporedno ali sočasno kemoterapijo in o uporabi gemcitabina.

Bolniki in metode. Retrospektivno smo analizirali podatke bolnikov z neresektabilnim nedrobnoceličnim rakom pljuč stadija III, ki so bili zdravljeni z durvalumabom po radikalnem obsevanju s sočasno ali zaporedno kemoterapijo od decembra 2017 do decembra 2020. Ocenili smo preživetje brez napredovanja bolezni (PFS), celokupno preživetje (OS) in toksičnost glede na značilnosti bolnikov.

Rezultati. V analizo smo vključili 85 bolnikov s srednjo starostjo 63 let, 70,6 % je bilo moških, 56,5 % v stadiju IIIB in 58,8 % s ploščatoceličnim rakom. Enaintrideset bolnikov je prejelo samo zaporedno kemoterapijo, 51 bolnikov je prejelo uvodno in sočasno kemoterapijo in 3 bolniki so prejeli samo sočasno kemoterapijo. Devetinsedemdeset bolnikov (92,9 %) je prejelo gemcitabin in cisplatin kot uvodno kemoterapijo, nato so sočasno z obsevanjem prejeli etopozid in cisplatin. Bolniki so začeli zdravljenje z durvalumabom po srednjem času 57 dni (razpon 12–99 dni) od zaključka obsevanja in smo jih zdravili s srednjim časom 10,8 (razpon 0,5–12 mesecev) mesecev. Enainštirideset bolnikov (48,2 %) je zdravljenje zaključilo z načrtovanim 12-mesečnim zdravljenjem z durvalumabom, 25 bolnikov (29,4 %) je predčasno zaključilo zdravljenje zaradi neželenih učinkov in 16 bolnikov (18,8 %) zaradi napredovanja bolezni. Srednji čas do napredovanja bolezni je bil 22,0 mesecev, 12- in 24-mesečni čas do napredovanja bolezni je bil 71 % (95 % interval zaupanja [IZ]: 61,2–80,8 %) in 45,8 % (95 % IZ: 32,7–58,9 %). S srednjim časom spremljanja 23 mesecev (razpon 2–35 mesecev) srednje preživetje ni bilo doseženo. Dvanajst- in ocenjeno 24-mesečno preživetje je bilo 86,7 % (95 % IZ: 79,5–93,9 %) in 68,6 % (95 % IZ: 57,2–79,9 %).

Zaključki. Podatki o preživetju v pričujoči raziskavi so primerljivi z objavljenimi randomiziranimi rezultati in z nedavno objavljenimi poročili iz kliničnih retrospektivnih raziskav. Zdravljenje s kemoterapijo na osnovi gemcitabina in platine kot uvodnega zdravljenja je bilo učinkovito in so ga bolniki dobro prenašali.

Radiol Oncol 2021; 55(4): 491-498.

doi: 10.2478/raon-2021-0021

Obvladovanje bolezni po zdravljenju s kemoterapijo na osnovi platine je napovedni dejavnik za preživetje pri bolnikih z metastatskim urotelnim rakom, ki so prejeli atezolizumab v redni klinični praksi

Mencinger M, Mangaroski D, Bokal U

Izhodišča. Atezolizumab, zaviralec imunskih kontrolnih točk, je nova možnost zdravljenja za bolnike z metastatskim urotelnim rakom. Raziskovali smo klinične napovedne dejavnike, preživetje in varnost bolnikov s takšnim rakom, ki so prejeli atezolizumab v redni klinični praksi.

Bolniki in metode. V raziskavo smo vključili 62 bolnikov z metastatskim urotelnim rakom, ki smo jih zdravili na Onkološkem inštitutu Ljubljana med 8. majem 2018 in 31. decembrom 2019. Beležili smo učinke zdravljenja in imunsko pogojene neželene dogodke. Z uporabo Kaplan-Meierjeve metode smo ocenili preživetje brez napredovanja bolezni in celokupno preživetje. Za določitev dejavnikov, ki vplivajo na preživetje, smo uporabili analizo po Coxu.

Rezultati. Od 62 bolnikov pet (8,1 %) še ni bilo ovrednotenih, 20 (32 %) pa jih je umrlo pred prvo radiološko oceno. Klinično dobrobit smo opazili pri 19 (33 %) bolnikih, objektivni odgovor pri 12 (21 %) in popoln odgovor pri 5 (9 %) bolnikih. Srednje celokupno preživetje za celotno populacijo je bilo 6,8 mesecev (CI 95 %, 2,6–11,0), za nezdravljene s platino 8,7 (CI 95 %: 0,8–16,5) in za predhodno zdravljene s platino 6,8 (CI 95 %, 3,7–10) mesecev. Po 5,8 (0,3–23,1) mesecev spremljanja še nismo dosegli mediano trajanja odziva. Imunsko pogojeni neželeni učinki so se pojavili pri 20 (32 %) bolnikih in 7 (11 %) od njih je zdravljenje prekinilo. Po multivariatni analizi je bil interval brez zdravljenja več kot 6 mesecev neodvisni dejavnik, ki je vplival na preživetje bolnikov z metastatskim urotelnim rakom.

Zaključki. Podskupina bolnikov z metastatskim urotelnim rakom je imela dolgo remisijo bolezni. Srednje preživetje celotne naše skupine bolnikov iz redne klinične prakse je bilo krajše zaradi velikega deleža bolnikov s slabšo splošno zmogljivostjo. Obdobje brez zdravljenja po kemoterapiji se je pokazalo kot dober napovedni dejavnik za preživetje bolnikov z metastatskim urotelnim rakom, predhodno zdravljenimi s platino, ki so v nadaljevanju prejeli atezolizumab.

Radiol Oncol 2021; 55(4): 499-507.
doi: 10.2478/raon-2021-0045

Nekoplanarna volumetrično modulirana ločna terapija levostranskega raka dojke z vključenimi notranjimi mamarnimi bezgavkami

Xu Y, Ma P, Hu Z, Tian Y, Men K, Wang S, Xu Y, Dai J

Izhodišča. Z obsevanjem dojke, zlasti leve, lahko povzročimo toksične učinke na srce in pljuča. Tako so za zmanjšanje obsevalne toksičnosti pri levostranskem raku dojke z vključenimi notranjimi mamarnimi bezgavkami (IMN) predlagali nekoplanarno volumetrično modulirano ločno terapijo (ncVMAT).

Bolniki in metode. V retrospektivno raziskavo smo vključili 10 bolnic z levostranskim rakom dojke, ki smo jih zdravili z radioterapijo po ohranitveni operaciji dojke. Za vsako bolnico smo izdelali obsevalni načrt za tehniko ncVMAT s štirimi delnimi loki – dvema koplanarnima in dvema nekoplanarnima, z rotacijo obsevalne mize 90°. S predpisano dozo 50 Gy v 25 frakcijah smo pokrili 95 % planirnega tarčnega volumna (PTV). Za vsak obsevalni načrt, izdelan za obsevalno tehniko ncVMAT, smo naredili tudi primerjavo dozimetričnih parametrov z obsevalnim načrtom za koplanarno volumetrično modulirano ločno terapijo (coVMAT).

Rezultati. Primerjava ncVMAT in coVMAT obsevalnih načrtov je pokazala, da sta bila pri ncVMAT obsevalnih načrtih izboljšana dozna konformnost in homogenost, kakor tudi V_{55} za celoten PTV ($p < 0,001$). Povprečne vrednosti V_{30} , V_{20} , V_{10} , V_5 in povprečna doza (D_{mean}) za srce so bile pomembno nižje ($p < 0,001$). Pomembno nižje so bile tudi vrednosti V_{20} , V_{10} , V_5 in D_{mean} za levo stran pljuč, kakor tudi V_{10} , V_5 in D_{mean} za desno stran pljuč ($p < 0,001$). Prav tako so bile pomembno nižje doze na levi sprednji descendentni koronarni arteriji (LAD) in na kontralateralni desni dojki ($p < 0,001$).

Zaključki. V primerjavi z obsevalno tehniko coVMAT zagotavlja tehnika ncVMAT boljšo dozno konformnost in homogenost celotnega PTV-ja, obenem pa zagotavlja nižjo prejeto dozo na srce, pljuča, LAD in desno dojko, s čimer potencialno znižuje tveganja za obsevalne poškodbe zdravih tkiv.

Radiol Oncol 2021; 55(4): 508-515.

doi: 10.2478/raon-2021-0046

Verifikacija optimizacijskega algoritma pri obsevalnih načrtih za intenzitetno modulirano ločno terapijo

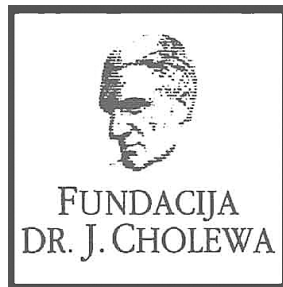
Pocza T, Szegedi D, Major T, Pesznyak C

Izhodišča. Ob uporabi obsevalnih načrtov, ki temeljijo na dinamičnih obsevalnih tehnikah, lahko različni predpisani obsevalni režimi (frakcionacije) vodijo do dozimetričnih razlik. Namen raziskave je bil, da ugotovimo, kako vpliva predpisana dnevna doza (doza na posamezno frakcijo) na kakovost obsevalnih načrtov in na obsevalno zdravljenje.

Materiali in metode. Obsevalne načrte smo izdelali za različne obsevalne režime. Namenjeni so bili 5 bolnikom z rakom pljuč v zgodnji fazi. Pri vseh bolnikih je bila skupna načrtovana doza 60 Gy, dnevni odmerki pa različni: 2, 3, 5, 12 in 20 Gy. Obsevalne načrte smo ponovno normalizirani tako, da smo spreminjali dnevno predpisano dozo po vsaki optimizaciji. Za določanje kakovosti in kompleksnosti obsevalnih načrtov smo izračunali ustrezne dozimetrične parametre. Natančnost dostavljene doze smo preverjali s pomočjo elektronske portalne dozimetrije.

Rezultati. Ugotovili smo, da je bila kakovost obsevalnega načrta neodvisna od uporabljenega obsevalnega režima (frakcionacije) in da smo lahko dnevni odmerek varno spreminjali po izvedeni optimizaciji. Rezultati meritev s pomočjo elektronske portalne dozimetrije so pokazali, da visoki dozni odmerki in visoke dozne hitrosti povzročijo zasičenje detektorjev sistema elektronske portalne dozimetrije, kar ima za posledico nižje mejne vrednosti pri analizi gama.

Zaključki. Kakovost obsevalnega načrta in izvedba obsevanja nista odvisni od doze posameznega odmerka (doze na frakcijo), kar pomeni, da lahko dozo posamezne dnevne frakcije varno spreminjamo po opravljeni dozni optimizaciji. Zasičenost detektorjev sistema elektronske portalne dozimetrije moramo upoštevati pri definiranju mejnih ravni sprejemljivosti v okviru sistema za zagotavljanje kakovosti.



FUNDACIJA "DOCENT DR. J. CHOLEWA"
JE NEPROFITNO, NEINSTITUCIONALNO IN NESTRANKARSKO
ZDRUŽENJE POSAMEZNIKOV, USTANOV IN ORGANIZACIJ, KI ŽELIJO
MATERIALNO SPODBUJATI IN POGLABLJATI RAZISKOVALNO
DEJAVNOST V ONKOLOGIJI.

DUNAJSKA 106
1000 LJUBLJANA
IBAN: SI56 0203 3001 7879 431

TANTUM VERDE®

benzidaminijev klorid

Za lajšanje bolečine in oteklin v ustni votlini in žrelu, ki so posledica radiomukozitisa



Bistvene informacije iz Povzetka glavnih značilnosti zdravila

Tantum Verde 1,5 mg/ml oralno pršilo, raztopina

Tantum Verde 3 mg/ml oralno pršilo, raztopina

Sestava 1,5 mg/ml: 1 ml raztopine vsebuje 1,5 mg benzidaminijevega klorida, kar ustreza 1,34 mg benzidamina. V enem razpršku je 0,17 ml raztopine. En razpršek vsebuje 0,255 mg benzidaminijevega klorida, kar ustreza 0,2278 mg benzidamina. **Sestava 3 mg/ml:** 1 ml raztopine vsebuje 3 mg benzidaminijevega klorida, kar ustreza 2,68 mg benzidamina. V enem razpršku je 0,17 ml raztopine. En razpršek vsebuje 0,51 mg benzidaminijevega klorida, kar ustreza 0,4556 mg benzidamina.

Terapevtske indikacije: **Samozdravljenje:** Lajšanje bolečine in oteklin pri vnetju v ustni votlini in žrelu, ki so lahko posledica okužb in stanj po operaciji. **Po nasvetu in navodilu zdravnika:** Lajšanje bolečine in oteklin v ustni votlini in žrelu, ki so posledica radiomukozitisa. **Odmerjanje in način uporabe:** Odmerjanje 1,5 mg/ml: Odrasli: 4 do 8 razprškov 2- do 6-krat na dan (vsake 1,5 do 3 ure). **Pediatrična populacija:** Mladostniki, stari od 12 do 18 let: 4-8 razprškov 2- do 6-krat na dan. Otroci od 6 do 12 let: 4 razprški 2- do 6-krat na dan. Otroci, mlajši od 6 let: 1 razpršek na 4 kg telesne mase; do največ 4 razprške 2- do 6-krat na dan. Odmerjanje 3 mg/ml: Uporaba 2- do 6-krat na dan (vsake 1,5 do 3 ure). Odrasli: 2 do 4 razprški 2- do 6-krat na dan. **Pediatrična populacija:** Mladostniki, stari od 12 do 18 let: 2 do 4 razprški 2- do 6-krat na dan. Otroci od 6 do 12 let: 2 razprška 2- do 6-krat na dan. Otroci, mlajši od 6 let: 1 razpršek na 8 kg telesne mase; do največ 2 razprška 2- do 6-krat na dan. **Starejši bolniki, bolniki z jetrno okvaro in bolniki z ledvično okvaro:** Uporabo oralnega pršila z benzidaminijevim kloridom se svetuje pod nadzorom zdravnika. **Način uporabe:** Za orofaringealno uporabo. Zdravilo se razprši v usta in žrelo. **Kontraindikacije:** Preobčutljivost na učinkovino ali katero koli pomožno snov. **Posebna opozorila in previdnostni ukrepi:** Če se simptomi v treh dneh ne izboljšajo, se mora bolnik posvetovati z zdravnikom ali zobozdravnikom, kot je primerno. Benzidamin ni priporočljiv za bolnike s preobčutljivostjo nasalicilno kislino ali druga nesteroidna protivnetna zdravila. Pri bolnikih, ki imajo ali so imeli bronhialno astmo, lahko pride do bronhospazma, zato je potrebna previdnost. To zdravilo vsebuje majhne količine etanola (alkohola), in sicer manj kot 100 mg na odmerek. To zdravilo vsebuje metilparahidroksibenzoat (E218). Lahko povzroči alergijske reakcije (lahko zapoznele). Zdravilo z jakostjo 3 mg/ml vsebuje makrogolglicerol hidroksistearat 40. Lahko povzroči želodčne težave in drisko. **Medsebojno delovanje z drugimi zdravili in druge oblike interakcij:** Študij medsebojnega delovanja niso izvedli. **Nosečnost in dojenje:** O uporabi benzidamina pri nosečnicah in doječih ženskah ni zadostnih podatkov. Uporaba zdravila med nosečnostjo in dojenjem ni priporočljiva. **Vpliv na sposobnost vožnje in upravljanja strojev:** Zdravilo v priporočenem odmerku nima vpliva na sposobnost vožnje in upravljanja strojev. **Neželeni učinki:** Neznana pogostnost (ni mogoče oceniti iz razpoložljivih podatkov): anafilaktične reakcije, preobčutljivostne reakcije, odrevenelost, laringospazem, suha usta, navzea in bruhanje, angioedem, fotosenzitivnost, pekoč občutek v ustih. Neposredno po uporabi se lahko pojavi občutek odrevenelosti v ustih in v žrelu. Ta učinek se pojavi zaradi načina delovanja zdravila in po kratkem času izgine. **Način in režim izdaje zdravila:** BRP-Izdaja zdravila je brez recepta v lekarnah in specializiranih prodajalnah.

Imetnik dovoljenja za promet: Aziende Chimiche Riunite Angelini Francesco – A.C.R.A.F. S.p.A., Viale Amelia 70, 00181 Rim, Italija **Datum zadnje revizije besedila:** 14. 10. 2019

Pred svetovanjem ali izdajo preberite celoten Povzetek glavnih značilnosti zdravila.

Samo za strokovno javnost.

Datum priprave informacije: oktober 2021

Odgovoren za trženje: Bonifar d.o.o.


ANGELINI

PRIBS/BEN/2021/019



EDINI zaviralec CDK4 & 6, ki se jemlje NEPREKINJENO VSAK DAN, 2x NA DAN^{1, 2, 3}

Verzenios + fulvestrant v 1. in 2. liniji¹

SKRAJŠAN POVZETEK GLAVNIH ZNAČILNOSTI ZDRAVILA

▼ Za to zdravilo se izvaja dodatno spremljanje varnosti. Tako bodo hitreje na voljo nove informacije o njegovi varnosti. Zdravstvene delavce naprošamo, da poročajo o katerem koli domnevnem neželenem učinku zdravila. Glejte poglavje 4.8, kako poročati o neželenih učinkih.

IME ZDRAVILA: Verzenios 50 mg/100 mg/150 mg filmsko obložene tablete **KAKOVOSTNA IN KOLIČINSKA SESTAVA:** Ena filmsko obložena tableta vsebuje 50 mg/100 mg/150 mg abemacicliba. Ena filmsko obložena tableta vsebuje 14 mg/28 mg/42 mg laktoze (v obliki monohidrata). **Terapevtske indikacije:** Zdravilo Verzenios je indicirano za zdravljenje žensk z lokalno napredovalim ali metastatskim, na hormonske receptorje (HR – *Hormone Receptor*) pozitivnim in na receptorje humanega epidermalnega rastnega faktorja 2 (HER2 – *Human Epidermal Growth Factor Receptor 2*) negativnim rakom dojke v kombinaciji z zaviralcem aromataze ali s fulvestrantom kot začetnim endokrinim zdravljenjem ali pri ženskah, ki so prejele predhodno endokrinno zdravljenje. Pri ženskah v pred- in perimenopavzi je treba endokrinno zdravljenje kombinirati z agonistom gonadolibarina (LHRH – *Luteinizing Hormone-Releasing Hormone*).

Odmerjanje in način uporabe: Zdravljenje z zdravilom Verzenios mora uvesti in nadzorovati zdravnik, ki ima izkušnje z uporabo zdravil za zdravljenje rakavih bolezni. **Zdravilo Verzenios v kombinaciji z endokrinim zdravljenjem:** Priporočeni odmerek abemacicliba je 150 mg dvakrat na dan, kadar se uporablja v kombinaciji z endokrinim zdravljenjem. Zdravilo Verzenios je treba jemati, dokler ima bolnica od zdravljenja klinično korist ali do pojavnega nesprejemljive toksičnosti. Če bolnica bruha ali izpusti odmerek zdravila Verzenios, ji je treba naročiti, da naj naslednji odmerek vzame ob predvidenem času; dodatnega odmerka ne sme vzeti. Obvladovanje nekaterih neželenih učinkov lahko zahteva prekinitve in/ali zmanjšanje odmerka. Zdravljenje z abemaciclibom prekinite v primeru povišanja vrednosti AST in/ali ALT >3 x ZMN SKUPAJ s celokupnim bilirubinom > 2,0 x ZMN v odsotnosti holestaze ter pri bolnicah z intersticijsko pljučno boleznijo (ILD)/pnevmonitis stopnje 3 ali 4. Sočasni uporabi močnih zaviralcev CYP3A4 se je treba izogibati. Če se uporabi močnih zaviralcev CYP3A4 ni mogoče izogniti, je treba odmerek abemacicliba znižati na 100 mg dvakrat na dan in pri katerih je bil odmerek znižan na 100 mg abemacicliba dvakrat na dan in pri katerih se sočasno dajanje močnega zaviralca CYP3A4 ni mogoče izogniti, je treba odmerek abemacicliba dodatno znižati na 50 mg dvakrat na dan. Pri bolnicah, pri katerih je bil odmerek znižan na 50 mg abemacicliba dvakrat na dan in pri katerih se sočasno dajanje močnega zaviralca CYP3A4 ni mogoče izogniti, je mogoče z odmerkom abemacicliba nadaljevati ob natančnem spremljanju znakov toksičnosti. Alternativno je mogoče odmerek abemacicliba znižati na 50 mg enkrat na dan ali prekiniti dajanje abemacicliba. Če je uporaba zaviralca CYP3A4 prekinjena, je treba odmerek abemacicliba povečati na odmerek, kakršen je bil pred uvedbo zaviralca CYP3A4 (po 3–5 razpolovnih časih zaviralca CYP3A4). Prilaganje odmerka glede na starost in pri bolnicah z blago ali zmerno ledvično okvaro ter z blago (Child Pugh A) ali zmerno (Child Pugh B) jetrno okvaro ni potrebno. Pri dajanju abemacicliba bolnicam s hudo ledvično okvaro sta potrebna previdnost in skrbno spremljanje glede znakov toksičnosti. **Način uporabe:** Zdravilo Verzenios je namenjeno za peroralno uporabo. Odmerek se lahko vzame s hrano ali brez nje. Zdravilo se ne sme jemati z grenivko ali grenivkinim sokom. Bolnice naj odmerke vzamejo vsak dan ob približno istem času. Tableto je treba zaužiti celo (bolnice je pred zaužitjem ne smejo gristi, drobiti ali deliti). **Kontraindikacije:** Preobčutljivost na učinkovino ali katero koli pomožno snov. **Posebna opozorila in previdnostni ukrepi:** Pri bolnicah, ki so prejemale abemaciclib, so poročali o nevtropeniji, o večji pogostnosti okužb kot pri bolnicah, zdravljenih s placebom in endokrinim zdravljenjem, o povečanih vrednostih ALT in AST. Pri bolnicah, pri katerih se pojavi nevtropenija stopnje 3 ali 4, je priporočljivo prilagoditi odmerek. Bolnice je treba spremljati za znake in simptome globoke venske tromboze in pljučne embolije ter jih zdraviti, kot je medicinsko utemeljeno. Glede na povečanje vrednosti ALT ali AST je mogoče potrebna prilagoditev odmerka. Driska je najpogostejši neželeni učinek. Bolnice je treba ob prvem znaku tekočega blata začeti zdraviti z antidiaroiiki, kot je loperamid, povečati vnos peroralnih tekočin in obvestiti zdravnika. Sočasni uporabi induktorjev CYP3A4 se je treba izogibati zaradi tveganja za zmanjšano učinkovitost abemacicliba. Bolnice z redkimi dednimi motnjami, kot so intoleranca za galaktozo, popolno pomanjkanje laktaze ali malapsorpcija glukoze/galaktoze, tega zdravila ne smejo jemati. Bolnice spremljajte glede pljučnih simptomov, ki kažejo na ILD/pnevmonitis, in jih ustrezno zdravite. Glede na stopnjo ILD/pnevmonitisa je morda potrebno prilaganje odmerka abemacicliba. **Medsebojno delovanje z drugimi zdravili in druge oblike interakcij:** Abemaciclib se primarno presnavlja s CYP3A4. Sočasna uporaba abemacicliba in zaviralcev CYP3A4 lahko poveča plazemsko koncentracijo abemacicliba. Uporabi močnih zaviralcev CYP3A4 sočasno s abemaciclibom se je treba izogibati. Če je močne zaviralce CYP3A4 treba dajati sočasno, je treba odmerek abemacicliba zmanjšati, nato pa bolnico skrbno spremljati glede toksičnosti. Pri bolnicah, zdravljenih z zmernimi ali šibkimi zaviralci CYP3A4, ni potrebno prilaganje odmerka, vendar jih je treba skrbno spremljati za znake toksičnosti. Sočasni uporabi močnih induktorjev CYP3A4 (vključno, vendar ne omejeno na: karbamazepin, fenitoin, rifampicin in šentjanževko) se je treba izogibati zaradi tveganja za zmanjšano učinkovitost abemacicliba. Abemaciclib in njegovi glavni aktivni presnovki zavirajo prenašalce v ledvicah, in sicer kationski organski prenašalec 2 (OCT2) ter prenašalca MATE1. *In vivo* lahko pride do medsebojnega delovanja abemacicliba in klinično pomembnih substratov teh prenašalcev, kot je dofelitid ali kreatinin. Trenutno ni znano, ali lahko abemaciclib zmanjša učinkovitost sistemskih hormonskih kontraceptivov, zato se ženskam, ki uporabljajo sistemske hormonske kontraceptive, svetuje, da hkrati uporabljajo tudi mehansko metodo. **Neželeni učinki:** Najpogostejši neželeni učinki so driska, okužbe, nevtropenija, anemija, utrujenost, navzea, bruhanje in zmanjšanje apetita. **Zelo pogosti:** okužbe, nevtropenija, levkopenija, anemija, trombocitopenija, driska, bruhanje, navzea, zmanjšanje apetita, disgevizija, omotica, alopecija, pruritus, izpuščaj, utrujenost, pireksija, povečana vrednost alanin-aminotransferaze, povečana vrednost aspartat-aminotransferaze **Pogosti:** limfopenija, povečano solzenje, venska tromboembolija, intersticijska pljučna bolezen (ILD)/pnevmonitis, suha koža, mišična šibkost **Občasni:** febrilna nevtropenija **Rok uporabnosti:** 3 leta **Posebna navodila za shranjevanje:** Za shranjevanje zdravila niso potrebna posebna navodila. **Imetnik dovoljenja za promet z zdravilom:** Eli Lilly Nederland BV, Papendorpseweg 83, 3528BJ, Utrecht, Nizozemska. Datum prve odobritve dovoljenja za promet: 27. september 2018 **Datum zadnje revizije besedila:** 19.7.2021 **Režim izdaje:** Rp/Spec - Predpisovanje in izdaja zdravila je le na recept zdravnika specialista ustreznega področja medicine ali od njega pooblaščenega zdravnika.

Reference:

1. Povzetek glavnih značilnosti zdravila Verzenios. Datum zadnje revizije besedila: 19.7.2021. **2.** Povzetek glavnih značilnosti zdravila Ibrance. Dostop preverjen 10.4.2020. **3.** Povzetek glavnih značilnosti zdravila Kisqali. Dostop preverjen 10.4.2020.

Pomembno: Predpisovanje in izdaja zdravila je le na recept zdravnika specialista ustreznega področja medicine ali od njega pooblaščenega zdravnika. Pred predpisovanjem zdravila Verzenios si preberite zadnji veljavni Povzetek glavnih značilnosti zdravil. Podrobne informacije o zdravilu so objavljene na spletni strani Evropske agencije za zdravila <http://www.ema.europa.eu>

Eli Lilly farmacevtska družba, d.o.o., Dunajska cesta 167, 1000 Ljubljana, telefon 01 / 580 00 10, faks 01 / 569 17 05

PP-AL-SI-0118, 15.10.2021, Samo za strokovno javnost.



Referenca: 1. Keytruda EU SmPC

SKRAJŠAN POVZETEK GLAVNIH ZNAČILNOSTI ZDRAVILA

Pred predpisovanjem, prosimo, preberite celoten Povzetek glavnih značilnosti zdravila!

Ime zdravila: KEYTRUDA 25 mg/ml koncentrat za raztopino za infundiranje vsebuje pembrolizumab. **Terapevtske indikacije:** Zdravilo KEYTRUDA je kot samostojno zdravljenje indicirano za zdravljenje: napredovalega (neoperabilnega ali metastatskega) melanoma pri odraslih; za adjuvantno zdravljenje odraslih z melanomom v stadiju III, ki se je razširil na bezgavke, po popolni kirurški odstranitvi; metastatskega nedrobnoceličnega pljučnega raka (NSCLC) v prvi liniji zdravljenja pri odraslih, ki imajo tumorje z $\geq 50\%$ izraženostjo PD-L1 (TPS) in brez pozitivnih tumorskih mutacij EGFR ali ALK; lokalno napredovalega ali metastatskega NSCLC pri odraslih, ki imajo tumorje z $\geq 1\%$ izraženostjo PD-L1 (TPS) in so bili predhodno zdravljeni z vsaj eno shemo kemoterapije, bolniki s pozitivnimi tumorskimi mutacijami EGFR ali ALK so pred prejemom zdravila KEYTRUDA morali prejeti tudi tarčno zdravljenje; odraslih in pediatričnih bolnikov, starih 3 leta ali več, s ponovljenim ali neodzivnim klasičnim Hodgkinovim limfomom (cHL), pri katerih avtologna presaditev matičnih celic (ASCT) ni bila uspešna, ali po najmanj dveh predhodnih zdravljenjih kadar ASCT ne pride v poštev kot možnost zdravljenja; lokalno napredovalega ali metastatskega urotelijskega raka pri odraslih, predhodno zdravljenih s kemoterapijo, ki je vključevala platino; lokalno napredovalega ali metastatskega urotelijskega raka pri odraslih, ki niso primerni za zdravljenje s kemoterapijo, ki vsebuje cisplatin in imajo tumorje z izraženostjo PD-L1 ≥ 10 , ocenjeno s kombinirano pozitivno oceno (CPS); ponovljenega ali metastatskega ploščatoceličnega raka glave in vratu (HNSCC) pri odraslih, ki imajo tumorje z $\geq 50\%$ izraženostjo PD-L1 (TPS), in pri katerih je bolezen napredovala med zdravljenjem ali po zdravljenju s kemoterapijo, ki je vključevala platino in za prvo linijo zdravljenja metastatskega kolorektalnega raka z visoko mikrosatelitsko nestabilnostjo (MSI-H – microsatellite instability-high) ali s pomanjkljivim popraviljem neujemanja pri podvojevanju DNA (dMMR - mismatch repair deficient) pri odraslih. Zdravilo KEYTRUDA je kot samostojno zdravljenje ali v kombinaciji s kemoterapijo s platino in 5-fluorouracilom (5-FU) indicirano za prvo linijo zdravljenja metastatskega ali neoperabilnega ponovljenega ploščatoceličnega raka glave in vratu pri odraslih, ki imajo tumorje z izraženostjo PD-L1 s CPS ≥ 1 . Zdravilo KEYTRUDA je v kombinaciji s pemetreksedom in kemoterapijo na osnovi platine indicirano za prvo linijo zdravljenja metastatskega neploščatoceličnega NSCLC pri odraslih, pri katerih tumorji nimajo pozitivnih mutacij EGFR ali ALK; v kombinaciji s karboplatinom in bodisi paklitakselom bodisi nab-paklitakselom je indicirano za prvo linijo zdravljenja metastatskega ploščatoceličnega NSCLC pri odraslih; v kombinaciji s akitinibom je indicirano za prvo linijo zdravljenja napredovalega raka ledvičnih celic (RCC) pri odraslih; v kombinaciji s kemoterapijo s platino in fluoropirimidinom indicirano za prvo linijo zdravljenja lokalno napredovalega neoperabilnega ali metastatskega raka požiralnika ali HER-2 negativnega adenokarcinoma gastroezofagealnega prehoda pri odraslih, ki imajo tumorje z izraženostjo PD-L1 s CPS ≥ 10 ; v kombinaciji s kemoterapijo indicirano za zdravljenje lokalno ponovljenega neoperabilnega ali metastatskega trojno negativnega raka dojki pri odraslih, ki imajo tumorje z izraženostjo PD-L1 s CPS ≥ 10 in predhodno niso prejeli kemoterapije za metastatsko bolezen. **Odmerjanje in način uporabe:** Testiranje PD-L1: Če je navedeno v indikaciji, je treba izbrati bolnika za zdravljenje z zdravilom KEYTRUDA na podlagi izraženosti PD-L1 tumorja potrditi z validirano preiskavo. Testiranje MSI-H/dMMR pri bolnikih s CRC: Za samostojno zdravljenje z zdravilom KEYTRUDA je priporočljivo opraviti testiranje MSI-H/dMMR statusa tumorja z validirano preiskavo, da se izbere bolnik s CRC. Odmerjanje: Priporočeni odmerek zdravila KEYTRUDA pri odraslih je bodisi 200 mg na 3 tedne ali 400 mg na 6 tednov, apliciran z intravensko infuzijo v 30 minutah. Priporočeni odmerek zdravila KEYTRUDA za samostojno zdravljenje pri pediatričnih bolnikih s cHL, starih 3 leta ali več, je 2 mg/kg telesne mase (do največ 200 mg) na 3 tedne, apliciran z intravensko infuzijo v 30 minutah. Za uporabo v kombinaciji glejte povzetek glavnih značilnosti sočasno uporabljenih zdravil. Če se uporablja kot del kombiniranega zdravljenja skupaj z intravensko kemoterapijo, je treba zdravilo KEYTRUDA aplicirati prvo. Bolnike je treba zdraviti do napredovanja boleznih ali nesprejemljivih toksičnih učinkov. Pri adjuvantnem zdravljenju melanoma je treba zdravilo uporabljati do ponovitve boleznih, pojava nesprejemljivih toksičnih učinkov oziroma mora zdravljenje trajati do enega leta. Če je akitinib uporabljen v kombinaciji s pembrolizumabom, se lahko razmislilo o povečanju odmerka akitiniba nad začetnih 5 mg v presledkih šest tednov ali več. Pri bolnikih starih ≥ 65 let, bolnikih z blago do zmerno okvaro ledvic, bolnikih z blago okvaro jeter prilagoditev odmerka ni potrebna. Odložitev odmerka ali ukinitve zdravljenja: Zmanjšanje odmerka zdravila KEYTRUDA ni priporočljivo. Za obvladovanje neželenih učinkov je treba uporabo zdravila KEYTRUDA zadržati ali ukiniti, prosimo, glejte celoten Povzetek glavnih značilnosti zdravila. **Kontraindikacije:** **Preobčutljivost na učinkovino ali katero koli pomožno snov.** **Povzetek posebnih opozoril, previdnostnih ukrepov, interakcij in neželenih učinkov:** Imunsko pogojeni neželeni učinki (pnevmonitis, kolitis, hepatitis, nefritis, endokrinopatije, neželeni učinki na kožo in drugi). Pri bolnikih, ki so prejeli pembrolizumab, so se pojavili imunsko

pogojeni neželeni učinki, vključno s hudimi in smrtnimi primeri. Večina imunsko pogojenih neželenih učinkov, ki so se pojavili med zdravljenjem s pembrolizumabom, je bila reverzibilnih in so jih obvladali s prekinitevami uporabe pembrolizumaba, uporabo kortikosteroidov in/ali podporno oskrbo. Pojavijo se lahko tudi po zadnjem odmerku pembrolizumaba in hkrati prizadanejo več organskih sistemov. V primeru suma na imunsko pogojene neželene učinke je treba poskrbeti za ustrezno oceno za potrditev etiologije oziroma izključitev drugih vzrokov. Glede na izrazitost neželenega učinka je treba zadržati uporabo pembrolizumaba in uporabiti kortikosteroide – za natančna navodila, prosimo, glejte Povzetek glavnih značilnosti zdravila Keytruda. Zdravljenje s pembrolizumabom lahko poveča tveganje za zavrnitev pri prejemnikih presadkov čvrstih organov. Pri bolnikih, ki so prejeli pembrolizumab, so poročali o hudih z infuzijo povezanih reakcijah, vključno s preobčutljivostjo in anafilaksijo. Pembrolizumab se iz obtoka odstrani s katabolizmom, zato presnovnih medsebojnih delovanj zdravil ni pričakovati. Uporabi sistemskih kortikosteroidov ali imunosupresivov pred uvedbo pembrolizumaba se je treba izogibati, ker lahko vplivajo na farmakodinamično aktivnost in učinkovitost pembrolizumaba. Vendar pa je kortikosteroide ali druge imunosupresive mogoče uporabiti za zdravljenje imunsko pogojenih neželenih učinkov. Kortikosteroide je mogoče uporabiti tudi kot premedikacijo, če je pembrolizumab uporabljen v kombinaciji s kemoterapijo, kot antiemetično profilakso in/ali za ublažitev neželenih učinkov, povezanih s kemoterapijo. Ženske v rodni dobi morajo med zdravljenjem s pembrolizumabom in vsaj še 4 mesece po zadnjem odmerku pembrolizumaba uporabljati učinkovito kontracepcijo, med nosečnostjo in dojenjem se ga ne sme uporabljati. Varnost pembrolizumaba pri samostojnem zdravljenju so v kliničnih študijah ocenili pri 6.185 bolnikih z napredovalim melanomom, kirurško odstranjenim melanomom v stadiju III (adjuvantno zdravljenje), NSCLC, cHL, urotelijskim rakom, HNSCC ali CRC s štirimi odmerki (2 mg/kg telesne mase na 3 tedne, 200 mg na 3 tedne in 10 mg/kg telesne mase na 2 ali 3 tedne). V tej populaciji bolnikov je mediana čas opazovanja znašal 7,6 mesece (v razponu od 1 dneva do 47 mesecev), najpogostejši neželeni učinki zdravljenja s pembrolizumabom so bili utrujenost (32 %), navzea (21 %) in diareja (21 %). Večina poročanih neželenih učinkov pri samostojnem zdravljenju je bila po izrazitosti 1. ali 2. stopnje. Najresnejši neželeni učinki so bili imunsko pogojeni neželeni učinki in hude z infuzijo povezane reakcije. Varnost pembrolizumaba pri kombiniranem zdravljenju s kemoterapijo so ocenili pri 2.033 bolnikih z NSCLC, HNSCC, rakom požiralnika ali TNBC, ki so v kliničnih študijah prejeli pembrolizumab v odmerkih 200 mg, 2 mg/kg telesne mase ali 10 mg/kg telesne mase na vsake 3 tedne. Pogostnosti, navedene v nadaljevanju in v preglednici 2, temeljijo na vseh poročanih neželenih učinkih zdravila, ne glede na raziskovalčevo oceno vzročnosti. V tej populaciji bolnikov so bili najpogostejši neželeni učinki naslednji: anemija (52 %), navzea (52 %), utrujenost (37 %), zaprtost (34 %), nevtropenija (33 %), diareja (32 %), zmanjšanje apetita (30 %) in bruhanje (28 %). Pojavnost neželenih učinkov 3. do 5. stopnje je pri bolnikih z NSCLC pri kombiniranem zdravljenju s pembrolizumabom znašala 67 % in pri zdravljenju samo s kemoterapijo 66 %, pri bolnikih s HNSCC pri kombiniranem zdravljenju s pembrolizumabom 85 % in pri zdravljenju s kemoterapijo v kombinaciji s cetuximabom 84 %, pri bolnikih z rakom požiralnika pri kombiniranem zdravljenju s pembrolizumabom 86 % in pri zdravljenju samo s kemoterapijo 83 % ter pri bolnikih s TNBC pri kombiniranem zdravljenju s pembrolizumabom 78 % in pri zdravljenju samo s kemoterapijo 74 %. Varnost pembrolizumaba v kombinaciji s akitinibom so ocenili v klinični študiji pri 429 bolnikih z napredovalim rakom ledvičnih celic, ki so prejeli 200 mg pembrolizumaba na 3 tedne in 5 mg akitiniba dvakrat na dan. V tej populaciji bolnikov so bili najpogostejši neželeni učinki diareja (54 %), hipertenzija (45 %), utrujenost (38 %), hipotiroidizem (35 %), zmanjšan apetit (30 %), sindrom palmarno-plantarne eritrodisezestije (28 %), navzea (28 %), zvišanje vrednosti ALT (27 %), zvišanje vrednosti AST (26 %), disfonija (25 %), kašelj (21 %) in zaprtost (21 %). Pojavnost neželenih učinkov 3. do 5. stopnje je bila med kombiniranim zdravljenjem s pembrolizumabom 76 % in pri zdravljenju s sunitinibom samim 71 %. Za celoten seznam neželenih učinkov, prosimo, glejte celoten Povzetek glavnih značilnosti zdravila. **Način in režim izdaje zdravila:** H – Predpisovanje in izdaja zdravila je le na recept, zdravilo se uporablja samo v bolnišnicah. **Imetnik dovoljenja za promet z zdravilom:** Merck Sharp & Dohme B.V., Waarderweg 39, 2031 BN Haarlem, Nizozemska.



Merck Sharp & Dohme inovativna zdravila d.o.o.,
Ameriška ulica 2, 1000 Ljubljana,
tel: +386 1/ 520 42 01, fax: +386 1/ 520 43 50;
Pripravljeno v Sloveniji, november 2021; SI-KEY-00328 EXP: 11/2023
Samo za strokovno javnost.

H – Predpisovanje in izdaja zdravila je le na recept, zdravilo pa se uporablja samo v bolnišnicah. Pred predpisovanjem, prosimo, preberite celoten Povzetek glavnih značilnosti zdravila Keytruda, ki je na voljo pri naših strokovnih sodelavcih ali na lokalnem sedežu družbe.

UČINKOVITOST, KI OMOGOČA DALJŠE ŽIVLJENJE¹

TECENTRIQ ▼
atezolizumab

ZDRAVILO TECENTRIQ JE INDICIRANO ZA ZDRAVLJENJE RAZLIČNIH VRST RAKA:



**NEDROBNOČELIČNI
RAK PLJUČ**



**DROBNOČELIČNI
RAK PLJUČ**



**TROJNO NEGATIVNI
RAK DOJK**



**UROTELIJSKI
KARCINOM**



**HEPATOCELULARNI
KARCINOM**

Vir: 1. Povzetek glavnih značilnosti zdravila Tecentriq je dosegljiv na povezavi: https://www.ema.europa.eu/en/documents/product-information/tecentriq-epar-product-information_sl.pdf

Skrajsan povzetek glavnih značilnosti zdravila Tecentriq

▼ Za to zdravilo se izvaja dodatno spremljanje varnosti. Tako bodo hitreje na voljo nove informacije o njegovi varnosti. Zdravstvene delavce naprošamo, da poročajo o katerem koli domnevnem neželenem učinku zdravila. Kako poročati o neželenih učinkih, si poglejte skrajšani povzetek glavnih značilnosti zdravila pod "Poročanje o domnevnih neželenih učinkih".

Ime zdravila: Tecentriq 840 mg/1200 mg koncentrat za infundiranje. Kakovostna in količinska sestava: 840 mg: ena 14-ml viala s koncentratom vsebuje 840 mg atezolizumaba. 1200 mg: ena 20-ml viala s koncentratom vsebuje 1200 mg atezolizumaba. Po redčenju je končna koncentracija razredčene raztopine med 3,2 mg/ml in 16,8 mg/ml. Atezolizumab je humanizirano monoklonsko protiteleso IgG1 z inženirano kitajskega hrčka s tehnologijo rekombinantne DNA in deluje na ligand za programirano celično smrt 1 (PD-L1). **Terapevtske indikacije:** **Urotelijski karcinom:** Zdravilo Tecentriq je kot monoterapija indicirano za zdravljenje odraslih bolnikov z lokalno napredovalim ali razsejanim urotelijskim karcinomom, ki: so bili predhodno zdravljeni s kemoterapijo na osnovi platine ali niso primerni za zdravljenje s cisplatinom in katerih tumorji izražajo PD-L1 v $\geq 5\%$. **Nedrobnocelični rak pljuč:** Zdravilo Tecentriq je v kombinaciji z bevacizumabom, paklitakselom in karboplatinom indicirano v prvi liniji zdravljenja odraslih bolnikov z razsejanim neploščatoceličnim nedrobnoceličnim rakom pljuč (NDRP). Pri bolnikih z EGFR mutiranim ali ALK pozitivnim NDRP je zdravilo Tecentriq v kombinaciji z bevacizumabom, paklitakselom in karboplatinom indicirano le, ko so izčrpana ustrezna tarčna zdravljenja. Zdravilo Tecentriq je v kombinaciji z nab-paklitakselom in karboplatinom indicirano kot prva linija zdravljenja odraslih bolnikov z razsejanim neploščatoceličnim NDRP, ki ni EGFR mutiran ali ALK pozitiven. Zdravilo Tecentriq je kot monoterapija indicirano v prvi liniji zdravljenja odraslih bolnikov z razsejanim nedrobnoceličnim rakom pljuč (NDRP), pri katerih je PD-L1 izražen na $\geq 50\%$ tumorskih celic (TC) ali $\geq 10\%$ imunskih celic (IC), ki infiltrirajo tumor, ter nimajo EGFR mutiranega ali ALK pozitivnega NDRP. Zdravilo Tecentriq je kot monoterapija indicirano za zdravljenje odraslih bolnikov z lokalno napredovalim ali razsejanim NDRP, ki so bili predhodno zdravljeni s kemoterapijo. Bolniki z EGFR mutiranim ali ALK pozitivnim NDRP morajo pred uvedbo zdravila Tecentriq prejeti tudi tarčna zdravljenja. **Drobnocelični rak pljuč:** Zdravilo Tecentriq je v kombinaciji s karboplatinom in etopozidom indicirano kot prva linija zdravljenja odraslih bolnikov z razsejanim drobnoceličnim rakom pljuč (DRP). **Trojno negativni rak dojke:** Zdravilo Tecentriq je v kombinaciji z nab-paklitakselom indicirano za zdravljenje odraslih bolnikov z inoperabilnim lokalno napredovalim ali razsejanim trojno negativnim rakom dojke (TNDR), katerih tumorji izražajo PD-L1 v $\geq 1\%$ in predhodno še niso prejeli kemoterapije zaradi razsejane bolezni. **Hepatocelularni karcinom:** Zdravilo Tecentriq je v kombinaciji z bevacizumabom indicirano za zdravljenje odraslih bolnikov z napredovalim ali neresektabilnim hepatocelularnim karcinomom (HCC), ki predhodno še niso prejeli sistemskega zdravljenja. **Odmerjanje in način uporabe:** Zdravilo Tecentriq morajo uvesti in nadzorovati zdravniki z izkušnjami pri zdravljenju raka. **Odmerjanje:** priporočeni odmerek zdravila Tecentriq je 840 mg, danim intraveno na dva tedna, ali 1200 mg, danim intraveno na tri tedne, ali 1680 mg, danim intraveno na štiri tedne, kot je navedeno v celotnem Povzetku glavnih značilnosti zdravila Tecentriq. **Zdravilo Tecentriq v kombinaciji:** kadar zdravilo Tecentriq dajete v kombinaciji, glejte tudi celotne informacije za predpisovanje zdravil, ki se uporabljajo v kombinaciji. **Prilagoditev odmerka med zdravljenjem:** odmerki zdravila Tecentriq ni priporočljivo zmanjševati. **Zapaznitev odmerka ali prenehanje uporabe:** glede na neželeni učinek je opisano v SmPC. **Način uporabe:** zdravilo Tecentriq je namenjeno za intravenosno uporabo. Infuzije se ne sme dajati kot hiter intravenosni odmerek ali bolus. Začetni odmerek zdravila Tecentriq je treba dati v 60 minutah. Če bolnik prvo infuzijo dobro prenese, je mogoče vse nadaljnje infuzije dati v 30 minutah. **Kontraindikacije:** Preobčutljivost na atezolizumab ali katero koli pomožno snov. **Posebna opozorila in previdnostni ukrepi:** **Sledljivost:** Za izboljšanje sledljivosti bioloških zdravil je treba lastniško ime in številko serije uporabljenega zdravila jasno zabeležiti v bolnikovi dokumentaciji. **Imunsko pogojeni neželeni učinki:** Večina imunsko pogojenih neželenih učinkov, ki so se pojavili med zdravljenjem z atezolizumabom, je bila po prekinitvi atezolizumaba in uvedbi kortikosteroidov in/ali podpornega zdravljenja reverzibilna. Opazili so imunsko pogojene neželene učinke, ki vplivajo na več kot en organski sistem. Imunsko pogojeni neželeni učinki, povezani z atezolizumabom, se lahko pojavijo po zadnjem odmerku atezolizumaba. Pri sumu na imunsko pogojene neželene učinke je treba opraviti temeljito oceno za potrditev etiologije oziroma izključitev drugih vzrokov. Glede na izrazitost neželenega učinka je treba uporabo atezolizumaba odložiti in uvesti kortikosteroide. Atezolizumab je treba trajno prenehati uporabljati pri vseh imunsko pogojenih neželenih učinkih 3. stopnje, in pri vseh imunsko pogojenih neželenih učinkih 4. stopnje, z izjemo endokrinopatij, ki jih je mogoče nadzorovati z nadomestnimi hormoni. Bolnike je treba spremljati glede znakov in simptomov pnevmonitisa ter izključiti druge možne vzroke, razen imunsko pogojenega pnevmonitisa. Bolnike je treba spremljati glede znakov in simptomov hepatitisa. Vrednosti AST, ALT in bilirubina je treba spremljati pred začetkom zdravljenja z atezolizumabom, redno med zdravljenjem in kot je potrebno glede na klinično oceno. Bolnike je treba spremljati glede znakov in simptomov kolitisa in endokrinopatij, meningitisa ali encefalitisa. V primeru meningitisa ali encefalitisa je treba zdravljenje z atezolizumabom trajno ukiniti ne glede na njuno stopnjo. Bolnike je treba spremljati glede znakov in simptomov motorične in senzorične nevropatije. V primeru miastenjskega sindroma/miastenije gravis ali Guillain-Barréjevega sindroma je treba zdravljenje z atezolizumabom trajno prekiniti ne glede na njihovo stopnjo. Bolnike je treba nadzorovati glede znakov in simptomov, ki kažejo na akutni pankreatitis. Bolnike je treba nadzorovati glede znakov in simptomov, ki kažejo na miokarditis. Imunsko pogojeni nefritis: Bolnike je treba nadzorovati glede sprememb v delovanju ledvic. Bolnike je treba nadzorovati glede znakov in simptomov, ki kažejo na miozitis. **Z infundiranjem povezane reakcije:** pri zdravljenju z atezolizumabom so opazili z infundiranjem povezane reakcije. Pri bolnikih, ki imajo z infundiranjem povezane reakcije 1. ali 2. stopnje, je treba zdravljenje z atezolizumabom trajno ukiniti. Bolniki, ki imajo z infundiranjem povezane reakcije 1. ali 2. stopnje, lahko še naprej prejemajo atezolizumab pod natančnim nadzorom: v poštev pride premedikacija z antipiretikom in antihistaminikom. Pri bolnikih, ki so prejeli atezolizumab, so poročali o imunsko pogojenih hudih neželenih učinkih, vključno s primeri Stevens-Johnsonovega sindroma (SJS) in toksične epidermalne nekrolize (TEN). Bolnike je treba spremljati glede sumov na hude kožne neželene učinke in izključiti druge vzroke. V primeru suma na hude kožne neželene učinke je treba bolnike napotiti k specialistu po nadaljnjo diagnozo in zdravljenje. Uporabo atezolizumaba je treba odložiti pri bolnikih s sumom na SJS ali TEN. Pri potrjenem SJS ali TEN je treba trajno prenehati z uporabo atezolizumaba. **Kartica za bolnika:** Zdravnik, ki predpiše zdravilo, se mora z bolnikom pogovoriti o tveganjih zdravljenja z zdravilom Tecentriq. Bolnike je treba dati kartico za bolnika in mu naročiti, naj jo ima vedno pri sebi. **Medsebojno delovanje z drugimi zdravili in druge oblike interakcij:** Formalni študiji farmakokinetičnega medsebojnega delovanja zdravljenja z atezolizumabom niso izvedli. Ker se atezolizumab odstrani iz obtoka s katabolizmom, ni pričakovati presnovnih medsebojnih delovanj med zdravili. Uporabi sistemskih kortikosteroidov ali imunosupresivov se je pred uvedbo atezolizumaba treba izogibati, ker lahko vplivajo na farmakodinamično aktivnost in učinkovitost atezolizumaba. Vendar pa se sistemske kortikosteroide ali druge imunosupresive lahko uporabi po začetku zdravljenja z atezolizumabom za zdravljenje imunsko pogojenih neželenih učinkov. **Neželeni učinki:** Informacije o varnosti atezolizumaba v monoterapiji: najpogostejši neželeni učinki ($> 10\%$) so bili utrujenost, zmanjšan apetit, navzea, zvišana telesna temperatura, izpuščaj, kašelj, diareja, dispneja, mišično-skeletna bolečina, bolečina v hrbtu, astenija, bruhanje, srbenje, artralgija, okužba sečil in glavobol. **Varnost atezolizumaba v kombinaciji z drugimi učinkovinami:** najpogostejši neželeni učinki ($> 20\%$) so bili anemija, nevropatija, navzea, utrujenost, trombotična diareja, izpuščaj, alopecija, zaprtost, zmanjšan apetit in periferna nevropatija. **Poročanje o domnevnih neželenih učinkih:** Poročanje o domnevnih neželenih učinkih zdravila po izdaji dovoljenja za promet je pomembno. Omočeno namreč stalno spremljanje razmerja med koristimi in tveganji zdravila. Od zdravstvenih delavcev se zahteva, da poročajo o katerem koli domnevnem neželenem učinku zdravila na: Javna agencija Republike Slovenije za zdravila in medicinske pripomočke, Sektor za farmakovigilanco, Nacionalni center za farmakovigilanco, Slovenčeva ulica 22, SI-1000 Ljubljana, Tel.: +386 (0)8 2000 500, Faks: +386 (0)8 2000 510, e-pošta: h-farmakovigilanca@jazmp.si, spletna stran: www.jazmp.si. Za zagotavljanje sledljivosti zdravila je pomembno, da pri izpolnjevanju obrazca o domnevnih neželenih učinkih zdravila navedete številko serije biološkega zdravila. **Režim izdaje zdravila:** II. **Imetnik dovoljenja za promet:** Roche Registration GmbH, Emil-Barell-Strasse 1, 79639 Grenzach-Wyhlen, Nemčija. **Verzija:** 5.0/21

ONIVYDE: IZDELAN POSEBEJ ZA BOJ PROTI RAKU TREBUŠNE SLINAVKE

ONIVYDE pegylated liposomal je odobren za zdravljenje metastatskega adenokarcinoma trebušne slinavke v kombinaciji s 5-fluorouracilom (5-FU) in levkovorinom (LV) pri odraslih bolnikih, pri katerih je bolezen po zdravljenju na osnovi gemcitabina napredovala.¹

ONIVYDE VSEBUJE PEGILIRANE LIPOSOME Z IRINOTEKANOM IN JE IZDELAN POSEBEJ ZA UČINKOVITO ZDRAVLJENJE METASTATSKEGA RAKA TREBUŠNE SLINAVKE²⁻⁵

KLINIČNI PODATKI ŠTUDIJE 3. FAZE POTRjujeJO EDINSTVENO KLINIČNO VREDNOST ZDRAVILA ONIVYDE V KOMBINACIJI S 5-FU/LV:

- skladni podatki o učinkovitosti pri vseh opazovanih dogodkih: pomembno podaljšanje preživetja in povečana stopnja odziva⁶⁻⁸
- ohranjena kakovost življenja^{6,9}
- dobro poznan varnostni profil^{1,6,7}

POMEMBNA UČINKOVITOST ONIVYDE + 5-FU/LV JE POTRjena V KLINIČNI PRAKSI¹⁰⁻¹²

ONIVYDE + 5-FU/LV PRIPOROČAJO VSE GLAVNE MEDNARODNE SMERNICE¹³⁻¹⁶

LITERATURA: 1. Povzetek glavnih značilnosti zdravila ONIVYDE pegylated liposomal. 2. Lamb YN, Scott LJ. *Drugs*. 2017;77:785-792. 3. Drummond DC et al. *Cancer Res*. 2006;66:3271-3277. 4. Kalra AV et al. *Cancer Res*. 2014;74:7003-7013. 5. Carnevale J, Ko AH. *Future Oncol*. 2016;12:453-464. 6. Wang-Gillam A et al. *Lancet*. 2016;387:545-557. 7. Wang-Gillam A et al. *Eur J Cancer*. 2019;108:78-87. 8. Chen LT et al. *Eur J Cancer*. 2018;105:71-78. 9. Hubner RA et al. *Eur J Cancer*. 2019;106:24-33. 10. Klier M et al. *The Adv Med Oncol*. 2019;11:1-13. 11. Yoo C et al. *The Adv Med Oncol*. 2019;11:1-9. 12. Pellino A et al. *ESMO*. 2019;P660. 13. Duceux M et al. *Ann Oncol*. 2015;25(suppl 5):v56-v68. 14. eUpdate Cancer of the Pancreas Treatment Recommendations. Objavljeno 20. junija, 2019. ESMO Guidelines Committee. 15. Okusaka T et al. *Pancreas*. 2020;49(3):326-335. 16. NCCN Guidelines Version 2. 2021. Pancreatic Adenocarcinoma. Objavljeno 25. februarja, 2021.



onivyde[®]
pegylated liposomal irinotecan

SKRAJŠAN POVZETEK GLAVNIH ZNAČILNOSTI ZDRAVILA Onivyde pegylated liposomal 4,3 mg/ml SESTAVA: Onivyde pegylated liposomal 4,3 mg/ml koncentrat za disperzijo za infundiranje: ena viala z 10 ml koncentrata vsebuje 43 mg brezvodnega irinotekana (v obliki irinotekanijeve soli saharoznega oktasulfata v pegilirani liposomski formulaciji). **TERAPEVTSKE INDIKACIJE:** Zdravljenje metastatskega adenokarcinoma trebušne slinavke v kombinaciji s 5-fluorouracilom (5-FU) in levkovorinom (LV) pri odraslih bolnikih, pri katerih je bolezen po zdravljenju na osnovi gemcitabina napredovala. **ODMERJANJE IN NAČIN UPORABE:** Onivyde pegylated liposomalnega bolnikom predpisati in dajati samo v zdravstveni delavci, ki imajo izkušnje pri uporabi zdravil za zdravljenje raka. Zdravilo Onivyde pegylated liposomal ni enakovredno drugim neliposomskim formulacijam irinotekana, zato jih ne smemo zamenjavati. Priporočeni odmerek in režim odmerjanja zdravila Onivyde pegylated liposomal je 70 mg/m² intravensko 90 minut, čemur sledi LV 400 mg/m² intravensko 30 minut in nato 5FU 2400 mg/m² intravensko 46 ur, vsaka 2 tedna. Zdravilo Onivyde pegylated liposomal se ne daje kot samostojno zdravilo. Pri bolnikih z znano homozigotnostjo za alel UGT1A1*28 je treba razmisлити o manjšem začetnem odmerku zdravila Onivyde pegylated liposomal 50 mg/m². Če zdravilo bolniki dobro prenašajo, lahko v naslednjih ciklih razmisliš o odmerku zdravila Onivyde pegylated liposomal 70 mg/m². Prilagajanje odmerka se priporoča za obvladovanje toksičnosti 3. ali 4. stopnje, povezane z zdravilom Onivyde pegylated liposomal. **KONTRAINDIKACIJE:** Anamneza hude preobčutljivosti na irinotekan ali katero koli pomožno snov. Dojenje. **POZORILA:** Zdravilo Onivyde pegylated liposomal ni enakovredno drugim neliposomskim formulacijam irinotekana, zato jih ne smemo zamenjavati. **Mielosupresija/nevtropenija:** Med zdravljenjem z zdravilom Onivyde pegylated liposomal se priporoča nadziranje celotne krvne slike. Bolniki se morajo zavedati tveganja za nevtropenijo in pomena povišane telesne temperature. Febrilno nevtropenijo je treba nujno zdraviti v bolnišnici s širokospektralnimi intravenskimi antibiotiki. Pri bolnikih, ki doživijo hude hematološke neželene učinke, se priporoča zmanjšanje odmerka ali prekinitve zdravljenja. Bolnikov s hudo odpovedjo kostnega mozga ne smemo zdraviti z zdravilom Onivyde pegylated liposomal. Anamneza predhodnega obsevanja trebuha poveča tveganje za hudo nevtropenijo in febrilno nevtropenijo po zdravljenju z zdravilom Onivyde pegylated liposomal. Pri bolnikih, ki hkrati prejemajo zdravilo Onivyde pegylated liposomal in so obsevani, je potrebna previdnost. Bolniki s pomembno povišano bilirubino, kot so bolniki z Gilbertovim sindromom, imajo med zdravljenjem z zdravilom Onivyde pegylated liposomal lahko večje tveganje za mielosupresijo. Bolniki azijskega porekla imajo večje tveganje za hudo in febrilno nevtropenijo. Posamezniki s homozigotnostjo 7/7 za alel UGT1A1*28 imajo povečano tveganje za nevtropenijo. **Imunosupresivni učinki in cepiva:** Dajanje živih ali atenuiranih cepiv bolnikom z oslabilnim imunskim sistemom lahko povzroči resne ali smrtne okužbe. **Interakcije z močnimi induktorji encima CYP3A4, močnimi zaviralci encima CYP3A4 in močnimi zaviralci encima UGT1A1:** Zdravilo Onivyde pegylated liposomal ne smemo dajati skupaj z močnimi induktorji encima CYP3A4, močnimi zaviralci encima CYP3A4 ali z močnimi zaviralci encima UGT1A1, razen če ni drugih terapevtskih možnosti. Zdravljenje z močnimi zaviralci encima CYP3A4 moramo prekiniti vsaj 1 teden pred začetkom zdravljenja z zdravilom Onivyde pegylated liposomal. **Driska:** Driska se lahko pojavi zgodaj (v ≤ 24 urah po začetku zdravljenja z zdravilom Onivyde pegylated liposomal) ali pozno (> 24 ur). Pri bolnikih, ki doživijo zgodnji pojav driske (v ≤ 24 urah po začetku zdravljenja z zdravilom Onivyde pegylated liposomal), je treba razmisлити o terapevtskem in profilaktičnem zdravljenju z atropinom, razen če je kontraindicirano. Bolnike je treba opozoriti na tveganje za zapoznelo drisko (> 24 ur), ki je izčrpačiva in v redkih primerih tudi življenjsko nevarna. Loperamid je treba uvesti ob prvem pojavu neoblikovane ali mehkega blata ali takoj, ko odvajanje blata postane pogostejše kot običajno. Loperamid je treba dajati, dokler bolnik ni brez driske vsaj 12 ur. Če driska traja tudi, ko bolnik prejema loperamid več kot 24 ur, je treba razmisлити o dodatni peroralni antibiotični podpori. Loperamida zaradi tveganja za paralični ileus ne smemo uporabljati več kot 48 ur zaporedoma. Zdravljenje z zdravilom Onivyde pegylated liposomal je treba odložiti, dokler se driska ne umiri do ≤ 1. stopnje (2-3 odvajanja/dan več kot pred zdravljenjem). Zdravilo Onivyde pegylated liposomal ne smemo dajati bolnikom z zaporo črevesja ali kronično vnetno črevesno boleznijo, dokler se ta ne pozdravi. **Holinergične reakcije:** Zgodnja driska lahko spremlja rinitis, povečano slinjenje, zardevanje, diaforeza, bradikardija, mioza in hiperperistaltika. Uporabiti je treba atropin. **Akutne infuzijske in povezane reakcije:** V primeru hudih preobčutljivostnih reakcij je treba zdravljenje z zdravilom Onivyde pegylated liposomal prekiniti. **Predhodna Whiplovska odziva:** Večje tveganje za resne okužbe. Bolnike je treba spremljati glede znakov okužbe. **Žilne bolezni:** Zdravilo Onivyde pegylated liposomal je bilo povezano s tromboemboličnimi dogodki, kot so pljučna embolija, venska tromboza in arterijska tromboembolija. Treba je pridobiti podrobno zdravstveno anamnezo, da bi prepoznali bolnike z več dejavniki tveganja poleg osnovne neoplazme. Bolnike je treba obvestiti o znakih in simptomih tromboembolije in jim svetovati, da se v primeru katerega od teh znakov ali simptomov takoj obrnejo na svojega zdravnika ali

medicinsko sestro. **Pljučna toksičnost:** Pri bolnikih, ki so prejeli neliposomski irinotekan, so se pojavili dogodki, podobni intersticijski pljučni bolezni (IPB), ki so vodili do smrtnih primerov. Pri bolnikih z dejavniki tveganja (obstoječo pljučno boleznijo, uporabo pnevmotoksičnih zdravil, kolonije stimulirajočimi dejavniki ali predhodnim zdravljenjem z obsevanjem) je treba pred zdravljenjem z zdravilom Onivyde pegylated liposomal in po njem skrbno nadzirati respiratorne simptome. Dokler ni opravljena diagnostična ocena, je treba ob pojavu nove ali napredovale dispneje, kašlja in povišane telesne temperature zdravljenje z zdravilom Onivyde pegylated liposomal začasno prekiniti. Pri bolnikih s potrjeno diagnozo IPB moramo zdravljenje z zdravilom Onivyde pegylated liposomal do končne prekinitve. **Jetrna okvara:** Bolniki s hiperbilirubinemijo so imeli povišane koncentracije skupnega SN-38, zato je tveganje za nevtropenijo povečano. Pri bolnikih z vrednostjo skupnega bilirubina 1,0-2,0 mg/dl je treba redno nadzirati celotno krvno sliko. Previdnost je potrebna pri bolnikih z jetrno okvaro (bilirubin > 2-kratna zgornja meja normalnih vrednosti [ULN]; aminotransferaze > 5-kratna ULN). Previdnost je potrebna, če zdravilo Onivyde pegylated liposomal dajemo v kombinaciji z drugimi hepatotoksičnimi zdravili. **Ledvična okvara:** Uporaba zdravila Onivyde pegylated liposomal pri bolnikih s pomembno ledvično okvaro ni bila ocenjena. **Bolniki s premajhno telesno maso (indeks telesne mase < 18,5 kg/m²):** Potrebna je previdnost. **Pomožne snovi:** To zdravilo vsebuje 33,1 mg natrija na vialo, kar je enako 1,65 % največjega dnevnega vnosa natrija za odrasle osebe, ki ga priporoča SZO in znaša 2 g. En mililiter zdravila Onivyde pegylated liposomal vsebuje 0,144 mmol (3,31 mg) natrija. **INTERAKCIJE:** **Previdnostni ukrepi:** Sočasno dajanje z induktorji encima CYP3A4 (npr. antikonvulzivi, rifampicin, rifabutin in šentjanževka) lahko zmanjša sistemsko izpostavljenost zdravilu Onivyde pegylated liposomal. Sočasno dajanje z zaviralci encima CYP3A4 (npr. grenivkinim sokom, klaritromicinom, indinavirjem, itraconazolom, lopinavirjem, nefazodonom, neflavinjem, ritonavirjem, sakvinavirjem, telaprevirjem, vorikonazolom) ali encima UGT1A1 (npr. atazanavirja, gemfibrozila, indinavirja, regorafeniba) lahko poveča sistemsko izpostavljenost zdravilu Onivyde pegylated liposomal. **PLODNOST*, NOSEČNOST*:** Uporaba ni priporočljiva. **DOJENJE*:** Zdravilo je kontraindicirano. **KONTRACEPCIJA*:** Ženske v rodni dobi morajo med zdravljenjem in še 1 mesec po zdravljenju z zdravilom Onivyde pegylated liposomal uporabljati učinkovito kontracepcijo. Moški morajo med zdravljenjem z zdravilom Onivyde pegylated liposomal in 4 mesece po zdravljenju uporabljati kondome. **VPLIV NA SPOSOBNOST VOZNIJE IN UPRAVLJANJA STROJEV*:** Bolniki morajo biti med zdravljenjem pri vožnji in upravljanju strojev previdni. **NEŽELENI UČINKI*:** Zelo pogosti: nevtropenija, levkopenija, anemija, trombocitopenija, hipokalemija, hipomagnezija, dehidracija, zmanjšan apetit, omotica, driska, bruhanje, navzea, bolečine v trebuhu, stomatitis, alopecija, pirsija, periferni edem, vnetje sluznic, utrujenost, astenija, zmanjšana telesna masa. **Pogosti:** septični šok, sepsa, pljučnica, febrilna nevtropenija, gastroenteritis, oralna kandidoza, limfopenija, hipoglikemija, hiponatremija, hipofosfatemija, nespečnost, holinergični sindrom, digizevija, hipotenzija, pljučna embolija, embolija, globoka venska tromboza, dispneja, disfonija, kolitis, hemoroidi, hipalbuminemija, akutna ledvična odpoved, z infuzijo povezana reakcija, edem, zvišana raven bilirubina, zvišana raven alanin-aminotransferaze, zvišana raven aspartat-aminotransferaze, zvišano mednarodno umerjeno razmerje. **Občasni:** biliarna sepsa, preobčutljivost, tromboza, hipoksija, ezofagitis, proktitis, makulopapulozni izpuščaji, obarvanje nohtov. **PREVELIKO ODMERJANJE*:** Za preveliko odmerjanje zdravila ni znanega antidota. Treba je uvesti maksimalno podporno nego, s katero preprečimo dehidracijo zaradi driske in zdravilno zaplete zaradi okužb. **FARMAKODINAMIČNE LASTNOSTI*:** Irinotekan (zaviralec topoisomerase I), inkapsuliran v vezikel z lipidnim dvoisoljem oziroma liposomom. Irinotekan je derivat kamptotecina. Kamptotecini delujejo kot specifični zaviralci encima DNA-topoisomerase I. Irinotekan in njegov aktivni presnovek SN-38 se reverzibilno vežeta na kompleks topoisomerase I in DNA ter sprožita poškodbe v enovrzični DNA, kar zaustavi replikacijske vilice pri podvajanju DNA in povzroča citotoksičnost. Irinotekan se presnavlja s karboksilesterazo do SN-38. SN-38 je približno 1.000-krat močnejši kot irinotekan kot zaviralec topoisomerase I, očističe iz tumorskih celic in linij človeka in glodavcev. **PAKIRANJE*:** Pakiranje vsebuje eno vialo z 10 ml koncentrata. **NAČIN PREDPISOVANJA IN IZDAJE ZDRAVILA:** H - Predpisovanje in izdaja zdravila je le na recept; zdravilo pa se uporablja samo v bolnišnicah. **DATUM ZADNJE REVIZIJE BESEDILA:** september 2021. Imetnik dovoljenja za promet: Les Laboratoires Servier, 50, rue Carnot, 92228 Suresnes cedex, Francija. *Pred predpisovanjem preberite celoten povzetek glavnih značilnosti zdravila. Celoten povzetek glavnih značilnosti zdravila in podrobnejše informacije so na voljo pri: Servier Pharma d.o.o., Podmilščakova ulica 24, 1000 Ljubljana, www.servier.si.

Zdravilo je na slovenskem trgu na voljo v tuji ovojnini. Za uporabnika so informacije v slovenskem jeziku dostopne na uradni spletni strani www.cbz.si. Navodila za uporabo v slovenskem jeziku so na voljo tudi na www.servier.si.

Instructions for authors

The editorial policy

Radiology and Oncology is a multidisciplinary journal devoted to the publishing original and high quality scientific papers and review articles, pertinent to diagnostic and interventional radiology, computerized tomography, magnetic resonance, ultrasound, nuclear medicine, radiotherapy, clinical and experimental oncology, radiobiology, medical physics and radiation protection. Therefore, the scope of the journal is to cover beside radiology the diagnostic and therapeutic aspects in oncology, which distinguishes it from other journals in the field.

The Editorial Board requires that the paper has not been published or submitted for publication elsewhere; the authors are responsible for all statements in their papers. Accepted articles become the property of the journal and, therefore cannot be published elsewhere without the written permission of the editors.

Submission of the manuscript

The manuscript written in English should be submitted to the journal via online submission system Editorial Manager available for this journal at: www.radioloncol.com.

In case of problems, please contact Sašo Trupej at saso.trupej@computing.si or the Editor of this journal at gsera@onko-i.si

All articles are subjected to the editorial review and when the articles are appropriated they are reviewed by independent referees. In the cover letter, which must accompany the article, the authors are requested to suggest 3-4 researchers, competent to review their manuscript. However, please note that this will be treated only as a suggestion; the final selection of reviewers is exclusively the Editor's decision. The authors' names are revealed to the referees, but not vice versa.

Manuscripts which do not comply with the technical requirements stated herein will be returned to the authors for the correction before peer-review. The editorial board reserves the right to ask authors to make appropriate changes of the contents as well as grammatical and stylistic corrections when necessary. Page charges will be charged for manuscripts exceeding the recommended length, as well as additional editorial work and requests for printed reprints.

Articles are published printed and on-line as the open access (<https://content.sciendo.com/raon>).

All articles are subject to 1200 EUR + VAT publication fee. Exceptionally, waiver of payment may be negotiated with editorial office, upon lack of funds.

Manuscripts submitted under multiple authorship are reviewed on the assumption that all listed authors concur in the submission and are responsible for its content; they must have agreed to its publication and have given the corresponding author the authority to act on their behalf in all matters pertaining to publication. The corresponding author is responsible for informing the coauthors of the manuscript status throughout the submission, review, and production process.

Preparation of manuscripts

Radiology and Oncology will consider manuscripts prepared according to the Uniform Requirements for Manuscripts Submitted to Biomedical Journals by International Committee of Medical Journal Editors (www.icmje.org). The manuscript should be written in grammatically and stylistically correct language. Abbreviations should be avoided. If their use is necessary, they should be explained at the first time mentioned. The technical data should conform to the SI system. The manuscript, excluding the references, tables, figures and figure legends, must not exceed 5000 words, and the number of figures and tables is limited to 8. Organize the text so that it includes: Introduction, Materials and methods, Results and Discussion. Exceptionally, the results and discussion can be combined in a single section. Start each section on a new page, and number each page consecutively with Arabic numerals. For ease of review, manuscripts should be submitted as a single column, double-spaced text, and must have continuous line numbering.

The Title page should include a concise and informative title, followed by the full name(s) of the author(s); the institutional affiliation of each author; the name and address of the corresponding author (including telephone, fax and E-mail), and an abbreviated title (not exceeding 60 characters). This should be followed by the abstract page, summarizing in less than 250 words the reasons for the study, experimental approach, the major findings (with specific data if possible), and the principal conclusions, and providing 3-6 key words for indexing purposes. Structured abstracts are required. Slovene authors are requested to provide title and the abstract in Slovene language in a separate file. The text of the research article should then proceed as follows:

Introduction should summarize the rationale for the study or observation, citing only the essential references and stating the aim of the study.

Materials and methods should provide enough information to enable experiments to be repeated. New methods should be described in details.

Results should be presented clearly and concisely without repeating the data in the figures and tables. Emphasis should be on clear and precise presentation of results and their significance in relation to the aim of the investigation.

Discussion should explain the results rather than simply repeating them and interpret their significance and draw conclusions. It should discuss the results of the study in the light of previously published work.

Charts, Illustrations, Images and Tables

Charts, Illustrations, Images and Tables must be numbered and referred to in the text, with the appropriate location indicated. Charts, Illustrations and Images, provided electronically, should be of appropriate quality for good reproduction. Illustrations and charts must be vector image, created in CMYK color space, preferred font "Century Gothic", and saved as .AI, .EPS or .PDF format. Color charts, illustrations and Images are encouraged, and are published without additional charge. Image size must be 2.000 pixels on the longer side and saved as .JPG (maximum quality) format. In Images, mask the identities of the patients. Tables should be typed double-spaced, with a descriptive title and, if appropriate, units of numerical measurements included in the column heading. The files with the figures and tables can be uploaded as separate files.

References

References must be numbered in the order in which they appear in the text and their corresponding numbers quoted in the text. Authors are responsible for the accuracy of their references. References to the Abstracts and Letters to the Editor must be identified as such. Citation of papers in preparation or submitted for publication, unpublished observations, and personal communications should not be included in the reference list. If essential, such material may be incorporated in the appropriate place in the text. References follow the style of Index Medicus, DOI number (if exists) should be included.

All authors should be listed when their number does not exceed six; when there are seven or more authors, the first six listed are followed by "et al.". The following are some examples of references from articles, books and book chapters:

Dent RAG, Cole P. In vitro maturation of monocytes in squamous carcinoma of the lung. *Br J Cancer* 1981; **43**: 486-95. doi: 10.1038/bjc.1981.71

Chapman S, Nakielny R. *A guide to radiological procedures*. London: Bailliere Tindall; 1986.

Evans R, Alexander P. Mechanisms of extracellular killing of nucleated mammalian cells by macrophages. In: Nelson DS, editor. *Immunobiology of macrophage*. New York: Academic Press; 1976. p. 45-74.

Authorization for the use of human subjects or experimental animals

When reporting experiments on human subjects, authors should state whether the procedures followed the Helsinki Declaration. Patients have the right to privacy; therefore the identifying information (patient's names, hospital unit numbers) should not be published unless it is essential. In such cases the patient's informed consent for publication is needed, and should appear as an appropriate statement in the article. Institutional approval and Clinical Trial registration number is required. Retrospective clinical studies must be approved by the accredited Institutional Review Board/Committee for Medical Ethics or other equivalent body. These statements should appear in the Materials and methods section.

The research using animal subjects should be conducted according to the EU Directive 2010/63/EU and following the Guidelines for the welfare and use of animals in cancer research (*Br J Cancer* 2010; 102: 1555 – 77). Authors must state the committee approving the experiments, and must confirm that all experiments were performed in accordance with relevant regulations.

These statements should appear in the Materials and methods section (or for contributions without this section, within the main text or in the captions of relevant figures or tables).

Transfer of copyright agreement

For the publication of accepted articles, authors are required to send the License to Publish to the publisher on the address of the editorial office. A properly completed License to Publish, signed by the Corresponding Author on behalf of all the authors, must be provided for each submitted manuscript.

The non-commercial use of each article will be governed by the Creative Commons Attribution-NonCommercial-NoDerivs license.

Conflict of interest

When the manuscript is submitted for publication, the authors are expected to disclose any relationship that might pose real, apparent or potential conflict of interest with respect to the results reported in that manuscript. Potential conflicts of interest include not only financial relationships but also other, non-financial relationships. In the Acknowledgement section the source of funding support should be mentioned. The Editors will make effort to ensure that conflicts of interest will not compromise the evaluation process of the submitted manuscripts; potential editors and reviewers will exempt themselves from review process when such conflict of interest exists. The statement of disclosure must be in the Cover letter accompanying the manuscript or submitted on the form available on www.icmje.org/coi_disclosure.pdf

Page proofs

Page proofs will be sent by E-mail to the corresponding author. It is their responsibility to check the proofs carefully and return a list of essential corrections to the editorial office within three days of receipt. Only grammatical corrections are acceptable at that time.

Open access

Papers are published electronically as open access on <https://content.sciendo.com/raon>, also papers accepted for publication as E-ahead of print.



TALZENNA[®]
talazoparib



Zdaj jim lahko ponudite več

Zdravilo **TALZENNA** je indicirano kot **monoterapija za zdravljenje odraslih bolnikov z germinalnimi mutacijami genov BRCA1 ali BRCA2**, ki imajo **lokalno napredovalega ali metastatskega HER2 negativnega raka dojk**. Bolniki so se morali predhodno že zdraviti z antraciklinom in/ali taksanom v okviru (neo)adjuvantnega zdravljenja lokalno napredovale ali metastatske bolezni, razen če bolniki za to zdravljenje niso bili primerni. Bolniki z rakom dojk, pozitivnim na hormonske receptorje, so se morali predhodno zdraviti z endokrinim zdravljenjem ali pa so morali biti neprimerni za endokrino zdravljenje.¹

BISTVENI PODATKI IZ POVZETKA GLAVNIH ZNAČILNOSTI ZDRAVILA

▽ Talzenna 0,25 mg, 1 mg trde kapsule

Za to zdravilo se izvaja dodatno spremljanje varnosti. Tako bodo hitreje na voljo nove informacije o njegovi varnosti. Zdravstvene delavce naprošamo, da poročajo o kateremkoli domnevem neželenem učinku zdravila. Glejte poglavje 4.8 povzetka glavnih značilnosti zdravila, kako poročati o neželenih učinkih. **Sestava in oblika zdravila:** Ena trda kapsula vsebuje talazoparibijev tosilat v količini, ki ustreza 0,25 mg oz. 1 mg talazopariba. **Indikacije:** Kot monoterapija za zdravljenje odraslih bolnikov z germinalnimi mutacijami genov BRCA1 ali BRCA2, ki imajo lokalno napredovalega ali metastatskega HER2 negativnega raka dojk. Bolniki so se morali predhodno že zdraviti z antraciklinom in/ali taksanom v okviru (neo)adjuvantnega zdravljenja lokalno napredovale ali metastatske bolezni, razen če za to zdravljenje niso bili primerni. Bolniki z rakom dojk, pozitivnim na hormonske receptorje (HR), so se morali predhodno zdraviti z endokrinim zdravljenjem ali pa so morali biti neprimerni za endokrino zdravljenje. **Odmerjanje in način uporabe:** Zdravljenje mora uvesti in nadzorovati zdravnik, ki ima izkušnje z uporabo zdravil za zdravljenje rakavih bolezni. Bolnike je treba izbrati na podlagi prisotnosti škodljivih ali domnevno škodljivih germinalnih mutacij gena BRCA, ki jih z validirano preskusno metodo določi izkušen laboratorij. **Odmerjanje:** Priporočeni odmerek je 1 mg enkrat na dan do napredovanja bolezni ali pojava nesprijemljive toksičnosti. **Izpušeni odmerek:** Če bolnik bruha ali izpusti odmerek, ne sme vzeti dodatnega odmerka. Naslednji predpisani odmerek mora vzeti ob običajnem času. **Prilaganja odmerkov:** Za obvladovanje neželenih učinkov je treba glede na resnost in klinično sliko razmisliti o prekinitvi zdravljenja ali zmanjšanju odmerka (glejte preglednico 2 v Povzetku glavnih značilnosti zdravila (PGZZ)). Za priporočena zmanjšanja odmerka glejte preglednico 1 v PGZZ. **Sočasno zdravljenje z zaviralci P-glikoproteina (P-gp):** Med zdravljenjem se je treba izogibati sočasni uporabi močnih zaviralcev P-gp. Sočasna uporaba pride v poštev šele po skrbni oceni morebitnih koristi in tveganj. **Posebne populacije: Okvara jeter:** Pri bolnikih z blago, zmerno ali hudo okvaro jeter prilaganje odmerka ni potrebno. **Okvara ledvic:** Pri bolnikih z blago okvaro ledvic prilaganje odmerka ni potrebno, pri bolnikih z zmerno okvaro je priporočeni začetni odmerek 0,75 mg enkrat na dan, pri bolnikih s hudo okvaro ledvic pa 0,5 mg enkrat na dan. Zdravila niso preučevali pri bolnikih s CrCl < 15 ml/min ali bolnikih, ki potrebujejo hemodializo. **Starejši bolniki:** Prilaganje odmerka ni potrebno. **Pediatrična populacija:** Varnost in učinkovitost pri otrocih in mladostnikih, starih < 18 let, nista bili dokazani. **Način uporabe:** Peroralna uporaba. Kapsulo je treba pogoltniti celo in se je ne sme odpirati ali raztapljati, lahko se jemlje s hrano ali brez nje. **Kontraindikacije:** Preobčutljivost na učinkovino ali katerokoli pomožno snov, dojenje. **Posebna opozorila in previdnostni ukrepi:** Mielosupresija: Poročali so o mielosupresiji, ki je zajemala anemijo, levkopenijo/nevтроpenijo in/ali trombocitopenijo. Zdravljenja ne smemo začeti, dokler bolniki ne okrevajo po hematološki toksičnosti, ki je posledica predhodnega zdravljenja. Treba je sprejeti previdnostne ukrepe za rutinsko spremljanje hematoloških parametrov ter znakov in simptomov, povezanih z anemijo, levkopenijo/nevтроpenijo in/ali trombocitopenijo. **Mielodisplastični sindrom/akutna mieloična levkemija (MDS/AML):** Pri bolnikih, ki so prejeli zaviralce PARP, vključno s talazoparibom, so poročali o MDS/AML. Ob izhodišču je treba pregledati celotno krvno sliko in bolnike med zdravljenjem mesečno spremljati glede znakov hematološke toksičnosti. Če potrdimo MDS/AML, je treba zdravljenje s talazoparibom prekiniti. **Kontracepcija pri ženskah v rodni dobi:** Če zdravilo dajemo nosečnicam, lahko škoduje plodu. Nosečnice je treba seznaniti z morebitnim tveganjem za plod. Ženske v rodni dobi med prejemanjem zdravila ne smejo zanositi in ob začetku zdravljenja ne smejo biti noseče, zato je treba pred zdravljenjem opraviti test nosečnosti. Bolnice morajo med zdravljenjem in še vsaj 7 mesecev po koncu zdravljenja uporabljati visokoučinkovito metodo kontracepcije. Bolnikom s partnerkami v rodni dobi ali nosečimi partnerkami je treba svetovati, naj med zdravljenjem in še vsaj 4 mesece po zadnjem odmerku uporabljajo učinkovito kontracepcijo. **Medsebojno delovanje z drugimi zdravili in druge oblike interakcij:** Učinkovine, ki lahko vplivajo na koncentracije talazopariba v plazmi: **Zaviralci P-gp:** Sočasni uporabi močnih zaviralcev P-gp (med drugim amjodaron, karvedilol, klaritromicina, kobicistata, darunavirja, dronedarona, eritromicina, indinavirja, itrakonazola, ketokonazola, lapatiniba, lopinavirja, propafenona, kinidina, ranolazina, ritonavirja, sakvinavirja, telaprevirja, tipranavirja, verapamil) se je treba izogibati. Če se sočasnemu dajanju ni mogoče izogniti, je treba zmanjšati odmerek talazopariba. **Induktorski P-gp:** Pri sočasnem dajanju z rifampicinom prilaganje odmerka ni potrebno. **Drugi induktorski (med drugim karbamazepin, fenitoin in šentjanževka)** lahko zmanjšajo izpostavljenost talazoparibu. **Zaviralci BCRP:** Učinka *in vivo* niso preučevali. Sočasni uporabi močnih zaviralcev BCRP (med drugim kurkumina in ciklosporina) se je treba izogibati. **Plodnost, nosečnost in dojenje:** Ženske v rodni dobi med prejemanjem zdravila ne smejo zanositi in ob začetku zdravljenja ne smejo biti noseče. Pred začetkom, med zdravljenjem in vsaj 7 mesecev (ženske v rodni dobi) oziroma 4 mesece (moški s partnerkami v rodni dobi/nosečimi partnerkami) po koncu zdravljenja je treba uporabljati visoko učinkovite kontracepcijske metode. Zdravilo lahko škoduje plodu, zato se naj ne uporablja pri nosečnicah in pri ženskah v rodni dobi, ki ne uporabljajo učinkovite kontracepcije. Dojenje med zdravljenjem in še vsaj 1 mesec po zadnjem odmerku ni priporočljivo. Zdravilo lahko oslabi plodnost pri moških s sposobnostjo razmnoževanja. **Vpliv na sposobnost vožnje in upravljanja strojev:** Ima blag vpliv na sposobnost vožnje in upravljanja strojev. **Neželeni učinki:** **Zelo pogosti:** trombocitopenija, anemija, nevтроpenija, levkopenija, pomanjkanje apetita, omotica, glavobol, bruhanje, diareja, navzeja, bolečina v trebuhu, alopecija, utrujenost. **Način in režim izdaje:** Rp/Spec - Predpisovanje in izdaja zdravila je le na recept zdravnika specialista ustreznega področja medicine ali od njega pooblaščenega zdravnika. **Imetnik dovoljenja za promet:** Pfizer Europe MA EEIG, Boulevard de la Plaine 17, 1050 Bruxelles, Belgija. **Datum zadnje revizije besedila:** 21.05.2021

Pred predpisovanjem se seznanite s celotnim povzetkom glavnih značilnosti zdravila.

Literatura: 1. Povzetek glavnih značilnosti zdravila Talzenna, 21.5.2021.

BRCA = (breast cancer susceptibility gene) gen dovzetnosti za raka dojk, HER2 = (human epidermal growth factor receptor 2) receptor humanega epidermalnega ravnega dejavnika 2.



Pfizer Luxembourg SARL, GRAND DUCHY OF LUXEMBOURG,
51, Avenue J. F. Kennedy, L-1855
Pfizer, podružnica Ljubljana, Letališka cesta 29a, Ljubljana

PP-TAL-EEP-0010
Datum priprave: september 2021.
Samo za strokovno javnost.

